

**NASA TECHNICAL
TRANSLATION**



NASA TT F-596

c.i



LOAN COPY: RETURN TO
AFWL (WLOL)
KIRTLAND AFB, NM MEX

TITANIUM ALLOYS FOR MODERN TECHNOLOGY

by N. P. Sazhin et al.

"Nauka" Press
Moscow, 1968

NATIONAL AERONAUTICS AND SPACE ADMINISTRATION • WASHINGTON, D. C. • MARCH 1970



0068948

TITANIUM ALLOYS FOR MODERN TECHNOLOGY

By N. P. Sazhin et al.

Translation of "Titanovyye splavy dlya novoy tekhniki"
"Nauka" Press, Moscow, 1968

NATIONAL AERONAUTICS AND SPACE ADMINISTRATION

For sale by the Clearinghouse for Federal Scientific and Technical Information
Springfield, Virginia 22151 — Price \$3.00

ANNOTATION

TITANIUM ALLOYS FOR MODERN TECHNOLOGY

The collection includes papers of a scientific-technical conference on the metallurgy, metalworking and use of titanium and its alloys (July, 1966). The following problems are considered: interaction of titanium with various elements of the periodic system (general problems of the metal chemistry of titanium); phase transformations in experimental and commercial titanium alloys; effect of new types of treatment (TMT, HTMT, etc.) of titanium alloys on the change of their physical-mechanical characteristics (including welding and soldering of alloys, studies connected with the investigation of oxidizability and gas saturation of a series of practically important titanium-based alloys). Phase diagrams for titanium mixtures with several elements are generalized, and recommendations are given for the selection of alloying admixtures in the development of titanium alloys with special mechanical and physical properties; new studies of a series of specific metallic systems Ti—Al—Mo—Zr, Ti—Al—V, Ti—Zr—Al, etc. are described.

The publication is addressed to a broad segment of researchers, designers, metal scientists, metallurgists and mechanical engineers and also to instructors, graduate students and students in metallurgical and mechanical engineering institutes and university departments.

EDITORIAL BOARD:

Academician N. P. Sazhin (Editor in Chief)
Doctor of Chemical Sciences I. I. Kornilov
Doctor of Technical Sciences V. I. Dobatkin
Doctor of Technical Sciences S. G. Glazunov
Candidate of Technical Sciences N. G. Boriskina (Chief Secretary of Editorial Board)
Candidate of Technical Sciences S. V. Ogurtsov
Candidate of Technical Sciences N. F. Anoshkin

INTRODUCTION

From the standpoint of its set of physicochemical and mechanical properties, titanium is one of the most promising new metals finding their way into the industry. Of particular importance are titanium alloys, which in a number of characteristics surpass the properties of high-alloy steels, at a specific gravity almost 1/2 that of iron and steel.

The development of the technology of production of metallic titanium was begun 20 years ago. The first semifinished samples of titanium sponge were obtained by magnesiothermic reduction of its tetrachloride. Having mastered this method of preparation of primary titanium, Soviet scientists and engineers soon developed and mastered the production of massive titanium by vacuum arc melting and organized the production of titanium and its alloys in our country.

The growing titanium industry was outfitted with the most modern industrial equipment for organizing scientific investigations and developing a continuous technology of production of semifinished products of all types from titanium and its alloys.

Today, our titanium industry is one of the foremost in the world, and it meets the country's demand for titanium at the level of world standards.

Research and experimental design studies on titanium and its alloys have been successfully carried on in many institutes and plants in the country. Studies in the area of chemical interaction of titanium with other elements, phase equilibria, structure and conversions in the solid state, patterns of change of all the properties, and a thorough study of the technological properties of titanium and its alloys have created the scientific base for the development and introduction of original brands of titanium alloys into production. Many of them have now found broad applications as structural, high-strength, heat-resistant and corrosion-resistant materials in various branches of the new technology.

Academician N. P. Sazhin
Professor, Doctor of Chemical Sciences I. I. Kornilov

TABLE OF CONTENTS

Annotation	iii
Introduction	iv
Chapter 1. Status and Prospects of the Production and Use of	
Titanium and Its Alloys	1
Status and Prospects of the Development of Production of	
Titanium Sponge, N. P. Sazhin	1
Status and Prospects of Development of the Production of	
Ingots and Semifinished Products from Titanium Alloys,	
A. F. Belov	8
Modern Titanium Alloys, S. G. Glazunov	11
Status and Prospects of Research in Metal Chemistry of Titanium,	
I. I. Kornilov	23
Improving the Technology of Production and Quality of Semifinished	
Products from Titanium Alloys, G. D. Agarkov, N. F. Anoshkin,	
V. I. Dobatkin, I. N. Kaganovich and V. A. Tsytsenko	36
Heat Treatment of Titanium and Its Alloys, V. A. Livanov,	
B. A. Kolachev and N. S. Lyasotskaya	41
Thermomechanical Treatment of Certain Titanium Alloys,	
I. M. Pavlov, A. E. Shelest and Yu. F. Tarasevich	55
Problem of Utilizing Titanium Scrap and Applications of	
Secondary Titanium, A. I. Kanyuk, E. M. Strikha and	
O. M. Shapovalova	68
Status and Prospects of Adoption of Titanium, A. I. Kanyuk,	
E. M. Strikha and N. F. Ivanova-Stepanova	76
Prospects for the Use of New Titanium Alloys in Chemical	
Machine Building, Yu. M. Vinogradov	84
Chapter 2. Metal Chemistry and Metallurgy of Titanium	89
Phase Diagram of a Part of the Ternary System Ti-Al-V	
(up to 45%Al), I. I. Kornilov and M. A. Volkova	89
Studies of the Phase Equilibrium and Certain Properties of Alloys	
of the System Ti-Al-Mo-Zr Rich in Titanium, I. I. Kornilov,	
N. G. Boriskina and M. A. Volkova	102
Study of the Equilibrium and Properties of Alloys of the Section	
Ti_3Sn - (Ti + 5%Zr) of the System Ti-Zr-Sn, N. I. Shirokova	
and T. T. Nartova	111
Study of the Phase Equilibrium and Properties of Alloys of the	
Titanium Corner of the System Ti-Zr-Al, N. I. Shirokova	
and T. T. Nartova	116
Nature of Hydrogen Brittleness of Titanium and Its Alloys,	
B. A. Kolachev and V. A. Livanov	123

Metastable Phases in the Alloys of Titanium with β -Alloying Metals, L. A. Petrova	138
Phase Transformations in Titanium Alloys Under Nonequilibrium Conditions, M. A. D'yakova and I. N. Bogachev	153
Effect of Tin and Zirconium on Transformations Accompanying the Heat Treatment of the Alloy Ti + 10% Cr, L. P. Luzhnikov, V. M. Novikova, A. P. Mareyev and I. S. Orlova	160
Study of Phase and Structural Transformations in Two-Phase Industrial Titanium Alloys, M. I. Yermolova, E. V. Polyak and O. P. Solonina	170
Changes in the Amount and Composition of the β Phase During Heat Treatment of the Alloy VTZ-1, Ye. I. Gus'kova, N. F. Lashko and L. M. Mirskiy	181
Decomposition of Titanium-Vanadium Martensite During Heating, S. G. Fedotov, K. M. Konstantinov and Ye. P. Sinodova	187
Study of Alloys of the System Ti-Al-Mo-Zr by the Bending Method at High Temperatures, N. G. Boriskina and M. A. Volkova	194
Study of the Properties of Alloys of the Systems Ti-Zr and Ti-Zr-Al, Ye. A. Borisova and I. I. Shashenkova	202
Some Problems of the Physicochemical Theory of High-Temperature Strength and the New High-Temperature Titanium Alloys ST-1, ST-3, ST-4 and ST-5, T. T. Nartova	208
Corrosion-Resistant Alloy of Titanium with 32% Mo, N. F. Anoshkin, N. G. Boriskina, P. B. Budberg, L. A. Yelyutina, S. I. Kushakevich, I. D. Nefedova, Ye. I. Oginskaya, Yu. M. Sigalov and G. L. Shvarts	221
Principal Properties of the Titanium Alloy AT-3 and the Prospects for Its Application, I. I. Kornilov, K. P. Markovich and V. S. Mikheyev	231
Parameters of the Diffusion of Oxygen in β -Titanium, L. F. Sokiryanskiy, D. V. Ignatov, A. Ya. Shinyayev, I. V. Bogolyubova, V. V. Latsh and M. S. Model'	239
 Chapter 3. Metallurgy and Technology of Titanium and Its Alloys	250
Magnesium Reduction of Titanium from Tetrachloride, N. P. Sazhin, S. V. Ogurtsov, K. N. Pavlova, V. L. Russo, V. S. Mirochnikov, Yu. N. Ol'khov, B. S. Gulyanitskiy, M. A. Losikova and V. D. Savin	250
Sodium Reduction of Titanium from Tetrachloride, S. V. Ogurtsov, V. D. Savin, A. Ye. Nikitin, O. V. Perfil'yev	264
Features of the Production Technology of Semifinished Products of Titanium and Its Alloys, I. N. Kaganovich	274
Production of Tubes from Titanium and Its Alloys, V. Ya. Ostrenko	289
Extrusion of Titanium Alloy Shapes, O. S. Mironov, M. F. Zakharov, Yu. I. Sobolev, L. A. Yelagina and A. A. Gel'man	301
Deformability of Certain ($\alpha + \beta$)- and β -Alloys of Titanium in Cold State, A. D. Lyuchkov, L. A. Il'vovskaya, V. I. Shevchenko and T. V. Kutsygina	305

Problems of the Welding of Titanium and Its Alloys, S. M. Gurevich	311
Abstracts	322

CHAPTER 1

STATUS AND PROSPECTS OF THE PRODUCTION AND USE OF TITANIUM AND ITS ALLOYS

N. P. Sazhin

Status and Prospects of the Development of Production of Titanium Sponge

In recent years, the production of metallic titanium has been successfully growing in the USSR. /5*

As recently as 20 years ago, metallic titanium was a rarity even in laboratories, but today the USSR is one of the first-rank producers of this metal in the world.

At the present time, the USSR possesses a powerful raw material base of various titanium ores. Geological organizations have revealed a considerable number of deposits. The exploitation of the Kusa deposit (Ural) and alluvial ilmenite deposits of the Ukraine (Samotkanskoye and Irshinskoye) has been started.

There are great reserves in the perovskite deposits of the Kola peninsula (Afrikanda) and titanomagnetites of the Ural and Transbaykal (Kruchina).

A study of the leucoxene ores of the northwestern regions of the European part of the Soviet Union has shown extensive possibilities of their industrial application.

The creation of the metallic titanium industry in the Soviet Union required an extensive development of research, design and planning.

At the Giredmet, the study of technological methods of production of metallic titanium began back in 1947.

After a thorough study of the sulfuric acid and chlorine methods of treatment of loparite, the Griedmet then recommended the adoption of the chlorine method in the industry; however, titanium tetrachloride (~50% of the chlorination products) thus remained unused. The most rational method for the production of metallic titanium turned out to be the use of tetrachloride.

After a study of a series of technological methods of reduction of titanium tetrachloride, the magnesiothermic method was chosen as the one most suitable for large-scale production.

In 1950, the Giredmet began a pilot-plant production of metallic titanium. At the same time, a study of the technology of titanium (magnesiothermic process

* Numbers in the margin indicate pagination in the foreign text.

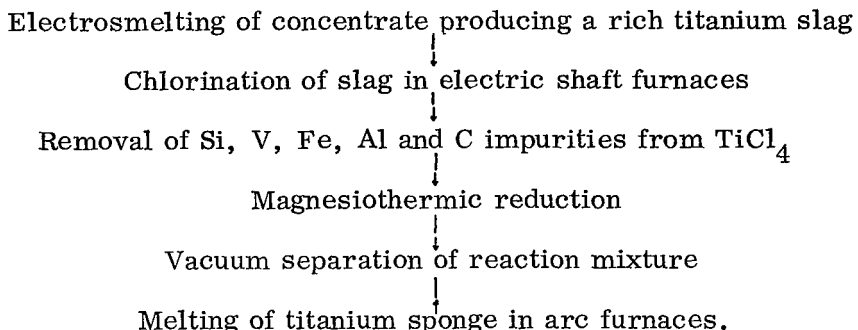
of production of titanium, particularly vacuum separation of titanium sponge and melting of titanium in arc furnaces) was started by the VIAM.

In 1954 it was found that loparite concentrates could not provide the necessary /6 amount of metallic titanium, and a search began for other types of raw material, primarily ilmenite concentrates.

Ilmenite concentrates contain a relatively small amount of titanium, and their chlorination involves the consumption of a large amount of chlorine, so that it was necessary to study the possibility of obtaining products with a high content of titanium dioxide from ilmenite concentrates.

In 1951, the Giredmet proposed a method of reduction of ilmenite concentrates in the course of melting in electric furnaces, resulting in the production of a rich titanium slag and cast iron. Pilot plant meltings of ilmenite concentrates were carried out; several tons of titanium slags, containing from 77 to 84% TiO_2 depending on the conditions, were thus melted. Chlorination in electric shaft furnaces of all slags obtained was also accomplished, and the possibility of chlorinating them satisfactorily was thus established.

These experiments were of extreme importance as the basis for the above-mentioned technological system of production of titanium. In 1952, the Giredmet and VIAM proposed the following flow sheet for the production of metallic titanium from ilmenite concentrates:



At the TsNIIChM, the possibility of smelting titanium slags and the calcium hydride method of producing metallic titanium were investigated. At the Baykov Metallurgy Institute, meltings of titanium slags were carried out, the composition of these slags was studied, and various methods of production of metallic titanium were investigated. Studies of titanium were developed with particular vigor in 1954, when the problem of titanium began to be considered by the VAMI, Gidroalyuminiy, VEI, GEOKhI, Mintsvetmet and several other organizations.

The Podol'sk chemical-metallurgical plant (PKhMZ), where the metallurgy of titanium is being studied, began operation in January, 1954.

The process of adoption of the magnesiothermic method of production of titanium was relatively complex. In the complexity of its technology, titanium is

a typical rare metal, but from the standpoint of the scale of production, it resembles minor metals and even certain nonferrous metals.

It was necessary to develop the apparatus of the process and test it on large pilot-plant installations. This required a considerable investment and long periods of time.

The supervision of the organization of the titanium industry was assigned to the Ministry of Nonferrous Metallurgy, which vigorously pursued many complex measures that achieved a rapid development of the titanium industry. The supervision of the new type of industry in the system of the Ministry of Nonferrous Metallurgy was assumed by a newly created administration, the Glavtitanredmet, ^{/7} which until 1957, i. e., until the liquidation of the ministry, supervised the development of the titanium industry. In the coordination of scientific research work carried on by the Glavtitanredmet and the Scientific Technical Council of the Ministry, considerable assistance was given by the Scientific Council on Titanium organized by the Academy of Sciences under the direction of Academician I. P. Bardin.

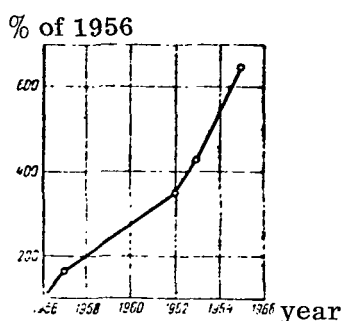


Figure 1. Increase of Cyclic Productivity of Reduction Units.

In the middle of 1954, titanium slags were smelted which contained about 80% TiO_2 . The introduction of such slags into the technology of titanium had a considerable influence on the economy of the titanium industry, and the problem of raw material was thus practically solved.

The work carried out at the Giredmet, VAMI, and later in other titanium plants made it possible to develop apparatus for chlorinators, and also for condensing and purifying technical-grade tetrachloride.

Up to now, two types of chlorinators have been developed and are being employed in the industry: electric shaft furnaces and high-capacity furnaces for chlorination in salt melts. Spraying with liquid tetrachloride has been introduced, a system of separation and utilization of the insoluble residue has been perfected, and the apparatus for the fractional distillation of the tetrachloride has been considerably modified.

The technology and apparatus of the magnesiothermic process of reduction and separation of titanium sponge has been perfected. Units of high cycle capacity have been created for the reduction and vacuum separation. The units "REDMET-500" and "REDMET-501", with a capacity of 1.5-2.0 ton of sponge per cycle, may be considered the best.

Figure 1 illustrates the growth of the productivity of reduction units in 1956-1966.

High capacity units made it possible to intensify the processes, in particular the low capacity and energy-consuming stage of vacuum separation of the reaction mixture, without lowering the quality of the titanium sponge produced.

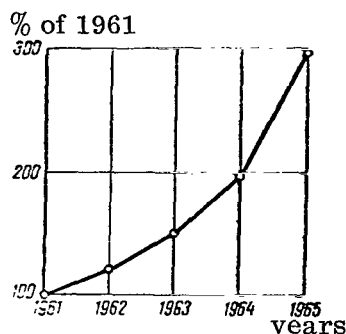


Figure 2. Growth of Production of Titanium Sponge in 1961-1965.

started. With the starting of the Usk'-Kamenogorsk plant (UKTMK) in 1965, the Soviet Union became one of the foremost producers of titanium in the world.

A data-processing and control machine (Mars 200 R) which governs 22 technological units or reduction and separation of titanium sponge, is being successfully employed. The use of Mars 200 R makes it possible to centralize the control process completely, makes the control and regulation more reliable, and reduces the role of subjective factors in the execution of a number of technological steps.

The magnesiothermic method of production of metallic titanium has been adopted in the planning of all the titanium plants in the USSR. In 1957, the Dnepr Titanium-Magnesium Plant (DTMZ) was put into operation, and in 1959, the first line of the Berezniki plant (BTMZ) was

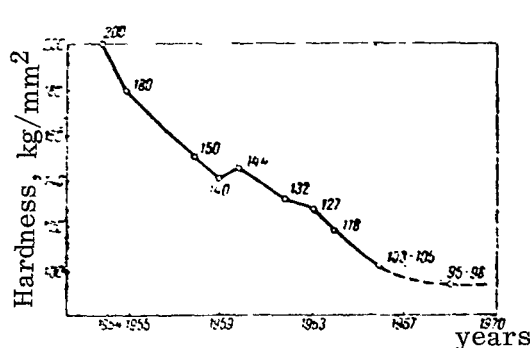


Figure 3. Change in the Hardness of Titanium Sponge Obtained in 1954-1966. (Ordinate Axis - Weighted Average of Hardness of Titanium Sponge of Commercial Batches).

Figure 2 illustrates the growth of titanium sponge production in 1961-1965.

The quality of titanium sponge has also increased continuously (Fig. 3), and now is as good as the best samples produced abroad, in particular, the best brands of titanium sponge obtained in Japan (see table).

At the Giredmet, further studies are continuing on the magnesiothermic method of production of metallic titanium; in particular, a continuous technological process has been developed in cooperation with the Paton Welding Institute.

Studies of a sodiothermic method of production of titanium are being made at the VAMI, Giredmet, The Baykov Metallurgy Institute, and DTMZ.

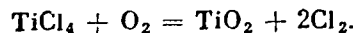
Brand	Fe	Chemical composition, %					Hardness, HB
		Si	C	Cl	N	O	
TG-100	0.07	0.04	0.03	0.03	0.02	0.04	100 and below
TG-105	0.08	0.05	0.03	0.03	0.025	0.05	101-105
TG-110	0.09	0.05	0.03	0.03	0.03	0.05	105-110
TG-120	0.11	0.05	0.04	0.03	0.03	0.065	110-120
TG-130	0.13	0.05	0.04	0.10	0.03	0.08	121-130

At the Giredmet, a two-step sodiothermic process of production of titanium is being developed in which a considerable part of the metal is obtained in the form of large high-purity crystals. The purity of such a metal is as good as that of titanium purified by iodide refining. The chief advantage of the two-step sodio-thermic method, as compared to the iodide method, is the possibility of organizing production of the pure metal on a large scale and thus of reducing cost several-fold.

Electrolytic methods of producing titanium and refining titanium waste are being studied at the Giredmet, VAMI, and TsNIIChermet.

At the Giredmet, a method has been developed for refining titanium by the thermal dissociation of iodide, which gives titanium with a purity of 99.8%. The method of iodide refining has been successfully applied in production.

Together with the Metallurgy Institute of the USSR Academy of Sciences, the Giredmet is carrying on studies of the chlorine method of production of pigment titanium dioxide. This excellent technological method of production is based on the reaction:



Using this reaction, one can create a continuous high capacity process of production of pigment titanium dioxide of high quality. Of great value is the possibility of recycling the chlorine for the chlorination of the initial raw material, i. e., titanium slags. /9

The following may be considered to be the major objectives of the development of the Soviet titanium industry:

- 1) improvement of the equipment used for dressing titanium ores;
- 2) development of a method of smelting of titanium concentrates mainly in the area of design of smelting units;
- 3) further modernization of equipment for the chlorination, condensation and purification of titanium tetrachloride;

- 4) improvement of apparatus for a batch magnesiothermic process;
- 5) development of a continuous magnesiothermic method;
- 6) development of methods for utilizing waste from titanium alloys;
- 7) development of a design of smelting furnaces for larger ingots;
- 8) improvement of methods of mechanical treatment of titanium alloys.

Tentative calculations show that if these measures are taken, in addition to an improvement in quality, it will be possible to achieve a considerable decrease of the cost of titanium sponge, semifinished products and articles made of titanium alloys, and also a considerable broadening of the scope of application of titanium in many areas of the national economy.

While the magnesiothermic process is being developed, it is necessary to continue the study of other methods, especially the electrolytic method of production of titanium.

REFERENCES

1. Pyatnov, V. I. Titanium minerals of the southern Timanskiy ore-bearing region. *Trudy Giredmeta*, XIII. "Metallurgiya," 1964.
2. Sazhin, N. P. Development of the metallurgy of rare and minor metals in the USSR. *Metallurgy of the USSR (1917-1957)*. Metallurgizdat, 1958.
3. Sazhin, N. P. and M. D. Khlystovskaya. New method of reprocessing perovskite concentrate. *Trudy Giredmeta*, I. Metallurgizdat, 1959.
4. Bardin, I. P. and V. A. Reznichenko. Studies in the metallurgy of titanium. Collection "40 years of Metallurgy in the USSR." Metallurgizdat, 1958.
5. Rapoport, M. B. Development of the technology of production of titanium slags. *Trudy VAMI*, 43, 1958.
6. Budneva, A. V., M. S. Model' and T. P. Ukolova. Solid solutions in high-titanium slags. Collection "Titanium and its Alloys," Issue 2. Metallurgy of Titanium. AN SSSR, 1959.
7. Reznichenko, V. A., M. B. Rapoport and V. A. Tkachenko. Metallurgy of titanium. Study of the electrosmelting of titanium slags. AN SSSR, 1963.
8. Ogurtsov, S. V. and V. A. Reznichenko. Study of the kinetic characteristics of the process of reduction of $TiCl_4$ with magnesium. Collection "Titanium and its Alloys," Issue 4. AN SSSR, 1960.
9. Reznichenko, V. A., S. V. Ogurtsov and P. S. Lopatin. Study of the process of production of titanium by the magnesiothermic method. Collection "Titanium and its Alloys," Issue 4. AN SSSR, 1960.
10. Dedkov, A. I. Reduction of $TiCl_4$ by a magnesium condensate at low temperatures in a vacuum. Collection "Titanium and its Alloys," Issue 8. AN SSSR, 1962.
11. Ageyev, N. V. et al. On the lower oxides of titanium. Collection "Titanium and its Alloys," Issue 2. Metallurgy of Titanium. AN SSSR, 1959.

12. Lipkes, Ya. M., K. N. Avertseva and I. N. Koptseva. Study of the nature of the process of condensation of magnesium and magnesium chloride vapors formed in the course of vacuum separation of the reaction mixture. Collection "Titanium and its Alloys," Issue 4, Metallothermy and Electrochemistry of Titanium. AN SSSR, 1961.
13. Sergeyev, V. V. and I. S. Kachanovskaya. Vacuum separation of titanium reaction mixture. Trudy VAMI, p. 51, 1963.
14. Savin, V. D. and V. A. Reznichenko. Study of the kinetics and mechanism of reduction of $TiCl_4$ by sodium. Collection "Titanium and its Alloys," Issue 9. AN SSSR, 1963.
15. Collection "Titanium and its Alloys." AN SSSR, 1963, Issue 9.
16. Strelets, Kh. L. et al. Titanium. Principles of Metallurgy, III. Metallurgizdat, /10 1963.
17. Sergeyev, V. V., N. V. Glaytskiy and V. P. Kiselev. Metallurgy of Titanium. "Metallurgiya," 1964.
18. Trudy Giredmeta, Vol. XV. Metallurgizdat, 1966.
19. Mishenev, M. A. et al. Smelting of ilmenite concentrates of various deposits into a rich titanium slag. Collection "Titanium and its Alloys," Issue 9, Metallurgy and Chemistry of Titanium. AN SSSR, 1963.
20. Kramnik, Yu. V. Smelting of ilmenite concentrate into a rich titanium slag. Tsvetnye metally, 1960, 5.
21. Movsesov, E. E. et al. Use of correlation analysis and computer in the study of the process of smelting of titanium slag. Tsvetnyye Metally, 1965, 9.
22. Forsblom, G. W. and R. A. Sandler. Effect of certain technological parameters on the indices of the process of magnesiothermic reduction. Tsvetnyye Metally, 1960, 10.
23. Kazain, A. A. and A. D. Khromov. Studies in the electrochemistry of titanium. Forty years of metallurgy in the USSR. Metallurgizdat, 1958.
24. Olesov, U. Yu. G. et al. Electrolytic refining of wastes of industrial titanium alloys. Tsvetnyye Metally, 5, 1966.
25. Rotyakin, V. V. Quality of titanium sponge obtained by using different forms of magnesium. Tsvetnyye Metally, 8, 1965.
26. Moroz, D. S. et al. Titanium and its alloys. Sudpromgiz, 1960.
27. Markov, V. F., E. B. Gitman and E. P. Belyakova. Electrolysis of $TiCl_4$ in fused salts. Ukr. khim. zh. 1, 1961.
28. Arutyunov, E. A. et al. Separation of a magnesiothermic reaction mixture in a unit with a bottom condenser. Tsvetnyye Metally, 6, 1966.
29. Reifman, M. B. et al. Production of titanium by the iodide method. Tsvetnyye Metally, 5, 1961.
30. Lozichniy, N. V. et al. Use of computer for centralized control in the production of titanium sponge. Tsvetnyye Metally, 10, 1966.
31. Vetrov, V. I. et al. Development of a standard process of production of titanium sponge. Zh. Prik. Khimii, 6, 1965.
32. Fal'kevich, E. S., E. A. Arutyunov and E. A. Lyukevich. Determination of the quality of titanium sponge from its hardness. Tsvetnyye Metally, 8, 1966.

STATUS AND PROSPECTS OF DEVELOPMENT OF THE PRODUCTION OF INGOTS AND SEMIFINISHED PRODUCTS FROM TITANIUM ALLOYS

A. F. Belov

In recent years, a completely new branch of metallurgy, the production of ingots from rolled stock and titanium alloys, has been created in the USSR. Titanium is one of the most important construction materials in modern technology. In the last few years, the development of the production and consumption of titanium has been particularly vigorous.

The industrial production capacity of titanium sponge has grown considerably. The output of sponge has increased by a factor of more than 10 in seven years. The Berezniki and Ust'-Kamenogorsk complexes have been put into operation. The purity of titanium sponge has been increased, and the fraction of higher grades (with a hardness < 120 units) exceeds 80% of the total output. Over one-half of all the sponge has a hardness of up to 100-105 units.

Industrial production of ingots from titanium alloys weighing from 0.5 to 5 tons has begun. This has required the solution of a large group of problems connected with the development of methods of fusion, construction of vacuum arc furnaces, methods of extrusion of electrodes, measures for preventing the danger of explosions, etc.

The technology has been developed and industrial production of deformed semifinished products-sheets and plates, rods, sections and forgings, stamped articles, rings, pipes and wires- have been achieved. The USSR now surpasses the United States in output of rolled stock from titanium. The cost and prices of semifinished titanium products have been considerably lowered in the course of the seven-year plan.

/11

The effort of scientific research institutes and plants have created a number of structural, heat resistant and special titanium alloys characterized by a high specific strength and heat resistance permitting the use of titanium at temperatures up to 500°C and in some cases higher temperatures; they are also characterized by corrosion resistance in various media, including very corrosive ones.

Processes of welding, brazing, cutting, sheet metal stamping and closed impression die forging, thermal and chemico-thermal treatment, intricate shape casting and many other operations have been adopted in machine-building plants with the participation of scientific research institutes.

The accumulated experience of production and application of titanium makes it possible to proceed with the realization of the program of further broad development of the titanium industry; in the immediate future, this development will follow two main directions:

1. Further increasing the production of titanium rolled stock (by a factor of 3-4), with the steadily increasing demands of machine building being satisfied.

2. Increasing the economy of production and bringing the cost of titanium parts (per unit volume) closer to the level of the cost of stainless steel parts (one-third of the level of the cost of heat-resistant nickel alloys).

A major task in the development of the capacities of production of ingots and rolled stock from titanium alloys is to boost the construction of new shops. It also becomes necessary to use large ingots (5-15 tons). In addition to the use of the method of section rolling of the intermediate billet in the forging-stamping, tube, section and extrusion operations, the switch to large ingots will provide a twofold increase in the volume of the metal from vacuum arc furnaces, a 3-4% increase of acceptable castings, a rise in the productivity of the machining shops, and an improvement in the quality of rolled stock.

As before, the problem of the most economic consumption of the metal remains a major one. In the last three years, much attention has been focused on the development and assimilation of methods of preparation of the most economic billets, the quantity of stamped items adopted per year has increased considerably, and the output of stampings in 1966 was 10 times that of 1964. The production of extruded sections have been adopted for preparing rings parts by welding, instead of forged or rolled parts. A 450 structural and merchant mill has started operation, and the production of rolled rods 26-60 mm in diameter and mechanically worked billets for stamping blades has been organized; the production of less economic forged and extruded rods of these dimensions has been completely discontinued.

All of this has made it possible to reduce the expenditure of metal considerably. However, even now the average coefficient of utilization of the metal, i.e., the ratio of the weight of the finished parts to the weight of the charge, amounts to only 18%, and for certain more intricate parts, 4-5%.

In the near future, it will be necessary to raise the coefficient of utilization of the metal by a factor of at least 2. To do this, it is necessary to solve such problems as the development of improved lubricants for extrusion and stamping, the creation of more resistant materials for the extruding and stamping tool, and many others.

It is necessary considerably to expand the nomenclature of rolled sections from titanium alloys.

A major source of reduction of the expenditure of the metal is the broad utilization of intricate shape casting. The technology of intricate shape casting of titanium alloys has now been adequately perfected. In institutes as well as many plants, intricate shape casting sections have been created, intricate castings have been assimilated, but the exceptional possibilities of this method are not yet in sufficient use. Intricate shape castings should be used for preparing intermediate shaped billets which are subsequently worked mechanically.

The problem of utilization of wastes has not been definitively solved either. In 1966, the amount of waste used in absolute terms increased considerably. However, the relative proportion of waste in the charge increased insignificantly (and amounts to about 29%). Metallurgical plants now utilize practically all of their waste, which can be purified by surface treatment, i.e., etching, tumbling and other operations. The processing of quality standardized waste obtained from consumers of rolled

/12

stock has also begun. However, in machine-building plants the grading of waste according to brand and alloys has been inadequately organized, and its processing becomes impossible or economically undesirable. As a result, the waste accumulates or is used for the production of ferrotitanium or directly in ferrous metallurgy with a much lower economic efficiency. Also formed in the plants is a significant fraction of so-called quality-ungraded waste, which is so contaminated with gases that it cannot be used in a charge without refining. However, the creation of the necessary productive capacities for refining waste has been intolerably protracted.

In the present five year plan, it is necessary to achieve a closed metallurgical balance in the entire industry by using all the waste of metallurgic and machine-building plants. To this end, during the five year plan in metallurgical plants preparing rolled stock, it is necessary to expand or create new sections for processing waste with the introduction of suitable capacities; to introduce the proper order with the collection, storage and unloading of waste in machine building plants; to introduce waste refining shops and sections into the system.

It is necessary to consider two more important problems of development of production of semifinished titanium products. As already noted, plants preparing titanium sponge have achieved a considerable increase in the purity of the sponge. However, no stable shipment of graded sponge has been achieved, and considerable fluctuations in the average hardness of sponge supplied to metallurgical plants are tolerated. The supply of sponge of not only soft grades but also great hardness, TG130, TG140, TG155, continues. This impairs the work of metallurgical plants directed at stabilizing the quality of rolled stock and composition of the alloys. It is necessary to obtain a more stable quality of the sponge in the immediate future. Incidentally, it should be noted that the improvement of the purity of the sponge has been associated with a considerable increase in the average price of a ton of sponge supplied to metallurgical plants. Thus, in 1961-1966 the average price of sponge rose by a factor of almost 1.5.

To date, various institutes working together with plants have developed a large number of alloys (about 40 titanium alloys have been developed and are in the stage of industrial or experimental production). This number of alloys greatly hinders the work of metallurgical plants, disperses the efforts of scientific research institutes which study, improve and adopt them, etc. It is clear that the existence of such an extensive nomenclature is in no way justified.

At one time, attempts were made to create a single commission for all the branches which would evaluate the need for developing and producing any given alloy. A commission of this kind existed for a time, but recently its activity has been practically discontinued. It is obviously advisable to entrust such a permanent commission with not only the supervision of the introduction of new alloys, but also with the study and a considerable reduction of the existing nomenclature of alloys.

/13

It would also be desirable to have a single coordinated plan of development and adoption of alloys which would exclude the repetition of research already done and parallelism in the work.

An indispensable condition for the introduction of an alloy into industry should be its preliminary testing under industrial conditions, on industrial products and not on laboratory specimens.

MODERN TITANIUM ALLOYS

S. G. Glazunov

In comparing titanium alloys, the most desirable criterion used should be the structural type instead of the technological indices (types of semifinished products, areas of application).

From the standpoint of the structural type, all industrial titanium alloys are solid solutions based on one of the allotropic modifications of titanium (α -Ti with a close-packed hexagonal lattice or β -Ti with a bcc lattice).

Attempts to develop industrial titanium alloys with an intermetallic type of hardening (similar to Duralumin type alloys) have been unsuccessful (the only exception is the binary alloy Ti-Cu). The intermetallic compounds encountered in industrial titanium alloys, for example the chemical compound of titanium with chromium, titanium carbide and hydride, etc., formed as a result of a eutectoid reaction, have an adverse effect on the mechanical and technological properties of titanium alloys, and for this reason special safety measures are usually taken to prevent the formation of these phases in the course of production of semifinished products.

In some cases, however, it may be assumed that useful intermetallic phases are present in industrial titanium alloys. Thus, the extremely strong influence of small admixtures of silicon (0.1-0.2%) on the heat resistance of titanium alloys containing molybdenum (VTZ-1, VT8, VT9) leads to the assumption that dispersed precipitates of a very stable and high melting phase, molybdenum disilicide, can be formed in this case. However, this assumption has not yet been successfully confirmed by direct experiments.

The practical use of the variable solubility of the intermetallic phase for the purpose of hardening is known only for a single low binary alloy containing 2% Cu and used in the British industry as a substitute for some grades of technical titanium. The alloy with 2% Cu in the annealed and quenched states is very soft and similar to unalloyed titanium in plasticity; after aging, its strength increases by 30-50%.

The strength of two-phase industrial titanium alloys may be increased with heat treatment by 50-100% as compared to the initial state (the strength of the alloy after annealing is usually implied) without the use of the mechanism of intermetallic hardening. The matrix and the hardening phase in this case are the solid solutions mentioned above, whose mechanical properties can be varied over a wide range depending on the alloying and on the technological factors (conditions of thermo-mechanical treatment).

It is most convenient therefore to retain the principle of classification of titanium alloys into three groups: α alloys, two-phase alloys and β alloys. Lately, alloys based on α -Ti containing a small amount of β phase and retaining all of the basic characteristics of pure α alloy have been applied more and more widely. A small amount of β phase improves the technological and mechanical properties of such alloys, which it is useful to refer to as "pseudoalpha alloys." In addition, alloys based on β -Ti, have appeared which are effectively hardened by quenching and aging owing to their small content of the α phase, which in this case plays the

/14

part of the hardener. Their properties are similar to those of pure β alloys, and they are, in the strict sense of the word, two-phase alloys; it will therefore be correct to refer to them as "pseudobeta alloys." Finally, α alloys can be subdivided into pure α alloys and alloys with an intermetallic phase.

The tables given below have been compiled on the basis of this principle.

Tables 1-3 give data on the chemical composition of industrial titanium alloys of the USSR, USA and England, and Tables 4-7 give their basic mechanical properties.

It is seen that alloys in these three countries are approximately equivalent in quality and variety of compositions, but there are certain differences in the general direction and trends of development of the various groups of alloys.

Comparing the literature data on the use of titanium alloys, one can realize which alloys are leading ones in each of the countries considered. The great majority of products from titanium alloys are prepared from 5-7 alloys, the fraction of the remaining alloys being very minor (10-15%).

In the USA, the leading alloys include technical titanium, alloys of types VT6 and VT5-1, Ti-8Al-1Mo-1V, Ti-4Al-4Mn, 11 alloy B-120V CA; the first three alloys in 1965-1966 comprised about 85% of the total tonnage of semifinished titanium products.

In England, where the production of titanium alloys is only a fraction of that in the USSR and USA, preference is given to Ti-2Al-2Mn, to an alloy of type VT5-1, to the alloy IMI 679, and to technical titanium.

Some interesting conclusions can be drawn from Tables 1-3. In quantity and variety of alloys, all three specifications are approximately equivalent. The oldest and broadest is the US specification, the United States having begun the development of titanium alloys before the USSR and England. For this reason, some of the most successful compositions of American alloys have found applications in other countries as well, particularly the α alloy Ti-5Al-2.5Sn, known in the Soviet Union as brand VT5-1, and in England as IMI 317, and also the two-phase alloy Ti-6Al-4V (our brand VT6, English brand IMI 318A).

Each of the three specifications considered (Table 1-3) has its characteristics which reflect the basic trends in the study of titanium alloys. The characteristic of the English specification is a trend toward multicomponent alloying (about one-half of the English alloys contain 4-5 alloying components in addition to titanium). The overwhelming majority of US alloys contain two alloying components each, more seldom there are alloys with three alloying additions and only one contains four alloying components. Multicomponent alloying of titanium is undoubtedly a progressive trend which is not fully appreciated in USA.* In the USSR, in addition to multicomponent alloying, so-called chains of alloys of the same type are used, as illustrated by a series of five alloys based on the system Ti-Al-Mn. For the same

/16

* This is confirmed by the fact that recently the USA has been purchasing licenses for the production of English heat-resisting alloys of such type, for example alloy IMI 679, used in jet engine compressors.

**TABLE 1. CHEMICAL COMPOSITION OF TITANIUM ALLOYS
 PRODUCED IN THE USSR (IN %; BALANCE - Ti)**

/15

Alloys with α -structure		Two-phase alloys (>2% β -stabilizers)
VT1-00	Technical titanium	BT6C 4.5 Al; 3.5 V
VT1-0	Same	BT6 6 Al; 4 V
VT5	5 Al	BT8 6.5 Al; 3.5 Mo; 0.2 Si
VT5-1	5 Al; 2, 5 Sn	BT9 6.5 Al; 3.5 Mo; 0.2 Si; 2 Zr
Pseudo- α -alloys (up to 2% β -stabilizers)		BT3-1 5.5 Al; 2 Mo; 2 Cr; 1 Fe; 0.2 Si
OT4-0	1 Al; 1.5 Mn	BT14 4 Al; 3 Mo; 1 V
OT4-1	2 Al; 1.5 Mn	BT16 2.5 Al; 7.5 Mo
OT4	3 Al; 1.5 Mn	BT22 2.5 Al; 7.5 Mo; 1 Cr; 1 Fe
BT4	4 Al; 1.5 Mn	
OT4-2	6 Al; 1.5 Mn	
AT3	3 Al; 1.5 (Fe + Cr + Si + B)	Pseudo- β -alloys
AT4	4 Al; 1.5 (Fe + Cr + Si + B)	BT15 3 Al; 8 Mo; 11 Cr
BT18	6 Al; 11 Zr; 1 Mo; 1 Nb	
BT20	6 Al; 2 Zr; 1 Mo; 1 V	

optimum content of manganese (1.5%), these alloys have variable contents of aluminum, which provide a broad range of strength characteristics. A one-type composition presents many advantages for metallurgical plants by facilitating the preparation of the charge and use of the waste.

It is also necessary to mention certain general trends in the development of titanium alloys, namely, the rapid development of the new subgroup of pseudoalpha alloys (they are termed "super-alpha" alloys in the USA). Titanium alloys with an alpha structure have a series of advantages: excellent weldability, high creep resistance, lack of sensitivity to hardening heat treatment, satisfactory thermal stability (ability to retain high plastic and strength properties after a long exposure to external stresses at high temperatures). However, to date, only one sheet alpha alloy of brand VT5-1 has been known which has a relatively low guaranteed hardness (75 kg/mm²), and this has restricted its applications. The pseudoalpha alloy of brand VT20 developed in the USSR has a strength of 95 kg/mm² owing to the addition of zirconium, molybdenum and vanadium. The properties of these two alloys are given in Fig. 1 a. The content of β -stabilizing elements is close to the limit of their solubility in α -Ti, and therefore the amount of the residual β phase in alloy VT20 is very low. This makes it possible to retain the basic advantages of α -alloys and at the same time slightly increase the plasticity and lower the sensitivity to hydrogen impurity as compared to pure α alloys. An analogous alloy in the USA is Ti-8Al-1Mo-1V (company brand 8-1-1). This alloy is inferior to VT20 in thermal stability, this being attributed to the high content of aluminum. Pseudo-alpha alloys are also used as heat-resisting materials for forgings and stampings (for example, alloy VT18, see Fig. 1 b).

Very frequently, old alloys are subjected to additional alloying, as for example alloy Ti-6Al-6V-2Sn, which may be considered to be a "reinforced variant" of the known alloy Ti-6Al-4V (USA). The same may be said for VT9, which is a further development of alloy VT8, and alloy VT22 was compounded from alloy VT16.

TABLE 2. CHEMICAL COMPOSITION OF TITANIUM ALLOYS
 PRODUCED IN THE USA (IN %; BALANCE - Ti)

Alloys with α -structure	Two-phase alloys (>2% β -stabilizers)
Ti - 35 A, Ti - 45 A . . . Technical titanium	Ti - 155 A 5 Al; 1,5 Fe; 1,4 Cr; 1,2 Mo
Ti - 50 A, Ti - 50 A . . . Same	Ti - 4 Al - 4 Mn 4 Al; 4 Mn
Ti - 65 A, Ti - 75 A . . . Same	Ti - 4 Al - 3 Mo - 1 V . . . 4 Al; 3 Mo; 1 V
Ti - 5 Al - 2,5 Sn 5 Al; 2,5 Sn	Ti - 3 Al - 2,5 V 3 Al; 2,5 V
Ti - 7 Al - 12 Zr 7 Al; 12 Zr	Ti - 3 Al - 5 Cr 3 Al; 5 Cr
Ti - 5 Al - 5 Sn - 5 Zr 5 Al; 5 Sn; 5 Zr	Ti - 2,5 Al - 16 V 2,5 Al; 16 V
Pseudo- α -alloys (<2% β -stabilizers)	Ti - 140 A 2 Fe; 2 Cr; 2 Mo
Ti - 8 Al - 1 Mo - 1 V 8 Al; 1 Mo; 1 V	Ti - 8 Mn 8 Mn
Ti - 8 Al - 2 Nb - 1 Ta 8 Al; 2 Nb; 1 Ta	Alloys with β -structure
Ti - 8 Al - 8 Zr - 1(Nb+Ta) 8 Al; 8 Zr; 1(Nb + Ta)	B-120 VCA 3 Al; 13 V; 11 Cr
Two-phase alloys (>2% β -stabilizers)	Ti - 12 Mo - (4-S) Sn 12 Mo; 4-S% Sn
Ti - 7 Al - 4 Mo 7 Al; 4 Mo	Ti - 1 Al - 8 V - 5 Fe 1 Al; 8 V; 5 Fe
Ti - 6 Al - 4 V 6 Al; 4 V	
Ti - 6 Al - 6 V - 2 Sn 6 Al; 6 V; 2 Sn	
Ti - 5 Al - 2,75 Cr - 1,25 Fe 5 Al; 2,75 Cr; 1,25 Fe	

Note. Alloys containing zirconium, niobium and tantalum and also the last two β alloys are experimental. Because of the great variety of company designations of alloys, a rational branding system (based on chemical composition) employed by the Titanium Metals Corporation of America has been adopted as the basis in this table.

TABLE 3. CHEMICAL COMPOSITION OF TITANIUM ALLOYS
 PRODUCED IN ENGLAND (IN %; BALANCE - Ti)

Alloys with α structure	Two-phase alloys (>2% β -stabilizers)
Ti-115, 120, 130, 150, 160 Technical titanium	IMI 314A . . 4 Al; 4 Mn
Ti-5 Al-2,5 Sn 5 Al; 2,5 Sn	IMI 318A . . 6 Al; 4 V
Ti-2 Cu 2 Cu (α -alloy-containing intermetallic phase)	Hy-50 4 Al; 5 Mo; 0,5 Si; 2 Sn
Hy-55 3 Al; 6 Sn; 5 Zr; 0,5 Si	IMI 680 2,25 Al; 4 Mo; 11 Sn; 0,2 Si
Pseudo- α -alloys (>2% β -stabilizers)	IMI 684 6 Al; 5 Zr; 1 W; 0,2 Si
IMI 314C 2 Al; 2 Mn	Pseudo- β -alloys
Hy-60 3 Al; 6 Sn; 5 Zr; 0,5 Si; 2 Mo	IMI 205 15 Mo
IMI 679 2,5 Al; 11 Sn; 5 Zr; 0,25 Si; 1 Mo	

TABLE 4. PROPERTIES OF VARIOUS ALLOYS

/17

Alloy	Use temperature, °C	Test temperature, °C	σ_B , kg/mm ²	$\sigma_{0.2/100}$, kg/mm ²	σ_{-1} , kg/mm ²
VT3-1 (USSR)	400—450	20	105	—	—
		300	83	65	32
		400	80	50	—
		450	75	28	—
Ti-155A (USA)		20	102	—	—
		300	74	—	—
		400	68	—	—
		450	63	—	—
IMI 318A (England) or Hy-45		20	100	—	—
		300	75	—	—
		400	71	—	—
		450	—	31	22
VT8 (USSR)	450—500	20	110	—	40
		300	88	—	—
		400	82	—	—
		450	80	43	—
Ti-7Al-4Mo (USA)		20	112	—	—
		300	88	—	—
		400	84	—	—
		450	77	—	—
Hy-50 (England)		20	126	—	39
		300	95	74	31
		400	89	53	26
		500	86	7	—
VT9 (USSR)	500—550	20	120	—	36
		300	99	—	—
		400	90	—	—
		500	85	38	25
Hy-60 (England)		20	110	—	34
		300	86	—	32
		400	80	—	30
		450	—	51	29
		500	77	41	28
VT18 (USSR)	550—600	20	110	—	—
		400	96	—	—
		500	90	37	—
		550	88	21	—
		600	77	11	33
IMI 679 (England)	—	20	105	—	—
		500	82	—	—
		540	76	—	—

Note. 1. All the alloys in the state following annealing, alloys Hy-50 and Hy-60 - after heat treatment. 2. Main heat-resisting alloys for tubojet engines in the USA - alloy Ti-6Al-4V (corresponds to English alloy IMI 318A) and in England - alloy IMI 679.

TABLE 5. WELDABLE TITANIUM ALLOYS (SHEET)
 USED AT (-252) - (+550°C)

/18

Alloy	Testing temperature, °C	σ_B , kg/mm ²	$\sigma_{0.2/100}$, kg/mm ²
VT5-1 (USSR)	20	80-100	—
	350	55	32
	400	54	—
	500	48	—
VT20 (USSR)	20	95-110	—
	350	75	55
	500	70	17
	550	60	5
IMI 317 (England)	20	80	—
	315	59	—
	427	52	—
	538	45	—
8-1-1 (USA)	20	95	—
	315	80	—
	427	73	—
	550	59	—

TABLE 6. HIGH STRENGTH TITANIUM ALLOYS (ROD, SHEET)
 IN STATE FOLLOWING HEAT TREATMENT,
 USED AT 20-400°C

Alloy	Testing temperature, °C	σ_B , kg/mm ²	σ_{100}	σ_{-1}
VT14 (USSR)	20	115-130	68	35
	400	95		
Ti-4Al-3Mo-1V (USA)	20	119	—	—
	400	93		
VT6 (USSR)	20	115	75	—
	400	82		
IMI 318 (England)	20	115	—	—
	425	83		

We should note the influence of the purity of the initial sponge titanium on the composition and properties of industrial titanium alloys.

TABLE 7. CAST TITANIUM ALLOYS (TESTS AT 20°C)

Alloy	$\sigma_B \cdot \text{kg/mm}^2$	$\delta, \%$	$\sigma_u \cdot \text{kgm/cm}^2$
VT5L(USSR)	70-90	8	5
VT3-1L (USSR)	100-110	5	3-5
IMI 318 (England)	80-95	7-10	5

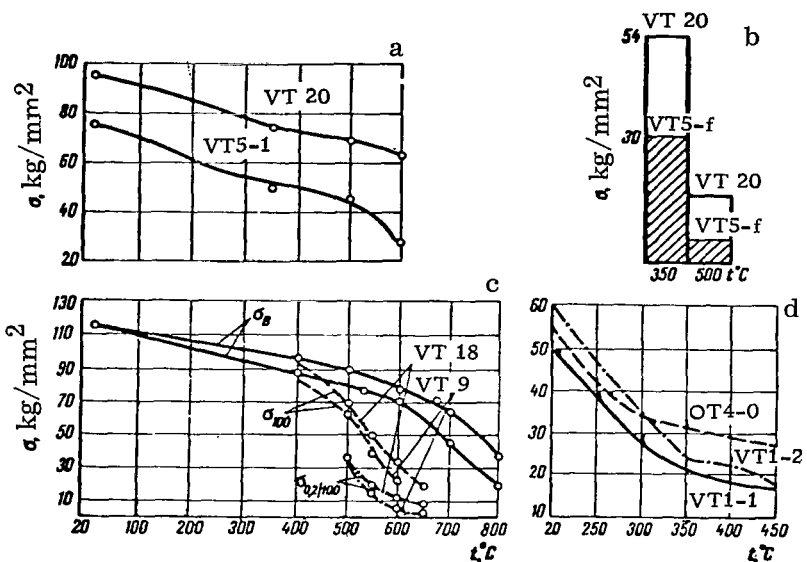


Figure 1. Mechanical Properties Versus Testing Temperature of Alloys.

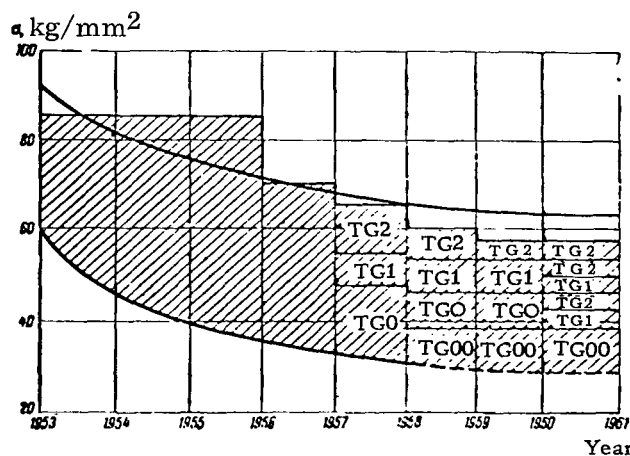


Figure 2. Change in the Quality of Sponge Titanium.

During the initial period of development of titanium metallurgy, the content of interstitial impurity elements (oxygen, hydrogen and carbon) was fairly significant. This substantially increased the strength and decreased the plasticity of technical titanium and titanium alloys.

The strength of titanium alloys is an additive property. It is made up of the strength of the initial titanium and the hardening effects of each alloying addition. This forms the basis of the calculation of the charge of titanium alloys in plants. As the strength of the initial titanium decreases, it becomes necessary to raise the content of alloying elements. This is illustrated by the graph of Fig. 2. It is evident that the strength of unalloyed titanium, which in 1953 reached 90 kg/mm^2 , is now $30-45 \text{ kg/mm}^2$ (for VT1-00 titanium) i. e., 2-3 times lower, whereas the plastic properties have been increased by approximately the same factor. When the strength requirements are higher, the use of low and medium-alloyed alloys is recommended, for example OT4-0 alloy of the system Ti-Al-Mn, whose characteristics are shown in Fig. 1 c.

/20

In the gradual increase of the purity of the initial titanium there is a negative side consisting in a drop of the strength of titanium and its alloys. In this connection, the question arose whether it was correct to try for an unlimited increase of the purity of the initial titanium, if this were associated with an increase of scrap at plants preparing sponge titanium, if the strength characteristics decreased and the expenditure of alloying elements (which are sometimes expensive) were increased in order to preserve the strength at the previous level. However, studies have shown that it is inadvisable to try to preserve the strength due to the presence of interstitial impurity elements, since this would result in a decrease of other important properties of the alloys: plasticity, heat resistance, thermal stability, weldability (see Table 8, cf. alloy VT3-1, melted on soft sponge of the 1964-1965 period and the same alloy from a 1957 batch).

TABLE 8. SOME PROPERTIES OF ALLOY VT3-1 (kg/mm^2)

Temperature, °C	Characteristic	1964-1965	1957
20	σ_B	100-120	95-120
	σ_{-1}	$53(2 \cdot 10^7)$ *	$48(10^7)$
	σ_{-1}^H	$42(2 \cdot 10^7)$	$38(10^7)$
400	σ_{-1}^H	$48(2 \cdot 10^7)$	$40(10^7)$
	σ_{100}	78	60
	σ_{2000}	7.5	—
	$\sigma_{0.2/100}$	50	30
	$\sigma_{0.2/2000}$	37	—

*Number of cycles.

An increase of alloying with the preservation of the number of elements present has limits which are determined by the structure of the phase diagrams. In alloy VT3-1 at $>6.5\%$ Al, $>3\%$ Mo and $>2\%$ Cr, the thermal stability decreases

at 400–450°C in long-term operation (about 2000 hr). A further increase of strength is possible only by introducing new elements (for example, zirconium in alloys of the system Ti-Al-Mo). This is responsible for the trend toward the development of multicomponent titanium alloys.

Thus, the increase of the purity of the initial titanium with respect to interstitial impurities is a gradual step, and the difficulties connected with changes of the chemical composition and calculation of the charge are compensated for by an improvement of the mechanical properties. Furthermore, titanium contaminated with oxygen cannot be used to prepare high thermally hardened alloys of satisfactory plasticity.

A study of the delayed fracture of specimens of titanium alloy VT6S and steel VKS-1 [2] has shown that notched specimens of high strength steel tested under load in water failed catastrophically fast, and that properties of specimens of titanium alloy of average strength (VT6S) do not change (Fig. 3). By analogy with aluminum alloys, it may be said that the Rebinder effect is not observed in aqueous media in the testing of notched specimens of titanium alloys under constant load. This difference is probably due to the higher corrosion resistance of titanium as compared to steel. Results of these studies are of great practical significance, since another important advantage of titanium as a structural material is thus revealed: it should be expected that under humid atmospheric conditions, bolts made of titanium alloys will function more reliably than those made of high strength steel without a special coating. In this case, notches on the specimens simulate sharp threads on the bolts.

/21

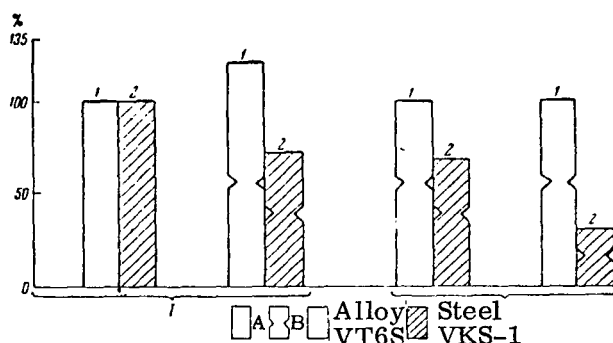


Figure 3. Effect of Notching and Medium on Short-Term (I) and Long-Term (II) Strength. Smooth (A) and Notched (B) Specimens.

1—Alloy VT6S; 2—Alloy VKS-1.

One of the major criteria of reliability is the sensitivity of the material to stress concentration at low temperatures. In a recent study [3], the sensitivity of a series of titanium alloys to curved notching and sharp cracking was studied at room temperature and low temperatures. It was definitely shown that the smaller the number of interstitial impurity elements (oxygen, nitrogen, hydrogen), the

lower the sensitivity of titanium alloys to stress concentration and to the action of low temperatures. Another valuable property of titanium alloys was established: in tensile testing of specimens with a previously applied sharp crack, titanium alloys showed a greater residual elongation, from 6 to 12%. The removal of the stress peak at the bottom of the crack, owing to local strain, holds up any further propagation of the cracks, and the strength is retained at the strength level of a smooth specimen. The strength of specimens with cracks (alloys OT4 and VT5-1) begins to decrease only at the liquid nitrogen temperature (-196°C).

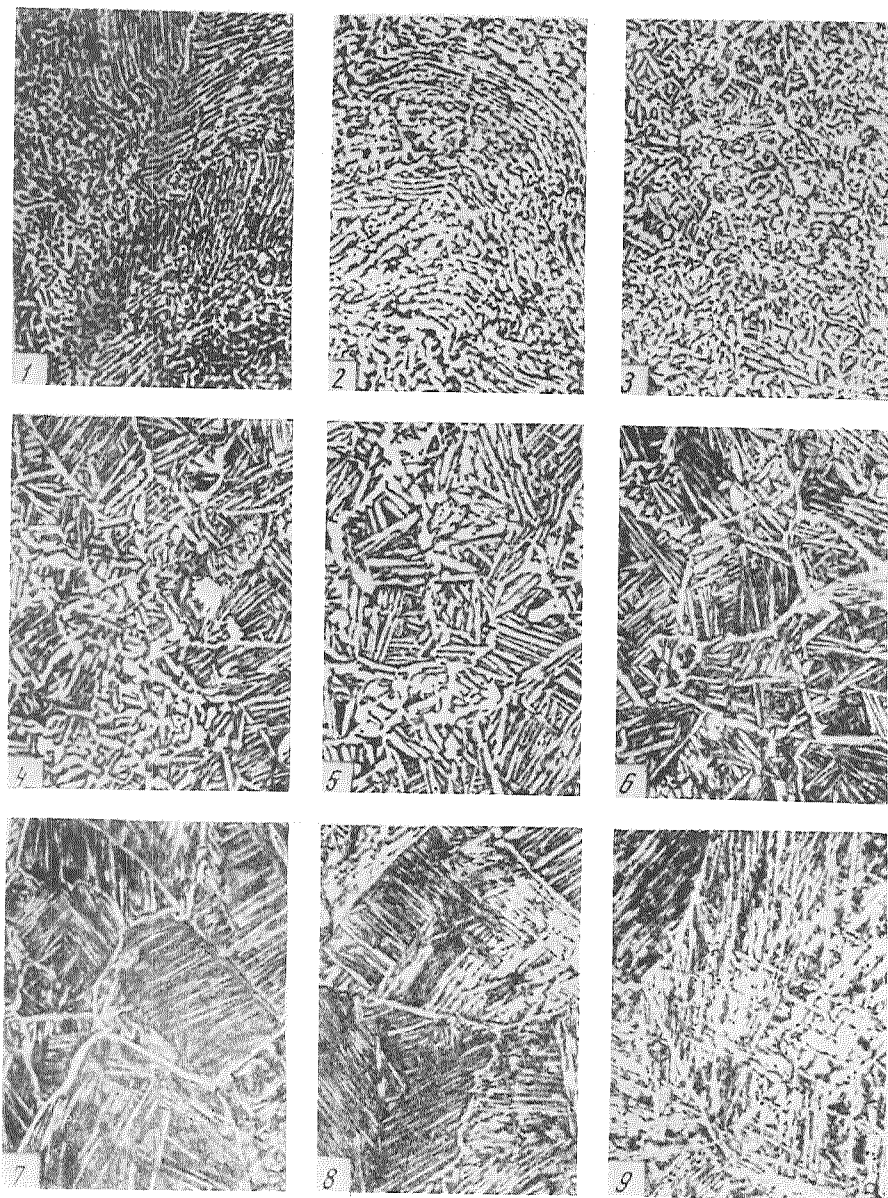
For comparison it may be indicated that in the quenched aluminum alloy D16, which is known to be one of the basic materials in modern aircraft construction, there is almost no residual elongation in specimens with a crack. Because of the lack of any appreciable plasticity (viscosity in the notch), the crack will gradually propagate and cause fracture in such a material.

This study again confirmed the great harmful influence of oxygen and other interstitial elements which increase the sensitivity to cracking and the cold brittleness of titanium alloys. Low titanium alloys with a small content of impurities, similar to alloy AT2 [4], are very valuable materials for cryogenic engineering.

/23

The problem of obtaining high strength characteristics continues to remain the major one in the development of industrial titanium alloys and, as in the case of other metals, for many branches of engineering the ultimate strength under unidirectional extension ceases to be a sufficiently reliable criterion for the choice of a material. Thus, for products such as containers operating under internal pressure, the decisive factor is the strength the usual strength limit is not linear but is expressed by a curve with a maximum [5]. In other words, as the ultimate strength of an alloy increases, the structural strength of the container prepared from it increases only up a certain limit, then begins to decrease, and the failure becomes brittle. The task facing metallurgists and technologists is to increase the structural strength by decreasing the sensitivity of the material to surface stress concentrators by plating with soft titanium [6, 7] or by using other technological methods, for example, local reinforcement of the weld or seamless shells [8].

Recent investigations have refined the relationship between the structure and properties of titanium alloys for various areas of application and made it possible to develop standard scales of macro- and microstructure which have become a part of mandatory requirements of technical conditions for semifinished products made of heat-resisting and high-strength titanium alloys. The optimum structure for obtaining a high fatigue resistance is the finest, so-called grainless macrostructure corresponding to points 1 and 2 of the scale. A 9-point scale has been established for the microstructure, and is used for evaluating the heat resistance and susceptibility of two-phase titanium alloys to hardening heat treatment (Fig. 4).



/22

Figure 4. Scale of Microstructure x 100:

1-4—Optimum Structure; 5—Permissible Structure; 6-9—Overheating Structure.

REFERENCES

1. Solonina, O. P. Collection "Titanium in Industry." Oborongiz, 113, 1961.
2. Borisova, E. A. and I. I. Shashenkova. "Vestnik Mashinostroyenia," 7, 56, 1961.
3. Koshelev, P. F. and S. E. Belayev. Strength and plasticity of structural materials at low temperatures. "Mashinostroyenia," 1967.

4. Kornilov, I. I. et al. Collection "Recent studies of titanium alloys." "Nauka," 1965.
5. Drozdovskiy, B. A. et al. "Metallovedeniye i termicheskaya obrabotka metallov," 5, 21, 1964.
6. Glazunov, S. G. and A. I. Khorev. "Metallovedeniye i termicheskaya obrabotka metallov," 8, 1964.
7. Khorev, A. I. et al. "Tsvetnyye metally," 9, 75, 1965.
8. Khorev, A. I., L. A. Gruzdeva et al. "Vestnik Mashinostroyeniya," 4, 8, 1965.

STATUS AND PROSPECTS OF RESEARCH IN METAL CHEMISTRY OF TITANIUM

I. I. Kornilov

In connection with the prospect of production and use of titanium and its alloys in various branches of the national economy, problems of further study and development of new titanium alloys are becoming increasingly urgent. /24

The chemical properties of titanium, the characteristics of its interaction with other elements of the periodic system, basic equilibrium diagrams of titanium systems and also ways of searching for and developing new titanium alloys have been discussed earlier [1, 2]. A study of the electronic structure of titanium atoms and of the behavior of titanium in binary, ternary, and more complex systems has enabled the authors to compile a table characterizing the metallochemical properties of titanium.

In this table, all the elements of the periodic system are divided into those forming solid solutions, compounds, and those which do not react with titanium. Using this table [1] as one would a good catalog in a comprehensive library, one can carry out calculations of the technically and practically important binary, ternary, and more complex multicomponent systems based on elements which form solid solutions and compounds with α and β titanium. Both solid solutions and metal compounds of titanium are of the greatest importance in the theory of titanium alloys and should serve as the basis for experimental studies.

Ideas on the influence of metallochemical properties of elements on the formation of metal solutions and compounds have been developed in monograph [3].

On the basis of these scientific premises, systematic studies of equilibrium diagrams, and gaseous transformations are being carried out and new titanium alloys are being created at the Institute of Metallurgy of the USSR Academy of Sciences. At the same time, detailed studies are made of the above-mentioned systems based on titanium, and also of the nature, structure and properties of α and β solid solutions of titanium, compounds of titanium and metallic phases conjugated between them.

Results of studies of the interaction of titanium with aluminum and oxygen [4, 5], of fundamental importance for titanium alloys, will be examined below.

Until recently, literature data on these systems have been far from accurate, and did not correspond to the true nature of the interaction of titanium with these elements. It is known from reference data [6, 7] that the regions of α and β solid solutions of titanium were widely distributed on the phase diagrams of the systems Ti-Al and Ti-O; the first recognized compounds (rich in titanium) were titanium monoaluminide (TiAl) and titanium monoxide (TiO).

The metallochemical properties of titanium, aluminum and oxygen indicate the great significance of the difference in the electronegative properties of the transition metal titanium. This allows one to assume the possibility of formation of a series of titanium aluminides and oxides in these systems instead of the broad regions (up to 25-32 at. %) of α solid solutions which are known from the literature.

This can be ascertained by examining the metallochemical properties of titanium, aluminum and oxygen (see Table 1).

TABLE 1

Properties	Ti	Al	O	Source
Atomic radius, A	1,46	1,43	0,68	[8]
Electronegativity*	1,12	1,48	3,5	[9]
First ionization potential of atoms, eV	6,82	5,94	13,61	[10]

*Relative units.

/25

It is evident from the table that in aluminum and particularly oxygen, the electronegativity values differ markedly from the electronegativity of titanium: as a nonmetal, oxygen has a markedly different ionization potential. In studying equilibria of the systems Ti-Al and Ti-O, we considered the chemical characteristics of these elements. The properties of titanium, considered in metal chemistry, of forming solid solutions and compounds should first and foremost be regarded as possibilities of interaction between the outer electrons of the atoms and their redistribution in the interaction products with different types of chemical bonds, i.e., metallic, covalent, ionic, or intermediate type bonds.

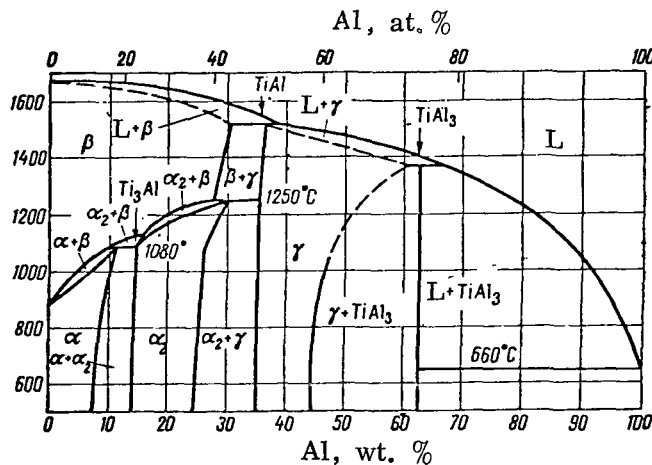


Figure 1. Equilibrium Diagram of the System Ti-Al.

In the last 3 to 4 years, we have worked out two new equilibrium diagrams of Ti-Al and Ti-O, which reflect the nature of the interaction of aluminum and oxygen with titanium. In light of these results, a new approach has been taken to the problem of the role of aluminum and oxygen in titanium alloys.

Figure 1 shows a new equilibrium diagram of the system Ti-Al [4]. It gives the composition of titanium aluminide Ti_3Al with an ordered structure. The conditions of its formation by the decomposition of the β solid solution and the region of propagation in the binary system, studied in [4], are of major importance for the determination of the limiting concentrations of aluminum in the α solid solution of titanium, above which the titanium alloys become less plastic. It is important to know exactly the region of appearance of the phase based on Ti_3Al and the degree of its dispersed separation in order to substantiate the compositions of titanium alloys from the region of α solid solutions, which are hardened by dispersed precipitates of Ti_3Al . It is shown in [11] that the aluminide Ti_3Al is important in itself as an individual chemical substance which can be used to develop new heat-resistant titanium alloys. In contrast to many other compounds, Ti_3Al has one characteristic: it is formed from the plastic β solid solution at $1080^{\circ}C$ (see Fig. 1); above this critical temperature in the state of the β solid solution, it is possible to forge and thus obtain semifinished products in the strained state from an alloy of this composition. Studies of the kinetics of formation, structure and properties of Ti_3Al and of the influence of alloying elements on its properties continue. Results of these investigations will permit the development of a new heat-resistant titanium alloys based on the aluminide Ti_3Al . Some properties of this alloy are discussed in the paper of T. T. Nartova [11].

/26

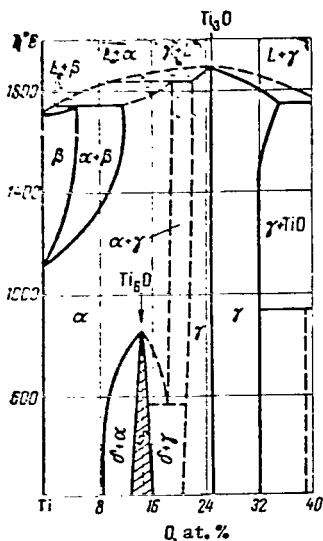


Figure 2. Equilibrium Diagram of the System Ti—O.

Another important study in the field of the metal chemistry of titanium is that of the equilibrium of the system Ti—O. According to reported data [6, 7] the equilibrium diagram of this system is characterized by a wide region of α solid solutions up to 32 at. % O. In the form cited it says nothing about the nature and properties of these solid solutions or their transformation. Some data on the anomalous changes of the properties of these α solid solutions associated with a change in composition [13], which have shown the complexity of the nature of interaction of titanium with oxygen, have led to the prediction, in the region of α solid solutions, of new compounds which have been observed in our study [5].

The literature has reported the existence of the compound Ti_2O [14], and to supplement this report, we have demonstrated the existence of two new suboxide-type compounds in this system: Ti_6O and Ti_3O , Ti_6O being formed from α solid solutions of titanium and Ti_3O separating on crystallization.

Thus, studies made by the author and his co-workers have resulted in a new equilibrium diagram of this system allowing for compositions of the new suboxides Ti_6O and Ti_3O phases based on them (Fig. 2).

The theoretical significance of the results of the study of the phase equilibrium of the systems Ti—Al and Ti—O cannot be over estimated; they offer a new treatment of the nature of the interaction of aluminum and oxygen with titanium, a new explanation of the role of aluminum and oxygen in titanium alloys, and prove the importance of these elements as alloying components in titanium. Furthermore, they make it possible to take a new approach to the solution of the problems of high temperature oxidation resistance and corrosion resistance of titanium. Accurate knowledge of the equilibrium diagrams of these important and basic binary titanium systems opens up great possibilities in the study of multicomponent titanium systems, which has been carried on by the laboratory for many years [1, 2, 15].

In the laboratory studies of the theory of titanium alloys, considerable attention is given to the nature and strength of the chemical bonding, physical and structural methods of investigation are employed, as well as methods of determination of the elastic modulus, characteristic temperatures, and study of the mechanism of the martensite-type transformation in titanium systems [15-17]. The use of neutron diffraction for the study of the structural ordering phenomena and formation of titanium and zirconium suboxides has been introduced.

Studies of the regularities characterizing changes in the high-temperature strength of titanium as a function of composition, structure, temperature and phase transformations have been undergoing a particularly rapid development. These studies make it possible to extend the physicochemical theory of high-temperature strength [18] as applied to titanium alloys and to establish the main types of "composition-high temperature strength" diagrams of titanium systems [19].

/27

In setting up the problems in the area of metal chemistry, in addition to theoretical studies on the interaction of titanium with other elements and the selection of systems important from the standpoint of technique for studying equilibria and phase transformations, specific practical requirements were considered.

In the development of new titanium alloys, the chief trend was the creation of the following materials:

- 1) highly plastic materials at cryogenic temperatures;
- 2) structural high-strength materials;
- 3) high temperature materials;
- 4) corrosion-resistant materials;
- 5) materials with special physical properties.

The new materials are designed for different purposes, and therefore the studies and development of titanium alloys have involved the use of simple and multicomponent titanium systems based on the following:

- 1) homogeneous α solutions;
- 2) α solid solutions with dispersion strengthening;

3) phases based on titanium aluminides;

4) α solid solutions stable at all temperatures.

For each of these groups of titanium alloys, the number of possible and most promising systems have been considered, on the basis of which optimum compositions of alloys satisfying specific practical requirements could be established by calculation and experiment [1, 2]. Alloys of these groups will be discussed below.

1. Titanium Alloys Highly Plastic at Cryogenic Temperatures

In selecting titanium systems from which highly plastic titanium alloys under cryogenic temperature conditions can be obtained by calculation, the authors proceeded from the idea of retention of homogeneous α solid solutions of titanium at low temperatures.

These alloys are those of the systems Ti-Zr, Ti-Hf, Ti-V, Ti-Nb, Ti-Ta, and Ti-Mo, where the components are either analogs or are situated close to titanium. Knowing the behavior of the components are either analogs or are situated close to titanium. Knowing the behavior of the components in similar binary and ternary systems of titanium-like type, one could readily calculate and show the possibilities and prospects of creation of similar plastic alloys from preselected ternary, quaternary and perhaps even more complex systems. As a result of detailed studies of the structure and properties of many possible compositions of titanium alloys of such type, in cooperation with V. S. Mikheev and O. K. Belousov, we developed a series of titanium alloys (AT-2-2, AT-2-3, AT-2-4, [20]); alloy of brand AT-2 was tested in the industry, it was granted a certificate, and the alloy was adopted.

AT-2 is a titanium alloy containing no aluminum, and in the temperature range from 0 to -196°C it retains the high plasticity characterizing it at room temperature. Figure 3 shows curves of the change of the impact strength of titanium alloys AT-2, OT-4, VT5-1, VT6S, AT-3, AT-6 and structural steel 17GS as a function of temperature (from $+100^{\circ}$ to -253°C). As is evident from the figure, alloy AT-2, whose impact strength at 20°C is 16 kgm/cm^2 , retains this strength down to -196°C , whereas the impact strength of other titanium alloys falls off smoothly as the temperature drops from 100 to -80°C , and the impact strength of structural steel 17GS, as the temperature drops below 0°C , falls off sharply and below -100°C amounts to only $1-2 \text{ kgm/cm}^2$.

/28

The study of the plasticity of alloy AT-2 and titanium alloys of many other brands at temperatures down to -253°C has shown that AT-2 is the only titanium alloy which retains a high plasticity down to the liquid hydrogen temperature [21, 22]. There is evidence that is plasticity remains fairly high down to the temperature of liquid helium (4.2°K).

The theoretical premises of the creation of similar highly plastic titanium alloys at liquid hydrogen temperatures consist in the fact that the metals which are the integral components of these systems are transition elements with a similar electronic structure and an unfilled d subshell. Some of them are direct analogs

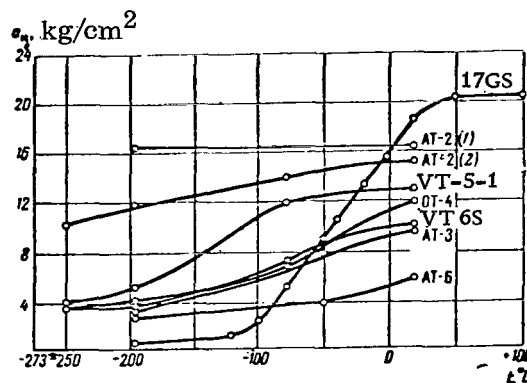


Figure 3. Impact Strength of Titanium Alloys and 17GS Steel.

(Zr, Hf) and others are elements located close to titanium (V, Nb, Ta, Mo). The chemical properties of all these elements are close to those of titanium (Table 2).

TABLE 2

Element	Properties		
	atomic radius, Å [7]	electronegativity* [7]	ionization potential, eV [8]
Ti	1,46	1,32	6,82
Zr	1,60	1,22	6,84
Hf	1,59	1,23	7,0
V	1,34	1,45	6,74
Nb	1,45	1,23	6,88
Ta	1,46	1,33	7,83
Mo	1,39	1,30	7,10

* In relative units.

None of these elements forms compounds with titanium; some (Zr and Hf) form continuous solid solutions with α β Ti, whereas others, isomorphous with β Ti (V, Nb, Ta, Mo), give continuous β solid solutions and are limitedly soluble in α Ti. At the same time, the temperature dependence of the maximum solubility in α Ti differs markedly from the similar dependence of other elements in α Ti. In contrast to the usual decrease of the solubility of the elements with decreasing temperature (see the system Ti-Si) in the systems Ti-V (Nb, Ta, Mo) the solubility increases (see Fig. 4). Such diverse physicochemical behavior of elements in terms of a decrease and increase in their solubility with decreasing temperature makes it possible to account for the low-temperature embrittlement of titanium alloys alloyed with elements whose solubility decreases with falling temperature, and for the retention of plasticity when alloying elements are used which increase the solubility as the temperature is lowered. The mechanisms of embrittlement

and preservation of plasticity under these conditions consist in the fact that in systems of the first group (for example, Ti—Si, Ti—B, Ti—Cr, Ti—Mn etc.), as the temperature is lowered, considerable internal stresses arise due to the formation of excess phases (silicides, borides, etc.), heterogenization of the structure of the alloys, and marked volume differences of the phases present; in systems of the second group (for example, Ti—Zr, Ti—V, Ti—Nb etc.), these internal stresses are either absent or insignificant because of the homogeneity of the structure and the great similarity between the metallochemical properties of Ti and those of Zr, Hf, V, Nb, Ta, Mo.

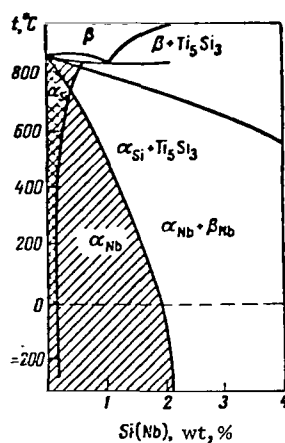


Figure 4. Limiting Solubility in the Systems Ti—Si (Decreases With Falling Temperature) and Ti—Nb (Increases With Falling Temperature).

high-temperature strength by the centrifugal and standard methods at 400–450°C, alloys of these composition have a greater high-temperature strength than many commercial titanium alloys, as indicated by the curves shown in Fig. 5. In addition, alloys of the AT series do not contain any scarce or expensive elements. The alloys are workable, and alloys of brands At-3, AT-4 and AT-6 have certificates; they are used in several branches of industry [1, 2, 25]. The problem of further raising the ultimate strength of titanium alloys (to 140–150 kg/mm²) while preserving the basic structure of α Ti is now being solved. This may be achieved by a rational selection of components in other multicomponent systems based on α solid solutions of titanium. A case in point is the new high-strength alloy based on the quaternary system Ti—Zr—W—Al, named St-6 ($\sigma_B \geq 130$ kg/mm², $\delta = 10-15\%$, $a_k = 2-3.5$ kgm/mm², which differs from many heat-treated high-strength alloys based on an unstable β structure in the fact that it is based on a stable α solid solution of titanium, and that no complex heat treatment is necessary for achieving a high strength.

Thus, the metallochemical properties of titanium enable one to understand the nature of its interaction with analog elements and to find and point out the routes of development of titanium alloys of many compositions with a predetermined high plasticity at cryogenic temperatures (for example, alloy AT-2).

2. High-Strength Structural Titanium Alloys

There also exist possibilities for the scientific development of high-strength alloys on the basis of α solid solutions of titanium; they are based on studies of multicomponent titanium systems with a wide region of α solid solutions and on the study of phase transformations in the solid state.

As long as five to six years ago, high-strength titanium alloys AT-3, AT-4, and AT-6 were prepared from the six-component system Ti—Al—Cr—Fe—Si—B [23–25]. The alloys are based on the structure of α solid solutions of titanium. With a constant content of the sum of elements – Cr, Fe, Si (1–1.5%) and a variable content of aluminum (from 3 to 8%), these alloys have a strength limit of 70–120 kg/mm² and a satisfactory plasticity. As was shown by a study of

/30

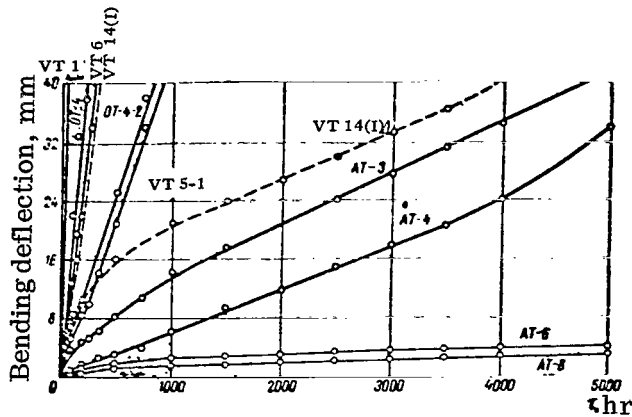


Figure 5. Creep Curves of Titanium and Titanium Alloys:

$$t = 450^{\circ}\text{C}, \sigma = 20 \text{ kg/mm}^2, \tau = 5000 \text{ hr.}$$

3. High-Temperature Titanium Alloys

As early as 1960, the physicochemical theory of high-temperature strength [18] made it possible to indicate the scientific routes of the development of heat-resisting titanium alloys and ways of increasing the temperature level of their use.

In 1963, the feasibility of reaching a $700\text{--}800^{\circ}\text{C}$ level of heat resistance was demonstrated, although it was then assumed that the temperature limit of the use of titanium alloys was $450\text{--}500^{\circ}\text{C}$.

According to physicochemical theory [18], two mechanisms are significant in high-temperature hardening:

1) formation of multicomponent solid solutions,

2) formation of dispersed precipitates of intermetallic compounds from supersaturated solid solutions of complex composition. An important and independent role in achieving high-temperature strength is played by intermetallic compounds and alloys based on them.

The most successful combinations in the structure of alloys of high-alloy α solid solutions of titanium with the formation of dispersed phases are achieved on the basis of the following binary, ternary, quaternary and more complex titanium systems: Ti-Zr with continuous α and β solid solutions; Ti-Al in a new variant of an equilibrium of phases based on an α solid solution and titanium aluminide Ti_3Al ; Ti-Sn with a wide region of α solution and compounds Ti_3Sn ; Ti-Mo (V, Nb) with a small region of α solid solution; Ti-Zr-Al; Ti-Al-Sn; Ti-Zr-Sn; Ti-Zr-Al-Sn; Ti-Zr-Al-Mo; Ti-Zr-Al-W; Ti-Sn-Al-Mo; Ti-Al-V-Mo and many other systems of similar type.

The enumerated systems make it possible to obtain highly concentrated α solid solutions in combination with dispersed phases based on such compounds as Ti_3Al , Ti_3Sn , $TiCr_2$, or solid solutions based on these intermetallic compounds.

Examples of new titanium alloy compositions developed by the staff of the Baikov Metallurgy Institute and in plants* are alloys based on the quaternary system $Ti-Zr-Al-Sn$ (ST-1) and the quinary system $Ti-Zr-Al-Sn-Mo$ (ST-4). According to the physicochemical theory of high-temperature strength, the maximum strength values are located near the saturation limit of α solid solutions of these complex systems.

Alloy ST-1 developed by T. T. Nartova is used for articles operating for short periods at $650-700^{\circ}C$, and alloy ST-4, at $700-800^{\circ}C$, having $\sigma_B = 80-60 \text{ kg/mm}^2$, has been adopted as the material for operation at working temperatures of $700-800^{\circ}$.

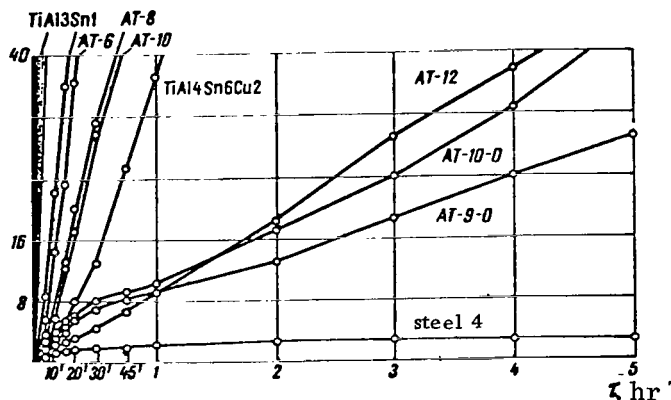


Figure 6. Creep Curves of Titanium Alloys.

$t = 700^{\circ}C$, $\sigma = 20 \text{ kg/mm}^2$, $\tau = 5 \text{ hr}$.

The basic properties of alloys ST-1 and ST-4 have been described by T. T. Nartova;* here we shall cite only the creep curves (taken by the bending method) of many commercial and experimental titanium alloys at $700^{\circ}C$ and $\sigma = 20 \text{ kg/mm}^2$, in comparison with the creep of ST-4 alloy under the same conditions (Fig. 6).

As is evidence by the curves, ST-4 alloy is the most heat-resisting of all the titanium alloys tested at $700^{\circ}C$. The alloys are workable. ST-1 alloy can be used to obtain forgings, rods and sheets, and ST-4 alloy can be used to make forgings and rods.

As a result of the mastering of the industrial production of these alloys, technical conditions have been established for the filling of orders of semifinished products from ST-1 and ST-4 alloys.

* See pp. [176-186].

It may be stated with confidence that similar compositions in these systems are not unique, i.e., they can be found in great numbers, and they all are to some extent included in the limited regions of α solid solutions of titanium and are located near the saturation limit with a dispersed separation of the excess phase.

Titanium aluminide Ti_3Al offers one possibility of creation of new high-temperature titanium alloys [11, 19].

A very interesting composition of a new heat-resistant alloy is a titanium-niobium alloy of the quaternary system $Ti-Nb-Mo-Cr$ (AN-5) with 52% Ti and a stable β structure [26]. A characteristic of this alloy is the fact that for a high-temperature strength up to $500-600^{\circ}C$, it has a high oxidation resistance, up to $800-1000^{\circ}C$. An alloy of this composition is of interest not only as a heat-resistant material at temperatures up to $600-650^{\circ}C$, but also as a material for protective coatings of high melting metals, especially niobium and its alloys, protecting them from oxidation up to $900-1000^{\circ}C$.

/32

It may be assumed that future investigations in the field of stable multicomponent α and β solid solutions of titanium will permit the creation of titanium alloys with an even greater high-temperature strength and oxidation resistance for use at higher temperatures and for longer service than has been possible until now.

One of the promising systems is the quaternary system $Ti-Mo-V-Al$, shown in Fig. 7 on the basis of data of [27, 28]. Figure 7 shows the region of the quaternary α solid solution and in space, the broad region of the quaternary β solid solution, both of which can undoubtedly be used as the basis for new compositions of heat-resistant titanium alloys.

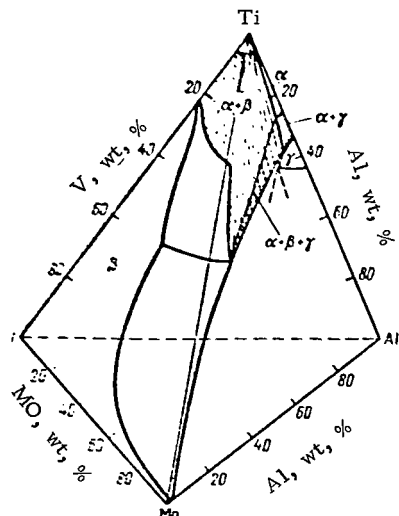


Figure 7. Spatial Configuration of the Quaternary System $Ti-Mo-Al-V$ at $600^{\circ}C$.

stable α and β solid solutions of titanium makes it possible to suggest ahead of time to the user which titanium system can give satisfactory results in terms of increasing the corrosion resistance. This problem has been specially treated in a survey [29] and in several other papers of the collection [15]. Studies have shown that the systems most important from the standpoint of corrosion resistance

4. Corrosion-Resistant Materials Based on Titanium

The corrosion resistance of pure titanium is generally known, but in chemical engineering there are a number of active corrosive media whose effect cannot be withstood by titanium and commercial titanium alloys.

The study of the metal chemistry of titanium, particularly the mechanism of formation of simple and multicomponent

are those with broad regions of α and β solid solutions, which were enumerated in the section on highly plastic and strong titanium alloys: Ti-Zr; Ti-Mo, Ti-Nb, Ti-Ta with regions of stable α and β solid solutions: Ti-Pd, Ti-Pt, Ti-Cu, Ti-Si, Ti-O with limited regions of α solid solutions.

On the basis of these systems, corrosion-resistant alloys with 0.2% Pd [30], with 32% Mo [31]*, stable in concentrated HCl on heating, and an alloy with 5% Ta replacing pure tantalum in chemical apparatus have been developed. The above-described titanium alloys At-3, AT-6 and ST-1 have proved to be corrosion-resistant in certain media. These alloys are described in detail in the collection [15].

5. Titanium Alloys With Special Physical Properties

/33

Among titanium alloys with special physical properties one should point out those compositions which are marked by extreme properties on "composition - property" diagrams. As follows from the theory of alloys, such properties are displayed primarily by intermetallic compounds of various stoichiometric compositions, formed in equilibrium systems. The intermetallic compounds have similar properties independently of the conditions and the medium of their formation; whether they are formed as a result of the decomposition of solid solutions in the form of Kurnakov-type compounds with an ordered structure, or directly upon crystallization, all the compounds on the composition - property diagrams are characterized by singular properties. Such extreme values of the properties have been observed in intermetallic compounds of the series of compositions enumerated below.

1. The titanium aluminides Ti_3Al and $TiAl$ are characterized by high elastic moduli considerably surpassing those of the constituents:

	E, kg/mm ²
Pure titanium.....	10 500
Aluminide Ti_3Al	15 000
Aluminide $TiAl$	19 000
Aluminum	6000-7000

2. A high corrosion resistance in sulfuric acid is displayed by titanium suboxides Ti_6O and Ti_3O , which differ greatly in stability from alloys of other compositions of the titanium - oxygen system [35].

3. As was shown by the studies [12, 32, 36, 37], the intermetallic compound $TiNi$ formed in the system Ti-Ni stands out from many compounds in a high plasticity even at cryogenic temperatures, a satisfactory strength, and a high damping capacity.

* See p. [74].

Without considering the special properties of metallic titanium compounds in detail, it should be pointed out that the properties cited which they possess are of major importance in practice, the possibilities of observing many extreme properties in compositions of many metallic compounds of titanium have been studied only very slightly, and the prospects of their practical applications have not been exhausted. The objectives of further studies will consist in a detailed investigation of the entire complex of properties of intermetallic compounds in connection with the general development of the metal chemistry of titanium.

Thus, in concluding this brief survey of investigations in the field of metal chemistry of titanium and objectives of further work in this direction, it may be stated that they are of current interest, are directed toward the solution of basic problems of interaction of titanium with other elements, establishment of the laws of formation of solid solutions and compounds of titanium, study of the dependence of the structure and properties on the composition, and study of equilibrium and metastable state of the phases. Using them, one can solve practical problems of development of new titanium alloys for various purposes and problems of their introduction into production.

REFERENCES

1. Kornilov, I. I. Collection "Titanium and its Alloys," issue VII. Metal chemistry and new alloys. AN SSSR, p. 5, 1962.
2. Kornilov, I. I. Collection "Titanium and its Alloys," issue X. Studies of new titanium alloys. AN SSSR, p. 5, 1963.
3. Kornilov, I. I. et al. Metallochemical properties of elements of the periodic system. "Nauka," 1966.
4. Kornilov, I. I. et al. Dokl. AN SSSR, 164, p. 843, 1965.
5. Kornilov, I. I. and V. V. Glazova. Dokl. AN SSSR, 150, 2, p. 313, 1963.
6. Hansen, M. and K. Anderko. Structure of binary alloys. Metallurgizdat, 1962.
7. Molchanova, E. K. Atlas of phase diagrams of titanium alloys. "Mashinostroyenie," 1964.
8. Bokiy, G. B. Introduction to crystal chemistry. MGU, 1954.
9. Astakhov, K. V. Collection "Electronegativity." Zap.-Sib. Izd., p. 5, 1965.
10. Vedeneyev, V. I. et al. Energy of rupture of chemical bonds. Ionization potentials and electron affinity. Handbook. AN SSSR, 1962.
11. Nartova, T. T. Properties of alloys based on the aluminide Ti_3Al . Poroshkovaya metallurgiya, No. 8, 1966.
12. Kornilov, I. I. and L. P. Dudkina. Izv. AN SSSR, Metally, 4, 184, 1964.
13. Bumps, E. S., H. D. Kessler and M. Hansen. Trans. ASM, 45, p. 1008, 1953.
14. Andersson, S. et al. Act. Chem. Scand., 11, 1641, 1957.
15. Collection "New Studies of Titanium Alloys." "Nauka," 1965.
16. Glazova, V. V. Alloying of titanium. Metallurgizdat, 1966.
17. Fedotov, S. G. Dependence of elastic properties of titanium alloys on composition and structure. Collection "Titanium and its Alloys," issue 10. Study of titanium alloys. AN SSSR, 1963.
18. Kornilov, I. I. Physicochemical principles of the high temperature strength of alloys. AN SSSR, 1961.
19. Kornilov, I. I. and T. T. Nartova. Dokl. AN SSSR, 172, 2, 1967.
20. Kornilov, I. I., V. S. Mikheyev and O. K. Belousov. Collection "Metal chemistry and new titanium alloys," issue VII. AN SSSR, p. 120, 1962.

21. Kornilov, I. I. et al. Izv. AN SSSR, Metally, 160, 1967.
22. Ul'yanov, R. A. and V. A. Moskalenko. Metallovedeniye i termicheskaya obrabotka, 10, 1966.
23. Kornilov, I. I., V. S. Mikheyev and T. S. Chernova. Izv. AN SSSR, OTN, Metallurgiya. No. 8, 1960.
24. Kornilov, I. I., V. S. Mikheyev and T. S. Chernova. Basic properties of new high-strength titanium alloys AT-3, AT-4, AT-6 and AT-8, issue II, VINITI, 1960.
25. Mikheyev, V. S. , K. P. Markovich and L. F. Tavadze. Collection "Titanium and its Alloys," issue X. AN SSSR, p. 24, 1963.
26. Grum-Grzhimaylo, N. V. and V. G. Gromova. Collection "Metal Chemistry and new Titanium Alloys," issue VII, AN SSSR, p. 35, 1962.
27. Pylayeva, E. N. and Dzhi-min, Ge. Studies of Alloys of the quaternary system Ti—Al—Mo—V. Abstract of candidate dissertation, Moscow, 1965.
28. Dzhi-min, Ge. Studies of alloys of the quaternary system Ti—Al—Mo—V. Abstract of candidate dissertation. Moscow, 1966.
29. Kornilov, I. I. and Yu. M. Vinogradov. Collection "New studies of titanium alloys." "Nauka," p. 102, 1965.
30. Domashov, N. D. and Yu. M. Ivanov. Zashchitnyye pokrytiya, 1, p. 32, 1966.
31. Andreyeva, V. V. and V. I. Kazarin. New chemically resistant structural metallic materials. Goskhimizdat, 1961.
32. Goldstein, D. M., W. J. Buchler and R. C. Wiley. The Nickel Bulletin, 3, 4, 1966.
33. Tavadze, F. N. et al. Titanium and its Alloys, issue 10. AN SSSR, p. 151, 1963.
34. Fedotov, S. G., T. T. Nartova and E. P. Sinodova. Dokl. AN SSSR, 146, 6, p. 1377, 1962.
35. Glazova, V. V. et al. Dokl. AN SSSR, 165, p. 136, 1965.
36. Buchler, W. J. and R. C. Wiley. Trans. ASM, 52, 1, 1962.
37. Rozner, A. G. and R. I. Wasilevski. Inst. Metals, 94, No. 5, 1966.

IMPROVING THE TECHNOLOGY OF PRODUCTION AND QUALITY OF SEMIFINISHED PRODUCTS FROM TITANIUM ALLOYS

G. D. Agarkov, N. F. Anoshkin, V. I. Dobatkin,
I. N. Kaganovich and V. A. Tsytsenko

/35

In the last 15 years, the efforts of a number of institutes and plants have resulted in the industrial production of semifinished titanium products; parts made of titanium alloys are successfully employed in various branches of the national economy. In describing the recent development of titanium production it is first of all necessary to mention a substantial increase in the nomenclature of the articles.

The technical requirements for all types of semifinished products have been recently reviewed (as a rule, made more strict). The standards of oxygen and hydrogen content have been considerably decreased: the oxygen content has been limited to 0.15% in the majority of alloys, and in some to 0.12% (earlier, 0.20-0.25%), the hydrogen content has been limited to 0.012% for most alloys, and for some to 0.006% (earlier, 0.015%). As a result of the introduction of analysis for oxygen, the standards of its content have become mandatory.

While the quality has improved, the cost of the semifinished products has decreased steadily; the fraction of waste utilized in the alloys, the yield of acceptable castings and the volume of output have increased, and the production technology has improved.

We shall discuss a few major trends in the improvement of the technology of production of semifinished products.

Economic Types of Semifinished Products

One of the major directions in the improvement of production technology has been the development of technological processes for producing economic types of semifinished products, i. e., stampings, sections and rods with reduced allowances, welded pipes and intricate shape castings.

The adoption of stampings instead of the less economical forgings is characterized by the following figures:

Years	1964	1965	1966
Number of items ...	12	154	320

In addition to stampings of small and intermediate weights, unique stampings weighing up to 1.2 t have been adopted. The effect of using stampings instead of forgings can be evaluated from the following data. The coefficient of utilization of the metal for the preparation of a set of parts for one article from forgings was 0.08 in 1960; for preparation from rough stampings, 0.11 in 1963, and for preparation from precision stampings obtained on presses, 0.26 in 1965.

The successful use of economic billets may be illustrated by the replacement of the old technology of preparation of ring parts from forgings and rolled rings by a new technology consisting in the production of pressed profiles of required cross sections and their butt welding. This made it possible to decrease expenditure of the metal per set of ring parts by a factor of more than 3. At the present time, the nomenclature of titanium profiles for ring parts exceeds 600 items. The development of a glass lubricant composition and technology of its application have contributed to a rapid introduction of more accurate profiles and a simultaneous improvement of their structure as a result of a lowering of the pressing temperature. The adoption of thin-walled titanium profiles of a high precision class is being successfully continued.

Mass production of longitudinally welded titanium tubes began two years ago. The welding is done on a specially designed mill in a medium of high purity argon. The production of tubes with a wall thickness of 1.0-2.0 mm and 25 to 100 mm in diameter has been adopted. These tubes are of course inferior in quality of precision seamless tubes. However, they have a number of advantages over extruded and rolled tubes for ordinary use. The quality of the outer and inner surfaces of these tubes is higher, the wall thickness tolerance is one-half that of seamless tubes, and the cost is 10-20% lower. Tests established a high quality of the welded seam. Such tubes can be used as billets for subsequent rolling, and this makes it possible to eliminate the cast structure in the weld zone.

/36

Unfortunately, the volume of production of shaped titanium castings is as yet entirely inadequate. The production technology of titanium castings is completely ready for adoption on a mass scale. Castings weighing up to 150 kg are being produced, and the production of larger sizes is feasible.

In discussing the economic types of semifinished products it should be emphasized that work on the latter brings us closer to the solution of one of the most important and complex problems, that of a closed metallurgical cycle. The solution of this problem implies a complete utilization of the waste formed in the process stages and by the machining of the billets, and thus a maximum saving of the metal and reduction of its cost.

Section Rolling - A Progressive Method of Obtaining Semifinished Products and Billets

Section rolling of titanium combines the possibilities of raising the quality of articles and reducing expenditures on their production. The introduction of section rolling has become particularly important in connection with the increase of the volume of production of rods and profiles. However, until recently this method was used for making profiles and rods of several types and also welding wire and rods for fasteners.

Experience in the production of the wire has shown that in the production of quality rolled articles, conditions of uniform deformation of the metal are of decisive importance. The problem of production of welding wire from technical titanium has now been solved.

Recently, mill 450 began operation at one of the plants. Mastering of the production of rods on this mill made it possible to improve the quality of the rods considerably, particularly in the area of tolerances and structure.

The diameter tolerances of rolled rods have been cut by almost one-half as compared to forged ones. For forged rods 30-45 mm in diameter, they are ± 2.0 mm, for rolled ones $(+0.8) - (-1.4)$ mm, and for rods 60 mm in diameter, respectively ± 3.0 and $(+1.0) - (-2.0)$ mm.

In the study of the macrostructure of rods in the majority of cases the permissible grain size is limited to point 2, increases to point 4 in some parts of the section, and in forged rods is limited by points 4-5. A local coarsening of the grain to point 4 in rolled rods is explained by an uneven heat effect due to the unevenness of deformation, and can be positively eliminated.

Rods up to 60 mm in diameter are now made chiefly by section rolling.

All of this leads to the conclusion that the production of not only all rods, but also all billets for forging, stamping and extrusion up to 200 mm in cross section can be switched to rolling on section and reduction mills using large ingots. Experience in rolling ingots 800 mm in diameter into rods 180 mm in diameter followed by preparation of stampings from them has shown the promise of such technology. Sections of simple shapes (angle, channel, T-connection) should also be prepared by section rolling.

Improvement of the Quality of Semifinished Products

/37

The study of the nature of metallurgical defects has made it possible to eliminate mass production spoilage due to defects. Effective means of preventing the formation of defects in ingots have been developed; sorting and standardization of sponge, separation of chips, special conditions of furnace cleaning and other steps.

As shown by the results of the studies, in the total number of defects observed, a large fraction consists at the present time of cold laps due to the breakage of parts of consumable electrodes. Defects of this kind are not particularly dangerous, since they are large and readily detectable by ultrasonic checking of the ingots; moreover, the nature, causes and ways of eliminating these defects are sufficiently known. The most dangerous are metallurgical defects which are difficult to detect. Among those observed by checking ready semifinished products or finished articles, the ones encountered most frequently are inclusions of high melting components, gas saturated areas, and areas of the metal differing from the base metal in content of the alloying components.

The most radical means of eliminating metallurgical inclusions would be the introduction of melting with a lining. In addition, the aluminothermic method of preparing titanium master alloys with high melting components should be widely introduced. The method of preparation of master alloys in use at the present time do not always afford a homogeneity of distribution of the high melting components in the master alloy. This may be why inclusions of molybdenum and niobium

articles are encountered most frequently among random metallurgical defects. The problem consists in setting up a centralized production of master alloys and their output in accordance with standards providing for a high quality. Immersion ultrasonic checking and, for more critical parts, additional x-raying should also be organized. Obviously, the most general and widespread method should be immersion ultrasonic control. An automated unit for checking ingots (Splav-1) involves checking of the alloy along the generatrix with the possibility of dividing the entire cross section of the ingot into 5 zones, which substantially increases the sensitivity of the control. The automated immersion unit Splav-2 is successfully used for controlling stampings of round cross section.

Major attention should be given to the protection of surfaces from oxidation and to the elimination of gas-saturated layers in the products. The billets should be prepared so that seams and folds during finished mechanical working operations are excluded. Thus, in many cases, working of the surface of the ingot should be excluded in order to make sure that the machining of the billet is more thorough if necessary.

The most acute problem in improving the quality of semifinished products made of titanium alloys is that of refining the grain, so that a controlled macro- and microstructure is obtained. In its general aspects, this problem is sufficiently clear and simple: a comparatively high degree of deformation of the material should be provided for without exceeding the temperature limits of the α or $(\alpha + \beta)$ -regions. However, it is very difficult to meet this condition, especially for large-sized articles. It is necessary to increase the power of the equipment employed; to develop equipment having greater capacities in regard to the deformation rate; to use new materials for the tool and to increase its stability; to develop lubricants which facilitate deformation as much as possible.

Three more trends of studies aimed at improving the structure of semifinished products may be mentioned.

1. Improvement of preliminary deformation of billets. The inherency of the structure was always considered, but the principal attention was focused on the conditions of the finishing mechanical working operation, and the importance of the conditions of deformation of the billet was sometimes underestimated. Experience shows that the optimum technological scheme for producing stampings with a fine grain structure and a high level of properties is one including uniform forging in the β region designed to produce a homogeneous microstructure by refining cast grains followed by recrystallization; a considerable deformation in the two-phase region in order to improve the microstructure; and carrying out the final operation, stamping in the two-phase region.

/38

Considering the necessity of a substantial pretreatment of the metal, a course directed toward enlarging an ingot, once formally adopted, appears to be quite correct. Planned work designed to increase the cross sections of smelted ingots to 1100-1200 mm should be completed, and efforts should be made to obtain billets for stamping and extrusion by rolling large ingots on reduction mills.

2. Securing a sufficiently uniform deformation of the metal and preventing substantial heating in the course of deformation in the two-phase region. Two factors are very important and are not yet always considered. To achieve

uniformity of deformation, it is sometimes necessary to take special steps (for example, using spiral blocks when mounting the billet for stamping discs, as successfully used in one of the plants).

Titanium alloys have a very low thermal conductivity and, what is particularly important, thermal diffusivity as compared to aluminum and iron. This gives rise to the possibility of considerable local heating due to the thermal effect of deformation. A considerable thermal effect is observed during forging, extrusion, rolling and other operations. Therefore, it is necessary to take steps to prevent a significant unevenness of deformation and to try to spread the thermal effect to the largest possible volumes of the metal.

3. Use of alloys possessing high technological properties. Alloys already exist which provide a guaranteed ultimate strength up to 110 kg/mm² without hardening heat treatment. Despite the great variety of alloys, their selection was determined only by the presence of definite mechanical and physicochemical properties. However, alloys with the same properties sometimes possess markedly different technological properties. In selecting alloys, preference must be given to those which, while possessing the necessary set of mechanical and physicochemical properties, have better technological properties (in particular, a structure which is least sensitive to changes in conditions of deformation).

The chief problems in the area of applied metal working of titanium alloys chiefly consist, at the present time, in a thorough investigation of the most widely employed industrial alloys, the study and improvement of their technological properties, their structural sensitivity the correlation between technological parameters, structure and properties, and on this basis, the development of new processes of molding and thermomechanical and thermal treatments.

A thorough study of industrial alloys should also become the basis for the unification and reduction of the number of mass produced alloys, resulting in an improvement of the technical-economic indices of production. This does not, of course, diminish the importance and urgency of research aimed at creating new alloys. However, such research should anticipate subsequent industrial introduction of only those alloys which differ substantially in properties from the ones already produced in industry.

HEAT TREATMENT OF TITANIUM AND ITS ALLOYS

V. A. Livanov, B. A. Kolachev and N. S. Lyasotskaya

Titanium and its alloys are subjected mainly to annealing, quenching, and aging. Titanium and alloys based on α -Ti are subjected to intermediate annealing or relieve the work hardening due to plastic deformation. The temperature of the heating should not exceed the boundary between the $(\alpha + \beta)$ and β regions, since the grain grows vigorously in the β region [1, 2]. In their grain growth tendency, titanium and its alloys resemble inherently coarse-grained steels. In addition, a considerable alpha phase containing layer is formed during annealing at high temperatures. Annealing is usually done in air, in an oxidizing medium, to avoid hydrogen absorption.

/39

The annealing of $(\alpha + \beta)$ alloys combines elements of intermediate annealing, based on recrystallization processes, and full annealing, based on phase recrystallization. The annealing temperature of titanium $(\alpha + \beta)$ alloys should be sufficiently high to relieve the work hardening, but at the same time sufficiently low to insure a content of alloying elements in the β phase that would not only prevent its decomposition in the course of cooling but also provide a sufficient stability during the operation of the finished product. The lower the annealing temperature in the $(\alpha + \beta)$ -region, the higher the concentration of β stabilizers in the β phase and its thermal stability.

At the same time, however, the amount of β phase given by the familiar lever rule does not decrease.

The simplest annealing schedule of $(\alpha + \beta)$ alloys consists in their heating at the lowest temperatures sufficient for relieving the work hardening. The temperature of simple annealing is usually 800°C . For $(\alpha + \beta)$ titanium alloys, in addition to simple annealing, use is made of isothermal annealing, which consists of heating a comparatively high temperatures sufficient for the occurrence of recrystallization processes, cooling to temperatures insuring a high degree of stability of the β phase (usually below the recrystallization temperature), holding at these temperatures, and air cooling. Such annealing provides a higher stability and long-time strength than simple annealing.

After annealing, titanium and its alloys are cooled in air. It should be noted that the cooling rate after annealing substantially influences not only the properties of $(\alpha + \beta)$ and β alloys, which is quite natural, but also the properties of titanium and α alloys. In [3-5] it was shown that by cooling α alloys after annealing in water, one can obtain an impact strength $1.5-2 \text{ kgm/cm}^2$ greater than after cooling in air, although with a slightly lower strength. Tempering at $300-600^{\circ}\text{C}$ of alloy VT5-1 cooled in water decreases the impact strength and raises the ultimate strengths and yield points.

The authors of [5] explain this effect by the fact that after quenching from temperatures above 700°C , dislocations in titanium and its alloys are free from impurity atmospheres of oxygen and nitrogen atoms, and after slow cooling or tempering at $300-600^{\circ}\text{C}$, Cottrell atmospheres, which increase the resistance to plastic deformation and decrease the viscosity, are formed on the dislocations. To relieve the internal stresses formed as a result of the mechanical treatment of

the work pieces, incomplete annealing is often employed at temperatures below the temperature of the start of recrystallization, lasting up to 1 hr and followed by cooling in air.

We have shown [6] that the coarse-grained structure of titanium and α titanium alloys can be corrected by heat treatment similar to that used for steel, mainly double phase recrystallization. Thus, quenching from 950°C followed by heating to 800°C and holding at this temperature for 6 hours made it possible to achieve an actual refinement of titanium grain and to increase its mechanical properties (coarse-grained titanium had $\sigma_B = 59.8 \text{ kg/mm}^2$; $\delta = 12\%$ and $\psi = 24.5\%$, while titanium after complete phase recrystallization had $\sigma_B = 68.5 \text{ kg/mm}^2$; $\delta = 18.6\%$; and $\psi = 39.8\%$).

/40

Grain refinement in such heat treatment is due to intra-phase work hardening during the quenching and subsequent recrystallization on second heating.

Unfortunately, the practical introduction of phase recrystallization for the purpose of an actual refinement of the grain of titanium and its alloys is complicated by the facts that a) because of the high tendency of the grain of titanium and its alloys to grow during heating for quenching to the β region (such heating is necessary for complete phase recrystallization), the original grain becomes so much coarser that subsequent heat treatment is frequently unable to decrease it even to the original size; b) the volume effect in the $\alpha \rightleftharpoons \beta$ transformation is slight and this does not produce a sufficiently strong intra-phase work hardening.

Apparently, titanium alloys can be developed whose grain can be effectively refined by phase recrystallization. To this end, it is necessary to alloy titanium with elements hindering grain growth, even over a narrow temperature range above the boundary $\alpha + \beta \rightleftharpoons \beta$, and elements increasing the volume effect of the $\beta \rightleftharpoons \alpha$ transformation.

Since it is difficult to improve the structure and properties of titanium by means of phase recrystallization, methods including work hardening through plastic deformation followed by recrystallization annealing have been developed for the purpose of refining coarse grain. Thus, Everhart [13] recommends that in order achieve grain refinement, cold deformation with shrinkages no less than 10% be carried out followed by annealing in the α region (of the order of 700°C) or short-time annealing at temperatures above the boundary between $(\alpha + \beta)$ and β regions. A second method consists in hot deformation of the material at $650-800^{\circ}\text{C}$ with a maximum degree of deformation of 9% followed by heat treatment (procedure analogous to the one described).

Recently, hardening treatment consisting of quenching and aging has been increasingly employed for titanium $(\alpha + \beta)$ alloys. This is undoubtedly due to the fact that the processes taking place during quenching and aging of titanium alloys are now better understood.

According to the classification first proposed by Uu. A. Bagaryatskiy, G. I. Nosova and T. V. Tagunova [7], the metastable phases α' , α'' , ω and β_{metast} are formed in titanium alloys during quenching. Although the nature of α' and β_{metast} phases is comparatively clear, there is as yet no consensus on the nature and mechanism of formation of α'' and ω phases.

Phase α'' has been observed in titanium alloys with β -isomorphous stabilizers in the system Ti-W.

Yu. A. Bagaryatskiy et al. [7, 8] have come to the conclusion that the α'' phase exists on the basis of two experimental facts:

- 1) As the content of β stabilizers increases above a certain definite concentration, the hardness of alloys quenched from the β region decreases;
- 2) Certain lines of the martensite phase on the x-ray powder patterns begin to split at approximately the same concentration.

Lately, studies by Soviet scientists have expressed the views that the α'' phase should not be regarded as a separate, individual martensite phase [9, 10]. S. G. Fedotov [9] comes to this conclusion on the grounds that the curves of elastic properties on the segment of martensite transformations are continuous in character. He points out that the decrease in the hardness of alloys of these compositions may be explained by a decrease in cohesive forces and by the appearance of a residual β phase. /41

L. P. Luzhnikov et al. [24] support this point of view and cite experimental data which show that in the presence of the α'' phase in the structure, decomposition during aging is accompanied by a marked hardening. Since the decomposition of martensite is usually associated with softening and the decomposition of the β phase with hardening, it is concluded that a residual β phase should be present in the structure.

The viewpoint of the authors of the present article concerning the nature of the α' phase amounts to the following. There is no doubt about the splitting of the lines of the martensite phase on x-ray powder patterns of quenched titanium alloys, due to a decrease of lattice symmetry from hexagonal to rhombic. This splitting was also observed by us in a study of the crystal structure of quenched Ti-Mo alloys; it begins to manifest itself at molybdenum concentrations above 4%.

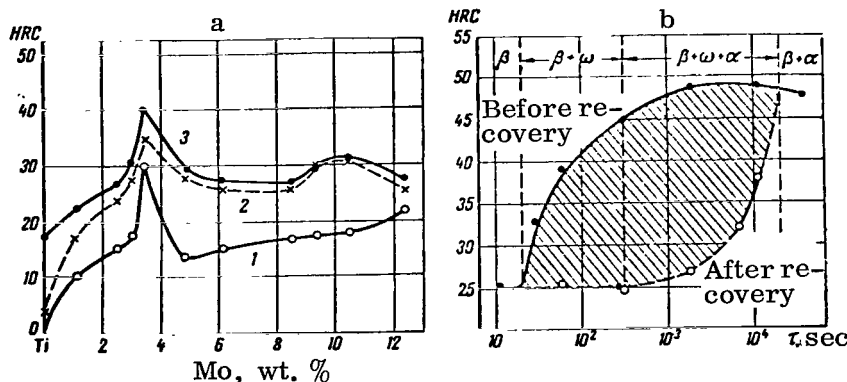


Figure 1. Hardness of Ti-Mo Alloys (a) After Quenching From Different Temperatures, °C: 650 (1), 850 (2), 1000 (3) and Ti-13% Mo (b) After Isothermal Treatment at 400°C Before and After Recovery.

This splitting may be interpreted as follows. At low molybdenum concentrations within the solubility range in the α phase, the martensite phase is not a supersaturated solid solution and its lattice remains hexagonal. As the molybdenum content increases above the maximum solubility in the α phase, supersaturation appears which is greater the higher the molybdenum content. As a result, the martensite lattice becomes rhombically distorted. In technically pure alloys of the Ti-Mo system, the maximum solubility in the α phase at 600°C is 1-1.86%. If the solubility line of molybdenum in the α phase is extrapolated to room temperature, the solubility becomes 3-5.5%. These concentrations are close to that at which splitting of the lines of the martensite phase begins in the Ti-Mo system.

This being the case, the change in the hardness of Ti-Mo alloys following quenching from the β region (Fig. 1) may be explained as follows. As the molybdenum content rises, the hardness increases as result of an increase in the alloying of martensite, and reaches a maximum at 3.5%. A further decrease of hardness is due to the appearance of a soft residual β phase. A certain increase of hardness at a molybdenum content of the order of 10% is due to the formation of the ω phase.

Since the lattice of martensite gradually changes from hexagonal to rhombic, and the indicated change of properties is due to the appearance of a residual β phase, we postulate that the system Ti-Mo contains a single martensite phase whose structure changes somewhat because of the increasing supersaturation with the β stabilizer. /42

A similar situation is observed in steels. Martensite in low carbon steels has a cubic structure. As the carbon content increases, the martensite lattice becomes distorted tetragonally, and the degree of tetragonality, i. e., the axis ratio c/a , gradually increases. Whereas in low carbon steels there is almost no splitting of the martensite lines, this splitting does exist in medium carbon steels, and as the carbon content rises, the splitting of x-ray lines due to the tetragonality of the lattice is reinforced.

Since, however, the crystal structure of martensite in Ti-Mo type alloys differs from the martensite structure in titanium alloys with β -eutectoid elements, it is useful to assume that in the first case a single martensite phase, for which the designation α'' can be retained, is formed over the entire molybdenum concentration range, and that a second phase (α') is formed in the second case.

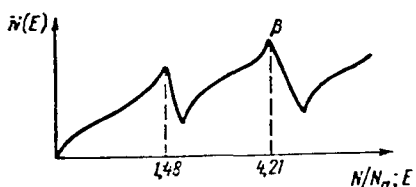


Figure 2. Density of Electron States for bcc Metals.

Still another metastable phase ω , which forms during quenching, is also produced in a diffusionless manner. Yu. A. Bagaryatskiy, G. I. Nosova and T. V. Tagunova treat it as a martensite phase of special type [8]. Recently, interesting ideas on the mechanism of formation of the ω phase were published by S. G. Fedotov [9]. He postulates that the ω phase is the product of an incomplete martensite transformation, $\beta \rightarrow \alpha'$.

Two basic views exist on the nature of the ω phase formed on quenching. Some researchers postulate that the ω phase has an electronic nature [8, 12, 17, 18], while others negate a decisive role of the electron concentration and contend that the main factor in this case are volume changes on alloying [11].

The authors of [17] as well as N. V. Ageev [18] have attempted to explain the role of the electron concentration in the freezing of the metastable phases in titanium alloys from the standpoint of metal physics. It is thought that the stability of the phases is determined by the density of the electron states, described by the $N(E)$ curve characterizing the number of electrons with energies from E to $E + dE$. Of several crystal structures differing in the shape of the $N(E)$ curve, the metal will have the structure with the highest density of electron states. The $N(E)$ curve or a bcc structure shows peaks at electron concentrations of 1.48 and 4.21. The first peak is associated with electron compounds of the type of β brass. The second peak apparently determines the freezing of the β phase in quenched titanium alloys at concentrations above 4.20 (Fig. 2).

N. A. Lashko [11] negates the decisive role of the electronic structure in the freezing of the β phase on quenching on the grounds that the maximum electron concentration above which a single β phase is frozen is not constant for different systems.

It should be noted that in calculating the electron concentration of alloys one should not identify the number of hybridized s-d electrons determining the electron concentration with the valence of the free atoms of transition elements, as was done in [11]. Furthermore, the role of the electron concentration should not be discussed without regard to the volume changes caused by the alloying. The shape of the Brillouin zones and hence the conditions of appearance of peaks on $N(E)$ curves depend substantially on the form of the unit cell of the crystal lattice. Consequently, the volume factor exerts its influence on the conditions of freezing of the phases via the electron concentration. This was pointed out by Hume-Rothery in a study of electron compounds of the type of β brass [15].

/43

Thus, we have no doubt as to the decisive role of the electron concentration in the freezing of the β phase on quenching.

The problem of the electronic nature of the ω phase is somewhat more complex. Generally speaking, the electronic structure of alloys always, in the final analysis, determines their structure. Even the appearance of the ω phase in pure titanium at high pressure may be explained by the influence of the electronic factor. The author of [14], who observed the ω phase in pure titanium at high pressure, shows that under the influence of pressure the electronic structure of titanium changes and approaches the electronic structure of alloys Ti-V and Ti-Nb of the composition at which the ω phase is formed therein on quenching.

Freezing of the ω phase in alloys may be explained by a change of the electron concentration due to a change in the electronic structure on alloying and to volume distortions.

Unfortunately, the electronic nature of the ω phase has not been theoretically validated thus far, since the $N(E)$ curve has not been plotted for this phase. It

should be noted that the $N(E)$ curve shown in Fig. 2 elucidates only the causes of freezing of the β phase on quenching of alloys with concentrations above 4.20, but gives no information whatever on the electronic nature of the ω phase.

The structures arising in titanium alloys after quenching from various temperatures may be represented in the form of metastable diagrams of the phase composition. These diagrams are plotted in the coordinates "temperature of heating for quenching vs. concentration of alloying element." The first published metastable diagrams [20-21] had nothing to do with equilibrium phase diagrams, although in point of fact metastable diagrams of the phase composition of titanium alloys should have a direct relationship to their equilibrium phase diagrams.

As an example, we shall consider the phase diagram of titanium with a β stabilizer represented by a transition element. Let us assume that the martensite transformation begins at a temperature M_I and ends at M_F . In keeping with the general pattern of such transformations, we shall assume that the temperatures of the beginning and end of the martensite transformation decrease with rising content of the β stabilizer and at certain concentrations C'_{cr} and C''_{cr} reach room temperature (Fig. 3 a). These concentrations may be designated the first and second critical concentrations respectively.

In quenching from the β region, the structure of alloys with a concentration of the alloying element less than C'_{cr} should be represented by the martensite phase α' (α'') and β , and finally, if the concentration of the β stabilizer is above the second critical concentration (C''_{cr}), only the β phase is frozen on quenching from the β region (Fig. 3).

In the two-phase ($\alpha + \beta$) region at temperatures below T_2 , the concentration of the β stabilizer in the β phase is higher than critical, and on quenching it does not undergo the martensite transformation, so that the structure of the alloys after quenching from temperatures below T_2 will be represented by α and β phases. In the T_2-T_7 range, the β stabilizer concentration in the β phase in the two-phase ($\alpha + \beta$) region is less than critical, and therefore on quenching, the β phase changes into a martensite-type phase. Since the martensite transformation in the β phase with a β stabilizer concentration from C'_{cr} to C''_{cr} does not go to completion, the final structure of the quenched alloys can be represented by the phases α , α' and β . On heating for quenching to the two phase ($\alpha + \beta$) region above temperature T_7 , and β stabilizer concentration in the β phase is less than C'_{cr} , and therefore the transformation $\beta \rightarrow \alpha'$ goes to completion, so that the final structure will be represented by the phases α and α' .

/44

In many binary titanium alloys with transition elements at concentrations of alloying elements close to the second critical concentration, on quenching from the β region, the ω phase is formed in the β phase. The metastable diagram of the phase composition of titanium alloys after quenching can then be represented by the graph of Fig. 3 a.

Thus, in a certain temperature range of heating for quenching, the ω phase may form even in low alloys of titanium. Actually, if the ω phase is formed in an

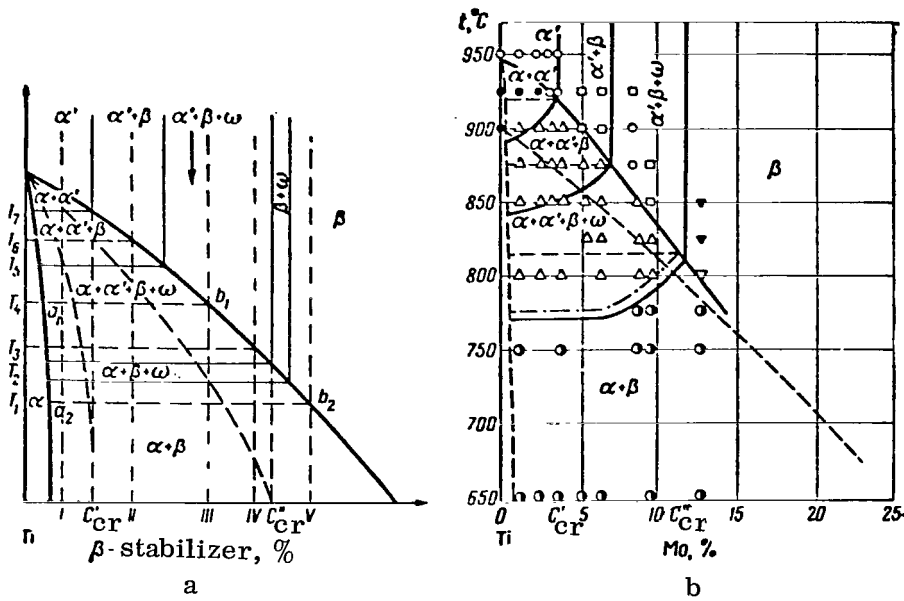


Figure 3. Metastable Diagrams of the Phase Composition of Titanium Alloys With 11 Stabilizers:

a—Scheme; b—System Ti-Mo.

alloy of composition b_1 on quenching from temperature T_4 , it should be formed in all alloys with concentrations of alloying elements from a_1 to b_1 on quenching from the same temperature T_4 , since on heating for quenching the structure of the alloys will be represented by an α phase of composition a_1 and β phase of composition b_1 . However, the amount of the β phase in the quenched composition and hence the amount of the ω phase will decrease with decreasing content of the β stabilizer in the alloy.

In [19], the above hypothetical metastable diagram for titanium alloys was confirmed experimentally by using alloys of the system Ti-Cr as examples. Figure 3 b shows a metastable diagram which we later plotted for the system Ti-Mo; this diagram provides a full confirmation of the scheme shown in Fig. 3 a. The $\beta + \omega$ region in this system is small and could not be detected experimentally.

On aging of quenched alloys, decomposition of the martensite phase takes place with the formation of a mixture of α and β phases, and there is also a decomposition of the metastable β phase if it is present. In the course of decomposition of the β phase above 500°C , separation of the α phase takes place, and at lower aging temperatures, the ω phase may form in the β phase.

There are at least three different viewpoints of the nature and mechanism of formation of the ω phase during aging. The first is that the formation of the ω phase during aging or isothermal treatment is similar to the bainite transformation in steel [7, 9, 22]. Investigators representing the second group assume

that holding below 500°C results in demixing of the β solid solution and that subsequent cooling in portions depleted of the alloying elements results in the martensite transformation $\beta_{\text{depl}} \rightarrow \omega$.

The third viewpoint has it that processes taking place in the β phase during aging or isothermal treatment are similar to those occurring during aging of aluminum alloys, and ω is the intermediate phase between β and α solid solutions.

It should be noted that many phenomena connected with the formation of the ω phase during aging may be accounted for by the first two viewpoints. However, some phenomena, in particular details of the recovery effect, the greater aging effect in β alloys caused by the presence of the ω phase as compared to the hardening of the alloy by the ω phase on quenching, are accounted for more logically on the basis of the third viewpoint. Thus, in alloys of the Ti-Mo system, which are close in composition to the second critical concentration, the maximum hardness after quenching from the β region amounts to 38HRC, and the hardness of the alloy Ti + 13% Mo after aging with formation of the ω phase is 49HRC. This experimental fact is difficult to explain by the bainite hypothesis of formation of the ω phase or by a martensitic mechanism of formation of the ω phase during aging.

Our study of the kinetics of decomposition of metastable phases in the course of aging and isothermal treatment has led to the necessity of refining the diagrams of isothermal transformations for titanium alloys proposed by I. N. Bogachev and M. A. D'yakova [22].

In the authors' studies [16, 23], alloys with 2, 6 and 9% Mo and the industrial alloy VT3-1 being used as examples, it was shown that in the interval between M_i and M_f decomposition into two phases (β and α') takes place, and that the decomposition rates are generally different. As an illustration, Fig. 4 shows the microstructure of the alloy Ti + 9% Mo after isothermal treatment. After quenching, the structure of the alloy is represented by α' and β phases. Isothermal treatment at 650°C for 30 sec led to a partial decomposition of martensite into the α phase (point precipitates) and β phase (matrix). Extension of the holding time to 1 min led to a complete decomposition of martensite and to the start of decomposition of the β phase: at the grain boundaries, there appeared laminar deposits of the α phase which grew with a further increase of the holding time. At the same time, the point α phase, which is the product of decomposition of martensite, dissolved, thus proving itself to be thermodynamically less stable than the laminar α phase growing from boundaries of β grains.

Thus, data of microstructural and electron microscope analyses showed that two phases, β and α' , decompose isothermally between M_i and M_f .

In the schemes given in [22], the $(\beta + \omega)$ region is at once replaced by the $(\beta + \alpha)$ region. However, the experimental data we obtained, in particular the use of the recovery effect for study transformations in alloys of titanium with chromium and molybdenum [23], indicate the simultaneous presence of alloys of α , β and ω phases in this structure in a definite range of temperatures and hold times. In the course of short-term heating at 600°C (recovery treatment), the ω phase formed during aging dissolves, and after quenching from 600°C the hardness of the alloy

returns to that of the alloy quenched from the β region. At the same time, the hardening caused by the α phase cannot be eliminated by the recovery treatment. Thus, as was first indicated by L. P. Luzhnikov et al. [10], the recovery effect can be used to evaluate the nature of the hardening phases. Figure 1 b illustrates the manner in which the recovery effect can be used to determine the phases formed in the quenched alloy Ti + 13% Mo in the course of aging at 450°C.

/46

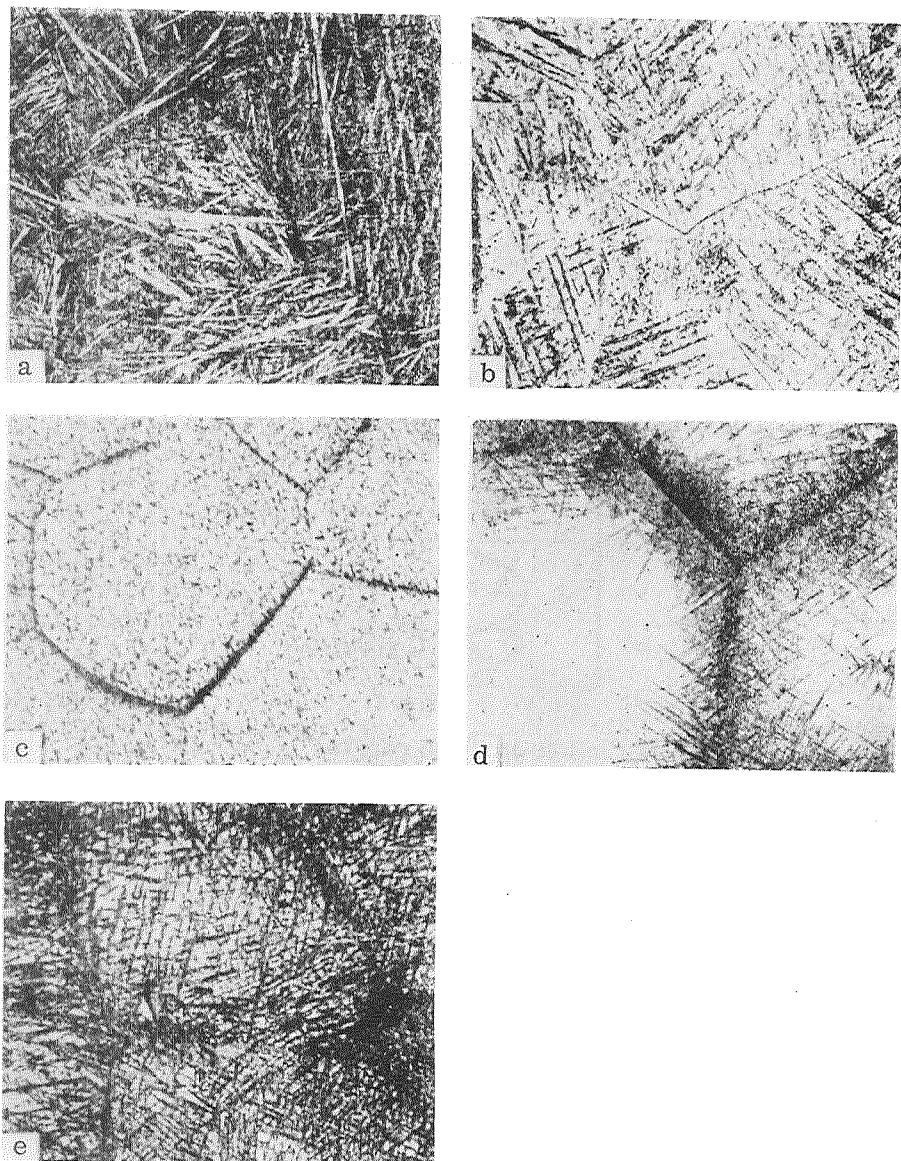


Figure 4. Microstructure of Alloy Ti + 9% Mo After Quenching (a) and After Isothermal Holding at 650°C (b-e) $\times 200$:

Hold Time: b—30 sec; c—1 min; d—5 min; e—30 min.

The transition from the $\beta + \omega$ structure to the $\beta + \alpha$ structure may be represented in two ways. It may be postulated that as the duration of the aging increases, the ω phase formed during aging gradually loses the coherence with the β matrix and changes into the α phase. Moreover, by analogy with aluminum alloys, one can postulate that the ω phase, being thermodynamically less stable, dissolves in the β phase and at the same time, nucleation of the α phase begins at other points of the β matrix. The second hypothesis appears to correspond to reality more closely. As was shown above, in the course of isothermal treatment at a temperature slightly below M_i , even laminar precipitates of the α phase (i.e.,

one form of the α phase) are not formed from fine point precipitates of the same α phase, but are generated at new points of the β matrix. This convinces us of the fact that in the transformation $\beta + \omega \rightarrow \beta + \alpha$, the α phase is not formed from the ω phase, but grows from new independent centers.

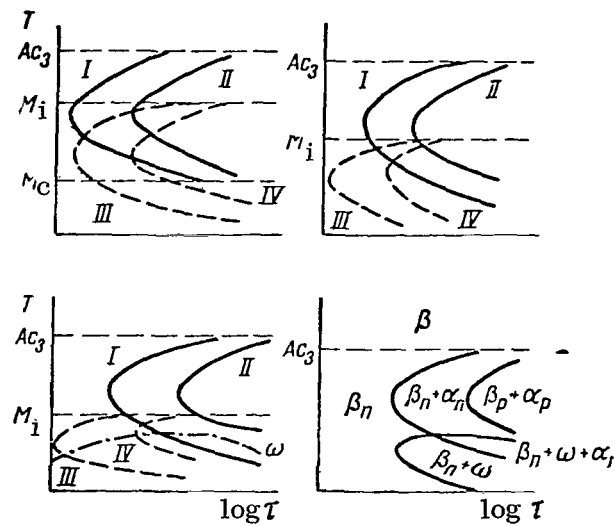


Figure 5. Graph of Change in Type of Diagrams of Isothermal Transformations With Increasing Content of β Isomorphous Stabilizers.

I, II—Beginning and End of Decomposition of β Phase; III, IV—Beginning and End of Decomposition of α' Phase; Dashed Line—Line of Existence of ω Phase.

Our experimental data permit the assumption that the change of the diagrams of isothermal transformations with increasing content of β isomorphous stabilizers may be described by the graphs shown in Fig. 5. For alloys with a content of β stabilizers less than the second critical concentration, the diagrams are represented by two series of lines describing the beginning and end of the decomposition of β and α' phases. In the interval between M_i and M_f , these series of lines

overlap. For alloys close in composition to the second critical concentration, the line of formation of the ω phase is superimposed on the lines in the lower portion of the diagram.

For supercritical alloys, the diagrams are represented by the lines at the beginning and end of the precipitation of the α phase and by the line bounding the region $\beta + \omega$. The region $\beta + \omega + \alpha$ is formed in a certain temperature interval.

The hardening of $\alpha + \beta$ titanium alloys during aging is caused by processes occurring in the metastable β phase [10, 24], and therefore during aging it will depend primarily on the amount of β phase and its ability to harden.

The amount of β phase formed on quenching may be found by means of the metastable phase composition diagram. As an example, we shall consider a metastable diagram for alloys of titanium with a β isomorphous stabilizer (Fig. 3 a). The amount of β phase in the alloys during heating for quenching to temperatures corresponding to the $\alpha + \beta$ region may be determined by means of the lever rule. As an example, the dashed line in Fig. 6 a shows the amount of β phase during heating for quenching for alloys I-V. An alloy V, all of the β phase which was present in the structure during heating for quenching is frozen after chilling at room temperature.

In alloys I-IV, the β phase is frozen completely on quenching without undergoing a martensite transformation, during heating for quenching only below T_2 . On quenching from temperatures above T_2 , part of the β phase is transformed into martensite. The amount of β phase retained in alloys I-IV on quenching from temperatures above T_2 may be determined if one knows the dependence of the amount of residual β phase on the content of β stabilizer on quenching from the β region. Experimental data obtained in [23] and other studies [20-21] indicate that this dependence may be described by a curve similar to the one given in Fig. 6 b. The amount of residual β phase, for example in alloy II after quenching from T_4 , can then be determined in the following manner. At T_4 the structure of alloy II is represented as follows: $(100 - x)\%$ of α phase of composition a_1 and $x\%$ of β phase of composition III. As is evident from Fig. 6 b, in alloy of composition III on quenching from the β region, $y\%$ of martensite phase is formed, and $(100 - y)\%$ of β phase is retained. Hence, the amount of residual β phase in alloy II will be

$$\frac{x(100 - y)}{100} \%,$$

and the amount of α' phase will be

$$x - \frac{x(100 - y)}{100} \%.$$

The amount of phases in alloy II after quenching from different temperatures (Fig. 6 c) may be determined in similar fashion. On the illustrated graphs, the amount of β phase as indicated along with the amount of the ω phase, since these two phases are coherent. Moreover, the ω phase takes part in the hardening of the β phase subjected to aging if the aging temperature is not high.

/48

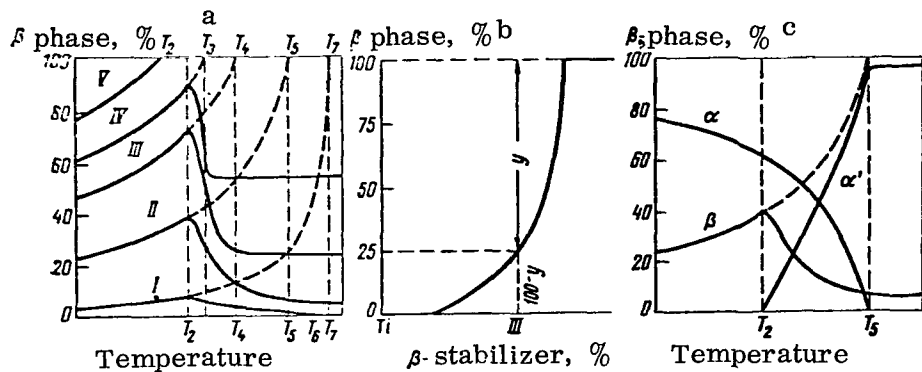


Figure 6. Dependence of the Amount of Residual β Phase on a) the Temperature of Heating for Quenching, b) the Content of β Stabilizing Element, c) Number of Phases in Alloy II.

In Fig. 6 a, solid lines indicate the amount of residual β phase in alloys of different composition. These data indicate that in all alloys with a content of β stabilizers lower than the second critical concentration, the largest amount of β phase is frozen on quenching from one and the same temperature. This is the temperature at which the composition of the β phase corresponds to the second critical concentration.

To illustrate how important it is to make a correct choice of the temperature of heating for quenching in order to obtain the maximum hardening, the alloy Ti + 9.41% Mo was subjected to quenching from different temperatures and aging at 400°C for 30 min. The aging effect was maximum after quenching from 800°C, and hence, the maximum amount of β phase is formed after quenching from this temperature. At this temperature (see Fig. 3 b), the β phase contains 12% Mo, and the second critical concentration corresponds to 11-12% Mo. Consequently, at the optimum temperature of heating for quenching, the composition of the β phase in alloys of the Ti-Mo system is indeed close to the second critical concentration. The maximum aging effect in the VT3-1 alloy is observed after quenching from 850-875°C. By analogy with data obtained for alloys of the system Ti-Mo, one can postulate that in alloy VT3-1 the composition of the β phase is close to the second critical concentration at 850-875°C.

/49

As we know, the hardening caused by the ω phase cannot be used for practical purposes because of considerable brittleness. In order to avoid brittleness associated with the ω phase, titanium alloys are subjected to aging under conditions which do not result in the formation of the ω phase, most frequently at 500-600°C. At these temperatures, the hardening is produced by the α phase. However, at these aging temperatures, relatively large precipitates of α phase appear, and the hardening during aging is comparatively slight.

Precipitates of the α phase may produce a relatively high degree of hardening if the aging is carried out at lower temperatures, when the α phase is highly dispersed. To eliminate brittleness caused by the presence of the ω phase, which unavoidably forms at low temperatures, use may be made of the recovery effect.

In the recovery, the ω phase dissolves, while the α phase is retained. To verify this possibility experimentally, VT3-1 alloy was subjected to quenching and aging under standard conditions, and also at 350-450°C for different periods of time, followed by treatment for 10 sec at 600°C. At 600°C, ready specimens for mechanical tests were subjected to treatment, since during the short time available, the billets were unable to heat up to the required temperature.

The data obtained show that after low-temperature aging and the recovery treatment, for VT3-1 alloy it was possible to obtain a strength 5-10 kg/mm² higher than after standard aging at practically the same plasticity. Thus, after quenching from 850°C, aging at 400°C for 15 hr and recovery at 600°C for 10 sec, VT3-1 alloy of the batch studied had the following properties: $\sigma_B = 144.8$ kg/mm², $\delta = 8.0\%$, $\psi = 26.8\%$, and after aging under standard conditions: $\sigma_B = 132.5$ kg/mm², $\delta = 10.9\%$, $\psi = 31\%$. It should be noted that the treatment leading to the recovery effect should be used only for small-sized articles. The duration of heating for the purpose of eliminating the ω phase may be increased, and this treatment can then be used for large-sized articles as well. Extension of the hold time leads to a certain drop of the ultimate strength and markedly increase the plasticity. Essentially, this treatment is used for alloy VT-15 (450°C, 25 hr + 560°C, 15 min).

The same conditions of thermal treatment can also be chosen for other $\alpha + \beta$ titanium alloys. It should be noted that the thermal stability after low-temperature aging followed by recovery treatment may be lower than after aging under standard conditions. Therefore, alloys after such treatment can be used at temperatures only up to 400°C, obviously if further studies confirm its advisability.

A number of papers point out that a better combination of mechanical properties can be achieved in aluminum alloys if, instead of quenching to room temperature and then aging, they are subjected to chilling directly in baths, down to the temperature of artificial aging. The better combination of mechanical properties resulting from such treatment is attributed to lower thermal stresses.

In principle, the same kind of heat treatment is also possible for titanium alloys. To check its usefulness, specimens of VT3-1 alloy of the same batch mentioned above were rapidly transferred from 850°C to a bath of Al-Cu-Si alloy heated to 550°C, held for 1-6 hr, then cooled in air. Similar specimens were quenched from 850°C in water then aged under the same conditions. In all cases, after the isothermal quenching, the plasticity turned out to be considerably higher than after ordinary quenching and aging, but with a somewhat lower strength. Thus, after isothermal treatment for 6 hr, VT3-1 alloy had $\sigma_B = 131.2$ kg/mm², $\delta = 14.2\%$, $\psi = 48.7\%$. /50

The studies which were carried out, particularly [25, 26], indicate that the thermomechanical treatment can be tested on an industrial scale. In evaluating the effectiveness of this treatment of titanium alloys it should be noted that the thermomechanical treatment of titanium alloys does not result in any substantial increase of strength, as in steels, but sharply increases the homogeneity of the structure and properties along the cross section and length of the articles, and the reproducibility of the properties of the articles from one and the same alloy but different batches.

REFERENCES

1. Kolachev, B. A. and N. Ya. Gusel'nikov. Trudy MATI, 55, 97, 1962.
2. Kolachev, B. A. and V. V. Shevchenko. Trudy MATI, No. 66, p. 63-75, 1966.
3. Glazunov, S. G. Collection "Titanium and its Alloys." AN SSSR, 99, 1958.
4. Dobatkin, V. I. Izv. vuzov. Tsvetnaya metallurgiya, 3, 1961.
5. Kolachev, B. A. and S. M. Faynbron. Trudy MATI, 66, 103, 1966.
6. Livanov, V. A., A. A. Bukhanova and B. A. Kolachev. Trudy MATI, 55, 78, 1962.
7. Bagaryatskiy, Yu. A., T. V. Tagunova and G. I. Nosova. Metallurgy and metal physics, issue 5. Metallurgizdat, 210, 1958.
8. Bagaryatskiy, Yu. A., G. I. Nosova and T. V. Tagunova. Physics of Metals and metallurgy. Metallurgizdat, Sverdlovsk, 3, 13, 145, 1962.
9. Fedotov, S. G. Collection "Study of Metals in the Solid and Liquid States." "Nauka," 207, 1964.
10. Luzhnikov, L. P. et al. Metallovedeniye i termicheskaya obrabotka metallov, No. 5, 1. 21, 1965.
11. Lashko, N. F. Collection "Physical Metallurgy of Titanium." "Nauka," 74, 1964.
12. Luke, C. A., R. Taggart and D. H. Polonis. Trans. ASM, 57, 1, 142, 1964.
13. Everhart. Titanium and its alloys. Metallurgizdat, 1956.
14. Jamilson, J. C. Science, 140, 3562, 1963.
15. Hume-Rothery, V. and G. V. Raynor. Structure of metals and alloys. Metallurgizdat, 1959.
16. Vishnyakov, D. Ya, B. A. Kolachev and V. S. Lyasotskaya. Metallovedeniye i termicheskaya obrabotka metallov, 2, p. 6, 1967.
17. Gridnev, V. N., V. A. Rafalovskiy and V. I. Trefilov. Voprosy fiziki metallov metallovedeniye, AN USSR, 14, 5, 1962.
18. Ageyev, N. V. Papers of conference "Nature of Metal Phases and Character of Chemical Bonding Therein." The A. A. Baykov Metallurgy Institute, p. 3, 1965.
19. Kolachev, B. A. and V. S. Lyasotskaya. Izv. Vuzov, OTN, Tsvetnaya metallurgiya, 2, 123, 1966.
20. Ageyev, N. V. and L. A. Petrov. Collection "Titanium and its Alloys," Metallurgy and Science of Metals," AN SSSR, p. 3, 1958.
21. Ageyev, N. V. and Z. M. Smirnova. Collection "Titanium and its Alloys," "Metallurgy and Science of Metals," AN SSSR, p. 17, 1958.
22. Bogachev, I. N. and M. A. D'yakova. Metallovedeniye i termicheskaya obrabotka metallov, 1, 1966.
23. Kolachev, B. A. et al. Sb. trudov MATI, 66, 39, 1966.
24. Luzhnikov, L. P., V. M. Novikova and A. P. Mareyev. Collection "Physical Metallurgy of Titanium." "Nauka," 80, 1964.
25. Novikov, I. I., I. S. Pol'kin and A. O. Barsukov. Physical metallurgy of light alloys. AN SSSR, 145, 1965.
26. Bernshteyn, M. L. et al. Metallovedeniye i termicheskaya obrabotka metallov, 5, 35, 1965.

THERMOMECHANICAL TREATMENT OF CERTAIN TITANIUM ALLOYS

I. M. Pavlov, A. E. Shelest and Yu. F. Tarasevich

The property of titanium alloys to combine a considerable strength with a low density and a high corrosion resistance accounts for their wide use in industry, and therefore it is of major interest to study the possibilities of improvement of their mechanical properties by methods of thermomechanical treatment without additional alloying. The positive effect of thermomechanical treatment for certain titanium alloys has been observed in many studies. In most cases, the investigations involved the use of various methods of plastic deformation for various temperature-rate conditions of deformation on specimens having different initial and final dimensions. This markedly hinders the comparison and analysis of the results obtained and does not permit one to obtain a complete picture of the effect of thermomechanical treatment of various titanium alloys. The authors made a study of the thermomechanical treatment of basic types of titanium alloys under identical conditions of treatment, the purpose of which was to determine the nature of the change in the mechanical properties of titanium alloys of different degrees of alloying starting with various initial structures under different conditions of thermomechanical treatment. The chief factors influencing the effect of thermomechanical treatment were the chemical composition of the alloys studied, the deformation temperature, the degree of deformation, and the degree of cooling after deformation. The authors studied the influence of these factors on the effect of thermomechanical treatment, which was evaluated from the change in the mechanical properties of the given alloys as compared to alloys subjected to thermal treatment.

/51

The following factors were considered:

1. Strength effect of thermomechanical treatment. The dependence of the tensile strength, yield point and their ratio on the conditions of thermomechanical treatment was determined.
2. Relationship between the chemical composition of the alloys studied and the effect of thermomechanical treatment.
3. Influence of thermomechanical treatment on the plastic limit of titanium alloys, evaluated by the magnitude of the reduction of area after rupture. The influence of thermomechanical treatment on the fracture of the metal was studied, and the relationship between the character of the rupture of titanium alloys and the magnitude of the reduction of area was determined.
4. Character of the change of the magnitude of elongation per unit length after rupture under thermomechanical treatment (an evaluation of uniform and concentrated deformations of the breaking specimens was made).

In addition, the failure of titanium alloys under thermomechanical treatment was studied. The thermomechanical treatment consisted of rolling at certain temperatures and degrees of deformation, followed by cooling at various rates.

Experimental Method

The following alloys with different degrees of alloying were chosen for the study: one-phase alpha alloy VT1, two phase ($\alpha + \beta$) alloys OT4, VT6C and VT14, and one-phase β alloy VT15.

The thermomechanical treatment was carried out by rolling with reductions of 20, 40 and 60% at 500–1100°C (every 100°C), followed by cooling of the specimens in water, air and under asbestos sheets. Two variants of retarded cooling made it possible to compare the mechanical properties of air-cooled specimens of various cross sections. It is known [1, 2] that high-temperature thermo-mechanical treatment produces a full effect only on specimens with cross sections of 10 x 12 mm, and the mean cooling rates of the schedules chosen, measured with thermocouples inserted into the specimen, amounted on 60.7 and 4 deg/sec respectively. The billets were prepared by rolling on a "200" mill at a linear rolling velocity of 0.5 m/sec. The mechanical properties were determined on fivefold specimens with a working-part diameter of 3 mm, and the extension rate was 2 mm/min.

/52

Hardening under HTMT may be regarded in a simplified view as the total result of hardening from quenching of the deformed high-temperature phase and from secondary hardening on aging. In order to evaluate these hardening factors separately, two series of specimens were subjected to rolling, and after rolling the specimens of one series were subjected to aging under the following conditions: VT1—350°C, 20 hr; OT4 and VT6S—400°C, 20 hr; VT14—480°C, 10 hr; VT15—500°C, 20 hr.

To compare the mechanical properties of the alloys after TMT with the properties after ordinary thermal treatment, the alloys were subjected to thermal treatment at 800–1100°C with the same cooling and tempering rates (specimens of the same cross section). A slight difference in the retarded cooling rates has virtually no effect on the mechanical properties of the two-phase titanium alloys. In alloy VT15, the retardation of cooling decreases the plasticity, probably as a result of some decomposition of the β phase, which manages to take place during the cooling. According to the data of M. Kh. Shorshorov [3], the decomposition of the β phase in alloy VT15 may take place during cooling at a rate of less than 9 deg/sec. Examination of the microstructure of specimens of alloy VT15 cooled from high temperatures in air and under asbestos showed precipitates of the α phase. Aging slightly increases (by 5–10 kg/mm²) the tensile strength of two-phase alloys and hardens alloy VT15.

Influence of Thermomechanical Treatment on the Strength Characteristics of Titanium Alloys

The effect of thermomechanical treatment is different in one-phase and two-phase alloys. In one-phase α titanium VT1, the tensile strength after rolling at 900–1100°C and quenching was 60–65 kg/mm², and after rolling and cooling in air, 55–60 kg/mm². An increase in the tensile strength of technical titanium to 70 kg/mm² is achieved only by rolling at 500–600°C, and an increase in the degree of deformation increases the plasticity. In alloy VT15, the effect

/53

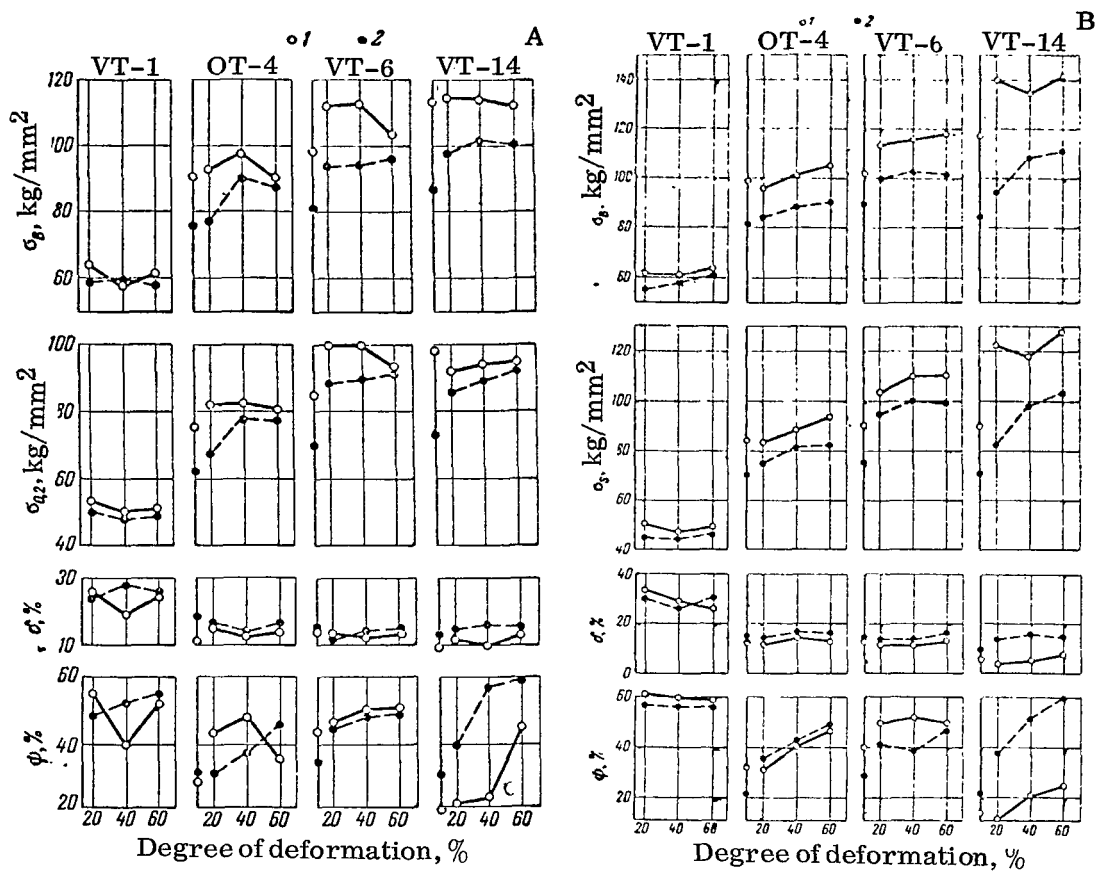


Figure 1. Effect of Degree of Deformation in Rolling on Mechanical Properties of Alloys Studied (Rolling Temperature 900°C):

a—Before Aging; b—After Aging, Cooling: 1—In Water; 2—In Air.

of hot working is also nearly absent — an increase in the degree of deformation in TMT hardens the alloy only slightly. After aging, its strength characteristics nearly correspond to the properties following thermal treatment (tensile strength about 165–170 kg/mm², and yield strength about 160–165 kg/mm²); the plasticity characteristics increase somewhat, but their absolute value is very low (reduction of area up to 7–9%). Thus, no appreciable increase of the strength characteristics of one-phase titanium alloys were noticed after the thermo-mechanical treatment.

The thermomechanical treatment of the two-phase alloys OT4, VT6S and VT14 at 800–1100°C substantially increases their mechanical properties as compared to the thermal treatment. The nature of the change in the properties is almost the same for all the alloys, and the optimum combination of strength and plastic characteristics was obtained after TMT at 900°C (Fig. 1). The effect of high-temperature work hardening is almost lacking, and the strength

characteristics even decrease somewhat with increasing degree of deformation. After aging, the tensile strength and yield point increase, as is evident from Fig. 2, are more appreciable the higher the degree of alloying of the alloys. Results of the thermomechanical treatment of titanium alloys support the prediction of N. N. Buinov and I. R. Zakharov [4]: hardening due to the refinement of blocks and to an increase of their disorientation even in alloys with large volume changes does not exceed 20-30% of age hardening. It is well known that after TMT, aging takes place more extensively. According to B. Chalmers [5], in regions of higher dislocation density, the growth of the precipitates becomes easier and faster in this case. The higher rate of their nucleation is explained by the formation of energy of elastic deformation in the dislocation rows, and the increased growth rate results from rapid diffusion along the line of dislocations. It was shown [6] that segregation of dissolved atoms on the dislocations plays a more important part in the hardening than the substructure does; this apparently explains the rise of the increase of tensile strength with increasing degree of alloying of two-phase alloys in the case of TMT followed by aging.

As the rolling temperature is lowered, the effect of hot work hardening appears. As is evident from Fig. 3, in the case of the thermomechanical treatment at 800°C, as the degree of deformation increases, the tensile strength also increases. Low yield point values after quenching from 800-850°C, characteristic of alloy VT14 [7], were also noted in alloys VT3-1 and VT6 [8, 9]. According to Jaffe [10], the yield point of titanium-molybdenum alloys depends on the structural transformations, and if the stress of formation of the martensite structure from the β phase is less than the critical stress, the formation of a martensite structure is possible in deformation. In addition, the decomposition of titanium alloys in deformation, associated with a strong decrease of the yield point, occurs in cases where the β phase has a composition determined by quenching from the β region (at 12% Mo and 15% V). Decomposition of the β phase on aging removes the effect of yield point lowering, and its value reaches 90 kg/mm². On the whole, the tensile strength of two phase alloys after IMI at 800°C and after aging increases by 5-20 kg/mm² as compared to the heat treatment.

/54

Rolling of alloys OT4 and VT6S at 700°C with high degrees of deformation can produce values of tensile strengths respectively above 90 and 110 kg/mm², and values of the yield point and reduction of area above those obtained after TMT at 800°C. As compared to the optimal mechanical properties obtained after thermomechanical treatment at 900°C, the tensile strength does not differ by more than 10 kg/mm² at almost the same values of the reduction of area and yield point. For alloys VT1, OT4 and VT6S, rolling at 500 and 600°C may be recommended, when the strength characteristics increase with the degree of deformation while the plasticity remains sufficient.

The comparatively slight hardening effect of HTMT obtained with these alloys (maximum increase of tensile strength as compared to the state following heat treatment did not exceed 20%) is probably due to the slight phase hardening on recrystallization, a hardening dependent on the effect of volume transformation of the high temperature phase into a low temperature phase, on the degree of alloying, temperature of the martensite transformation, and magnitude of

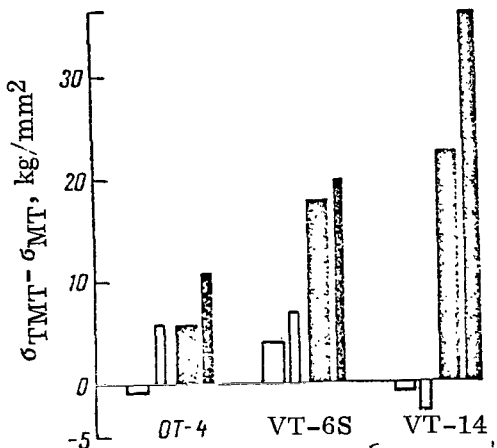


Figure 2. Hardening of Two-Phase Titanium Alloys in Thermomechanical Treatment:

$\sigma_{TMT} - \sigma_{MT}$ —Difference Between Values of Tensile Strengths and Yield Points of Alloys After TMT (Rolling at 900°C, $\epsilon = 60\%$) and After Heat Treatment. Black Columns—Quenching + Aging, White Columns—Quenching, Wide Columns— σ_u kg/mm², Narrow Columns— σ_u 0.2 kg/mm².

hysteresis of the temperatures of the start and end of the transformation [11]. As was shown by V. D. Sadovskiy et al. [12], the volume effect of the polymorphous transformation is insignificant (about 0.17%); the temperature of the martensite transformation on quenching is fairly high and not as distant from the recrystallization temperature as in the case of steels, thus facilitating the transformation in accordance with martensite kinetics, according to M. Kh. Shorshorov [3]. In contrast to the martensite of steels, the large interatomic "pores" of the low-temperature phase cause a peritectoid reaction with the interstitial elements instead of a eutectoid reaction. Moreover, it is known that in the case of a coherent transformation of the body-centered lattice of the β phase into a hexagonal lattice of the α phase, a slight inheritance of defects takes place. Thus, in titanium alloys in the case of thermomechanical treatment, the contribution of "mechanical" hardening (due to the creation of obstacles to the movement of dislocations such as grain boundaries, blocks, increase of their disorientation), is insignificant, and the TMT effect is determined primarily by a "chemical" hardening (precipitates on dislocations). Using the experimental data on the thermomechanical treatment of various titanium alloys, we shall arrange them in order of increasing tensile strength: VT1, OT4, VT6S, VT8 and VT14, VT3-1; an examination of this series shows that the degree of alloying of alloys with β stabilizers also increases in the same order.

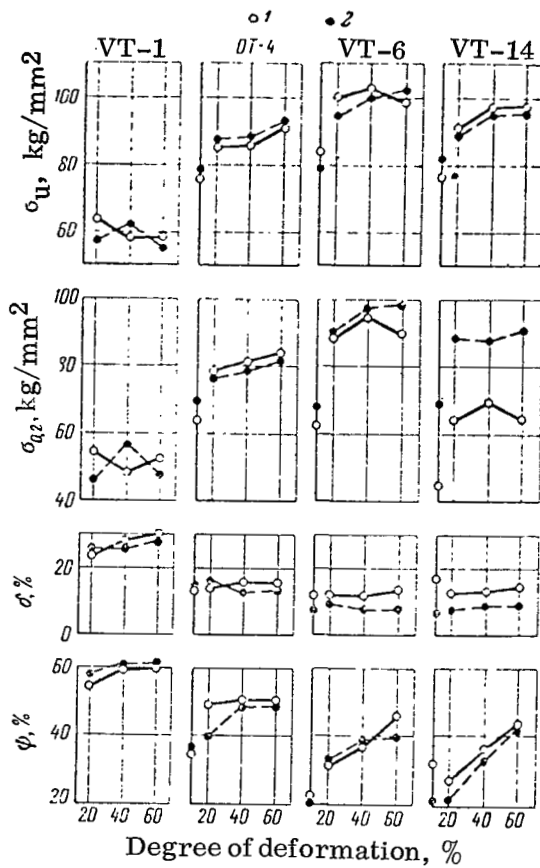


Figure 3. Effect of Degree of Deformation in Rolling on Mechanical Properties of Alloys Studied. Rolling Temperature 800°C:

1—Cooling in Water; 2—In Air.

It is well known that a preliminary cold deformation of the metal substantially increases the resistance to slight plastic deformations and raises the ratio of the yield point to the tensile strength. As can be seen from Fig. 2, under certain conditions of thermomechanical treatment, the yield point increases more appreciably than the tensile strength. Taking this ratio as an indirect indicator of work hardening (strain hardening), we may assume that the conditions of thermomechanical treatment which provide for higher values of this ratio than ordinary heat treatment partially freeze the hardened state of the metal.

As the temperature is lowered, this ratio in alloys after heat treatment essentially decreases; after rolling, it increases, and after rolling at temperatures below 900°C, it is greater than after heat treatment. As the degree of alloying increases, the ratio of the yield point to the tensile strength increases. However, in the case of titanium alloys, in contrast to pure metals, structural

effects can additionally superimpose themselves, as for example in alloys VT6S and VT14 in certain cases of thermomechanical treatment at temperatures of 800 and 900°C. /56

Influence of Thermomechanical Treatment on the Reduction of Area Following Rupture and on the Character of the Fracture

The influence of thermomechanical treatment on plastic characteristics determined in subsequent tension may vary. Thermomechanical treatment, by creating additional interfaces inside the grains, such as boundaries of blocks with a high angular disorientation, hinders the possibility of easy propagation of microcracks in the metal and prevents the migration of impurities toward the grain boundaries. However, numerous obstacles to the movement of dislocations may promote the formation of microcracks during subsequent deformation. The increase of the degree of deformation in TMT should have a favorable effect, primarily on the character of the fracture of coarse-grained structures, namely, in the case of rolling at high temperatures. /57

In alloys VT6S, VT14 and VT15, as the degree of deformation in the course of rolling at 1100-1000°C increases, the character of the fracture changes from intercrysalline to intracrysalline and from brittle intracrysalline (breakoff) to ductile intracrysalline (by shear). For instance, in alloy VT6S, the intercrysalline fracture of undeformed specimens cooled from 1100° is completely or partially replaced by intracrysalline fracture (by shear) after TMT at this temperature (Fig. 4a). In treatment of alloys in the two-phase region, deformation causes a fine subdivision of plates of the primary α phase and orients them in the direction of the main deformation. In ductile fracture, TMT may change the type of break. Thus, it is apparent from Fig. 4b that fracture by shear may be replaced by fracture by a "cup", in which the reduction of area is usually higher.

The magnitude of the reduction of area following rupture, commonly used to evaluate the deformation of specimens in tension to fracture, is closely related to the character of their fracture. Although no definite dependence of the reduction of area on the degree of deformation in rolling was observed in one-phase alloys, in the two-phase alloys OT4, VT6S and VT14 the reduction of area in most cases increases with increasing degree of deformation, but the character of its change is different in the case of different TMT conditions. Thus, in alloys VT6S and OT4, quenched after rolling at 1000-1100°C with 60% deformation, the reduction of area is 2-3 times less than after ordinary quenching, and in slowly cooled specimens, approximately 1.5 times less. After rolling at 900°C, the increase of the reduction of area is not so large, but after TMT at 800°C it may again be more than twice as high as the reduction of area of these alloys following heat treatment. In alloy VT14, as the degree of deformation in rolling increases in this temperature range, the reduction of area increases by an average factor of 1.5-2 regardless of the dependence on the cooling rate.

The observed increase of reduction of area with increasing degree of deformation in the case of rolling at low temperatures may be explained by the bending and interweaving of structural components, and also by the polygonization occurring at these temperatures.

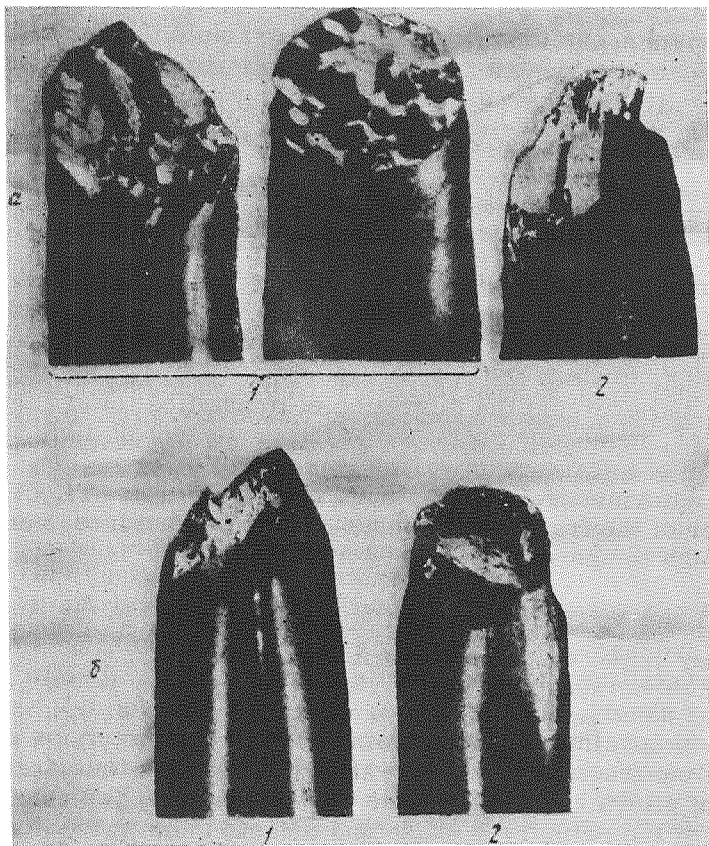


Figure 4. Change of the Character and Type of Fracture in TMT:

a—Alloy VT6S (1000°C); b—Alloy VT14 (900°C) Without Deformation (1) and After 60% Deformation (2).

Influence of Thermomechanical Treatment on Elongation Per Unit Length and Character of the Distribution of Deformation Along the Length of Tensile Test Specimens

No definite relationship was observed in this study between the degree of deformation in rolling and the magnitude of elongation per unit length after rupture. The elongation per unit length of a specimen is made up of uniform elongation (δ_u) and concentration elongation (δ_c), and for this reason the change of these components of elongation during thermomechanical treatment were examined separately. It is well known that the magnitude of these characteristics is related to the history of the preparation of the specimens and in particular to the work hardening of the metal [11, 13]. To determine these components of elongation, lines of distribution of the elongation deformation were plotted on the

calculated length of the specimens by using a method described in [4]. The deformation of the specimen itself was evaluated by means of three coefficients.

The uniform deformation of the specimen was evaluated from the coefficient of uniformity (stability) of the deformation K_e , indicating the fraction of uniform elongation in full elongation: $K_e = \frac{\delta_u}{\delta}$.

The concentrated deformation of a specimen was evaluated by means of two coefficients: K_c , indicating the portion of the calculated length of the specimen on which a neck develops ($K_c = \frac{l_n}{l_0}$, the segment of calculated length l_0 of the specimen where the elongation was higher than δ was arbitrarily taken as the neck length l_n), and K_B , showing how many times the maximum elongation deformation exceeds the elongation per unit length after rupture ($K_B = \frac{\delta_{max}}{\delta}$).

/58

As the degree of deformation increases in the case of TMT at 1000–1100°C, the uniform deformation may increase (alloy OT4), remain constant (alloy VT14) or decrease (alloy VT6S). After rolling at 900°C, no definite dependence of these quantities was observed either, but after rolling at temperatures up to 800°C, the uniform deformation in all alloys was less than after heat treatment, and decreased continuously with increasing degree of deformation (Fig. 5).

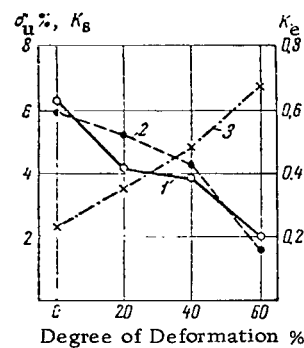


Figure 5. Effect of Degree of Deformation on Uniform Elongation of Alloy VT6S (Rolling at 800°C:)

1— δ_u —Uniform Deformation, %; 2— K_e ; 3— K_B .

The amount of concentrated strain is proportional to the volume displaced in the region of the neck. Statistical treatment of the experimental data showed that the dependence of the concentrated elongation δ_c and of the reduction of area ψ is linear in character: $\delta_c = 0.2\psi - 1$ (δ_c and ψ in per cent). The magnitude of standard deviation from the given line amounts to $\pm 1\%$, and the region of scatter, including 95% of all the experimental points, amounts to $\pm 2\%$ of the given line.

The absolute change of the total elongation of the specimen after TMT is determined by changes of δ_u and δ_c . If δ_c basically increases with increasing degree of deformation in rolling, δ_u may decrease, and the total effect of TMT may vary. For example, the elongation per unit length of alloy VT6S subjected to aging after quenching from 800°C, equal to 8%, consists of uniform elongation to the extent of 3/4, and the elongation equal to 10% after TMT and aging is mainly caused by concentrated elongation ($\delta_u = 1\%$).

For this reason, the change of elongation per unit length after TMT will be different in specimens of different calculated lengths.

The change of coefficient K_e with temperature, degree of deformation and rate of cooling is not always similar to the change of δ_u . For example, δ_u of alloy VT1 on lowering the rolling temperature from 900 to 500°C is cut by 1/2 while coefficient K_e remains almost unchanged. Coefficient K_B basically increases with rising degree of deformation and decreasing rolling temperature in two-phase alloys. In alloy VT1 and two-phase alloys, the length of the neck decreases with rising degree of deformation and decreasing rolling temperature.

The magnitude of uniform deformation may be used for comparing strain hardening (work hardening) obtained by thermomechanical treatment at low temperatures. For instance, after rolling alloy OT4 at 500°C with 20% degree of deformation and at 600°C with 40% degree of deformation, the uniform elongation will be the same. Aging decreases the work hardening to some extent, and the same kind of uniform elongation was obtained after rolling of an aged alloy at 500°C with a 40% reduction of area. In 20% deformed alloys VT6S and VT14, δ_u increases somewhat after tempering, and decreases after 40% deformation; at the same time, a change of δ_u does not always correspond to the change of the tensile strength. Smaller δ_u and higher σ_u values correspond to higher alloys. On the whole, it may be stated that the change of δ_u accompanying a decrease of rolling temperature or an increase in the degree of deformation can yield a qualitative picture of the hardening of alloys.

/59

Fracture of Titanium Alloys in Rolling

The diverse nature of fracture in the rolling of specimens of low and high titanium alloys was observed in [15]. In low alloys, cracks arose mainly on the lateral surface in a vertical direction, and in high alloys, on the lateral and end surfaces at an angle of approximately 45° to the plane of rolling.

Considerable deformation in thermomechanical treatment is associated with a certain irregularity. As was shown by A. Nadai [16], in the deformed volume there are always slip lines with a considerable shear strain. Friction on the surface of contact between the tool and the metal reinforces the unevenness of the strain, causing the formation of hindered strain, on the outside of which are located regions (bands) of macrolocalization of plastic strain [17]. N.N. Davidenkov et al. [18] proposed the following mechanism of formation of these bands in steels: as a result of strong shear strain, an intense heating of the metal, whose temperature may exceed the critical value, takes place in areas of macrolocalization of strain, creating the possibility of a polymorphic transformation. The adjacent mass of metal conducts the heat away at a rapid rate, causing quenching of this layer. This band has the hardness of martensite and a needle-free structure. M.V. Rastegaev [19] has shown that the band itself is inhomogeneous over the cross section because of its uneven temperature distribution. A local thermal effect along the grain boundaries is sometimes used to explain the lowering of the ductility of high alloy steels in forging [20, 21]. Zener [22] refers to this mechanism of deformation as adiabatic shear.

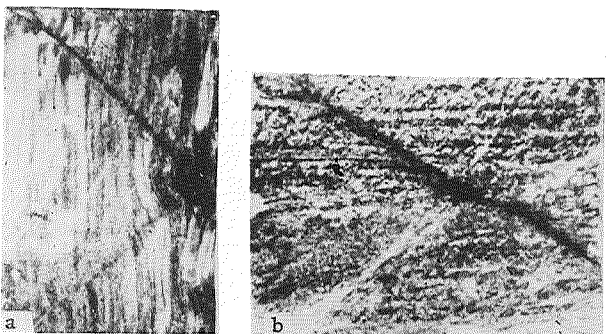


Figure 6. Bands of Macrolocalization of Deformation in Titanium Alloys:

a—Alloy VT14, Rolling at 600°C , 20%; b—Alloy OT4, Rolling at 500°C , 40%.

/60

In the titanium alloys studied, after rolling at $500\text{--}800^{\circ}\text{C}$, bands were observed similar to strain macrolocalization bands in steels (Fig. 6), along which fracture took place in high alloys. In alloy VT14, microcracks were formed in these bands, in rolling at 800°C with 20% reduction (Fig. 7).

/61

In all variants of the treatment, the microhardness of the band surpassed that of the base metal. A considerable increase of microhardness in the bands, observed in certain cases, should not be attributed to strain hardening, since, as the degree of deformation in rolling increased, the tensile strength increased by no more than 15%. It may be assumed that in certain variants of the treatment, the mechanism of formation of bands of strain macrolocalization in titanium alloys is similar to the mechanism of their formation in steels. In our study, local overheating of the metal is fostered by the low thermal conductivity of titanium alloys and high rate of deformation in rolling. A number of indications supporting this assumption can be cited: 1) the microhardness of bands of titanium alloys increases with the degree of alloying and reaches the microhardness of titanium martensite; 2) the microhardness in bands of alloy VT15 increases only slightly, 3) the structure of the bands differs from that of the base metal; 4) impressions of the pyramid in the bands of the alloys are in the shape of squares, although one should expect their distortion in a metal which has been subjected to strong plastic deformation and should possess a substantial anisotropy of the properties; 5) the microhardness of bands of strain macrolocalization increases with rising temperature of rolling, when the simultaneous increase of the heat effect and cooling rate reinforces the quenching effect. In addition to the bands of strain macrolocalization, observed on macrosections and located diagonally along the cross section of the specimens, there are always thinner bands also located predominantly at a 45° angle to the surface of the specimens (Fig. 7a), where the cracks are chiefly formed. Cracks caused by the presence of bands of strain macrolocalization are formed more frequently not in the bands themselves, but at their boundaries. In the view of R. Low [23], ductile fracture involves, at first, deformation of many parallel microcracks, between which the metal fails as a result of plastic shear. To decrease the

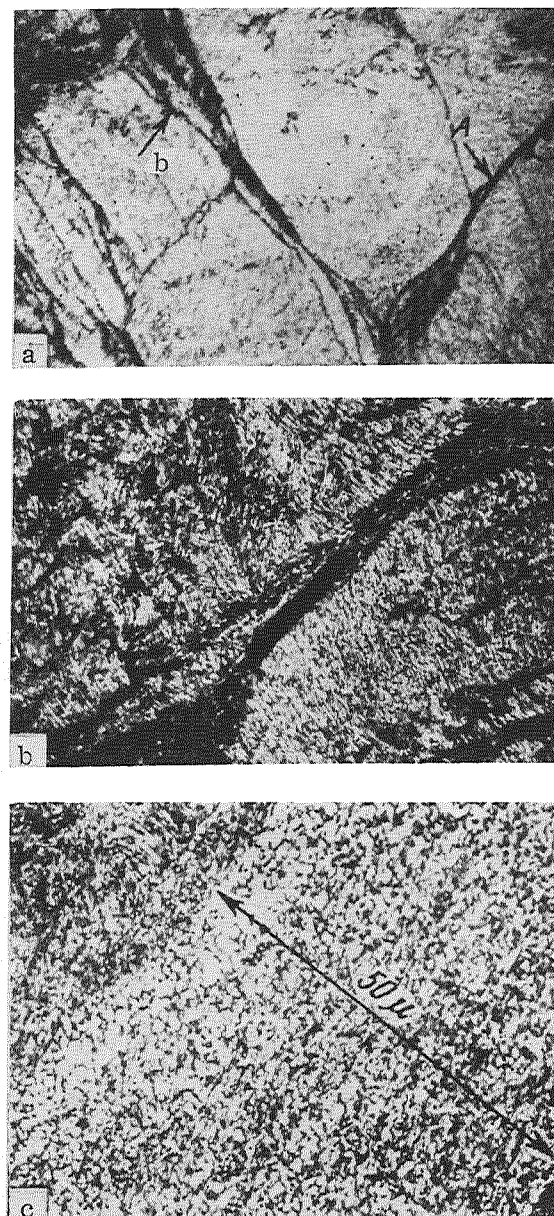


Figure 7. Bands of Macrolocalization of Deformation in Alloy VT14 After Rolling at 800°C:

a—Microcracks, Shown By Arrows A and B $\times 160$; b—Microcrack B $\times 500$; c — Structure of Band of Macrolocalization of Deformation $\times 1000$.

possibility of formation of these bands in thermomechanical treatment with considerable degrees of deformation, it is preferable to carry out fractional deformation (with a sufficient stability of the high temperature phase), and in order to eliminate undesirable tensile strains in the bands, use should be made of deformation processes with a triaxial compressible schedule [24].

It should be noted that thermomechanical treatment substantially increases the plasticity of $\alpha + \beta$ -alloys, determined by the magnitude of reduction of area following rupture, and may produce a metal with satisfactory properties after plastic deformation at higher temperatures. As the degree of alloying of two-phase titanium alloys increases, a large increase of tensile strength and yield point is observed. It would be advisable to work out a composition of titanium alloys designed specifically for thermomechanical treatment.

REFERENCES

1. Lozinskiy, M.G. Structure and Properties of Metals and Alloys at High Temperatures. Metallurgizdat, 1963.
2. Ivanova, V.S. and L.K. Gordiyenko. New Ways of Increasing the Strength of Metals. "Nauka," 1961.
3. Shorshorov, M.Kh. Metallurgy of the Welding of Steel and Titanium Alloys. "Nauka," 1965.
4. Buinov, N.N. and R.R. Zakharova. Decomposition of Supersaturated Metal Solid Solutions. "Metallurgiya," 1964.
5. Chalmers, B. Physical Metallurgy. Metallurgizdat, 1963.
6. Fleischer, R.L. Acta Met., 8, 32, 1960.
7. Glazunov, S.G. and V.N. Moiseyev. Collection "Titanium in Industry." Oborongiz, 232, 1961.
8. Solonina, O.P. Collection "New Investigations of Titanium Alloys." "Nauka," 206, 1965.
9. Zwicker, U. Z. f. Metallkunde, 47, 535, 1956.
10. Jaffe, R.I. UMF. Issue IV, Metallurgizdat, 77, 1961.
11. Moroz, L.S. Fine Structure and Strength of Steel. Metallurgizdat, 1957.
12. Sadovskiy, V.D. et al. FMM, 10, Issue 3, 38, 1960.
13. Pavlov, I.N. Theory of Rolling. Metallurgizdat, 1950.
14. Pavlov, I.M., A.E. Shelest and Yu.F. Tarasevich. Trudy, MISiS, MEI, Issue LXI. Mechanical Working of Metals, Part 1, MEI, 17, 1965.
15. Pavlov, I.M. et al. Mechanical Working of Metals and Alloys. ONTI, VILS, 95, 1965.
16. Nadai, A. Plasticity and Failure of Solids. IL, 1954.
17. Gubkin, S.I. Plastic Deformation of Metals. I, Metallurgizdat, 1960.
18. Davidenkov, N.N. and I. Mirolyubov. Vestnik metallopromyshlennosti, 9-10, 132, 1960.
19. Rastegayev, M.V. Izv. AN SSSR, OTN, 8, 1183, 1950.
20. Dzugutov, M.Ya. and B.F. Vakhtanov. Kuznechno-shtampovoye proizvodstvo '11, 5, 1959.
21. Osipov, V.G. Plastic Deformation of Metals. "Nauka," 63, 1964.
22. Zener, C. Fracturing of Metals, ASM Symp., 3, 1948.
23. Low, R.J. J.U.T.A.M. Madrid Colloquium, Deformation and Flow of Solids. Berlin; Springer, p. 20, 1956.
24. Pavlov, I.M. Collection "Studies of Heat Resistant Alloys." AN SSSR, 98, 1956.

PROBLEM OF UTILIZING TITANIUM SCRAP AND APPLICATIONS OF SECONDARY TITANIUM

A. I. Kanyuk, E. M. Strikha and O. M. Shapovalova

The USSR is one of the world's foremost producers of titanium [1]. The growth of the production of titanium and articles made from it presents the industry with the problem of efficiently utilizing all the scrap being formed. /62

The problem of utilizing titanium scrap arose simultaneously with the start of its industrial production. In the USA, as early as 1953, the problem of finding methods of processing of titanium scrap was termed one of the most important in a description of the status of the titanium industry [3, 4].

In the USSR, the problem of utilizing titanium scrap is being given major attention, but so far it has not been solved.

According to the data of Soviet literature, the production of titanium sponge forms up to 10% of scrap, while in this production of semifinished titanium alloys and articles from them, the scrap and loss amount to about 80% of the weight of the metal charge [5, 6].

The ratio of quality-certified to uncertified scrap in the total scrap resources (at the "charge-part" stage in the industry as a whole) is 2:1. Quality-certified scrap is considered to the scrap that is unoxidized or has an oxidized surface, and which, when appropriate processing methods are used, can be included in the charge for melting ingots of commercial titanium alloys. Uncertified scrap is considered to the scrap oxidized over the entire cross section or with visually detectable cracks, tears and laminations, which, with the existing processing methods, cannot be included in the charge for melting ingots of commercial titanium alloys.

To determine the trends of efficient processing of titanium scrap, an analysis of the present-day status of their utilization is necessary. Titanium sponge scrap is used in ferrous metallurgy for alloying and deoxidizing steel in place of ferrotitanium, and in small amounts, for the production of shaped titanium castings. The use of briquets of titanium sponge scrap results in a considerable reduction of the cost of the metal and improves its quality.

Thus far, the use of sponge scrap in the production of shaped castings amounts to only 0.5% (of all the sponge scrap). This is obviously insufficient: calculations show that each ton of sponge scrap utilized in the production of shaped castings produces a yearly saving (taking related industrial branches into consideration), that is approximately 20 times the value obtained when it is used for alloying steel.

About one-third of all the scrap of titanium alloys formed is used for satisfying the needs of ferrous metallurgy, i.e., in the production of standard and high-percentage ferrotitanium, and also for direct alloying of steel. Small amounts of scrap are used for alloying ferrous metal alloys. The literature gives data on the use of titanium scrap for alloying steel and for the production of ferrotitanium in the USA, England and Canada [7, 8].

The scrap from titanium alloys is also used for the production of ingots.

The use of titanium scrap for the production of ingots constitutes the most efficient processing method among those adopted by the industry. As shown by calculations, a 1% increase of the content of scrap in the charge of ingots reduces the cost of the charge by 0.7% (taking the cost of preparation of the scrap into consideration), and the use of one ton of titanium scrap for melting ingots yields a saving of about 2700 rubles to the plant, owing to a decrease in the consumption of the sponge and alloying components.

Comparison of Soviet and foreign data [7, 9] shows that the use of scrap for melting ingots in the USSR is at a higher level than in the USA. /63

Research done by a number of institutes and plants shows the practical feasibility of utilizing up to 50% of scrap in the charge of ingots of commercial titanium alloys. This is also confirmed by US data [10]. It is interesting to note that up to 50% of titanium scrap (mainly chips) is already being used at one of the Soviet plants in the melting of ingots of a commercial alloy.

Analysis shows that the main reason for the poor utilization of scrap is the lack of metallurgy of secondary titanium.

It should be noted that in the Soviet literature [5, 6], titanium scrap is defined as secondary titanium. It is more correct to refer to the waste as secondary raw material or secondary resources, and to secondary titanium as the metal obtained from scrap, in contrast to primary metal obtained from ores.

To determine the desirable trends of processing of the scrap into secondary titanium, a technical-economic evaluation of available Soviet and foreign data on the production and use of secondary titanium is necessary.

Economically, the most favorable method of returning titanium scrap into production is its processing into secondary alloys close in composition to the initial raw material. The fullest utilization of all the valuable components present in titanium alloys (V, Mo, Zr, etc.) is thus achieved. Analysis of the quality of titanium scrap shows that the most realistic and desirable processing is that of secondary alloys, taking into consideration the mixing of alloy brands taking place in the plants.

Soviet and foreign data on the processing of titanium scrap show the technical feasibility and economic advisability of producing secondary titanium alloys. Table 1 lists the mechanical properties of secondary titanium melted from 100% scrap of commercial alloys.

According to foreign data, only titanium scrap is used in many cases in the production of ingots [10]. A major US firm processing titanium scrap, the Frenkel Company of Detroit, remelts the bulk of the scrap it receives the casts it into ingots.

It is reported that a further reduction of the cost of titanium castings is achieved by the Oregon Metallurgical Company by substituting scrap for sponge

TABLE 1. MECHANICAL PROPERTIES OF SECONDARY
 TITANIUM (INGOTS)

Scrap used	σ_B kg/mm ²	δ , %	ψ , %	σ_y kg/mm ²
Turnings of alloy of technical titanium (100%)	51.1	21.7	47.8	7.5
Turnings of alloy Ti-Al-V of black stripping of alloy (100%)	83.2-83.6	12.6-13.6	35.7-37.8	10.1-11.0
Scrap from tube products of etching (100%)	44.3-58.1	21.2-33.7	56.2-58.2	7.8-11.5

titanium. As a result, the cost of titanium castings produced by the company for the chemical industry is only 10% higher than analogous parts from stainless steel. After the remelting of pretreated titanium scrap, the metal has the same purity as the primary metal (with a somewhat higher oxygen content) [11].

/64

Research carried out by one of the organizations on an experimentally industrial scale showed that when 100% of large-sized sheet scrap and also up to 70% of lump scrap of rolled stock and small-sized forgings of a commercial alloy were used in the charge, the castings obtained satisfied the requirements of technical conditions for castings melted from a primary charge. Castings from 100% scrap had $a_n = 4-7$ kg/cm².

At the Titanium Institute, investigations are being carried out on the processing of sponge titanium scrap and chips by the method of remelting into ingots. Ingots of laboratory batches 120 mm in diameter and weighing up to 7 kg, melted in a vacuum arc furnace with a consumable electrode from titanium sponge scrap of various fractions (-2+0 mm bloom; -25+12 mm bottom; -12+10 bottom; -12+10 mm side; -70+25 mm bottom and side; -70+12 mm bottom and side) had satisfactory mechanical properties in the forged state.

The mechanical properties of fine fractions (-12+0 mm) of bottoms and sides of the titanium block were lower.

In the course of forging (920°C + annealing 0.5 hr at 700°C) and rolling at different temperatures (20, 500, 700, 900, 1000°C) it was noted that secondary titanium from sponge scrap had a satisfactory ductility. Maximum reduction in hot rolling was 77.4% after 5 passes; maximum reduction after successive total rolling (hot and cold) was 99%. Foil 0.12 mm thick was obtained.

After rolling, trimming and vacuum annealing, the sheet had fully satisfactory mechanical characteristics: tensile strength 64 kg/mm², elongation per unit length 24.0%, and hardness 202 HB.

In the laboratory rolling of templates of industrial ingots from 100% chip scrap of an alloy of the system Ti-Al-V, it was found that the alloy had a satisfactory plasticity in hot, warm and cold rolling. The first cracks in the process of cold

without intermediate annealing appeared at a reduction of 30%, in warm rolling at 77-82%, and in hot rolling at 78-85%.

The mechanical properties of industrial alloys from sponge titanium scrap of different fractions and different degrees of contamination with impurities were found to be within the range of standards specified for commercial titanium alloys (Table 2).

Secondary titanium from scrap may find applications in industry primarily as a corrosion resistant material, and it was therefore subjected to prolonged corrosion tests in corrosive media at room temperature.

Specimens of industrial ingots melted from sponge titanium scrap of different fractions were studied (Table 3).

As is evident from the data cited, secondary titanium from sponge scrap has a high corrosion resistance in corrosive media (like technical titanium) and a lower corrosion resistance in sulfuric acid, in which technical titanium is also unstable.

Corrosion tests of specimens from sponge titanium scrap and from 100% chips of an alloy of the system Ti-Al-V in technological media at the Saki Chemical Plant, Krasnovodsk Petroleum Refinery, "Severonikel" combine, Derbenev Chemical Plant etc., established a high corrosion resistance of secondary titanium-at the level of primary titanium and its alloys.

The studies show that titanium scrap can be used to obtain corrosion-resistant secondary alloys.

One of the Soviet enterprises of the titanium-magnesium industry has adopted the production of cast parts of TN-70 pump from extruded consumable electrodes TGChM (sponge scrap of the fraction -70+12 mm). The pumps operate successfully in a number of corrosive media of the titanium-magnesium, coking and other industries.

The NIOKhIM institute used secondary titanium (forged billets from TGChM sponge) to prepare a shaft for the pump and caps for titanium valves. The parts were installed in the ammonium chloride shop of the Donets soda plant and had been in operation for over 7 months without any indications of corrosion. Under the same conditions, a pump made of chromium nickel molybdenum steel operated for only 22 days and went out of order due to intense corrosion, and the shutoff valves, made of 1Kh18N9T steel, were dismantled after 7 days because of deep pitting corrosion.

A widespread use of titanium is still being held up by its high cost. The production of semifinished products and articles from secondary titanium may considerably reduce this cost.

Preliminary calculations show that even with the existing cost of the charge - ingot conversion, the production of ingots from scrap will permit a reduction of

TABLE 2. CHEMICAL COMPOSITION AND MECHANICAL PROPERTIES OF INGOTS OF SECONDARY TITANIUM MELTED FROM SCRAP OF SPONGE TITANIUM

Characteristics of scrap		Impurities, %				
Fractions, mm	Hardness, HB	Fe	C	Si	N ₂	O ₂
-25+12	205 (bottoms and sides)	0.80	0.024	0.04	0.047	0.13
-70+12	195 (bottoms and sides)	0.80	0.025	0.05	0.066	0.13
-2+0	229 (bloom)	0.37	0.054	0.03	0.054	—
-4+5	207 (bottoms and sides alloyed with aluminum up to 1.25%)	1.0	0.041	0.03	0.042	—
-70+25	246 (bottoms and sides)	0.908	0.025	0.043	0.058	—

Characteristics of scrap		Mechanical properties				
Fractions, mm	Hardness, HB	Hardness, HB kg/mm ²	σ_B , kg/mm ²	δ , %	ψ , %	σ_u , kg/cm ²
-25+12	205 (bottoms and sides)	226	75.8	25.2	56.2	6.4
-70+12	195 (bottoms and sides)	229	77.5	24.1	55.4	6.4
-2+0	229 (bloom)	241	78.1	20.9	44.9	5.1
-4+5	207 (bottoms and sides alloyed with aluminum up to 1.25%)	252	81.8	23.8	39.4	5.4
-70+25	246 (bottoms and sides)	257	84.9	24.2	42.0	3.7

their cost by a factor of 2.0-2.5. Actually, the cost of conversion in the melting of ingots of secondary titanium will be considerably lower owing to the elimination or sharp decrease of the sputtering of titanium in the course of melting because of the presence of $MgCl_2$ and other residues in the consumable electrode.

It should be noted that the costlier the titanium alloys, the cheaper will be ingots from the scrap of these alloys, since the cost of the scrap is independent of the alloy brand.

Calculations show that in the production of castings in the amount of 500-1000 t/year, their cost will be 2-3.5 times less than the cost of a casting from a fresh charge.

Preliminary data on the mechanical properties of secondary titanium permit some conclusions on the feasibility and desirability of its use for the preparation of corrosion-resistant equipment.

The use of titanium for the preparation of matrices instead of stainless steel yields an annual economy for 100,000 rubles to the "Severonikel" combine. The cost of sheet titanium used for these purposes is 5-6 thousand rubles per ton.

TABLE 3. CORROSION RESISTANCE IN VARIOUS CORROSIVE MEDIA

Corrosive medium	Duration of tests, hr	Corrosion rate g/m ² · hr	Corrosion intensity, mm/year	Corrosion resistance, points*
HNO ₃ , %				
10	3000	0.0002	0.0004	0
15	3000	0.0002	0.0004	0
20	3000	0.0002	0.0004	0
30	3000	0.0002	0.0004	0
40	3000	0.0001	0.0002	0
50	3000	0.0002	0.0004	0
60	3000	0.0003	0.0006	0
70	3000	0.0002	0.0005	0
H ₂ SO ₄ , %				
0,5	1500	0.0006	0.001	0
1,1	1286	0.0006	0.0012	1
3	1286	0.0509	0.0991	4
5	1286	0.0677	0.1317	5
10	1286	0.1740	0.3386	5
15	1286	0.2320	0.4515	5
20	1286	0.3546	0.6901	6
30	1286	0.3421	0.6657	6
40	1286	0.0025	0.0049	1
50	1286	0.0166	0.0323	3
60	1286	0.0017	0.0033	1
70	1286	0.4719	0.9183	6
HCl, %				
0,5	1624	0.0001	0.0001	0
1,0	1624	0.0006	0.001	0
2,0	1624	0.0004	0.0008	0
3,0	1624	0.0002	0.0004	0
5,0	1624	0.0003	0.0005	0
7,0	1640	0.0002	0.0002	0
HCl : HNO ₃				
1 : 3	1100	0.0007	0.001	0
1 : 7	1100	0.0021	0.004	1
10% AlCl ₃	1100	0.0004	0.0008	0
25% CaCl ₂	1100	0.0007	0.001	1
30% NiCl ₂	1100	0.0017	0.0030	1
10% FeCl ₃	2000	0.0024	0.0047	2
50% FeCl ₂	2000	0.0003	0.0017	1
10% H ₂ C ₂ O ₄	1624	0.0005	0.0009	0
(CH ₃ CO ₂)O (10%)	1624	0.0003	0.0005	0
(CO ₂ H)CH (50%)	1624	0.0019	0.004	1

*On a 10-point scale.

Pumps cast from titanium sponge scrap at one of the plants of the titanium-magnesium industry and used instead of pumps from acid resistant steel meet

the production requirements from the standpoint of mechanical properties. The service life amounts to 2 years, versus 1-1.5 months for pumps from acid-resistant steel. Despite the higher initial cost of titanium pumps, the plant realizes savings every year as a result of their adoption.

The use of secondary titanium will make it possible to decrease the cost of equipment by 15-30% and thus considerably increase the economic effectiveness of its use.

Secondary titanium may be widely employed in the national economy, primarily for the production of parts of pumps, fittings, and tanks designed for transportation and storage of corrosive liquids.

Secondary titanium alloys will find applications in many parts under light loads operating in corrosive media (in heating and cooling systems, evaporators, tube sheets of condensers, vacuum systems for pumping out corrosive gases, in mufflers, etc.).

Analysis of the requirements of enterprises for corrosion resistant equipment, carried out by the Titanium Institute, showed that in 1966-1968, nonferrous metallurgy, the chemical industry, ferrous metallurgy and the pulp-and-paper industry will be able to utilize effectively ~3.0-4.0 thousand tons of titanium semifinished products from secondary titanium for the production of containers, column and heat exchange apparatus, pumps and fittings.

It should be noted that it will be possible to use part of the scrap that is off-grade for the titanium industry in the production of secondary titanium, provided there is an appropriate pretreatment of the scrap, the assortment is improved, the scrap is stored, and a number of progressive methods of treatment of titanium are introduced (for example, blasting the cutting zone with compressed air).

On the basis of preliminary data, use can thus be made of up to 70% of sponge scrap, up to 70% of lump scrap that is off-grade at the present time, and up to 35% of off-grade turnings.

The remaining titanium scrap, contaminated with interstitial impurities over the entire cross section, and scrap having no definite chemical composition, should be subjected to treatment by methods of electrolytic and thermal refining.

The creation of metallurgy of secondary titanium and the organization of the development, production and application of secondary titanium alloys will considerably increase the technical-economic indicators of the titanium industry.

REFERENCES

1. Lomako, P. F. Five Year Plan of Nonferrous Metallurgy. *Ekonomicheskaya Gazeta*, 23, 1966.
2. Dobatkin, V. N. et al. Ingots of Titanium Alloys. *Metallurgizdat*, 1966.

3. Report on examination in the US Senate of the question about the state of the titanium industry (Mellon Commission). Modern Metals, I, IX, 12, 70, 1954.
4. Cook, M. A. Amer. Soc. Eng. Inc., 66, 2, 400, 1954.
5. Sycheva, S. I. and G. D. Zykov-Batyrev. Titanium in Industry. Oborongiz, 282, 1961.
6. Gopiyenko, V. G. and R. A. Sandler. "Legkiye Metally," Issue V. TsNIITsvetmet, 138, 1965.
7. Krucher, G. N. Collection "Production and Use of Titanium Semifinished Products." TsNIITsvetmet, 90, 1966.
8. Titanium in Steel by a Correspondent "A Metal Bulletin", Special Issue, Nov. 1965.
9. Nonferrous Metallurgy of the Capitalist Countries in 1958-1965. TsNIITsvetmet, 198, 1966.
10. Titanium: Ready for Commercial Breakthrough. Mill Technology "Steel", 155, 16, 106, 1964.
11. Wood, N. Titanium Castings. "Foundry", 66, 1965.

STATUS AND PROSPECTS OF ADOPTION OF TITANIUM

A. I. Kanyuk, E. M. Strikha and N. F. Ivanova-Stepanova

Titanium possesses a rare combination of different physicomechanical and anticorrosive properties, which makes it one of the most promising metals in modern technology.

In the national economy of the USSR, titanium is used in civil aviation and also in relatively small amounts in nonferrous metallurgy and chemical industry in the production of corrosion-resistant equipment.

The improvement of the technology of various branches of industry requires the use of more corrosive reagents, high temperatures and pressures. In this connection, the problem of selection of structural material of high corrosion resistance becomes particularly urgent. The high technological and corrosion properties of titanium make it one of the most promising structural materials for almost any branch of industry.

In many cases, the use of titanium is economically justified despite its high cost, and for many industries titanium is the only material suitable for the manufacture of equipment.

The most extensive experience in the use of titanium equipment has been in nonferrous metallurgy. Hydrometallurgical and electrochemical processes of nonferrous metallurgy involve the use of corrosive solutions and high temperatures. The requirements set for commercial production do not permit contamination of the solutions with corrosion products of the apparatus.

Studies made by branch scientific research institutes and plants have shown an adequate corrosion resistance and also mechanical strength of titanium and its alloys in technological media of the nickel, cobalt, copper, zinc, lead, titanium and other industries.

A pioneer in the introduction of titanium equipment into nonferrous metallurgy was the nickel-producing combine. In 1960, it began a mass production of titanium pumps and their installation in the most important production facilities, where the maximum service life of pumps made of high alloy steel 1Kh18N25M2T was no more than two months, and that of 1Kh18N12M2T, 5-15 hr.

In 1964, the saving realized from the introduction of titanium pumps amounted to 300,000 rubles.

This combine was the first in the USSR to use titanium matrices for the preparation of nickel bases instead of stainless steel matrices, giving the combine /69 an annual saving of 100,000 rubles. The successful experience in the exploitation of titanium matrices has created the basis for producing continuous-action electrolyzers.

Candle titanium pressure filters are used in combines in place of plate-and-frame filterpresses. One such filter replaces 4-7 plate-and-frame

filterpresses in output, the use of candle-shaped filter excludes expenses on filtering cloths, improves the operating conditions, and permits programmed automatic control. The annula saving from the use of each titanium candle filter amounts to 10.3 thousand rubles.

In planning and adopting new autoclave processes in all branches of industry and in the corresponding apparatus employed, the valuable experience of the above-mentioned combine in utilized in the operation of the first autoclave unit in the USSR in which titanium autoclaves are employed. The autoclave unit, designed for the oxidative dissolution of nickel sulfide concentrate, has a high output and replaces 12-15 earlier baths for electrochemical dissolution of nickel anodes.

Experience in the use of titanium equipment at a nickel combine is used at other plants of the nickel-cobalt industry: at one of the mining-metallurgical combines, titanium equipment with a total titanium weight up to 120 t and at another, 100 t, is employed.

Titanium-magnesium plants have had a successful experience in the use of titanium pumps.

Titanium-magnesium industries utilize the pumping of considerable quantities of corrosive liquids containing hydrochloric and sulfuric acids, and iron, aluminum and magnesium chlorides. The use of titanium pumps instead of cast iron ones has cut down the cost of transportation of corrosive liquids by a factor of 2.5.

Cast pumps were used at one of the plants of the titanium-magnesium industry. Despite their comparatively high cost, the operational expenses per pump were reduced from 3,000 to 15 rubles per year. The annual saving realized from the operation of 30 cast titanium pumps amounted to ~70,000 rubles.

Titanium is used with a high economic effectiveness at a copper-sulfur combine.

The cost of parts of titanium pumps operating in the pumping of sulfuric acid, whose concentration ranges from 5 to 35%, slightly exceeds the cost of similar parts of pumps from ferrosilicide and hard lead, used earlier. However, the service life of titanium parts is 30 times longer than that of cast iron parts and 10 times longer than that of parts from hard lead.

At the combine, titanium also replaces nonferrous metals, particularly lead in scrubbing-aided electrostatic precipitators.

Over 16 t of lead rolled stock per battery of spray-type electric separators is expanded in the preparation of ionizing and dust-attracting electrodes, gas distributing screens and upper lid.

The filter operates satisfactorily for only 1-1.5 years, and then, because of the fitting of the lead parts, the mud from the precipitating blocks flows down poorly, and the quality of the cleaning of the gases decreases; after 3-4 years, the lead parts break down completely.

The consumption of titanium on the overhaul of electric separators amounts to 4 t.

Experience in the operation of titanium parts installed in electrostatic precipitations leads to the assumption that scrubbing-aided electrostatic precipitators do not require an overhaul for 8-12 years.

At the combine, titanium is also used in electrical apparatus.

In an atmosphere saturated with SO_2 and SO_3 gases, the copper and silver contacts of automatic units become coated in 2 to 3 weeks with a thin film of oxides whose conductivity is very low. Special cleaning of the contacts causes their rapid wear, breakdown of the apparatus and considerable investment of labor. Titanium contacts do not lose their initial properties, and their use, despite their low electric conductivity, is very efficient, since apparatus having such contacts is operationally reliable.

/70

Analysis of the results of the use of titanium at the copper-sulfur combine shows the effectiveness of its use not only in replacing parts with service lives of less than a year but also in replacing materials which last longer under these conditions (service life > 3 years).

We should mention one more area of application of titanium electrodes. At the lead-zinc plant, titanium is used as the cathode in the production of pure lead and indium, and also for preparing other parts.

According to preliminary data, even with the titanium prices now in effect, the nonferrous metallurgy of the USSR can effectively utilize in 1966-1968 several thousand tons of rolled stock and hundreds of tons of shaped castings for the production of corrosion-resistant equipment.

Of the foreign experience in the use of titanium, it is of interest to mention its use in the manufacture of apparatus of the titanium-magnesium industry. According to the statement of the TMCA Company, the plant for leaching magnesium and magnesium chloride from titanium sponge replaces 14 gold units and yields savings of \$370, 000 per year [1].

Titanium is widely employed in electrochemical processes of the metallurgical production.

Almost all of the electrolytic manganese in the USA is obtained in baths with titanium cathodes [2].

In the German Federal Republic, titanium cathodes are used for the preparation of high purity metals (indium, copper, tin, etc.) [3].

Titanium equipment is widely employed to satisfy the needs of the chlorine industry, where titanium is the only corrosion-resistant material. Titanium is stable in such basic media of the chlorine industry as wet chlorine, aqueous and acid solutions of chlorine, various chlorides, oxygen compounds of chlorine, and

in chlorinated organics. The economic desirability of using titanium equipment for operation in wet chlorine is confirmed by the experience of the Sumgait Chemical Plant.

According to the Titanium Metals Corporation of America, the use of titanium in equipment for cooling chlorine has led to a new technology. Titanium equipment has lasted for over 3 years without signs of corrosion or erosion, whereas stainless steel with a vinyl coating operates for no more than one year under the same conditions. Because of lower downtime and operational costs, the more expensive titanium equipment pays for itself in 2.5 years.

Titanium heat exchangers used in the production of chlorine are 30% cheaper than glass heat exchangers and take up 8 times less floor area [4].

According to the Allied Chemical Co. the replacement of graphite tubes in heat exchangers for cooling chlorinated hydrochloric acid solutions by titanium tubes should yield a saving of \$9,000 in 6 years of operation. Thin-walled titanium tubes insure a higher level of heat transfer during the entire service life and do not require any maintenance [5].

Particular mention should be made of the prospects of utilizing titanium for electrodes in electrolysis processes in the production of chlorine and its various derivatives.

The use of platinized titanium anodes is very promising. According to reports of the E.I. du Pont de Nemours Co., such anodes cost 4 times as much as ordinary ones, but serve 20 times as long [4]. Platinized anodes are used in place of carbon and lead anodes for protecting seagoing ships and equipment from corrosion.

/71

A major saving should be obtained by using titanium in electrolytic metallurgy. Titanium is used abroad in electrolytic metallurgy for preparing suspensions, baskets and coils. The high initial cost of the articles pays for itself in the course of service [6].

At a domestic chemical plant in the production of dyes, titanium coils instead of lead or stainless steel coils, which had to be replaced every year, have been in operation for several years without any signs of corrosion. The calculated service life of titanium coils is 30 years. The cost of a lead coil made of tubing with a wall thickness of 7 mm and weighing 945 kg is 800 rubles, and that of a titanium coil made of tubing with a wall thickness of 3 mm and weighing 117 kg is 1050 rubles. The operation of 32 titanium coils in this plant yields an annual saving of 70,000 rubles, increases the output of dyes and improves their quality.

The use of titanium equipment in the production of caprolactam is promising. The shops being currently constructed and designed are equipped chiefly with imported apparatus with a glass-enamel coating. At the same time, research and experimental industrial tests show the high, practically absolute resistance of titanium and its alloys in the technological media used in the production.

According to the results of tests carried out by the Armniikhimprojekt, a part of the equipment has been designed to consist of titanium for an experimental

industrial unit being constructed for the production of caprolactam, but the project also specifies enameled pipes and fittings.

Titanium will be widely employed in the production of alcohols, and in the production of acetaldehyde at a synthetic rubber plant, the use of a considerable amount of titanium equipment has been specified.

Despite its comparatively low coefficient of thermal conductivity, titanium is economical for manufacturing heat exchange and evaporation apparatus thanks to its high corrosion resistance, which permits the reduction of the wall thickness to a minimum, and a lack of scaling tendency. The Marston Co. reports a successful replacement of a 400 kg lead coil by a 24 kg titanium coil. It should also be noted that a titanium coil has a longer service life in many media.

According to the calculations of the Niukhimmash, 2% of all the heat exchange and evaporation apparatus made of stainless steel operates in a medium containing the chloride ion. According to the data of plants using this apparatus, the service life of stainless steel pipe stills does not exceed two years. In 1965, just the replacement of steel pipe stills with titanium ones, whose service life under these conditions is estimated at 20 years, will give an annual saving of 350,000 rubles per year due to the decrease of the maintenance costs.

Of great promise is the use of titanium for plate heat exchangers, which have better technological characteristics and a minimum metal volume.

According to the calculations of Ukrniukhimmash, in the next few years the demand for plate heat exchangers from titanium will amount to $1000 \text{ m}^2/\text{year}$ (the specific consumption of titanium in plate heat exchangers per 1 m^2 is 7 kg). About 25% of the heat exchange apparatus now produced (1 million m^2) will be made of titanium.

Titanium plate heat exchangers are manufactured in Japan, Sweden, the German Federal Republic.

The pulp-and-paper industry has great prospects for the use of titanium. According to a project of the Giprobum, a large amount of titanium equipment is included in the production of pulp at the combine under construction. Bleaching towers for another combine have been built but are not yet being used.

/72

Foreign sources contain many indications of extensive use of titanium in equipment for the pulp-and-paper and textile industries.

The use of chlorine dioxide in certain processes make titanium an irreplaceable equipment material. According to preliminary estimates, in 1966-1968 the pulp-and-paper industry may require up to 500 t of titanium rolled stock and up to 1000 t of titanium rolled stock and up to 1000 t of the "titanium-steel" bimetal.

Such large-sized equipment as cooking boilers and bleaching towers of the pulp-and-paper industry and column and tank apparatus of the petrochemical and metallurgical industries should combine an adequate corrosion resistance with a high mechanical strength and an acceptable cost. Most of all, these conditions

are met by equipment made of carbon steel lined with titanium or of the "titanium-steel" bimetal. According to preliminary technical-economic calculations, a ton of the "titanium-steel" bimetal (10-20% Ti) will cost ~ 2200-2500 rubles. The demand for the bimetal in 1968 will be 1500 t.

The use of titanium in the pharmaceutical and food industries is limited at the present time, but it is very promising.

Thus, an extractor from AT-3 alloy for a chemico-pharmaceutical plant, manufactured on the recommendation and with the participation of the Metallurgy Institute of the USSR Academy of Sciences gives the plant a saving of 142,000 rubles per year.

An evaporation unit from titanium installed at an industrial wine-making combine in place of stainless steel units, whose service life did not exceed 1-3 months, yields a saving of 15,000 rubles per year (prospective service life of the unit, 10 years).

The Metallurgy Institute of the USSR Academy of Sciences has tested titanium and its alloys in a number of media of the food industry, particularly in the canning industry [7].

The possible uses of titanium in the petroleum industry have been insufficiently studied thus far. The existing studies are fragmentary.

Abroad, titanium is widely employed in the petrochemical industry of the USA, England and Japan.

In Japan, titanium is used to manufacture reflux columns, heat exchangers, pumps, fittings, measuring instruments, etc.

It may be assumed that the introduction of titanium apparatus into various branches of industry will cause the national economy to gain savings of up to 20-40,000 rubles per ton of titanium and up to 10-15,000 rubles from the introduction of pumps and fittings.

Analysis of the present state of production of titanium equipment shows that there are considerable prospects for lowering its cost and improving its quality; the achievement of these objectives will make it necessary to organize the manufacture of titanium equipment in specialized plants on an industrial scale, to work out uniform distribution prices for titanium equipment, and adopt on an industrial scale of titanium-lined equipment using the "titanium-steel" bimetal.

There are bright prospects for the use of titanium alloys in the construction of steam turbines. In two large SREPP, two steam turbines are in operation in which the stainless steel vanes alternate with vanes from a titanium alloy. Operational experience shows that titanium vanes do not undergo corrosion and are subject to much less erosion than steel vanes.

The use of high-strength titanium alloys for vanes of the last stage makes it possible to improve the design of the low-pressure cylinder of a steam turbine.

/73

According to the calculation of TsKTI im. Polzunov, the adoption of such turbines will yield an annula saving of 149,000 rubles per turbine unit [8].

However, extensive use of titanium in the construction of steam turbines will be possible only when the cost of titanium semifinished products is reduced. By reducing the cost of rolled stock by a factor of 2 to 3, by 1970 it will be possible effectively to utilize 4.0-5.0 thousand tons of titanium semifinished products in steam-turbine construction.

Thanks to its ability to retain high mechanical and anticorrosive properties under stress, titanium will be used for manufacturing plates in compressors operating with corrosive media and also in automobile compressors for manufacturing valves and piston sleeves.

An experimental specimen of a compressor, TsKS-390/0.1, with wheels from VT3-1 alloy, was made at a compressor plant. Tests made at a coking plant in media containing hydrogen sulfide showed high service qualities of the compressor. According to preliminary calculations, the saving from the use of one TsKS-390/0.1 compressor will amount to 49,000 rubles. In its physiomechanical and anticorrosion properties at low temperatures, titanium surpasses high alloy steels and special alloys used in compressore os refrigerating units.

According to the data of VNIIKhOLODMASH, the use of titanium alloy AT6 in ammonia compressors of refrigerating units makes it possible to create a machine with a single unit.

The annual saving from the reduction of the metal volume of machines and decrease of the area occupied by the structure of the station (by a factor of more than 2) per machine even at the existing cost of titanium will be 67,000 rubles.

The demand for titanium in the refrigeration industry may reach 2.0-3.0 thousand tons in 1970.

Of great interest is the experience of the All Union Scientific Research Institute of Drilling Technology in the use of tubes from high-strength titanium alloys for drilling high-depth holes 10-15 km deep. The studies performed confirmed the advisability of using titanium tubes.

Abroad, titanium is used in automobile construction in the manufacture of connecting rods, needles of flap valves, etc. [9].

Analysis of the present state and prospects of the use of titanium shows that the titanium industry has a great potential. The widespread adoption of titanium is delayed by its high cost and scarcity. This may result in a situation where, even if the cost of titanium is decreased, its adoption will be held up for many years.

Starting in 1957, permission was given in the USA to release 25% of rolled stock to the consumer sector, and in 1958 this restriction was removed. However, until 1960, the fraction of titanium used in the chemical industry was no more than 3%, since the plants were not prepared for its use.

The creation of titanium production on a large scale will result in technical progress in the leading branches of the national economy.

REFERENCES

/74

1. Titanium Producer Buys His Own Product FCP. "Chemical Engineering". 72, 9, 80, 1965.
2. Iron-Titanium Curtain. "Chemical Week", 17, Sept. 1966.
3. May, M. et al. Titanium and Titanium Alloys. "Chemische Technik", Vol. 13, 5, 280, 1961.
4. Titanium Ready for Commercial Breakthrough, "Steel", 155, 16, 105, 1964.
5. Boost for Titanium. "Chemical Week", 94, 3, 5, 1964.
6. Wud, A. Several Examples of Application of Titanium in Electrolytic Industry. "Metalloberfläche", 18, 1, 525, 1964.
7. Tavadze, F. N. et al. Collection: "Titanium and its Alloys," Issue VII. AN SSSR, 246, 1962.
8. Robert, L., K. Preece and W. Bowen. Applications and Uses of Titanium and its Alloys. "Metallurgical Reviews", 6, 22, 271, 1961.

PROSPECTS FOR THE USE OF NEW TITANIUM ALLOYS IN CHEMICAL MACHINE BUILDING

Yu. M. Vinogradov

The high corrosion resistance of titanium alloys, their strength and light weight make them valuable and occasionally irreplaceable materials in chemical machine building, and for this reason from the very beginning of the adoption of titanium production in the USSR, chemical machine building became one of the consumers of the new material in the construction of chemical equipment.

The corrosion resistance of titanium and its alloys in many inorganic acids and solutions containing chloride, in moist chlorine and in reducing media justifies the advisability of using titanium in the production of toxic chemicals for agriculture, organic intermediates of dyes, in the chlorine industry and in hydro-metallurgy.

In plants building chemical equipment for the chemical industry, a whole series of articles made of VT-1 titanium have been used. Such for example are the horizontal and vertical sheet filters LV-5OT with vibratory unloading of the residue. These filters are used for filtering pulp from molybdenum trisulfide and other mixtures obtained in the metallurgy of rare and nonferrous metals.

A complex automatic filterpress, containing a chamber and a mechanical clamp, is used for filtering corrosive suspensions.

As we know, until recently the problem of welding titanium to carbon steel had not been solved, and therefore the shells of housings of heat exchangers operating with corrosive media in a tubular space and tubular grids were made entirely of titanium. When housings of heat exchangers with tubular grids are made of the "steel-titanium" bimetal for the production of acetaldehyde in the amount of 100 t (without tubes), the economy of titanium will amount to 50 t (this signifies an economy of about 3000,000 rubles).

A centrifugal reactor-separator with housing made of Kh18N9T steel lined with sheet titanium was constructed for the mining metallurgical industry. The reactor is used for purifying the nickel electrolyte and has a capacity of 30 m³/hr.

Experience in the industrial operation of the reactor has shown that it meets all the technical requirements and can replace reactors made completely of titanium. This will make it possible to reduce the consumption of titanium by almost 400 kg for each unit, resulting in a saving of 4375 rubles.

The production of chemical equipment from titanium alloys, primarily from VT-1 alloy, has now been adopted at several chemical machinery plants. /75

The development of chemical machine building and the necessity of manufacturing equipment for new technological processes constantly require the use of new structural materials. Furthermore, as new processes appear in which highly corrosive chemical compounds are used, the requirements for the chemical resistance of materials used in building the chemical equipment are raised (for

example, in the production of mineral fertilizers, which require the use of sulfuric, hydrochloric, nitric and phosphoric acids, in the production of plastics and synthetic fibers, etc.).

The immediate objectives include the development of alloys possessing a sufficient corrosion resistance in hydrochloric acid up to 30% at 160°C and a pressure up to 50 atm, in hydrochloric and sulfuric acids containing oxidants (chlorine, oxygen containing compounds) up to 100°C, in solutions of nitric acid (35-60%) up to 200°C. Such alloys should also have sufficiently high mechanical properties: $\sigma_u \approx 60 \text{ kg/mm}^2$, $\sigma_s \approx 40-45 \text{ kg/mm}^2$ at $\delta \geq 20\%$ and $a_k \approx 6-12 \text{ kg/cm}^2$.

Joint studies made at the Metallurgy Institute, Niikhimmash and VILS led to the creation of new titanium alloys.

1. Ti + 32% Mo, stable to boiling hydrochloric acid of up to 21% concentration (Fig. 1a).
2. Ti + 32% Mo and 1.5-2.5% Nb, stable to boiling hydrochloric acid of up to 10% concentration (Fig. 1 b).
3. Ti + 0.2% Pd, stable in hydrochloric acid solutions up to 5% (Fig. 1 c).
4. Ti + 5% Ta for 18% hydrochloric acid containing oxidants; this alloy should be used as a substitute for pure tantalum.

The workability of the new titanium alloys was tested by preparing experimental specimens of chemical equipment. The titanium-palladium alloy was used to make a shell-and-tube heat exchanger with a lined tubular grid in accordance with the design of the DIAP (Fig. 2), and alloy of titanium with molybdenum and with molybdenum and niobium were used to prepare parts for a refluxing column (Fig. 3).

The corrosion resistance of the base metal and of the weld joints of alloys of titanium with molybdenum and niobium is characterized by the following data for test in boiling 21% hydrochloric acid (Tables 1 and 2).

The lowest corrosion rate of weld joints is achieved in automatic agron-arc welding. In its corrosion rate in boiling hydrochloric acid, this alloy is the most stable of all known alloys. Results of corrosion tests show that from the standpoint of their corrosion rate in boiling 21% hydrochloric acid, the alloys Ti + 32% Mo and Ti + 32% Mo + 1.5-2.5 Nb are equivalent to nickel-molybdenum alloy EP496 (type B Hastelloy).

This makes the new titanium alloys competitive with hastelloy, since the cost of one ton of hastelloy is 1.5 times higher (when the savings are taken into consideration, it should also be noted that the density of titanium alloys is 1.6 times less than that of Hastelloy). Thus, the use of titanium alloys particularly in the chlorine industry, may become one of the means of economizing the scarce nickel.

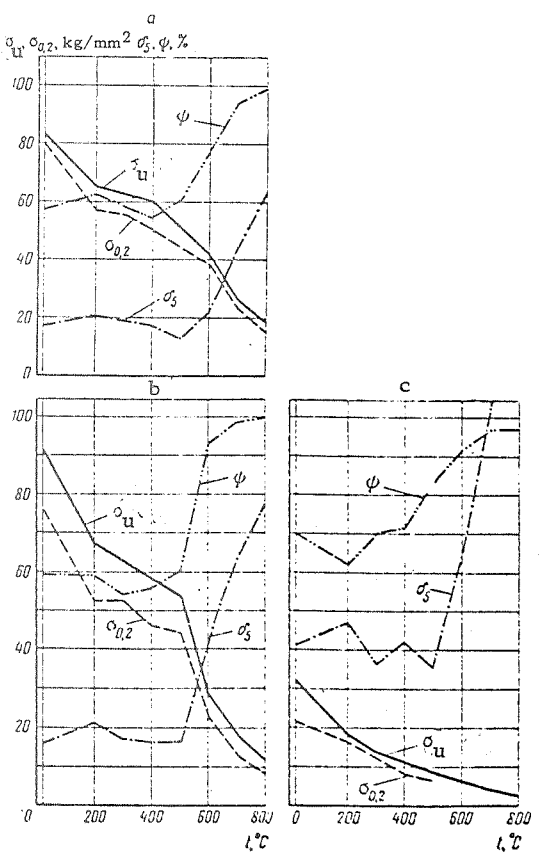


Figure 1. Mechanical Properties of the Alloys Ti + 32% Mo (a), Ti + 32% Mo +(1.5-2.5)% Nb (b) and Ti + 0.2% Pd (c).

/76

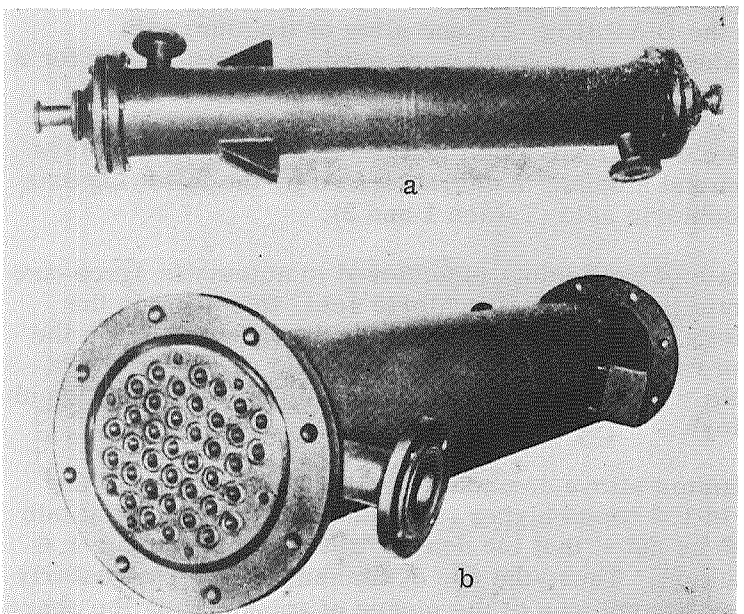


Figure 2. Shell-and-tube heat exchanger made of Titanium-Palladium alloy. a) closed b) open

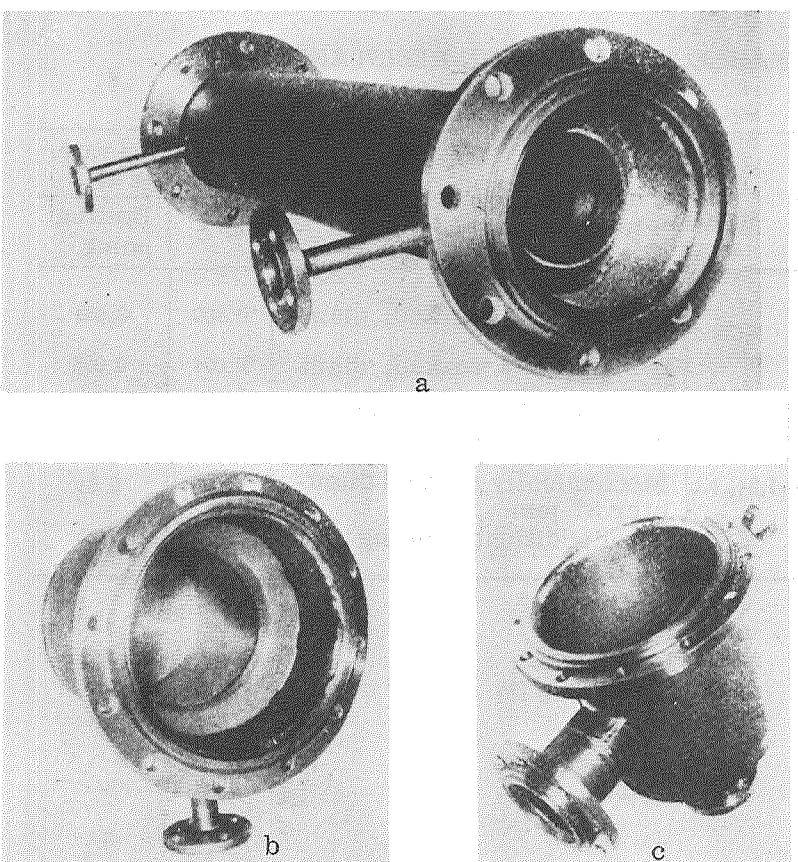


Figure 3. Parts of Refluxing Column Made of Titanium-Molybdenum Alloy.

TABLE 1. CORROSION RESISTANCE OF ALLOY
 Ti + 35% Mo

Characteristic of Specimen	Corrosion Rate, mm per year	
	100 hr	250 hr
Base metal.....	0.026—0.125	0.042—0.172
Seam of manual argon-arc welding with additive by a degassed welding strip...	0.084	0.105
Seam of manual argon-arc welding with additive by a nondegassed welding strip	0.126	0.136
Seam with automatic argon-arc welding (without additive).....	0.123	0.097

**TABLE 2. CORROSION RESISTANCE OF
 TUBE METAL (500 hr)**

Alloy	Characteristic of tube	Corrosion rate, mm/year at	
		90° C	Boiling point
Ti + 35% Mo	Mechanically worked, diameter 38 mm	0.100	0.081
	Mechanically worked, diameter 30 mm	0.091	0.053
	Without mechanical working	0.935	1.165
Ti + 32% Mo + 1,5% Nb	Mechanically worked diameter 37 mm	0.16	0.61
	After additional rolling	0.41	6.25

CHAPTER 2

METAL CHEMISTRY AND METALLURGY OF TITANIUM PHASE DIAGRAM OF A PART OF THE TERNARY SYSTEM Ti-Al-V (up to 45% Al)

I. I. Kornilov and M. A. Volkova

/78

Phase equilibria in alloys of the ternary system Ti-Al-V have been studied in several papers [1-4]. However, the study of the phase diagrams of binary systems Ti-Al and V-Al has yielded new data which should be taken as the basis for plotting a phase diagram of the ternary system Ti-Al-V; in this connection, the system Ti-Al-V requires further investigation.

The object of the present work was to supplement and refine the phase diagram of the ternary system Ti-Al-V (up to 45 wt. % Al), using the latest data on the phase diagrams of the binary systems Ti-Al [5], V-Al [6] and Ti-V [7].

Results of a study of the titanium corner of the phase diagram of this system have been partially published earlier [8], and the present study is a continuation of the earlier one.

The phase diagram of the binary system Ti-Al, according to the data of [5], is characterized (Fig. 1) by the presence of a wide region of β solid solutions. In the system of the β solid solution, the metallic compound Ti_3Al is formed, which has a hexagonal ordered structure of type Mg_3Cd . Paratectoid reactions take place in the system at $1080^\circ C: \alpha_2 + \beta \rightarrow \alpha$, and at $1250^\circ C: \beta + \gamma \rightarrow \alpha_2$. The solubility of aluminum in α -Ti at $550^\circ C$ is 7.5%.

Titanium and vanadium form a continuous series of β solid solutions and limited α solid solutions [9]. The boundaries of the two-phase region $\alpha + \beta$ at $510^\circ C$ pass at 2 and 40% V [7].

Vanadium and aluminum form a wide region of β solid solutions based on a body-centered cubic structure and a series of aluminides: V_5Al_8 , VAl_3 , etc. [6]. The authors of [10] postulate that the system contains the compound V_3Al , which is formed from the β solid solution. However, the study indicates that it is difficult to obtain this compound since it exists in a narrow temperature range. To determine its distribution in the ternary system Ti-Al-V, it is necessary to carry out a separate study.

In plotting the phase diagram of the ternary system Ti-Al-V, the diagram of the system V-Al, based on the data of the authors of [6], was taken as the starting point.

/79

Alloys were selected for the study whose compositions are located on radial sections emanating from the vertex of pure titanium at aluminum-to-vanadium ratios of 1:3 (1), 1:1 (2), and 3:1 (3), and alloys of sections parallel to the Ti-V side with constant aluminum contents from 5 to 45%. The compositions of the alloys

studied are shown in Fig. 1. In addition, alloys of the section between the compounds $TiAl-V_5Al_8$ were studied. An equilibrium was found to exist in the system between these compounds.

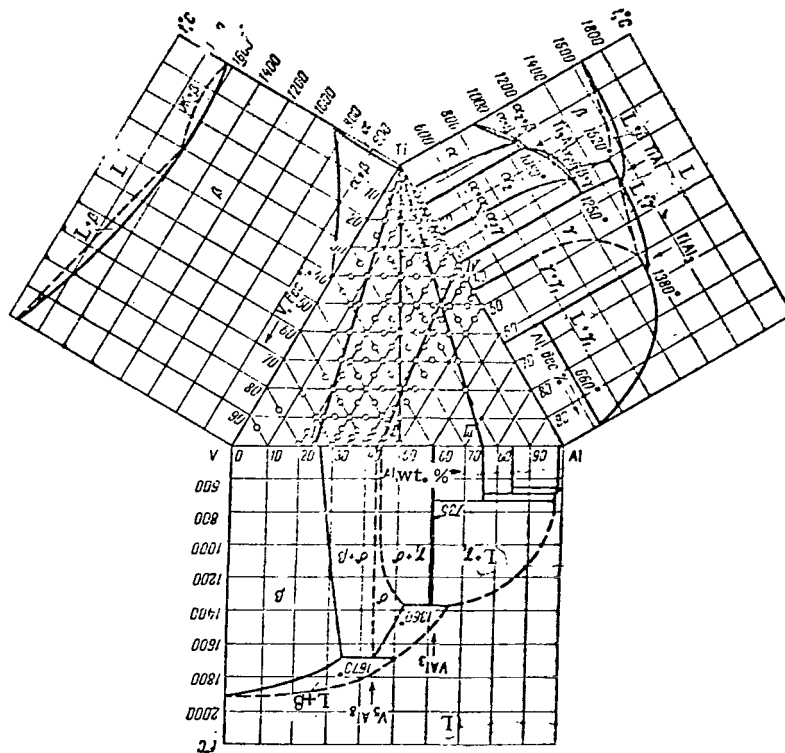


Figure 1. Concentration Triangle of the Ternary System Ti-Al-V.

Methods of thermal, microstructural and x-ray analyses and measurements of electrical resistance and hardness were used in the study.

The x-ray patterns were taken with copper radiation. Hardness was measured with a diamond pyramid at a load of 10 kg. The electrical resistance was measured potentiometrically.

The starting materials employed were iodide titanium, AV-000 aluminum, and carbothermic vanadium (99.7% V). The alloys were melted in an arc furnace in an argon atmosphere and by floating fusion in the suspended state. Heat treatment of the alloys followed the schedules: 1100°-25-75 hr, 1000°-100-150 hr, 800°-250-300 hr, 600°-550-1000 hr.

Alloys of the section with 5% Al and a variable vanadium content (from 0 to 40%) were studied by the centrifugal bending method at $l = 15 \text{ kg/mm}^2$ and $t = 550^\circ\text{C}$. Alloys for the study of high-temperature strength were prepared from titanium sponge; melting was done in an arc furnace in argon. Castings 12 mm in diameter and 60 mm high were obtained and subjected to forging (heating for forging 1000°C) to a diameter of 8 mm. The specimens were vacuum-annealed according to the schedule: $1100^\circ\text{C}-2\text{hr}$, $600^\circ\text{C}-200 \text{ hr}$.

Results

/80

Thermal analysis (differential recording of heating and cooling curves with an N. S. Kurnakov pyrometer) was used to obtain the temperatures of transformation in the solid state for alloys of radial sections of the system. The compositions of the alloys studied and the transition points obtained are given in Table 1.

TABLE 1. TRANSITION POINTS OF ALLOYS OF THE TERNARY SYSTEM Ti-Al-V IN THE SOLID STATE

Chemical composition, wt. %			Transition point, °C.
Al	V	Ti	
0.75	0.25	99	870 ($\alpha \rightarrow \alpha + \beta$)
3.75	1.25	95	980 ($\alpha + \beta \rightarrow \beta$)
5.62	1.87	92.5	970 ($\alpha + \beta \rightarrow \beta$)
7.5	2.5	90	1010 ($\alpha + \beta \rightarrow \beta$)
11.25	3.75	85	1100 ($\alpha + \alpha_2 + \beta \rightarrow \beta$)
15	5	80	1100 ($\alpha_2 + \beta \rightarrow \beta$)
18.75	6.25	75	1150 ($\alpha_2 + \beta \rightarrow \beta$)
2.5	2.5	95	940 ($\alpha_2 + \beta \rightarrow \beta$)
20	20	60	1160 ($\alpha_2 + \beta \rightarrow \beta$)
0.25	0.75	99	880 ($\alpha + \beta \rightarrow \beta$)
3.75	11.25	85	880 ($\alpha + \beta \rightarrow \beta$)
7.5	22.5	70	820 ($\alpha + \beta \rightarrow \beta$)

These data were used in plotting the polythermal sections of the system.

Results of microstructural and x-ray analyses of alloys of the titanium corner of the system containing 0-60% Σ Al, V, were given earlier [8]. The present paper gives mainly a description of the remaining portion of the diagram, adjacent to the corner of pure vanadium and to the V-Al side.

After solidifying, alloys of the ternary system whose compositions are located on sections parallel to the Ti-V side, at aluminum contents from 0 to 30% and vanadium contents from 0 to 100%, have the structure of either a converted β solid solution (since the β phase does not become fixed in alloys of the binary system Ti-Al), or of a stable β solid solution.

Alloys adjacent to the region of the γ phase (based on the compound TiAl) containing from 0 to 40-45% Al and from 0 to 22-25% V, have the one-phase structure of a γ solid solution in the cast and the homogenized states.

The γ phase is formed in the binary system Ti-Al by the peritectic reaction $L + \beta \rightarrow \gamma$. This process also takes place in alloys of the ternary system Ti-Al-V. Figure 2, a shows the microstructure of the alloy, where traces of the peritectic reaction $L + \beta \rightarrow \gamma$ are evident. Light areas represent the dissolving β phase enriched with titanium; the field of grey color is the γ solid solution.

In the binary system V-Al, the peritectic process $L + \beta \rightarrow \delta$ takes place, as a result of which the metallic compound V_5Al_8 is formed. This process is also characteristic of alloys of the ternary system Ti-Al-V. Alloys containing 36 and 40% Al and 0-5% Ti have in their structure a β solid solution and a δ phase formed by a peritectic reaction. The alloy shown in Fig. 2, b has a two-phase structure ($\beta + \delta$), the δ phase being present in a large amount. Figure 2, c shows the micro- /81
structure of an alloy from the region of the δ phase (V_5Al_8).

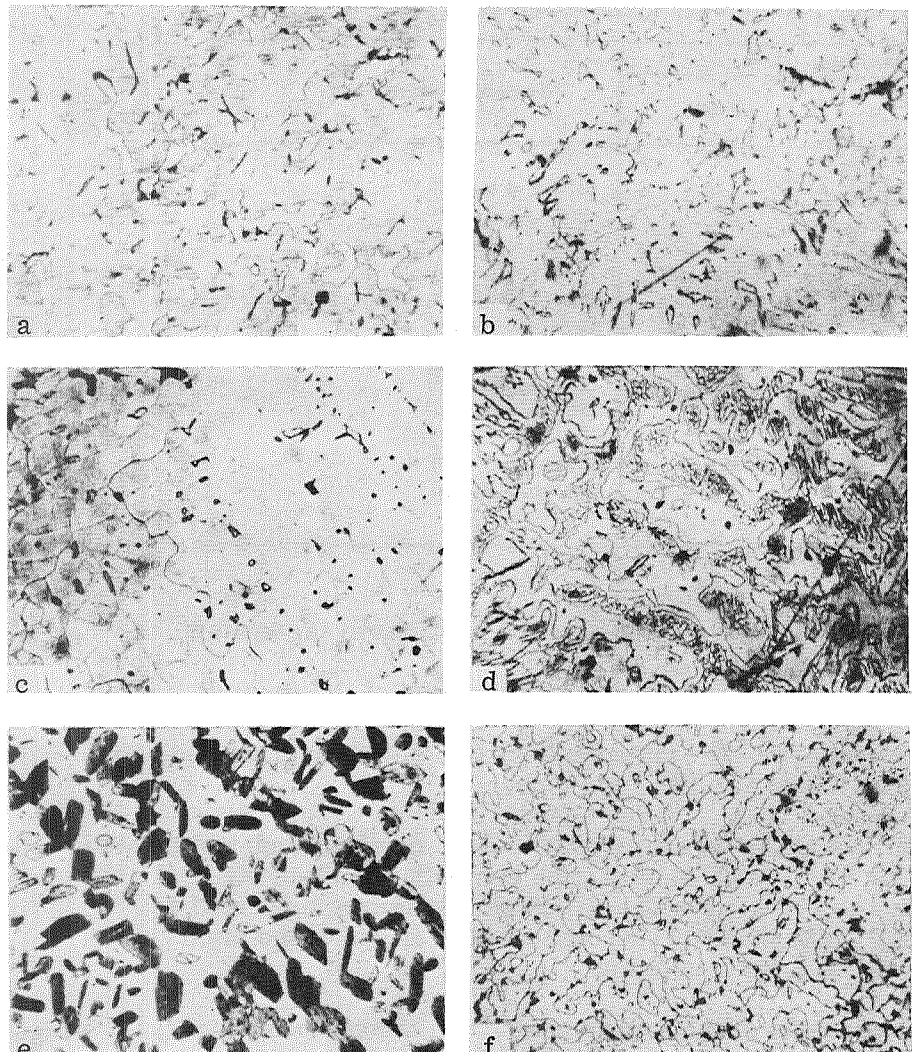


Figure 2. Microstructure of Alloys of the Ternary System Ti-Al-V
 $\times 200$:

a-40% Al, 30% V, 30% Ti(cast); b-43% Al, 56% V, 1% Ti(cast); c-45% Al, 55% V (cast); d-40% Al, 50% V, 10% Ti (cast); e-30% Al, 30% V, 40% Ti (quenching from 1100°C); f-40% Al, 58% V, 2% Ti (quenching from 1100°C).

Alloys of sections with 36 and 40% Al containing over 40% and 5-20% Ti in the cast and homogenized state display a three-phase structure ($\beta + \gamma + \delta$). In the structure of these alloys one can detect a conglomerate of two phases resembling a eutectic. Apparently, the crystallization process of these alloys involves the following reactions: $L + \beta \rightarrow \gamma$ or $L + \beta \rightarrow \delta$; $L + \beta \rightarrow \gamma + \delta$. A study of alloys of the section $TiAl-V_5Al_8$ in ternary system Ti-Al-V revealed only these phases, and therefore it may be assumed that γ and δ phases are simultaneously formed in the alloys when one phase dissolves (β); i.e., $L + \beta \rightarrow \gamma + \delta$.

Figure 2, d shows the microstructure of an alloy in which a β solid first separated, then the process, $L + \beta \rightarrow \delta$ took place, and finally, the crystallization ended in the separation of two phases: $L + \beta \rightarrow \delta + \gamma$. /82

In alloys of the ternary system containing from 60 to 100% Σ Al, V and containing no more than 45% aluminum, after quenching from 1100, 800 and 550°C, the following phases were detected: β , γ , δ , $\beta + \gamma$, $\beta + \delta$, $\delta + \gamma$, $\beta + \delta + \gamma$.

The microstructure of alloys from the two-phase regions is shown in Fig. 2, e-f. The structure of an alloy from the two-phase region ($\beta + \gamma$) is shown in Fig. 2, e: dark grains of the δ phase show up against the light background of the β solid solution. X-ray analysis shows lines corresponding to β and γ phases. /83

Figure 2, f shows the structure of an alloy from the two-phase region ($\beta + \delta$).

An x-ray analysis was performed in order to determine the phase composition of the alloys.

Table 2 shows compositions of alloys subjected to x-ray analysis and also the phase observed.

X-ray analysis confirmed that an equilibrium exists between the δ and γ phases in the system Ti-Al-V.

To determine the distribution of the γ solid solution in the ternary system Ti-Al-V, the lattice constants of the γ solid solution based on the compound TiAl were determined by x-ray structural analysis.

Table 3 shows data on the lattice constants of the γ solid solution.

Figure 3 shows the change of the lattice constants of the γ phase as a function of the composition of alloys of the section $TiAl-V_5Al_8$.

As is evident from the graph, lattice constant a decreases with increasing vanadium content, then remains constant in the two-phase region ($\gamma + \delta$). Values of constant c remain unchanged at all vanadium concentrations. The axis ratio c/a increases with the vanadium content. As is evident from the graph, the boundary of the two-phase region ($\gamma + \delta$), is located at 19 at. % (26 wt. %) V. These data are in accord with those obtained by measuring the hardness and microhardness and also by studying the microstructure.

TABLE 2. RESULTS OF X-RAY PHASE ANALYSIS OF ALLOYS
 OF THE TERNARY SYSTEM Ti-Al-V

Chemical composition, wt. %			Phases after quenching from temperature, °C.		
Ti	Al	V	1100	800	550
85	10	5		$\alpha + \beta$	—
85	12	3		—	α_2
78	12	5		$\alpha + \alpha_2 + \beta$	—
85	14	1		—	α_2
83	16	1		—	α_2
81	16	3	α_2	—	—
79	16	5	—	$\alpha_2 + \beta$	$\alpha_2 + \beta$
74	16	10	—	$\alpha_2 + \beta$	$\alpha_2 + \beta$
60	20	20	$\alpha_2 + \beta$	—	—
52.5	20	27.5	—	—	$\alpha_2 + \beta$
50	20	30	—	—	$\alpha_2 + \beta$
40	20	40	$\alpha_2 + \beta$	—	—
75	25	0	α_2	—	—
72	25	3	α_2	α_2	—
70	25	5	α_2	α_2	—
55	25	20	$\alpha_2 + \beta$	—	—
70	30	0	$\alpha_2 + \gamma$	—	$\alpha_2 + \gamma$
65	30	5	$\alpha_2 + \gamma$	—	$\alpha_2 + \gamma$
45	36	19	—	—	$\beta + \gamma$
40	36	24	$\beta + \gamma$	—	—
25	36	39	$\beta + \gamma + \delta$	—	—
10	36	54	$\beta + \gamma + \delta$	$\beta + \gamma + \delta$	$\beta + \gamma + \delta$
5	36	59	$\beta + \delta$	—	—
0	36	64	$\beta + \delta$	—	—
60	40	0	—	—	γ
15	40	45	$\gamma + \beta$	—	—
10	40	50	$\gamma + \delta + \beta$	—	—
5	40	55	$\beta + \delta$	—	$\beta + \gamma + \delta$
30	45	25	—	—	γ
20	45	35	$\gamma + \delta$	—	—
10	45	45	—	$\gamma + \delta$	—
0	45	55	δ	δ	δ
2	45	53	$\gamma + \delta$	—	—
47.99	38.45	13.56	γ	—	γ
38.39	39.91	21.70	γ	—	—
25.59	41.86	32.55	$\gamma + \delta$	—	$\gamma + \delta$
12.80	43.80	43.40	$\gamma + \delta$	—	—
6.40	44.78	48.82	$\gamma + \delta$	—	—
1.93	45.45	52.62	$\gamma + \delta$	—	—
0	45.75	54.25	δ	—	δ

As a result of a study of the alloys by methods of microstructural and x-ray analyses, isothermal sections of the ternary system Ti-Al-V were plotted.

/84

TABLE 3. CHANGE OF THE LATTICE CONSTANTS OF THE γ SOLID SOLUTION BASED ON THE COMPOUND TiAl OF ALLOYS OF THE SECTION TiAl-V₅Al₈ QUENCHED FROM 1100°C

Composition, wt. % (at. %)			TiAl	V ₅ Al ₈	$a, \text{Å}$	$c, \text{Å}$	c/a
Ti	Al	γ					
63.98 (50)	36.02 (50)	0 (0)	100	0	3.998	4.062	1.018
47.99 (37.24)	38.45 (52.90)	13.56 (9.86)	75	25	3.947	4.059	1.028
38.39 (29.60)	39.91 (54.70)	21.7 (15.70)	60	40	3.917	4.057	1.035
25.59 (19.63)	41.86 (56.95)	32.55 (23.42)	40	60	3.890	4.061	1.044
6.40 (4.86)	44.78 (60.30)	48.82 (34.84)	10	90	3.890	4.054	1.042

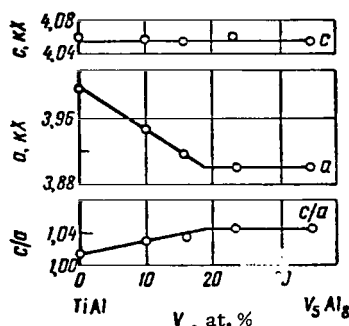


Figure 3. Change in the Lattice Constants of the γ Solid Solution Based on the Compound TiAl of Alloys of the Section TiAl-V₅Al₈ Quenched From 1100°C.

the compound V₅Al₈ extends from 44.5 to 47% Al and contain up to ~3% Ti. In correspondence with the one-phase regions, the system contains two- and three-phase regions: $\alpha_2 + \beta$, $\alpha_2 + \gamma$, $\beta + \gamma$, $\gamma + \delta$, $\beta + \gamma + \delta$, $\alpha_2 + \beta + \gamma$.

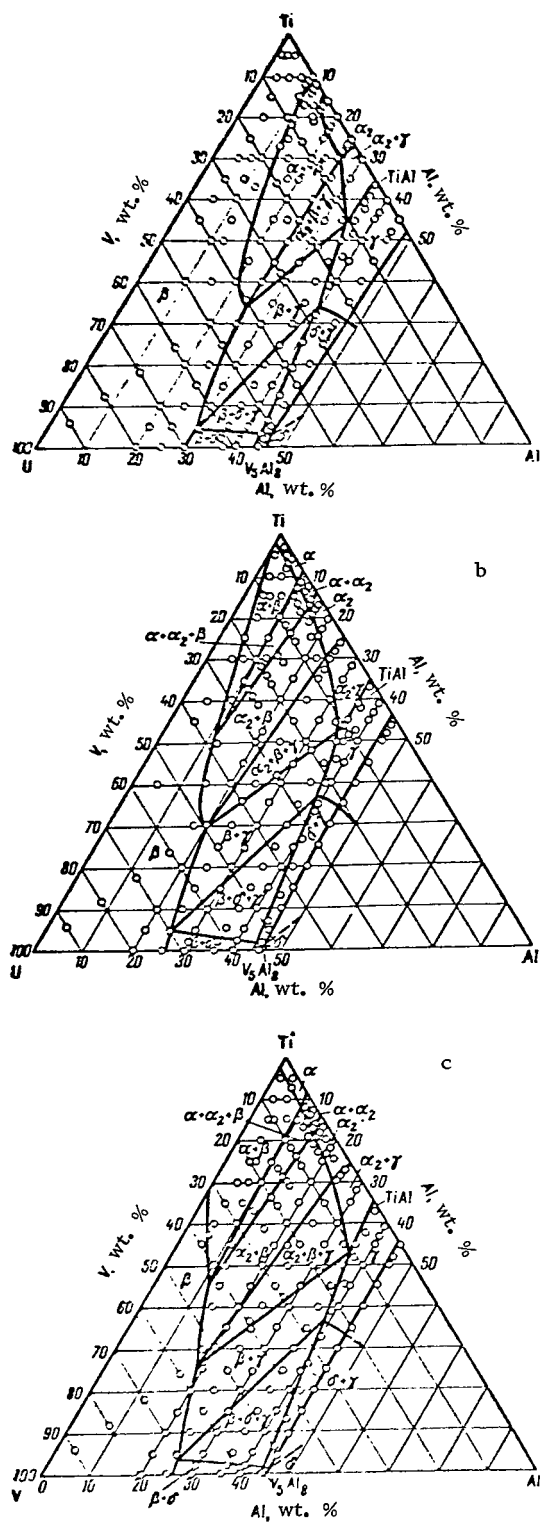
Isothermal section of the system at 800°C. The following phases were found in the system at 800°C: β , α , α_2 , γ and δ . Comparison of the isothermal sections at 1100°C (Fig. 4, a) and 800°C (Fig. 4, b) shows that the region of the β solid solution is substantially shifted toward the vanadium side and contains from 0 to 97% Ti and up to 27.5% Al on the V-Al side. The solid solution based on α -Ti extends from 0 to 9% Al and contains up to 2% V. The solid solution based on the compound Ti₃Al contains up to 5% V at 24% Al. The region of the ternary β solid solution as compared to the section at 1100°C narrows somewhat (extends from 35.5 to 44.5% Al) and contains up to 24% V. Compared to the section at 1100°C, the three-phase region ($\alpha_2 + \beta + \gamma$) broadens.

Isothermal Sections of the System Ti-Al-V

Isothermal section of the system at 1100°C. Figure 4, a shows the isothermal section of the system at 1100°C. At this temperature, the following phases were detected in the alloys: β , α_2 (Ti₃Al) γ (Ti Al) and δ (V₅Al₈).

As can be seen from Fig. 4, a the β solid solution based on a bcc structure extends from the Ti-V side and contains 11% Al on the side of the binary system Ti-Al and ~30% Al on the side of the system V-Al. A solid solution based on the compound Ti₃Al extends from the Ti-Al side from 14.5 to 25.5% Al and contains up to ~5% V at 25% Al; a γ solid solution based on the tetragonal face-centered structure of the compound TiAl extends from 35.5 to 47% Al and contains up to 26% V. A solid solution based on the compound V₅Al₈ extends from 44.5 to 47% Al and contain up to ~3% Ti. In

/85



Isothermal section at 550°C.
 At 550°C, the same phases were found in the alloys of the system as at 800°C. The isothermal section of 550°C is shown in Fig. 4, c. The region of the ternary β solid solution extends from the corner of pure vanadium; the regions $\alpha + \beta$ and $\alpha + \alpha_2 + \beta$ broaden. The remaining phases of the region do not undergo any substantial changes.

Polythermal Sections of the System

Results of thermal, microstructural and x-ray analyses with the use of the given isothermal sections were used to plot the polythermal sections of the system, i. e., radial sections originating from the vertex of pure titanium at aluminum to vanadium ratios of 3:1, 1:1 and 1:3 (Fig. 5, a-c).

Figure 5, a shows the section of the system at an aluminum-to-vanadium ratio of 3:1. As the content Σ Al, V increases, the temperature of the start of fusion of the alloys of this section decreases to 1600°C for the alloy with 40% Σ Al, V. The transition temperature $\alpha \rightarrow \beta$, $\alpha + \beta \rightarrow \beta$ increases from 882°C for pure titanium to 1100°C for the alloy with 20% Σ Al, V. The region of the α solid solution extends from 0 to 10% Σ Al, V. The region of the ternary γ solid solution extends from 49 to 60% Σ Al, V.

Figure 4. Isothermal Sections of the Ternary System Ti-Al-V at Various Temperatures:

a—1100°C, b—800°C, c—550°C.

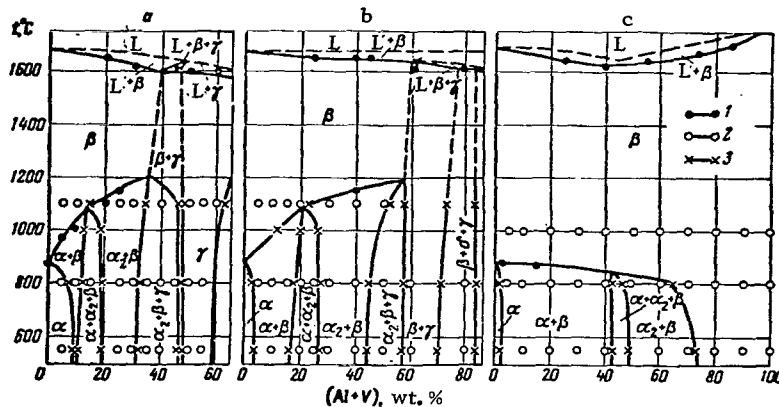


Figure 5. Polythermal Sections of the Ternary System Ti-Al-V at Ratio of Aluminum to Vanadium of 3:1 (a), 1:1 (b) and 1:3 (c):

1—Rate of Thermal Analysis; 2—Composition of Alloys Studied; 3—Phase Boundaries Transposed from Isothermal Sections.

The section for the aluminum-to-vanadium ratio of 1:1 is shown in Fig. 5, b. In this section as compared to the preceding one, the region of the β solid solution extends along the concentration axis up to 58% Σ Al, V at 1200°C , and in the preceding section at this temperature β solid solution extends up to 35% Σ Al, V at 1200°C . The region of the α solid solution (up to 5% Σ Al, V) narrows, the region $(\alpha + \beta)$ expands, and the one-phase region of the γ solid solution is absent. The three-phase region $(\beta + \gamma + \delta)$ appears.

The section for an aluminum-to-vanadium ratio of 1:3 is shown in Fig. 5, c. The section contains a continuous series of β solid solutions. The temperature of the transition $\alpha + \beta \rightarrow \beta$ with increasing content of Σ Al, V decreases and at 800°C amounts to 62% Σ Al, V. The boundaries of $\alpha/\alpha + \beta$ and $\alpha_2 + \beta/\beta$ pass at 2 and 72% Σ Al, V (for 550°C). Comparing these radial section at the ratio $\text{Al:V} = 3:1$ is largely determined by the phase diagram of the binary system Ti-Al, and in alloys of the section with the ratio $\text{Al:V} = 1:3$, by the nature of the chemical interaction in the binary system Ti-V.

/86

Electrical Resistivity and Hardness of Alloys

The electrical resistivity was studied on alloys of sections parallel to the Ti-V side, with a constant content of V from 2 to 5% (Fig. 6, a, b). As is evident from Fig. 6, for both sections the resistivity values increase with rising aluminum content in the alloys up to 10-12%, which corresponds to the aluminum concentration at which the appearance of a phase based on the aluminide Ti_3Al is possible in the alloys. The resistivity values increase as a result of saturation of the α solid solution with aluminum. As the aluminum content of the alloys increases further, the resistivity values decrease, reaching a minimum at 16% Al,

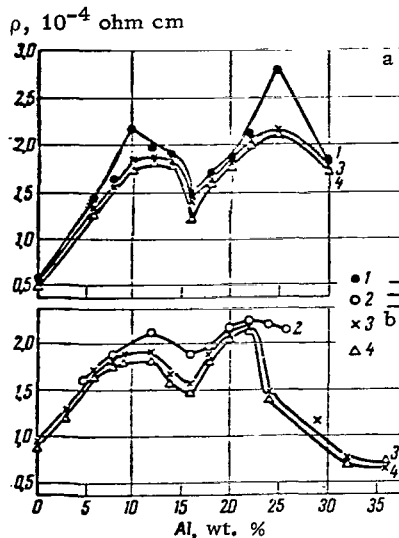


Figure 6. Electrical Resistivity of Alloys of the Ternary System Ti-Al-V for Sections with Constant Content of 2% V (a) and 5% V (b):

Quenching From 1200 (1), 1100 (2), 800 (3) and 550°C (4).

curve go through a minimum, owing to the appearance of a solid solution based on the compound TiAl.

In alloys of the section Al:V = 1:3 the hardness changes along curves with a broad maximum (Fig. 7, b). For most alloys, the hardness values range from 350 to 400 kg/mm². The presence of a maximum at 3-10% ΣAl, V, is apparently due to the instability of the β solid solution under quenching conditions and to the appearance of intermediate metastable phases.

The hardness of alloys of sections with constant contents of 20, 25, 30, 36, 40 and 45% Al is shown in Fig. 8.

/87

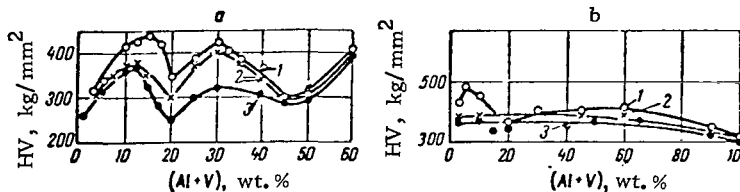


Figure 7. Hardness of Alloys of the Ternary System Ti-Al-V for Radial Sections at Al:V = 3:1 (a) and Al:V = 1:3 (b):
 1—1100°, 2—800°, 3—550°C.

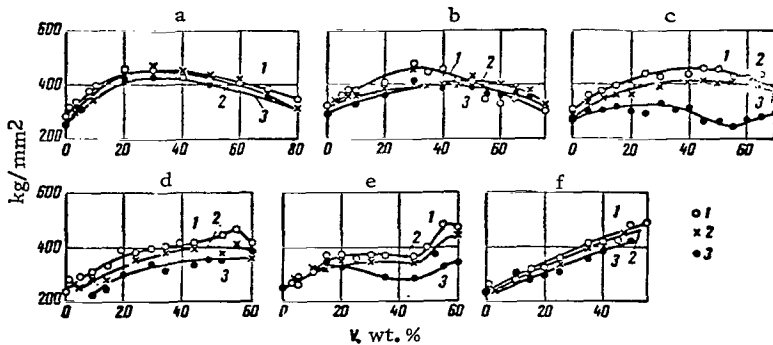


Figure 8. Hardness of Alloys of the Ternary System Ti-Al-V of Sections with Constant Aluminum Content, % : 20 (a), 25 (b), 30 (c), 36 (d), 40 (e) and 45 (f): Quenching From 1100 (1), 800 (2) and 550°C (3).

The hardness of the alloys of the illustrated sections is determined by the nature and relative amounts of the phases present.

The hardness of alloys of these sections changes along curves with a broad maximum after quenching from all the indicated temperatures. Among alloys of the section with 20% Al, the greatest hardness (up to 460 kg/mm²) is displayed by alloys containing 20-40% V. These alloys are located in the two-phase region ($\alpha_2 + \beta$). Alloys of the section with 25% Al have a maximum hardness (400-460 kg/mm²) at 20-50% V.

Among alloys of the sections with 20, 25, 30 and 36% Al, the greatest hardness is displayed by alloys containing 20-50% V.

The hardness of alloys of all these sections after quenching from 550°C is less than that of alloys quenched from 1100 and 800°C. This is apparently due to the less stressed state of alloys after their annealing at 550°C.

The hardness of alloys of sections with 40 and 45% Al in the region of the δ solid solution increases to 460-470 HV after quenching from any temperature, this being obviously due to the appearance of the δ phase in the alloys and to an increase of its quantity.

High-Temperature Strength of Alloys

The adopted measure of temperature strength was the time taken to reach a specified bending deflection of 5 and 7 mm. Figure 9 shows the results of the series of tests.

As is evident from Fig. 9, an increase of vanadium content to 0.5-3% slightly increases the time necessary for a bending deflection of 5 and 7 mm to be reached. As the vanadium content increases further, the curve goes through a minimum,

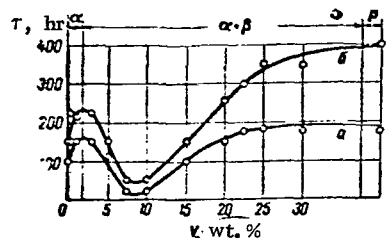


Figure 9. Time Necessary for Reaching a Bending Deflection of 5 mm (a) and 7 mm (b) for Alloys of the Section with 5% Al; $t = 550^{\circ}\text{C}$, $\sigma = 15 \text{ kg/mm}^2$.

region of the β solid solution with a considerable degree of saturation with vanadium.

apparently owing to an increase in the degree of heterogeneity of the alloys and an associated increase in the intensity of the processes of interaction of the phases at their interface.

In the vicinity of the phase boundary $\beta/(\alpha + \beta)$ of the phase regions, the high-temperature strength of the alloys increases.

Thus, among alloys of the section with 5% Al (after thermal treatment following the indicated schedules) at $t = 550^{\circ}\text{C}$ and $\sigma = 15 \text{ kg/mm}^2$, the maximum high-temperature strength is displayed by alloys located near the boundaries of the phase regions $\alpha/(\alpha + \beta)$ and $\beta/(\alpha + \beta)$ in the presence of a small amount of a second phase, and also alloys from the

Summary

1. Alloys of the ternary system Ti-Al-V containing from 0 to 45% Al were studied by methods of thermal, microstructural, and x-ray analyses, and also by measurements of electrical resistivity and hardness.

2. As a result of the study, isothermal sections of the system at 1100° , 800 and 550°C were plotted, as well as polythermal sections of the system at aluminum-to-vanadium ratios of 1:3, 1:1 and 3:1. The existence of α -, α_2 -, γ - and δ solid solutions were established. Equilibrium between the compounds TiAl (γ) and V_5Al_8 (δ) was observed in the part of the system studied. The existence of the following phase regions was established: $\alpha + \beta$, $\alpha + \alpha_2$, $\alpha_2 + \gamma$, $\beta + \gamma$, $\beta + \delta$, $\gamma + \delta$, $\alpha + \alpha_2 + \beta$, $\alpha_2 + \beta + \gamma$, $\beta + \delta + \gamma$.

3. On curves of the resistivity versus composition of alloys of sections with a constant vanadium content (2 and 5%), there is a minimum at 16% Al, which confirms the existence of the compound Ti_3Al in the binary system Ti-Al.

4. The hardness of alloys of the sections with 20-45% Al changes along curves with broad maxima. The greatest hardness is displaced by alloys containing 30-40% V, and also alloys located in the region of the δ solid solution (V_5Al_8).

5. A study of the high-temperature strength of alloys of the section with 5% Al with a variable vanadium content from 0 to 40%, determined by the centrifugal bending method, showed that the greatest high-temperature strength is displayed by alloys whose compositions are close to the $\alpha/(\alpha + \beta)$ and $\beta/(\alpha + \beta)$ boundaries of the phase regions.

REFERENCES

1. Rausch, J.J., F.A. Crossley and H.D. Kessler. J. Met., Vol. 8, No. 2, p. 211, 1956.
2. Jordan, C.B. and P. Duwes. Trans. ASM, No. 48, p. 783, 1956.
3. Kubaschewski, O., C. Wainwright and F.J. Kirby. J. Inst. Met., Vol. 4, No. 12, p. 139, 1960-1961.
4. Farrar, P.A. and H. Margolin. Trans. Met. Soc. AIME, Vol. 221, No. 6, p. 1214, 1961.
5. Kornilov, I.I. et al. Dokl. AN SSSR, Vol. 161, No. 4, p. 843, 1965.
6. Carlson, O.N., D.J. Kenny and H.A. Wilhelm. Trans. ASM, No. 47, p. 520, 1954.
7. Ermanis, F., P.A. Farrar and H.M. Margolin. Trans. Met. Soc. AIME, Vol. 221, p. 904, 1961.
8. Kornilov, I.I., M.A. Volkova and E.I. Pylayeva. Collection "Recent Studies of Titanium Alloys." Proceedings of 6th conference on the metal chemistry, metallurgy and use of titanium and its alloys. (Sb. "Novyye issledovaniya titanovykh splavov". Trudy 6-go soveshchaniya po metallokhimii, metalovedeniyu i primeneniyu titana i yego splavov. "Nauka," No. 8, p. 92, 1965.
9. Pietrokowsky, P. and P. Duwez. J. Metals, Vol. 4, No. 6, p. 627, 1952.
10. Holleck, H., F. Benesovsky and H. Nowotnej. Mon. Chémie, No. 94, 2, p. 477, 1963.
11. Kornilov, I.I. Physicochemical Principles of High-Temperature Strength of Alloys. (Fiziko-khimicheskiye osnovy zharoprochnosti splavov). AN SSSR, 1961.

/89

STUDIES OF THE PHASE EQUILIBRIUM AND CERTAIN PROPERTIES OF ALLOYS OF THE SYSTEM Ti-Al-Mo-Zr RICH IN TITANIUM

I. I. Kornilov, N. G. Boriskina and M. A. Volkova

A study was made of the quaternary system Ti-Al-Mo-Zr along two sections passing through an edge of the tetrahedron Ti-Al and intersecting the plane of the tetrahedron Ti-Mo-Zr at Mo:Zr = 3:1 (I) and 1:3 (II) up to 30-35% ll Al, Mo, Zr. The systems Ti-Al, Ti-Mo and Ti-Zr were the most interesting among binary diagrams for studying the selected region of alloys. The system Ti-Al has been studied by many authors. In the present paper, a variant of the phase diagram proposed in [1] was used. In [1] it was found that a broad region of β solid solution exists in the Ti-Al system in the region of alloys rich in titanium. At 1120°C, only one compound of the composition Ti_3Al (16 wt. % Al), having a hexagonal ordered structure of type Mg_3Cd , is formed from the β solid solution. The system contains a broad region of solid solutions based on this compound (α_2 phase). At 1080°C in the concentration range ~9-14% Al, the α phase is formed by the paritectoid reaction $\beta + \alpha_2 \rightarrow \alpha$. At 550°C, the solubility of aluminum in α Ti is ~7.5%. The two-phase region $\alpha + \alpha_2$ at the same temperature lies in the range of 7.5-14% Al, and the region of the α_2 phase, in the range of 14-24.5% Al.

Titanium with molybdenum form a continuous series of solid solutions based on the body-centered lattice of molybdenum and β -Ti. The solubility of molybdenum in α -Ti, according to the data of [2], amounts to about 0.8%. Titanium and zirconium form a continuous series of solid solutions based on β - and α' - modifications of the crystal lattices of these elements [3].

In ternary systems making up the four-component system Ti-Al-Mo-Zr, in the portion rich in titanium, the following phases are in equilibrium: in the system Ti-Mo-Zr, α - and β - phases (according to the author's data), and in the systems Ti-Al-Mo [4] and Ti-Al-Zr [5-7], α , α_2 (Ti_3Al) and β .

In order to study the phase composition and properties of alloys of the system Ti-Al-Mo-Zr of both sections, groups of six sections each were selected with constant aluminum contents of 3, 6, 9, 12, 16 and 22%. The composition of the alloys is given in the Table, and also shown on corresponding isothermal sections.

The initial materials used were iodide titanium (99.7% Ti) and zirconium (99.8% Zr), AV-000 aluminum (99.99% Al), and molybdenum in bars (99.9% Mo). The studies were made by using microstructural analysis and partially x-ray analysis, and also measurements of hardness and electrical resistivity of the alloys.

/90

A microstructural study and measurements of hardness were carried out on alloys prepared by arc melting with a nonconsumable electrode in an argon atmosphere. The specimens of alloys for studying the resistivity were prepared by floating fusion in a helium atmosphere. TG00 titanium sponge (99.6% Ti) was used for the preparation of these specimens. The composition of the alloys was checked by accurate weighing of the bead. Specimens were chosen whose weight did not deviate from the calculated value by more than 0.5%.

TABLE 1. COMPOSITION OF STUDIED ALLOYS OF THE SYSTEM Ti-Al-Mo-Zr, wt. %

3Al		6Al		9Al		12Al		16Al		22Al		Section I		Section II	
Ti	Mo	Zr	Mo	Zr											
97.0	94.0	91.0	88.0	84.0	78.0	0	0	0	0	0	0	0	0	0	0
96.5	93.5	90.5	87.5	83.5	77.5	0.38	0.13	0.125	0.375	—	—	0.187	0.563	—	—
96.25	93.25	90.25	87.25	83.25	77.25	—	—	—	—	—	—	—	—	—	—
96.0	93.0	90.0	87.0	83.0	77.0	0.75	0.25	0.25	0.25	0.5	0.5	0.5	0.75	0.75	0.75
95.0	92.0	89.0	86.0	82.0	76.0	1.5	0.5	0.5	0.5	1.5	1.5	1.5	1.5	1.5	1.5
94.0	91.0	88.0	85.0	81.0	75.0	2.25	0.75	0.75	0.75	2.25	2.25	2.25	2.25	2.25	2.25
92.0	89.0	86.0	83.0	79.0	73.0	3.75	1.25	1.25	1.25	3.75	3.75	3.75	3.75	3.75	3.75
89.5	86.5	83.5	80.5	76.5	70.5	5.62	1.88	1.88	1.88	5.625	5.625	5.625	5.625	5.625	5.625
87.0	84.0	81.0	78.0	74.0	68.0	7.5	2.5	2.5	2.5	7.5	7.5	7.5	7.5	7.5	7.5
84.5	81.5	78.5	75.5	71.5	65.5	9.38	3.12	—	—	—	—	—	—	—	—
—	—	—	—	70.0	—	—	—	—	—	—	—	3.50	10.50	—	—
82.0	79.0	76.0	73.0	69.0	63.0	11.25	3.75	3.75	3.75	11.25	11.25	11.25	11.25	11.25	11.25
79.5	76.5	73.5	70.5	66.5	—	13.14	4.38	—	—	4.38	—	—	—	—	—
—	—	—	70.0	—	—	—	—	—	—	—	—	4.5	13.5	—	—
77.0	74.0	71.0	68.0	—	—	—	15.0	5.0	5.0	5.0	5.0	5.0	15.0	15.0	15.0
—	—	70.0	—	—	—	—	—	—	—	—	—	5.25	15.75	—	—
74.5	71.5	—	—	—	—	—	16.88	5.63	—	—	—	—	—	—	—
—	70.0	—	—	—	—	—	—	—	—	—	—	6.0	18.0	—	—
72.0	69.0	—	—	—	—	—	18.75	6.25	6.25	6.25	6.25	6.25	18.75	18.75	18.75
70.0	—	—	—	—	—	—	—	—	—	—	—	6.75	20.25	—	—
69.5	66.5	—	—	—	—	—	20.63	6.88	—	—	—	—	—	—	—
67.0	—	—	—	—	—	—	22.5	7.5	—	—	—	—	—	—	—
64.5	—	—	—	—	—	—	24.4	8.1	—	—	—	—	—	—	—

Alloys sealed into double evacuated quartz ampules were subjected to heat treatment under the following schedules: 1100°C, 10 hr → 1000°C, 25 hr → 900°C, 75 hr → 800°C, 400 hr → 700°C, 200 hr → 600°C, 400 hr → 500°C, 1000 hr (alloys of intersection section II) and 1100°C, 50 hr → 1000°C, hr → 800°C, 200 hr → 600°C, 300 hr → 500°C, 500 hr (alloys of intersection section I).

The study of the microstructure and also measurements of the hardness and resistivity of the alloys were made after quenching from 1100, 800 and 500°C. The etchant used was a mixture of hydrofluoric and nitric acids and glycerin. The resistivity was measured potentiometrically. The hardness values were obtained with a Vickers instrument at a load of 10 kg.

Figure	Section	Alloy		Quenching temperature, °C	Phases	Figure	Section	Alloy		Quenching temperature, °C	Phases
		Al, %	(Mo + Zr), %					Al, %	(Mo + Zr), %		
a b c d	I	3	12.5	1100	β	e	II	6	10	800	α + β
	II	16	5	1100	α _s	f	II	12	0.75	800	α + α _s
	II	12	10	1100	α _s + β	g	II	12	3	800	α + α _s + β
	I	3	12.5	900	α + β	h	I	12	7.5	500	α + α _s + β annealing

Figure 1 (Cont'd) on next page.

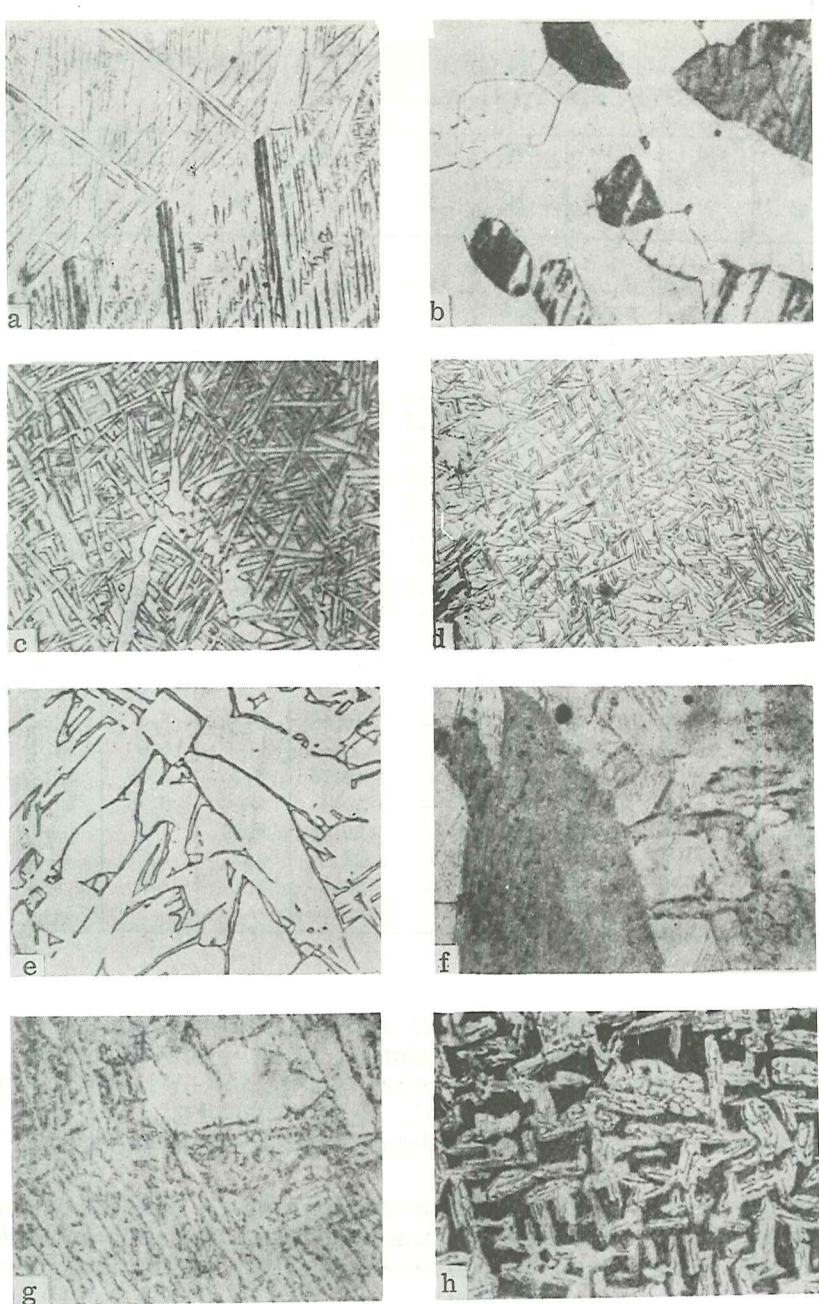


Figure 1. Microstructure of Alloys of the System Ti-Al-Mo-Zr.

Results of Microstructural Study

A study of the microstructure of cast alloys showed that over the entire range of component concentrations of the part of the phase diagram studied, solid solutions based on the bcc lattice of molybdenum, β -Ti and zirconium crystallize from the liquid. Most of the alloys have the structure of a transformed β phase.

After quenching from 1100°C, the region of alloys studied is characterized by the presence of three types of microstructures: transformed or stable β -phase, solid solution based on the compound Ti_3Al (α_2 phase), and two-phase ($\alpha_2 + \beta$) alloys. The characteristic microstructure of some alloys is shown in Fig. 1, a, b, c.

Isothermal sections of both cross sections at 1100°C, plotted from data of microstructural analysis, are given in Fig. 2, a and 2, d.

The region of the four-component solid solution based on β -Ti (cross sections I and II) extends from the side of Ti (Mo:Zr = 1:3, 1:1), encompassing all the alloys of the section with 9% Al. The regions of $\alpha_2 + \beta$ and α_2 phases extend in correspondence with the binary system Ti-Al as the aluminum content of the alloys of the cross section II causes an expansion of the region of the α_2 phase in the concentration triangle.

Thus, up to 1.5% Σ Mo, Zr dissolves along the section with 16% Al in the solid solution based on the α_2 phase in alloys of cross section I, and in alloys of cross section I, and in alloys of cross section II, 5% of Σ Emo, Zr dissolves. Identification of the α_2 phase was also confirmed by data of x-ray analysis of alloys of sections with 22 and 16% Al, containing up to 5% Mo + Zr. X-ray patterns of these alloys, obtained with Cu_{α} radiation, showed reflection lines corresponding to the ordered hexagonal structure of the α_2 phase (Ti_3Al) with a superstructure line (101) characteristic of this compound.

According to data of microstructural analysis, in the course of annealing at 800°C, the β solid solution of most alloys of both cross sections of sections of 3, 6 and 9% Al decomposes with the formation of the α phase as a result of a polymorphic transformation.

In alloys of both cross sections of the section with 12% Al (and in cross section II also partly in alloys of the section with 9% Al), the α phase is formed by the peritectoid reaction $\beta + \alpha_2 \rightarrow \alpha$, as in the system Ti-Al.

The microstructure of alloys with $\alpha + \beta$, $\alpha + \alpha_2$ and $\alpha + \alpha_2 + \beta$ is shown in Fig. 1, d-g.

In a certain range of molybdenum and zirconium concentrations, this interaction leads to the formation of two-phase ($\alpha + \alpha_2$) and three-phase ($\alpha + \alpha_2 + \beta$) structures. The formation of the α phase in the peritectoid reaction of α_2 and β phases is associated with an increase of the dispersity of the phase components of the alloys as compared to the state after quenching from 1100°C (Fig. 1, f-g). The phase composition of the alloys of sections with 16 and 22% Al after quenching from 800°C did not change as compared to alloys quenched from 1100°. /94

In accordance with the data of microstructural analysis, regions of homogeneous four-component solid solutions based on α -, α_2 - and β -phases were noted on the

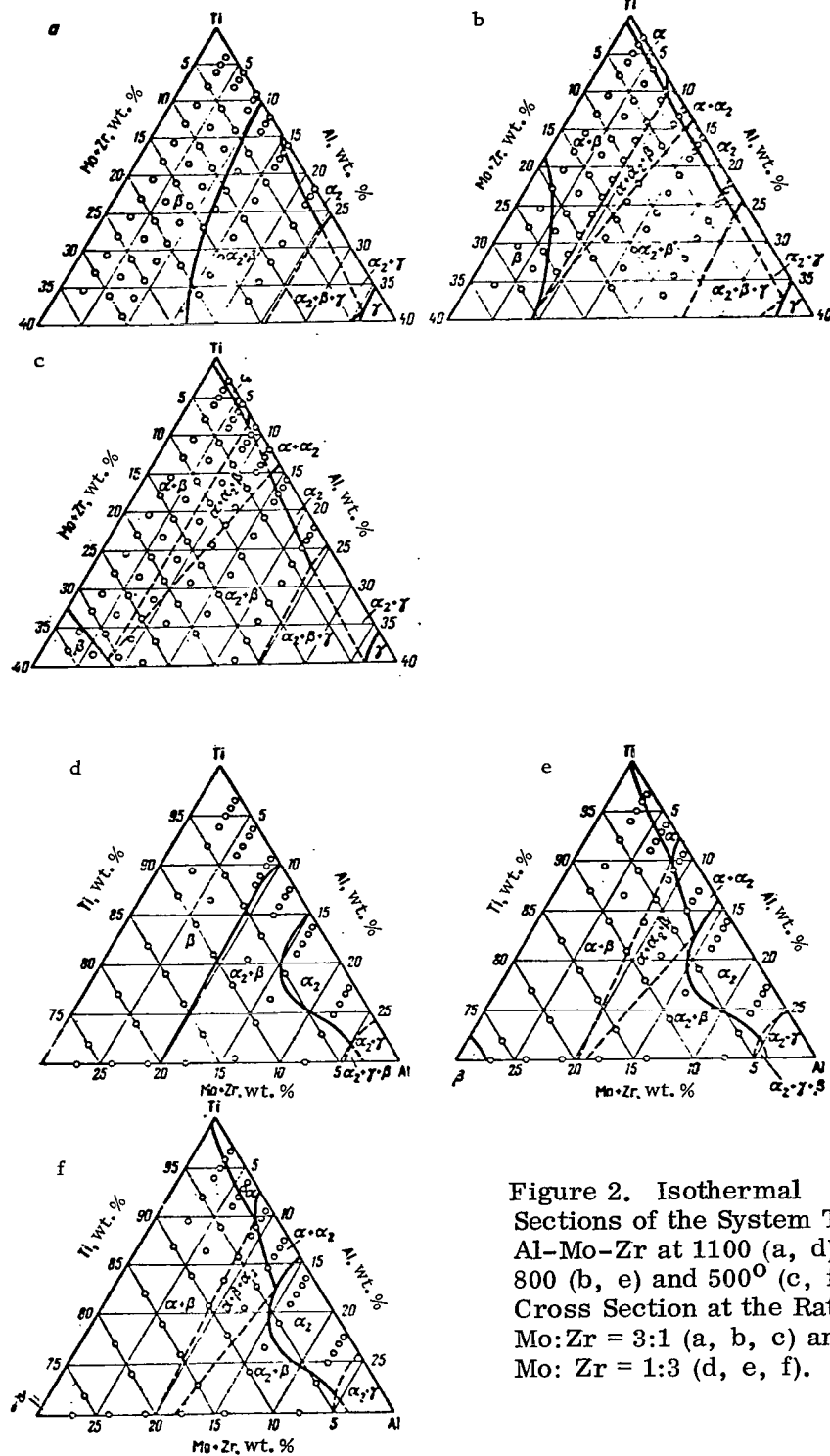


Figure 2. Isothermal
 Sections of the System Ti-
 Al-Mo-Zr at 1100 (a, d),
 800 (b, e) and 500° (c, f).
 Cross Section at the Ratio
 Mo:Zr = 3:1 (a, b, c) and
 Mo: Zr = 1:3 (d, e, f).

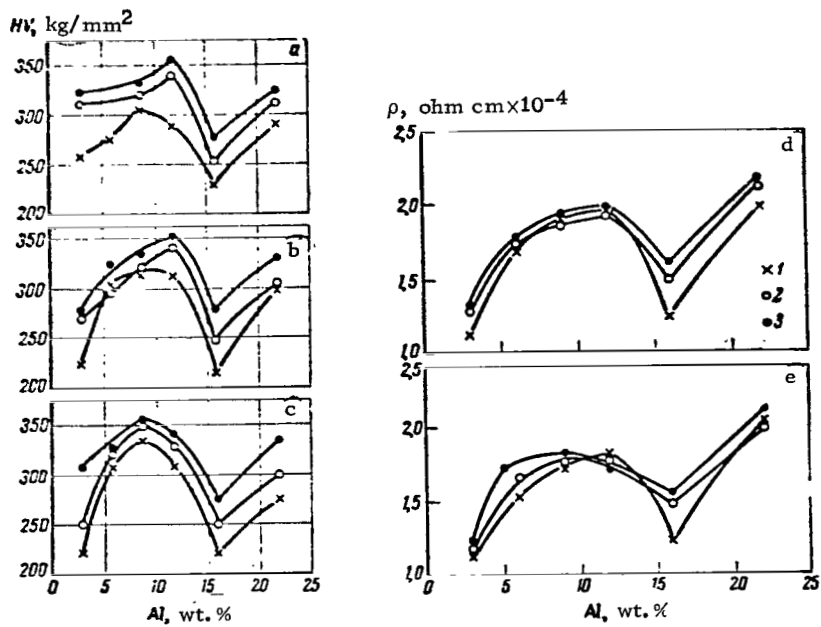


Figure 3. Hardness and Electrical Resistivity of Alloys of the Cross Section Mo:Zr = 3:1 Versus Aluminum Content.

Quenching from 1100 (a), 800 (b, d), 500°C (c, e) of Alloys with 1-1% Mo + Zr, 2-3% Mo + Zr, 3-5% Mo + Zr.

isothermal sections of both cross sections (Fig. 2, b and 2, e). At 800°C, these solid solutions form three regions of a two-phase equilibrium ($\alpha + \beta$, $\alpha + \alpha_2$ and $\alpha_2 + \beta$) and one three-phase region ($\alpha + \alpha_2 + \beta$) marked with a dashed line, since its boundaries have not been precisely established. The higher molybdenum content in alloys of intersection I promotes an expansion of the region of homogeneous β solid solutions. It should be noted that the propagation of the phase regions in the system Ti-Al-Mo-Zr is in good agreement with the results of a study of alloys of the corresponding radial sections with ratios Mo:Zr = 3:1 and Mo:Zr = 1:3 of the system Ti-Mo-Zr.

A microstructural examination of alloys subjected to prolonged annealing at 500°C showed that their phase composition remained practically unchanged, and that there was a decrease in the amount of the β solid solution, which decomposed additional with the formation of α - and α_2 -phases. At a low content of the sum of molybdenum and zirconium in alloys of intersection I of the section with 16 and 22% Al, this decomposition went to completion, so that the region of the α_2 -phase expanded.

After prolonged annealing at 500°C, alloys of the sections with 9 and 12% Al displayed the peritectoid character of the formation of the α -phase most distinctly (Fig. 1, h). Decomposition of the β -phase was associated with the appearance of a large amount of acicular grains of the α -phase, as a result of which the structure of such alloys is marked by a considerable heterogeneity.

The isothermal sections of both cross sections at 500°C (Fig. 2, c and 2, f) are similar to the corresponding sections at 800°C and are distinguished only by a certain shift of the boundaries of the phase regions (intersection I).

The region of the β -solid solution of alloys of cross section I narrowed considerably. All the alloys of this cross section with 9% Al shifted into the region of the three-phase equilibrium $\alpha + \alpha_2 + \beta$.

Thus, the study confirmed the role of zirconium as a stabilizing element promoting the expansion of regions of solid solutions based on α and α_2 -phases in alloys of cross section II, richer in zirconium. On the other hand, molybdenum, being a strong stabilizer of the β modification of titanium, promotes a wider propagation of the region of β solid solutions in alloys of cross section I.

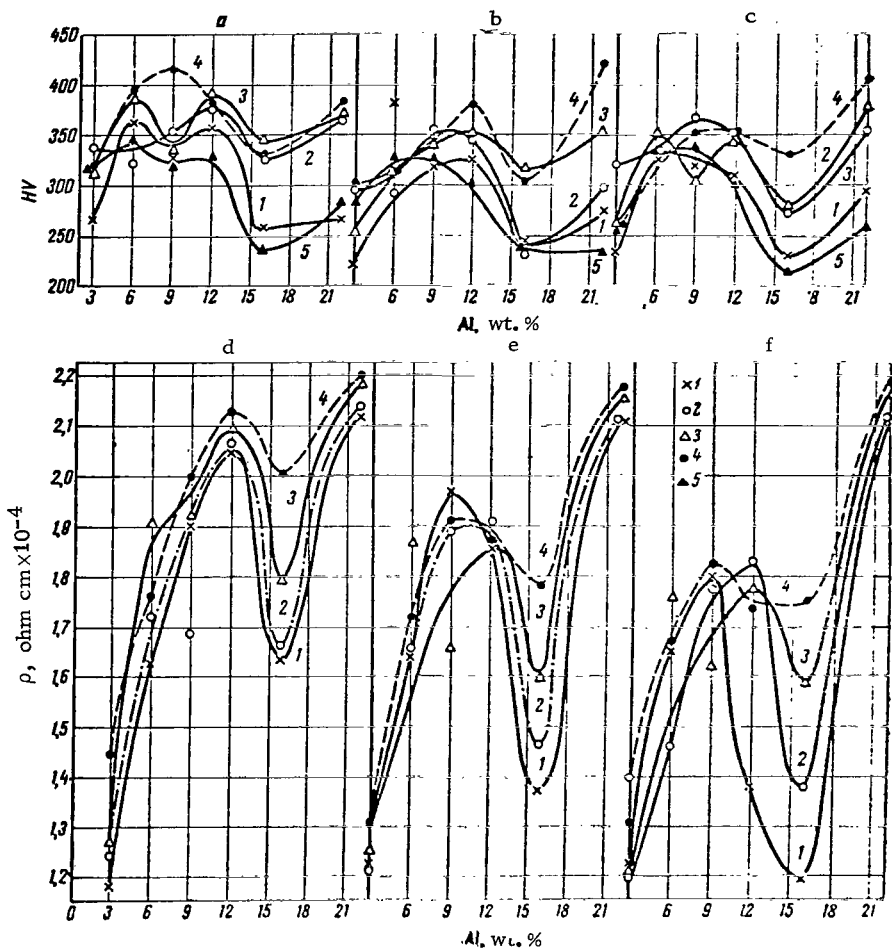


Figure 4. Hardness (a-c) and Electrical Resistivity (d-f) of Alloys of the Cross Section Mo + Zr = 1:3 Versus Aluminum Content After Quenching from 1100°C (a, d), 800°C (b, e) and 500°C (c, f).

1—1% Mo + Zr, 2—3% Mo + Zr, 3—5% Mo + Zr, 4—10% Mo + Zr, 5—0.5% Mo + Zr. Numbers Marking Curves — Sum of Mo + Zr.

Properties of Alloys of the System Ti-Al-Mo-Zr

/96

The hardness of alloys of both cross sections was measured on specimens which had already been subjected to microstructural analysis. As may be seen from diagrams plotted in the coordinates "wt. % Al vs. hardness," in a number of alloys with a constant content of the sum of molybdenum and zirconium (Fig. 3 and 4), the hardness changes along curves with a distinct minimum corresponding to alloys with 16% Al, this being related to the existence of the compound Ti_3Al .

At the same time, an increase in the content of the sum of molybdenum and zirconium in the alloys is associated with a certain increase of their hardness, particularly noticeable in alloys of cross section II in the 3-10% range of Mo + Zr. It should be noted that the hardness of alloys of cross section I depends little on the annealing temperature. In alloys of intersection II, the hardness gradually decreases after annealing at $1100-800-500^{\circ}C$, owing to the decomposition of the β solid solution accompanying the formation of the α phase (although this decrease is generally slight).

The electrical resistivity of alloys of both cross sections changes like the hardness. The lowest resistivity was displayed by alloys containing 3 and 16% Al (Fig. 3, 4). At the same time, the increase of the content of the sum of molybdenum and zirconium in the alloys promotes a certain increase of their resistivity. A decrease of the annealing temperature from 1100° and 500° leads to a decrease of the " ρ " of the alloys, owing to an additional decomposition of the β solid solution, associated with the separation of α or α_2 phases.

The particularly rapid decrease of resistivity of alloys with 16% Al and 1% (Mo + Zr) after annealing at $500^{\circ}C$ is obviously due to the presence in these alloys of a large portion of an ordered solid solution α_2 based on the compound Ti_3Al , which has a low resistivity.

Summary

1. A study of a portion of the four-component system Ti-Al-Mo-Zr along two cross sections of the tetrahedron passing through the Ti-Al edge and the plane Ti-Mo-Zr and Mo-Zr-Al at a ratio of Mo:Zr = 3:1 and 1:3 showed that both cross sections are characterized by the existence of solid homogeneous solutions based on β -Ti, α -Ti and α_2 -phase and the presence of corresponding two-phase and three-phase regions.

Solid solutions based on β -Ti were crystallized from the liquid in the investigated portion of the quaternary system.

At $1100^{\circ}C$, the region of the β solid solution, extending from the titanium vertex, encompasses alloys adjacent to the Ti-Mo-Zr plane. At the same time, the β region narrows toward the aluminum vertex from the Al-Mo edge (13% Al) to the Al-Zr edge (~ 7 % Al). The region of solid solutions based on the α_2 -phase gradually expands from the Ti-Al-Mo system (~ 1 % Mo dissolves in the α_2 -phase) to systems of the corresponding intersections of the tetrahedron and Ti-Al-Zr

(at Mo:Zr = 3:1, up to 1.5% Mo + Zr dissolves in the α_2 -phase at 1100°C, and at Mo:Zr = 1:3, up to 6-4% Mo + Zr dissolve). At 800°C, because of the polymorphic transformation of the β -solid solution, the region of the β -phase narrows considerably. It extends mainly from the Ti-Mo edge to the Ti-Al-Mo system into the body of the tetrahedron, encompassing alloys adjacent to the Ti-Mo-Zr plane and narrowing considerably toward the intersection Mo:Zr = 1:3. The region of the α -phase at 800°C expands from the Ti-Al-Mo system to the Ti-Al-Zr system.

At 500°C, the region of the β -phase narrows even more, and the regions of the α - and α_2 -phases expanded slightly toward alloys with a higher content of molybdenum and zirconium. The one-phase regions are separated by corresponding volumes of two-phase and three-phase equilibria in the four-component system. /97

2. The chief conclusion reached from a comparison of the properties of alloys of the two intersections studied along sections with constant aluminum contents of 3, 6, 9, 12, 16 and 22% at three quenching temperatures is the presence on the surface of properties of folds of minimum values of hardness and resistivity, originating from the compound Ti_3Al . Such a dependence of the properties of alloys on the composition confirms the existence of the compound Ti_3Al in the binary system and made it possible to conclude that a region of solid solutions based on this compound exists in the four-component system. Values of the hardness and resistivity for alloys of sections with the same aluminum content lie in approximately the same range and are relatively independent of the ratio of molybdenum to zirconium, in the alloys. A certain difference in the course of the curves of alloys of the intersections of the tetrahedron is in agreement with different qualitative relationships of the same phase components and with the shift of the boundaries of the phase regions.

REFERENCES

1. Kornilov, I. I. et al. Dokl. AN SSSR, Vol. 164, No. 4, p. 843, 1965.
2. Hansen, M. a. o. J. Met., Vol. 3, No. 10, p. 881, 1961.
3. Fast, J. D. Rec. Trav. Chim., Vol. 58, No. 9/10 p. 973, 1939.
4. Pylayeva, E. N. and Ge. Dzhi-min. Collection "Metallurgy of Titanium." (Sb. "Metallovedeniye titana"), "Nauka," p. 236, 1964.
5. Pylayeva, E. N. and M. A. Volkova. Collection "Metallurgy of Titanium." (Sb. "Metallovedeniye titana"), "Nauka," p. 26, 1964.
6. Kornilov, I. I., T. T. Nartova and M. M. Savel'yeva. Collection "Metallurgy of Titanium." (Sb. "Metallovedeniye titana"), "Nauka," No. 43, 1964.
7. Kornilov, I. I. and N. G. Boriskina. Collection "Metallurgy of Titanium." (Sb. "Metallovedeniye titana"), "Nauka," No. 47, 1964.

STUDY OF THE EQUILIBRIUM AND PROPERTIES OF ALLOYS OF THE SECTION Ti_3Sn - (Ti + 5% Zr) OF THE SYSTEM Ti-Zr-Sn

N. I. Shirokova and T. T. Nartova

Titanium, one of the transition metals with six unfilled d electron shells and two crystalline modifications, has a tendency to enter into various reactions with other elements. It forms continuous solid solutions with the close analogs zirconium and hafnium, etc. It forms broad regions of α and β solid solutions with many elements. In addition, titanium has a tendency to form many refractory intermetallic compounds (aluminides, beryllides, carbides, silicides, stannides, etc.) with properties of practical importance [1].

Many of these compounds have a marked high temperature strength, high temperature oxidation resistance and corrosion resistance.

The compound Ti_3Sn formed in the Ti-Sn system and corresponding to the composition 45.24 wt. % Sn, has a high creep resistance at 500-650°C [2]. However, the marked brittleness of the compound and its high oxidizability limit its use. In this connection, it becomes particularly important to study the influence of these elements on the phase equilibrium and the properties of this intermetallic compound of titanium. /98

Zirconium was selected as one of the elements for studying its influence on Ti_3Sn . In selecting this element it was considered that zirconium as an analog of titanium can have a favorable influence on some physicochemical and mechanical properties of the compound Ti_3Sn .

The reaction of titanium with tin has been studied by only a few authors, who proposed four fundamentally different variants for the equilibrium between α -Ti and the δ -phase based on the compound Ti_3Sn [3-8]. Since there is no unified view on the nature of the solid state equilibrium in the titanium rich region of the Ti-Sn system, it was of interest to study the equilibrium in this part of the system in the presence of a third element, zirconium.

This being taken into consideration, the portion of the ternary system Ti-Zr-Sn along the section Ti_3Sn - solid solution of titanium with 5% Zr was chosen for the study. The radial section which we studied is shown in Fig. 1. This figure also gives a polythermal phase diagram of the part of the binary system Ti-Sn up to the compound Ti_3Sn based on data of [7].

The alloys were melted by using a master alloys corresponding to the stoichiometric ratio of the atoms in the compound Ti_3Sn (25 at. % Sn), prepared by quadruple remelting in an arc furnace with a nonconsumable tungsten electrode made of iodide titanium and tin of brand ChDa. The specimens for the study were prepared by inductive floating fusion in the suspended state [9] in an atmosphere of purified helium. Waste from the alloys amounted to no more than 0.7%.

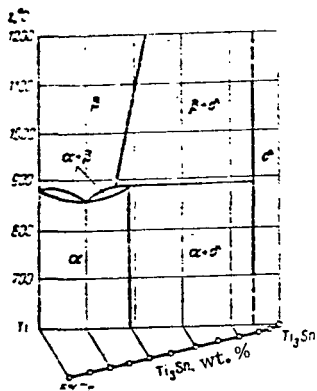


Figure 1. Part of Concentration Triangle of the System Ti-Zr-Sn in the Region Bounded by the Compound Ti_3Sn , the Alloy of Titanium With 5% Zr and Titanium.

range. At the same time, alloys with 40-90% Ti_3Sn undergo a peritectoid transformation at about 860°C; in alloys containing over 90% Ti_3Sn , no transformations were observed in the temperature range studied.

The microstructural study of alloys subjected to annealing in accordance with the above-indicated schedule showed that alloys containing up to 30% Ti_3Sn had the one-phase polyhedral structure of the α solid solution (Fig. 2, a); alloys with 40–90% Ti_3Sn had a two-phase structure consisting of a mixture of solid solutions based on titanium (α) and the compound Ti_3Sn (δ) (Fig. 2, b); alloys containing over 90% Ti_3Sn had the one-phase structure of the δ solid solution (Fig. 2, c). Similar structures were also observed in binary alloys Ti–Sn after annealing for 2500 hr.

/99

After quenching from 800°C, the microstructure was analogous to that obtained after annealing, with the exception of the alloy with 90% Ti₃Sn, whose structure is a mixture of the three phases α , δ and β (Fig. 2, d).

After quenching from 1000°C, the alloys containing up to 40% Ti_3Sn have in their structure a transformed β -phase of a circular texture (Fig. 2, e); those with 50 to 90% Ti_3Sn have a mixture of δ and β solid solutions (Fig. 2, f).

/100

On the basis of experimental data of the study of alloys of the section $Ti_3Sn - (Ti + 5\% Zr)$ of the ternary system Ti-Zr-Sn using methods of microstructural and thermal analyses, the peritectoid character of the transformation was established and the polythermal cross section shown in Fig. 3 was plotted.

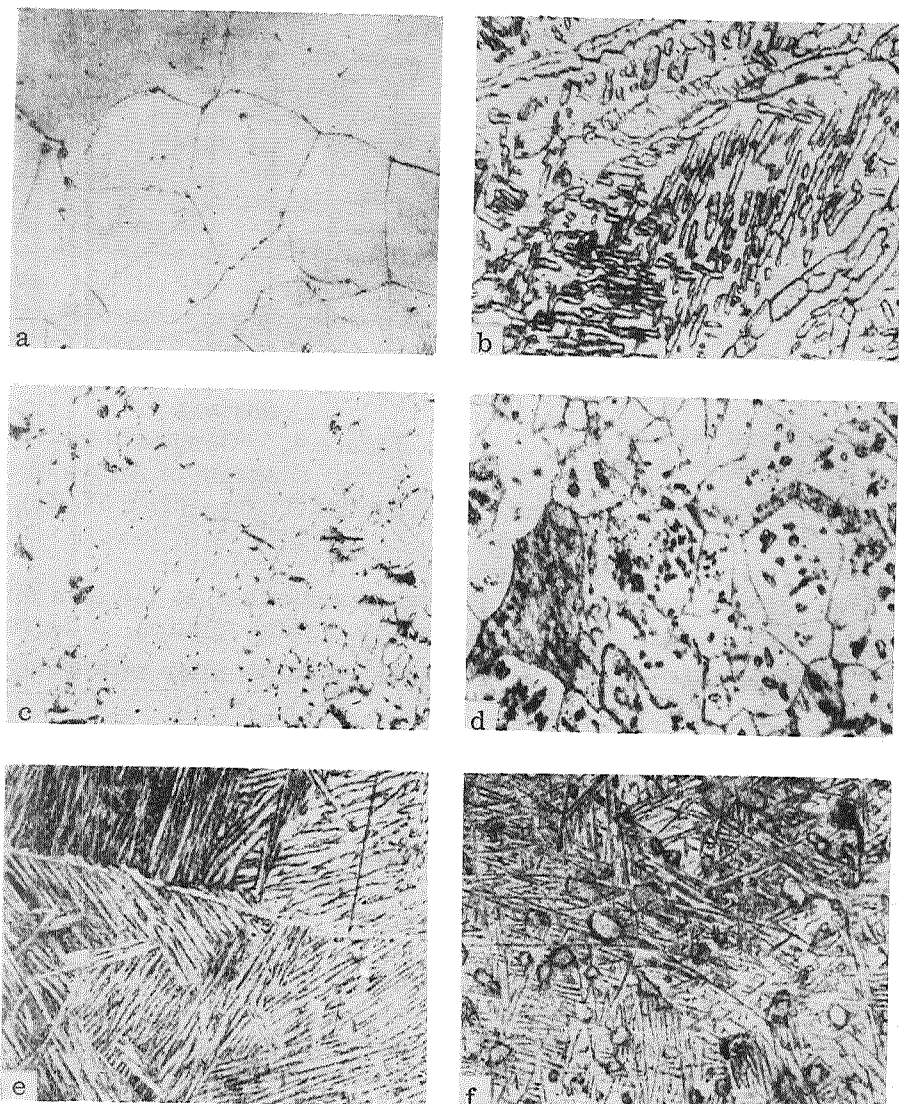


Figure 2. Microstructure of Alloys of the System Ti-Zr-Sn x 200.

Figure	Ti ₃ Sn, %	Treatment	Phases	Figure	Ti ₃ Sn, %	Treatment	Phases
a	10	Annealing	α	d	90	Quenching from 800°C	$\alpha + \delta + \beta$
b	60	:	$\alpha + \delta$	e	10	Quenching from 1000°C	β
c	100	:	δ	f	60	Same	$\beta + \delta$

Figure 4 gives some data on the properties of the alloys as a function of the composition. It is apparent that the resistivity within the confines of the region of the solid solution δ increases smoothly from 1.04 ohm mm²/m for the alloy corresponding to the compound Ti₃Sn to 1.4 ohm mm²/m for the alloy with 90% Ti₃Sn.

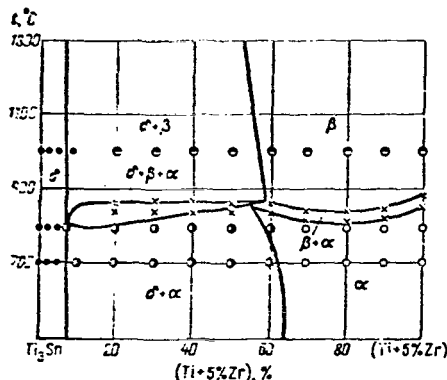


Figure 3. Polythermal Section $Ti_3Sn - (Ti + 5\% Zr)$ of the System $Ti-Zr-Sn$.

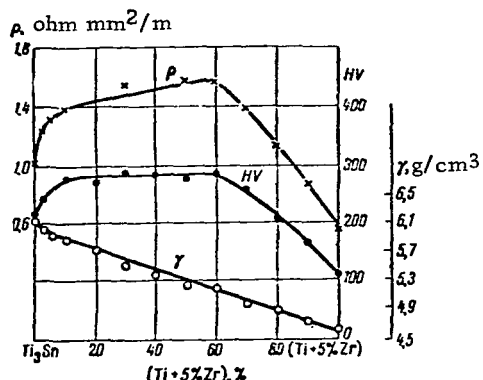


Figure 4. "Composition - Property" Diagram of Alloys of the Section $Ti_3Sn - (Ti + 5\% Zr)$.

In the two-phase region, the resistivity decreases somewhat (to 1.6 ohm mm^2/m for the alloy with 40% Ti_3Sn). In the region of the α solid solution, ρ decreases considerably - to 0.54 ohm mm^2/m for the binary titanium alloy with 5% Zr.

A similar change of hardness is observed within the confines of the one-phase regions. In the two-phase region, the hardness of all the alloys remains perfectly constant.

Within the sensitivity of the method, the density of the alloys decreases linearly from 6.2 g/cm^3 for the compound Ti_3Sn to 4.6 g/cm^3 for the alloy of titanium with 5% Zr.

Thus, the character of the chemical interaction of the elements of the section studied, investigated by methods of thermal and microstructural analyses, was confirmed by the regular change of the properties of the alloys with changing composition and structure.

CONCLUSION

Methods of thermal and microstructural analyses were used to establish the phase regions in the portion of the ternary system $Ti-Zr-Sn$ along the radial section $Ti_3Sn - (Ti + 5\% Zr)$. The established nature of chemical interaction of the elements, analogous to the interaction of titanium with the compound Ti_3Sn in the binary system $Ti-Sn$, was confirmed by studying the dependence of certain properties on the composition and structure of the alloys.

REFERENCES

1. Kornilov, I. I. Izv. Akad. Nauk SSSR, Metallurgiya i gornoye delo, 6, p. 19, 1964.
2. Kornilov, I. I. and T. T. Nartova. Trudy Instituta Metallurgii im. A. A. Baykova, No. 8, Press of Ac. Sci. USSR, 1961.

3. Worner, H.N. J. Inst. Met., No. 81, p. 521, 1953.
4. Finlay, N.L. and R.I. Jaffee. J. Inst. Met., No. 6, p. 25, 1954.
5. Pietrokowsky, P. TASM, No. 49, p. 339, 1957.
6. McQuillan, M.K. J. Inst. Met., No. 84, p. 307, 1956.
7. Kornilov, I.I. and T.T. Nartova. ZhNKh; Vol. 5, No. 3, p. 622, 1960.
8. Glazova, V.V. and N.N. Kurnakov. Collection "Titanium and its Alloys," (Sb. "Titan i yego splavy"), Issue VII, AN SSSR, 1962.
9. Fogel', A.A. Izd. AN SSSR, OTN, Metallurgiya i toplivo, Vol. 2, No. 24, 1959.

STUDY OF THE PHASE EQUILIBRIUM AND PROPERTIES OF ALLOYS OF THE TITANIUM CORNER OF THE SYSTEM Ti-Zr-Al

N. I. Shirokova and T. T. Nartova

An increase in the high-temperature strength of titanium is caused most effectively by elements which form broad regions of solid solutions and intermetallic compounds with titanium.

Such elements include primarily: 1) aluminum, whose role in titanium alloys is as important as that of carbon in steels; 2) zirconium, which forms a continuous series of solid solutions with titanium; 3) tin, which like aluminum forms a broad region of solid solutions and a series of intermetallic compounds with α -Ti.

One of the most promising systems as the base for heat resistant alloys is the ternary system Ti-Zr-Al.

Binary phase diagrams of titanium with zirconium and aluminum have been studied in detail. The structure of the Ti-Zr phase diagram does not leave any doubt: the analog elements form a continuous series of solid solutions of α and β modifications [1]. Thus far, there is no single view regarding the structure of the Ti-Al phase diagram, particularly in the portion rich in titanium. However, all subsequent studies indicate the presence in this system, in addition to the known compounds $TiAl$ and $TiAl_3$ [1], of the intermetallic compound Ti_3Al , characterized by an ordered structure and belonging to Kurnakov-type compounds [2].

The structure and properties of alloys of the ternary system Ti-Zr-Al have been studied by many authors [3-9]. However, the literature contains no data on the phase equilibrium of alloys adjacent to the titanium corner and having the greatest practical importance. For this reason, a part of the ternary system Ti-Zr-Al along the following two sections was chosen for the study:

1) from the composition of a binary alloy of titanium with 5 wt. % Zr on the aluminide Ti_3Al (I); 2) with a constant zirconium content (5 wt. %) and a variable aluminum content up to 16 wt. % (II).

The sections studied are shown in Fig. 1, which also gives a polythermal phase diagram of a portion of the binary system Ti-Al based on data of [2].

The alloys were prepared by using iodide titanium and zirconium of 99.9% purity and aluminum of brand AV000 as the starting materials.

The specimens were prepared by inductive floating fusion in suspension [10] with preliminary melting of the components in an arc furnace with a nonconsumable tungsten electrode in an atmosphere of purified helium. The chemical composition of all the alloys was checked by weighing the ingots after melting in the arc furnace. The waste amounted to no more than 0.6%. Selective chemical analysis of certain alloys showed insignificant deviations from the calculated composition. /102

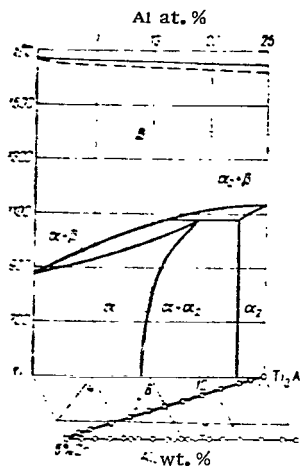


Figure 1. Portion of Concentration Triangle of the System Ti-Zr-Al and Binary System Ti-Al.

In order to achieve equilibrium, cast alloys were subjected to prolonged homogenization at 100°C for 100 hr followed by stepwise annealing according to the following schedule: 900°C, 200 hr, cooling to 800°C, at 800°C soaking for 300 hr, cooling to 700°C at 700°C soaking for 500 hr, cooling in air. Thus, the total anneal time at 1000-700°C was 1100 hr. The heat treatment was carried out in ordinary electric heating furnaces and the specimens were placed in double evacuated quartz ampules.

In the investigation of the phase equilibrium of alloys of the sections studied, use was made of methods of thermal analysis, study of the microstructure, and measurement of certain properties as a function of the composition. The temperature of the start of fusion was determined by the drop method with the aid of an optical pyrometer [11].

In order to plot the boundaries of the phase regions of polythermal sections, data of differential thermal analysis obtained with a Kurnakov parameter were employed. The specimens, previously annealed in accordance with the above-indicated schedule, were heated in air in a resistance furnace at a rate of about 500 deg/hr.

To check the transition points determined by thermal analysis carried out in air, certain alloys were subjected to dilatometric analysis in a vacuum of about 10⁻⁴ mm Hg. Results of this study show a 5-10°C discrepancy with the data of thermal analysis, i.e., a discrepancy within the experimental accuracy. It should be noted that as the aluminum content of the alloys rises, the phase transformations are detected dilatometrically with less accuracy, and above 10% Al, are not detected at all.

The location of the solubility limits was determined by a microstructural study of the specimens subjected to annealing and quenching from different temperatures. After prolonged annealing and quenching from 800°C, specimens of alloys containing up to 40% Ti₃Al (cross section I) and up to 6% Al (cross section II) have the polyhedral structure of an α solid solution (Fig. 2, a). The one-phase structure of the α₂ solid solution based on the compound Ti₃Al is displaced by alloys containing > 90% Ti₃Al (I) and 14% Al (II) (Fig. 2, b). Alloys with 50-80% Ti₃Al (I) and 7-14% Al (II) have the two-phase structure of the mixture of (α + α₂) phases (Fig. 2, c, d). After quenching from 1000°C, the alloys containing up to 30% Ti₃Al (I) and up to 3% Al (II) have a transformed β phase of acicular structure; alloys with 30-50% Ti₃Al (I) and 4-5% Al (II) have the two-phase structure of (α - β) phases (Fig. 2, e); the structure of alloys containing 50-100% Ti₃Al (I) and 7-16% Al (II) is similar to the structure of annealed alloys. Alloys quenched from 1100°C with < 60% Ti₃Al (I)

and < 3% Al (II) have a two-phase structure $\alpha_2 + \beta$ (Fig. 2, f); > 90% Ti_3Al (I) and 15% Al (II) have the structure of the α_2 phase. All the alloys quenched from $1200^{\circ}C$ have a transformed β -phase (Fig. 2, g) of acicular structure.

/105

The form of polythermal cross sections I and II, plotted by using data of thermal and microstructural analysis, is shown in Fig. 3, a and b. In both cross sections, the temperature of the polymorphic transformation rises with increasing aluminum content, and at about 1020 and $1060^{\circ}C$ a peritectoid transformation is observed.

Some data on the properties of alloys of cross sections I and II as a function of composition are shown in Fig. 4, a and b. As is evident from the curves, the electrical resistivity and hardness of the alloys increase smoothly with the range of the α -phase, change only slightly in the two-phase region $\alpha + \alpha_2$, and decrease smoothly in the α_2 region. The density of the alloy decreases linearly with rising aluminum content.

For alloys of cross section II, with a constant zirconium content of 5% and an aluminum content of up to 12%, the high-temperature strength was determined by the centrifugal bending method at $700^{\circ}C$ and $\sigma = 20$ kg/mm². The specimens were prepared by arc melting followed by forging of the ingots into rods 8 mm in diameter at 1000 - $1200^{\circ}C$. After forging, the rods were subjected to annealing at $800^{\circ}C$ for 1 hr with cooling in air. Results of tests shown in Fig. 5 indicate that alloys having the structure of a homogeneous α solid solution of zirconium and aluminum in titanium (with < 8% Al) have an increased creep. The alloy located near the boundary of the two-phase region $\alpha + \alpha_2$ (9 wt. % Al) and after annealing at $800^{\circ}C$ for 1 hr having finally divided separations of the α_2 -phase in the structure, together with α solid solution, has considerably less creep [12]. In the alloy with 10 wt. % Al, the separations of the α_2 -phase are much coarser, and therefore the high-temperature strength of this alloy is considerably less than that of the alloy with 9% Al. In the alloy with 12% Al, the amount of the α_2 -phase is so large that its high-temperature strength becomes predominant.

Alloys containing > 10% Al have an increased brittleness and undergo plastic deformation with difficulty, and for this reason the alloy with 5% Zr and 9% Al was selected for the detailed study. Figure 6 shows results of testing of this alloy for short-time rupture at various temperatures, indicating that the alloy possesses a considerable strength up to $700^{\circ}C$ (80 kg/mm²) with a satisfactory combination of strength and plasticity under room temperature conditions ($\sigma_u \approx 100$ kg/mm², $\delta \approx 5\%$). The data obtained are in good agreement with the results of test performed earlier [6].

SUMMARY

1. Two polythermal sections were plotted in the portion of the ternary system $Ti-Zr-Al$ adjacent to the $Ti-Al$ side, and phase regions of this portion of the equilibrium diagram were established by concerning the formation of the aluminide Ti_3Al in the system $Ti-Al$.

/103

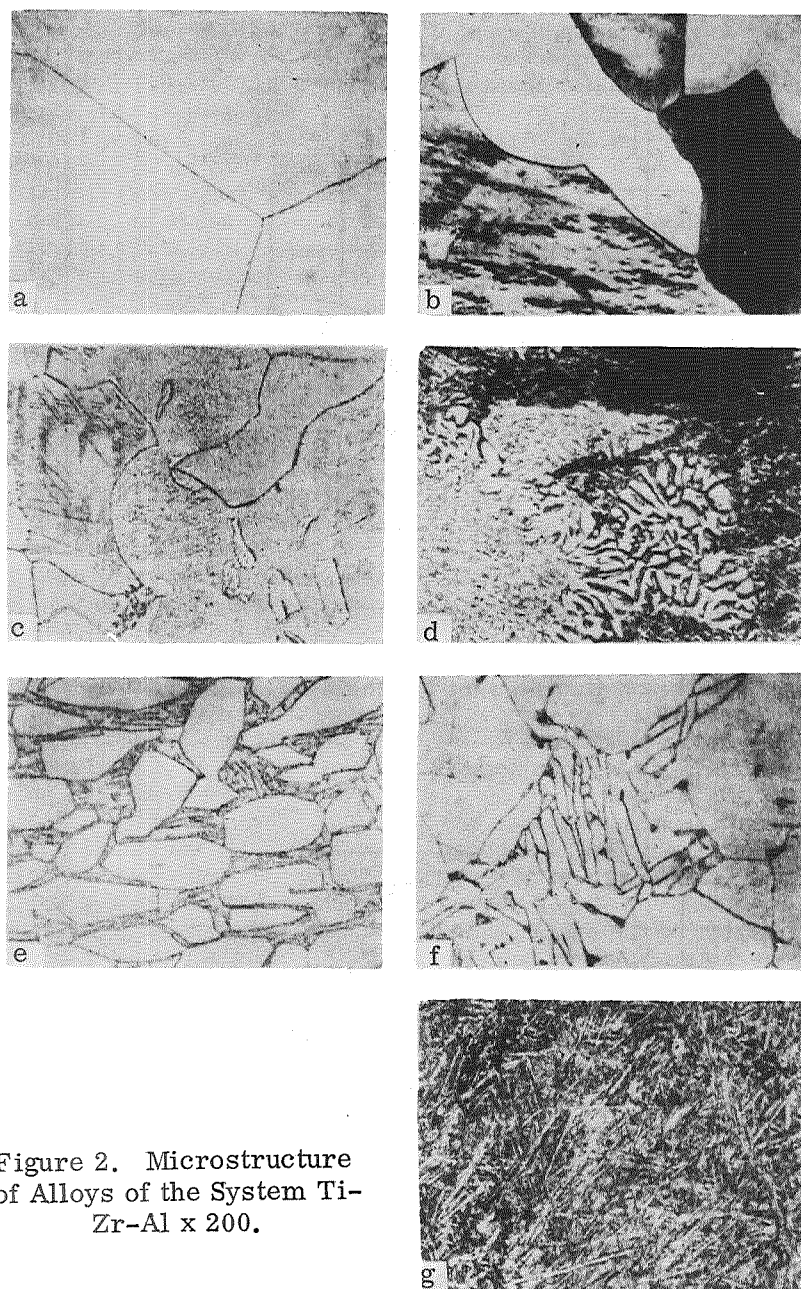


Figure 2. Microstructure of Alloys of the System Ti-Zr-Al x 200.

Figure	Composition, %	Treatment	Phases
a	5% Zr + 4% Al	Annealing	α , α_2
b	95 Ti ₂ Al	•	
c	50 Ti ₂ Al	•	$\alpha + \alpha_2$
d	5% Zr + 13.5% Al	•	$\alpha + \alpha_2$
e	30 Ti ₂ Al	Quenching 1000° C	$\alpha + \beta$
f	90 Ti ₂ Al	from 1100° C to 1200° C	$\alpha_2 + \beta$
g	10 Ti ₂ Al		β

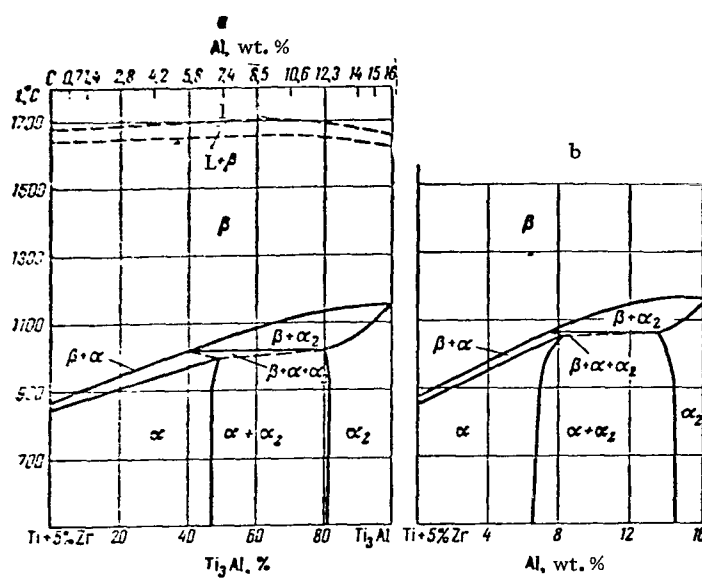


Figure 3. Polythermal Sections of the Systems
 Ti-Zr-Al:
 a—(Ti + 5% Zr) - Ti_3Al ; b—Constant Zirconium
 Content (5%).

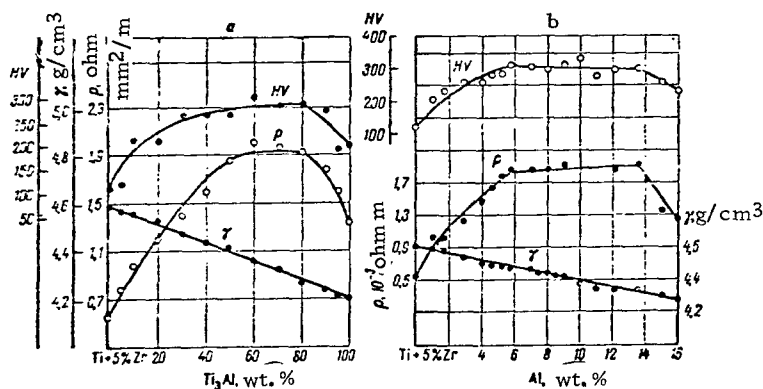


Figure 4. "Composition vs. Property" Diagrams.

a—Cross Section I; b—Cross Section II.

2. The interaction of titanium with zirconium and aluminum in the ternary system Ti-Zr-Al along the sections studied is similar to the interaction of titanium with aluminum in the binary system Ti-Al.

3. The established character of chemical interaction of the components of the sections studied in the ternary system Ti-Ar-Al was confirmed by investigating the properties as a function of the composition.

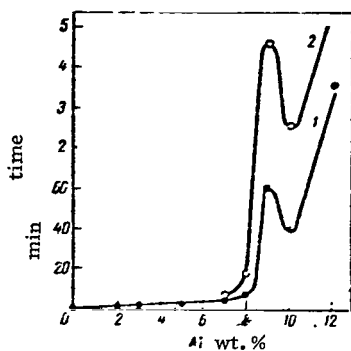


Figure 5. Time Necessary for Quenching a Bending Deflection of 5 (1) and 7 (2) mm Alloys of Section With 5% Zr With Different Aluminum Contents.

$$t = 700^{\circ}\text{C}, \sigma = 20 \text{ kg/mm}^2.$$

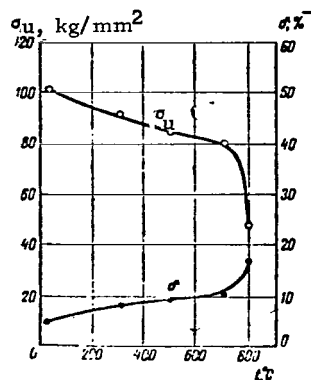


Figure 6. Mechanical Properties of an Alloy of Titanium With 5% Zr and 9% Al at Various Temperatures.

On the basis of centrifugal tests at 700°C and $\sigma = 20 \text{ kg/mm}^2$, the composition was established for an alloy which at 700°C had a short-time strength of 80 kg/mm^2 and at room temperature $\sigma_u \approx 100 \text{ kg/mm}^2$ and $\delta \approx 5\%$. Studies of the alloy continue in order to increase the high-temperature strength by making its chemical composition and structure more complex.

REFERENCES

1. Hansen, M. and K. Anderko. Structure of Binary Alloys, (Struktura dvoynikh splavov), I, II. Metallurgizdat, 1962.
2. Kornilov, I. I. et al. Phase Structure of Alloys of the Binary System Ti-Al Containing from 0 to 30% Al, (Fazovoye stroyeniye splavov dvoynoy sistemy Ti-Al soderzhaschikh ot 0 do 30% Al. Sb. "Novyye issledovaniya titanovykh splavov". (Collection "New Studies of Titanium Alloys.") "Nauka," 1965.
3. Pylayeva, Ye. N. and M. A. Volkova. Collection "Metallurgy of Titanium." (Sb. "Metallovedeniye titana") "Nauka," No. 38, 1964.
4. Kornilov, I. I., T. T. Nartova and M. M. Savel'yeva. Collection "Metallurgy of Titanium," (Sb. "Metallovedeniye titana") "Nauka," No. 43, 1964.
5. Kornilov, I. I. and N. G. Boriskina. Collection "Metallurgy of Titanium." (Sb. "Metallovedeniye titana") "Nauka," No. 4, 1964.
6. Mikheyev, V. S. and K. T. Markovich. "Titanium and its Alloys," (Titan i ego, splavy"), Issue VII. AN SSSR, 1962.
7. Glazunov, S. G. and L. P. Solonina. Collection "Titanium in Industry." (Sb. "Titan v promyshlennosti") Oborongiz, No. 73, 1961.
8. Ingram, A. G., D. N. Williams and H. R. Ogden. Effect of Zr and Hf ternary additions on the tensile and creep properties of titanium-aluminum alloys. Trans. Quarterly, Vol. 55, No. 1, March, 1962.
9. Williams, D. N. a. o. "The development of high-strength alpha-titanium alloys containing aluminum and zirconium". Trans. Metallurgical Society of AIME, No. 227, 1963.

10. Fogel', A.A. Izv. Akad. Nauk SSSR, ONT, Metallurgiya i toplivo, Vol. 2, No. 24, 1959.
11. Meyerson, G.A., G.V. Samsonov and M.M. Borisov. Zavodskaya Laboratoriya, Vol. 19, No. 2, p. 243, 1959.
12. Kornilov, I.I. Physicochemical Principles of High-Temperature Strength of Alloys, (Fiziko-khimicheskiye osnovy zharoprochnosti splavov), AN SSSR, 1961.

NATURE OF HYDROGEN BRITTLENESS OF TITANIUM AND ITS ALLOYS

B. A. Kolachev and V. A. Livanov

Analysis of experimental data obtained by the authors in a study of the influence of hydrogen on the structure and properties of metals [1, 2] and their comparison with results obtained by other authors [3-18] show that materials display different types of hydrogen brittleness according to the different nature of their interaction with hydrogen and the difference in the nature of the phases thus formed. The types of brittleness may be classified according to the dependence on the deformation rate of the tendency toward a given type of hydrogen brittleness, and according to their reversibility or irreversibility of the process of fracture. However, the fullest and most logical classification may be worked out if the sources of hydrogen brittleness are taken as the reference. A classification of the types of hydrogen brittleness of metals based on this criterion is given in Table 1.

The table also indicates the dependence of the type of brittleness on the deformation rate, its nature, and also the metals in which brittleness of a given type is observed.

In titanium and its alloys, the pressure of molecular hydrogen in a discontinuity within the metal is negligibly low, and for this reason brittleness types caused by a high hydrogen pressure are not observed therein. The development of hydrogen disease in titanium and its alloys is also excluded. The remaining forms of hydrogen brittleness in titanium and its alloys can develop to their full extent.

1. Nature of Brittleness of the First Kind

/107

a) Hydride Brittleness (Brittleness of Third Type)

In titanium and α -titanium alloys, the predominant form of hydrogen brittleness is hydride brittleness. The solubility of hydrogen in titanium and α -titanium alloys is low, and therefore at hydrogen concentrations prevailing in practice, separations of hydride phase appear in their structure which cause brittleness. Hydride brittleness manifests itself most distinctly in impact strength tests (Fig. 1); it begins to develop at the concentration at which hydride separations appear in the structure. Hydride brittleness manifests itself in tests for impact strength, but it has little effect on the properties of the metal in tensile tests at low rates. The authors of [23] explain this regularity by postulating that titanium hydrides possess a certain plasticity and therefore, when the specimens are stretched at a low rate, the lamellae of hydrides are bent, and the stress concentration decreases. Metallographic analysis of characteristic areas of the deformed zone at various stages of the breakdown showed that the hydride lamellae do indeed possess a certain pliability and, at a low bending rate, are deformed together with the matrix without forming cracks at the ends of the hydride lamellae.

/108

At a high bending rate, cracks develop along the interface between the metal and the hydride lamella. Thus, hydride lamellae in the microstructure are the

TABLE 1. HYDROGEN BRITTLENESS

Type	Relationship to deformation rate	Character	Sources
Brittleness of first kind, caused by sources which are created by hydrogen in the original metal	Reinforced with increasing deformation rate	Irreversible	<ol style="list-style-type: none"> 1. Products of interaction of hydrogen with impurities with formation of a high pressure gas within the metal (hydrogen disease, hydrogen corrosion, Cu, Ag, Fe, Steels). 2. High pressure of molecular hydrogen (steel, Ni, Cu, Mg). 3. Hydride brittleness (U, Ta, Zr, Nb, V, Ti, titanium alloys). 4. Cold shortness caused by dissolved hydrogen (nb, V, ($\alpha + \beta$) - and β- titanium alloys).
Brittleness of second kind caused by sources arising in the metal with an elevated hydrogen concentration in the course of plastic deformation	Manifests itself in a certain range of deformation rates	Irreversible Reversible	<ol style="list-style-type: none"> 5. Breakdown of solid solutions supersaturated relative to hydrogen (Zr, Ti; α- and ($\alpha + \beta$)-titanium alloys). 6. Transport of hydrogen atoms by dislocations (all metals with appreciable solubility of hydrogen). 7. Directed diffusion of hydrogen atoms (all metals with appreciable solubility of hydrogen)

source of Griffiths cracks which develop upon application of stress because of weak bonding between the precipitate and the main phase and as a result of differences in their elastic and plastic properties. The formation and propagation of cracks are facilitated in this case by tensile stresses which appear at the ends of the hydride precipitates because the specific volume of the hydrides is greater than that of the base metal.

The data listed in Fig. 2 show that the dependence of the breaking stresses σ_p on the linear dimensions of the grain d may be described by Pech's equation

$$\sigma_p = \sigma_0 + Kd^{-1/2}; \quad K = \left(\frac{6\pi G_1}{1-\mu}\right)^{1/4}. \quad (1)$$

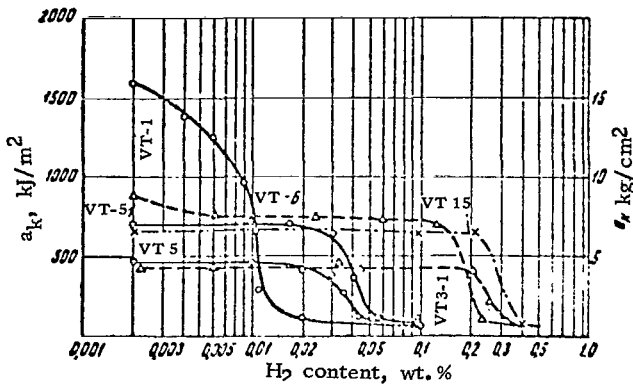


Figure 1. Effect of Hydrogen on the Impact Strength of Titanium and Its Alloys.

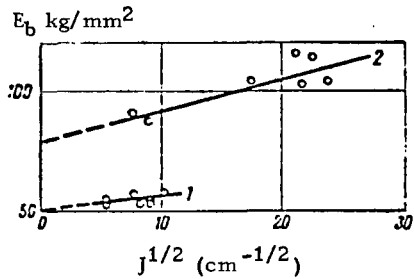


Figure 2. Dependence of True Breaking Stresses of Titanium with 0.03% Hydrogen on the Length of Hydride Lamellae at a Deformation Rate of $2.7 \times 10^{-3} \text{ sec}^{-1}$;

1 - Hydrides Impregnating All of the Grain; 2 - Length of Hydrides Less than the Grain Size.

where σ_0 is a stress independent of the grain size; G is the shear modulus; γ is the surface energy; μ is Poisson's ratio. In this case, when the hydrides impregnate all of the grain, the quantity σ_0 characterizes the breaking stress along the hydride - titanium interface. The magnitude of σ_0 turns out to be 50 kg/mm^2 at a surface energy $\gamma = 300 \text{ erg/cm}^2$. For titanium, the surface energy is equal to 1000 ; 200 erg/cm^2 , so that the fracture along the titanium-hydride interface takes place with more ease than along the spalling planes in titanium.

If the hydrides are smaller than the size of the micrograin, they facilitate the propagation at cracks only with the grain and have little influence on the effective surface energy determining the propagation of cracks across grain boundaries. The breaking stresses in this case can also be described by the Pech's equation but σ_0 and γ no longer characterize the hydride-titanium interface, but titanium itself.

The experimental points are in good agreement with this equation at $\sigma_0 = 87 \text{ kg/mm}^2$ and $\gamma = 1350 \text{ erg/cm}^2$ (this value is fairly close to the surface energy of titanium).

b) Cold Shortness Caused by Dissolved Hydrogen (Brittleness of Fourth Type)

The hydrogen brittleness which develops at high deformation rates in $(\alpha + \beta)$ - and β -titanium alloys and also in niobium begins to manifest itself at concentrations much longer than those at which hydride separations appear. Thus, in VT-15 alloy, hydrogen brittleness develops at 0.25% hydrogen, and the first separations of hydrides appear at 0.5 wt. % hydrogen.

The following two regularities are characteristic of hydrogen brittleness of this type: 1) the impact strength of the specimens remains almost unchanged up to certain hydrogen concentrations, then decreases abruptly to very slow values; 2) the hydrogen

concentration at which the plasticity decreases markedly diminishes with dropping temperature (Fig. 3).

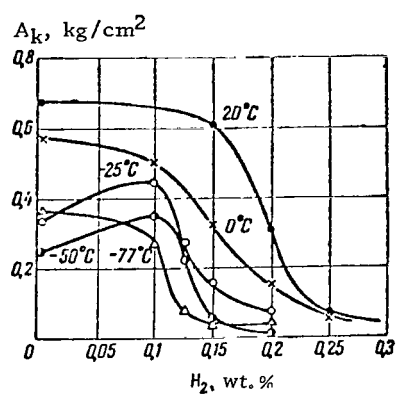


Figure 3. Dependence of the Impact Strength of VT-15 Alloy on the Hydrogen Content and Testing Temperature.

dislocations; t_0 is the time necessary for generating the crack; b is the Burgers vector; u is the activation energy of extraction of dislocations from Cottrell atmospheres.

Because of the double exponential dependence, this equation explains the marked decrease of viscosity with decreasing temperature: the probability of brittle fracture changes sharply from negligibly low values at high temperatures to values close to unity at low temperatures.

Unfortunately, no analytical expression has thus far been derived for the dependence of the temperature of cold shortness on the impurity content, although this interrelationship can be readily explained in qualitative terms. According to Cottrell [19], the temperature T_c of condensation of impurity atmospheres is given by the equation

$$T_c = \frac{u}{k \ln 1/C_0},$$

where u is the energy of interaction of impurity atoms with dislocations and C_0 is the average content of impurities in atomic fractions. It follows from this equation that as the temperature is lowered, there is decrease in the impurity concentration at which the formation of Cottrell atmosphere blocking dislocations begins, and cold shortness begins to manifest itself.

Figure 4 shows the dependence of the temperature of condensation of Cottrell atmospheres on the average hydrogen concentration of the metal, assuming that $u = 0.08$ eV (curve 1). The same figure shows the dependence of the temperature

These regularities are characteristic of cold shortness caused by such impurities as oxygen and nitrogen, and therefore the decrease of the impact strength of $(\alpha + \beta)$ - and β -alloys and also of niobium can be explained by drawing an analogy between the hydrogen brittleness of the type considered and cold shortness.

Stroh [21] has shown that the probability of brittle fracture may be expressed by the equation

$$P = \exp \left[-\frac{v l t_0}{b} \exp \left(-\frac{u}{kT} \right) \right], \quad (2)$$

where v is the vibration frequency of the atoms; l is the length of the source of

dislocations; t_0 is the time necessary for generating the crack; b is the Burgers

vector; u is the activation energy of extraction of dislocations from Cottrell

atmospheres.

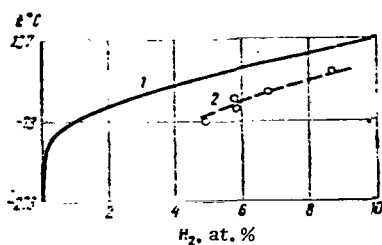


Figure 4. Dependence of the Temperature of Cold Shortness of VT-15 Alloy on the Hydrogen Content.

of cold shortness of VT-15 alloy on the hydrogen content (curve 2). The criterion taken for cold shortness was the temperature at which the impact strength is cut by one-half. These two dependences are qualitatively similar, but the cold shortness temperatures lie considerably below the temperatures of condensation of Cottrell atmospheres. Obviously, this discrepancy is due to the fact that the cold shortness begins to manifest itself only when the density of the hydrogen atmosphere is sufficiently high (at least greater than 1 atom of impurity per atom of metal at the edge of the extraneous half-plane).

2. Hydrogen Brittleness of the Second Kind

a) Irreversible Brittleness of the Second Kind (Hydrogen Brittleness of Fifth Type)

If a solid solution saturated with hydrogen becomes fixed in the specimens, they have no tendency toward hydrogen brittleness in high rate deformation. In low rate deformation, solid solutions decompose with the formation of lamellar separates of hydrides, which cause brittleness. Brittleness of this type may also develop under prolonged action of stresses in static loading.

In titanium and its alloys, the diffusion of hydrogen takes place at high rates, and therefore on quenching from the one-phase region, the hydrides may partially separate from the solid solution. In this case, hydrogen brittleness is observed in deformation at a high as well as a low rate. Excess separations of hydrides cause the appearance of hydrogen brittleness of metals in deformation at high rates, and a solid solution supersaturated with hydrogen leads to brittleness in deformation at low rates.

In quenched specimens of α -alloys of VT5 and VT5-1 after deformation at a low rate, a considerable amount of hydrides oriented perpendicular to the axis of extension was observed in the vicinity of the surface of fracture. The same type of oriented separation of hydrides was observed by Louthan in titanium [24] in hydrogenation of specimens with simultaneous action of stresses. The density of hydrides is less than that of metals, and therefore the separation of hydride lamellae perpendicular to the tensile stresses removes the stresses in the matrix and thereby decreases the free energy of the system. In tensile tests, hydride lamellae perpendicular to the axis of tension embrittle metals more markedly than lamellae oriented parallel to the tensile stresses.

b) Hydrogen Brittleness Caused by the Transport of Hydrogen by Dislocations (Hydrogen Brittleness of Sixth Type)

/111

The most complex is the nature of reversible brittleness of the sixth type, which develops in most characteristic form in $(\alpha + \beta)$ - and β -titanium alloys in deformation at low rates.

The following regularities are characteristic of hydrogen brittleness of this type.

1. A decrease in plasticity shows up in a certain temperature range.
2. The plasticity drop is most pronounced at a certain definite deformation rate. A decrease and increase of deformation rate as compared with this value leads to a decrease of the plasticity drop.
3. The plasticity drops are shifted toward higher temperatures with increasing deformation rate.
4. As the hydrogen content rises, the plasticity drops are reinforced, and the upper temperature at which hydrogen brittleness appears is shifted to higher values.

The hypotheses of hydrogen brittleness given in [7, 16, 18] for $(\alpha + \beta)$ alloys do not explain all the basic regularities of the hydrogen brittleness of the sixth type, and particular arise when attempts are made to explain its reversibility.

In refining the nature of reversible hydrogen brittleness of the sixth type, the authors proceeded from the fact that brittleness of this type develops in many metals independently of their crystal structure. Brittleness of this type is observed in metals which absorb hydrogen endothermically, for example, in iron and nickel, and in exothermically absorbing metals such as titanium, vanadium, niobium and tantalum. In the first case, at temperatures at which reversible brittleness develops, hydrogen generates huge internal pressures, and in the second case this pressure is negligibly low. The basic problems of reversible hydrogen brittleness are the same for all the metals regardless of whether hydrides are or are not formed therein. The specific electronic structure of the transition metals has no determining significance either, since brittleness of this type is also observed in nontransition metals, particularly in magnesium alloys [5].

There should be a common feature in the mechanism of the hydrogen brittleness of these metals, a feature independent of their crystal structure or internal hydrogen pressure or the presence of hydrides or the electronic structure, although there is no doubt that these factors have substantial influence on the details of this mechanism.

In [6, 9], an attempt was made to explain the basic features of reversible hydrogen brittleness from the standpoint of dislocation theory. According to the hypothesis given in the study, reversible hydrogen brittleness of the sixth type is due to the fact that the new dislocations formed in plastic deformation at low deformation rates interact with hydrogen atoms, forming Cottrell atmospheres, which they carry along behind them in their motion. The plasticity of the metals decreases: a) because the hydrogen atmospheres slow down the motion of dislocations and thereby increase the glide resistance of the dislocations, b) because of transport of hydrogen atoms by dislocations on the grain boundaries or other obstacles where, if dislocations pile up, the concentration of hydrogen becomes sufficient for a marked acceleration of the generation and propagation of cracks leading to fracture of the metal.

The reversible nature of this brittleness may be explained by the fact that if the load is removed prior to the instant of appearance of cracks, thermal diffusion will gradually equalize the hydrogen concentration throughout the volume of the metal.

Hydrogen brittleness which develops at low deformation rates manifests itself in a definite temperature range. At temperatures that are too low, the mobility of hydrogen atoms is so small that they are not carried along by the moving dislocations and do not affect the plasticity of the metal. As the temperature rises, the mobility of hydrogen atoms increases, and at a certain temperature becomes comparable to the rate of motion of dislocation at the same deformation rate $\dot{\varepsilon}$. Beginning at this temperature, the dislocations partially carry along the hydrogen atmospheres behind them, and the plasticity decreases (Fig. 5). At a certain temperature, the hydrogen atmospheres are completely carried along by the dislocations and hydrogen brittleness develops to its fullest extent.

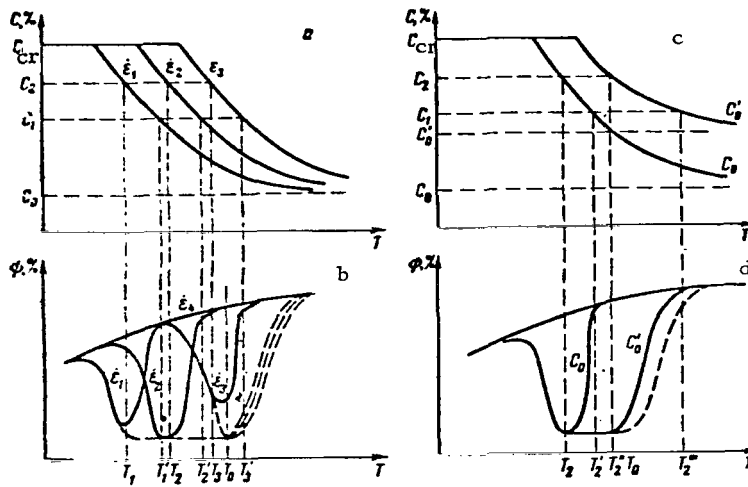


Figure 5. Hydrogen Concentration in the Region of Pile-Up of Dislocations (a) and Plasticity of Hydrogenated Specimens (b) Versus Testing Temperature, c and d-Dia-grams.

The critical rate $\dot{\varepsilon}_{cr}$ at which the atmospheres are completely entrained by the moving dislocations is given by the equation

$$\dot{\varepsilon}_{cr} = \frac{4D_0Nb}{A} kTe^{-\frac{Q}{kT}}, \quad (3)$$

where A is a quantity connected with the energy of interaction of the impurities with the dislocations (u_0) by the relation $A = u_0 d$ (d is the dislocation width); E_0 is the exponential factor in the expression relating the diffusion coefficient of the impurity and the temperature; N is the density of dislocations participating in the

slip; b is Burger's vector; k is Boltzmann's constant; T is the absolute temperature; Q is the activation energy in the diffusion of hydrogen in the metal.

At sufficiently high temperatures, hydrogen brittleness of the sixth type does not develop. The temperature at recovery of plasticity of metals may be estimated as follows. Let us assume that the region of higher hydrogen concentration around the dislocation pile-up is in the shape of a cylinder of radius r_0 . If the rate of displacement of dislocations is v , the number of dislocations reaching the pile-up in time $d\tau$ is $\frac{v}{a}d\tau$ where a is the distance between dislocations in the glide plane. In time $d\tau$, these dislocations will supply $\beta n \frac{v}{a} dld\tau$ of hydrogen to a pile-up of length dl , where β is the weight of the hydrogen atom and n is the number of hydrogen atoms transported by a dislocation of unit length. According to [22], the amount of hydrogen n , transported by a unit length of dislocation line, may be expressed as $n_0 p$, where n_0 is the density of hydrogen atmospheres under saturation conditions and p is the probability that the impurity atoms will be located at the edge of the extraneous half-plane. The quantity p is given by the equation

$$p = \frac{1}{\frac{1}{C_a} e^{-\frac{u_0}{kT}} + 1} \quad (4)$$

where C_a is the average atomic fraction of hydrogen in the metal.

Considering that $\dot{\epsilon} = N\dot{v}$, we find that the following amount of hydrogen is supplied to the volume of pile-up dV in time $d\tau$

$$dm_1 = B_1 p \dot{\epsilon} d\tau dV,$$

where

$$B_1 = \frac{\beta n_0}{\pi r_0^2 N b a}.$$

Simultaneously with the transport of hydrogen atoms by dislocations toward the pile-up, there is the action of diffusion, which tends to distribute hydrogen uniformly over the entire volume. This factor will decrease the hydrogen concentration in the cylinder. The amount of hydrogen escaping from the cylinder considered in time $d\tau$ will be, according to the diffusion laws,

$$dm_2 = -D \Delta c dV d\tau$$

The remaining hydrogen will increase the hydrogen concentration by an amount dc in time $d\tau$ in volume dV . Thus,

$$B_1 n \dot{\epsilon} d\tau dV = -D \Delta c dV d\tau + dc dV,$$

whence we find

$$\frac{dc}{d\tau} = B_1 n \dot{\epsilon} + D \Delta c. \quad (5)$$

If equation (5) is translated into cylindrical coordinates and considering that $dc/dr = 0$ and $d^2c/dr^2 = 0$, the differential equation determining the change of hydrogen concentration in a cylinder of radius r_0 will assume the form

$$B_1 n \dot{\epsilon} + D \frac{1}{r} \frac{dc}{dr} + D \frac{d^2c}{dr^2} = \frac{dc}{d\tau}. \quad (6)$$

This equation is in full agreement with the differential equation of thermal conductivity in the presence of internal heat sources with the following conditions:

initial condition at $\tau = 0$ with $(0, r) = c_0$,

boundary condition for any $\tau dc/dr = 0$ (at $r = 0$)

To simplify the problem, we shall assume that at least in a cylinder of radius r_0 a steady-state distribution of hydrogen is established fairly rapidly, and for any τ , $c(r_0) = c_0 + \frac{c(r=0) - c_0}{2}$. In this case, the solution of equation (6) give the following expression for the maximum hydrogen concentration in the region of the dislocation pile-up: 114

$$C_{\max} = C_0 + \frac{\frac{Q}{B \dot{\epsilon} n_0 e^{-\frac{Q}{kT}}}}{1 + \frac{1}{C_0} e^{-\frac{Q}{kT}}} \quad (7)$$

$$B = \frac{503}{\pi N b D_0 \rho},$$

where C_0 is the average concentration of hydrogen in the metal (wt. %); ρ is the density of the metal.

It follows from this equation that as the deformation temperature is lowered, the hydrogen concentration in the region of pile-ups increases. Figure 5, a shows the basic shape of the curves illustrating the change of hydrogen concentration in the region of a dislocation pile-up in accordance with the equation (7) for three deformation rates. Essentially, the explanation of brittleness of the sixth type amounts to the following: owing to the transport of hydrogen atoms by dislocations in the region of a dislocation pile-up, a hydrogen concentration is generated before the obstacles at which the development of brittleness of the first kind is possible. Therefore, brittleness of the sixth type begins to develop when the hydrogen concentration in the pile-up reaches the same value c_1 at which under conditions of

uniform distribution of hydrogen throughout volume of the metal, brittleness of the first kind begins to appear and develops to a full extent if the hydrogen concentration in the pile-up reaches a value c_2 , when a pronounced brittleness of the first kind appears.

Thus, the relationship between the temperature corresponding to the minimum plasticity and the deformation rate may be expressed by the equation

$$\dot{\varepsilon} = \frac{(c_2 - c_0) \left(\frac{1}{C_a} e^{-\frac{u}{kT}} + 1 \right)}{B n_0 e^{Q/kT}}. \quad (8)$$

The temperature of complete recovery of plasticity may be found from a similar expression by substituting c_1 for c_2 .

The diagram given in Fig. 5, b shows that as the deformation rate increases, the plasticity drops caused by reversible hydrogen brittleness should lift toward higher temperatures, and at the same time their magnitude decreases.

Analysis of equations (3) and (8) shows that the temperature at which the hydrogen atmospheres begin to be completely trapped decreases less sharply with decreasing deformation rate than the temperature at which the hydrogen concentration in the region of the pile-up, because of thermal diffusion, becomes less than the value necessary for the complete development of brittleness. Thus, as the temperature of the test (deformation at relatively low rates) is raised, the thermal dissipation of hydrogen segregations in the region of the dislocation pile-up begins to exert its influence before the moving dislocations completely trap the hydrogen atoms, and the plasticity drop will be completely absent or will be less.

Thus, the plasticity should be restored not only in the course of tests at very low temperatures, but also during deformation at rates that are too low. In other words, brittleness of the type considered should be observed not only in a certain range of temperatures but also in a certain range of deformation rates.

We shall now examine the manner in which the hydrogen content effects the nature of the curves illustrating the dependence of plasticity on the temperature of the tests. From equation (7) it follows that for hydrogen contents c_0 and c'_0 , the hydrogen concentration in the region of pile-ups will change in accordance with the curves shown in Fig. 5, c.

As the temperature of the tests for a given hydrogen content is raised, the plasticity begins to decrease at approximately the same temperature, since in the first approximation the critical deformation rate is independent of the hydrogen content. However, in specimens with a lower average hydrogen concentration, the thermal dissipation decreases the hydrogen concentration in the region of the dislocation pile-up to values which do not result in brittleness, at lower temperatures than in specimens with a higher average concentration. In summary, as the hydrogen content increases, the curves illustrating the dependence of plasticity on the testing temperature will change in accordance with the diagram shown in Fig. 5, d.

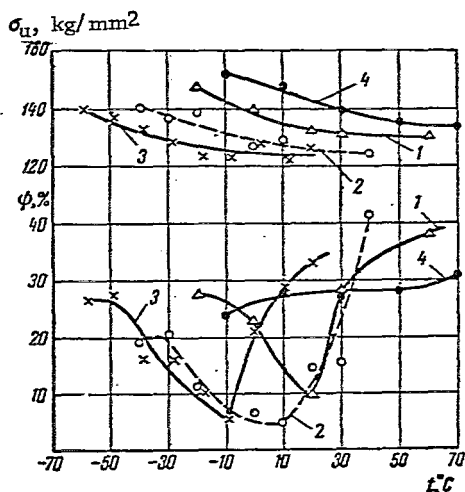


Figure 6. Effect of Temperature of the Specimen on the Properties of Alloy VT3-1:

Deformation Rate, sec^{-1} : 1. 35×10^{-2} (1); 2.7×10^{-3} (2); 2.7×10^{-4} (3); 4×10^{-2} (4).

obstacles may facilitate the opening of cracks for at least three reasons: a) hydrogen distorts the metal lattice and thus prevents the scattering of energy of pile-up of dislocations because of plastic deformation, b) as a result of absorption of hydrogen on the surface of the crack, the surface energy decreases, c) the local hydrogen concentration in the region of the dislocation pile-up becomes sufficient for the formation of the submicroscopic hydride separations.

The decrease of cohesive forces upon introduction of hydrogen cannot account for the easier generation of cracks in hydrogen-saturated specimens, at least in the case of titanium, titanium alloys and niobium, since our experiments have shown that hydrogen has little influence on the elastic moduli of these materials.

/116

Hydrogen also facilitates the growth of a crack which has formed. Orován [25] and Mac Lean [26] contend that cracks in metals grow as a result of attraction of dislocations to the mouth of the cracks. Emergence of dislocations at the surface of the crack increases its size. In this case, hydrogen may facilitate the propagation of the crack for the same reason as it facilitates its generation, i. e., because of the transport of hydrogen atoms by dislocation to the mouth of the growing crack.

Of great interest are data on the influence of hydrogen on the nature of propagation of cracks in β -titanium alloy VT15, obtained by N. Ya. Gusel'nilov. In specimens of VT15 alloy within hydrogen in the vicinity of surface of fracture, no additional cracks were present, and in hydrogen specimens they are fairly numerous, and the dimensions of the cracks are frequently circumscribed by the boundaries of a single grain (Fig. 7). This indicates that hydrogen markedly facilitates the generation and propagation of cracks within the confines of a single grain.

Thus, the proposed hypothesis explains all the basic features of hydrogen brittleness of the sixth type. As an example concerning this hypothesis, Fig. 6 shows the influence of the temperature of the specimen on the properties of alloy VT3-1 with 0.03% H_2 in deformation at different rates. In plotting the graph given in Fig. 6, account was taken of the fact that heat is evolved during the deformation, and therefore in deformation at high rates, the temperature of the specimen is higher than that of the cooling medium.

The nature of the influence of hydrogen on the dislocation mechanism of generation of cracks should be different metals. In titanium and other metals which absorb hydrogen exothermically, the internal pressure is very low and cannot stimulate the formation and propagation of cracks. In these metals, hydrogen transported by the dislocations toward



Figure 7. Characteristic Cracks in VT15 Alloy with 0.03% Hydrogen in the Vicinity of the Surface of Fracture After a Tensile Test at a Rate of $2.7 \times 10^{-4} \text{ sec}^{-1}$ at -18°C .

Cracks in hydrogenated specimens of VT15 alloy are not generated along the grain boundaries but within them, apparently because of displacement of dislocations in intersecting glide planes and their coalescence at the point of encounter (according to Cottrell's mechanism).

In hydrogenated specimens there is a simultaneous development of a number of cracks, each of which constitutes a complex branched structure with a single main crack from which numerous cracks of various sizes branch out. Comparison of this pattern with the character of stress-strain diagrams shows that the process of development of cracks in VT15 alloy with hydrogen should be regarded as a sequential alternation of brittle development of cracks owing to the accumulation of elastic energy with viscous development of cracks due to plastic deformation at the mouth of the crack.

c) Reversible Hydrogen Brittleness Caused by Directed Hydrogen Diffusion (Brittleness of Seventh Type) /117

In tests for static fatigue in tension or bending, the presence of hydrogen sharply decreases the time to fracture at stresses lower than the yield point.

The following characteristics are typical of brittleness of this type [15]:

- 1) the decrease of durability is reversible in character;
- 2) the long-time strength decreases only in a certain range of temperatures and stresses. Accelerated static fatigue in the presence of hydrogen disappears at temperatures and stresses that are too high and too low.

In keeping with the ideas of B. Ya. Pines [20], brittle fracture under static load at stresses below the yield point is explained by the growth of incipient cracks determined by the diffusion of vacancies toward them.

The decrease of the static fatigue of hydrogenated specimens may be explained by the fact that the behavior of hydrogen atoms and vacancies is similar: the combined diffusion of hydrogen atoms and vacancies toward metal defects including grain boundaries decreases the long-time strength more extensively than the diffusion of the vacancies alone does. As was shown by studies made by the authors, in the course of tests for static bending at stresses less than the yield point, the hydrogen atoms are displaced into the stretched portion of the specimens as a result of ascending diffusion (Table 2), and the progressing segregation of hydrogen in the region of the stretching accelerates the fracture.

TABLE 2. HYDROGEN CONCENTRATION ON
 THE SURFACE OF TITANIUM SHEETS 2 mm
 THICK AFTER BENDING AT DIFFERENT
 TEMPERATURES IN THE COURSE OF 500 hr
 (DISTANCE BETWEEN SUPPORTS 100 mm)

Temperature, °C,	Load, kg,	Hydrogen concentration (wt. %) on the surface	
		Convex (region of extension)	Concave (region of compression)
20	6	0.019	0.014
20	12	0.024	0.017
100	6	0.025	0.019
200	6	0.024	0.018

The directed diffusion of hydrogen in a stress field may be responsible for the appearance of cracks in weld joints and ingots. Cracks in ingots and weld joints begin to arise at average hydrogen concentrations at which hydrogen brittleness does not develop [14]. However, because of the directed diffusion of hydrogen atoms in the field of thermal stresses in certain volumes of the metal, the local hydrogen concentration may be considerably below the average value. The combined action of the segregation of hydrogen, promoting the development of brittleness, and of thermal stresses leads to the generation of cracks.

An uneven distribution of hydrogen in the metal also arises from an inhomogeneous thermal field. As was shown by studies made by the authors, hydrogen in titanium and its alloys moves from regions of higher temperature to regions of lower temperature (Table 3). The progressing migration of hydrogen into colder parts of the specimen or article may also lead to brittleness at average concentrations which are considered safe. Thermal diffusion of this kind may occur in the welding and operation of finished articles.

TABLE 3. HYDROGEN CONCENTRATION (wt. %)
 AT THE ENDS OF RODS 100 mm LONG AFTER
 HEATING FOR 250 hr IN AN INHOMOGENEOUS
 THERMAL FIELD

Temperature of ends of specimen, °C	Alloy		
	VT1-1	VT3-1	VT15
600	0.011	0.0137	0.0117
400	0.0143	0.0160	0.0183

SUMMARY

Hydrogen brittleness observed in titanium and its alloys may be subdivided into five types:

1. Hydride brittleness developing at high deformation rates in the presence of visible precipitates of hydrides in titanium and its alloys.
2. Cold shortness, caused by the presence of dissolved hydrogen. This brittleness is observed at high deformation rates in $(\alpha + \beta)$ - and β -titanium alloys at high hydrogen concentrations without hydride separations visible under optical magnification.
3. Irreversible hydrogen brittleness developing at low extension rates as a result of decomposition of solid solutions supersaturated with hydrogen.
4. Reversible hydrogen brittleness developing in titanium alloys under deformation at relatively low rates over a certain temperature range as a result of transport of hydrogen atoms by dislocations in the region of generation of cracks.
5. Reversible brittleness caused by directed diffusion of hydrogen in fields of various types (inhomogeneous stresses, thermal gradients).

REFERENCES

1. Livanov, V. A., A. A. Bukhanova and B. A. Kolachev. Vodorod v titane (Hydrogen in Titanium), Metallurgizdat, 1962.
2. Kolachev, B. A. Vodorodnaya khrupkost' tsvetnykh metallov (Hydrogen Embrittlement of Nonferrous Metals), Metallurgizdat, 1966.
3. Karpenko, G. A. and R. I. Kripyakevich. Vliyaniye vodoroda na svoystva stali (Effect of Hydrogen on the Properties of Steel), Metallurgizdat, 1962.
4. Cottrell. Vodorodnaya khrupkost' metallov (Hydrogen Embrittlement of Metals), Metallurgizdat, 1963.
5. Kolachev, B. A. et al. Tsvetnyye metally (Nonferrous Metals), No. 8, 1966.
6. Kolachev, B. A., V. A. Livanov and A. A. Bukhanova. Sb. Metallovedeniye titana (Collection "Metallurgy of Titanium"), "Nauka," No. 88, 1964.

7. Kornilov, I. I., S. G. Glazunov and L. M. Yakimova. FMM, 370, 1959.
8. Moroz, L. S. and Yu. D. Khesin. Sb. Nekotoryye problemy prochnosti tverdogo tela (Collection "Some Problems of the Strength of Solids"), AN SSSR, 140, 1959.
9. Kolachev, B. A. et al. Sb. Novyye issledovaniya titanovykh splavov (Collection "New Studies of Titanium Alloys"), "Nauka," 212, 1965.
10. Yagunova, V. A. and K. V. Popov. Sb. Issledovaniya po zharoprochnym splavam (Collection "Studies of Heat Resistant Alloys"), AN SSSR, Issue VIII, 199, 1962.
11. Moroz, L. S. and T. E. Mingin. Metallovedeniye i termicheskaya obrabotka metallov (Physical Metallurgy and Heat Treatment of Metals), Vol. 4, No. 2, 1962.
12. Shorshorov, M. Kh. and G. V. Nazarov. Sb. Titan i yego splavy (Collection "Titanium and Its Alloys"), Issue X, AN SSSR, 284, 1963.
13. Chechulin, B. B. and M. B. Bodunova. Sb. Metallovedeniye titana (Collection "Metallurgy of Titanium"), "Nauka," 196, 1964.
14. Mikhaylov, A. S. and B. S. Krylov. Metallovedeniye i termicheskaya obrabotka metallov (Physical Metallurgy and Heat Treatment of Metals), Vol. 4, No. 48, 1962.
15. Daniell, R. D., R. I. Quigg and A. R. Troiano. Trans. ASM, No. 60, p. 843, 1959.
16. Williams, D. N. J. Inst. Metals, No. 91, p. 147, 1962-1963.
17. Moroz, L. S. et al. FMM, Vol. 16, No. 5, p. 737, 1963.
18. Jaffee, R. I., G. A. Lenning and C. M. Craighead. J. Metals, Vol. 8, No. 8 (11), p. 923, 1957.
19. Cottrell, A. H. Dislokatsii i plasticheskoye techeniye v kristallakh (Dislocations and Plastic Flow in Crystals), Metallurgizdat, 1958.
20. Pines, B. Ya. ZhTF, Vol. 25, No. 8, p. 1399, 1955.
21. Stroh, A. N. Phil. Mag., Vol. 46, No. 380, p. 968, 1955.
22. Louat, N. Proc. Phys. Soc., Vol. 69, p. 459, 1956.
23. Moroz, L. S. et al. Sb. Titan i yego splavy (Collection "Titanium and Its Alloys"), Sudpromgiz, 1960.
24. Louthan, M. R. Trans. AIMME, No. 10, p. 1166, 1963.
25. Orovyan. Sb. Atomnyy mekhanizm razrusheniya (Collection "Atomic Mechanism of Fracture"), "Metallurgiya," 1964.
26. McLean, D. Mekhanicheskiye svoystva metallov (Mechanical Properties of Metals), "Metallurgiya," 1965.

METASTABLE PHASES IN THE ALLOYS OF TITANIUM WITH β -ALLOYING METALS

L. A. Petrova

In practice titanium alloys usually are not equilibrium compositions; hence it is important to know what metastable phases are present in these alloys. /119

Metastable phases in titanium alloys are best investigated with reference to phase diagrams for metastable states. Diagrams of this kind for alloys with β -alloying elements illustrate the phase state of the alloys following rapid cooling from various temperatures, and they are usually constructed on the coordinates "pre-quenched temperature — concentration of alloying element."

From the standpoint of the presence of metastable phases in titanium alloys, metastable phase diagrams can be divided into two types [1]. The first type is characterized by the fact that alloys quenched from the β -region have the structure of metastable α' , ω and β phases.

Figure 1, a illustrates the first type of the metastable phase diagram of alloys of titanium with iron [2]. Diagrams of this type also include analogous diagrams of alloys of titanium with nickel, manganese, chromium, cobalt [2, 3].

Figure 1, b illustrates the second type of the metastable phase diagram of alloys of titanium with molybdenum [4]. Diagrams of this type also include analogous diagrams of alloys of titanium with vanadium [5], tantalum, niobium and tungsten [6]. In metastable phase diagrams of these alloys the phase α'' is present in addition to the aforementioned metastable phases characteristic of diagrams of the first type.

In the literature no doubts are raised as to the existence of metastable α' , ω and β phases in titanium alloys. As for the existence of the α'' phase in titanium alloys, it is reported only by Yu. A. Bagaryatskiy [7, 8] and N. V. Ageyev [1, 4, 6]. Moreover, S. G. Fedotov [9] points out that the α'' phase should not be treated as an independent phase since the variation of elastic properties in alloys of titanium with vanadium, niobium and molybdenum quenched from the β region (in the concentration range in which the α' and α'' phases should be observed) is continuous and gradual due to supersaturation. It should be noted that this is not convincing evidence to us, since in the regions which follow the β region the variation in elastic properties is also continuous but Fedotov still distinguishes β and ω phases. Moreover, Fedotov refrained from using x-ray phase analysis to investigate the alloys in general and the alloys with α'' structure in particular, although, as will be shown below and as is known in the literature, α' and α'' phases have a similar martensitic structure, and thus can be distinguished only by radiographic analysis, in terms of their line systems. /120

F. L. Lokshin [10] criticized certain views of S. G. Fedotov concerning the formation of metastable phases and proved can form an independent convincingly that the α'' phase.

L. P. Luzhnikov et al. [11] note that the data on binary Ti-Mo alloys obtained by those presented in the literature (the work of S. G. Fedotov, as well as

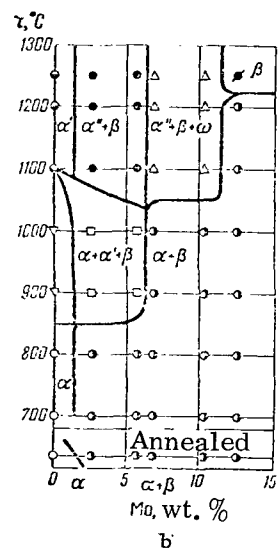
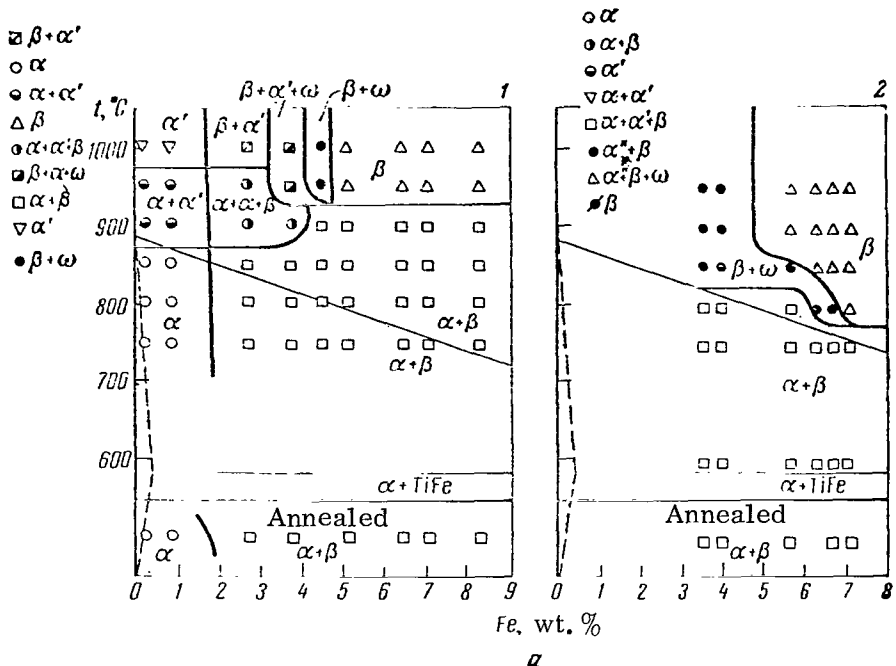


Figure 1. Metastable Phase Diagrams of Alloys of the First (a) and Second (b) Types. Alloys Based on Titanium Obtained by Thermal Reduction with Magnesium (1) and From Titanium Iodide (2).

of Bungardt and Rüdinger [12]) lead one to doubt the existence of the α'' phase. However, Luzhnikov et al. believe that the data of Bungardt and Rüdinger [12] cannot be used to demonstrate the absence of the α'' phase in alloys of titanium with β isomeric elements, since Bungardt and Rüdinger investigated only one alloy of titanium with 8% Mo which, on quenching from the β region, must have the structure $\beta + \omega$ or $\beta + \omega + \alpha_{\text{res}}$. (depending on the mass of the specimen

/121

investigated). L. P. Luzhnikov [11] did not specify which compositions of Ti-Mo alloys were investigated and what methods of analysis were employed, and hence it is not possible to assess these data and, a fortiori, to infer any conclusions concerning the possibility of existence of the α'' phase.

Currently the α'' phase has been detected in the Soviet industrial titanium alloys VTZ-1 and VT14 [10, 13].

In foreign literature, too, reports on the existence of the α'' phase have appeared [14, 15]. The α' phase forming in Ti-based low-alloy compositions represents a supersaturated solid solution of β alloying elements in α -Ti and, like α -Ti, it has a hexagonal lattice. By contrast with α -Ti, the lines of the α' phase on the x-ray diffraction pattern are more blurred due to higher internal stresses.

Considering the low solubility of β alloying elements in α -Ti — that is elements whose atomic dimensions are smaller than the atomic radius of titanium, i. e., elements forming eutectoids — the supersaturation of the α -solid solution with these elements will be lower and, as a result, there will be no marked displacement of lines of the α' phase on the x-ray pattern with respect to lines of the α phase. The lines of the α' phase are considerably blurred and hence their displacement on the x-ray patterns cannot be observed even in the alloys for which solubility in α -Ti and supersaturation are substantial, i. e. in alloys of Ti with β alloying elements whose atomic radii exceed the atomic radius of Ti.

Figure 2, a is a radiograph of an alloy of Ti with 2.08% Mo, water-quenched from 1000°C; the α and α' phases display an identical line system corresponding to a hexagonal lattice. The difference between α and α' phases in this case is that the α phase is represented by sharply defined spots and the α' phase (because of internal stresses) by blurred lines. The α -phase spots (from the large grains in the microscope specimen) are superposed on the blurred lines of the fine-grained α' phase; thus we can say that in this alloy the compositions of α and α' phases are virtually identical.

The microstructure of the α' phase is displays acicular crystals, and resembles a martensitic structure; the α' phase may either exist separately or coexist with α and β phases, depending on the alloy, its composition and pre-quench temperature.

Figure 3, a-f, shows the microstructure of the phases α'' , $(\alpha + \alpha'')$, $(\alpha + \alpha' + \beta)$ and $(\beta + \alpha')$, respectively.

The α'' phase is an even more supersaturated solid solution of the alloying element in α -Ti than the α' phase. According to the theory developed by Yu. A. Bagaryatskiy et al. [7] the α'' phase forms from the α phase but its atomic arrangement is somewhat different so that the hexagonal symmetry of the α phase is disrupted and it converts to a lower, rhombic symmetry. Radiographs of alloys having an α'' -phase structure display the splitting of certain α -phase lines and their displacement with increase in the content of the alloying element or rise in pre-quench temperature.

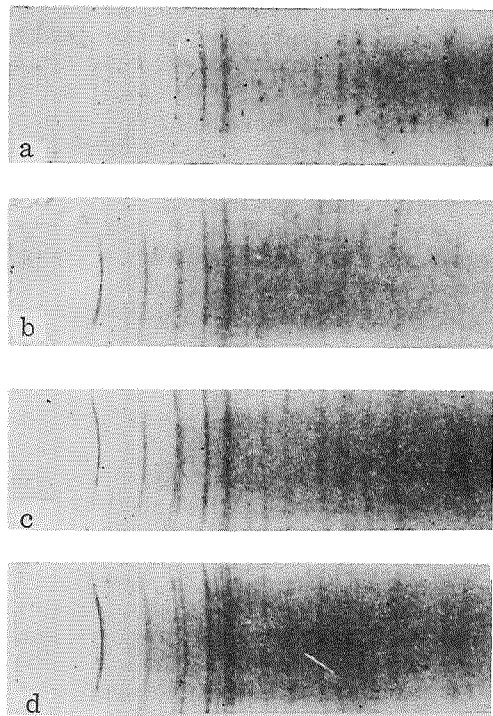


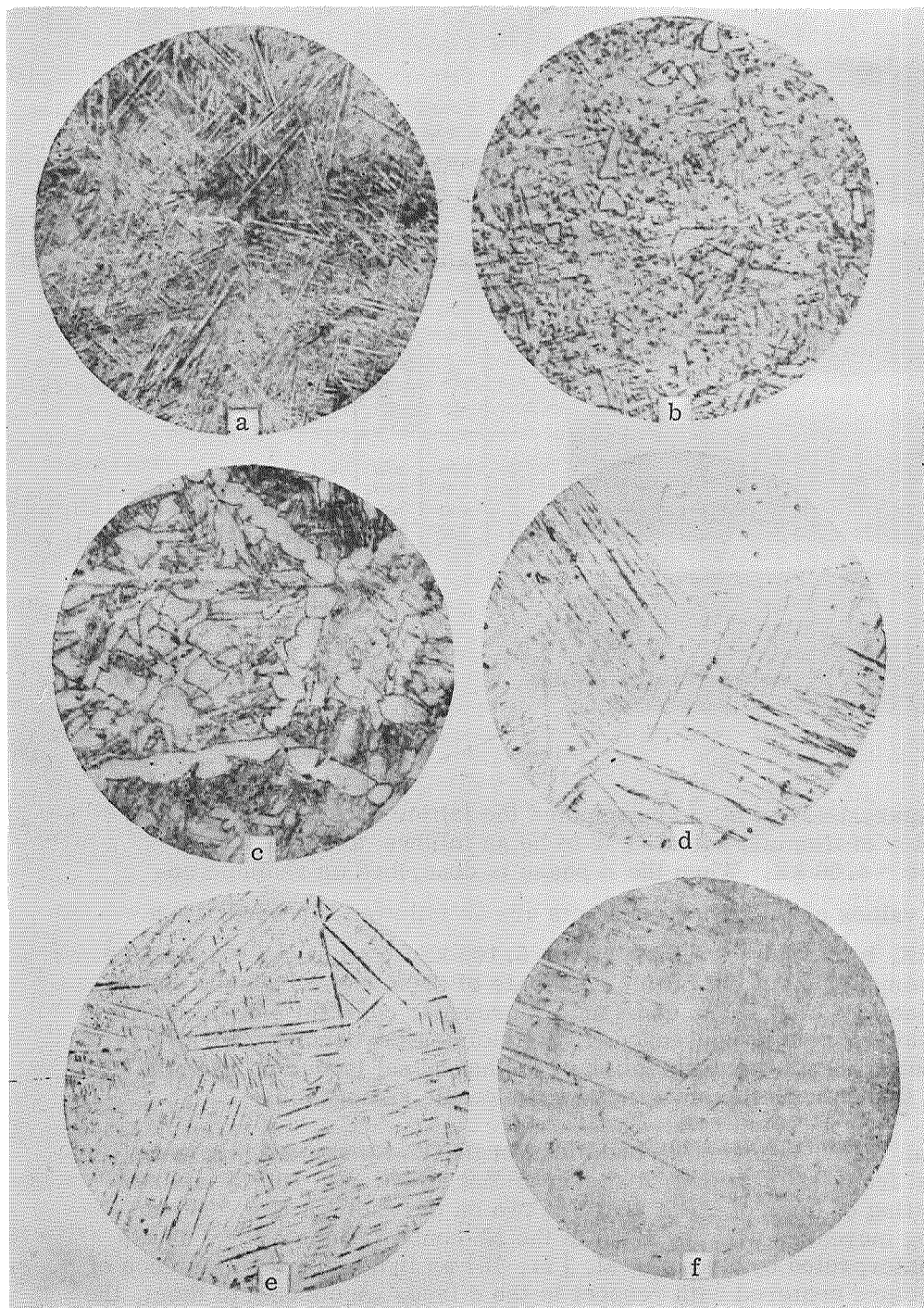
Figure 2. Radiographs of Alloys of the System Ti-Mo.

	Mo, %	Pre-quench temperature, °C	Composition
a	2,03	1000	$\alpha + \alpha'$
b	2,08	1100	$\alpha'' + \beta$ (weak)
c	4,97	1100	$\alpha'' + \beta$ (weak)
d	7,02	1100	$\alpha'' + \beta$ (weak) + ω (weak)

Yu. A. Bagaryatskiy et al. [7] computed the lattice constants of the α'' phase in the alloy of titanium with 15% W to be as follows: $a = 3.01$ kX, $b = 4.96_{\frac{4}{4}}$ kX, and $c = 4.66$ kX. When the α phase is described on rhombic coordinates, the values of its lattice constants are as follows: a (rhomb.) = a (hex.) = 2.93 kX, b (rhomb.) = a (hex.) $\sqrt{3} = 5.105$ kX, c (rhomb.) = c (hex.) = 4.675 kX. A comparison of the lattice constants of the α and α'' phases shows that on transition to the α'' phase constant a increases, constant b decreases and constant c remains virtually unchanged. This violates the condition $a = b/\sqrt{3}$, which is characteristic of the description of the hexagonal lattice on rhombic coordinates, and thus causes the splitting of lines on the radiograph.

Brown et al. [14], in investigating alloys of the Ti-Nb system that were water-quenched from the β region, discovered that alloys with 10, 15 and 20% Nb exhibit splitting of lines of the α phase in two on the radiographs. The degree of splitting increases with increase in the Nb content of the alloy. These findings were interpreted by Brown et al. [14, 15] as indicating the existence of a rhombic structure centered with respect to the c face. According to them, the rhombic structure is a simple distortion of the hexagonal lattice.

Brown and Jekson [14, 15] calculated the lattice parameters of the rhombic α'' phase in the alloy with 20 at. % Nb to be as follows: $c = 3.159_{\frac{6}{6}}$ kX, $b = 4.844_{\frac{2}{2}}$ kX, $c = 4.642_{\frac{6}{6}}$ kX. The rhombic axis c corresponds to the c -axis of the hexagonal cell, while the rhombic axes a and b correspond to the rectangular axes of the



/123

Figure 3. Microstructure of Titanium Alloys, Magnification
340x.

Fig. 3 (Cont'd) on next page.

	Composi- tion, %	Pre- quench temp. $^{\circ}\text{C}$	Composi- tion		Composi- tion, %	Pre- quench temp. $^{\circ}\text{C}$	Composi- tion
a	Ti - 0.19 Fe	1000	α'	d	Ti - 4.74 Ni	900	$\delta + \alpha'$
b	Ti - 0.52 Ni	950	$\alpha + \alpha'$	e	Ti - 2.63 Mo	1100	$\alpha'' + \beta$ (weak)
c	Ti - 5.88 Mo	950	$\beta + \alpha + \alpha'$	f	Ti - 40% Ta	900	α''

hexagonal cell. The structure of the rhombic α'' phase resembles the structure of α -U (Cmcm); the α'' phase was also observed by the authors of [15] in the systems Ti-V, Ti-Mo, Ti-Ta.

In the alloys Ti-6Al-4V quenched from 980°C , two martensitic phases, denoted by the authors of [16] as α' and α'' , were observed. Both phases were identified as hexagonal phases with practically equal constants c and different constants a (2.89 and 2.92 kX, respectively).

It may be that the observed effect is analogous to that described above, but considering that in an alloy of this composition we are dealing with very low supersaturation and hence also limited distortion of the hexagonal lattice, the authors of [16] could interpret it as the coexistence of two hexagonal phases.

Figure 2, b-d, presents radiographs of alloys of Ti with 2-7% Mo, quenched from 1100°C ; these indicate that the lines gradually split with increase in Mo content. On the radiographs of the alloys with 2.08 and 4.97% Mo (Fig. 2, b, c) line splitting is observed only for one plane (11.0). On the radiograph of the alloy Ti + 7.02% Mo (Fig. 2, d) line splitting is observed for as many as four planes (01.0), (01.1), (01.2) and (11.0), and line displacement is visible.

We calculated the lattice parameters of the α'' phase in the alloy with 7.02% Mo, quenched from 1000°C , i.e., for the case where line splitting on the radiograph is maximum. The lattice periods of the α'' phase were found to correspond to: $a = 3.01$ kX, $b = 4.96$ kX, $c = 4.61$ kX. They were measured from line positions on the radiographs over an angle range of up to 40° , and hence these data are relative.

Figure 4 presents the sketch of a radiograph of the alloy with 7.02% Mo quenched from 1000°C , within the range of reflection angles from 15 to 45° ; the lattice parameters of the α'' phase were derived from this sketch. Under the sketch are given the descriptors of the planes of the hexagonal α -phase and their variation with rhombic distortion of the lattice (the α'' phase). From this radiograph, as well as from the radiographs shown earlier in Fig. 2, it can be seen that in lieu of the single line of the α phase we now have two lines each for some planes.

The distance between the line pairs depends on the rhombic distortion of the lattice, and it is greater the higher the Mo content or the quenching temperature.

The rhombic distortion of the hexagonal α -phase lattice in titanium alloys as a function of the molybdenum content and pre-quench temperature is analogous to the tetragonal distortion of the body-centered lattice of α -Fe upon formation of

/124

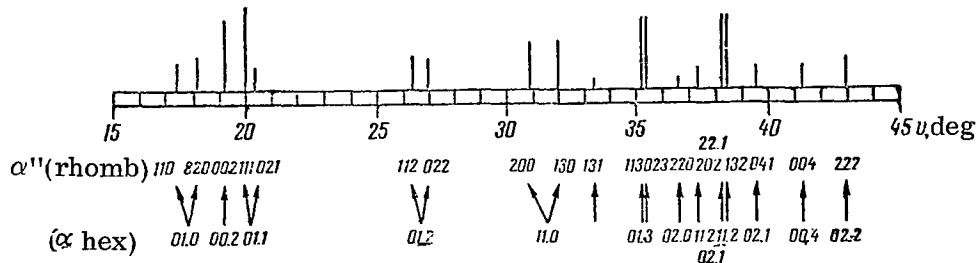


Figure 4. Sketch of Radiograph of the Alloy Ti + 7.02% Mo, Quenched From 1000°C.

martensite; the latter is a function of the carbon content of the steel and the pre-quench temperature. When the C content of the steel is 0.6-0.7%, the tetragonality of the martensite is very low and the line pairs blend together into single blurred lines. When the pre-quench temperature is extremely low, the carbides remain almost undissolved and this will result in loss from carbon austenite. As a consequence, the tetragonality of the martensite forming during quenching will be very low, and the line pairs will merge into single lines corresponding to the α -Fe lattice [17].

The microstructure of the α'' phase (Fig. 3, e, f) resembles the microstructure of the α' phase (α'' phase is finer) and the decomposed β -solid solution. These also involve alloys of titanium with tantalum and hence, to avoid errors in microstructural examination, x-ray analysis should be carried out in parallel to the metallographic analysis.

The α'' phase can exist separately or it can coexist with β and ω phases whose presence in the alloys is manifested in the form of one or two weak lines on the radiographs. Yu. A. Bagaryatskiy et al. [7, 8] observed separate existence of the α'' phase (separately from other metastable phases) in the alloy. N. V. Ageyev and associates found that the α'' phase exists separately in the system Ti-Nb [6], and that it also coexists with β - and ω phases [1, 4]. Brown and Jekson [15] also made this observation.

/125

This discrepancy (the observation of the α'' phase separate from the other phases or coexisting with the β and ω phases) in the studies of alloys of identical composition by different investigators [1, 4, 6-9, 14, 15] apparently is traceable to the difference in the dimensions of the investigated specimens. Titanium and Ti-base alloys exhibit a low thermal conductivity and hence large specimens cool more slowly than small specimens. As a result, in larger specimens the metastable α'' phase decomposes into $\alpha'' + \beta$, or into $\alpha'' + \beta + \omega$, depending on the content of the β -alloying element.

In alloys with a still higher content of alloying elements, (though not so high as to cause fixation of all of the β phase on quenching) it is possible to observe the ω phase, which at normal pressure always coexists with the β -solid solution. Under a hydrostatic pressure of 90,000 kg/mm² plus, a temperature of 20-600°C, and pure titanium, the α phase converts to the ω phase [18] which persists at 20°C following removal of pressure. The ω phase is not an intermediate phase during

the formation of α ; neither is it an α phase + chemical compound substance [19]. Rather, it is a form of titanium stable with respect to β -Ti within a certain range of concentrations, given rapid cooling from the β -region. Yu. A. Bagaryatskiy and associates [8] considered the ω phase as a metastable low-temperature modification of the β solid solution, representing a compound of electronic type and assumed that during quenching the ω phase forms in a diffusionless manner, owing to oriented displacement of atoms. In all the investigated alloys the formation of the ω phase during quenching occurred in the presence of a concentration of the alloying element corresponding to the following value of the lattice constant of the β solid solution: 3.255-3.260 kX [7].

In certain early foreign works [20-26] the ω phase was regarded as an intermediate phase forming through diffusion owing to the redistribution of alloying elements in the β solid solution during quenching and tempering.

Now that the crystal structure of the ω phase has been established more precisely and the extent of the atom displacements required for the $\beta \rightarrow \omega$ transition has been determined [27], it can be unequivocally stated that the ω phase forms during quenching in a diffusionless manner and represents a martensitic phase.

In the literature various opinions are voiced concerning the detection of the ω phase under the microscope.

Yu. A. Bagaryatskiy et al. [27] believe that the ω phase lacks the relief characteristic of ordinary martensitic transformations inasmuch as the $\beta \rightarrow \omega$ transition occurs through collective displacement of atoms in diametrically opposite directions and hence it cannot be observed under the microscope.

Austin and Doig [28] point out that since the ω phase is coherently associated with the β matrix, the phase interface cannot be clearly observed by metallographic means. However, they also note that the presence of a mottled β structure, observable under an optical microscope, is associated with the presence of the ω phase.

Knorr and Scholl [29] pointed out that alloy specimens containing the ω phase displayed surface roughness when examined with the aid of an electron microscope.

The ω phase was observed under an electron microscope by Frost et al. [20] in an alloy of titanium with 7.54% Cr following tempering for 4 hours at 370°C. They identified as particles of this phase the tiny equiaxial segregations whose size was of the order of one micron. Later Frost [20] expressed doubt concerning the identity of these segregations.

V. N. Gridnev et al. [31] observed the ω phase in alloys of titanium with 5 and 8% Cr and 5% Fe following their quenching from the β -phase region, as well as in tempered β -alloys. In the quenched alloys the ω phase was present in the form of very small discrete particles.

A study of titanium alloys in quenched and tempered states by Gridnev et al. showed that the presence of the ω phase in an alloy is signaled by the presence

/126

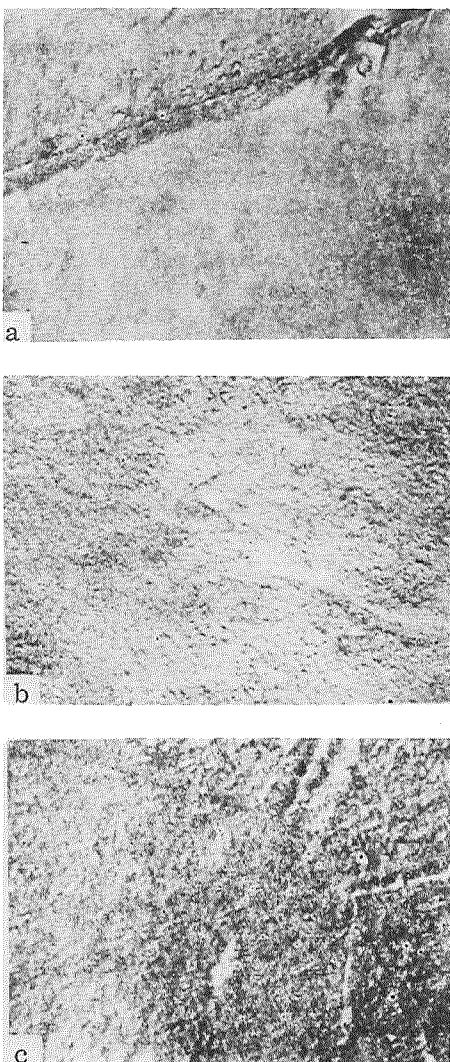


Figure 5. Electron Microphotographs of Alloys. Colloidal Replica Shadowed with Chromium at the Angle of 10°. Magnification 12,000 x.

a—Ti + 5.37% Fe + 7.39% V, Quenching from 900°C, β phase;
b—Ti + 14.17% V, Quenching from β Region, $\beta + \omega$; c—Ti + 15.11% Mo, Quenching and Aging at 200°C, 100 hours.

lines of the bcc β phase, while those lines which complement the lines of the β phase divide the distance between the lines of the β phase roughly into three

of a rough, mottled surface of β grains when examined under an optical microscope. An electron-microscopic examination of quenched alloys in β and $(\beta + \omega)$ -states and, even more so, of aged alloys in $(\beta + \omega)$ state, made it possible to observe the ω phase. Figure 5 presents electron microphotographs of the alloys in various states; these show that the β alloy has a smooth surface. The quenched alloy with $(\beta + \omega)$ structure (Fig. 5, b) displays a structure from which particles seem to have been torn out (pockmarked structure). An aged specimen with the same structure displays convex particles of the ω phase, located over the surface of the β matrix, which differ in nature from the ω phase in the quenched alloy (Fig. 5, c).

Croutzeilles et al. [32] have also detected the ω phase under the electron-microscope in an alloy of titanium with 15% Mo (after quenching and aging). On analysis of structure with the aid of carbon replicas, the ω phase was found to exist in the quenched alloys as a dense mass of particles with a low contrast, having a size of about 200 Å; these were oriented with respect to the β solid solution. Transillumination of films, prepared by thinning sheet specimens by means of electrolytic dissolution made possible a more precise detection of ω phase particles: as on the carbon replicas, these particles were found to be located in dense accumulations on the matrix surface and oriented with respect to it. The ω -phase particles resembled lamellae measuring ~200 Å in length and 40 Å in thickness. Following tempering the appearance of the ω phase changes very insignificantly but it exhibits a still higher contrast.

The most reliable method for identifying the ω phase in an alloy is the x-ray method. On the radiograph of a section quenched from the β region some of the ω -phase lines coincide with the

/127

subsections. Figure 6 shows radiographs of alloys quenched from the β region. It can be seen from this figure that the interference lines of the ω phase (denoted by arrows), which forms due to the drastic quenching, are fairly blurred, whereas the lines of the β phase (also denoted by arrows) are relatively distinct and sharp.

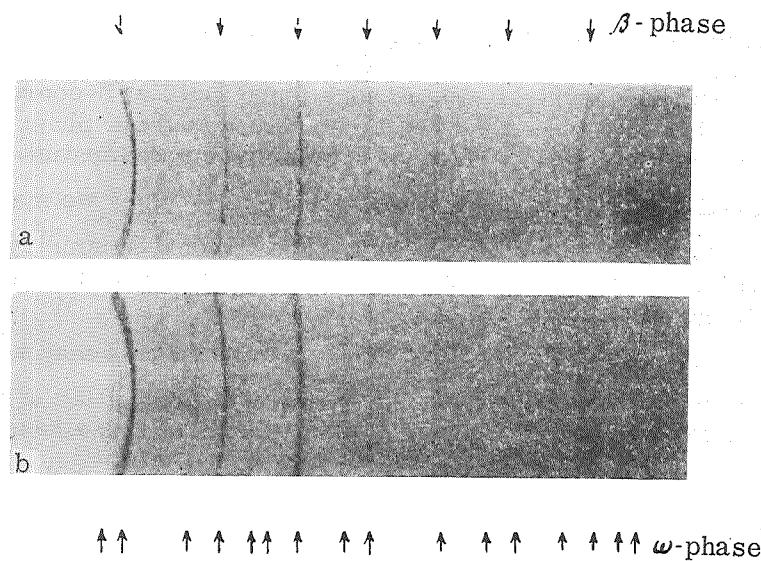


Figure 6. Radiographs of Titanium Alloys Quenched from the β Region:
 a— β Phase; b— $\beta + \omega$.

Concerning the crystal lattice of the ω phase, several different opinions are expressed in [33-41]. Certain investigators [35, 36, 38] assume that the ω phase has a cubic lattice with a lattice constant triple that of the original cubic β phase; some of them [35, 38] assume that the ω phase has a cubic structure with 58 atoms in a cell while others [36] state that this phase has a cubic lattice with $a = 9.76 \text{ \AA}$ (space group 1 m 3 m). Spachner [37] in his study of powder specimens of Ti + 8% Cr alloy established that the ω phase exists in two modifications: ω_A , conventional, coexisting with the β phase, and ω_B , coexisting with the α phase and forming on tempering.

In [37] a rhombic lattice with the parameters $a = 6.203 \text{ \AA}$, $b = 6.498 \text{ \AA}$, $c = 13.63 \text{ \AA}$ and $a/b = 0.95$ and $b/c = 0.48$ is ascribed to the ω phase.

X-ray studies on single crystals in monochromatic radiation [34, 41] established that the crystal structure of the ω phase is the same on quenching and tempering, and is characterized by a hexagonal symmetry with virtually constant lattice parameters for different alloys ($a = 4.60$ and $c = 2.82 \text{ \AA}$). The ω phase has a lattice with three atoms per unit cell, and is regularly oriented with respect to the original cubic β phase: $(00.1)\omega \parallel (111)\beta$, $(11.0)\omega \parallel (110)\beta$; on radiographs of polycrystalline specimens, the ratio between the axes ($c/a = 0.613 = \sqrt{3/8}$) produces the impression that this phase has a cubic lattice.

Later findings by Yu. A. Bagaryatskiy and G. I. Nosova [42] confirmed again that the lattice of the ω phase is structurally equivalent to the bcc lattice described in hexagonal axes, since $a_{\text{hex}} = \sqrt{2}a_{\text{cub}}$; $c_{\text{hex}} = \sqrt{3/4}a_{\text{cub}}$ and $c_{\text{hex}}/a_{\text{hex}} = 0.612$. Yu. A. Bagaryatskiy and G. I. Nosova calculated the exact positions of atoms in the unit cells, finding them to be somewhat different from those specified by Silcock [40, 41]. Instead of the atomic positions $000, \pm(1/3, 2/3, 1/2)$ found by Silcock, Bagaryatskiy and Nosova found that the Z-coordinate differs somewhat from $1/2$ ($Z = 0.48 \pm 0.001$) the structure of the ω phase can thus be described more accurately in a trigonal system having the spatial group $P\bar{3}m1$ than in a hexagonal system with the space group $P/\frac{6}{mmm}$. Thus we may assume as a fact that the ω phase in titanium alloys has trigonal symmetry, is regularly oriented with respect to the original β phase and displays the following structural base in hexagonal axes for the space group: $P3m\ 1:1$ (Ti, Me)... 000 (position a), $2(\text{Ti, Me})... \pm \frac{1}{2} \frac{2}{3} z$ (position d) [43]. The value of Z may vary in various alloys, remaining close to $1/2$. A study of the structure of the ω phase by the electron diffraction method [32] confirmed that this phase has a hexagonal lattice.

In alloys with a still higher content of alloying elements, a metastable β phase can be obtained once a certain critical content of β alloying elements (specific for each system) is reached. The table below gives the minimum concentrations of alloying elements needed to obtain a single-phase structure of β solid solution in a state that is metastable at room temperature [44]. The alloying elements in Table 1 are presented in terms of decreasing effectiveness of stabilization of the β solid solution.

TABLE 1

Alloying element	Critical stabilizing concentration		Alloying element	Critical Stabilizing concentration	
	at. %	el./at.		at. %	el./at.
Iron.....	4.5*, 4.9**	4.2	Chromium ..	8.4 **	4.2
Cobalt....	4.9**	4.2	Tungsten ...	8.7 **	4.2
Manganese	5.0*	4.2	Vanadium ...	18.4 **	4.2
Nickel....	5.8*-6.3**	4.2-4.3	Tantalum ...	21.0 ***	4.2
Molybdenum	5.8***	4.1	Niobium	23.0 **	4.2
Rhenium ...	6.0 **	4.2			

NOTE: The titanium used as the alloy base was obtained by: reduction with magnesium (*), iodide process (**), calcium hydride process (***)�

The minimum critical content of alloying element needed to stabilize the β phase depends on a number of factors which must be elucidated in order to derive the general laws governing the stabilization of the β solid solution in the titanium alloys. The elements stabilize the β phase the more effectively the further removed they are from titanium in the Periodic Table (Fig. 7). Thus in group IV the effectiveness of stabilization decreases from nickel, cobalt and iron to chromium and vanadium; in group V, from molybdenum to niobium; in group VI, from rhenium and tungsten to tantalum. This relationship is due to the effect of the dissolving solid solution component on the lattice rearrangement of the solvent (titanium) during rapid cooling. The lattice rearrangement of the β phase will be hindered by the introduction of an extraneous atom, to an extent that will increase with the difference in the chemical nature of the atoms of titanium and the second component of the solid solution, and with the difference in the dimensions of these atoms. Hence, the greater these differences, the more decisive will be the effect of the alloying element on the stabilization of the β phase and the lower will be the concentration of this element needed to obtain a metastable β phase.

/129

The chemical nature of an atom and its size depend on the number of electrons in that atom, i. e., on the electronic concentration. This permits to derive a relationship between the critical stabilizing concentration of the β phase during quenching and the electronic concentration in the solid solution.

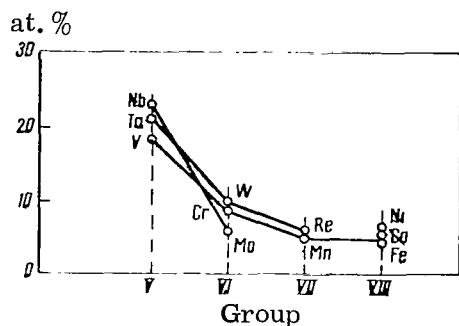


Figure 7. Effectiveness of β Alloying Elements as a Function of Their Position in the Periodic Table (Ordinate: Critical Stabilizing Concentration, at. %).

high-temperature β phase at room temperature.

McQuillan [47] pointed out that the electron concentration required to stabilize the β solid solution, which Ageyev and Petrova [44] fixed at 4.2 el./at., is not in very good agreement with experimental findings (the limit of the scatter is given at 0.1 el./at. and the system Ti-Nb is cited by way of an example). However, we believe that the system Ti-Nb is not a very felicitous example, since in this system the critical content of Nb required to stabilize the β phase is 23 at. %, and thus the electron concentration calculated for an alloy of this composition is 4.23 el./at. (i. e. 4.2 el./at.).

The table given earlier also shows the electron concentration corresponding to the critical stabilizing concentration of the β phase; here it was assumed that the number of electrons in the atom corresponds to the number of the group in which the given element belongs. These calculations show that all the β phases in metastable state in Ti-base alloys are obtained at virtually identical electron concentrations which average 4.2 electrons per atom.

In addition to the study by N. V. Ageyev and L. A. Petrova [44], the literature includes a number of works dealing with the effect of the valence of the substance being dissolved [45] and the electron concentration [46-49] on the stability of the

A scatter of 0.1 el./at. in the values of electron concentration holds only for nickel and, up to a point, for molybdenum, since the electron concentration for the system Ti-Mo is 4.12 el./at. The critical concentration of molybdenum (system Ti-Mo) was determined in alloys based on titanium obtained by the calcium hydride method, and hence the impurities present in such titanium undoubtedly accounted for some error. This, however, could only result in reducing rather than increasing the amount of the alloying element. In view of this, we can assume that alloys based on pure titanium require a greater amount of molybdenum and therefore the electron concentration will be greater than 4.12 el./at. (4.1 el./at.).

In alloys of titanium with nickel, the critical concentration of nickel is 5.8-6.3 at. % (depending on the purity of titanium), and the electron concentration is 4.23-4.25 el./at.

In certain systems for which the limit of the scatter in the 4.2 el./at. value of electron concentration is 0.1 el./at., it is nevertheless possible (in theory) to select such compositions of alloys of not only binary but also multicomponent systems which retain the structure of the β solid solution following quenching from the β region. /130

Recently, the "transillumination" method of electron microscopy has been developing rapidly, and methods of electron diffraction are being utilized; hence new data on previously unknown metastable phases have appeared in the literature.

Thus, the alloy of titanium with 3 wt. % Fe quenched from the β region showed, along with the residual β phase, the existence of martensite of two types with hexagonal close-packed lattice as well as with fcc lattice [50]. The authors of [50] point out that, owing to the small-particle nature of their acicular grains, the martensitic phases, and particularly the new martensitic phase with fcc lattice, cannot in some instances be detected by electron diffraction.

The alloy of titanium with 5.45% Ni shows, following quenching from the β region, only the β -residual and α' phases on the x-ray radiograph, whereas electron diffraction reveals an additional ω phase [51].

Tempering of alloys having the structure $\beta + \alpha' + \omega$ results in the appearance (some time afterwards), of the metastable ω' phase along with the above-mentioned phases. The authors of [51] ascribe to the ω phase a bcc lattice with the constant $a = 9.80 \text{ \AA}$, which is three times as high as the lattice constant of the β phase ($a = 3.26 \text{ \AA}$); to the ω' phase they also ascribe a bcc lattice, but one whose constant is roughly double that of the β phase ($\sim 6.53 \text{ \AA}$).

In [50] it is assumed that the ω' phase can exist in alloys of titanium with chromium as well as in other alloys, but so far it has not been detected in them due to failure to use electron-microscopic "transillumination" of films and electron diffraction analysis.

REFERENCES

1. Ageyev, N. V. and L. A. Petrova. In the collection *Titan i yego splavy* (Titanium and Its Alloys) No. VII, USSR Acad. Sci. Press, 26.
2. Ageyev, N. V. and L. A. Petrova. *Zh. Neorgan. Khimii*, Vol. 4, No. 5, p. 1092, 1959.
3. Ageyev, N. V., O. G. Karpinskiy and L. A. Petrova. *Zh. Neorgan. Khimii* Vol. 8, p. 1976, 1961.
4. Ageyev, N. V. and L. A. Petrova. In the collection *Titan i yego splavy* (Titanium and Its Alloys) USSR Acad. Sci. Press, Vol. 3, 1958.
5. Ageyev, N. V. and L. A. Petrova. *Zh. Neorgan. Khimii*, Vol. 5, No. 3, p. 615, 1960.
6. Ageyev, N. V., O. G. Karpinskiy and L. A. Petrova. In the collection *Fiziko-khimicheskiy analiz Trudy yubileynoy konferentsii* (Physicochemical Analysis, Proceedings of Jubilee Conference) Novosibirsk, Publ. House of the Siberian Department of the USSR Acad. Sci., Vol. 5, 1963.
7. Bagaryatskiy, Yu. A., T. V. Tagunova and G. I. Nosova. *Problemy metallovedeniya i fiziki metallov* (Problems of Metallography and Physics of Metals) coll. No. Vol. 5, Metallurgizdat, p. 210, 1958.
8. Bagaryatskiy, Yu. A., G. I. Nosova and T. V. Tagunova. *Dokl. Akad. Nauk SSSR*, Vol. 122, No. 4, p. 593, 1958.
9. Fedotov, S. G. In the collection: *Issledovaniya metallov v zhidkem i tverdom sostoyaniyakh* (Studies on Metals in Liquid and Solid States), Nauka Press, No. 207, 1964.
10. Lokshin, F. L. *Metallovedeniye i Termicheskaya Obrabotka Metallov*, Vol. 9, No. 55, 1966.
11. Luzhnikov, L. P., et al. *Metallovedeniye i Termicheskaya Obrabotka Metallov*, Vol. 5, No. 21, 1965.
12. Bungardt, K. and K. Rüdinger. *Z. Metallkunde*, Vol. 52, No. 2, p. 120, 1961.
13. Ivanov, A. N. and Ya. S. Umanskiy. *Tsvetnyye Metally*, Vol. 7, No. 91, 1966.
14. Brown, A. R. G. et al. *Nature*, Vol. 29, No. 4922, p. 915, 1964.
15. Brown, A. R. G. and K. S. Jekson. *Mem. scient. Rev. métallurgie*, Vol. 6, No. 63, p. 575, 1966.
16. Griest, A. Y., J. K. Doig and P. D. Frost. *Trans. AIME*, No. 215, p. 627, 1959.
17. Katsanov, N. N. and L. I. Mirkin. *Rentgenostrukturnyy analiz* (X-Ray Structural Analysis), Metallurgizdat, 1960.
18. Bundy, F. *New Materials and Methods for Research Into Metals and Alloys*; Rumanian transl. Metallurgiya Press, No. 230 1966.
19. McQuillan, M. K. *Met. Rev. Inst. Metals*, Vol. 8, No. 29, p. 41, 1963.
20. Frost, P. D. et al. *Trans. ASM*, No. 46, p. 231, 1954.
21. Brotzen, F. R., E. L. Harmon and A. R. Troiano. *J. Metals*, Vol. 7, No. 2, Section 2, p. 431, 1955.
22. Zwicker, U. *Z. Metallkunde*, Vol. 47, No. 8, p. 535, 1956.
23. Zwicker, U. *Z. Metallkunde*, Vol. 49, p. 179, 1958.
24. Böhm, H. and H. Westphal. *Z. Metallkunde*, Vol. 47, No. 8, p. 558, 1956.
25. Böhm, H. *Z. Metallkunde*, Vol. 49, No. 4, p. 190, 1958.
26. Löhnberg, K. and H. Westphal. *Z. Metallkunde*, Vol. 49, No. 9, p. 443, 1958.

/131

27. Bagaryatskiy, Yu.A. and G.I. Nosova. *Fizika metallov i metallovedeniye*, Vol. 13, No. 3, p. 415, 1962.
28. Austin, A.E. and J.R. Doig. *Trans. AIME*, No. 209, p. 27, 1957.
29. Knorr, W. and H. Scholl. *Z. Metallkunde*, Vol. 51, No. 10, p. 605, 1960.
30. Frost, P.D. *J. Met.*, Vol. 8, No. 1, Section 1, p. 35, 1956.
31. Gridnev, V.N., et al. *Voprosy fiziki metallov i metallovedeniye* (Problems of Metals Physics and Metallography), USSR Acad. Sci. Press, Vol. 11, No. 32, 1960.
32. Croutzeilles, M. et al. *Compt. Rend.*, No. 23, p. 2685, 1961.
33. Silcock, J.M., M.N. Davies and H.K. Hardy. *Nature*, Vol. 175, No. 731, p. 4460, 1955.
34. Bagaryatskiy, Yu.A., G.I. Nosova and T.V. Tagunova. *Dokl. Akad. Nauk SSSR*, Vol. 105, No. 6, p. 1225, 1955.
35. Austin, A.E. and J.R. Doig. *J. Metals*, Vol. 9, No. 1, 1957.
36. Voshida, H. *J. Japan Inst. Metals*, Vol. 20, No. 5, p. 292, 1956.
37. Spachner, S.A. *Trans. Met. Soc. AIME*, Vol. 212, No. 1, p. 57, 1958.
38. Raub, E. and H. Beeskow. *Z. Metallkunde*, Vol. 49, No. 4, p. 185, 1958.
39. Bagaryatskiy, Yu.A. and G.I. Nosova. *Kristallografiya*, Vol. 3, No. 15, p. 17., 1958.
40. Silcock, J.M. *Acta Met.*, Vol. 6, No. 7, p. 481, 1958.
41. Silcock, J.M., M.N. Davies and H.K. Hardy. *The Mechanism of Phase Transformations in Metals*, Inst. Metals, Monographia, Report Ser., Vol. 18, No. 93, 1956.
42. Bagaryatskiy, Yu.A. and G.I. Nosova. *Kristallografiya*, Vol. 3, No. 15, 1959.
43. Bagaryatskiy, Yu.A. and G.I. Nosova. *Fizika metallov i metallovedeniye*, Vol. 13, No. 3, p. 415, 1962.
44. Ageyev, N.V. and L.A. Petrova. *Dokl. Akad. Nauk SSSR*, Vol. 138, No. 2, p. 359, 1961.
45. Hy, J.C. and A.A. Burr. *Trans. AIME*, No. 224, p. 204, 1962.
46. Bychkov, Yu.F., V.N. Maskalets and A.N. Rozanov. *Inzh.-Fiz. Zh.* Vol. 3, No. 4, p. 95, 1960.
47. McQuillan, M.K. *Metallurgical Reviews*, Vol. 8, No. 29, p. 41, 1963.
48. Luke, C.A., R. Taggart and D.H. Polonis. *Trans. ASM*, No. 57, p. 142, 1964.
49. Luke, C.A., R. Taggart and D.H. Polonis. *J. Nucl. Mater.*, Vol. 16, No. 1, p. 7, 1965.
50. Jeni Nusiyama, Muneo Oka and Hiroshi Nakagawa. *J. Japan Inst. Metals*, Vol. 30, No. 1, p. 16, 1966.
51. Lee, E.U., E.E. Underwood and O. Johari. *Electron Microscopy*, 1966, 1, Tokyo, Maruzen Co, Ltd., 1966, 433.

PHASE TRANSFORMATIONS IN TITANIUM ALLOYS UNDER NONEQUILIBRIUM CONDITIONS

M. A. D'yakova and I. N. Bogachev

In titanium alloys with transition elements (Mn, Cr, Fe, V, Mo, Co, Ni, W, etc.) the metastable phases α' , α'' , ω may form under conditions in which the formation and growth of nuclei of the stable α phase are hindered: during rapid cooling, during supercooling of the high-temperature β phase within a specific temperature range, and under high pressures [1-9]. In addition, a major condition for the formation of metastable α' , α'' , ω phases in titanium alloys is obviously the thermodynamic factor: the free energies of the metastable phases are lower than those of the high-temperature phase (Fig. 1). The predominant formation of metastable rather than stable phases under nonequilibrium conditions during rapid cooling or during supercooling to specific temperatures is attributable to the marked structural correspondence and similarity of chemical composition between the metastable phases and the original phase.

/132

In pure titanium and in Ti-based low-alloy compositions, the thermodynamic conditions for the existence of the phases are such that depending on the rate and temperature of cooling, both the stable α phase and the martensite α' may form (see Fig. 1, a). Raising the pressure results in changing the thermodynamic conditions and makes possible the formation of the ω phase in pure titanium. Bundy experimentally established that in pure titanium under a pressure of 90 kbar at any temperature below 600°C, the hexagonal close-packed α phase is transformed into the more dense ω -phase modification. He observed a similar transformation of the hexagonal close-packed phase into the ω in pure zirconium under a pressure of the order of 50 kbar [5]. When the content of transition elements in titanium alloys increases, this also causes a change in the thermodynamic conditions for phase existence. In alloys with moderate transition element contents either the stable α phase may form or the metastable phases such as martensite (α' , α'') and the intermediate ω phase, depending on the rate and temperature of cooling (see Fig. 1, b). In high-alloy compositions the thermodynamic conditions are such that, depending on the cooling rate and temperature, the high-temperature β phase may decompose with the formation of either the stable α phase or the intermediate ω phase (see Fig. 1, c).

Titanium alloys display a martensitic structure of two types: martensite with distorted hexagonal close-packed α' lattice and martensite with rhombohedral α'' lattice whose crystal lattice distortion is different. In alloys containing small amounts of V, Mo, Nb, Re, or W the martensite has a distorted hexagonal close-packed α' lattice, whereas in high-alloy compositions the resulting martensite has the rhombohedral α'' lattice [1]. For Ti-Mo alloys the limiting concentration for the formation of the martensite with hexagonal close-packed lattice is 6.0 wt. % Mo, and for Ti-V alloys, 12.0 wt. % V [8]. Thus, depending on the degree of supersaturation of the α solid solution (martensite) with alloying elements, the crystal lattice symmetry varies from hexagonal to rhombohedral. Radiographically the martensitic α'' phase is characterized by the "splitting" of certain interference lines of the α phase, which increases with the concentration of alloying elements.

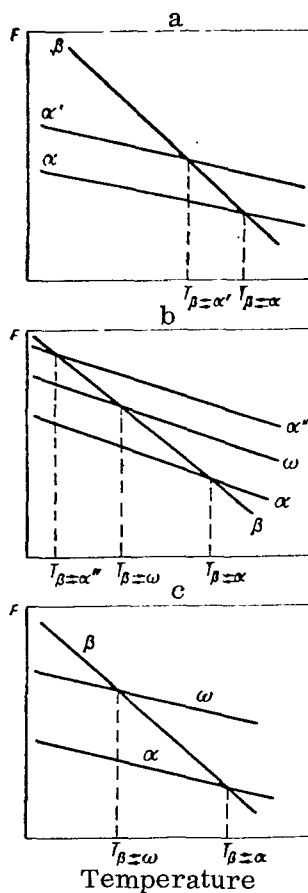


Figure 1. Variation in the Ratios of Free Energies of the (α , β , ω) Titanium Phases as a Function of the Content of Transition Element in the Titanium Alloys:

a—Technical Titanium and Low-Alloy Compositions;
 b—Medium-Alloy Compositions;
 c—High-Alloy Compositions.

formation [1, 7, 9, 15] point to a shift-type martensitic nature of the transformation under these conditions. It should be noted that Bundy observed reversibility of the $\beta \rightleftharpoons \omega$ transformation at 600–700°C under high pressures even in pure titanium [5]. The $\beta \rightarrow \omega$ transformation in critical-concentration titanium alloys displays all the principal features of martensitic transformation except one: the formation of a macrorelief on the specimen surface. This macrorelief in martensitic transformations is the result of the pile-up of displacements caused by transition from one form of unit cell to the next. There

The high rate of martensitic transformation [1], its reversibility [10] and the possibility of the formation of deformation martensite [10-11] are all proofs of a diffusionless shift mechanism for martensitic transformation in titanium alloys.

The starting temperature for martensitic transformation in titanium alloys depends on the content of the alloying elements and on their nature. All transition elements lower the start temperature, and Fe, Mn, or Cr are particularly notable in this respect. When the concentration of these elements is of the order of 6.5–7.0 wt. %, the martensite transformation temperature drops below room temperature. Aluminum hardly affects the starting temperature but in the presence of β stabilizing elements it also lowers it [13].

The process of formation of the ω phase in titanium alloys is of a dual nature. When the ω phase forms during quenching, the $\beta \rightarrow \omega$ transformation is of a martensitic nature, whereas in the case of isothermal transformation at 300–500°C this process displays much in common with the intermediate (bainitic) transformation in steels.

The $\beta \rightarrow \omega$ rearrangement of crystal lattices requires only insignificant shift of atoms, of the order of 1/6 of the interatomic distance [1]. According to Yu. A. Bagaryatskiy, the ω phase arises during the quenching of alloys containing that amount of transition elements when the lattice parameter of the β solid solution is 3.255–3.266 Å. At such a composition, the ω phase forms during cooling at extremely fast rates (of the order of 3000–11,000 deg/sec). The formation of the ω phase in alloys of critical composition during quenching [1] and under strain, that is, in alloys with an unstable β phase [1, 14, 15], as well as the reversibility of the $\beta \rightleftharpoons \omega$ trans-

exists an opinion that during $\beta \rightarrow \omega$ transformation relief cannot form on the specimen surface because then the atomic displacements, even though parallel, go in opposite directions, and hence transition from one unit cell to another is not accompanied by a pile-up of displacements. Bagaryatskiy and Klassen-Neklyudova therefore ascribe the $\beta \rightarrow \omega$ transformation during quenching to martensitic transformations occurring without change in form [1, 16].

The $\beta \rightarrow \omega$ transformation in alloys with a critical content of transition elements may be regarded as an allotropic transformation, and the ω phase may be considered a low-temperature modification differing from the β phase in thermodynamic, physical, magnetic and other properties.

It has been postulated that the $\beta \leftrightarrow \omega$ transformation develops owing to instability of the electronic structure of the unstable β phase, which results in electron exchange between s- and d-shells [1]. Ageyev and associates also suggest that electronic structure is a decisive factor in the stabilization of the β solid solution [17, 18, 24].

In its crystal structure the ω phase is an intermediate phase between the equilibrium α and β phases.

Under isothermal conditions the process of decomposition of the β solid solution with formation of the ω phase in alloys containing large amounts of transition elements exhibits an induction period, which makes possible the suppression of this transformation by means of rapid cooling. In this case the $\beta \rightarrow \omega$ transformation requires a redistribution of the alloying elements to assure formation of depleted regions of β solid solution, in which the $\beta \rightarrow \omega$ rearrangement of crystal lattice can occur via atomic displacement. The transformation rate is then controlled by the rate of redistribution of the alloying elements. Experimental data of Harmon and Troiano [19], Knorr and Scholl [20] and Krisement [21], obtained on Ti-Mo and Ti-V alloys, indicate that below 270-280°C there exists a preliminary stage prior to the segregation of the ω phase; during this stage the transition elements become redistributed in the solid solution, and this results in the formation of regions enriched in and depleted of alloying elements.

/134

According to R. I. Entin, the intermediate transformation represents a special type of transformations, in which the martensitic polymorphic transformation combines with diffusive redistribution of some chemical element [22]. Such a definition encompasses both the bainitic transformation in steels and the decomposition of high-temperature β phase with formation of the ω phase in alloys based on titanium, zirconium, etc.

In titanium alloys containing Cr, Fe, Ni, or Co, one observes the segregation of titanides. The lack of reactions in the eutectoid transformation in Ti-based alloys and particularly in the Ti-Mn alloys is worth noting.

The decomposition of the high-temperature β phase may occur either through diffusion or through diffusionless displacement or through intermediate transformation.

The behavior of alloys under nonequilibrium conditions is described by isothermal and thermokinetic diagrams of decomposition of the supercooled high-temperature phase [23].

In titanium alloys, the β solid solution decomposes at the upper temperature limit with the formation of the α phase and titanides. This decomposition is diffusion-controlled and is described by c-shaped curves (first stage of transformation).

Upon supercooling of the β solid solution below 550°C , the diffusion of alloying elements slows down, the induction period for stability of the β solid solution increases, and the rate of decomposition (with formation of the α phase) decreases. When the temperature is lowered below 450°C , the rate of transformation of the β solid solution again increases markedly, owing to the change in the transformation mechanism. In this case the decomposition of the β solid solution with formation of the intermediate ω phase proves to be thermodynamically favored. At such temperatures the diffusional redistribution of alloying elements occurs within microvolumes of the solid solution, accounting for the formation of solid solution regions depleted of alloying elements. It is in these regions that the $\beta \rightarrow \omega$ lattice rearrangement is possible. Under isothermal conditions, the decomposition of the β solid solution with formation of the ω phase is described by C-shaped curves and displays features characteristic of both diffusive and non-diffusive transformations; it can be classified as an intermediate transformation (second stage of transformation).

If diffusion processes do not develop when the β solid solution is very stable (in the temperature range of the first and second stages of transformation) because of a specific degree of alloying with transition elements, then on rapid cooling the $\beta \rightarrow \alpha$ transformation may be of a displacive martensitic nature, resulting in the formation of the martensitic structures α' or α'' (third stage of transformation).

This may be illustrated by the diagrams of isothermal decomposition of the high-temperature β phase in several alloys investigated by us (Fig. 2). These diagrams are derived on the basis of data of dilatometric, metallographic, hardness and x-ray structural analyses.

In the Ti4Al3Mo1V alloy, which contains small amounts of transition elements, supercooling from the β -phase region starting from 1000°C results in two stages of decomposition of the β solid solution: above 500°C , the decomposition is accompanied by diffusive formation of the α phase and below 500°C , by formation of the α' martensite (Fig. 2, a). Diffusive transformation becomes superposed on martensitic transformation. Prolonged exposure to 500 – 450°C causes the decomposition of martensite with attendant decrease in hardness and resistivity.

/135

In the Ti2.5Al7Mo alloy the temperature of martensitic transformation drops to 380°C due to molybdenum higher content, and thus lies in the range of thermodynamic stability of the ω phase; this accounts for the complex kinetics of decomposition of the β solid solution. This alloy displays all three stages of transformation (Fig. 2, b), with the diffusive transformation superposed on the

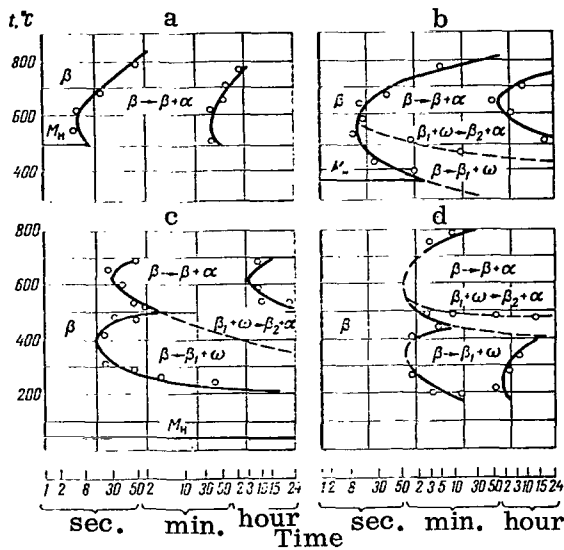
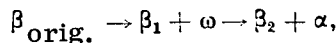


Figure 2. Diagrams of Isothermal Decomposition of the High-Temperature β Phase of Titanium Alloys (Cooling From the Region of the β Solid Solution):

a—Ti4Al3Mo1V; b—Ti2.5Al7Mo; c—Ti3.4Al8Mo; d—Ti9Mn.

intermediate transformation in the 500–450°C range; in this range the decomposition of the high-temperature β phase occurs via the formation of the intermediate ω phase, followed by the segregation of the α phase:



Here, the β_2 solid solution is more highly alloyed than the β_1 solid solution and the latter, in turn, is more highly alloyed than the original $\beta_{\text{orig.}}$ solution. In this alloy the intermediate transformation is also superposed on the martensitic transformation at 380–350°C. Prolonged exposure to 380–350°C assures the decomposition of the residual β phase with formation of the ω phase, which results in an increase in hardness and brittleness.

In the Ti3.4Al8Mo alloy, in which the temperature of martensitic transformation is below the thermodynamic stability range of the ω phase ($M_s = 80^\circ\text{C}$), all the three stages of transformation are distinct (Fig. 2, c).

In the Ti9Mn alloy, the transformation of which starts markedly below room temperature, one can distinguish only two stages of transformation (Fig. 2, d). In

/136

the last two cases diffusive transformation is also superposed on the intermediate transformation.

CONCLUSIONS

The results of our investigations, as well as an analysis of kinetics of phase transformations in titanium alloys [9, 19, 20, 23] warrant the following general conclusions:

1. The kinetics of decomposition of the high-temperature β phase in titanium alloys are controlled by the degree of alloying and by the nature of alloying elements; these factors determine the relationship between the temperature ranges of diffusive, intermediate and martensitic transformations, and the specific rates of diffusive and intermediate transformations.
2. All transition elements (Mn, Cr, Fe, V, Mo, Ni, Co, etc.) enhance the stability of the β solid solution within the temperature range of diffusive and intermediate transformations, and virtually do not affect the temperature range of intermediate transformation (—except for molybdenum, which somewhat increases this range). Aluminum retards the decomposition of the β solid solution, while oxygen and nitrogen accelerate it. The transition elements exert particularly marked effect on the temperature range of martensitic transformation (by lowering this range).
3. The temperature of martensitic transformation may vary markedly, depending on the amount and nature of alloying elements. It may lie within the temperature range of diffusive and intermediate transformations, and it also may be below room temperature.
4. Titanium alloys containing transition elements are characterized by the superposition of one type of transformation upon another. In low-alloy compositions, the diffusive transformation is superposed on the martensitic transformation; in medium- and high-alloy compositions, in which intermediate transformation occurs the diffusive transformation is, as a rule, superposed on intermediate transformation. If the martensite transformation starting temperature is in the range of thermodynamic stability of the ω phase, intermediate transformation is superposed on martensitic transformation.
5. Varying the temperature of heating in the β phase region does not markedly affect the nature of the decomposition kinetics of the high-temperature β phase. Varying the temperature of heating in the two-phase region, on the other hand, produces changes in the decomposition kinetics of the β solid solution, owing to the change in its content of alloying elements.

REFERENCES

1. Bagaryatskiy, Yu.A., T.V. Tagunova and G.I. Nosova. Problemy metallovedeniya i fiziki metallov (Problems of Metallography and Metal Physics) 5, Metallurgizdat, 210, 1958.
2. Bagaryatskiy, Yu.A. and G.I. Fizika metallov i metallovedeniye, Vol. 13, No. 3, p. 415, 1962.

3. Ageyev, N. V. and L. A. Petrova. In the collection: *Titan i yego splavy* (Titanium and Its Alloys) No. 3, USSR Acad. Sci. Press, 5, 1958.
4. Ageyev, N. V. and Z. M. Smirnova. In the collection: *Titan i yego splavy* (Titanium and Its Alloys), No. 3, USSR Acad. Sci. Press, 7, 1958.
5. Bundy, F. In the collection: *Novyye materialy i metody issledovaniya metallov* (New Materials and Methods for Research Into Metals and Alloys), Metallurgiya Press, 230, 1966.
6. D'yakova, M. A. and I. N. Bogachev. *Fizika metallov i metallovedeniye*, Vol. 10, No. 6, p. 896, 1960.
7. Bogachev, I. N. and M. A. D'yakova. *Fizika metallov i metallovedeniye*, 961, 12, 4, 607.
8. Nosova, G. I. Authors's abstract of Candidate Thesis, 1961.
9. Bundgardt, K. and K. Rüdinger. *Z. f. Metallkunde*, Vol. 52, No. 2, p. 120, 1961.
10. Zwicker, U. *Z. f. Metallkunde*, Vol. 50, No. 5, p. 261, 1959.
11. J. Japan Inst. Metals, Vol. 25, No. 9, p. 568, 1961.
12. Jaffe, R. I. In the collection: *Uspekhi fiziki metallov* (Advances in Metal Physics), Vol. 4, No. 77, 1951.
13. Kossler, H. D. and M. Hansen. *Trans. ASM*, Vol. 46, No. 585, p. 609, 1954.
14. Bogachev, I. N. et al. *Fizika metallov i metallovedeniye*, Vol. 10, 11, No. 4, p. 557, 1961.
15. Gridnev, V. N. et al. In the collection: *Voprosy fiziki metallov i metallovedeniye* (Problems of Physics of Metals and Metal Science), Vol. 10, UkrSSR Acad. Sci. Press, Vol. 77, 1959.
16. Klassen-Neklyudova, M. V. *Mekhanicheskoye dvoynikovaniye kristallov* (Mechanical Twinning of Crystals), USSR Acad. Sci. Press, 1960.
17. Ageyev, N. V. and Z. M. Rogachevskaya. *Zh. Neorgan. Khimii*, Vol. 10, No. 4, p. 2323, 1959.
18. Ageyev, N. V. and L. A. Petrova. In the collection: *Titan i yego splavy* (Titanium and Its Alloys), Vol. 7, USSR Acad. Sci. Press, No. 26, 1962.
19. Harmon, E. L. and A. R. Troiano. *Trans. ASME*, Vol. 53, No. 43, 1961.
20. Knorr, W. and H. Scholl. *Z. f. Metallkunde*, Vol. 51, No. 10, p. 605, 1960.
21. Krisement, O. *Z. f. Metallkunde*, Vol. 52, No. 10, p. 695, 1961.
22. Entin, R. I. *Prevrashcheniya austenita v stali* (Transformations of Austenite in Steel), Metallurgizdat, 1960.
23. Popov, A. A. and L. Ye. Popova. *Izotermicheskiye i termokineticheskiye diagrammy raspada pereokhlazhdennogo austenita* (Isothermal and Thermokinetic Decomposition Diagrams for Supercooled Austenite), Metallurgiya Press, 1965.
24. Ageyev, N. V. and Z. M. Rogachevskaya. *Zh. Neorgan. Khimii*, Vol. 3, No. 5, p. 619, 1960.

/137

**EFFECT OF TIN AND ZIRCONIUM ON TRANSFORMATIONS
 ACCOMPANYING THE HEAT TREATMENT OF
 THE ALLOY Ti + 10% Cr**

L. P. Luzhnikov, V. M. Novikova, A. P. Mareyev and
 I. S. Orlova

The earlier investigation [1] dealt with the effect of aluminum on transformations occurring during the heat treatment of the alloy Ti + 10% Cr.

The present investigation is concerned with the effect of tin and zirconium on this alloy.

The methods for preparing the alloys, their heat treatment and study were the same as described in [1, 2].

The alloys were prepared from OP2 rod tin (GOST All-Union State Standard 860-41) and zirconium iodide, as well as from TG120 titanium sponge ($\sigma_B = 35$ kg/mm²).

The chemical composition of the alloys is given in Table 1.

**TABLE 1. CHEMICAL COMPOSITION OF ALLOYS WITH
 VARYING CONTENT OF TIN AND ZIRCONIUM, % (BAL. Ti)**

Alloy Brand	Cr	Sn	Zr	Alloy Brand	Cr	Sn	Zr
A1	10,2	—	—	A18	10,0	—	1,9
A14	9,6	1,2	—	A19	9,5	—	4,0
A15	9,9	4,0	—	A20	10,0	—	8,0
A16	10,0	10,4	—	A21	10,0	—	16,4
A17	9,9	14,0	—				

Note: Oxygen content of alloys: 0.15-0.17%.

The following methods of investigation were employed: dilatometric, construction of kinetic curves of aging, analysis of recovery during aging and, partially, the metallographic method.

TIN-CONTAINING ALLOYS

Figure 1, a-e presents dilatometric and hardness curves of the alloy Ti + 10% Cr containing varying amounts of tin (0, 1, 4, 10 and 14%).

The hardness curves correspond to aging for 1.5 hr at temperatures shown on the abscissa.

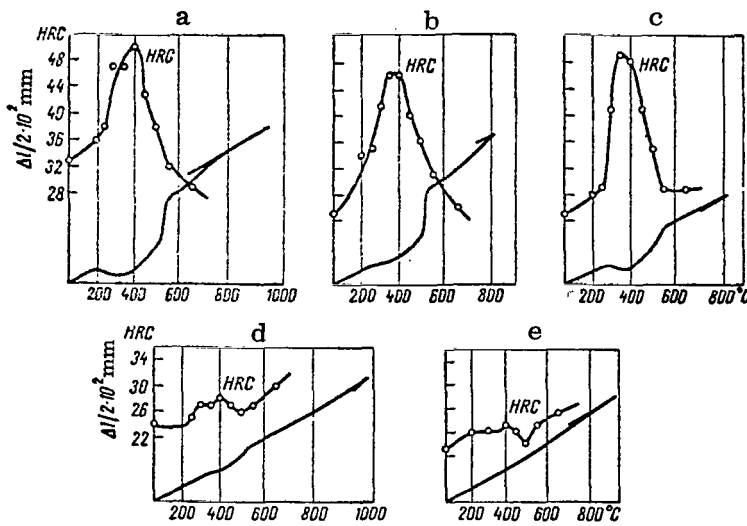


Figure 1. Effect of Tin on Hardness Following Aging for 1.5 Hours (Broken Line) and Variation of Duration of Heating (Solid Lines) of Quenched Ti + 10% Cr Alloy Containing: a—0.17% O₂; b—1% Sn; c—4% Sn; d—10% Sn; e—14% Sn.

The specimens used for hardness measurements and the dilatometric specimens of all the alloys except the alloy Al were quenched from 900°C (heating for 40 min) in water at room temperature. Specimens of the alloy Al (Sn- and Zr-free) were quenched from 800°C.

Following quenching, all the alloys had the structure of a homogeneous β solid solution, as shown by metallographic analysis.

Cooling following aging was carried out in water.

The tin- and zirconium-containing alloys were primarily compared with the alloy lacking these elements (the alloy A1, which is a Ti + 10% Cr alloy containing 0.15–0.17% oxygen).

Let us examine the hardening due to the alloying of the β solid solution, i.e. the hardness of the hardened tin- and zirconium-containing alloys (Table 2).

The hardened Sn- and Zr-containing alloys clearly are more correctly compared with the alloy lacking these elements and having the structure of the β -solid solution when hardness, i.e. with the "pure" alloy (containing 0.02% oxygen). As can be seen from Table 2, treatment of the β -solid solution with Sn or Zr does not harden it.

Thus, alloying of the metastable β solid solution with fairly large amounts of aluminum (up to 7.5%) [1], of tin (up to 14%) or zirconium (up to 16%) does not result in its hardening.

TABLE 2. EFFECT OF TIN AND ZIRCONIUM ON THE HARDNESS OF THE HARDENED ALLOY Ti + 10% Cr

/139

Sn, % (Brand of Alloy)	Rockwell hardness after quenching	Zr, % (Brand of alloy)	Rockwell hardness after quenching
0 (A0)	27 (33)	0 (A0)	27 (33)
1 (A14)	27	2 (A18)	27
4 (A15)	25	4 (A19)	29
10 (A16)	24	8 (A20)	28
14 (A17)	25	16 (A21)	26

Note: The hardness of the Sn- and Zr-free alloy is specified for the case of an 0.02% O₂ content on which the ω phase virtually never occurs during quenching, as well as for the case of an 0.15-0.17% O₂ content (in parentheses), in which a large amount of the ω phase arises during hardening (the alloy A1).

Moreover, it can be seen that introduction of 1% Sn or 2% Zr into the alloy Ti + 10% Cr containing 0.15-0.17% O₂ suppresses the formation of the ω phase during quenching.

The hardness of the alloy A1 (Fig. 1, a) increases slightly (from 33 to 36 H_{RC} units) following aging at $\leq 200^{\circ}\text{C}$.

As the aging temperature is raised, a hardness maximum is observed at 400°C , above which the hardness sharply decreases.

The slight increase in hardness following aging at 200°C is due to the presence of substantial amounts of the ω phase in this alloy following aging, i. e. to the attendant existence of the ($\beta + \omega$) structure in this alloy.

Comparatively brief (1.5 hr) aging at this temperature has very little effect on the ($\beta + \omega$) structure, and the $\beta \rightarrow \omega$ transformation occurs but slightly during this aging. Prolonging the aging at 200°C , on the other hand leads to a more complete $\beta \rightarrow \omega$ transformation and to a marked rise in hardness, as shown by kinetic hardening curves. The variation in hardness (Fig. 1, a) tallies with the shape of the dilatometric curve for this alloy. At $\leq 200^{\circ}\text{C}$ a very weak negative effect is observed. As the temperature is further raised, this effect (contraction) increases steadily until it reaches the temperature of the hardness maximum (400°C), beyond which it decreases (expansion) owing to the $\omega \rightarrow \beta$ recovery and the precipitation of the α phase from the β solid solution. Above 530°C there exists only the ($\beta + \alpha$) two-phase structure. The general pattern of variation of the dilatometric and hardness curves of alloys with the tin content is fundamentally the same, particularly for the alloys containing up to 4% Sn (inclusively).

These curves point to the following specific effects of the tin. The negative effect on the dilatometric curves, as well as the maximum on the hardness curves

diminish with tin content and particularly sharply when the Sn content exceeds 10% Sn. A marked negative effect begins to appear at the following temperature, (°C):

In the Sn-free alloy	200
1% Sn	200-250
4% Sn	250-300
10% Sn	300-350

In the alloy containing 14% Sn this effect is insignificant and hence it is difficult to determine its temperature range. These data appear to indicate a higher stability of the β solid solution containing tin. On the other hand, the maximum hardness (in H_{RC} units) is observed in the Sn-free alloy (at 400°C, 50 H_{RC} units) and in the alloys containing only small amounts of Sn (1 and 4% Sn, at 350-400°C — 48 and 49 H_{RC} units, respectively).

The hardness maximum corresponds to the temperature of the most $\beta \rightarrow \omega$ complete transformation and to the maximum contraction of dilatometric specimens. Above this temperature there commences the $\omega \rightarrow \beta$ transformation and the segregation of the α phase from the β solid solution.

Two weak hardness maxima are observed in alloys with 10 and 14% Sn in the alloy with 10% Sn, at 300-350°C and at 400-450°C; in the alloy with 14% Sn, at 200-300°C and at 400°C. The maximum hardness of the alloy with 10% Sn is $H_{RC} = 27-28$ and that of the alloy with 14% Sn, $H_{RC} = 28-29$. Thus, on alloying with 1-4% Sn, the temperature corresponding to the hardness maximum as well as hardness itself decrease only insignificantly.

The weak first maximum observable on alloying with 10-14% should apparently be identified with the maximum for the alloys containing 1-4% Sn. A sharp decrease in the temperature of the first maximum as well as in the corresponding hardness can then be discerned. In the Sn-free alloy, the hardness maximum (50 H_{RC}) lies at 400°C and in the alloy with 14% Sn (28-29 H_{RC}), at 200-300°C.

Thus, adding to the alloy Ti + 10% Cr more than 4% Sn markedly lowers the temperature of the most complete manifestation of the $\beta \rightarrow \omega$ transformation and this transformation itself is then markedly suppressed. On comparing the temperatures at which the negative effect begins to manifest itself appreciably with the temperatures corresponding to the hardness maximum after aging, one can observe a marked contraction of the temperature range in which the ($\beta + \omega$) structure can exist at high Sn contents of the alloy. For the Sn-free alloy this range is approximately 200°C (200-400°C), while for the alloy with 10% Sn it does not exceed 50°C (300-350°C). The dilatometric curves also point to a reduction (on treatment with tin) in the expansion effect associated with the precipitation of the α phase from the β solution.

The presence of two hardness maxima in the alloys with 10 and 14% Sn is confirmed by the kinetic curves of aging of these alloys. Following aging for

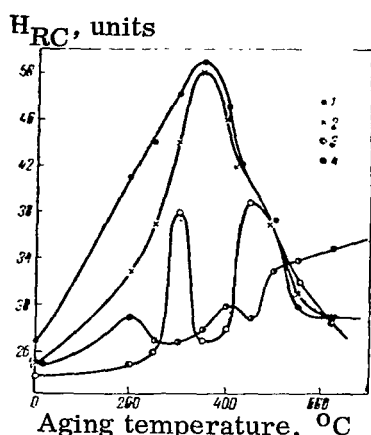


Figure 2. Variation (After Aging for 20 Hours) in Hardness of the Alloy Ti + 10% Cr Containing the Following Amounts of Sn, %: 1 (1), 4 (2), 10 (3), 14 (4).

distinctly observed in the alloy Ti + 10% Cr: at low aging temperatures owing to the formation of the $(\beta + \omega)$ structure, and at high temperatures owing to the formation of the $(\beta + \alpha)$ structure.

Thus, in the alloy with 10% Sn the three-phase $(\beta + \omega + \alpha)$ mixture, in which hardening is due to the presence of two products of decomposition of the β solid solution (the ω and α phases), is apparently absent following aging for 20 hours. It appears that this is the first time that such an effect of tin on the processes of transformation in the β -alloy Ti + 10% Cr has been discovered.

/142

Figure 3, a-d presents "aging-recovery" diagrams for alloys without tin as well as with 1, 10 and 14% Sn [3].

In aging for 1.5 hours, maximum hardening at 400°C occurs in the Sn-free alloy and in the alloy with 1% Sn; at this temperature, the alloys with 10 and 14% Sn do not harden. This shows that alloying 10% Sn completely suppresses the formation of the $(\beta + \omega)$ structure in the alloy Ti + 10% Cr on aging; on the diagrams the hatched region characterizing hardening with formation of the ω phase, shrinks in area. The diagram for the alloy with 1% Sn (Fig. 3, b) points to increased hardening on precipitation of the α phase from the solution and increase in aging time (the region between the recovery curve and the broken line which specifies the ranged hardness of the quenched alloy, widens).

This is also characteristic of the alloy with 10% Sn (Fig. 3, c), but in this alloy the prolongation of aging time is accompanied by intensification of the $\beta \rightarrow \omega$ transformation (hatched region broadens). In the alloy with 14% Sn (Fig. 3, d) this transformation is not observed even after aging for 80 hours. In this case, following aging at up to 400°C and following recovery the hardness is virtually identical to that of the hardness alloy. The recovery effect is also absent.

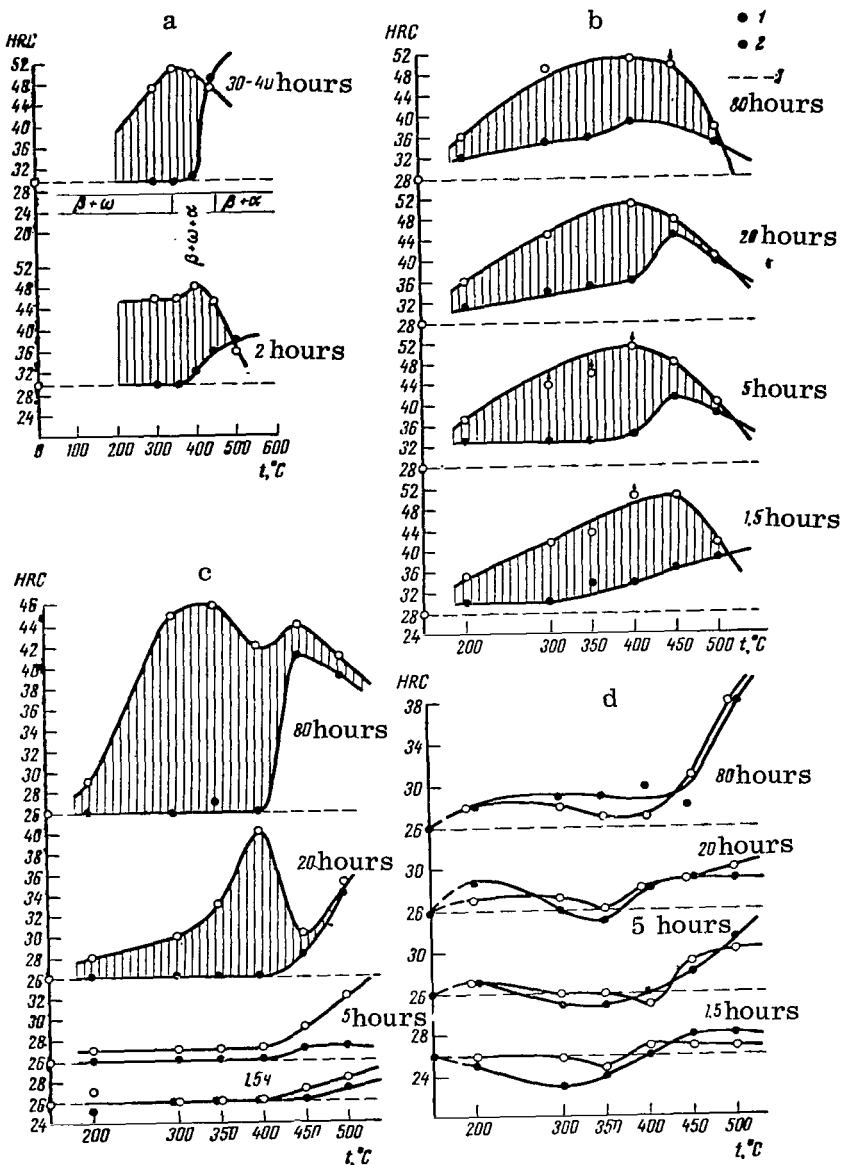


Figure 3. "Aging-Recovery" Diagrams of the Alloy Ti + 10% Cr Containing 0.17% O₂ (a), 1% Sn (b), 10% Sn (c) and 14% Sn (d):

O—Aging (Aging Time in Hours is Specified on Curves);
 o—Recovery at 550°C for 45 sec (a, b), 60 sec (c) and 3 sec (d). Broken Line Shows Hardness Following Quenching From 800 (a) and 900°C (b-d).

On aging at 20 and 80 hours, the alloy with 10% Sn displays two distinct hardness peaks; the temperatures at which these peaks occur decrease with increase in the aging time. These findings confirm the presence of the two maxima pointed out earlier. It should be pointed out, however, that the hardness maxima in Fig. 2 occur at 300 and 475°C, whereas in Fig. 3, c they correspond to 300-400°C and 450-550°C, depending on the aging time.

It may be that the reason for this difference is that the data in Fig. 2 were obtained on rods 12 mm diameter, and the data in Fig. 3, c were obtained on 1.5 mm thick strips (differences in quenching rate, condition of material, etc.).

As far as the alloy with the maximum tin content is concerned, it can be only stated that the effect of hardening due to the formation of the $(\beta + \alpha)$ structure increases with increase in aging time at $> 400-450^\circ\text{C}$.

ZIRCONIUM-CONTAINING ALLOYS

Figure 4, a presents dilatometric and hardness curves of the alloy Ti + 10% Cr containing 2, 4, 8 and 16% Zr. These should be compared with the curves in Fig. 1, a (alloy A1).

As can be seen, the nature of these curves resembles the curves for the (Sn- and Zr-free) alloy A1.

However, a number of special features associated with the effect of zirconium can be pointed out. The failure of Zr to harden the β solid solution has already been mentioned when comparing the hardness of quenched alloys (Table 2).

The negative effect contraction on dilatometric curves, as well as the hardness maximum, vary little on alloying with up to 16% Zr.

An appreciable negative effect begins to manifest itself at 200°C in the Zr-free alloys and in the alloys with 2 and 4% Zr, and at 220-250°C in alloys with 8 and 16% Zr.

The hardness maximum for all the alloys (from 0 to 16% Zr) is observed at 350-400°C (49-51 Rockwell units).

The positive effect (expansion), due to the precipitation of the α phase from the β solution, is not affected by alloying with 2% Zr (Fig. 1, a and 4, a) but it is markedly and sharply increased (more than twice) by alloying with 4 and 8% Zr (Fig. 4, b and 4, c), and is drastically reduced by alloying with 16% Zr (Fig. 4, d). In this last case it is almost half of that in the Zr-free alloy (Fig. 1, a). The starting point for the sharp increase in length [the temperature at which the two-phase $(\beta + \alpha)$ decomposition region begins to appear and the three phase $(\beta + \omega + \alpha)$ region ceases to appear] decreases with increasing Zr content from 530°C for the Zr-free alloy to 520, 510 and finally to 480°C for the alloy with 16% Zr. The beginning of the three-phase region corresponds to the hardness maximum ($\sim 350-400^\circ\text{C}$). Below this temperature the alloys display the two-phase $(\beta + \omega)$

/143

structure. Thus alloying the β solid solution with Zr results in the narrowing of the region of existence of the $(\beta + \omega + \alpha)$ structure.

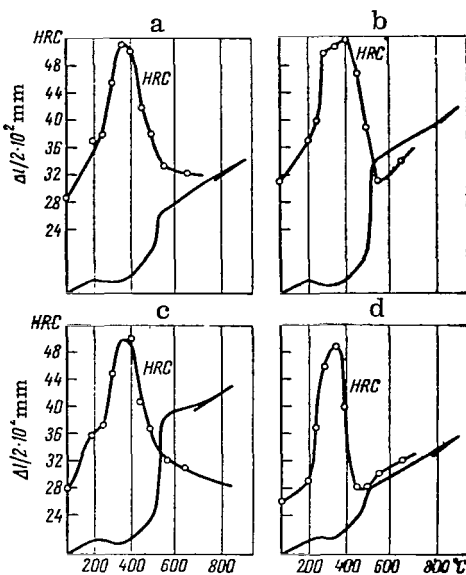


Figure 4. Effect of Zirconium on Hardness Following Aging for 1.5 Hours (Broken Line) and on Variation in Length During Heating (Solid Lines) of Hardened Ti + 10% Cr Alloy Containing:

a—2% Zr; b—4% Zr; c—8% Zr;
 d—16% Zr.

400°C) is unaffected by alloying with 0, 4 and 8% Zr ($H_{RC} = 16, 18$ and 18 units).

The maximum hardness does not change on alloying with up to 8% Zr even when aging time is prolonged 80 hours.

The aging of alloys with 4 and 8% Zr for 80 hours results in a gradual decrease in the hardening due to the formation of the $(\beta + \omega)$ structure and an increase in the hardening due to the formation of the $(\beta + \alpha)$ structure. Following recovery, the alloys with 4 and 8% Zr, aged below 400°C, display a somewhat lower hardness than after quenching.

At the same time, the alloy with 1% Sn (Fig. 3, b) exhibits incomplete recovery following aging even at 200°C; as aging time is prolonged this effect tends to increase. These findings require further separate investigation with the object of elucidating the causes of the observed "anomalies."

The hardness curves do not show any marked changes when the aging time is prolonged to 20 hours. In this case the hardness maximum for all the alloys lies at 350°C. Only the curve for the alloy with the maximum content of zirconium (16%) displays inflection points at 250–300°C and at 450–500°C. The first of these inflection points is apparently due to a retardation of the $\beta + \omega$ transformation, and the second to the transition from the three-phase $(\beta + \omega + \alpha)$ structure to the two-phase $(\beta + \alpha)$ structure.

It may be that if the aging time were prolonged beyond 20 hours, two hardness maxima would be observed as in the alloy with 10% Sn described earlier.

Figure 5 presents "aging-recovery" diagrams for the alloys with 4 and 8% Zr. The diagram for the Zr-free alloy is given in Fig. 3, a. We will examine the data obtained after aging for 1.5–2 hours. The degree of the hardening due to the $(\beta + \omega)$ structure diminishes (hatched area) following aging below 200°C and alloying with 4 and 8% Zr. The maximum hardening (aging at

400°C) is unaffected by alloying with 0, 4 and 8% Zr ($H_{RC} = 16, 18$ and 18 units).

/144

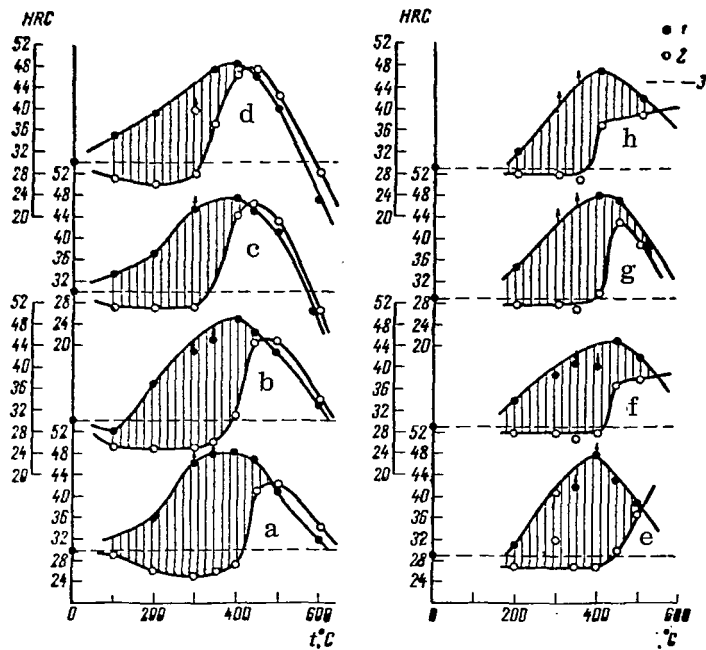


Figure 5. "Aging-Recovery" Diagrams of the Alloy Ti + 10% Cr Containing 4% Zr (a-d) and 8% Zr (e-h):

1—Aging for 1.5 Hours (a, c), 5 hours (b, f), 20 Hours (c, g), 80 Hours (d, h); 2—Recovery at 550°C, 30 Sec; 3—Hardness Following Quenching From 900°C.

CONCLUSIONS

1. The effect of tin (up to 14%) and zirconium (up to 16%) on the transformations accompanying the heat treatment of the alloy Ti + 10% Cr was investigated.
2. Alloying with 1% Sn or 2% Zr suppresses the formation of the ω phase during hardening.
3. Alloying Ti + 10% Zr with tin or zirconium does not harden the quenched alloy. Earlier it was shown that aluminum produces a similar effect [1].
4. Tin or zirconium affect appreciably the processes of decomposition of the β solid solution of the alloy Ti + 10% Cr; however, the maximum hardening that can be attained by means of heat treatment (quenching + aging) is not affected by alloying with tin or zirconium.
5. These experimental data show that alloying of the β alloys of titanium with α stabilizers is a promising direction for obtaining high-strength and, probably, high-temperature alloys with various combinations of strength and plasticity.

REFERENCES

/145

1. Luzhnikov, L. P. et al. Effect of Aluminum on Transformation in the Alloy Ti + 10% Cr), Izvestiya Akad. Nauk SSSR, Metally, No. 3, 1967.
2. Luzhnikov, L. P. et al. Transformations in Titanium Alloys During Heat Treatment. Metallovedeniye i termicheskaya obrabotka metallov, Vol. 5, pp. 21-29, 1965.
3. Luzhnikov, L. P. et al. Recovery During Aging in Industrial Titanium Alloys. Metallovedeniye i termicheskaya obrabotka metallov, Vol. 12, No. 3, 1967.

STUDY OF PHASE AND STRUCTURAL TRANSFORMATIONS IN TWO-PHASE INDUSTRIAL TITANIUM ALLOYS

M. I. Yermolova, E. V. Polyak and O. P. Solonina*

Changes in Phase Composition and Structure During Quenching

The phase composition, structure and mechanical properties of two-phase titanium alloys of the $\alpha + \beta$ type may vary markedly depending on the regime of heat treatment employed. Hardening of these alloys is accomplished in the course of their aging owing to the decomposition of the metastable β , α' or α'' phases and the formation of a mixture of highly disperse segregations of the α and β phases. The quantitative ratio between the phases and the form, distribution and dispersion of the decomposition products are determined by the heating temperature, cooling rate and aging conditions. This article presents the results of an investigation of the kinetics of phase and structural transformations accompanying the quenching and aging of the alloys VTZ-1, VT6, VT8, VT14 and VT16. The methods of investigation employed were: x-ray structural analysis, electron microscopy and hardness measurements. The chemical composition of the above-mentioned alloys were nominal and corresponded to the specifications [1]. The most thorough study was done on alloys VTZ-1 and VT-8. The investigation was performed on specimens cut out of 14-mm diameter forged rods. The specimens were water-quenched after 30-min heating to 700-1050°C and subsequently aged for 2 hours at 200-700°C.

It is known that in all two-phase titanium alloys the curve of the dependence of strength and plastic properties on the quenching temperature exhibits a minimum of the yield point following quenching from a specific temperature [2, 3]. Thus for the VTZ-1 alloy quenched from 850-870°C the difference between ultimate strength and yield point reaches 30-35 kg/mm² (Fig. 1).

Similar changes in mechanical properties following quenching from various temperatures are observed in the other investigated alloys. The only difference exists in the pre-quench temperature at which the yield point reaches its minimum. For the VT8 alloy this temperature is 900°C; for the VT14 alloy, 800°C, and so on.

According to a number of investigators [5-7] the decrease in yield point and ultimate strength following quenching from the above temperatures is due to "freezing" of the maximum amount of the metastable β phase by quenching from the two-phase ($\alpha + \beta$) region.

With the aid of x-ray structural analysis it proved possible in this investigation to demonstrate that the yield point minimum in two-phase titanium alloys is due to "freezing" of the martensitic-type α'' phase during quenching from the $\alpha + \beta$ -region. The presence of this phase is characteristic not only of alloys with 146

* Other participants in this project were: V. I. Bezgina, V. A. Koroleva, V. N. Moiseyev and I. A. Timonina.

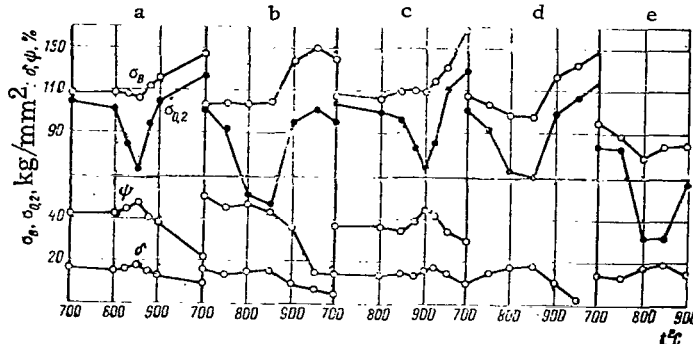


Figure 1. Relation of the Mechanical Properties of the Alloys VTZ-1 (a), VT6 (b), VT8 (c), VT14 (d) and VT16 (e) to the Pre-quench Temperature (Quenching in Water).

a high molybdenum content, as was established earlier for the VT-16 alloy [4], but also of other two-phase titanium alloys at corresponding quenching temperatures. The α'' phase has been detected on radiographs where it shows up as splitting of the diffraction lines of α -Ti. By way of illustration, Fig. 2 presents sections of x-ray diffraction patterns obtained for the alloys VTZ-1 and VT-8 with the aid of an URS-50I diffractometer using monochromatized Cu K_{α} -radiation within the angle ranges

$\theta = 17 - 19^\circ$ and $\theta = 25 - 29^\circ$. The rate of motion of the counter was 1 deg/min and the rate of motion of the strip chart, 1600 and 600 mm/hr. These x-ray diffraction patterns reveal the presence of additional diffraction lines associated with the larger reflection angles during quenching of the VTZ-1 alloy from $850 - 900^\circ\text{C}$ and the VT8 alloy from $880 - 950^\circ\text{C}$. They also reveal the presence of the diffraction line of the β phase (200); the intensity of the latter at first increases, reaching its maximum for the VTZ-1 alloy quenched from 800°C and the VT-8 alloy quenched from 850°C , and thereupon sharply decreases, indicating a decrease in the amount of the β phase on quenching of VTZ-1 from 850°C and VT-8 from 880°C . It is exactly at these pre-quench temperatures that the yield point reaches its minimum.

In the above range of temperatures we detected the α'' phase, as well as the lines of residual α and β phases, with the amount of the β phase not exceeding 7%. Raising the pre-quench temperature from $850 - 880^\circ\text{C}$ to $900 - 950^\circ\text{C}$ resulted in more of the α'' phase, whose chemical composition resembles that of the α' phase but whose crystal structure differs from the latter, since it displays a rhombic lattice [8]. Quenching from the β -region fixes the α' phase, which displays a hexagonal close-packed lattice. In two-phase ($\alpha + \beta$) alloys with high molybdenum content, the α'' phase occurs on quenching from the β region. For example, in the alloy VT22 quenching from the β region freezes the α'' phase. The change in the phase composition of the alloys VTZ-1 and VT-8 on quenching from various temperatures is illustrated in Table 1. A comparison of the results of the radiographic determination of the amount of β phase (Table 1) in the alloy VTZ-1 with measurements of Brinell hardness following quenching from various temperatures showed that the minimum hardness point does not coincide with the maximum content of the β phase (28%). Thus the minima of hardness and yield point correspond to the region of existence of the α'' phase, and not of the β phase.

147

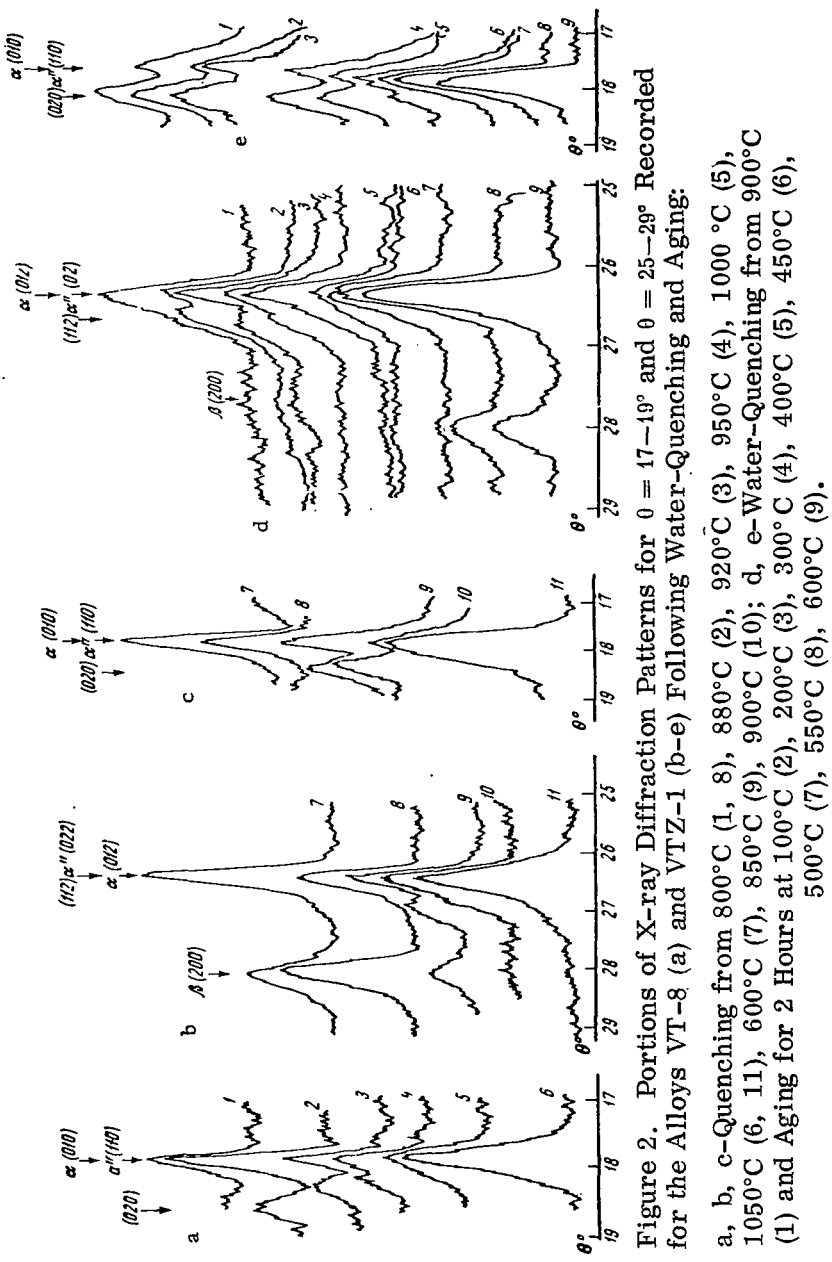


Figure 2. Portions of X-ray Diffraction Patterns for $\theta = 17-19^\circ$ and $\theta = 25-29^\circ$ Recorded for the Alloys VT-8 (a) and VTZ-1 (b-e) Following Water-Quenching and Aging:

Depending on the content of molybdenum and other β -stabilizing elements, the temperature ranges of existence of the metastable β , α'' and α' phases become displaced by quenching in accordance with the variation in the temperature of polymorphic transformation.

TABLE 1

/148

Pre-quench temperature $^{\circ}\text{C}$	Phase composition	Amount of β phase, %	H_B , kg/mm^2
VTZ-1 alloy			
After forging	$\alpha + \beta$	19	340
200	$\alpha + \beta$	17	340
400	$\alpha + \beta$	15	360
600	$\alpha + \beta$	13	360
800	$\alpha + \beta$	28	340
850	$\alpha + \alpha'' + \beta$	7	290
900	$\alpha'' + \alpha + (\beta)$	~ 2	300
940	$\alpha'' (\alpha) + \alpha'$	0	—
1050	α'	0	400
VT-8 alloy			
After forging	$\alpha + \beta$	9	—
500	$\alpha + \beta$	—	—
600	$\alpha + \beta$	—	—
800	$\alpha + \beta$	—	—
850	$\alpha + \beta$	18	—
880	$\alpha + \alpha'' + (\beta)$	—	—
900	$\alpha + \alpha''$	—	—
950	$\alpha' (\alpha'') + \alpha$	0	—
1050	α'	0	—

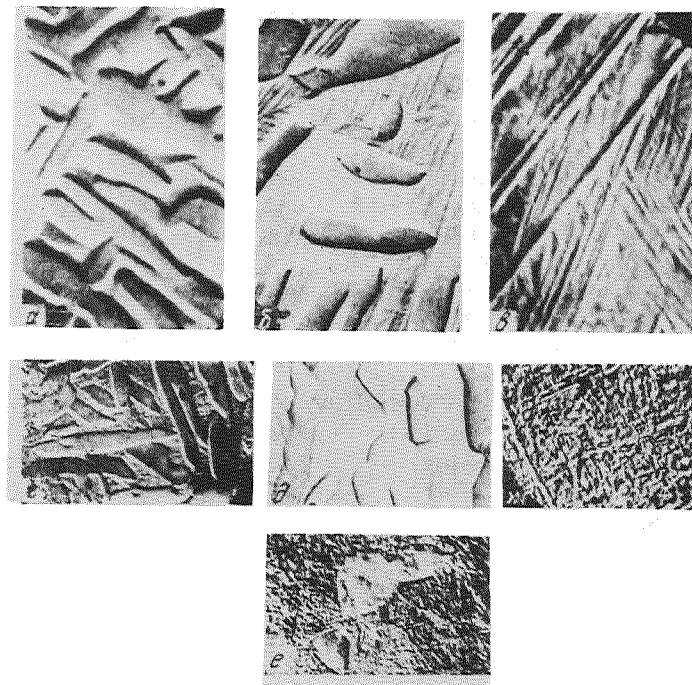
Table 2 presents data on the phase composition of alloys following quenching from various temperatures.

TABLE 2

Alloy	Pre-quench température $^{\circ}\text{C}$	Phase composition	Alloy	Pre-quench température $^{\circ}\text{C}$	Phase composition
VTZ-1	Up to 800—840	$\alpha + \beta$	VT-8	Up to 850—860	$\alpha + \beta$
	Up to 850—900	$\alpha + \alpha'' + \beta$		Up to 880—920	$\alpha + \alpha'' + \beta$
	Up to 940—960	$\alpha' (\alpha'', \beta) + \alpha$		Up to 950—980	$\alpha' (\alpha'', \beta) + \alpha$
	Above 980	α'		Above 1000—1020	α'
			VT-16	Up to 820	$\alpha + \beta$
				830—870	$\alpha + \alpha'' + \beta$

Examination under an electron microscope revealed that the quenching of two-phase titanium alloys is accompanied not only by phase transformations but also by marked changes in structure.

Figure 3 shows the structure of VTZ-1 alloy following quenching from 800-960°C. The photographs were obtained by the silver-carbon replica method.



/149

Figure 3. Structure of VTZ-1 Alloy Specimens Following Quenching (a-c) and Following Quenching + Aging (d-f), Magnification 9000 x.

Fig.	Temperature of quenching and aging, °C	Phases	Fig.	Temperature of quenching and aging, °C	Phases
a	800	$\alpha + \beta$	e	900 + (450, 2 hr.)	$\alpha + \alpha''$
b	900	$\alpha + \alpha''$	f	900 + (550, 2 hr.)	$\alpha + \beta$
c	960	α'	g	960 + (550, 2 hr.)	$\alpha + \beta$
d	800 + (450, 2 hr.)	$\alpha + \beta$			

On quenching from temperatures not exceeding 800°C segregations of the β phase are frozen, along with the primary α phase; their amount is estimated at 28-30% by the x-ray structural analysis method.

As the pre-quench temperature is raised to 850-900°C, the photographs begin to show, along with the primary α phase and the (7%) β phase (determined

by x-ray structural analysis), thin needles of an additional phase in the β sections. This apparently represents a martensitic type phase of α'' , detected by x-ray structural analysis. Its structure differs from that of the martensitic α' phase by having a finer relief and a high dispersion of needles, as is readily seen from a comparison of Figs. 3, b and 3, c. Quenching from the β region (960°C) results in a martensitic transformation and the formation of the macroacicular α' phase. Similar structural changes were also observed during the quenching of other two-phase titanium alloys (VT-16, VT-8, etc.).

The mechanism of formation of the metastable β , α' and α'' phases during quenching of $\alpha + \beta$ titanium alloys may be described with the aid of the diagram shown in Fig. 4, which relates the amount of the β phase and the concentration of β -stabilizing elements in it to the heating temperature. The curves were plotted on the basis of a general phase diagram for composition with 5% of β -stabilizing elements. This diagram is satisfactorily confirmed by the experimental findings obtained for the VTZ-1 alloy [9] by N. V. Lashko and associates.

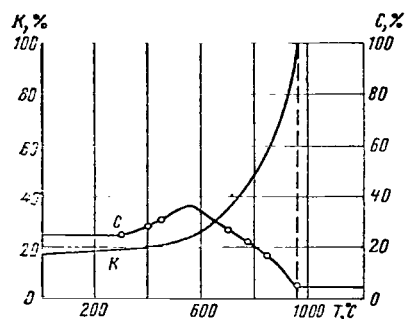


Figure 4. Relation of the Amount of β Phase (K) and Concentration of β -Stabilizing Elements Therein (C) to the Heating Temperature. Ti + 5% Cr Alloy (Theoretical Calculation).

($\text{Mo} > 10\%$). The other part of the β phase (48-68%), which represents a more dilute solid solution, should seemingly have transformed into the metastable α'' phase with a hexagonal crystal lattice. However, for this transformation the β phase would have to contain less than half the alloying element actually present, considering that the $\beta \rightarrow \alpha$ transformation goes to completion in quenching from the β region when the content of β -stabilizing elements in the alloy is 5%. Therefore, the high temperature β phase becomes, during quenching from $850-900^{\circ}\text{C}$, the metastable α'' phase with a rhombic crystal lattice; the latter arises from the β phase with a cubic crystal lattice during transformation of the β phase to the hexagonal α -Ti lattice. The rhombic crystal lattice may be treated as a distorted hexagonal lattice.

On heating between $20-600^{\circ}\text{C}$, the β -phase content and the concentration of β -stabilizing elements in the β phase change little. Hence water cooling from these temperatures results in freezing roughly the same amount of the stable β phase (14-17%). Heating to 800°C increases the amount of the β phase to 48% and reduces in half the concentrations of Cr, Mo and Fe in that phase. Quenching from this temperature results in fixing 28% of the metastable β phase, depleted of β -stabilizing elements ($a_{\beta} = 3.250 \text{ kX}$). As the heating

temperature is further raised to $850-900^{\circ}\text{C}$, the content of the β phase in the alloy rises to 55-70% and the concentration of β -stabilizing elements in this phase falls below critical. Therefore, during quenching the β phase becomes virtually completely transformed into α'' , with only a small (2-7%) residual amount of the β phase surviving owing to fluctuations in the concentration of the alloying elements

/150

In the VTZ-1 alloy, which contains alloying elements having shorter atomic radii than titanium, this distortion of the hexagonal crystal lattice is possible. As calculations showed, the replacement of a titanium atom ($r_{Ti} = 1.47$ kX) by a molybdenum atom ($r_{Mo} = 1.39$ kX) in a unit α -Ti cell results in an alteration of the crystal lattice parameter a of titanium from 2.95 to 2.85 kX; the latter value corresponds to one of the latter parameters of the α'' phase, amounting to $b/\sqrt{3} = 2.84$ -2.85 for the VTZ-1 alloy following quenching from 850-900°C. Thus, quenching results in the following transformation sequence: $\alpha + \beta \rightarrow \alpha + \alpha'' + \beta$.

Heating above the temperature of allotropic transformation results in the dissolution of all the alloying elements in the β phase, and that phase is so weakly saturated that quenching causes its transformation into the hexagonal α' phase (transformation sequence $\beta + \alpha'$).

Phase and Structural Transformations Accompanying the Aging of Quenched VTZ-1 Alloy

Changes in the phase composition and structure are determined not only by the conditions of aging but also by the temperature of quenching prior to aging, as was shown above. The kinetics of decomposition of the solid solution depends largely on the type of the metastable phase (β , α'' or α') that is frozen by quenching. Aging at 450-600°C of an alloy that was water quenched from 200-700°C causes only a limited redistribution of alloying elements between the α and β phases; this does not appreciably affect the mechanical properties of the alloy. On the other hand, aging of the alloy which was quenched from 800-950°C markedly changes the phase composition as well as the crystal lattice parameters of the phases. Thus, aging of VTZ-1 alloy quenched from 800°C is accompanied by decomposition of the β solid solution and the formation of a highly disperse mixture of α - and β -phase segregation. Thus the amount of the β phase decreases, as shown by x-ray structural analysis, from 28 (in hardened state) to 11%. The β phase content reaches its minimum following aging at 450-550°C (Fig. 5, a). This residual β phase is saturated with β -stabilizing elements (Mo, Cr, Fe), as is readily seen from the decrease in the crystal lattice parameter of the β phase (from $a = 3.25$ kX to $a = 3.20$ kX). Here the crystal lattice parameter of the α phase also decreases, which points to the saturation of this phase by β -stabilizing elements. This last may be attributed to the formation of a more enriched α phase during the decomposition of the metastable β phase. Moreover, the residual α phase apparently also becomes enriched with alloying elements through diffusion. /151

Following aging at 300-450°C the diffraction lines of the β phase become blurred, which may be explained by the presence of a β phase having a nonuniform composition. At > 300 °C the hardness of the alloy also increases (from 360 to 400 H_B). The hardness maximum is achieved following aging at 500°C.

The rise in the hardness of the alloy is associated with the decomposition of the metastable β phase, its maximum saturation by β -stabilizing elements and the formation of a highly disperse heterophase structure, which will be discussed below.

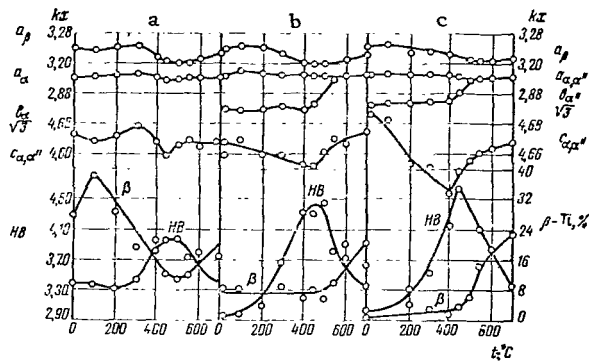


Figure 5. Variation in Crystal Lattice Parameters of the α , α'' and β Phases, of the Amount of β Phase and of Brindell Hardness (H_B) in the VTZ-1 Alloy Following Water Quenching From 800°C (a), 850°C (b), 900°C (c) and Aging.

Certain investigators attribute the increase in the hardness of quenched ($\alpha + \beta$) titanium alloys following their aging at 280 – 380°C to the decomposition of the β phase via the ω phase. However, radiographic analysis of VTZ-1 alloy that was quenched and aged under similar conditions did not show any ω phase. This phase was observed in the VT22 alloy, which contains approximately 10% β -stabilizing elements.

As the aging temperature of the VTZ-1 alloy is raised to 700°C , the amount of the stable β phase (which is less saturated than the β phase following aging at 500°C) increases. Here, the α phase also reaches a stable state. The hardness of the alloy then falls to a level close to the hardness of quenched material.

Electron microphotographs reveal decomposition of the β phase during aging at $\geq 300^{\circ}\text{C}$. The decomposition product is a finely dispersed mixture of α and β phases (Fig. 3, g).

Most interesting are the data obtained following quenching from 850 – 900°C . The process of decomposition of the metastable α'' and β phases frozen by water quenching from these temperatures can be traced during the aging process in terms of the variation in x-ray diffraction patterns recorded at angles $\theta = 25$ – 29° (Fig. 2). Following quenching, the line (022) of the α'' phase can be detected* on the x-ray pattern along with the lines of the β phase (200) and α phase (012).* Following aging at 100°C the angular distance between the x-ray lines of the α and α'' phases increases, which points to an increase in the distortion of the crystal lattice of the α'' phase. On the plot illustrating the relative variation in

/152

* The x-ray lines (012) and (010) of the α phase coincide with the lines (112) and (110) of the α'' phase, respectively [8].

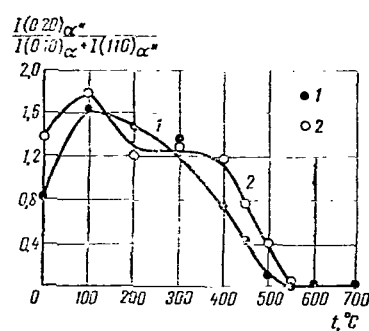


Figure 6. Relative Variation in Integral Intensities of the X-ray Diffraction Lines: $I_{(020)} \alpha''$, $I_{(010)} \alpha + I_{(110)} \alpha''$. Quenching From 850°C, 1 Hour, Water (1), From 900°C, 1 Hour, Water (2).

phase. On this basis it may be assumed that during decomposition the α'' phase goes through a state corresponding to the α' phase. In the final analysis, this phase decomposes with the formation of stable α and β phases. This decomposition of the α'' phase ends at 500°C. On electronmicroscopic photographs the decomposition of the α'' phase is observed later than by the x-ray method (following aging at 550°C, which corresponds to the terminal stage of decomposition (Fig. 3, f).

Along with the decomposition of the α'' phase the β phase also becomes altered. Its lines become blurred on aging at 300-450°C and become displaced in the direction of wider reflection angles. This is attributable to the change in the concentration of Cr, Mo and Fe in the β phase. The alloying elements liberated during the decomposition of the α'' phase pass into the β phase. Apparently the decomposition of the α'' phase occurs through diffusive migration of atoms. This is also confirmed by the change in the crystal lattice parameter a_{β} of the β phase (Fig. 5, b, c.). The parameter a_{β} reaches its minimum at temperatures corresponding to the ending of decomposition of the α'' phase.

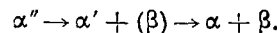
As the aging temperature of the alloy quenched from 850-900°C is raised to 600-700°C, the amount of β phase in this alloy also increases and its composition becomes stabilized.

As can be seen from Fig. 5, aging at 200-450°C increases Brinell hardness from 300 to 430-460 units. As the aging temperature is further raised, however, the hardness of the alloy decreases; then the amount of the β phase in the alloy is very small and hence the rise in hardness cannot be attributed to the formation of the ω phase. Considering that the ultimate decomposition product of the α'' phase is a fine-disperse mixture of the phases α and β , as in the decomposition of the metastable β phase except that the volume is greater (since a greater amount of the α'' phase is fixed), the rise in hardness may also be due to the fine-disperse

the content of the α'' phase in the specimen (Fig. 6) during low temperature aging, the amount of the α'' phase becomes relatively larger. The crystal lattice parameters of the α and α'' phases (a_{α} and $b_{\alpha}/\sqrt{3}$) display the maximum difference — 0.01 kX (Fig. 5, b, c). This points to completion of the $\beta \rightarrow \alpha''$ transformation during aging. Aging at 200-300°C produces only an insignificant decomposition of the α'' phase, as indicated by the slight variation in the ratio between the x-ray line intensities

$I_{(020)} \alpha'' / I_{(010)} \alpha + I_{(110)} \alpha''$ of the phases α and α'' . The x-ray lines of these phases in Fig. 2, d, e come somewhat closer together. Aging at $\geq 400^\circ\text{C}$ results in an intense decomposition of the α'' phase: its parameter ($b/\sqrt{3}$) decreases and its amount in the alloy drastically diminishes. Following aging at 450°C the x-ray lines which have been observed to split during the formation of the α'' phase became blurred like the lines of the α'

nature of the decomposition products. Another reason for the rise in hardness may be the formation during the decomposition of a phase resembling the α' phase (in its concentration of alloying elements) and having a high hardness compared with the α phase, i. e. in the case where the decomposition kinetics of the α'' phase during aging may be represented by the sequence



According to Bagaryatskiy [8] the phases α'' , α' (α) and β differ somewhat in the extent of atom displacements in the crystal lattice: in the α'' phase atom displacements with respect to the β phase are smaller than in the α phase. On this basis the $\beta + \alpha''$ transformation during quenching may be regarded as an incomplete $\beta + \alpha'$ transformation. It is completed by aging at 400–450°C. This transformation is initiated by diffusion processes causing the migration of atoms of β -stabilizing elements from the α'' phase to the β phase. The diffusive nature of the transformation of the α'' phase during aging may also be the reason why electron microphotographs fail to reveal the decomposition of this phase.

The hypothesis of the diffusive nature of the formation of the intermediate α' phase does not conflict with the pattern of transformations in titanium alloys. As is known, the ω phase, which belongs in the martensitic class, also may arise during tempering as an intermediate phase between the metastable β phase and the α phase. To conclusively resolve the question of the existence of the intermediate α' phase it is necessary to broadly investigate phase transformations on a number of alloys of the $\alpha + \beta$ type.

Following quenching from the region of existence of the β phase there forms a metastable α' phase which aging decomposes into the α and β phases.

Thus, the decrease in ultimate strength and yield limit of the VTZ-1 alloy following its quenching from 850°C is attributable to the formation of the metastable phase α'' . The rise in strength, accompanied by a low plasticity that is observed following quenching from temperatures exceeding the critical temperature of the $\alpha + \beta \rightarrow \beta$ transformation is due to the formation of the α' phase.

Aging at 450–500°C of the VTZ-1 alloy quenched from 800–1050°C results in a sharp increase in hardness and decrease in plasticity [2] to an extent that increases with increase in quenching temperature, regardless of which phase is fixed by the quenching (β , α'' or α').

Decomposition of the metastable phases occurs at 300–600°C and is accompanied by a redistribution of alloying elements which results in marked saturation of the β phase by Cr, Mo and Fe during aging at 450–500°C. The temperature range of existence of the supersaturated β phase coincides with the hardness maximum of the alloy. The decomposition of the metastable phases results in the formation of a fine-disperse mixture of stable α and β phases whose amount is greater the higher was the quenching temperature. This may account for the rise in the hardness of the alloy aged following quenching from high temperatures.

The literature provides indications of the possibility of formation, during tempering, of the intermediate ω phase causing the embrittlement of the titanium alloys treated with transition elements. In the investigated binary alloys the formation of the ω phase during tempering is accompanied by a shrinkage in the volume of the metal and by a rise in hardness; thus these characteristics were taken to the principal signs of the existence of the ω phase [7]. However, hardness in the investigated alloy increases (400-440 H_V) during aging at temperatures higher than the temperature of the formation and decomposition of the ω phase. Moreover, the maximum hardness (470 H_V) is attained during the formation and decomposition of the α'' phase rather than the β phase.

/154

Therefore, the hardening of the alloy VTZ-1 cannot be explained by the formation of the ω phase. As is pointed out in [10, 11], the ω phase can be unambiguously determined only by the x-ray structural method. However, not one of the regimes of heat treatment employed has made it possible to detect diffraction lines of the ω phase on the radiographs.

Thus a more likely reason for the hardening of the alloy following aging of quenched material is the decomposition of the metastable β , α'' and α' phases and the formation of fine-disperse particles of the decomposition products.

Similar kinetics of decomposition of metastable phases may be observed during the aging of other two-phase industrial alloys.

REFERENCES

1. Entsiklopediya sovremennoy tekhniki "Konstruktionskiye materialy" [Encyclopedia of Modern Technology, Structural Materials, 3.] Sovetskaya Entsiklopediya Press, 1965.
2. Zwicker, U. Z. Metallkunde, Vol. 47, No. 8, p. 535, 1956.
3. Solonina, O. P. In the collection: "Novyye issledovaniya titanovykh splavov" [New Research into Titanium Alloys], Nauka, 206, 1965.
4. Lashko, N. F. Doklady AN UkrSSR, Vol. 4, p. 502, 1964.
5. Glazunov, S. G., G. M. Kokhova and O. P. Solinina. Aviatsionnaya Promyshlennost' [Aviation Industry], Vol 6, No. 43, 1958.
6. Verigina, Z. V. and B. G. Lifshits. Izvestiya Vuzov "Chernaya Metallurgiya" [Ferrous Metallurgy], Vol. 5, p. 163, 1960.
7. Luzhnikov, L. P., V. N. Novikova and A. P. Mareyev. In the collection: "Metallovedeniya titana" [Metallography of Titanium], Nauka Press, No. 80, 1964.
8. Bagaryatskiy, Yu. A., T. V. Tagunova and G. I. Nosova. Metallovedeniya i vizika metallov [Metallography and Metal Physics], No. 5, Metallurgidat, p. 210, 1958.
9. Lashko, N. F. et al. "Titan v promyshlennosti" [Titanium in Industry], Oborongiz, No. 112, 1961.
10. Bagaryatskiy, Yu. A. and G. I. Nosova. Fizika metallov i metallovedeniye [Metal Physics and Metallography], Vol. 13, No. 3, p. 415, 1962.
11. Fedotov, S. G. In the collection: "Metallovedeniye titana" [Metallography of Titanium], Nauka Press, 308, 1964.

CHANGES IN THE AMOUNT AND COMPOSITION OF THE β PHASE DURING HEAT TREATMENT OF THE ALLOY VTZ-1

Ye. I. Gus'kova, N. F. Lashko and L. M. Mirskiy

So far no acceptable explanation has been found for the processes of hardening and softening that occur in $\alpha + \beta$ titanium alloys (in particular in the VTZ-1 alloy and similar alloys). There exist sharply conflicting opinions on the phase composition of this alloy and the processes occurring in it during its quenching from the region of $\alpha + \beta$ or β phase, as well as on the processes of the decomposition of the metastable quenched structures during subsequent aging.

Basically, there exist the following three views on the nature of phase transformations in the alloy VTZ-1:

1. The high strength and low plasticity of the alloy VTZ-1 are conditioned by the formation of the metastable ω phase during quenching and low-temperature aging [1].

2. The change in mechanical properties of the alloy VTZ-1 is attributed to the change in the amount of the β phase and decrease in grain size during thermo-mechanical treatment. Low-temperature aging results in decomposition of the β phase [2, 3] regardless of the quenching regime. /155

3. The properties of the alloy VTZ-1 are determined by the mutual ratio, dispersity and distribution of the α , α' , α'' and β phases. Low-temperature aging results in the decomposition of the metastable α' , α'' and β phases and the formation, stabilization and change in composition of the β phase [4].

Of special significance of the hardening of the alloy VTZ-1 is the β phase, its amount, composition, degree of stability, form of segregation and distribution. The amount of the β phase in $\alpha + \beta$ alloys is determined by two methods: x-ray structural, no intact specimens [5], and chemical analysis of anodic residues isolated by methods of electrochemistry.

The composition of the β phase in heterogeneous alloys can be directly determined only by the latter method. The determination of the amount of this phase by the x-ray structural method reduces to finding the integral intensities of diffraction from selected reflection planes of the α and β phases [3, 5].

The accuracy of determination of the diffraction intensities markedly diminishes in polycrystalline, mosaic and textured alloys, since it is highly difficult to make proper allowance for the effects of extinction and texture: in the presence of texture the determination of the amount of β phase is practically impossible, and hence the β phase was chiefly investigated only after it had been isolated.

Earlier investigations [4] showed that following quenching of the VTZ-1 alloy from the $\alpha + \beta$ region, regardless of the cooling rate, a residual β phase with a varying content of alloying elements and varying stability is always detected. On quenching from the β region ($960-970^{\circ}\text{C}$), the β phase is detected following cooling in air and in oil and in some cases in water (when the content

of β forming elements verges on its lower limit). The elementary-lattice parameter of the residual β phase increases with increase in quenching temperature, which points to a decrease in the content of β -forming elements in this phase. The residual β phase is the least stable following quenching in water from 800°C (during subsequent aging it decomposes); following quenching from 840°C it is more stable—its amount increases during subsequent aging.

Quenching of the alloy in water from 840°C results in partial nondiffusive transformation into the α'' phase.

In specimens of the alloy VTZ-1 water-quenched from 845°C the β phase was isolated together with the metastable rhombic α'' phase in one of the electrolytes.

The data of the x-ray analysis of the anodic residue are presented in Table 1.

TABLE 1

/156

<i>I</i>	<i>h</i> <i>l</i>	<i>d</i>	Phase	<i>I</i>	<i>h</i> <i>l</i>	<i>d</i>	Phase
Weak	110	2.56	α''	Weak	021	2.186	α''
Medium	020	2.46	α''	Medium	200	1.640	β
Strong	002	2.326	α''	»	130	1.443	α''
»	110	2.326	β	Strong	211	1.332	β
»	111	2.242	α''	Medium	{ 221 132	1.233	α''

Thus the existence of the metastable martensitic α'' phase following acute quenching of the alloy VTZ-1 from specific temperatures was confirmed. Following water-quenching from $950\text{--}1000^{\circ}\text{C}$ the α' phase appears.

During aging, owing to the decomposition of the martensitic α' and α'' phases, as well as of the most metastable β phase, the alloying elements get redistributed between the α and β phases and this is accompanied, up to definite temperatures ($\sim 550^{\circ}\text{C}$) by the enrichment of the β phase with β -forming elements in the process of stabilization of the alloy (the parameter of the β phase then decreases). A typical change in the lattice parameter of the β phase (intact [non-electrolyzed] etched specimens) following quenching and aging is illustrated in Fig. 1.

The isolation of the β phase was accomplished with the aid of a specially selected electrolyte and mode of electrolysis assuring an active state of the α , α' and α'' phases and a passive state of the β phase (isolation in powder form). The curve of anodic polarization of the alloy, which is chiefly determined by the α , α' and α'' phases, as well as the curve of the β phase* in the selected

*The potentials of the alloy VTZ-1 are determined by the high content of the α phase which resembles in composition the α phase of alloy VT-5, while the

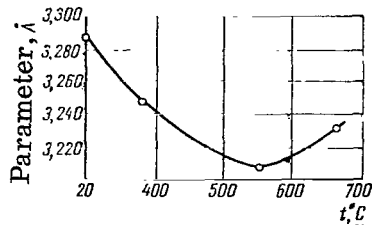


Figure 1. Variation in the Lattice Parameter of the α Phase of VTZ-1 Following Water-Quenching From 800°C and Aging for 2 Hours at Various Temperatures. Intact Specimens of the Alloy VTZ-1.

5.9% Al, 0.5% Fe, 0.2% Si, 0.03% N_2 , 0.015% H_2 .

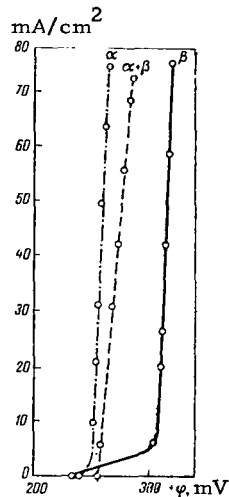


Figure 2. Anodic Polarization Curves of an α -Alloy (VT-5) an $\alpha + \beta$ Alloy (VTZ-1) and a β -Alloy (VT-15) in an Electrolyte Containing 3 g of Succinic Acid and 1 ml of Sulfuric Acid Per Liter of Methanol.

In the alloy quenched in helium from 870°C a highly disperse β phase was detected (weak, blurred lines on Debye powder diagrams); following quenching from 1000°C (from β -region) the β phase was much less disperse (distinct, strong lines). The relatively large size of its particles may be due to the fact that the concomitantly forming α' phase is macroacicular, whereas the α' phase forming after quenching from 870°C is either structureless or microacicular. Following quenching from 870°C and from 1000°C and following subsequent aging for 5 hr at 550°C the lines of the β phase are distinct, which points to its coagulation.

The anodic residues isolated from specimens following thermomechanical treatment (without aging) contain, along with the β phase, a small amount of the $\alpha(\alpha')$ phase and hence their chemical composition does not precisely correspond to that of the β phase. The results of chemical analysis of the anodic residues are presented in Table 2.

The amount of the β phase following conventional quenching from 1000°C and following thermomechanical treatment from 920°C is smaller than following

/157

*Footnote (cont'd). potentials of the β phase of the alloy are close to the potentials of the single-phase β alloy VT-15 (system Ti-Al-Cr-Mo).

quenching from 870°C. Thermomechanical treatment of the alloy contributes to a more intense formation of the residual β phase following aging than following conventional quenching.

TABLE 2

Treatment	Phase	Amount of phase, %	Composition of β and α Phases, %				
			Ti	Al	Cr	Mo	Fe
Quenching from 870°C, cooling in helium	β	4.90	83.06	3.47	3.47	8.16	1.83
	α	95.10	89.93	6.02	1.51	2.10	0.43
As above + aging for 5 hr at 550°C	β	6.1	69.49	2.28	8.97	14.20	5.05
	α	93.87	90.92	6.13	1.11	1.63	0.20
Quenching in vacuo, from 1000°C cooling in helium	β	3.65	82.19	3.56	4.10	8.49	1.65
	α	96.35	89.87	5.93	1.60	2.16	0.45
As above + aging for 5 hr at 550°C	β	8.14	71.86	1.59	8.11	13.51	4.92
	α	91.86	91.29	6.28	1.02	1.4	0.10
Thermomechanical treatment (TMT) (870°C, cooling in helium + 30% deformation)	$\beta+\alpha$ (c.p.)	5.29	85.79	3.22	4.35	5.31	1.32
	α	94.72	89.81	6.04	1.44	2.24	0.46
TMT (870°C + 30 deformation), cooling in helium + 500°C for 5 hr	β	7.61	76.3	1.83	6.70	12.40	2.76
	α	92.39	90.72	6.23	1.08	1.67	0.31
Vacuum TMT (1000°C + 30% deformation), cooling in helium	$\beta+\alpha$	5.78	87.71	2.60	4.15	4.50	1.03
	α	94.22	89.71	6.10	1.43	2.37	0.45
As above + aging for 5 hr at 500°C	β	9.43	70.20	2.01	8.16	15.38	4.24
	α	90.57	91.61	6.31	0.91	1.04	0.11
Forging at 920°C with 70% deformation, cooling in water	β	6.52	78.52	5.06	7.05	9.35	
	α	93.48	90.84	5.89	1.51	1.73	
As above + aging for 2 hr at 550°C	β	7.82	73.78	4.73	8.95	12.52	
	α	92.18	91.48	6.01	0.987	1.54	
As above + sizing	β	8.52	74.41	3.75	8.85	13.02	
	α	91.48	91.56	6.09	0.91	1.42	

The chemical composition of the β phase isolated from the specimens is roughly the same regardless of the quenching regime (Table 2); following aging the β phase contains a higher concentration of β -forming elements (Cr, Mo and Fe) than following quenching. The content of Cr, Mo and Fe in the specimens aged following their thermomechanical treatment (TMT) also is higher than following conventional quenching and aging.

The results of phase analysis may be explained by assuming that aging causes the metastable phase α' (or α'') to partially decompose into α and β phases with the attendant coagulation of the residual β phase.

This is accompanied by the redistribution of β -forming elements between the α and β phases, with the β phase becoming enriched with Cr, Mo and Fe and the phases becoming commensurately depleted of these elements. Then the alloy VTZ-1 stabilizes. All this is in agreement with the data of x-ray structural analyses.

/158

High-temperature deformation during TMT contributes to an intense formation of the residual β phase and intensifies the decomposition of the $\alpha'(\alpha'')$ phase during aging.

TABLE 3

Conditions of treatment			Mechanical properties		
Temp- erature °C	Deg. of de- formation %	Subsequent treatment	σ_B , kg/mm ²	δ , %	Φ , %
870	0	Cooling in helium	115.0	16.0	40
	60		143.0	22.5	60
	0		120.0	7.5	10
	60		168.0	11.0	14.0
1000	0	Cooling in helium + aging at 500°C for 5 hr	125.0	12.0	30.0
	60		162.0	17.0	36.0
	0		130	5.0	7.0
	60		178	6.5	7.5

The increase in the amount and degree of dispersity of the β phase should, in accordance with the theory of the inhibition of dislocations in two-phase alloys, increase ultimate strength and reduce plasticity. The results of short-time tensile tests (Table 3) of the alloy VTZ-1 following various modes of its cold and hot working are in agreement with the variation in the phase composition of this alloy. The higher plasticity of this alloy following its thermomechanical treatment is apparently associated with the attendant greater homogeneity of structure. The residual plastic deformation (permanent set) accompanying TMT should, as is usually the case, at high temperatures lead to predomination of softening processes over hardening processes (owing to the increase in the intensity of diffusion processes); the characteristics of the high-temperature strength of the alloy above a certain temperature should be lower following TMT than following heat treatment.

CONCLUSIONS

1. A residual β phase was detected in the alloy VTZ-1 following its quenching from the $\alpha + \beta$ region as well as from the β -phase region; in the latter case the amount of the β phase is smaller. The dispersity and amount of the β phase following quenching from 1000°C usually are smaller than those following quenching from 870°C. When quenching is carried out as part of TMT, the β phase is highly disperse regardless of the pre-quench temperature.

2. Aging at 550°C results in decomposition of the $\alpha'(\alpha'')$ phase into $\alpha + \beta$ phases. The residual β phase then coagulates. High-temperature deformation during TMT contributes to a more intense decomposition of the $\alpha'(\alpha'')$ phases during aging than following conventional quenching.

3. Aging at 550°C causes the residual β phase to become markedly enriched with β -forming elements (Cr, Mo, Fe).

4. The hardening of the alloy VTZ-1 following its TMT (compared with its heat treatment at relatively low temperatures) depends to a large degree on the state of the β phase (its amount, dispersity and distribution). At above-critical temperatures ($\geq 500^\circ \text{C}$), softening processes, which are associated with the fine structure of the alloy and the rise in the intensity of diffusion processes, must predominate.

/159

REFERENCES

1. Luzhnikov, L. P., V. M. Novikova and A. P. Mareyev. In the collection: "Metallovedeniye titana" [Metallography of Titanium], Nauka Press, 80, 1964.
2. Shigarev, A. S. Metallovedeniye i termicheskaya obrabotka metallov [Metallography and Thermal Treatment of Metals], Vol. 1, No. 42, 1962.
3. Gulyayev, A. P. and A. S. Shigarev. In the collection: "Issledovaniya po vysokotemperaturnym i nitevidnym kristallam" [Research into High-Temperature and Filamentous Crystals], USSR Acad. Sci. Press, 142, 1963.
4. Blok, N. I. et al. In the collection: "Titan i yego splavy" [Titanium and Its Alloys], Oborongiz, 112, 1961.
5. Yermolova, M. I. Zavodskaya Laboratoriya [Plant Laboratory], Vol. 5, p. 577, 1965.

DECOMPOSITION OF TITANIUM-VANADIUM MARTENSITE DURING HEATING

S. G. Fedotov, K. M. Konstantinov and Ye. P. Sinodova

This investigation deals with the decomposition kinetics of a supersaturated α -solid solution of titanium (martensite) containing 4, 8, 10, 11 and 12 wt. % V. The principal method of investigation employed was the determination of elasticity moduli, which proved to be highly sensitive to the phase structure of titanium alloys, particularly in quenched state, and to its variation during heating [1-3]. Moreover, the temperature dependence of the resistivity of the alloys also was investigated. In addition, x-ray phase analysis and microstructural analysis were carried out.

The alloys were prepared from TG-118 titanium sponge and 99.51% pure vanadium. Ingots weighing 30-40 g were melted in a vacuum arc furnace with a nonconsumable tungsten electrode. The composition of the alloys was monitored by measuring the losses of burden during melting and the hydrostatic density, on resorting to chemical analysis of a number of alloys as well. The ingots were forged in air at 900-1000°C into cylindrical billets from which specimens were turned. The alloys were annealed in evacuated quartz ampoules following the regime: 1000°C, 24 hr; 800°C, 100 hr; 600°C, 150 hr; 400°C, 200 hr, cooling in ampoules. The heating of the alloys to the pre-quench temperature of 1000°C and exposure to this temperature for 24 hr were also carried out in evacuated quartz ampoules. Quenching was accomplished by shattering the specimen-containing ampoules in water at room temperature.

Elastic properties (Young modulus and shear modulus) were determined by the dynamic method with the aid of an Elastomat type device [4]. During investigation of the temperature dependence of elastic properties of specimen was heated in a special furnace including a massive stainless steel block assuring a uniform heating of the specimen. The heating rate was near-linear and amounted to ~ 3 deg/min. The temperature was measured with the aid of a Pt/PtRh thermocouple readings of which were recorded on an EPP-09 electronic potentiometer, as well as with the aid of a more sensitive Ni/NiCr thermocouple and an extension potentiometer. The thermocouple junctions were embedded in the massive steel block near the specimen.

During investigation of the temperature dependence of resistivity the specimen was heated in vacuo to 1000°C. Resistivity was measured by the method of automatic recording of the voltage drop in the specimen during the passage of rectified, smoothed and stabilized 920-ma current across it [5]. /160

Radiographs of the 0.5-0.6 mm diameter cylindrical specimens were recorded following their heat treatment by the same regime as that applied to the specimens used to investigate elastic properties. Evacuated ampoules containing the cylindrical specimens heated to the desired temperature were shattered in room-temperature water. The radiographs were recorded in Cu radiation on using a Ni filter. Exposure time was 2.5-3.0 hr.

Figure 1 presents the results of measurements of elasticity moduli during the heating of vanadium-containing martensite. Figure 2 presents the temperature

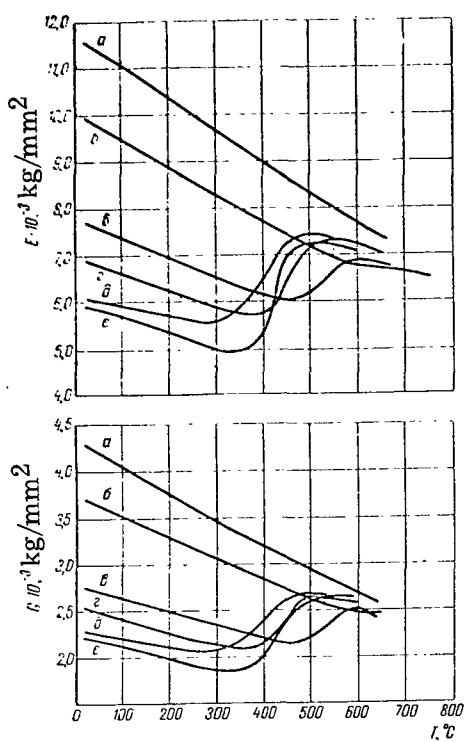


Figure 1. Variation in Elastic Moduli During Heating of Martensite Containing:
 1 wt. % V (a); 4 wt. % V (b), 8 wt. % V (c); 10 wt. % V (d), 12 wt. % V (e)
 11 wt. % V (f).

10% V following quenching and annealing are illustrated in Fig. 3. The temperatures of the $\alpha + \beta \rightarrow \beta$ transition are indicated on the curves of resistivity of alloys in annealed state. The values of these temperatures for alloys of the above and other investigated compositions satisfactorily lie along the curve of the $\alpha + \beta \rightarrow \beta$ transformation of the phase diagram shown in Fig. 4. The pattern of variation in the resistivity of the quenched alloys is more complicated

Figure 5 presents radiographs of the alloy with 10% V following quenching from 1000°C (a), subsequent heating of 350°C and cooling in water (b) and also following heating of the quenched alloy to 550°C and cooling in water (c). These and other radiographs indicate that heating to 350°C does not alter the state of the martensite, whereas heating of the martensite to 450, 500 or, particularly, 550°C affects its state substantially. As the martensite heating temperature increases, the blurring of the lines, characteristic of the original supersaturated α -solid solution of titanium, decreases and new lines pointing to the presence of the β phase in the alloy structure begin to appear.

dependence of elasticity moduli for alloys containing 4 and 10% V following annealing and following quenching to martensite. The annealed alloys of all compositions are marked by a monotonic decrease in Young and Shear moduli on heating within the investigated range of temperatures. The quenched alloys display a different response. Initially their elastic properties decrease during heating but after a specific temperature—which depends on the chemical composition of the alloy—is reached, the moduli E and G rise, to an extent that is greater the higher is the vanadium content of the alloy, i. e. higher is the supersaturation of α -Ti with V. This rise occurs within a specific range of temperatures.

The data presented above also imply that the greater the supersaturation, the lower is the temperature at which the rise in elastic moduli begins and ends. The values of these temperatures are given on the curves.

In the quenched alloy with 1% V whose content of the alloying element does not exceed the limit of its solubility in α -Ti in equilibrium state, elastic properties vary during heating as in the annealed alloys shown in Fig. 1, a. The characteristic features of the variation in resistivity during heating of the alloy with

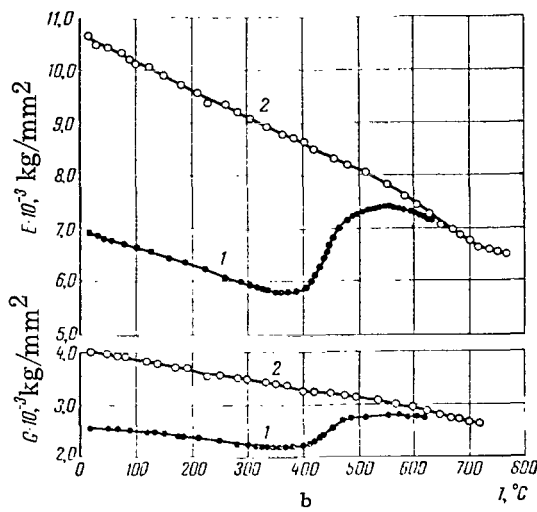
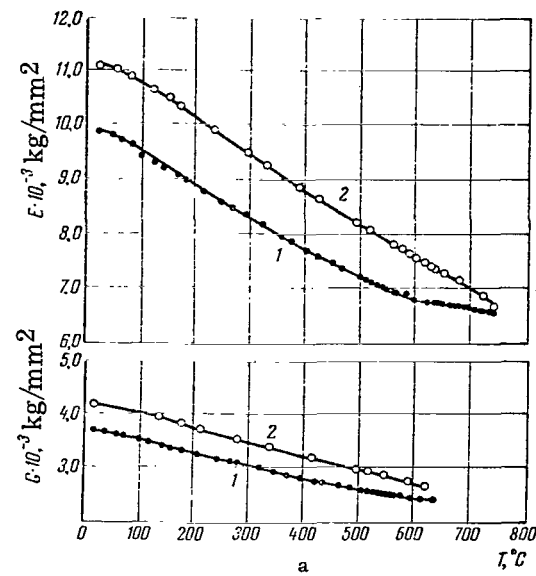


Figure 2. Variation in Elastic Moduli of the Alloys of Titanium with Vanadium in Quenched (1) and Annealed (2) States:

a—4% V; b—10% V.

Thus the observed structural changes accompanying the heating of alloys previously quenched to martensite, when such heating is carried out at temperatures corresponding to the rise in elasticity moduli, point to the decomposition of martensite. It follows hence that the temperatures at which the rise in elastic

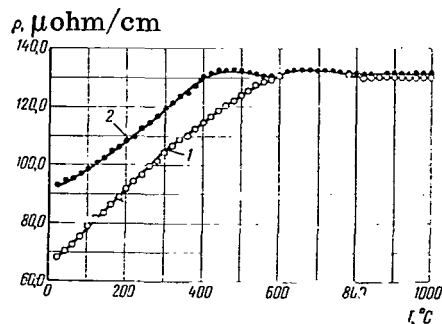


Figure 3. Variation in Resistivity During Heating of the Alloy of $Ti + 10$ wt. % V in Annealed (1) and Quenched (2) States.

moduli is small, since the β phase itself displays extremely low elastic moduli.

moduli begins and ends correspond to the temperatures at which the decomposition of martensite begins and ends.

These temperatures, plotted on the phase diagram of the system Ti - V (Fig. 2, lines 1 and 2), reflect the relation of the initial and final temperatures of the decomposition of martensite to the composition of martensite.

The rise in elastic moduli during the decomposition of heated martensite is primarily associated with the decrease in the supersaturation of the α -solid solution by vanadium. The contribution made by the newly forming β phase to the rise in these

moduli is small, since the β phase itself displays extremely low elastic moduli.

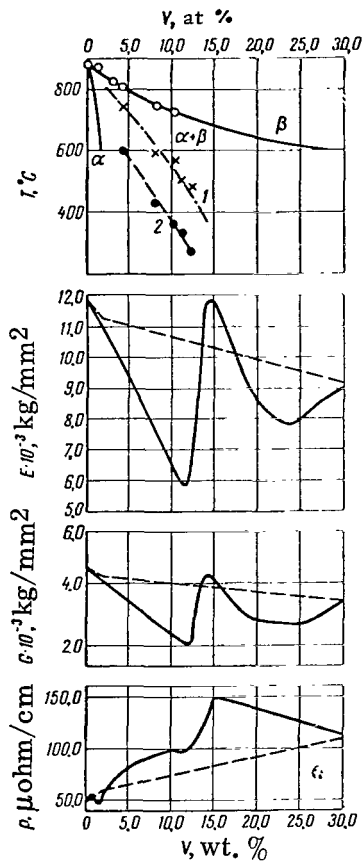


Figure 4. Phase Diagram of the System Ti-V and the Properties of Alloys in Annealed (Broken Lines) and Quenched (Solid Lines) States.

1, 2—Start and End Points of the Decomposition of Martensite.

The role of vanadium in reducing the elastic moduli of α -Ti during the formation of supersaturated α -solid solutions is graphically demonstrated by a comparison of the dependence of these properties on composition in annealed and in quenched (to martensite) states (Fig. 4).

It is interesting to note that the curve reflecting the dependence of the final temperature of martensite decomposition on composition (Fig. 4, curve 1) practically coincides with the curve of the initial temperatures of martensitic transformation (martensite start point M_s) of these alloys. It may be assumed that the initial temperature of martensite decomposition is close to the final temperature of martensitic transformation (martensite end point) for these alloys. As is known, martensitic transformation occurs within a specified range of temperatures. Since the initial temperature of martensite decomposition depends on the composition of the martensite, and this decomposition itself occurs within a range of temperatures that differs for

/163

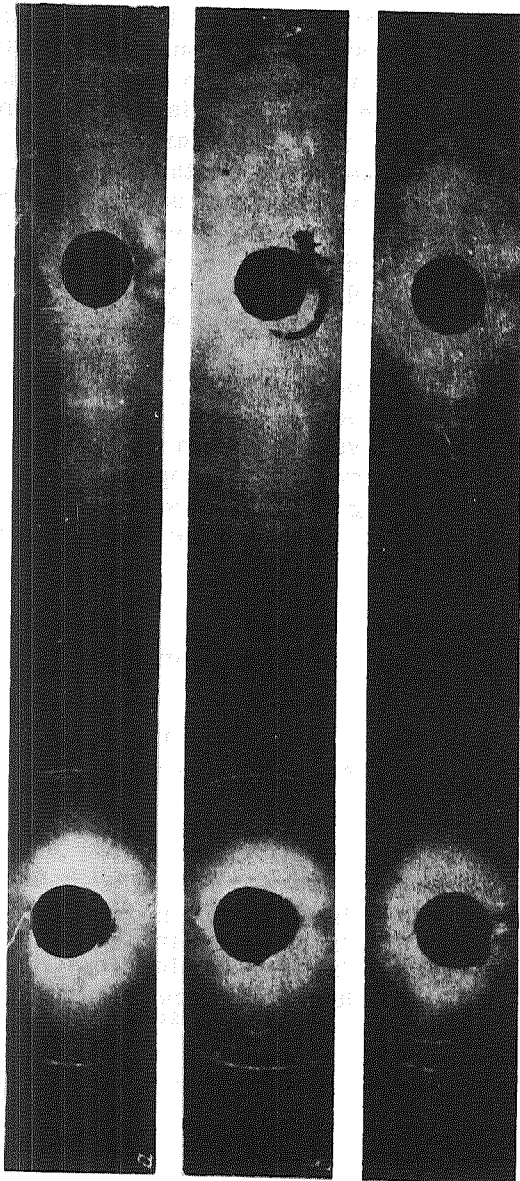


Figure 5. Radiographs of the Alloy Containing 10 wt. %: a—Quenching from 1000°C; b—Quenching Followed by Heating to 350°C; c—Quenching Followed by Heating to 550°C.

each alloy, it may be assumed that the martensite itself represents a phase of variable composition and the decomposition of martensite occurs within a specific range of temperatures.

The interrelationship between the temperatures of the decomposition and formation of martensite as well as the minimally low values of elastic moduli of the alloys in these two extreme states of phase structure may point to similarity of the mechanisms of these processes. An indeed, the metastable β -solid solution during the stage preceding martensitic transformation is characterized by extremely low values of elastic moduli and an extremely high Poisson ratio [6], and it is this that accounts for the displacive mechanism of the transformation. Martensite is also characterized by a sharp decrease in elastic moduli and rise in Poisson ratio with increase in supersaturation of α -Ti [7]. Depending on the degree of supersaturation, heating results in a still greater decrease in the moduli and rise in Poisson ratio to its upper limits beyond which martensite begins to decompose, also by the displacive mechanism. The oriented displacive decomposition of the original acicular crystals of martensite manifests itself in the microstructure of the alloy following the tempering of martensite.

It should also be pointed out that the tempered titanium-vanadium martensite displays a high ultimate strength. This will be illustrated with results of the determination of ultimate strength of the alloys of titanium with 4 and 10 wt. % V following prolonged annealing, quenching from various temperatures of the region of existence of the β -solid solution, quenching to martensite and subsequent tempering. As can be seen, aging of martensite increases the ultimate strength of the alloys by at least 30%:

Heat treatment	σ_B , kg/mm ²	Heat treatment	σ_B , kg/mm ²
Ti + 4 wt. % V		'Ti + 10 wt. % V	
Multistage annealing		Multistage annealing	
1050° C - 48 hr		1050° C - 48 hr	
800° C - 72 hr		800° C - 72 hr	
600° C - 72 hr		600° C - 72 hr	
400° C - 24 hr	81.2	400° C - 24 hr	64.2
Water-quenching from 1200° C	69.2	Water-quenching from 1200° C	63.4
Water-quenching from 1000° C	68.4	Water-quenching from 1000° C	63.7
Water-quenching from 875° C	64.7	Water-quenching from 850° C	63.1
Quenching from 1000° C and tempering at 650° C	97.1	Quenching from 1000° C and tempering at 40° C	95.9

CONCLUSIONS

1. The decomposition of martensite during heating occurs within a specific temperature range.

2. The initial and final temperatures of martensite decomposition depend on the chemical composition of martensite. As supersaturation increases, the initial temperature of martensite decomposition decreases.

3. The initial and final temperatures of the decomposition of martensite during heating are associated with the start and end points of martensite during quenching.

4. Martensite has a variable composition.

5. The decomposition mechanism of martensite is displacive.

6. The aging of titanium martensite leads to a sharp hardening of the alloys.

REFERENCES

1. Knorr, W. and Scholl. Z. Metallkunde, No. 51, p. 609, 1960.
2. Fedotov, S.G. In the collection: "Titan i yego splavy" [Titanium and Its Alloys], No. 10, USSR Acad. Sci. Press, 188, 1963.
3. Fedotov, S.G. and O.K. Belousov. Fizika metallov i metallovedeniye [Metal Physics and Metallography], Vol. 17, No. 5, p. 732, 1964.
4. Forster, F. Industrie Anzeiger, Vol. 64, No. 77, 1955.
5. Kornilov, I.I., V.S. Mikheyev and K.M. Konstantinov. Fizika metallov i metallovedeniye [Metal Physics and Metallography], Vol. 16, No. 1, p. 57, 1963.
6. Fedotov, S.G. Issledovaniya metallov v zhidkem i tverdom sostoyaniyakh [Studies of Metals in Liquid and Solid States], Nauka Press, 207, 1964.
7. Fedotov, S.G., K.M. Konstantinov and Ye.P. Sinodova. In the collection: "Novyye issledovaniya titanovyakh splavov" [New Studies of Titanium Alloys], Nauka Press, 189, 1965.

STUDY OF ALLOYS OF THE SYSTEM Ti-Al-Mo-Zr BY THE BENDING METHOD AT HIGH TEMPERATURES

N. G. Boriskina and M. A. Volkova

Research into the high-temperature strength of alloys of the system Ti-Al-Mo-Zr is of considerable practical interest inasmuch as there exist in this system regions of α -, α_2 - and β -solid solutions which may be used as the basis for developing alloys for high temperature performance.

Phase equilibria in this system have been investigated earlier.

To investigate high-temperature strength a series of alloys of this system was prepared over two cross sections passing across the edge of the tetrahedron Ti-Al and the face Ti-Mo-Zr with the Mo/Zr ratio amounting to 3:1 and 1:3 over the sections with 3, 6, 9, 12, 16 and partially 22% Al, containing an aggregate amount of Mo and Zr reaching 25-30%.

/165

In addition, the high-temperature strength of alloys of the system of the radial section Ti-Al-Zr running from the pure Zr corner to the alloy of the binary system Ti-Al containing 9% Al was also investigated. Phase equilibria in this system are described in the work [1].

The alloys were prepared by the crucibleless melting method. The test specimens had the shape of cylinders measuring 4 mm in diameter and 50-60 mm in length. The raw materials used were TG00 titanium sponge, AV000 (99.99% pure) aluminum, molybdenum rods (99.9% pure) and iodide zirconium.

The high-temperature strength tests were carried out in air by the centrifugal bending method [2] under the load $\sigma = 15 \text{ kg/mm}^2$, with the test duration reaching at least 300 hr. the test temperatures were selected in accordance with the temperature level of high-temperature strength of binary alloys of titanium with aluminum and were as follows:

Alloy	Temperature, $^{\circ}\text{C}$
Section with 3 and 6% Al	500
with 9 and 12% Al	700
with 16 and 22% Al	750
System Ti-Al-Zr	700

Prior to tests the alloys were subjected to the following regimes of heat treatment: 1100°C , 2 hr \rightarrow 800°C , 50 hr \rightarrow 700°C , 150 hr \rightarrow 550°C , 250 hr.

Following exposure to test temperatures the alloys of the corresponding sections were cooled in air.

The adopted criterion of high-temperature strength was the variation in the bending deflection of the specimens during tests of varying duration and the time taken to attain specified bending deflections of 1, 2, 3, 4 and 5 mm for alloys of

the cross section Mo:Zr = 3:1 and 2, 5, 7 and 10 mm for alloys of the cross section Mo:Zr = 1:3.

STUDY OF HIGH-TEMPERATURE STRENGTH OF ALLOYS OF THE TERNARY SYSTEM Ti-Al-Zr OVER THE RADIAL SECTION Zr (91% Ti, 9% Al)

According to Pylayeva and Volkova [1] in alloys of this section the phases $(\alpha + \alpha_2)$ - α -, $(\alpha + \beta)$ exist in an equilibrium at 700°C . The two-phase region $(\alpha + \alpha_2)$ exists within the limits of 0-6% Zr; the region of α -solid solutions, within the range of 6-55% Zr; and the region of $(\alpha + \beta)$ phases, within the range of 55-80% Zr. Tests of the alloys in selected conditions showed (Fig. 1, a) that the alloys containing 0-7% Zr display the greatest high-temperature strength (it takes them 80 and 125 hr to reach a bending deflections of 3 and 4 mm, are reached within fewer than 25 hr). Tests of alloys with $>30\%$ Zr were not carried out due to their intense oxidation at high temperatures.

The maximum high-temperature strength of the alloys in the concentration range of 0-7% Zr is attributable to the decomposition of the α -solid solution accompanied by the segregation of a slowly coagulating α_2 phase (solid solution based on the compound Ti_3Al). Comparison of this finding with the high-temperature strength of the binary alloy of titanium with 9% Al implies that zirconium in amounts of up to 7% does not lower the level of high-temperature strength of the binary alloy but even tends to increase it slightly.

The cause of the lower high-temperature strength of alloys containing $> 10\%$ Zr may be their lower heat resistance, due to the increase in Zr concentration. /166

STUDY OF ALLOYS OF THE SYSTEM Ti-Al-Mo (CROSS SECTION WITH THE Mo:Zr RATIO OF 3:1)

Alloys of the section with 3 and 6% Al were tested for 300 hr at 550°C and subsequently for 50-100 hr at 600°C , under the load $\sigma = 15 \text{ kg/mm}^2$. As can be seen from Fig. 1, b, alloys of the section with 3% Al which contain 0-5% (Mo + Zr) display the greatest high-temperature strength and basically have the structure of an α -solid solution with a small amount of the β phase. They reach bending deflections of 3 and 4 mm after 330-340 hr of tests. Roughly the same level of high-temperature strength is displayed by the alloy with 35% (Mo + Zr) which has the structure of a β -solid solution and is located in the neighborhood of the $(\alpha + \beta)/\beta$ phase interface. Alloys containing 25 and 30% Mo + Zr and having the distinct two-phase structure of $(\alpha + \beta)$ -solid solutions display the lowest high-temperature strength among the alloys investigated. A similar relationship between phase composition and high-temperature strength is also observed for alloys containing 6% Al (Fig. 2, a). It should be noted that at 550°C the alloys of this section are practically undeformable. The bending deflection of these alloys following 300 hr tests reaches 1-2 mm. At 600°C the greatest high-temperature strength is displayed by the alloy containing 2% (Mo + Zr) which has the structure

of an α -solid solution with a small amount of the β phase. The increase in the amount of the β phase in alloys with a higher content of Mo and Zr is accompanied by a decrease in their high-temperature strength.

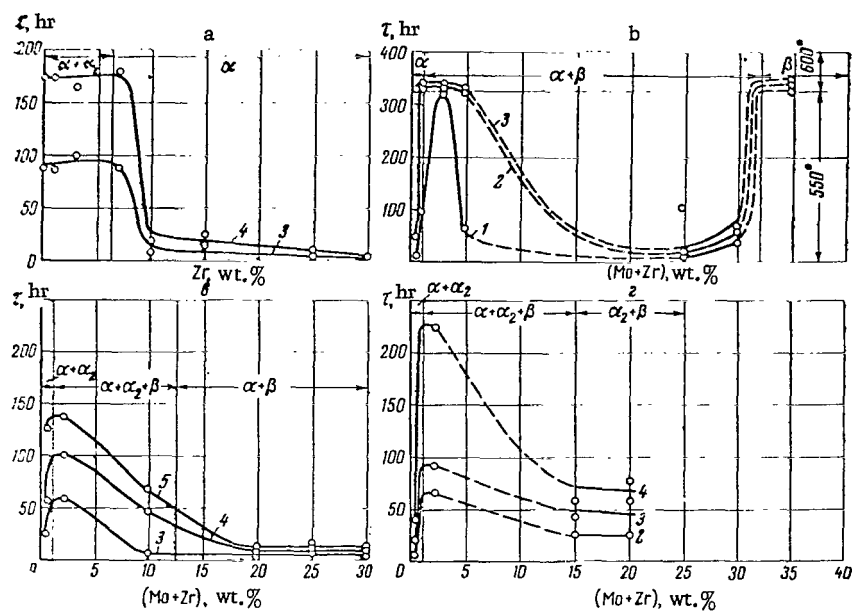


Figure 1. Relation of the Time (τ) of Reaching Specific Bending Deflections (in mm) to the Composition of Alloys of the Ti-Al-Zr Section (a) as Well as of Sections of the Ti-Al-Mo System of the Cross Section Mo:Zr = 3:1 With 3% Al (b), 9% Al (c) and 12% Al (d):

1—5—Bending Deflections of 1, 2, 3, 4, 5 mm, Respectively.

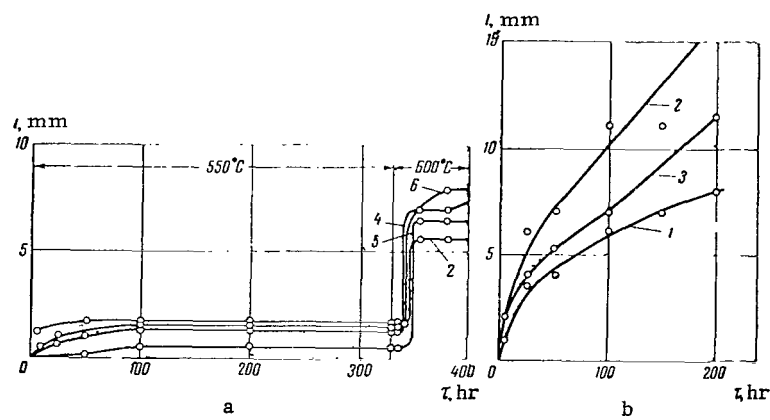


Figure 2. Relation of Bending Deflection (l) to the Duration of Tests of Alloys of the Cross Section Mo:Zr = 3:1. Alloys of Sections with 6% Al (a) and 16% Al (b). (Mo + Zr) % = 1 (1); 2 (2); 3 (3); 5 (4); 10 (5); 20 (6).

/167

Alloys of the Sections With 9 and 12% Al

In alloys of the section with 9% Al with varying aggregate content of Mo and Zr the $(\alpha + \alpha_2)$ and $(\alpha + \alpha_2 + \beta)$ phases exist in an equilibrium at 700°C. As can be seen from the curves of the relation of the high-temperature strength of these alloys to their composition (Fig. 1, c), the greatest high-temperature strength is displayed by the alloy with (Mo + Zr), located at the boundary between the regions $(\alpha + \alpha_2)$ and $(\alpha + \alpha_2 + \beta)$: it reached a bending deflection of 3 mm only after 125-130 hr of tests. Alloys containing 20-30% (Mo + Zr) and having the three-phase structure $(\alpha + \alpha_2 + \beta)$ with a marked degree of heterogeneity display a lower high-temperature strength: they reached a bending deflection of 3 mm after 10-15 hr of tests.

A similar pattern of the relation of high-temperature strength of composition was observed for alloys of the section with 12% Al (Fig. 1, d). In this section the greatest high-temperature strength was displayed by the alloy containing 2% (Mo + Zr). As the aggregate content of Mo and Zr increases to 10-20% the high-temperature strength of the alloys decreases; this is associated with the increase in the amount of β phase in their structure. Comparison of the high-temperature strength values of alloys of the sections with 9 and 12% Al shows that alloys of the section with 12% Al have a greater high-temperature strength: the alloy containing 2% (Mo + Zr) and 12% Al reaches a bending deflection of 3 mm after 250 hr of tests, while the same alloy with 9% Al reaches it within as little as 140 hr of tests.

Alloys of the Section With 16% Al

Only alloys of this section containing 1, 2 and 3% (Mo + Zr) were investigated ($t = 750^\circ\text{C}$, $\sigma = 15 \text{ kg/mm}^2$). Other alloys of this section were not investigated in detail, since alloys in this region are brittle and the specimens fracture during their preparation. Following 200-hr tests the smallest bending deflection was attained for the alloy containing 1% (Mo + Zr) (see Fig. 2, b). This alloy is located in the single-phase region of the α_2 -solid solution. Alloys containing 2 and 3% (Mo + Zr) have the two-phase structure $(\alpha_2 + \beta)$ and following tests of the same duration get deformed to a greater degree. Analysis of the findings on the high-temperature strength of alloys of the system Ti-Al-Mo-Zr over the cross section with Mo:Zr = 3:1 and consideration of the results from the standpoint of the physicochemical theory of high-temperature strength [3] indicates that the decrease in the high-temperature strength of the alloys having the structure of $(\alpha + \beta)$ - and $(\alpha + \alpha_2 + \beta)$ - phases is associated with the considerable heterogeneity of these alloys compared with alloys of the boundary regions $\alpha/(\alpha + \beta)$, $(\alpha + \alpha_2)/(\alpha + \alpha_2 + \beta)$.

STUDY OF ALLOYS OF THE TETRAHEDRON CROSS SECTION WITH A RATIO OF 1:3 BETWEEN ZIRCONIUM AND MOLYBDENUM

/168

Alloys of Sections With 3 and 6% Al

At 550°C the phases α and $(\alpha + \beta)$ exist in an equilibrium in alloys of these sections, with the region of the α -solid solution being bounded by the 1% (Mo + Zr) content. All the other investigated alloys had the structure of $(\alpha + \beta)$ -solid solutions. As implied by Figs. 3 and 4 the alloys of the section with 3% Al and 5-7% (Mo + Zr), having the structure of $(\alpha + \beta)$ -solid solutions with a small amount of β phase, display the greatest high-temperature strength. They reach a bending deflection of 5 mm after 80 hr of tests, whereas alloys in which the (Mo + Zr) content is 10, 15, 20 or 25%, and the proportion of β phase in the structure is larger, reach this deflection after roughly 10 hr. Alloys containing 0.5-1.0% (Mo + Zr) and having the structure of the α -solid solution display a similarly low level of high-temperature strength. It is known that under the same test conditions the binary alloy of Ti + 3% Al reaches a bending deflection of 5 mm within approximately 15-20 hr. Thus, treatment with 5-7.5 (Mo + Zr) somewhat enhances the high-temperature strength of the binary alloy. It should be noted that this is a highly conditional comparison, considering that Kornilov [4] tested alloys prepared by the powder-metallurgical method. The high creep rates of alloys of the section with 3% Al clearly indicate that the selected test temperature (550°C at $\sigma = 15 \text{ kg/mm}^2$) is high for these alloys.

Under the same conditions alloys of the section with 6% Al display markedly lower creep rates (Fig. 3, b and 4, b). Treatment with 6% Al appreciably enhances the high-temperature strength of the alloys with 1 and 3% (Mo + Zr) located at the boundary between the solid solutions α /($\alpha + \beta$). Then the alloy with 1% (Mo + Zr) does not reach the bending deflection of 2 mm even after 500-hr tests, while alloys with 3 and 5% (Mo + Zr) still do not reach it after 250 and 100 hr, respectively, of tests. Increasing the Mo and Zr content of the alloys to 10, 15 and 24% (Mo + Zr) shortens the time of this bending deflection the range of the alloys with the greatest high-temperature strength extends from 1 to $\sim 7.5\%$ (Mo + Zr).

The binary alloy of Ti + 6% Al under these test conditions [4] reaches a bending deflection of 2 mm after approximately 80 hr and treatment with 1, 3 and 5% (Mo + Zr) increases its high-temperature strength. The diagrams of phase -high-temperature strength (Fig. 4) for this and the other sections are characterized by a maximum of high-temperature strength corresponding to alloys deriving chiefly from the range of $(\alpha + \beta)$ -solid solutions with a slightly heterogeneous structure; the diagrams are of the second type [3].

Alloys of the Sections With 9 and 12% Al

At 700°C in alloys of these sections the $(\alpha + \alpha_2)$ -, $(\alpha + \alpha_2 + \beta)$ - and $(\alpha + \beta)$, $(\alpha_2 + \beta)$ -solid solutions exist in an equilibrium. The $\alpha + \alpha_2$ region of the solid solutions reaches 2 and 3% (Mo + Zr) and the $\alpha + \alpha_2 + \beta$ region, 3 and 10% (Mo + Zr). Alloys of the section with $> 3\%$ (Mo + Zr) have the structure of $(\alpha + \beta)$ phases while alloys of the section with 12% Al, containing $> 10\%$ (Mo + Zr)

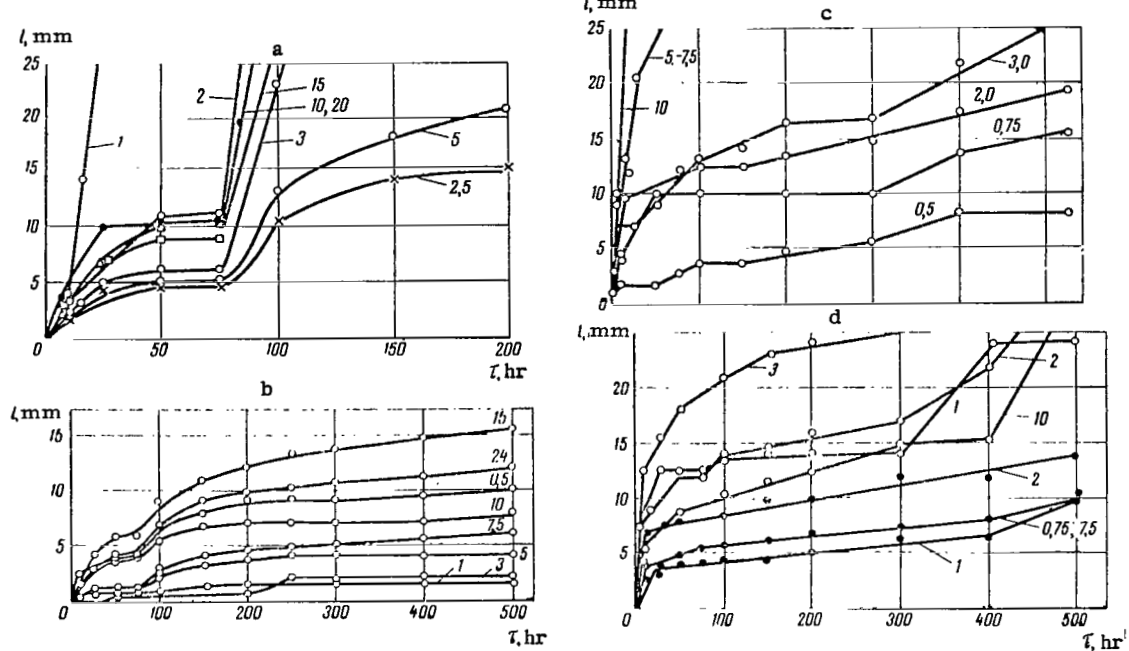


Figure 3. Bending Deflection (l) as a Function of Duration of Tests of Alloys of the Cross Section Mo:Zr = 1:3 Over the Section With 3% Al (a), 6% Al (b), 9% Al (c), 16% Al (d, Solid Lines) 22% Al (Broken Line):
 The Numerals on the Curves Give the $(Mo + Zr)$ Content in %.

have the structure of $(\alpha_2 + \beta)$ phases. Alloys of the section with 9% Al are characterized by a gradual increase in creep rate with increase in their content of Mo and Zr (Fig. 3, c). The highest deformation rates are displayed by alloys containing 5-10% $(Mo + Zr)$ and having the structure of $(\alpha + \beta)$ -solid solutions, while the lowest rates are displayed by the alloy with 0.5% $(Mo + Zr)$ as well as by the alloys with 0.75 and 2.0% $(Mo + Zr)$, from the region of $(\alpha + \alpha_2)$ -solid solutions. A bending deflection of 5 mm is reached by the alloy with 0.5% $(Mo + Zr)$ after 250 hr of tests, while the other alloys reach it after 25 hr.

Comparison of these data with the findings on the binary alloy of $Ti + 9\%$ Al tested under the same conditions (Fig. 1, a) clearly reveals that treatment with 0.5% $(Mo + Zr)$ does not merely lower the level of the high-temperature strength of the binary alloy. Treatment with 0.75% $(Mo + Zr)$ adversely affects the high-temperature properties of the binary alloy, although within the range of 50-300 test hours they are relatively stable and persist at a single level. As for the dependence of high-temperature strength of the alloys of the section with 12% Al on their content of Mo and Zr, this is difficult to assess, since it proved possible to test only alloys of three compositions: with 2, 7.5 and 18% $(Mo + Zr)$. Of these alloys the one with 7.5% $(Mo + Zr)$, having the structure of $(\alpha + \alpha_2 + \beta)$ -solid solutions with a small amount of β phase, proved to display the greatest

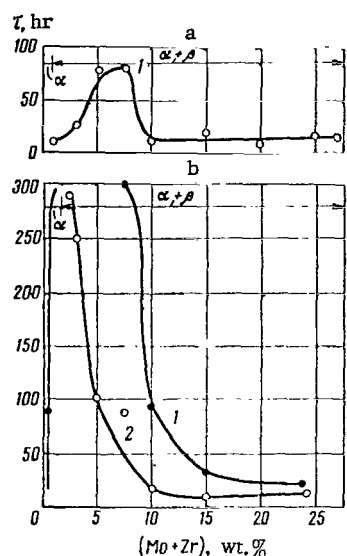


Figure 4. Time (τ) Taken to Reach Specified Bending Deflections (1, 2-2 and 6 mm, Respectively) as a Function of Composition of Alloys of the Section Mo:Zr = 1:3 With 3% Al (a), and 6% Al (b).

presence of the load applied.

The investigation of the high-temperature strength of alloys of the system Ti-Al-Mo-Zr revealed that when Mo:Zr = 1:3, in the selected test conditions, the most intense hardening is accomplished by increasing the content of aluminum—an element which markedly raised the temperature of the polymorphic transformation of titanium. Treatment of binary Ti-Al alloys with Mo and Zr apparently enhances their high-temperature strength only if the aluminum content is low, of the order of 3.6% (i. e. for undersaturated solid solutions). If the aluminum content of the alloys is any higher, treatment with molybdenum and zirconium—as preliminary findings indicate—does not enhance the high-temperature strength of binary alloys. Apparently, all that can then be expected is the preservation of the original level of high-temperature strength following treatment with small amounts of Mo and Zr. However, the addition of these elements may contribute to improving the technological properties of the alloys.

CONCLUSIONS

1. Alloys of the ternary system Ti-Al-Zr of the section (Zr—9% Al, 91% Ti) are high-temperature alloys when their Zr content is 0-7%.

2. The greatest high-temperature strength at 550 and 600°C is displayed by alloys of the cross section Mo:Zr = 3:1 in the sections with 3 and 6% Al, containing 2% (Mo + Zr), whose compositions are located in the two-phase region ($\alpha + \beta$) in the presence of a small amount of the β phase, as well as by alloys from the region of the saturated β -solid solution.

3. In sections with 9 and 12% Al at 700°C the alloys displaying the greatest high-temperature strength are those containing 0.5-2% (Mo + Zr) and having compositions located close to the phase interface $(\alpha + \alpha_2)/(\alpha + \alpha_2 + \beta)$ and in the region $(\alpha + \alpha_2 + \beta)$ in the presence of a small amount of the β phase.

4. The greatest high-temperature strength among the alloys of the section with 16% Al tested at 700°C is displayed by the alloy containing 1% (Mo + Zr). /171

5. Analysis of the relative high-temperature strength of alloys of the cross section Mo:Zr = 1:3 established that the maximum of this strength is displayed by alloys of the section with 3% Al at 550°C, located in the region of 5-7.5% (Mo + Zr) as well as by alloys of the section with 6% Al and (1-7.5)% Mo. + Zr.

Among the alloys of the section with 9% Al the greatest high-temperature strength is displayed at 700°C by the alloys with 0.5 and 0.75% (Mo + Zr) and among the alloys with 16 and 22% Al, by the alloys containing 1 and 10% (Mo + Zr) and 1 and 0.75% (Mo + Zr).

6. Analysis of the findings on the high-temperature strength of alloys of the two cross sections (Mo:Zr = 3:1 and 1:3) showed that the temperature level of their high-temperature strength is chiefly determined by their aluminum content. Alloys with an identical aluminum content and the ratio Mo:Zr = 3:1 display, under the same test conditions, a greater high-temperature strength than alloys with the same aggregate amount of Mo and Zr but a reversed ratio (Mo:Zr = 1:3).

7. The compositions of the alloys displaying the maximum values of high-temperature strength generally correspond either to homogeneous solid solutions in the neighborhood of the solubility boundary or to two-phase alloys with a small amount of β phase the structure, located near the phase interfaces $\alpha/(\alpha + \beta)$, $(\alpha + \alpha_2)/(\alpha + \alpha_2 + \beta)$.

REFERENCES

1. Pylayeva, Ye. N. and M. A. Volkova. In the collection: "Metallovedeniye titana" [Metallography of Titanium], Nauka Press, 38, 1964.
2. Kornilov, I. I. Izvestiya SFKhA, Vol. 18, No. 72, 1949.
3. Kornilov, N. I. Fiziko-khimicheskiye osnovy zharoprochnosti splavov [Physicochemical Foundations of the High-Temperature Strength of Alloys], USSR Acad. Sci. Press, 1961.
4. Kornilov, I. I., Ye. N. Pylayeva and M. A. Volkova. Izvestiya AN SSSR, OKhN, Vol. 7, p. 771, 1956.

STUDY OF THE PROPERTIES OF ALLOYS OF THE SYSTEMS Ti-Zr AND Ti-Zr-Al

Ye. A. Borisova and I. I. Shashenkova

Research into the alloys of titanium treated with zirconium and aluminum is highly important in developing alloys suitable for performance over a broad temperature range, from -253°C to $500\text{--}600^{\circ}\text{C}$, since zirconium forms with titanium a continuous series of α - and β -solid solutions. It is known that single-phase alloys having the structure of the α -solid solution display the maximal high-temperature strength and at low temperatures (down to -253°C) their plasticity is optimal as well.

This investigation deals with alloys containing 2, 4, 8, 12, 20, 40 and 65% Zr without aluminum as well as alloys treated with 4, 6 and 7% Al. Ingots of the experimental alloys were first forged into square 50 x 50 mm billets at temperatures that were selected with allowance for the phase composition of the alloys so that the maximum temperature would not exceed by more than 50°C the temperature of the $\alpha + \beta \rightarrow \beta$ transformation. It was observed that the alloys with 40 and 65% displayed a sharp decrease in oxidation resistance during forging — the billets continued to burn in air until complete burnout of the metal was effected.

All the alloys were subjected to tensile tests at from -196 to $+700^{\circ}\text{C}$. Impact strength was determined on Menager-notch specimens; these specimens also were used to measure hardness. Prior to the tests all specimens were annealed in a vacuum furnace at α region temperatures, $50\text{--}100^{\circ}\text{C}$ below the temperature of the $\alpha \rightarrow \alpha + \beta$ transformation. The test results are presented in Figs 1 and 2. It can be seen that the ultimate strength and hardness of the alloys at room temperature increase with increasing content of zirconium, while plasticity at the same time decreases. The lowest plasticity was observed for the alloys containing $>40\%$ Zr. Alloys containing 2-4% Zr display a slight strength minimum and a plasticity maximum. In the Al-free alloys this strength minimum corresponds to 2% Zr and in the alloys containing 4 and 6% Al, to 4% Zr. It should be noted that the authors of [2, 3] obtained similar results. It may be that this effect is due to the decrease in grain size owing to treatment with small amounts of zirconium. These findings also show that aluminum in the alloys Ti-Zr-Al also is a much more effective hardening agent than zirconium. Treatment with 1% Zr increases the ultimate strength of the alloys by $2\text{--}3 \text{ kg/mm}^2$, whereas treatment with 1% Al increases it by $5\text{--}7 \text{ kg/mm}^2$. /172

The relation of the variation in mechanical properties to the content of zirconium in the alloys at 20 and at 500°C is similar. In both cases a maximum is observed in the presence of 65% Zr. At higher temperatures (600 and 700°C) the ultimate strength of the alloys increases with increase in Zr content up to a point (40% at 600°C and 20% at 700°C) beyond which it sharply decreases. The decrease in strength in this case is associated with the formation in the structure of the alloys, along with the α phase, of the less strong and more plastic β phase. Alloys with an intermediate Zr content (20-40%) were not investigated, and hence it is possible that the ultimate strength maximum at 600 and 700°C will in their case be somewhat displaced in the direction of the higher Zr content. The pattern of variation in mechanical properties in the alloys containing 4 and 6% Al and up /173

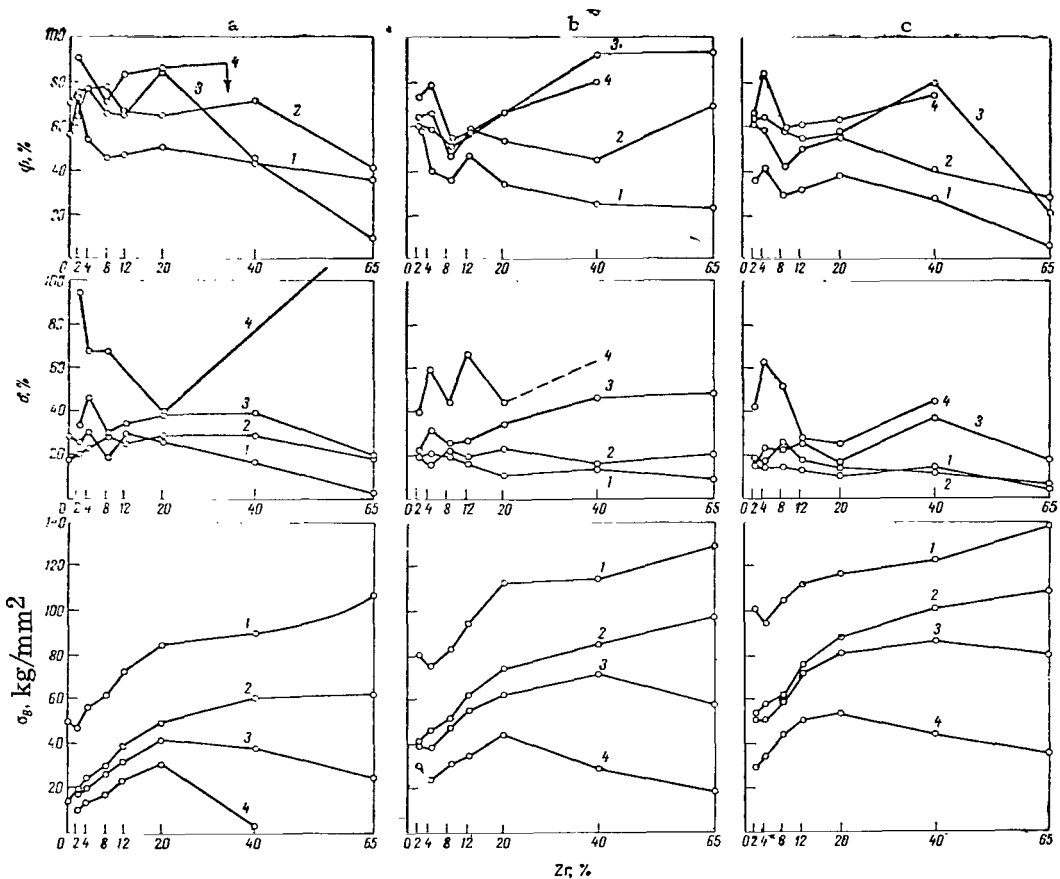


Figure 1. Mechanical Properties of the Alloys Ti-Zr (a) and Ti-Al-Zr With 4% Al (b) and With 6% Al (c). Arrow Points to the Case in Which Burnout of Specimen Occurred. Tests Carried Out at 20 (1), 500 (2), 600 (3) and 700°C (4).

to 65% Zr is independent of the Al content. At 600°C treatment with 4 and 6% Al displaces the ultimate strength maximum in the direction of higher Zr content (20% Zr for Al-free Alloys and 40% Zr for alloys containing 4 and 6% Al). At 700°C the ultimate strength of the Al-containing alloys, while decreasing when the Zr content exceeds 20%, still remains at least 20 kg/mm², which is 10 times as high the ultimate strength of the Al-free alloys of this system. Aluminum raises the temperature of allotropic transformation; alloys containing 4 and 6% Al and 20-65% Zr at 600 and 700°C prove to lie in the region of the α -solid solution. It should also be noted that the addition of up to 4% Al to Ti-Zr alloys reduces their plasticity to a level that, however, still remains sufficiently high. On the other hand, addition of 6% Al reduces this plasticity fairly sharply. Test results at -196°C show (Fig. 3) that alloys containing up to 8% Zr display at -196°C a high plasticity but their strength level does not exceed 45-65 kg/mm². Increasing the Zr content above 8% makes it possible to obtain alloys with an ultimate strength of 80-90 kg/mm² but their plasticity then sharply decreases at -196°C, which makes these alloys less promising compared to standard industrial alloys having

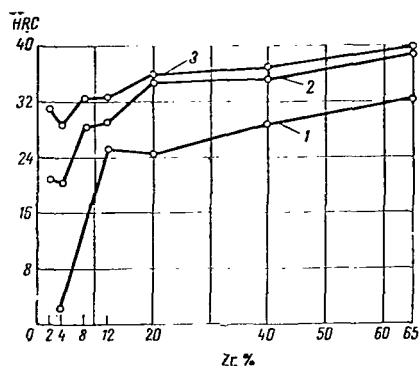


Figure 2. Rockwell Hardness (Under 150 kg Load) of Titanium Alloys Containing Varying Amounts of Zirconium and Aluminum:

1, 2, 3—0, 4, and 6% Al Respectively.

was 49.5 kg/mm^2) which, as is known, sharply reduces the plasticity of alloys at low temperatures, and hence the plasticity characteristics will be somewhat higher if the alloys are melted from softer sponge.

/174

In addition, the microstructure of alloys of the systems Ti-Zr and Ti-Zr-Al following their annealing and quenching was investigated, the temperature boundaries of the phase regions were determined by metallographic and dilatometric methods and the coefficient of linear thermal expansion of the alloys Ti-Zr was determined. The conducted investigation showed that the structure of the annealed alloys of titanium with 2, 4 and 8% Zr is typical of single-phase α -alloys (Fig. 6), except that the grains of the α phase are somewhat smaller. Alloys containing 12 and 20% Zr display a highly disperse structure resembling the structure of two-phase titanium alloys of the VT6 type. Alloys with 40 and 65% Zr have an acicular structure characteristic of the α' phase. The boundaries of the $\alpha \rightarrow \alpha + \beta$ phase transformation, as determined by the dilatometric method, and of the $\alpha + \beta \rightarrow \beta$ transformation, as determined by the metallographic method, for the alloys Ti-Zr and Ti-Zr-Al are shown in Fig. 5. In addition, the coefficients of linear thermal expansion for the alloys Ti-Zr also were calculated:

/175

Zr, %	$\alpha \cdot 10^4$ (100-20) $1/\text{^{\circ}C}$	Zr, %	$\alpha \cdot 10^4$ (100-20) $1/\text{^{\circ}C}$
0	8.05	12	7.43
2	6.35	20	6.23
4	7.44	40	6.23
8	7.43	65	6.17

As can be seen, with increase in Zr content the coefficient of linear thermal expansion decreases from $8.05 \cdot 10^{-6} \text{ }^{\circ}\text{C}^{-1}$ for technical titanium to $6.17 \cdot 10^{-6} \text{ }^{\circ}\text{C}^{-1}$

/176

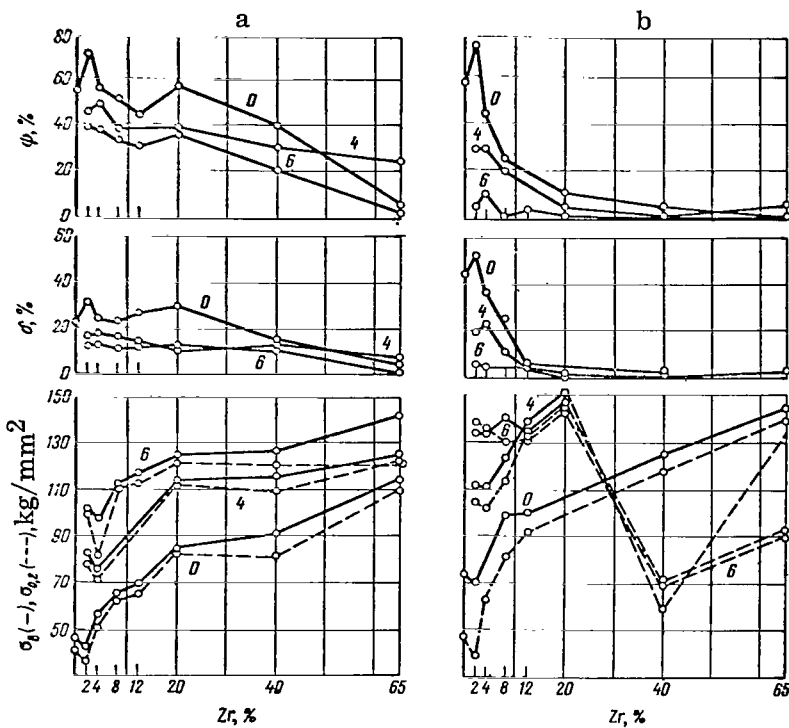


Figure 3. Mechanical Properties of the Alloys Ti-Zr and Ti-Zr-Al At $+20^{\circ}\text{C}$ (a) and -196°C (b):

The Numerals on the Curves Denote Al Content in %.

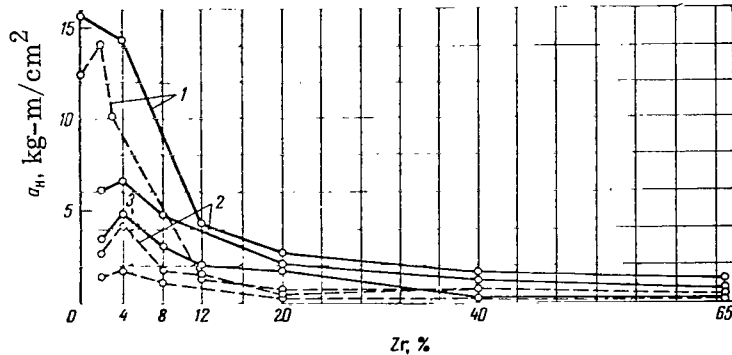


Figure 4. Impact Strength of the Alloys Ti-Zr and Ti-Zr-Al at $+20^{\circ}\text{C}$ (Solid Lines) and -196°C (Broken Lines).
 Content of Al in %: 0 (1), 4 (2), 6 (3).

for the alloy containing 65% Zr. Thus, binary Ti-Zr alloys can, if needed, becomes the basis for developing an alloy having a lower thermal linear expansion coefficient than technical titanium.

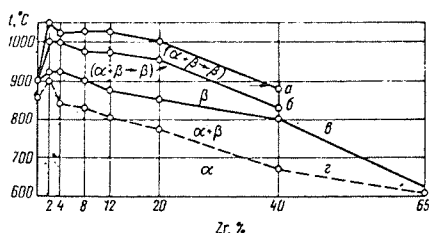


Figure 5. Phase-Transformation Boundaries in the Alloys Ti-Zr and Ti-Zr-Al, Determined by the Metallographic (a, b, c) and Dilatometric (d) Methods:

Al Content, %: 0 (c, d); 4(b); 6 (a).

It should also be pointed out that the aforementioned decrease in oxidation resistance observed for alloys of the systems Ti-Zr and Ti-Zr-Al implies that, compared with alloys of other systems, these alloys have a greater ability to form surface layers during their chemothermal treatment [metal plating], e.g. during oxidation, resulting in layers with a higher surface hardness and satisfactory wear resistance.

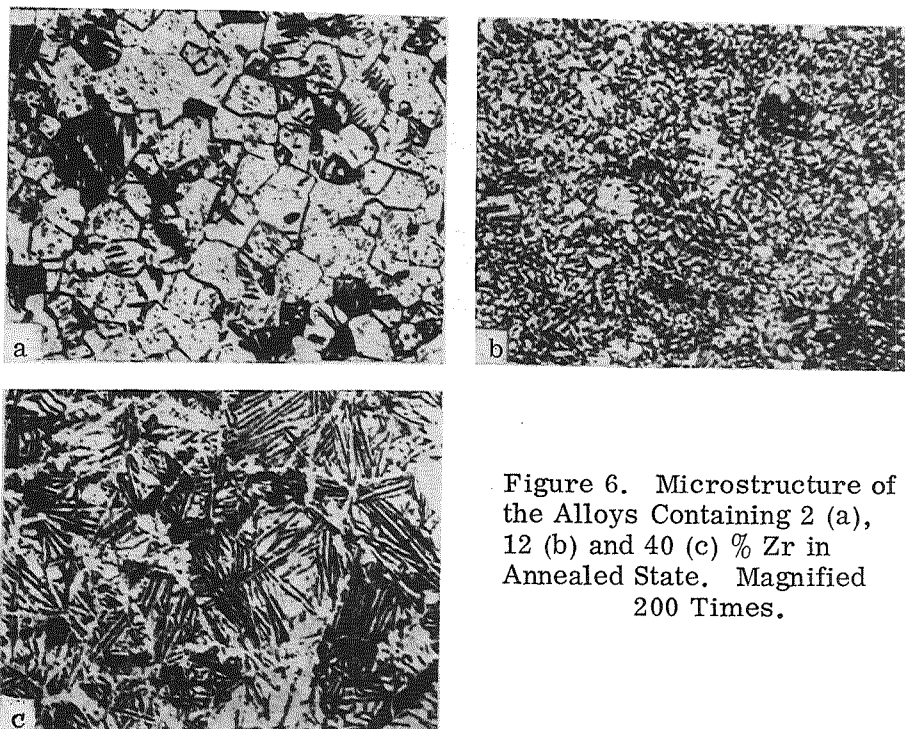


Figure 6. Microstructure of the Alloys Containing 2 (a), 12 (b) and 40 (c) % Zr in Annealed State. Magnified 200 Times.

CONCLUSIONS

1. It was shown that alloys of the system Ti-Zr-Al with 2-4% Al and 6-8% Zr display a high plasticity at low temperatures and are promising materials for further investigation with the object of developing a single-phase alloy with an ultimate strength of 80-90 kg/mm².

2. It was established that alloys containing 6% Al and up to 20% Zr can be used for prolonged performance at temperatures of up to 500°C.

3. It was shown that in Ti-Zr alloys increasing the Zr content reduces their coefficient of linear thermal expansion so that when the Zr content reaches 65% this coefficient drops to $6.17 \cdot 10^{-6} \text{ }^{\circ}\text{C}^{-1}$.

4. It was observed that the oxidation resistance of the alloys Ti-Zr and Ti-Zr-Al decreases with increase in their Zr content.

REFERENCES

1. Fast, J. D. Rec. Trav. Chim., Vol. 58, No. 9, p. 10, 1939.
2. Glazunov, S. G. and O. P. Solonina. Splavy sistemy titan-tsirkoniya-alyuminiiy [Alloys of the System Titanium-Zirconium-Aluminum]. In the collection: (Titanium in Industry) Oborongiz, 73, 1961.
3. Luzhnikov, L. P. and V. M. Novikova. Dvoynyye splavy system titan-olovo i titan-tsirkoniya. Sb. Titan v promyshlennosti [Binary Alloys of the Systems Titanium-Tin and Titanium-Zirconium]. In the collection: (Titanium in Industry), Obornogiz, 31, 1961.
4. Kornilov, I. I. Metallovedeniye i termicheskaya obrabotka metallov [Metallurgy and Heat Treatment of Metals]. Vol. 2, No. 7, 1963.

SOME PROBLEMS OF THE PHYSICOCHEMICAL THEORY OF HIGH-TEMPERATURE STRENGTH AND THE NEW HIGH-TEMPERATURE TITANIUM ALLOYS ST-1, ST-3, ST-4 AND ST-5

T. T. Nartova

High-temperature technology is a major field of application of titanium-based high-temperature alloys.

According to the physicochemical theory of high-temperature hardening [1] it may be stated that two mechanisms of metal hardening are of major significance concerning high-temperature titanium alloys: the solution mechanism and the dispersion mechanism, both being in agreement with the solution-precipitation mechanism of high-temperature strength [2]. A separate role in this respect is played by a refractory compounds of titanium, whose plasticity is especially satisfactory.

Considering the postulates of the physicochemical theory of high-temperature strength it may be assumed that high-temperature titanium alloys can be developed on the basis of:

- 1) α -solid solutions of titanium with hexagonal crystal lattice;
- 2) β -solid solutions of titanium with bcc lattice;
- 3) certain intermetallic compounds of titanium.

All these approaches are feasible and their adoption depends only on practical requirements for the properties of the alloys.

High-temperature strength is highly sensitive to composition, degree of equilibrium state, homogeneous and heterogeneous structures, and the distribution and extent of the phases coexisting in the system. Therefore, the laws governing the high-temperature strength of titanium alloys have to be determined on the basis of the nature of chemical interaction between titanium and other elements, the formation of solid solutions and intermetallics of titanium, the phase transformations in solid state and the degree and final state of the phase equilibrium in titanium-based systems.

When analyzing the pattern of interaction between titanium and other elements their positions in the Periodic Table must be taken into account.

If allowance is made for the metallochemical properties of titanium, all elements of the Periodic Table can be classified according to the nature of their interaction with titanium into elements forming four types of equilibrium diagrams [3, 4]. Diagrams of this kind are shown in Fig. 1.

Proceeding from these types of equilibrium diagrams and from the special features of the metastable states of the system, various changes in high-temperature strength that depend on the composition and structure of titanium systems can apparently be reduced to four basic types of "composition—high-temperature strength" diagrams [5] (see lower part of Fig. 1).

/177

/178

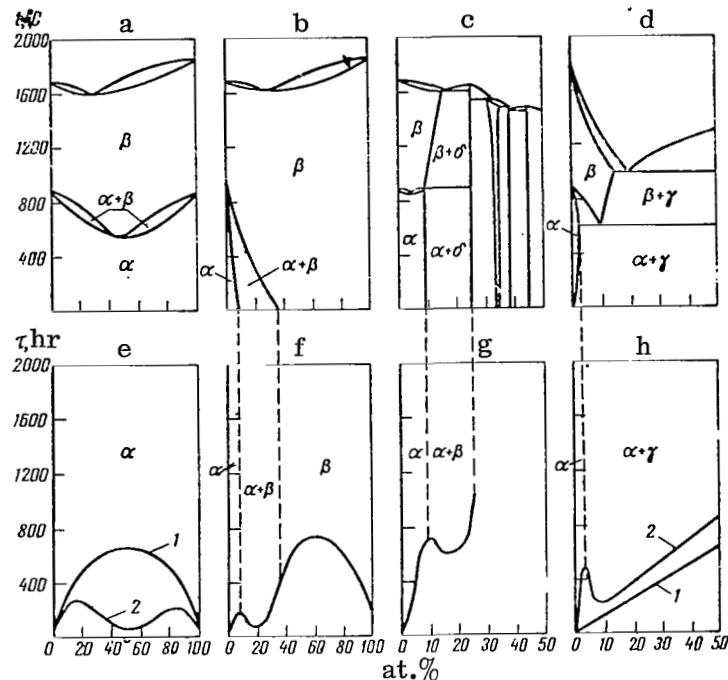


Figure 1. Equilibrium and "Composition-High-Temperature Strength" Diagrams of Titanium System [5]:
 Ordinate: Temperature, $^{\circ}\text{C}$ (a-d) and Time Taken to Reach Specified Bending Deflection, hr (e-h).

In this connection, it was of interest to analyze certain available experimental data on the high-temperature strength of binary titanium systems.

Of the two possible equilibrium diagrams of systems of the first type (Ti-Zr, Ti-Hf) the most adequately investigated is the high-temperature strength in the system Ti-Zr in the regions of α - and β -solid solutions [6, 7].

In the system Ti-Zr at moderately high temperatures (300-400 $^{\circ}\text{C}$) in the region of α -solid solutions of titanium the curve of variation in high-temperature strength has a gently sloping maximum (30 at. % Zr) (Fig. 1, e, curve 1). With increase in temperature (e.g. to 500 $^{\circ}\text{C}$) and approach to the temperature of the $\alpha \rightleftharpoons \beta$ transformation (525 $^{\circ}\text{C}$) in the region of 50 at. % Zr high-temperature strength begins to be influenced by the activated state of atoms in the α -solid solution [6]. This leads to an increase in the creep rate of the alloys corresponding to this part of the diagram (cf. Fig. 1, e).

The dependence of the high-temperature strength of these systems on their composition is attributable to the solution mechanism of hardening and the disruption of periodicity of the crystal lattice due to the substitution of titanium atoms in the solid solutions with atoms of zirconium or hafnium.

During variation of composition of alloys corresponding to phase diagrams of the second type, their high-temperature strength should somewhat increase at temperatures below the temperatures of polymorphic transformation—in the region of limited α -solid solutions—and reach a small maximum in the neighborhood of the boundary of the two-phase $\alpha + \beta$ region. In the two-phase $\alpha + \beta$ region itself of the phase diagram high-temperature strength decreases; this is associated with the unstable state of the phases under conditions of high-temperature tests and, as a consequence, with the greater mobility of atoms in the lattice of α and β phases, which accelerates the process of the creep of alloys under load.

With transition to the region of β -solid solutions and with increase in the concentration of elements in these solutions the high-temperature strength of the alloys again increases (cf. diagram in Fig. 1, f).

It may be assumed that in such systems the curve of high-temperature strength in the region of β -solid solutions will, on passing through a gentle maximum, gradually dip with approach to the second component. Hardening in this case is conditioned by the rise in the strength of the chemical bonding between heteronymous atoms in the solid solutions.

Such a dependence of high-temperature strength on composition and phase structure in phase diagrams of the second type is attributable to the solutive mechanism of hardening of the alloys in the region of α - and β -solid solutions and to the accelerated diffusive processes of the displacement of atoms in the region of $\alpha + \beta$ -solid solutions under the test conditions. This type of variation in high-temperature strength has been demonstrated for alloys of the systems Ti-V and TiNb [9].

"Composition—high-temperature strength" diagrams of this nature are, according to our data, characteristic of the system Ti-Mo and probably also of the system Ti-Ta as well as the corresponding ternary systems in which $\alpha \rightarrow \alpha + \beta$ transitions and β -solid solutions are observed.

The elements creating diagrams of the third type, with a broad range of bounded β - and α -solid solutions and with intermetallic compounds, enhance most effectively the high temperature strength of the α -modification of titanium. In this case we may expect a maximum effect of solution and precipitation hardening, a gradual rise in the high-temperature strength of titanium in the region of α -solid solutions and a maximum of this strength in the neighborhood of the boundaries of saturation and compositions of the compounds (cf. Fig. 1, g).

Depending on the content of the elements which together with titanium create "composition—high-temperature strength" diagrams of the third type, the degree of the hardening of titanium, in α -solid solutions, is determined by the degree of the difference in electronic structure between the atoms of titanium and the atoms of the other elements, as well as by the strength of the chemical bonding between the solid solutions of titanium and these elements.

In this respect, of the greatest interest are the system Ti-Al, Ti-Sn and Ti-O, in which exist regions β and α with an ordered structure [10-13]. The systems Ti-Cu, Ti-Si and certain others also may be included in this group.

/179

Less well investigated are the patterns of variation in high-temperature strength of systems of the fourth type with low solubility in α -Ti and with an eutectoid reaction.

Diagrams of this fourth type have a characteristic feature: as the eutectoid temperature decreases in alloys of these systems, the possibility also decreases of attaining a hardened state at medium and high temperatures. It should be pointed out, however, that in many systems with this type of interaction there form intermetallic compounds of various composition which, as in the preceding types of diagrams, are of two-fold significance to the hardening of titanium alloys. Many of these systems are characterized by low temperatures of eutectoid transformation [14].

The factors associated with the insignificant solubility of these metals in α -Ti and with the temperatures of eutectoid transformations should affect the high-temperature strength of alloys of binary systems of this kind. The low concentration of α -solid solutions in systems of this kind may in some cases prove to be relatively ineffective, and their high-temperature strength will probably be determined by the strength of the excess phase and will linearly increase with increase in the amount of that phase (Fig. 1, h, curve 1). However, in most systems forming equilibrium diagrams of the fourth type, in which the broad region of α -solid solutions has a varying solubility (varying with temperature), high-temperature strength will increase in the presence of the solution mechanism of hardening, and possibly also of the precipitation mechanism of hardening, as shown in Fig. 1, h. With increase in temperature a comparatively rapid softening may be expected in the systems Ti-Mn and Ti-Fe, due to the negligible solubility in α -Ti and the low temperature of the eutectoid reaction, whereas on transition to systems with Co, Ni, Cu and Si with their high temperatures of eutectoid transformation and greater solubility of components in α -Ti a gradual rise in high-temperature strength may be expected. In the systems Ti-Cu and Ti-Si some increase in high-temperature strength may be expected also due to the possible precipitation mechanism of the hardening of supersaturated α -solid titanium solutions and the formation of a disperse phase based on the intermetallic compounds Ti_2Cu and Ti_5Si_3 . In all these systems approach to eutectoid temperature will result in a decrease in the high-temperature strength of alloys of eutectoid composition. However, experimental data on the high-temperature strength of such binary systems are not available.

Thus many binary titanium systems may be divided into four groups according to the effect of the second component on the high-temperature strength of titanium.

Of the Ti-based ternary systems the most promising to the development of new high-temperature alloys are systems with zirconium, aluminum, tin, molybdenum, niobium, vanadium, copper and other elements.

If the nature of the interaction between titanium and the alloying elements is known and if the pattern of variation in high-temperature strength in relation to the composition and structure of binary titanium systems is determined, it is possible to solve the problems of synthesizing more complex multicomponent α -solid solutions and to develop on their basis new high-temperature titanium alloys of optimal composition.

Studies of the equilibrium diagrams and properties of alloys of certain multicomponent systems have resulted in establishing optimal compositions of the new high-strength high-temperature titanium alloys: ST-1, based on the system Ti-Zr-Al-Sn; ST-3, based on the system Ti-Zr-Al-Mo-Fe; ST-4, based on the system Ti-Zr-Al-Sn-Mo; and ST-5, based on the intermetallic compound Ti_3Al [15].

The aforementioned alloys were melted by the techniques currently used in the production of serial titanium alloys to somewhat modify the cooling regime of the ingots. The weight of the ingots was 450-500 kg.

Semifinished products were prepared by the free-forging method. Of major importance in determining the optimal regimes of heat treatment is knowledge of the temperatures of crystallization and phase transformations in solid state. The melting points and phase-transformation temperatures of the alloys were determined by the method of contactless thermal analysis in the device of N. A. Nedumov by recording the curves of heating and cooling [6] of specimens subjected to prolonged annealing (150 hr at $1000^{\circ}C$, cooling to $800^{\circ}C$ with exposure to this temperature for 300 hr, cooling to $600^{\circ}C$ for 500 hr and cooling in air). The radiographs were taken in Cu radiation.

The data on thermal analysis of the alloys are presented in Table 1.

TABLE 1

Alloy	Transformation temperature, $^{\circ}C$		
	Liquidus	Solidus	Solid state
ST-1	1620	—	1040, 990
ST-3	1610	—	1010, 880
ST-4	1680	1630	1040, 1020, 990, 920
ST-5	1665	1600	1150, 1000

As can be seen from Table 1, the alloys undergo transformations in solid state, associated with the polymorphic transformation in titanium: $\beta \rightarrow \alpha$, and hence also with transformations in the binary system Ti-Al: $\beta + \alpha_2 \rightarrow \alpha$.

The alloy ST-1 undergoes the polymorphic $\beta \rightleftharpoons \alpha$ transformation across the two-phase region $\alpha + \beta$ within the $1040-990^{\circ}C$ range.

The thermogram of the alloy ST-3 reveals two effects corresponding to transformations in solid state: $\beta \rightleftharpoons \alpha$ at $1010^{\circ}C$ and $\alpha + \beta \rightarrow \alpha + \alpha_2 + \beta$ at $880^{\circ}C$.

As the temperature is further reduced, the $\beta \rightarrow \alpha + TiFe$ transformation, associated with the eutectoid decomposition of the β phase in the binary system Ti-Fe, should also be expected in the alloy ST-3.

In the microstructure of the alloy ST-3 segregations of the intermetallic compound (TiFe) are observed following annealing at $\leq 700^{\circ}\text{C}$.

The alloy ST-4 undergoes the following three phase transformations when the temperature is lowered: $\beta \rightarrow \alpha_2 + \beta \rightarrow \alpha + \beta + \alpha_2 \rightarrow \alpha + \alpha_2$ at 1040, 990 and 920°C , respectively.

The alloy ST-5 at 1150°C , in the course of its cooling, passes from the β region to the two-phase $\beta + \alpha_2$ region, which at 1000°C is followed by transition to the single-phase region of α_2 -solid solutions based on the intermetallic compound Ti_3Al .

Alloys cooled in water following exposure to 800°C for 300 hr and 600°C for 500 hrs were subjected to x-ray phase analysis.

Table 2 presents the brands of the alloys and the identified phases.

TABLE 2

/181

Quenching temperature, $^{\circ}\text{C}$	Phase composition of alloy			
	ST-1	ST-3	ST-4	ST-5
800	α	$\alpha + (\alpha_2) + \beta$	$\alpha + (\alpha_2)$	α_2
600	α	$\alpha + (\alpha_2) + \beta$	$\alpha + (\alpha_2)$	α_2

Radiographs of the alloy ST-3 revealed the presence of reflections corresponding to the phases α and β .

The radiograph of the alloy ST-5 is characterized by the presence of lines of the α_2 phase based on the aluminide Ti_3Al .

Proceeding from the phase diagrams of the systems Ti-Al, Ti-Al-Fe and Ti-Al-Zr, taken as the basis for developing the alloys ST-3 and ST-4, and also proceeding from the results of their thermal and microstructural analysis, it may be expected that the α_2 phase should also be present in the alloys ST-3 and ST-4.

The strong lines of the α and α_2 phases coincide and hence they can be differentiated only according to the superlattice line (101) whose intensity is very low. In view of this, and also considering the small amount of ordered phase, the presence of the α_2 phase could not be established on radiographs of the alloys ST-3 and ST-4 (and hence in Table 2 the α_2 phase, for which the superlattice line (101) was not detected but which should exist in the alloys ST-3 and ST-4, was denoted as (α_2)).

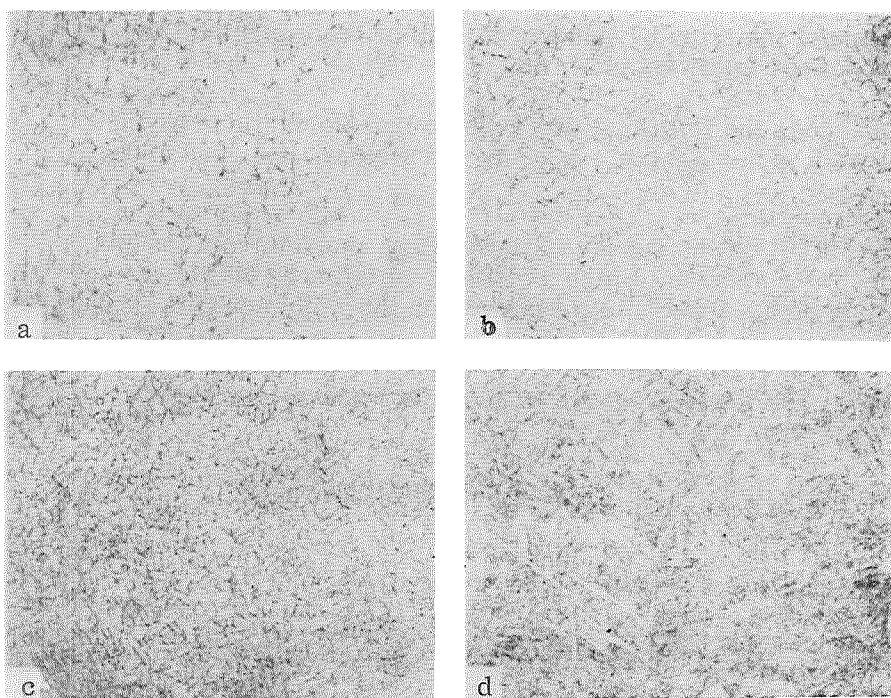


Figure 2. Microstructures of Alloys Following Optimal Regimes of Their Heat Treatment:

a—ST-1; b—ST-3; c—ST-4; d—ST-5.

For the very same reason, due to its small amount, the presence of the compound TiFe in the alloy ST-3 could not be established by means of x-ray phase analysis; this compound is detectible by microstructural examination. Segregation of the compound TiFe at 600–500°C may cause additional hardening of the alloy ST-3.

/182

Thus the alloy ST-1 is based on α -solid solutions of titanium, while the alloy ST-5 is based on the aluminide Ti_3Al . The alloy ST-3 at $> 700^\circ C$ has the two-phase structure $\alpha + \beta$. The stable phase in this alloy is chiefly the phase α . As for the structure of the alloy ST-4, it consists mainly of α -solid solutions of titanium.

Microstructural examination of the alloys ST-1, ST-3, ST-4 and ST-5 following various regimes of their heat treatment confirms the phase transformations specified above. Figure 2 presents the characteristic microstructures of the alloys ST-1, ST-3, ST-4 and ST-5 following their heat treatment by optimal regimes.

The optimal regime of heat treatment of these titanium alloys was selected after taking into account the information on critical points and on the effect of heat treatment on the structure and mechanical properties at room temperature.

To this end, the specimen billets were heated at various temperatures (from 700 to 1200°C) for 1 hr and cooled in air (ST-1), in oil and air (ST-3 and ST-4) and in oil (ST-5).

The dependence of ultimate strength on the temperature of heat treatment for all the investigated alloys in oil (and for ST-1 in air) is given in Fig. 3, a.

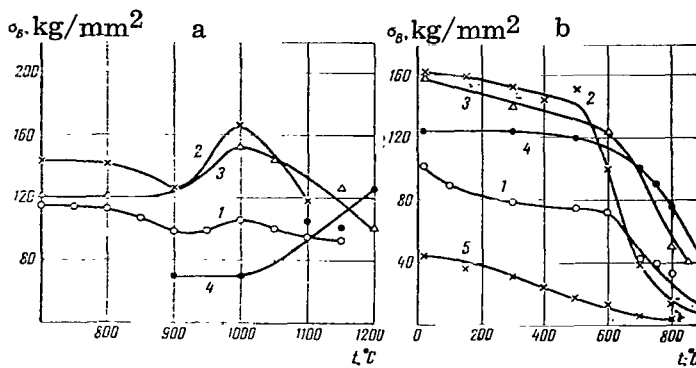


Figure 3. Relation of the Ultimate Strength of the Investigated Alloys to the Temperature of Heat Treatment (a) and Test Temperature (b):

1—ST-1 (Air); 2—ST-3 (Oil); 3—ST-4 (Oil); 4—ST-5 (Oil); 5—VT-1.

The conducted investigation showed that annealing at 700–800°C does not appreciable affect the strength of the alloy ST-1 but does enhance its plasticity. At 800°C recrystallization and insignificant growth of grains of the α phase are observed (Fig. 2, a). As the temperature of heat treatment is further raised (above 850°C) the strength and plasticity characteristics of the alloy ST-1 deteriorate; this is due to the marked growth of grains of the α phase and the formation of the martensitic α' phase ($> 1000^\circ\text{C}$) causing a decrease in plasticity.

The optimal regime of heat treatment assuring a maximally favorable ratio between strength and plasticity for the alloy ST-1 is heating at 800°C with cooling in air. Heating at 600, 700 and 800°C with cooling in air or in oil causes a decrease in the plastic properties of the alloy ST-3. This alloy displays improved plasticity characteristics ($\delta = 3.2\text{--}5.2\%$; $\psi = 10.7\text{--}13.2\%$; $\alpha_{\text{impact}} = 1.8\text{--}2.1$ kg-m/cm²) and an ultimate strength of 131–138 kg/mm² when heated at 900–950°C and cooled in air.

The maximum ultimate strength (166 kg/mm²) along with satisfactory plasticity characteristics ($\delta = 1.5\%$; $\psi = 4.5\%$) was obtained when quenching the alloy ST-3 in oil from 1000°C (Fig. 3). /183

Thus the optimal regime of heat treatment of the alloy ST-3, assuring its maximal ultimate strength is quenching in oil from 1000°C, and its plastic properties can be increased by heating it to 900–950°C with cooling in air. Following

such heat treatment the microstructure of the alloy ST-3 consists of two phases, α and α' (Fig. 2, b).

A study of the mechanical properties of the alloy ST-4 following various regimes of its heat treatment showed that the highest mechanical properties are obtained on quenching this alloy in oil rather than on cooling it in air. Then the maximum strength ($154-160 \text{ kg/mm}^2$) is attained by quenching from 1000°C (Fig. 2) and the plasticity characteristics are (Fig. 2): $\delta = 3-5\%$, $\psi = 8-10\%$ and $a_{\text{impact}} = 1.5 \text{ kg-m/cm}^2$.

The microstructure of the alloy ST-4 following this optimal regime of its heat treatment consists of microacicular martensite α' with tiny elongated and round segregations of the α phase (Fig. 2, c).

A study of the mechanical properties of the alloy ST-5 showed that its cooling in air results in low mechanical properties. Following cooling in oil the mechanical properties of the alloy ST-5 at room temperature increase. Ultimate strength of this alloy increases with increase in the temperature of heat treatment and with the formation in the structure of this alloy of the martensitic phase α' which is fixed by quenching from the region of the β -solid solution (Fig. 3, a). The plasticity characteristics of this alloy then also somewhat increase.

The optimal regime of heat treatment of the alloy ST-5, assuring a high strength and some plasticity, is quenching in oil from 1200°C . Treatment by this regime assures the following mechanical properties: $\sigma_B = 118-122 \text{ kg/mm}^2$, $\delta = 1-2\%$, and $\psi = 2-5\%$. The microstructure of the alloy in this state is martensitic and acicular (Fig. 2, d).

Thus, on the basis of the results of this investigation of the effect of heat treatment on the structure and mechanical properties at room temperature, the following should be considered the optimal regimes of heat treatment assuring the most favorable combination of strength with plasticity: for the alloy ST-1, heating at 800°C , * cooling in air; for the alloys ST-3 and ST-4, heating at $1000-1020^\circ\text{C}$, cooling in oil; and for the alloy ST-5, heating at 1200°C , also with cooling in oil. Following these regimes of heat treatment the residual internal stresses due to previous pressure working are maximally eliminated while at the same time appreciable grain growth still does not occur.

The mechanical properties of the alloys ST-1, ST-3, ST-4 and ST-5 at room temperature following these optimal types of heat treatment are presented in Table 3.

/184

The mechanical properties of the alloys ST-1, ST-3, ST-4 and ST-5 were investigated at various temperatures within the $20-950^\circ\text{C}$ range. Figure 3, b presents the curves of the temperature dependence of these new titanium alloys (specimens taken from industrial melts) as compared with technical-purity titanium VT-1. The tests were carried out on specimens subjected to the optimal regimes of heat treatment.

*The heating time for the 12-mm diameter specimens of all the alloys is taken at 1 hr.

TABLE 3

Alloy	σ_B , kg/mm ²	δ , %	ψ , %	α impact, kg-m/cm ²
ST-1	112-113	12-16	40-43	4-5
ST-3	131-166	2-5	5-13	0.6-1.8
ST-4	140-160	4-5	8-10	1-2
ST-5	118-122	1-2	2-5	0.5

As Fig. 3, b implies, commercial-purity titanium VT-1 rapidly softens with rise in temperature; at 800°C its ultimate strength is not more than 5-6 kg/mm².

The alloy ST-1, the ultimate strength of which at room temperature is comparatively low (112 kg/mm²) retains a high strength at up to 700°C (45-50 kg/mm²); at 800°C this strength is 30-35 kg/mm².

The ultimate strength of the alloy ST-3 at 20-500°C remains practically constant (150-160 kg/mm²). At 600°C short-time strength is ~100 kg/mm², while at 700°C it sharply decreases to 40 kg/mm² and at 800°C, to 15 kg/mm².

The alloy ST-4 display an insignificant degree of softening even at high temperatures. At 600°C its ultimate strength remains ~ 120 kg/mm²; at 750°C, it is 75 kg/mm²; and at 800°C, 50 kg/mm².

The alloy ST-5 is characterized by a relatively low ultimate strength at room temperature. With rise in temperature the softening of this alloy is smaller than for the other investigated alloys in the series, and it reaches its maximum ultimate strength at high temperatures of the order of 700-900°C (Fig. 3, b). At 800°C its ultimate strength is 75 kg/mm² and at 900°C, 40 kg/mm². The high-temperature strength of the alloys ST-1, ST-3, ST-4 and ST-5 was investigated by the method of determining stress-rupture strength at 600, 700 and 800°C as well as by the method of variable stresses with construction of curves of stress-rupture strength. The findings are presented in Fig. 4.

On the basis of the findings on high-temperature strength the limiting stresses for the investigated alloys can be established (Table 4).

Figure 4, c presents the results of stress-rupture strength tests of the alloy ST-5 at 600, 700 and 800°C. Specimens of this alloy at 600°C withstood without fracturing the stress $\sigma = 23-27$ kg/mm² for 1500-2000 hr, after which their tests were discontinued. The stress-rupture strength of the alloy ST-5 after 100 hr at 700°C is 20 kg/mm². These findings show that the alloy ST-5 can be used for prolonged performance at 600-700°C and for temporary performance at 800°C.

/185

Thus, the new titanium alloys ST-1, ST-3, ST-4 and ST-5 represent high-temperature materials which can perform at the following temperatures, °C:

ST-3 600 ST-4 700-800
 ST-1 600-700 ST-5 750-850

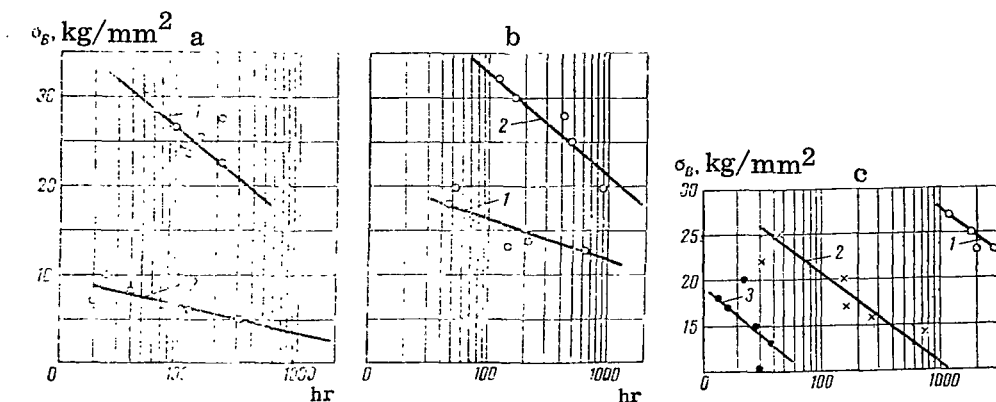


Figure 4. Stress-Rupture Strength of the Alloys:
 a—ST-1 at 600 (1) and 700°C (2); b—ST-3 (1) and ST-4 (2) at 600°C;
 c—ST-5 at 600 (1), 700 (2) and 800°C (3).

TABLE 4

Alloy	τ hr	$t, ^\circ\text{C}$	$\sigma, \text{kg/mm}^2$	Alloy	τ hr	$t, ^\circ\text{C}$	$\sigma, \text{kg/mm}^2$
ST-1	100	600	25,5	ST-3	100	600	16,5
	200	600	22,0		1000	600	11,5
	1000	600	14,0		100	600	33
	100	700	6,0		1000	600	21
	300	700	5,0				
	15 min	750	18,0				

CONCLUSIONS

1. In accordance with the four principal types of equilibrium diagrams four types of "composition—high-temperature strength" diagrams of titanium systems were established. Binary titanium systems were classified into these four types of diagrams according to the nature of the effect of the alloying element on the high-temperature strength of titanium.
2. The established patterns of dependence of high-temperature strength on the composition and structure of the binary titanium systems are of significance to research into multicomponent titanium systems and to the determination of the optimal compositions of new high-temperature titanium alloys.
3. The temperatures of phase transformations of the titanium alloys ST-1, ST-3, ST-4 and ST-5 were determined at temperatures ranging from crystallization temperature to room temperature. These alloys undergo in solid state the polymorphic transformation $\beta \rightarrow \alpha$ or the transformation associated with the formation of the aluminide Ti_3Al (ST-5) or solid solutions on its basis (ST-3 and ST-4) as well as the eutectoid transformation (ST-3).

4. The optimal regimes of heat treatment of the alloys ST-1, ST-3, ST-4 and ST-5 were determined; these regimes assure the most favorable combination of strength with plasticity:

ST-1 heating at 800°C, cooling in air
 ST-3 and ST-4 heating at 1000-1020°C, cooling in oil
 ST-5 heating at 1200°C, cooling in oil

5. The alloys ST-1 and ST-3 display a high short-time strength up to 600°C and the alloys ST-4 and ST-5, up to 800°C. The ultimate short-time strength of the alloy ST-1 at 600°C is ~ 70 kg/mm², while the alloy ST-3 it reaches 100 kg/mm². The alloy ST-4 has an ultimate strength of 75 kg/mm² at 750°C and 50 kg/mm² at 800°C. The ultimate strength of the alloy ST-5 at 800°C is 75 kg/mm² and at 900°C, 40 kg/mm².

6. At 600°C the ultimate stress-rupture strength of the alloy ST-1 after 100 and 1000 hr is $\sigma_{100} = 25.5$ kg/mm² and $\sigma_{1000} = 14$ kg/mm², respectively. At 700°C, $\sigma_{100} = 6$ kg/mm², and at 750°C following 15-min test this strength is 18 kg/mm².

At 600°C after 100 hr the ultimate stress-rupture strength of the alloy ST-3 is 16.5 kg/mm² and of the alloy ST-4, 33 kg/mm². /186

The alloy ST-5 at 700°C after 100 hr has an ultimate stress-rupture strength of 20 kg/mm².

7. The alloy ST-1 may be recommended for prolonged service up to 600°C and temporary service up to 750°C; the alloy ST-3, for prolonged service up to 550-600°C; and the alloys ST-4 and ST-5, up to 800-850°C.

REFERENCES

1. Kornilov, I. I. Fiziko-khimicheskiye osnovy zharoprochnosti splavov [Physico-chemical Principles of the High-Temperature Strength of Alloys], USSR Acad. Sci. Press, 1961.
2. Bochvar, A. A. Metallovedeniye [Metallography], Metallurgizdat, 1956.
3. Kornilov, I. I. Zhurnal neorganicheskoy khimii [Journal of Inorganic Chemistry], Vol. 111, No. 2, p. 360, 1958.
4. Kornilov, I. I. Doklady AN SSSR, Vol. 91, No. 3, p. 549, 1953.
5. Kornilov, I. I. and T. T. Nartova. Doklady AN SSSR, Vol. 172, No. 2, p. 135, 1967.
6. Osipov, K. A., Ye. M. Miroshkina and A. L. Sotnichenko. Izvestiya AN SSSR: Metallurgiya i gornoye delo [Metallurgy and Mining], Vol. 2, p. 146, 1963.
7. Glazova, V. V. and N. N. Kurnakov. Izvestiya AN SSSR, OTN: Metallurgiya i toplivo [Metallurgy and Fuel], Vol. 4, No. 81, 1960.
8. Kornilov, I. I. ISFKhA, AN SSSR, Vol. 18, No. 72, 1949.
9. Kornilov, I. I. and V. S. Vlasov. Izvestiya AN SSSR, OTN, Vol. 4 No. 32, 1958.

10. Kornilov, I. I. et al. In the collection: *Novyye issledovaniya titanovykh splavov* [New Studies of Titanium Alloys], Nauka Press, 1965.
11. Kornilov, I. I. and T. T. Nartova. *Izvestiya AN SSSR, OTN: Metallurgiya i toplivo* [Metallurgy and Mining], Vol. 5, No. 133, 1960.
12. Kornilov, I. I. and V. V. Glazova. *Doklady AN SSSR*, Vol. 150, No. 2, 1963.
13. Kornilov, I. I., Ye. N. Pylayeva and M. Z. Volkova. *Izvestiya AN SSSR*, Vol. 7, p. 771, 1956.
14. Kornilov, I. I. *Uspekhi khimii* [Achievements in Chemistry], Vol. 34, No. 1, p. 103, 1965.
15. Nartova, T. T. *Poroshkovaya metallurgiya* [Powder Metallurgy], No. 8, 1966.
16. Nedumov, N. A. *Zhurnal fizicheskoy khimii* [Journal of Physical Chemistry], Vol. 34, No. 1, p. 184, 1960.

CORROSION-RESISTANT ALLOY OF TITANIUM WITH 32% Mo

N. F. Anoshkin, N. G. Boriskina, P. B. Budberg, L. A. Yelyutina,
S. I. Kushakevich, I. D. Nefedova, Ye. I. Oginskaya,
Yu. M. Sigalov and G. L. Shvarts

Titanium and its alloys are among the new structural materials which are beginning to be used as corrosion-resistant materials in chemical machine building and in types of production associated with high temperatures.

The corrosion resistance of pure titanium in hydrochloric acid media (0-30% HCl) is markedly higher (at room and high temperatures) than the corrosion resistance of stainless chromium-nickel steels [1], but it remains satisfactory only in solutions of hydrochloric acid of low concentration.

Chemical machine building requires structural materials that are more resistant in hydrochloric acid media than pure titanium.

From literature data it was known that alloys of titanium containing a high content of molybdenum display a higher corrosion resistance in hydrochloric acid. In 1957 in a patent of the Rem-Cru Company [2] it was stated that the alloys of titanium containing 30-40% Mo are not inferior to tantalum, platinum and gold in resistance in boiling solutions of 20% hydrochloric acid and 40% sulfuric acid.

A series of studies by Soviet investigators [3, 4] showed that molybdenum markedly reduces the susceptibility of titanium to anodic dissolution. These works established that the corrosion resistance of Ti-based alloys in sulfuric acid solutions of various concentration markedly increases with increase in the molybdenum content of these alloys. These investigators also pointed out that the alloy of Ti + 30% Mo is the most corrosion-resistant in solutions of hydrochloric and phosphoric acids as well as in boiling solutions of CuCl_2 , FeCl_3 , AlCl_3 .

/187

Hydrofluoric acid, on the other hand, corrodes this alloy.

In accordance with the structure of the phase diagram of Ti-Mo [5], alloys of titanium with 30-40% Mo are alloys based on the body-centered lattice of β -Ti and molybdenum. At 500-400°C, however, the β -solid solution may decompose owing to the polymorphic transformation of the β -modification into the α -modification. In view of their closeness to the boundary of the $\beta \rightleftharpoons \alpha$ transformation, the amount of the α phase in alloys containing 32-34% Mo will be low.

The literature lacks information on the mechanical and technological properties of alloys in this series. Yet data of this kind are needed to develop materials for use in chemical machine building.

Laboratory studies of corrosion resistance and mechanical properties of a series of Ti-Mo alloys treated with various elements made it possible to establish that the alloys containing 32-34% Mo display the most appropriate combination of corrosion resistance with mechanical properties.

TECHNOLOGICAL AND MECHANICAL PROPERTIES OF THE ALLOY

In view of the high molybdenum content of the alloy it was to be expected that its technological properties would differ markedly from the properties of the series-produced titanium alloys and also that the technology of the production of ingots and semifinished products of this alloy would have specific features of its own. The principal difficulty in ingot production consists in assuring a sufficiently complete dissolution of molybdenum in titanium and its uniform distribution throughout the ingot. By now a technology assuring the production of ingots with a sufficiently homogeneous chemical composition lacking molybdenum inclusions has been developed.

The technological process of the production of semifinished products is complicated by the high deformation resistance of the alloy.

However, the alloy displays a good technological plasticity (Table 1) and hence it can be processed into various semifinished products: forgings, extruded rods, plate, sheets, tubes.

Industrial trials showed that the optimal method of deformation of this alloy is extrusion, such that the deformation pattern is characterized by isostatic compression which assures smooth flowage of the metal. In this case the danger of surface oxidation and cracking of the billet during deformation also is reduced.

/188

TABLE 1

Tempera- ture, °C	Mechanical properties			Tem- pera- ture, °C	Mechanical properties		
	σ_B , kg/mm ²	δ , %	ψ , %		σ_B , kg/mm ²	δ , %	ψ , %
20	65.6	1.4	1.9	800	26.0	27.0	56.0
200	55.0	11.0	27.0	900	16.0	42.0	40.0
400	49.5	15.0	47.0	1000	11.5	52.0	59.0
500	47.0	12.0	40.0	1100	7.5	95.0	90.0
600	44.0	15.5	42.0	1200	4.8	104.0	90.0
700	36.5	21.0	56.0				

Experience in the production of extruded rods of various diameter (from 230 to 15 mm) has shown that the temperature of extrusion and the rate of cooling from that temperature are of decisive importance during deformation to the structure and properties of these rods.

To obtain rods with a large cross section (diameter 230-100 mm) high temperature of the order of 1100-1200°C must be applied. The rate of cooling from extrusion temperature over the cross sectional area of these rods is non-uniform and is sufficiently high only in the peripheral zone, which is narrower the larger is the diameter. The central zone of the rods cools very slowly. The mechanical properties of large-diameter rods, and particularly their plasticity

characteristics, are not uniform over the cross sectional area, and their mean level is extremely low (Table 2).

TABLE 2

Rod di- ameter, mm	Site of excision of specimens	Mechanical properties			
		σ_B , kg/mm ²	δ , %	ψ , %	a_{impact} , kg-m/mm ²
230	Periphery	102.4	1.2	8.6	1.17
	Central zone	87.1	0.4	—	0.36
110	Periphery	86.9	15.4	33.8	0.46
	Central zone	86.7	3.6	5.6	0.25
45	Over entire cross section	89.5	16.8	50.2	1.2
15	Ditto	75.6	25.5	60.2	5.65

A special feature of the structure of large-diameter extruded rods is the presence of a macrograined structure as well as of second-phase segregations (Fig. 1, a). In accordance with the equilibrium diagram of the system Ti-Mo the formation of this structure and segregations is clearly linked to the partial decomposition of the β -solid solution with formation of the α phase or of some of their metastable modifications.

Following quenching from 1000–1100°C the segregations disappear and the plasticity of the alloy sharply increases (Fig. 1, b). For example, in rods of 230 mm diameter following quenching from 1000°C, unit elongation reaches 13.3% and contraction, 54.2%.

For rods of ≤ 60 mm diameter, which are extruded from an intermediate deformed billet, the deformation temperature can be reduced to 900–950°C. The rate of cooling of small-diameter rods is much higher, and it increases with decrease in diameter.

The mechanical properties of these rods are distinguished by their uniformity, their extremely high plasticity, and their structure which is more homogeneous and relatively micrograined (Fig. 1, c).

On slow cooling from temperatures exceeding 1100°C the alloy loses plasticity, which obviously is due to structural transformation. Rapid cooling from these temperatures, on the other hand, is accompanied by a rise in plasticity. The alloy is less sensitive to the cooling rate when cooled from temperatures below 1000°C, although even then its plasticity is higher when the cooling rates are more rapid.

When working out the technology of sheet production it was necessary to study in detail the conditions of deformability and the principal energy and force parameters of the rolling process: deformation resistance, spread and friction coefficient.

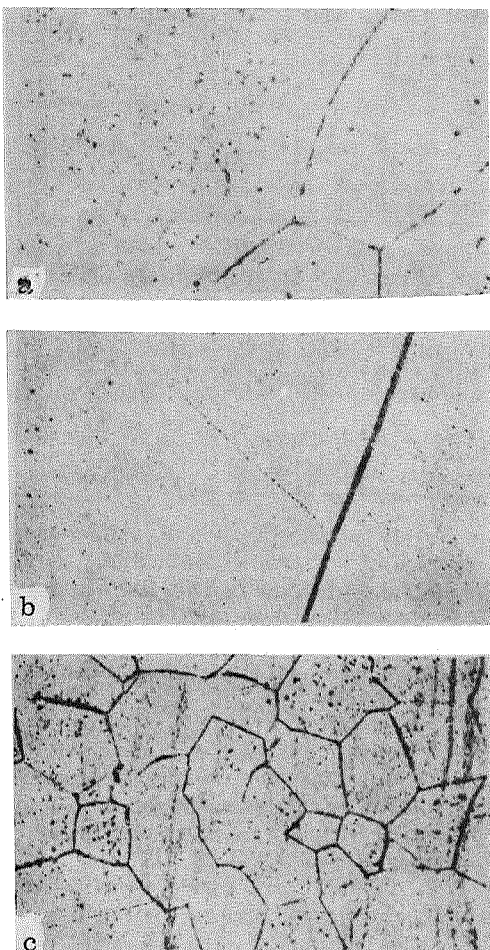


Figure 1. Microstructure of Rods:
a—Diameter 230 mm, Hot-Extruded State; b—Diameter 230 mm, Quenched From 1100°C; c—Diameter 45 mm, Hot-Extruded State.

than for the series-produced titanium alloys, rising from 0.33-0.36 at 300°C to 0.50-0.53 at 900-1000°C. This is probably associated with the special features of the composition and properties of the oxidized surface layer.

These findings made it possible to determine the principal rolling parameters needed to develop the production technology of plate and sheets of the investigated alloy.

The mechanical properties of hot-rolled plate are close to the properties of hot-extruded small-diameter rods, as are the conditions of their deformation and cooling.

The experiments were carried out on a 175/425 x 300 mm quarto mill by rolling flat specimens at 300-1000°C with a fixed 30% reduction in area at the rate of 0.167 m/sec. A 260 duo mill was used to roll wedge-shaped specimens at 500-1000°C with $\leq 60\%$ reduction in area at the rate of 0.4 m/sec. Deformability, total and unit pressure of the metal on the rolls, spread and the friction coefficient were investigated.

The deformation resistance of this alloy during its rolling throughout temperature range investigated markedly exceeds the deformation resistance of the series-produced titanium alloys (Fig. 2, a). The curves of the relation of deformation resistance to relative reduction in area (Fig. 2, b) reach a maximum when the reduction in area is approximately 40-45%.

The spread index increases with increase in rolling temperature until it reaches a maximum at 900°C, beyond which it tends to fall somewhat. In absolute value the spread index amounts to 0.36-0.47 at 300°C and 0.53-0.62 at 900°C. The temperature dependence and magnitude of the spread index for this alloy basically coincide with the data on the series-produced titanium alloys.

The friction coefficient of this alloy during rolling is markedly higher than for the series-produced titanium alloys, rising from 0.33-0.36 at 300°C to 0.50-0.53 at 900-1000°C. This is probably associated with the special features of the composition and properties of the oxidized surface layer.

Sheets 4-2.5 mm thick in the state following warm rolling and pickling display an extremely low plasticity (Table 3). The loss of plasticity under these conditions is due both to some work hardening and to the susceptibility of the alloy to embrittlement at 400-700°C (Table 4). The factors responsible for the low plasticity of the sheets in their original warm-rolled state are the final operations of the technological process of their production—warm skin rolling and pickling.

/190

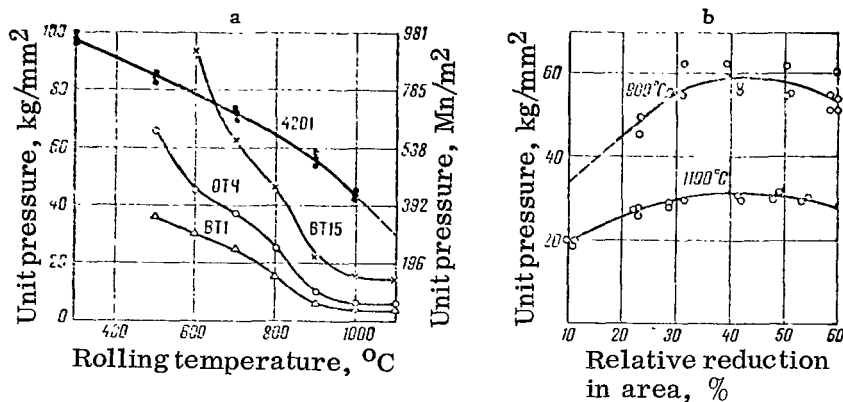


Figure 2. Relation of Unit Pressures of Metal on the Rolls to Temperature During Rolling with 30% Reduction in Area (a) and to Relative Reduction in Area (b).

Warm skin rolling of the sheets is carried out after heating to 850°C. Then the deformation occurs at 500-700°C, i.e. within the possible temperature range of decomposition of the β -solid solution, and it may stimulate structural transformations, causing a decrease in plastic properties. Thereupon the alloy is exposed to 430-460°C during the pickling of sheets. Special investigation (Table 4) established that exposure to these temperatures also leads to a marked loss of plasticity.

Annealing at 850°C prior to pickling removes work hardening but does not improve mechanical properties, while quenching from this temperature, carried out prior to pickling, even intensifies the embrittling effect of the subsequent exposure to 430-460°C.

In the event of vacuum annealing at 850°C, which makes it possible to avoid oxidation of the sheet surface and which hence is carried out after pickling, the plasticity of the alloy increases sharply while its strength remains unchanged. As the temperature of vacuum annealing is further increased, the effect of the low rate of subsequent cooling begins to manifest itself and the alloy undergoes sharp embrittlement which is also accompanied by a decrease in strength.

/191

The effect of the temperature and time of heating on mechanical properties of the alloy was investigated in greater detail on specimens prepared from 15 mm diameter extruded rods. Their aging was carried out at 200, 350, 400, 500,

TABLE 3

State of specimens	Mechanical properties			
	c_b , kg/mm ²	σ_s , kg/mm ²	δ , %	ψ , %
Plate				
Hot rolling	89.1	87.2	13.7	31.8
Hot rolling, pickling and vacuum annealing	90.3	85.8	15.7	43.1
Sheets				
Warm rolling and pickling ..	93.8	90.8	7.0	—
Warm rolling, annealing at 850°C in air and pickling ...	86.5	84.0	10.5	—
Warm rolling, quenching from 850°C and pickling ...	87.2	82.6	5.7	—
Warm rolling, pickling and vacuum annealing at 850°C	86.0	84.0	17.1	—
Warm rolling, pickling and vacuum annealing at 1200°C	58.7	—	0.4	—

600°C for 25-1000 hr. The results of this investigation are presented in Table 4 and they point to the following: at 200 and 350°C the strength and plasticity characteristics of the alloy do not change following aging from 100 to 1000 hr. Ultimate strength remains within the limits of 75.5-81 kg/mm² at 200°C and it changes even less at 350°C compared with the quenched state. Unit elongation remains within the limits of 23-24% at 200°C and 24-28% at 350°C throughout aging time, contraction of area is 60-63% and impact strength is 10 kg-m/cm².

Following aging at 400°C for 1000 hr the strength and plasticity characteristics of the alloy still remain at the level of the properties of the quenched alloy. However, impact strength then decreases to 2.7 kg-m/cm², which indicates the occurrence of structural changes. Raising the aging temperature to 500°C and prolonging the aging time leads to a continuous decrease in contraction of area as well as to a sharp decrease in impact strength, which after 300 hr of aging dropped to 0.81 kg-m/cm².

/ 192

At 600°C the processes leading to embrittlement of the alloy occur within the first 25-100 hr of tests. This is accompanied by a decrease in contraction of area, unit elongation and impact strength of the alloy. Following aging at this temperature for 300 and 500 hr plasticity increases, but the values of δ , ψ and α_{impact} then reached still are markedly lower than for the alloy in quenched state. Alloy specimens tested for impact strength following various regimes of their aging were also tested for corrosion resistance by the NIIKhIMmash method in 21% hydrochloric acid for 500 hr at 90°C. Analysis of the test findings (Table 4) shows that only the alloys aged at 200°C do not change in corrosion resistance compared to the quenched alloy. Aging at 350, 500 and 600°C leads to an insignificant increase in corrosion rate. Aging at 400°C for 100-500 hr markedly reduces the corrosion resistance of the alloy although then the properties of the alloy still

TABLE 4

Aging time, hr	σ_B , kg/mm ²	σ_S , kg/mm ²	δ , %	ψ , %	σ_{impact} , kg-m/cm ² mm/year	Corrosion rate, mm/year
Original state (extruded rod, 15 mm diameter)						
	75.6	75.1	25.5	60.2	5.65	0.071
Quenching from 900°C						
	75.5	75.0	23.6	64.1	8.72	0.069
Aging at 200°C						
100	79.3	78.9	23.5	62.6	9.22	0.068
300	77.7	77.4	23.0	63.4	10.38	0.066
500	81.2	80.5	24.11	60.09	7.65	—
1000	81.0	80.6	24.51	61.48	9.1	—
Aging at 350°C						
100	78.1	77.8	28.1	62.2	11.72	0.167
300	77.7	77.5	25.7	62.15	12.0	0.086
500	76.2	75.8	24.7	63.9	10.8	0.094
1000	79.1	78.5	25.8	61.0	10.3	0.092
Aging at 400°C						
100	75.0	73.9	25.9	66.2	8.96	0.157
300	74.1	73.3	26.3	66.0	8.67	0.118
500	74.6	73.5	26.5	66.8	7.75	0.181
1000	76.0	74.6	23.1	62.3	2.71	0.091
Aging at 500°C						
25	76.1	74.9	24.1	58.6	—	—
50	75.4	74.9	23.9	54.5	1.57	0.073
100	74.8	73.6	24.8	55.3	1.25	0.074
300	75.8	74.7	20.6	37.2	0.81	0.078
500	74.9	73.6	20.6	40.0	3.49	0.074
Aging at 600°C						
25	75.4	75.0	16.4	33.0	—	—
50	74.6	73.6	18.1	34.4	3.36	0.102
100	74.7	74.4	17.7	36.0	2.61	0.083
300	74.9	74.2	20.1	46.5	4.42	0.084
500	74.1	73.6	21.8	45.1	4.88	0.084

remain practically unchanged. Aging at 600°C and particularly at 500°C, when the processes leading to loss of plasticity by the alloy reach their peak intensity, hardly affects corrosion resistance. Microstructural examination of the aged alloys showed that they all have the polyhedral structural of the β -solid solution. Following aging at 500 and 600°C a small amount of point segregations of the second phase appears in the structure. Radiographs of these alloy specimens display only reflection lines corresponding to the β phase. Thermograms of the specimens lacked any distinct thermal effects corresponding to phase transformation of the oxide MoO_3 is observed.

WELDABILITY OF THE ALLOY AND THE CORROSION RESISTANCE OF ITS WELDED JOINTS

The welding was carried out manually as well as with the aid of welding jigs by the nonconsumable tungsten electrode method in argon or in a controlled-atmosphere chamber.

Of special significance to the quality of the welded joint was the purity of the surfaces being joined and the proper preparation of the edges for joining. Following their cleaning the edges of the alloy specimens were inspected by the dye-penetrant method. If surface cracks were detected the cleaning was repeated until they were completely eliminated.

The regimes of manual and automatic argon-arc welding (4 mm thick sheets) are given in Table 5.

TABLE 5

/193

Argon-arc welding	Current intensity, amp	Voltage, v	Welding rate, m/hr	Argon consumption for shielding, liters/min	
				Weld	Back side of weld
Manual	170	11-16	—	12-14	2-4
Automatic	200-220	11-13	14	12-14	2-4
	200-220	11-13	19	12-14	2-4

Note: The numerator pertains to single-pass welding and the denominator, to double-pass welding.

The strength properties of the base metal and welded joints are given in Table 6.

The figures given in the tables indicate that the ultimate strength of joints of the alloy welded by both manual and automatic argon-arc methods was at least 90% of the ultimate strength of the base metal. Fracture during mechanical tests of the welded joints occurred in the base metal. The bending angle of the weldments was not stable, ranging from 0 to 180°C.

Corrosion tests of the base metal and welded joints of the alloy were carried out in boiling 21% hydrochloric acid. Table 7 presents data on the corrosion rate of the sheet metal and welded joints of three melts of the alloy, containing a varying amount of molybdenum: 29.3, 31.7 and 35.8%.

The corrosion rate of the alloy markedly increases when its molybdenum content is below 30%.

TABLE 6

Test temperature, °C	Base metal (4 mm thick sheet)	σ_B	
		Welded joints	
		Manual argon-arc welding	Automatic argon-arc welding
20	82.6—83.5 83.1	81.4—81.4 81.4	80.0; 63.0; 92.0
200	63.7—66.4 65.2	63.7—62.0 62.9	61.8; 64.7; 67.7
300	62.1—63.0 62.6	60.8—62.0 60.9	63.0; 60.0; 64.7
400	60.5—61.0 60.7	55.0—54.9 55.0	55.8; 63.7
500	50.8—54.6 52.4	47.0—50 48.5	37.2; 38.0
600	42.5—43.4 42.9	40.2—41.0 40.6	30.4; 20.0
700	26.1—26.8 26.3	23.4—26.4 26.9	24.5; 29.4
800	17.5—18.7 18.1	18.5—17.9 18.2	13.7; 14.7

/ 194

Note: The test data pertaining to automatic argon-arc welding are given for different specimens.

TABLE 7

Specimen	Corrosion rate (mm/year) for a Mo content of		
	29.3	31.7	35.8
Base metal	0.863	0.090	0.123; 0.042
Welded joint			
manual argon-arc welding	0.758	0.097	0.136
automatic argon-arc welding	0.718	0.095	0.097

Thus while for the alloys containing 31.7—35.8% Mo the rate of corrosion in boiling 21% HCl is 0.1 mm/year, for the alloy containing 29.3% Mo this rate increases by a factor of 8.5 times (corrosion rate 0.863 mm/year). Welded joints do not differ in corrosion rate from the base metal.

The welding regimes developed above were experimentally verified when manufacturing components for a tetrochloroalkane rectification column (cf [Russian] p. 76, Fig. 3, a); in the course of these trials certain technological operations of the processing of this alloy into finished products also were refined. It was established that the blanks can also be cut with the aid of guillotine shears provided that the edges are machined. Flame cutting is inappropriate in this case. The parts can be produced in cold state by the pressure working method, following heating to 150–300°C, as well as in hot state at 600–700°C. For forging in cold state the die must be heated to 300°C. The minimum permissible bending radius for sheet metal in cold and hot states is three times the thickness of the blank (for 4 mm thick sheet). Rolling of skelp into shells, tube sections and other shapes must be carried out in cold state in a direction transverse to the original rolling direction of the sheet. Pressure working of weldments of the alloy is not recommended.

It should be noted that all the tests and the production of shapes were carried out on the basis of sheet material which was carefully inspected with the aid of x-ray and visual inspection methods.

CONCLUSIONS

1. Mechanical and corrosion properties of the alloy with 32–34% Mo were investigated. It is shown that this alloy has a high corrosion resistance in 21% boiling hydrochloric acid (corrosion rate ≤ 0.1 mm/year). Following its heat treatment by the optimal regime the strength of the sheet material is 84–86 kg/mm² and its plasticity, 15–17%.
2. A technology for the production of semifinished products from this alloy in the form of forgings, rods and sheets was developed.
3. The weldability of this alloy by different welding methods was investigated and the mechanical and corrosion properties of the welded joints were determined. It was established that weldability is satisfactory and the corrosion resistance of the welded joints is similar to the resistance of the base metal.

REFERENCES

/195

1. Tablitsy korroziionnoy stoykosti titana i yego splavov v razlichnykh agressivnykh sredakh [Tables of Corrosion Resistance of Titanium and Its Alloys in Various Corrosive Media], NIIKhimMash, 1961.
2. Margolin, H. J. J. Met. Progr., Vol. 71, No. 2, p. 86, 1957.
3. Tomashov, N. D. et al. In the collection: Korroziya i zashchita konstruktsionnykh materialov [Corrosion and Protection of Structural Materials], Mashgiz, No. 173, 1961.
4. Andreyeva, V. V. and V. I. Kazarin. Novyye konstruktsionnyye khimicheski stoykiye metallichесkiye materialy [New Chemically Resistant Structural Metal Materials], Goskhimizdat, 1961.
5. Nausen, M. et al. J. Metals, Vol 3, No. 10, p. 881, 1951.

PRINCIPAL PROPERTIES OF THE TITANIUM ALLOY AT-3 AND THE PROSPECTS FOR ITS APPLICATION

I. I. Kornilov, K. P. Markovich and V. S. Mikheyev

Systematic studies of the phase diagrams of part of the six-component system Ti-Al-Cr-Fe-Si-B and a detailed analysis of the dependence of the properties of alloys of this system on their composition and phase structure has resulted in the development of the new titanium alloys AT-3, AT-4, AT-6 and AT-8 [1-3].

Of the aforementioned alloys the alloy AT-3 finds the broadest application in various branches of technology. The physical, mechanical, technological and high-temperature properties of this alloy have been investigated in detail [4, 5]. The technologicity (processability) and comparatively high plasticity of this alloy composition make possible its industrial processing into forgings, sheets, tubes and foil. The alloy is satisfactorily weldable and the properties of its welded joints reach 94-96% of the properties of the base metal.

The present work reports on the results of an investigation of the creep, stress-rupture strength and thermal stability of the alloy AT-3 having the following composition: 2.7% Al, 0.6% Cr, 0.3% Fe, 0.36% Si, 0.01% B, bal. Ti.

The investigation was carried out on rod and sheet material at 300-600°C for up to 15,000-20,000 hr. Stress-rupture strength tests were carried out on VP-8 machines and creep tests, on an IM-5 machine using standard specimens. Rod specimens (14 x 14 mm and 25 mm in diameter) were annealed at 880°C for 30 min and cooled in air. The structure of the alloy following annealing consisted chiefly of the α -solid solution and a small amount of residual metastable β phase. The mechanical properties of the alloy at elevated temperatures are given in Table 1.

TABLE 1

Tempera- ture, °C	Ultimate strength, kg/mm ²	Yield point, kg/mm ²	δ, %	ψ, %	^a impact strength, kg-m/cm ²
20	86.3	85.0	14.0	47.7	
350	60.9	58.5	14.8	56.8	8.5
400	58.8	54.6	15.8	58.5	12.6
500	50.5	48.3	16.4	70.3	14.3
600	35.7	31.8	25.3	74.0	18.8

Stress-rupture strength was investigated with the object of determining ultimate strength after 100 hr of tests at 400, 500, 600 and 650°C and after 20,000 hr at 350 and 500°C. The values of stress-rupture strength determined after 100 hr at 350-650°C are given below:

/196

$t, {}^\circ\text{C}$ 350, 400, 500, 600, 650
 $\sigma_{100}, \text{kg/mm}^2$ 55, 45, 30, 10, 2

Analysis of the results of tests of stress-rupture strength of the alloy at 350 and 500°C under various loads resulted in constructing the curve of stress-rupture strength (Fig. 1). This curve shows that during tests at 350°C the alloy undergoes little softening and its stress-rupture strength is high. This is demonstrated by the similarity between stress-rupture strength and short-time strength as well as by the slope of the curve of stress-rupture strength toward the ordinate.

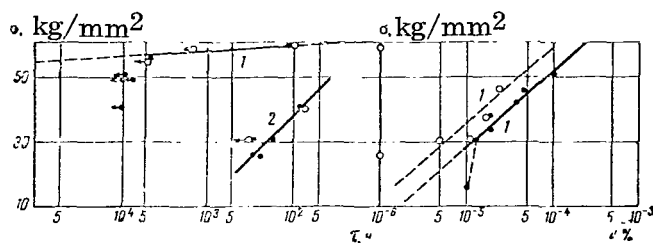


Figure 1. Curve of Stress-Rupture Strength of the Alloy AT-3 at 350°C (1) and 500°C (2).

Data of TsKTI (Central Boiler and Turbine Institute) (●) and IMET (Baykov Institute of Metallurgy) (O).

The stress-rupture strength at 350°C thus lies at 56 kg/mm² while ultimate strength at the same temperature 61 kg/mm² (i.e. stress-rupture strength is 90% of ultimate strength). It is known that for many austenitic steels at these test temperatures after 1000 hr stress-rupture strength corresponds to 50-60% of ultimate strength.

The alloy softens appreciably at > 500°C; then its stress-rupture strength drops to 22 kg/mm².

These findings, as can be seen from Fig. 1, are in good agreement with the test results for this alloy obtained at the Central Boiler and Turbine Institute [6].

The investigation of the creep of the alloy reduced to determining the creep limit at 350-500°C with a total elongation of 0.2%, as well as to obtaining more detailed data for 300 and 350°C:

$t, {}^\circ\text{C}$ 350, 400, 450, 500
 $\sigma_{0.2/100}, \text{kg/mm}^2$ 50, 30, 20, 5-6

At 350°C creep was investigated under various loads: 15, 30, 33 and 37 kg/mm^2 , for 5000 hr (after which the specimens remained intact), and under loads of 40, 45 and 50 kg/mm^2 for 20,000 hr. A specimen fractured under the 50 kg/mm^2 load following service for 17,898 hr. At 300°C the tests were carried out under the load $\sigma = 30 \text{ kg/mm}^2$ for 5000 hr (after which the specimen remained intact). Analysis of the obtained data made it possible to construct the creep curves given in Fig. 2 (a-c).

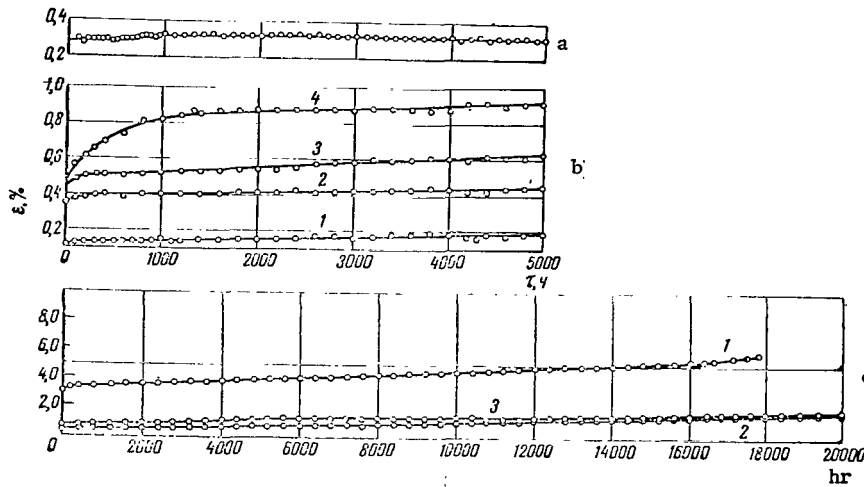


Figure 2. Creep Curves of the Alloy AT-3 for:

a— $T = 300^{\circ}\text{C}$, $\sigma = 30 \text{ kg/mm}^2$, v_c (Creep Rate) = $0.45 \cdot 10^{-6}$; b— $T = 350^{\circ}\text{C}$, $\sigma = 15$ (1), 30 (2), 33 (3), 37 (4) kg/mm^2 , $v_c = 1 \cdot 10^{-5}$ (1), $1.6 \cdot 10^{-5}$ (2), $2 \cdot 10^{-5}$ (3, 4); c— $T = 350^{\circ}\text{C}$, $\sigma = 50$ (1), 45 (2), 40 (3) kg/mm^2 .

The shape of the creep curve at $T = 300^{\circ}\text{C}$ and $\sigma = 30 \text{ kg/mm}^2$ (Fig. 2, a) as well as at $T = 350^{\circ}\text{C}$ and $\sigma = 15$ and 30 kg/mm^2 (Fig. 2, b) is nearly rectilinear. The stage of unsteady-state creep is brief, not longer than 200 hr. As the load is increased to 37 kg/mm^2 at 350°C , the length of the state of unsteady-state creep increases to 1200 hr. The state of steady-state creep at 300 and 350°C under all the loads applied is fairly long and after 5000 hr it still does not terminate. For this selected regime of testing, the third state (the stage of accelerated creep) is absent. On the creep curve for $\sigma = 50 \text{ kg/mm}^2$ (specimen fractured after 17,890 hr of service) the segment pertaining to the accelerated stage of creep is short, only about 10% of the curve (Fig. 2, c).

The accumulated deformation after 5000 hr of tests at 300°C is only 0.02%, while at 350°C it increases with increase in load from 0.18% for $\sigma = 15 \text{ kg/mm}^2$ to 0.92% for $\sigma = 37 \text{ kg/mm}^2$.

A characteristic feature of the alloy AT-3 during creep at 350°C is the relatively small change in creep rate with change in the load applied within the limits investigated, thus causing the slope angle of the curve of the relation of

load applied to the logarithm of creep rate to be fairly steep in the direction toward the ordinate (Fig. 1). This represents a positive quality of the alloy, as this means that in the presence of considerable overloads during tests the creep rate will not vary substantially. Plastic deformation (permanent set) accumulates chiefly during the stage of accelerated creep. As for deformation during the stage of steady-state creep, it amounts to only tenths of a percent.

Combined analysis of test data on creep and stress-rupture strength indicates that the alloy AT-3 at 350-400°C is most suitable for prolonged performance (up to 15,000-20,000 hr).

These conclusions completely correspond to the microstructural data which revealed the high stability of structural state of this alloy under conditions of extremely prolonged testing.

The alloy's microstructure following creep tests at 350°C under varying loads for 18,000 hr was not found to undergo any changes compared with its initial state (Fig. 3, a and b).

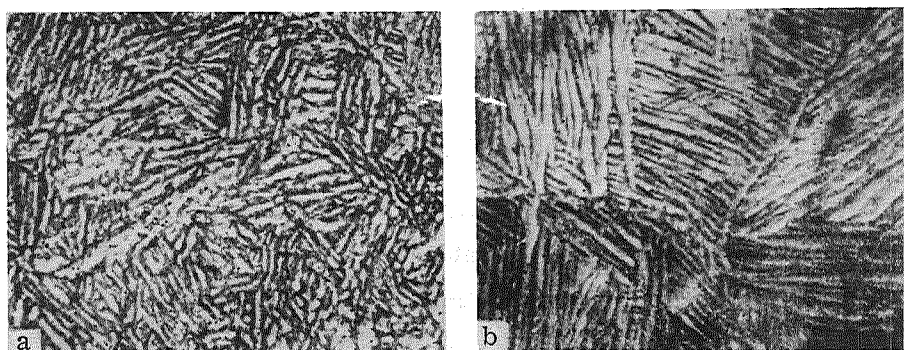


Figure 3. Microstructure of the Alloy AT-3 Following Creep Tests,
Magnified 600 Times:

a— $T = 350^\circ\text{C}$, $\sigma = 37 \text{ kg/mm}^2$, $\tau = 5215 \text{ hr}$; b— $T = 350^\circ\text{C}$, $\sigma = 50 \text{ kg/mm}^2$, $\tau = 17,890 \text{ hr}$.

The radiograph of the specimen subjected to creep tests for 17,890 hr at 350°C under the loads $\sigma = 50 \text{ kg/mm}^2$ and 50 kg/mm^2 in an RKU chamber in Cu radiation reveals only the reflection lines of the hexagonal lattice of the α -solid solution.

The relative stability of structure of the alloy in the course of such prolonged tests at elevated temperatures under load is apparently due to the high stability of the basic multicomponent α -solid solution, considering that diffusion processes occur very slowly at these temperatures.

Tensile tests of specimens excised from the specimens subjected to creep tests at 350°C under various loads for 5000-10,000 hr (Table 2) showed that the plasticity of the alloy following such prolonged tests remains close to its initial

TABLE 2

Creep tests			σ_B kg/mm ²	σ_s kg/mm ²	δ , %	Φ , %
t , °C	t , hr	σ , kg/mm ²				
		Original state	87.4 86.4	84.4 85.4	14.4 14.0	44.7 41.8
350	584	15	86.0 87.36	80.24 81.25	17.6 18.4	38.2 43.45
350	6632	30	86.09 85.07	80.99 79.72	15.2 14.4	38.81 38.51
350	5125	37	87.11 87.4	84.05 82.02	18.0 16.0	43.75 36.93
350	9939	43	85.17 84.38	81.18 81.18	16.0 18.0	39.93 28.0
350	17890	50*	92.67 93.00	87.00 88.50	16.0 16.4	42.0 43.46

*In all cases except the one denoted by the asterisk the specimen did not fracture.

value: unit elongation in original state is 14% whereas after creep tests for 5454 and 9936 hr it is 16-18%. Ultimate strength also did not decrease following the creep tests. These findings point to the high stability of structural state and absence of embrittlement of the alloy in the creep process. The alloy AT-3 under these conditions is thermally stable. A special investigation of prolonged aging of the alloy AT-3 at 350 and 400°C for 10,000 hr also confirms its thermal stability, as can be seen from the curves of variation in strength and plasticity shown in Fig. 4 for aging for 10,000 hr at 400°C. At 500°C the properties of the alloy AT-3 change. The creep curve (Fig. 5) recorded for $\sigma = 15$ kg/mm² is of a shape different from the shape of the curves recorded at 350°C. The specimen fractured after 1500 hr; during the final 500 hr creep occurred at an accelerated rate. The softening of the alloy at 500°C is due to the attendant thermal instability of its structure. During tests under load at this temperature the six-component α -solid solution of titanium undergoes decomposition resulting in the formation of a phase based on the compound Ti_5Si_3 [8]. Metallographically this compound manifests itself in the form of light inclusions which in the course of creep become disposed along the active slip planes, thus contributing to the acceleration of the creep process.

/ 199

Electronmicroscopic examination by the carbon replica method reveals these inclusions existing in the form of irregularly shaped formations (Fig. 6).

The radiograph of a section of the specimen tested for creep at 500°C under the load of 15 kg/mm² for 1500 hr displays the reflection lines of the hexagonal closely packed lattice (α -phase) as well as very weak reflection lines of the hexagonal lattice of the compound Ti_5Si_3 . The conducted analysis shows that the

softening at 500°C is due to instability of the structure of the α -solid solution of the alloy AT-3 at this temperature.

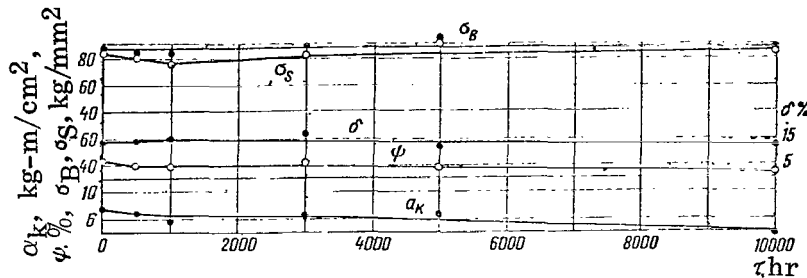


Figure 4. Variation in Mechanical Properties of the Alloy AT-3 During Aging For 10,000 hr at 400°C.

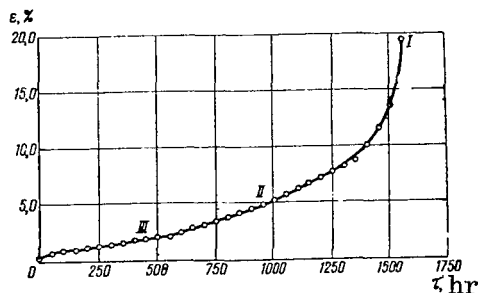


Figure 5. Creep Curve of the Alloy AT-3.

$t = 500^\circ\text{C}$ and $\sigma = 15 \text{ kg/mm}^2$, $v_c = 28$ (II), 6.6 (II), $3.4 \cdot 10^{-3}\% \text{ hr}$ (III).

mending the alloy AT-3 for use as a structural material in atomic power engineering.

The alloy AT-3 displays a high corrosion resistance when used as the material of equipment for the production of tartaric acid as then the acid is not contaminated with ions of nickel, maganese, iron and chrominum and, moreover, the service life of the equipment is prolonged.

This alloy also displays a high corrosion resistance in caustic soda, ammonia liquer, nitric acid, perchloric acid and acetic acid, as well as in media containing sulfur at 50°C. This alloy may be recommended for the construction of equipment performing under these conditions as well as a structural material for the reaction vessels used to produce perchloric acid.

The alloy AT-3 also displays a high corrosion resistance in sulfur concentrate media treated with 3% magnesium chlordide solution.

The alloy AT-3 is recommended for broad introduction into production as a structural material for products of the New Technology, as well as a corrosion-resistant material for equipment performing in corrosive media at up to 450°C.

Tests of the corrosive properties of the alloy AT-3 were performed in many media, including a medium containing a sulfuric acid solution at 350°C. Over a prolonged period of time these tests, performed in the presence of radiation on specimens of the alloy, revealed no signs of corrosion nor of stress-corrosion cracking. This warrants recom-

/200

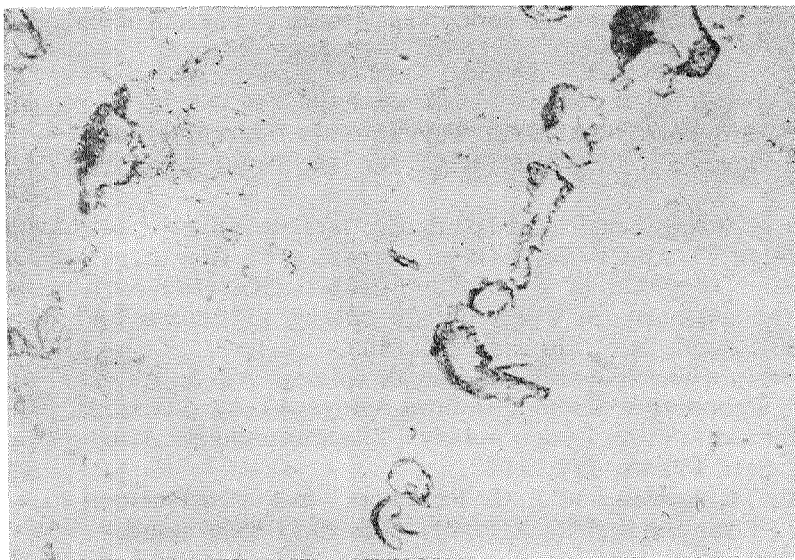


Figure 6. Microstructure of the Alloy AT-3 Following Creep Tests at $T = 500^{\circ}\text{C}$, $\sigma = 15 \text{ kg/mm}^2$, $\tau = 1500 \text{ hr}$. Magnified 10,000 Times.

CONCLUSIONS

1. The titanium alloy AT-1 is an alloy of medium strength which performs as a high-temperature alloy at up to 450°C and is thermally stable. It is satisfactorily welded as well as deformed in cold and hot states.
2. The high-temperature strength of this alloy was investigated by the method of determining stress-rupture strength and creep at $300\text{--}600^{\circ}\text{C}$.
3. Curves of stress-rupture strength at 350 and 500°C were plotted and the limits of stress-rupture strength at 350°C were found to be: $\sigma_{10,000} = 56 \text{ kg/mm}^2$; $\sigma_{20,000} = 55.5 \text{ kg/mm}^2$; $\sigma_{100,000} = 54 \text{ kg/mm}^2$.
4. The alloy AT-3 has a high stress-rupture strength; $\sigma_{10,000}$ at 350°C is close to the limit of short-time strength at the same temperature ($\sigma_B = 60 \text{ kg/mm}^2$).
5. The closeness between the values of the limits of stress-rupture and short-time strength points to an insignificant softening of the alloy under conditions of prolonged creep at $300\text{--}400^{\circ}\text{C}$.
6. Analysis of the creep curves at 350°C established that creep rate at this temperature is relatively independent of load. /201
7. It is shown that at 500°C occurs softening of the alloy due to the change in the structure of its α -solid solution.
8. The alloy can be used as a corrosion-resistant structural material for a number of equipment types.

REFERENCES

1. Mikheyev, V. S., K. P. Markovich and L. F. Tavadze. In the collection: *Titan i yego splavy* [Titanium and Its Alloys], No. 10, USSR Acad. Sci., Press, 42, 1963.
2. Mikheyev, V. S., T. S. Chernova and N. M Dzhibuti. *Issledovaniye chastichnoy diagrammy sostoyaniya Ti-Al-Cr-Fe-Si-B po razrezu s 6% Al* [Investigation of the Partial Phase Diagram of Ti-Al-Cr-Fe-Si-B Over the Section With 6% Al]. In the collection: *Titan i yego splavy* [Titanium and Its Alloys], No. 10, USSR Acad. Sci., Press, 48, 1963.
3. Kornilov, I. I. et al. *Osnovyye svoystva titanovykh splavov AT-3, AT-4, AT-6, AT-8* [Basic Properties of the Titanium Alloys AT-3, AT-4, AT-6, AT-8]. In the collection: *Titan i yego splavy* [Titanium and Its Alloys], No. 7, USSR Acad. Sci. Press, 174, 1962.
4. Mikheyev, V. S., K. P. Markovich and Z. G. Fridman. In the collection: *Titan i yego splavy* [Titanium and Its Alloys], No. 10, USSR, Acad. Sci. Press, 214, 1963.
5. Markovich, K. P., V. S. Mikheyev and Z. G. Fridman. In the collection: *Metallovedeniye titana* [Metallography of Titanium], Nauka Press, 204, 1964.
6. Nikitina, L. P. In the collection: *Titan i yego splavy* [Titanium and Its Alloys], No. 10, USSR Acad. Sci., Press, 204, 1963.
7. Mikheyev, V. S. et al. *Izvestiya An SSSR: Metallurgiya i gornoye delo* [Metallurgy and Mining], Vol. 2, No. 156, 1964.
8. Kornilov, I. I. et al. In the collection: *Novyye issledovaniya titanovykh splavov* [New Studies of Titanium Alloys]. *Trudy 6-go soveshchaniya po metallokhimii, metallovedeniyu i primeneniyu titana i yego splavy* [Proceedings of the Sixth Conference on Metal Chemistry, Metallography and Uses of Titanium and Its Alloys], Nauka Press, 221, 1965.

PARAMETERS OF THE DIFFUSION OF OXYGEN IN β -TITANIUM*

L. F. Sokiryanskiy, D. V. Ignatov, A. Ya. Shinyayev,
I. V. Bogolyubova, V. V. Latsh and M. S. Model'

Research into the diffusion of oxygen in titanium has previously been producing highly contradictory results. At the temperatures being compared the difference in the diffusion coefficients specified by different investigators reaches two orders of magnitude. The most unexpected proved to be the results of an investigation of the diffusion of oxygen in the high-temperature β -modification of titanium. On the basis of general theoretical premises it might be expected that the diffusion coefficients of oxygen in the bcc lattice of the β phase would be several times as high as the diffusion mobility of oxygen in the closely packed hexagonal lattice of the α phase. Yet Reynolds and associates [1] observed no difference whatever in the diffusion rates of oxygen in these two titanium modifications. The authors of two other works ([2, 3]) did detect a more rapid diffusion of oxygen in the β phase but they reported unusually high values of activation energy (about 70 kcal/mole) which are roughly twice as high as the values of activation energy of interstitial elements in the other metals with bcc lattice. According to Reynolds and associates such high values of activation energy indicate that the kinetics of the diffusion absorption of oxygen by titanium is determined not by diffusion but by some other process (surface reaction, self-diffusion of titanium, etc.).

Parr [4] suggested that the mechanism of the diffusion of oxygen in β -titanium is not interstitial, contrary to what is usually assumed, but substitutional. The authors of [7], on analyzing the results of previous investigations, pointed out that the aforementioned anomalies may be due to certain methodological errors, and particularly to insufficient reliability of the methods for the analysis of diffusion layers.

/202

The investigation whose results are presented in this article was intended to determine more precisely the numerical values of the diffusion parameters.

The method used here to investigate the structure of the gas-saturated layers is based on the utilization of the marked effect of the concentration of the oxygen dissolved in titanium on the parameters of its crystal lattice. The lattice parameters were measured for a series of plane surfaces parallel to the oxidized surface, which were obtained by means of successive etchings of the test specimen to specific depths. X-ray structural analysis was carried out with the aid of somewhat modified URS-50I ionization apparatus, as well as by the photographic method with the aid of an URS-70 camera. The greater part of the investigations was carried out by the ionization method, since this method produces more precise results. The distribution of oxygen over the depth of the diffusion zone was characterized by the displacement of the position of the intensity maximum of the reflection from the plane (114) in K_{α} -radiation of cobalt

* The participants in this project also included the engineers L. V. Gubanova, L. G. Maksimova and N. F. Kharlamova.

$$\Delta 2\vartheta_{114} = |2\vartheta_{114}(x) - (2\vartheta_{114})_{\text{base}}|,$$

where $(2\vartheta_{114})_{\text{base}}$ is the position of the intensity maximum of the interference line corresponding to the base of the analyzed sample (on plots this position is conditionally taken as zero position); $2\vartheta_{114}(x)$ is the position of the intensity maximum during analysis of the layer occurring at the distance x from the specimen surface.

The investigation was carried out on specimens of technical titanium (VT1-1 alloy) oxidized in air, as well as on specimens of iodide titanium annealed in pure oxygen. The chemical composition of the alloys is given in the table below.

TABLE 1

Material	Impurity content, %						
	Fe	Si	Mg	C	H ₂	N ₂	O ₂
VT1-1 Iodide ti- tanium	0.13 0.01	0.06 0.01	— 0.01	0.04 0.015	0.005 0.002	0.02 0.02	0.1 0.02

Ground specimens of VT1-1 alloy measuring 20x20x20 mm were heated in vacuo to the desired temperature and thereupon oxidized in the atmosphere of non-dried laboratory air. The experiments were performed at 950, 1000, 1050, 1100 and 1150°C for 0.5-4 hr each time. The layers for layer x-ray structural analysis were removed by the method of anodic electrolytic polishing.

The structural pattern of the diffusion zone is shown in Fig. 1. Zone I, which is rich in interstitial impurities, directly adjoins the specimen surface. It is followed by the gas-saturated layer sector II which at the oxidation temperature represents the β phase. The extent of this sector is much greater than the extent of sector I, but the concentration gradient therein is much smaller — this undoubtedly points to a more rapid diffusion of oxygen in β -Ti than in the α phase.

The method used to calculate the diffusion coefficients was so designed as to avoid, insofar as possible, assumptions the validity of which is difficult to verify experimentally. When deriving the working formulas allowance was made for the following features of the process of the absorption of gases.

1. In the initial sector (sector I) of the diffusion zone the x-ray reflection are greatly blurred, which is primarily due to the high concentration gradient of oxygen in the layer, thus affecting the formation of the diffraction pattern. In the neighborhood of the surface this blurring is so considerable that it leads to merging of the components of the α_1 - and α_2 -doublet. The marked effect of the concentration gradient manifests itself throughout this sector (Fig. 1). Moreover, the outer layers of metal when oxidized in air may get enriched with other

/203

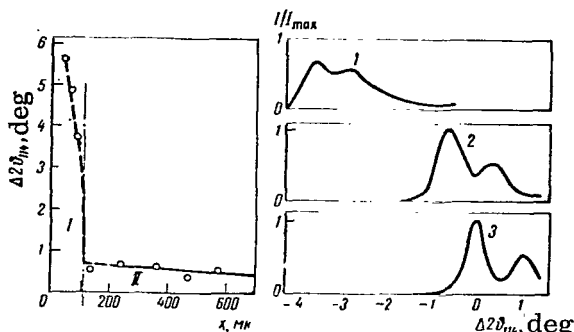


Figure 1. Variation in the Position (a) and Shape (b) of the (114) Reflection Over the Depth of the Diffusion Zone:

Oxidation Regime: $T = 1050^{\circ}\text{C}$, 2 Hr.
 Depth of Occurrence of the Analyzed Layer (x) Below the Surface, in Microns:
 80 (1), 360 (2), 2000 (3).

in β -Ti and the experimental results for this layer are most reliable, it is precisely the data pertaining to this part of the diffusion zone that should be used to calculate the diffusion coefficients of oxygen.

2. The dependence of the position of the intensity maximum of the (114) reflection in K_{α} -Co on the oxygen content of titanium is not linear. The nature of this dependence could be established from the known, published data on the effect of oxygen on the parameters "a" and "c" of titanium lattice [8-12]. However, these data do not completely coincide, which complicates deriving from them the relation $\Delta 2\theta_{114} = f(c)$. At the same time, in the presence of low concentrations of oxygen that do not exceed its limiting solubility in the β phase, this dependence is linear, which makes it possible to operate in the calculations not with concentrations but with experimentally directly derivable values of $\Delta 2\theta_{114}$, thereby precluding the additional errors entailed in the use of insufficiently reliable calibration data.

3. The solubility of oxygen in titanium is quite high (up to 35 at. %). When analyzing the process of gas absorption it is usually assumed that the diffusion coefficient of oxygen throughout the range of the variation in oxygen content within the limits of the solid solution of α -Ti or β -Ti is independent of the oxygen concentration. The validity of this assumption is, generally speaking, not evident, but within the range of relatively diluted solid solutions of oxygen in β -Ti this assumption is justified, as was confirmed by the experimental findings of Claisse and Koenig [6].

4. Usually the mathematical description of diffusion processes is constructed by solving Fick's differential equation for corresponding boundary conditions. Given certain simplifying assumptions, this method may be also used to derive the relations for calculating the coefficients of the diffusion of oxygen in β -Ti [13]. Under real conditions of gas absorption, however, the conditions at the phase

interstitial impurities (particularly with nitrogen). Allowance should also be made for the possibility of the accumulation in the layer underneath the scale of certain impurities present in the technical titanium itself, during oxidation. All this complicates the interpretation of the results of layer analysis of sector I of the diffusion zone. By contrast, layer analysis of sector II yields extremely distinct reflections with a high degree of resolution of the doublet. In this sector the concentration gradient practically no longer affects the position of the intensity maximum. Since the displacement of reflections in sector II of the gas-saturated layer directly characterizes the diffusion of oxygen

interference are of a much more complex nature than is assumed in the idealized mathematical model. Thus the rate of delivery of oxygen to the metal surface. During exposure to elevated temperatures various processes develop in the oxide film and alter its properties (internal stresses lead to cracking, peeling, the film gets sintered, etc.). The nature of these processes is insufficiently well-investigated and hence a rigorous formulation of the boundary conditions at the oxide film-metal phase interface is difficult. The boundary conditions at the interface between the α and β phases also are not wholly clear. The magnitude of the concentration jump at this interface is usually determined by the width of the two-phase region on the phase diagram, although it is not unlikely that some degree of supersaturation is needed to shift the front of the $\beta \rightarrow \alpha$ transformation. As for the experimental determination of the conditions at the phase interface, this is complicated by the marked blurring of reflections, due to the sharp concentration drop. The use of boundary conditions as uniqueness conditions is a commonly accepted but not the sole possible path for the solution of the differential equation of diffusion.

We will consider the segments of diffusion curves which at gas-absorption temperature corresponds to the β phase during exposure to high temperatures over various time periods (Fig. 2).* We will draw a series of straight lines parallel to the abscissa and construct for various values of $(\Delta 2\theta_{114})$, the coordinate of the points of intersection of the straight line by the curves as a function of the exposure time. For all the investigated temperatures these dependences represent straight lines passing through the coordinate origin (Fig. 3). This demonstrates that the analyzed process for $x > x_0$ (Fig. 1) obeys the Boltzmann rule, according to which concentration may be regarded as the function of a single variable: $\lambda = x/\sqrt{\tau}$. Utilizing this circumstance as well as the aforementioned validity of the assumption $D_\beta(c) = \text{const}$, the formula for Fick's second law

$$\frac{\partial c}{\partial \tau} = \frac{\partial}{\partial x} \left(D_\beta \frac{\partial c}{\partial x} \right). \quad (1)$$

may be rewritten as

$$\frac{d^2 c}{d \lambda^2} + \frac{\lambda}{2D_\beta} \cdot \frac{dc}{d\lambda} = 0. \quad (2)$$

The order of Eq. (2) is reduced by the substitution of the new variable

/205

$$P = \frac{dc}{d\lambda}. \quad (3)$$

* The experimental points in Figs. 2, 3, 5, 7 are denoted by different symbols because different specimens were used in calculating diffusion coefficients by the statistical method.

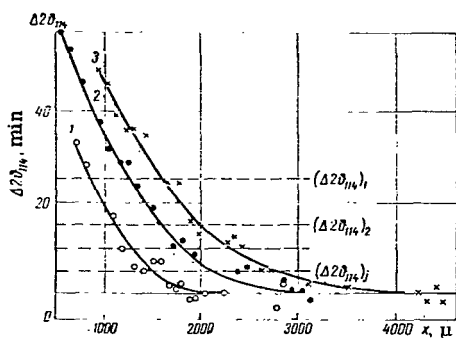


Figure 2. Structure of Section II of the Diffusion Zone.

Oxidation Regimes: $T = 100^{\circ}\text{C}$, $\tau = 1$ (1), 2 (2), 4 hr (3).

Then we have

$$\frac{dP}{d\lambda} + \frac{\lambda}{2D_\beta} P = 0. \quad (4)$$

This last equation is readily solved by the method of the separation of variables

$$P = A \exp(-\lambda^2/4D_\beta), \quad (5)$$

or, allowing for (3),

$$dc = A \exp(-\lambda^2/4D_\beta) d\lambda. \quad (6)$$

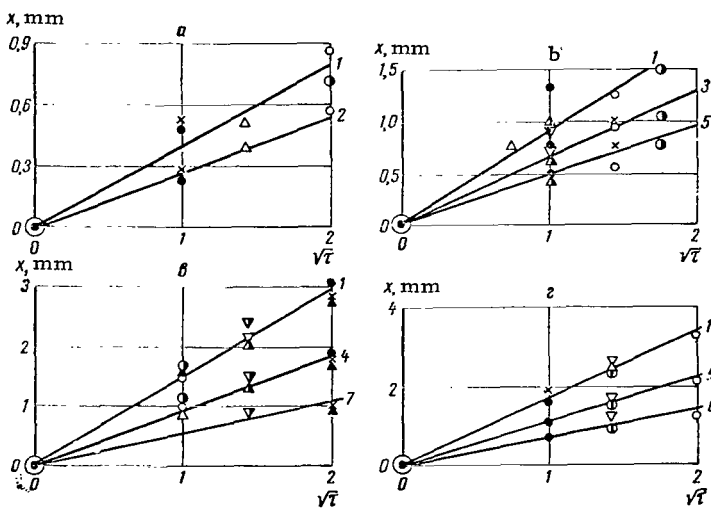


Figure 3. Isoconcentration Dependences for 950 (a), 1050 (b), 1100 (c) and 1150°C (d).

Lines 1-7 Correspond to Different Displacements of the Diffraction Maximum: 5' (1), 10' (2), 15' (3), 20' (4), 25' (5), 35' (6), 45' (7).

/ 206

Integrating relation (6) within corresponding limits, we have

$$c = A \operatorname{erfc} \left(\frac{x}{2} \sqrt{D_\beta \cdot \tau} \right) + B. \quad (7)$$

The values of the Kramp function

$$\operatorname{erfc}\left(\frac{x}{2} \sqrt{D_\beta \cdot \tau}\right) = 1 - \frac{2}{\sqrt{\pi}} \int_0^{x/2} \exp(-z^2) dz$$

have been tabulated and are given in a number of reference books.* Since the thickness of the specimen is known to exceed the thickness of the gas-absorption layer, the constant B in relation (7) equals the concentration c_0' of oxygen in the original sample. Therefore,

$$\Delta c = c - c_0' = A \operatorname{erfc}\left(\frac{x}{2} \sqrt{D_\beta \tau}\right), \quad (8)$$

or, after taking into account proportionality (within the investigated range of variation in Δc) of the concentration to the displaced position of the intensity maximum of the reflection (114), we ultimately have

$$\Delta 2v_{114} \propto (\Delta 2v_{114})^* \operatorname{erfc}\left(\frac{x}{2} \sqrt{D_\beta \tau}\right) \text{ for } x \geq x_0. \quad (9)$$

Relation (8) coincides in form with the conventional solution of the Fick equation for a semi-infinite isotropic medium with a constant concentration at the surface. The principal difference lies in that the constant A is a complex function of a number of parameters characterizing a given diffusion system and cannot be equated with the limiting solubility of oxygen in β -Ti at a given temperatures. The constants $(\Delta 2v_{114})^*$ and D_β can be determined from experimental data by various methods. In this work they were estimated as follows: Suppose that, for given temperature and duration of exposure there exists the experimental dependence $\Delta c = f(x)$ which in the presence of a certain value of the diffusion coefficient $D_\beta = D_1$ is described by relation (8). Then the dependence

$\Delta c = f\left[\operatorname{erfc}\left(\frac{x}{2 \sqrt{D_\beta \tau}}\right)\right]$ in the cartesian coordinate system will be represented by a

straight line passing through the coordinate origin (Fig. 4, b). If another value of D_β , such as $D_\beta = D_2 < D_1$, is ascribed to these experimental points, the dependence $\Delta c = f\left[\operatorname{erfc}\left(\frac{x}{2 \sqrt{D_2 \tau}}\right)\right]$ will no longer be rectilinear. The points will then

form a convex curve (Fig. 4, a) and if a straight line is drawn along these points, the points located in the neighborhood of the coordinate origin will lie above that line while for higher values of Δc the points will lie below the dot-and-dash line.

* See for example, Tables of Probable Functions, Vol. 1, USSR Acad. Sci., Press, 1958; Segal, B.I. and Semendyayev, K.A., Five-Digit Mathematical Tables, Fizmatgiz, 1962.

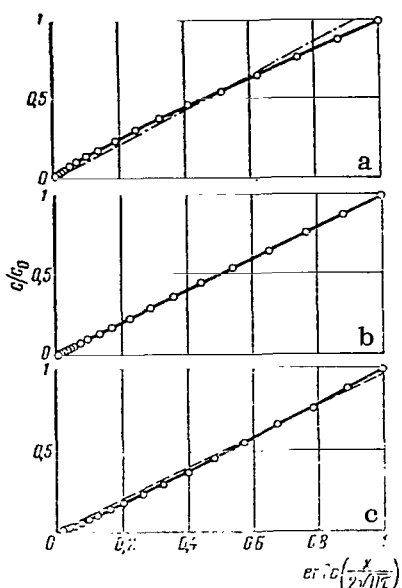


Figure 4. Concerning the Method of Calculating Diffusion Constants.

and $D_{\beta, \min}$ for which the tendencies illustrated in Fig. 4 (a and c) begin to manifest themselves markedly. The theoretical curves corresponding to Eq. (9) and to the thus established range of values of D_{β} satisfactorily describe the experimental data at all the temperatures investigated (see for example Fig. 5, b).

/207

Figure 6 shows the relation of diffusion coefficients to absolute temperature, for which was derived the equation

$$D_{\beta} = 0.63 \exp(-37000/RT) \text{ cm}^2/\text{sec.} \quad (10)$$

The error in determining the activation energy of the diffusion of oxygen in β -Ti does not exceed 20%. To assess the effect of the purity of original components on the parameters of oxygen diffusion, control experiments with iodide titanium and pure oxygen were carried out.

Polished specimens of iodide titanium, measuring 20x20x8 mm were, following their degreasing, subjected to recrystallization annealing in a vacuum of 10^{-5} - 10^{-6} mm Hg at 850°C for 30 min. During the annealing the weight of the specimens did not change by more than 0.0001 g. The microhardness of the annealed specimens was 90-100 kg/mm². The pure oxygen was obtained by decomposing potassium permanganate in vacuo. Chemically pure KMnO_4 was purified by means of recrystallization. Heating to 300 - 400°C was accomplished in a cylindrical furnace. To absorb CO_2 the oxygen was passed through granulated KOH,

If, on the other hand, $D_{\beta} = D_3 > D_1$, the picture will be reversed (Fig. 4, c). Thus the correctness of the selection of the value of the diffusion coefficient D_{β} can be determined from the shape of the experimental curve in the above-mentioned coordinate system.

When processing experimental data the results of layer analyses of all the specimens exposed to a given temperature over various periods of time were initially recorded on a common plot depending on the ratio $x/\sqrt{\tau}$ (Fig. 5, b). The tentative value of D_{β} was determined from two selected points and from Eq. (9). Further, on considering near D_{β}^* a number of the values of D_{β} differing not more than 15-20% from each other, the experimental data were framed in the coordinate system shown in Fig. 5, a. The shape of the resulting curves is fairly sensitive to the value of $(D_{\beta})_i$, and hence a small number of tests proved sufficient to determine that value of D_{β} for which the experimental points are optimally aligned with respect to the straight line, as well as to determine the limiting values $D_{\beta, \max}$

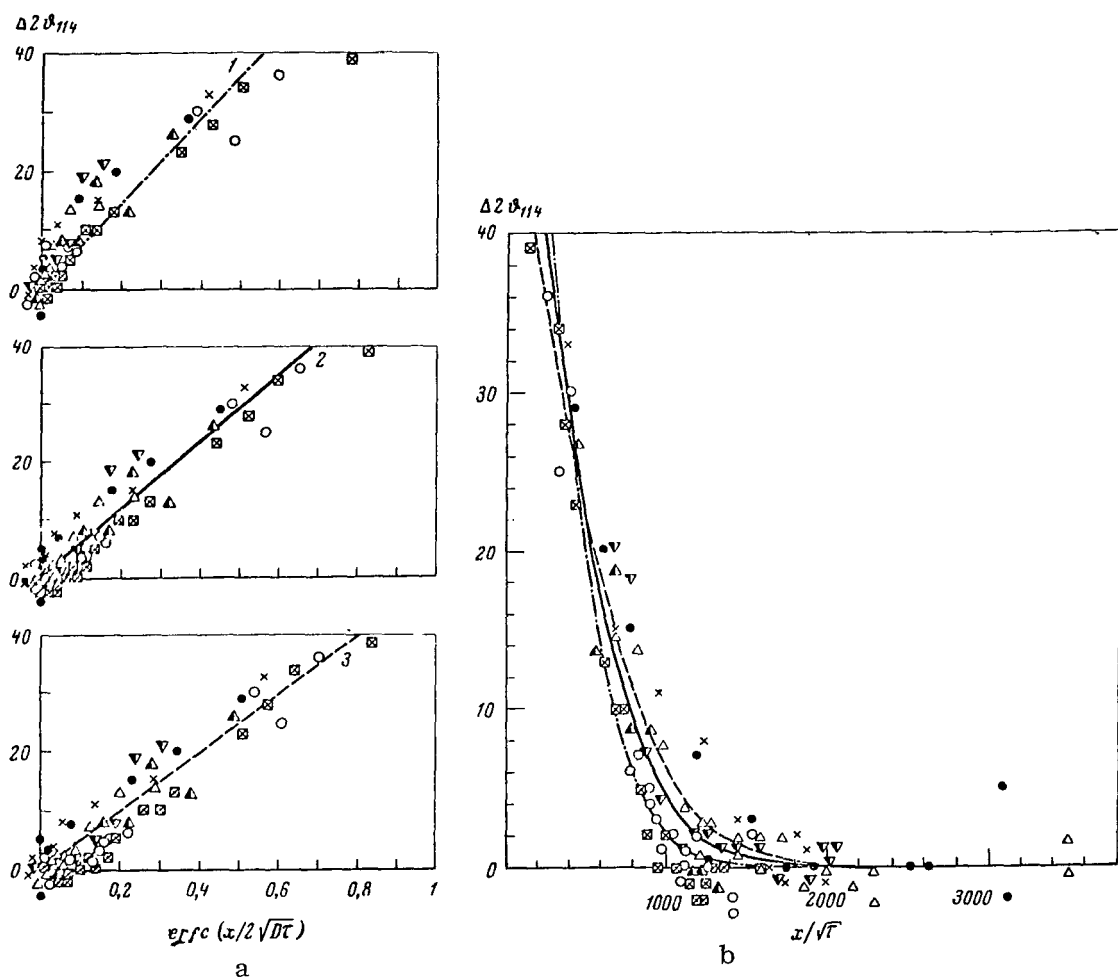


Figure 5. Results of Mathematical Processing of the Data of Layer Analysis of Specimens of the Alloy VT1-1 Oxidized at 1050°C in Air.

and to purify it of water vapors it was subjected to liquid-nitrogen treatment. The purified oxygen was collected in two 5-liter cylinders from which subsequently the needed portions of the gas were taken to fill the work tube. The pressure of oxygen was determined with the aid of a V-shaped mercury manometer. The mercury vapors were frozen out with the aid of liquid oxygen, while the oil vapors of the forevacuum and diffusion pumps were frozen out during evacuation with liquid nitrogen.

The specimens were annealed in a quartz tube with a useful space of 950 cm³. The specimen was suspended in the tube on a thin platinum wire, whereupon the tube was evacuated to a vacuum of 10⁻⁴ mm Hg, flushed several times with small portions of oxygen and filled with oxygen up to a pressure of 200 mm Hg.

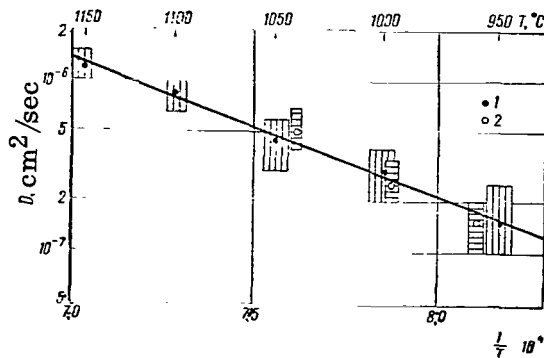


Figure 6. Temperature Dependence of Diffusion Coefficients.

Data for Technical Titanium (1) and Iodide Titanium (2). Hatched Regions Pertain to Measurement Error.

for 5-7 min, which should not introduce distortion into the results. /209

Diffusion annealing was carried out in an electrical resistance furnace. The temperature in the working zone was monitored by means of Pt/PtRh thermocouples and maintained with the aid of a special heat controller. The thermocouples were previously calibrated with respect to such reference temperatures as the melting points of pure silver (960.5°C) and pure copper (1085°C). In the oxidation process the temperature deviations from the desired level did not exceed $\pm 3^{\circ}\text{C}$.

The experiments were performed at 907 , 960 , 997 and 1030°C for 1-4 hr each time. The specimens were heated to the desired temperature

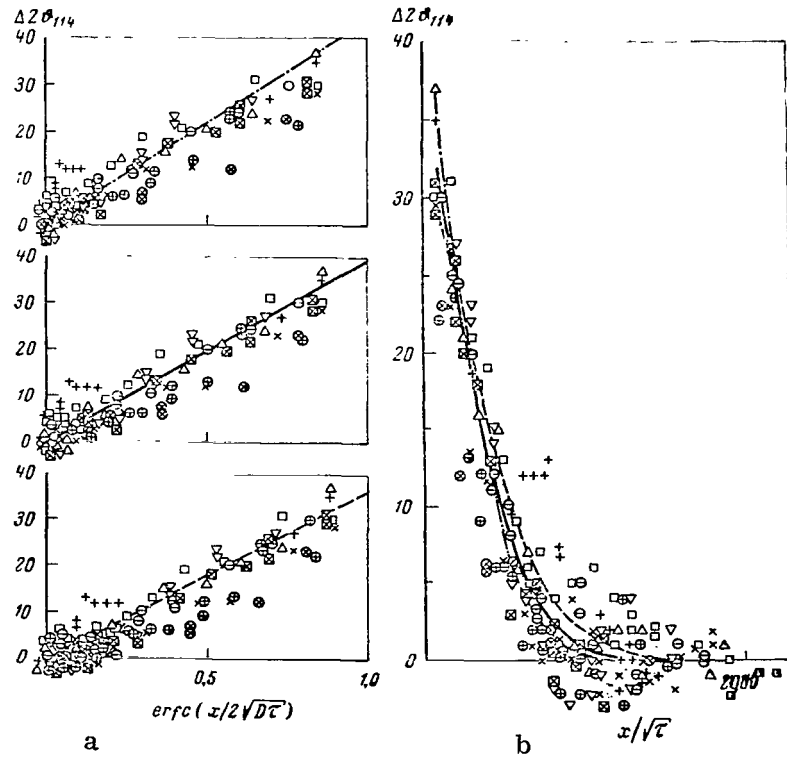


Figure 7. Results of the Processing of Data on Layer Analysis of Specimens of Iodide Titanium Oxidized in Oxygen at 997°C .

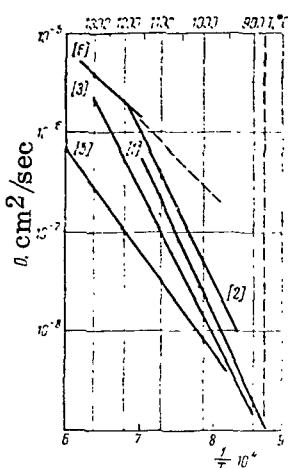


Figure 8. Temperature Dependence of the Diffusion Coefficient of Oxygen in β -Titanium According to the Published Literature (Solid Lines) and According to the Present Authors (Broken Line).

Of the data published in the earlier literature the data of Claisse and Koening [6] are in best agreement with the results obtained in this investigation (Fig. 8). The titanium used in [6] was considerably contaminated with copper, but the original technique of obtaining and analyzing layers that was employed by these investigators is apparently sufficiently reliable, which warrants greater credence in their findings than in the findings of later investigators [1-5].

The value of the activation energy of the diffusion of oxygen in β -Ti obtained in the present work ($Q_\beta = 37$ kcal/mole) is qualitatively in good agreement with the activation energy values of diffusion of the interstitial elements (N, O, C) in other bcc transition metals (Zr, Nb, Ta, V). For these systems the authors of [14-18] derived values of activation energy ranging from 25 to 40 kcal/mole. In the course of this investigation no data indicating any anomalous nature of the diffusion of oxygen in β -Ti were obtained.

REFERENCES

1. Reynolds, J., H. Ogden and R. Jaffe, TASM, XLIX, 280, 1957.
2. Roe, W., H. Palmer and W. Opie, TASM, No. 52, p. 191, 1960.
3. Elliot, R. Nucl. Sci. Abstr., Vol. 17, No. 20, p. 33859, 1963.
4. Parr I.—TASM, 198 (Discussion), 1960.
5. Wasilewski, R. and G. Keel, J. Inst. Met., Vol. 83, No. 3, p. 94, 1954.
6. Claisse, F. and H. Koening, Acta Met., Vol. 4, p. 650, 1956.

7. Mozhayev, S.S. and L.F. Sokiryanskiy. In the collection: *Podivizhnost' atomov v kristallicheskoy reshetke* [Mobility of Atoms in Crystal Lattice], Naukova Dumka Press, Kiev, 110, 1965.
8. Clark, H.T. *Trans. AIME*, Vol. 185, No. 588, 1949.
9. Rostoker, W. *J. Metals*, Vol. 4, No. 9, p. 981, 1952.
10. Bumps, E.S., H.D. Kessler and M. Hansen. *TASM*, Vol. 45, p. 1008, 1953.
11. Andersen, S. et al. *Acta Chem. Scand.*, Vol. 11, p. 1641, 1957.
12. Makarov, Ye.S. and L.M. Kuznetsov. *Zhurnal strukturnoy khimii* [Journal of Structural Chemistry], Vol. 1, No. 2, p. 170, 1960.
13. Mozhayev, S.S. and L.F. Sokiryanskiy. *Inzh. Fiz. Zhurnal*, Vol. 6, No. 9, p. 81.
14. Powers, R. and M. Doyle. *J. Appl. Phys.*, Vol. 30, p. 514, 1959.
15. Mallett, M. V.S. *Atomic Energy Commission Report BMI-1154*, 1957.
16. Mallett, M., J. Bella and B. Cleland. *J. Electrochem. Soc.*, Vol. 101, No. 1, 1954.
17. Pavlikov, L.V. and V.N. Bykov. *Fizika metallov i metallovedeniye* [Metal Physics and Metallography], Vol. 19, No. 3, p. 397, 1965.
18. Andriyevskiy, R.A., V.N. Zagryazkin and G.Ya. Meshcheryakov. *Fizika metallov i metallogedeniye* [Metal Physics and Metallography], Vol. 21, No. 1, p. 140, 1966.

PART III

/211

METALLURGY AND TECHNOLOGY OF TITANIUM AND ITS ALLOYS

MAGNESIUM REDUCTION OF TITANIUM FROM TETRACHLORIDE

N. P. Sazhin, S. V. Ogurtsov, K. N. Pavlova, V. L. Russo,
V. S. Mirochnikov, Yu. N. Ol'khov, B. S. Gulyanitskiy,
M. A. Losikova and V. D. Savin

The reduction of titanium from tetrachloride by magnesium is a complex and varied process. The sites of the deposition of the reaction mass, the pattern of formation and structure of the titanium sponge, and the question of whether the process will occur mostly in the gas phase or at the surface of the reaction mass due to the interaction between the chlorides and molten magnesium all practically depend on the design execution of the process and the technological regimes of its conduct. Improvements in existing processes of this kind and the development of new processes are inconceivable without studying the processes occurring in the reduction apparatus. Studies carried out in industrial reduction apparatus under conditions permitting the obtaining of commercial-purity metal are to be regarded as the most topical studies.

The present investigation, carried out by co-workers of the Giredmet (State Institute of the Design and Planning of the Rare Metals Industry), made it possible to relate the data of laboratory research to the results of research into reduction processes under industrial conditions, conducted with the aid of a number of new methods in the presence of a broad variation in the values of the principal technological parameters characterizing reduction processes.

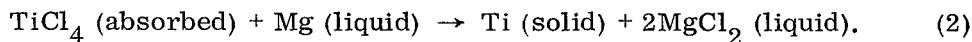
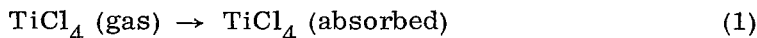
PURPOSES OF INVESTIGATION

The existing variety of views on the mechanism of reduction by magnesium appears to be due primarily to the complexity of the processes that may occur in the system $TiCl_4-TiCl_3-TiCl_2-MgCl_2-Mg$. The overall reaction for the production of titanium, $TiCl_4 + 2Mg = Ti + 2MgCl_2$, is almost completely displaced in the direction of the formation of the metal and the equilibrium pressure of the vapors of titanium tetrachloride with magnesium at the process temperatures is about 10^{-5} atm; thus in this complex system a large number of secondary processes is possible.

Among the first to interpret the mechanism of the magnesium-reduction process were Wartman, Baker, Nettle and Homme [1]. The developer of this process, W. J. Kroll [2] shares the opinions of these investigators, which basically reduce to the following. The process occurs between molten magnesium and the tetrachloride at the surface of the sponge growing on the walls of the apparatus above the original level of the reducing agent, which is in agreement with the data of [3]. Due to capillary action magnesium ascends in the porous sponge and covers its surface with a continuous film. The gas-phase reaction is thus precluded. This mechanism is confirmed by experiments with metal bars which do not come in contact with magnesium and do not become covered with the reaction mass, as well as by analysis of the distribution of reaction products according to the data on the distribution of impurities in the sponge.

These views on the process largely coincided with the conclusions of S. Ogurtsov and V. Reznichenko who had at approximately the same time been investigating the formation of titanium sponge at the Institute of Metallurgy, USSR Academy of Sciences [4-7].

Ogurtsov and Rezanichenko [4-7] investigated in greater detail the kinetic conditions of the process as well as the distribution of reaction products in the course of the process, relating it to the structure of the sponge and the effect of individual parameters. They arrived at the conclusion that the principal parameter of the process is the rate of admission of titanium tetrachloride, which conditions the rate of evolution of the process, the formation of the reaction mass, its structure, etc. Programming of the admission rate of $TiCl_4$ makes it possible to standardize the process [8]. It was shown that the process is of an auto-catalytic nature, as demonstrated by the decrease in the values of apparent activation energy from $\sim 25\ 000$ to ~ 8000 cal/mole and the increase in the process rate with increase in the admission rate of $TiCl_4$. Reduction occurs on active (not covered by magnesium chloride) sectors of the growing sponge which acts as a catalyst. The molecules of titanium tetrachloride pass through a stage of activated adsorption and then they may dissociate, whereas magnesium enters, as it were, into a multistage interaction with the lower chlorides [5]. Under certain conditions, however, the catalytic reaction occurs at once, as it were, in the absence of the theoretically possible stages. The principal process on the active sectors is



Magnesium enters into the reaction chiefly in liquid form. Its successive portions envelop the particles of titanium thus protecting them from secondary processes, cause conglomeration of the sponge and proceed to the shifting front of the reaction. The spongy structure of titanium is determined by heterogeneous catalysis. The authors believe that in the absence of excess magnesium secondary processes occur not only between titanium and the tetrachloride but also between titanium and magnesium chloride, with formation of titanium dichloride. Predominance of the reaction between the tetrachloride (at sufficiently high rates of its admission) and magnesium in the gas phase is admissible only at the very beginning of the process.

V. T. Musiyenko [9] in his discussion of the work of Wartman and associates [1] also does not attach any great importance to interaction in the gas phase and to the possibility of multistage reduction in industrial reduction apparatus.

Gillemot [10] believes that the reaction of the reduction of titanium tetrachloride by magnesium practically does not occur in the gas phase. But he admits the possibility of the development of side reactions toward the end of the process with interaction in the gas phase.

R. A. Sandler [11, 12] assumes that a large part of the sponge in the reduction apparatus may form due to multistage reduction of titanium tetrachloride by both liquid and gaseous magnesium, particularly during the second half of the process. Then the process may develop in the gas phase at the surface of the newly forming titanium as well as in the molten pool. One has to agree with E. Ye. Lukashenko et al [13] who arrived at the conclusion that the effects occurring in the reduction apparatus are highly complex and that the opinions of various investigators complement rather than conflict with each other.

The aim of this investigation was to study the kinetic features of the occurrence of the process under both laboratory conditions (it is worth noting that the literature lacks information on research into the use of solid magnesium with simultaneous admission of reagents) and industrial conditions on using new techniques such as the determination of the partial vapor pressures of the tetrachloride, the investigation of heat fluxes across the top of the reduction apparatus, collection of samples of the reaction mass from various zones of the apparatus and monitoring of the level of this mass in the course of the reduction process, investigation of the physical properties of the sponge and reaction mass, etc. The data thus obtained make it possible to determine more precisely the reduction mechanism and to successfully carry out research into improvements in the existing methods of the reduction of titanium tetrachloride by magnesium and development of new methods of this kind for the production of titanium.

/213

LABORATORY PART

Here the investigation dealt with the kinetic features of the reduction of titanium tetrachloride by solid (in the form of chips or return condensate) and molten magnesium with simultaneous admission of the reduction agent, as measured thermographically. The nature of this method consists in measurements of the heat flux generated by the thermal effect of the process, comparison of this flux with a standard heat flux, and photographic recording of the result of this comparison on a thermobarogram with the aid of Kurnakov's pyrometer. The reaction vessel was conditionally divided into two zones over its height, with each zone being equipped with its own heat flux meter, and hence analysis of thermobarograms yielded data on the rates of interaction between reagents, the magnitude of the thermal effect and the relative position of the reaction front over the height of the apparatus. At the same time pressure in the apparatus also was recorded. The experimental method and the analysis of thermobarograms are described in the work [14]. Values of apparent activation energy of the process were derived from the Arrhenius equation by the graphic method.

Data characterizing the process are presented in the table below.

Figure 1 (see also the table below) shows the relation of the values of apparent activation energy to the admission rate of $TiCl_4$ for normal pressures and identical fractions of magnesium when this reducing agent is supplied in solid and liquid forms.

Analysis of reaction products and experimental data (see table below) for processes occurring at $< 650^\circ C$ showed that the interaction is determined by

TABLE 1

Delivery of $TiCl_4$, g	Conditions of experiment			E_A , cal/mole	
	(Magnesium chips)	Fractions, mm	Load Weight, g	Residual pressure in apparatus, mm Hg	Below 650°C
0.5	—800+560	2.0	780	12 400	—
1.0	—800+560	2.0	780	7 280	18 700
2.0	—800+560	2.0	780	4 250	12 900
3.0	—800+560	2.0	780	2 920	7 550
2.0	—800+560	2.0	560	4 960	—
2.0	—800+560	2.0	1	8 600	—
2.0	—1250+800	2.0	780	3 100	—
2.0	—560+280	2.0	780	2 630	—
2.0	Return condensate	10.0	1	6 500	—

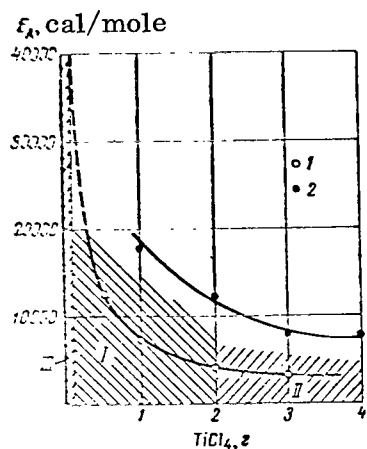


Figure 1. Variation in Values of Apparent Activation Energy With Increase in Admission Rate of Titanium Tetrachloride; Temperature $< 650^\circ\text{C}$ (1) and $> 760^\circ\text{C}$ (2).

exothermic nature of the interaction. The greater is the admission rate of $TiCl_4$, the more complete becomes the development of heterogeneous catalysis (Fig. 1, region II). When the admission rate of $TiCl_4$ is quite low, the process apparently may occur completely in the gas phase (Fig. 1, region III); in this case the values of the apparent activation energy begin to exceed the heats of evaporation and sublimation of magnesium. For 0.05-0.1 g portions (Fig. 1)

the conditions of experiment, occurs in the kinetic region at the surface of the reducing agent and is determined by the size of its fraction (unit surface area). Thus, when the fraction of the reducing agent is reduced from 1250-800 μ to 560-280 μ (resulting in a 15% increase in unit surface area), the interaction rate is increased by 15.3% (at 500°C) while at the same time the values of apparent activation energy decreases (see table above). As the admission rate of titanium tetrachloride is increased, interaction rate increases while activation energy decreases (see table above and Fig. 1).

/214

These findings are in good agreement with the data of the studies [4-6] which were carried out with molten magnesium; by analogy they may be attributed to the autocatalytic nature of the process, with the segregating titanium metal representing the catalyst. It appears that the process, which commences at the surface of the reducing agent and in the gas phase, may lead to the melting of magnesium due to the

these values rise to 45-50 kcal/mole. As the delivery rate is reduced from 2 to 0.05-0.1 g, along with heterogeneous catalysis there increasingly develops the interaction between the tetrachloride and vapor-like magnesium, as indicated by the rise in the values of apparent activation energy. This region (region I, Fig. 1) is considered a transition region.

The presence of the smaller fractions of magnesium and a low residual pressure in the apparatus cause the interaction between gaseous components to become appreciable even when the tetrachloride is supplied in portions of 2 g each (activation energy rises from 4250 to 8600 cal/mole).

When return condensate is used, the process slows down due to the presence of magnesium chloride in that condensate.

The determining role of heterogeneous catalysis is also indicated by the good agreement between the curves of the differential recording of the heat flux, the pressure variation and the accumulation of the reaction product — which represents the catalyst in this autocatalytic process. It appears that the reduction of titanium tetrachloride by solid magnesium is accompanied by some development of secondary processes.

The interaction between the tetrachloride and molten magnesium (table above, Fig. 1) also is in good agreement with that described in [4-6] and is characterized by a rise in process rate and a decline in the values of apparent activation energy with increase in the admission rate of titanium tetrachloride. In the course of the process the interaction rate increases while the activation energy somewhat decreases.

Specific values of apparent activation energy determined by this method (18,700-7550 cal/mole) correspond with the findings of [4-6] 25,000-8000 cal/mole).

At the beginning of the process (as in the works [4-6]) the reactions of interaction between the tetrachloride and magnesium vapors develop to some extent. This is confirmed by the data on some displacement of heat fluxes into the upper zone of the apparatus. When approximately 20% of the reducing agent is utilized, the gas reaction ceases to be of any practical importance. Increasing the admission rate of titanium tetrachloride reduces the role of gas reactions but it provides the conditions for the displacement of the reaction zone to the upper part of the apparatus due to the greater upward development of the lining (sponge). This last also corresponds satisfactorily with the data of [4-6].

/215

The laboratory investigations also dealt with the features of the interaction between titanium tetrachloride and magnesium during simultaneous admission of the original reagents to the reduction apparatus. The experiments were carried out in the presence of a fixed vapor pressure of the tetrachloride. In accordance with the conditions of experiment, magnesium was admitted to the reaction vessel at a specific fixed rate. The admission rates of titanium tetrachloride and magnesium were used to derive the degree of utilization of magnesium, which was taken as the apparent degree of its utilization. (The actual degree of utilization of magnesium was determined by chemical analysis of the reaction mass.)

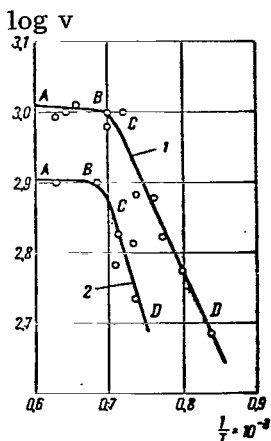


Figure 2. Inverse Logarithmic Temperature Dependence of Reaction Surfaces of Different Size.

(Reaction Surface in Case 1 is Larger than in Case 2).

temperatures ($1150-1300^{\circ}\text{C}$) are quite low, of the order $500-700^{\circ}\text{C}$ and the process rate is high, which is characteristic of heterogeneous processes occurring at the catalyst surface. It appears that in this region the process may be considered occurring in the diffusion region of heterogeneous catalysis, in which the surface of the catalyst is highly developed and the rate of chemical interaction is so high that the transport of reagents to the reaction zone becomes the limiting link in the process.

At the same time, further research into the features of the interaction between magnesium and titanium tetrachloride after taking into account the published data on the mechanism of the interaction between such metals as sodium, rubidium, cesium, magnesium and zinc, on the one hand, and the halogens and halogen salts [15-16] (particularly chlorine and its compounds), on the other, indicates that the process considered may be referred to the class of heterogeneous catalytic processes which pass through the state of electronic excitation. These processes are characterized by a low apparent activation energy (horizontal segment of the curve in Fig. 2). Such a mechanism is confirmed by the results of experiments formulated as observation of the processes accompanying the interaction between a drop of molten magnesium and the vapors of titanium tetrachloride, in which during the interaction was observed the formation of a glowing cloud, the diameter of which varied depending on the conditions of experiment as well as depending on the calculated amount of energy required to excite the magnesium atoms.

/216

Calculations show that the heat released during the reaction suffices for the formation of excited atoms of magnesium having the wavelength of 4600 \AA

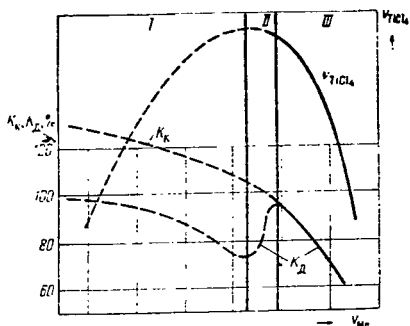


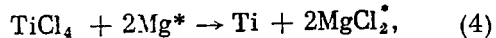
Figure 3. Relationship Between the Parameters Characterizing the Basic Laws Governing the Processes Occurring During Simultaneous Admission of Reagents to the Reduction Apparatus.

Since the process in question is heterogeneous, occurring in the presence of a catalyst, it can be represented in general form by Eqs. (1) and (2) which take into account activated adsorption.

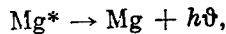
When allowance is made for the passage of interaction through the electronically excited state, the equations may be supplemented as follows:



and



where Mg^* corresponds to the excited state of magnesium. The additional transition



is possible, which coincides with the possibility of observing glow during interaction between titanium tetrachloride and magnesium in the experiments described above.

Depending on concrete conditions the interaction mechanism may differ and the process may exist in the kinetic or diffusion regions.

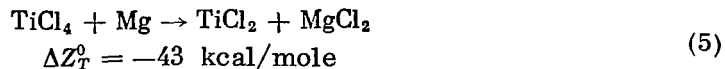
The autocatalytic nature of the process is additionally confirmed by the results of special experiments during which the active surface of the newly forming reaction product was withdrawn from the reaction zone. In this case the process rate sharply decreased and interaction practically ceased.

The principal interrelationship of process parameters (rate of admission of titanium tetrachloride, rate of admission of magnesium and the degree of utilization of magnesium) is illustrated in Fig. 3.

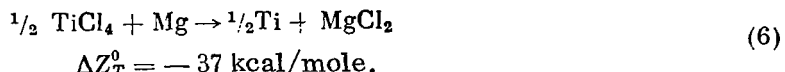
The mechanism of occurrence of the processes corresponding to the left-hand part of Fig. 3 (low admission rates of magnesium and $\alpha > 90\%$ apparent degree of its utilization) can, to a known approximation, be attributed to the occurrence of secondary reactions of the interaction between the newly forming titanium metal and TiCl_4 and MgCl_2 .

On this sector (Fig. 3, region I) the admission rate of TiCl_4 increases while the apparent and actual degrees of magnesium utilization decrease.

Thermodynamic analysis of the equations of the formation of titanium metal and lower chlorides (by way of an example, $TiCl_2$ is taken) shows that in the event of a magnesium shortage the thermodynamic probability of occurrence of the reaction

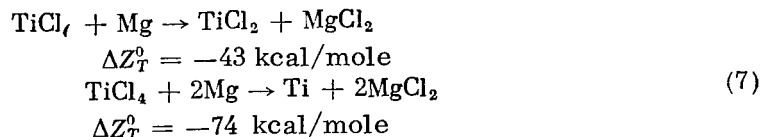


at $1050^{\circ}C$ is higher than for the fundamental process



When the apparent degree of magnesium utilization is 105-90% (region II, Fig. 3) the admission rate of titanium tetrachloride is practically unchanged but the amount of magnesium admitted continues to increase.

In this case thermodynamic analysis should be carried out with allowance for the actual excess of magnesium, and the following coefficients are introduced into the reactions



Then the negative significance of the isobaric-isothermal potential to the basic process expressed by Eq. (7) is much greater. It is precisely the predominant occurrence of the basic process that accounts for the rise of the actual degree of magnesium utilization in this region. However, the conditions for the formation of the lower chlorides of titanium (reaction (5)) still persist until the 90% apparent degree of magnesium utilization is reached.

When the degree of magnesium utilization is 90-70% (region III, Fig. 3) the interaction is characterized only by the fundamental reaction — the formation of titanium metal in the apparatus, and the apparent and actual degrees of magnesium utilization begin to coincide.

Thus, region III in Fig. 3 is the optimal region for the chemical reduction of $TiCl_4$ by magnesium during simultaneous admission of the original reagents; it is in this region that the conditions for the occurrence of the principal chemical reaction (reaction (7)) of the formation of titanium metal occur in the virtual absence of the lower chlorides of titanium.

STUDY OF REDUCTION PROCESSES IN INDUSTRIAL APPARATUS

This was the first study of its kind in which the technological parameters characterizing the occurrence of processes in industrial magnesium reduction apparatus were varied within very broad limits: pressure, from excess pressure (0.2-0.3 gauge atm) to residual pressures (100-200 mm Hg); $TiCl_4$ admission rates, from 60 to 700 kg/hr.

The newly developed techniques of technological monitoring made it possible during the processes of reduction to measure the partial pressure of titanium tetrachloride, to collect samples of the reaction mass, to record the heat transfer across the cover plate of the apparatus, to determine the formation sites of the reaction mass and to investigate the variation in the level of the reaction products in the apparatus.

/218

The partial pressure of titanium tetrachloride was determined in a specially designed setup with the aid of which the vapors of $TiCl_4$ and argon in the samples collected from underneath the cover plate of the reaction vessel could be separated by means of evacuation of air and freezing. The heat fluxes were measured with the aid of special pickups represented by brass plates with nichrome heaters. The nature of this method consisted in compensation of the temperature of the pickup and the unperturbed surface of heat transfer. Under industrial conditions these pickups were used in the form of thermal feelers making it possible to trace the mechanism of sponge formation and record the heat balance in the reaction vessel. Samples of the reaction mass for various coefficients of utilization of the reducing agent were collected with the aid of special devices which made it possible to obtain specimens for analysis of chemical composition and physical properties of the obtained sponge. Porosity was determined by the method of hydrostatic weighing and unit surface area, by the volumetric method of low-temperature adsorption (BET method) [17, 18].

Special experiments were carried out to pinpoint the sites of formation of the reaction mass. Cylindrical perforated cups were placed in the central zone of the reaction vessel, in which they were coaxially positioned on a false bottom so that their upper rim was located below the original level of the molten magnesium. The process was carried out with incomplete utilization of the reduction agent, and the lower part of the apparatus was filled with magnesium chloride. A special method was developed to measure the level of the reaction products: the variation in pressures underneath the lid of the apparatus as well as in a dome placed in the bottom part of the apparatus and filled with an inert gas was measured with the aid of a differential manometer, thus making it possible periodically or continuously to measure the level of the molten pool.

The partial pressures of titanium tetrachloride are extremely low (5-30 mm Hg) and the gas phase in the upper part of the apparatus consists of ~ 93-98% argon. Figure 4 shows the pressure region of $TiCl_4$ (hatched region) and the total pressure in the apparatus (upper section of diagram). It can be seen from this figure that for most of the time during the process the partial vapor pressure of $TiCl_4$ does not exceed 13-15 mm Hg. It rises only at the very beginning and at the end of the process, due to the attendant absence of reaction mass and shortage of reducing agent. The partial pressures of $TiCl_4$ are independent of

its admission rate and, as Fig. 5 shows, they average 8-10 mm Hg. The same level of pressures persisted in the processes accompanying the admission of $TiCl_4$ at various rates in the presence of a residual pressure of argon amounting to 100-150 mm Hg. These data are in good agreement with the theory that the process is self-accelerating and self-adjustable and that the increase in the admission rate of $TiCl_4$ is accompanied by such an increase in interaction rate that $TiCl_4$ does not have the time to evaporate and raise the pressure in the apparatus. The constancy of partial pressure of $TiCl_4$ in the apparatus makes it possible, in studies of the magnesium reduction process, to assume that the admission rate of the liquid to the apparatus equals the rate of the reduction process. This last is particularly important in research into the kinetic features of the occurrence of processes of this kind in industrial apparatus.

/219

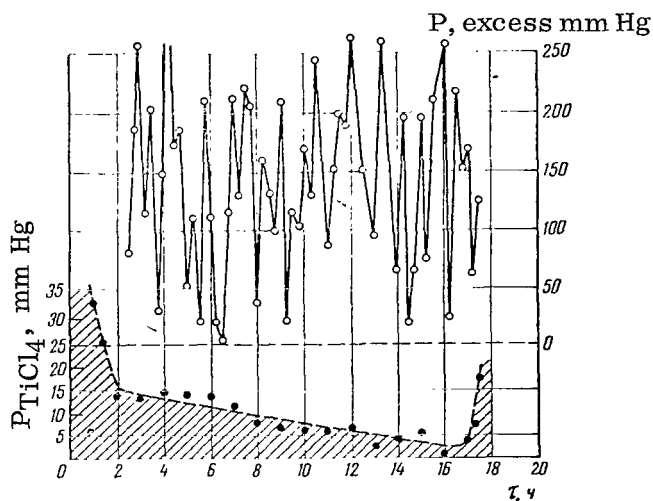


Figure 4. Pattern of Variation of Pressure in the Apparatus and of the Partial Pressure of Titanium Tetrachloride During the Reduction Process with a Fixed Admission Rate of the Liquid.

The investigation of sponge-formation in experiments with perforated cylinders established that the sponge begins to form by lining the walls of the apparatus. In the course of the process part of the sponge continually separates from the walls of the apparatus and falls onto the bottom of the reaction vessel. The perforated cylinders installed in the central zone of the apparatus remain empty during the first half of the process, which points to the absence of reaction at the surface of the reducing agent and in the gas volume occupying the central zone of the apparatus. This pertains to processes carried out under excess pressure and at a residual pressure of 100-150 mm Hg, in which the formation of the reaction mass was in both cases of similar nature.

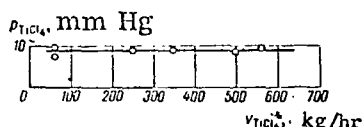


Figure 5. Relation of the Vapor Pressure of Titanium Tetrachloride to Its Admission Rate (Averaged Values of Pressure).

increased to 30-40%. Chemical analysis of the samples shows that during the initial period of the process the sponge lining the walls of the reaction vessel is enriched with magnesium which levitates to the reaction zone. If the proportion of magnesium utilized is 40%, the concentration of magnesium chloride in the sponge substantially increases.

Measurements with the aid of a level gauge showed that during the initial period of the processes the fluctuation in levels is insignificant and due only to the descent of magnesium chloride and accumulation of reaction products. Later on, however, as the reaction mass further accumulates while the amount of the descending magnesium chloride remains the same, the level of the molten pool sharply falls. While during the first half of the process only a minor part of the sponge lining the walls of the reaction vessel protruded above the melt, roughly half-way through the process the surface of the block of newly grown sponge occupying the central zone of the apparatus begins to appear during the descent of magnesium chloride. Subsequently active sectors of the reaction surface may be present both on the sponge lining the walls of the reaction vessel and on the surface of the growing block of sponge-like titanium masses. The amount of sponge protruding above the level of the molten pool could be estimated with the aid of the level gauge. At the beginning of the process the volume of the protruding reaction mass was 20-50 liters, while in the second half of the process it grew to as much as 200-600 liters. These figures are in good agreement with the mechanism of the process as presented above, with the increase in interaction rate in the course of the process and with the decrease in the values of apparent activation energy.

/220

The study of the porosity and unit surface area of the reaction mass and sponge following vacuum separation revealed that they generally tend to increase with increase in the admission rate of titanium tetrachloride to the reduction apparatus (this pertains to processes carried out both under excess pressure and at a residual pressure of 100-500 mm Hg). Figure 6 presents the findings on porosity of the sponge and reaction mass in relation to various admission rates of the liquid. The hatched region characterizes the data on the reaction mass subjected to hydrometallurgical treatment. The porosity of the reaction mass is higher than the porosity of the sponge following vacuum separation, and it ranges from 74 to 91%. The data on the separated sponge are of a somewhat conditional nature, since the time of exposure of high temperatures was not rigorously maintained. But in this case, too, there can be observed a general tendency to increase in porosity with increase in the admission rate of $TiCl_4$.

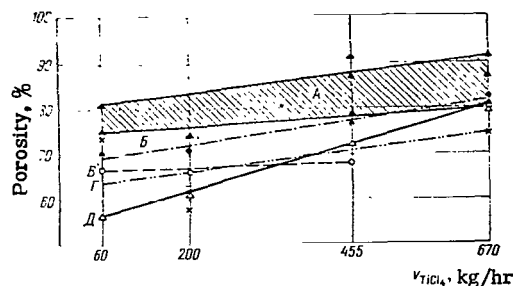


Figure 6. Total Porosity of Sponge and Reaction Mass in Relation to Admission Rate of Liquid:

A—Reaction Mass; B—Uppermost Section of the Sponge Lining the Walls (Lining Sponge); C—Collapsed Lining Sponge; D—Lower Section of Lining Sponge; E—Molten Pool.

from 52-67 to 92-126 kg/hr resulted in increasing the unit surface area of the newly forming sponge from 1-1.18 to 1.16-2.5 m²/g.

Measurements of heat fluxes across the cover plate of the apparatus showed that the process is of a focal nature. Zones (foci) of higher temperature were detected on the cover plate, and in the course of the process they shifted over its surface. During the initial period of the process these foci were detected only at the edges of the cover plate, corresponding to the sponge formation around the walls of the reaction vessel. Half-way during and toward the end of the process these foci shifted toward the central region. These findings are in good agreement with the postulate that the process occurs only in the active sectors of the reaction surface.

The focal nature of the process was also confirmed by visual observations as well as by photography of the exposed reaction surface in a laboratory apparatus enclosed within a large argon chamber. The observed active sectors may be characterized as composing a field of point sources of radiation.

The measurement of heat fluxes also made it possible to plot the dependence shown in Fig. 7, relating heat release to the admission rate of TiCl₄. Lines 1-7, which represent isotherms constructed on the basis of thermodynamic data, characterize the heat release of the process carried out at various temperatures. Line 1 was plotted for the case of the maximum possible temperature of the adiabatic process, 1414°C. The curve a-a is plotted on the basis of an investigation of actual heat loss in the reaction space of the apparatus during variation from 150 to 570 kg/hr in the admission rate of titanium tetrachloride.

/221

The points of the intersection of the isotherms by the curve a-a refer to the mean heat-balance temperature and can be taken as the temperature of the reaction surface. Above it was shown that the admission rate of titanium

tetrachloride represents the rate of the process itself, and from Fig. 7 the value of the corresponding temperatures can be found; therefore, the value of the apparent activation energy was derived by the graphic method in accordance with Arrhenius law, and was found to be approximately 8000 cal/mole. Such an energy value characterizes processes occurring at an already formed reaction surface, and therefore it is in good agreement with the data presented above as well as with the results of [4-6] where for a 20% utilization of reducing agent the apparent activation energy was found to be ~ 8400 cal/mole.

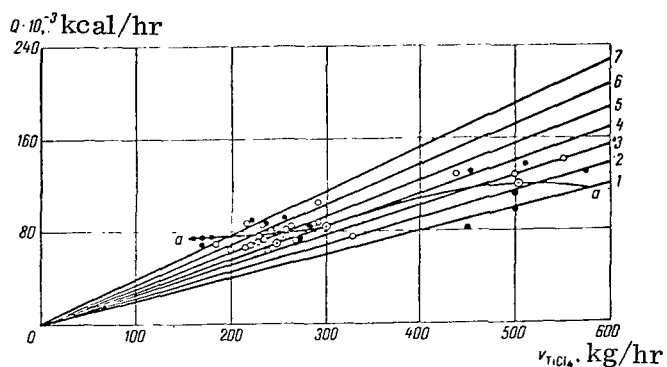


Figure 7. Analysis of Mean Heat-Balance Temperatures in the Processes of the Magnesium Reduction of Titanium Tetrachloride:

Isotherms: 1414 (1), 1300 (2), 1200 (3), 1100 (4),
 1000 (5), 900 (6), 800°C (7).

DISCUSSION OF FINDINGS

The kinetic features of reduction processes at $< 650^\circ\text{C}$ as well as of the process carried out with simultaneous admission of reagents at $800\text{--}1300^\circ\text{C}$ were investigated for the first time. The obtained data made it possible to confirm and markedly complement the views on the mechanism of magnesium-reduction.

In particular, the possibility of the transition of the heterogeneous catalytic process of reduction through the electronic excited states was demonstrated. The results of the investigation are in satisfactory agreement with the data of works carried out earlier [4-6].

A study performed under industrial conditions made it possible to elucidate the mechanism of sponge-formation in industrial apparatus, to determine the reaction surface temperatures, to establish a relationship between physical characteristics of the sponge and the admission rate of titanium tetrachloride, and to clarify the mechanism of the magnesium reduction of titanium from titanium tetrachloride in industrial reaction vessels. The pertinent data, obtained by various techniques, are in good mutual agreement and correspond satisfactorily with the results of earlier studies [1-9]. The increase in the surface area of contact between the reaction mass and the gas space in the apparatus toward the

end of the process, as indicated by level gauges, confirms the possibility of the development of secondary reactions toward the end of the process — reactions to which considerable importance is attached in the works [10-12].

This comprehensive investigation confirmed the validity and applicability of the working hypotheses based on the autocatalytic nature of the process, which make it possible to perfect under semi-industrial and industrial conditions the methods and apparatus used in the existing processes as well as to work to develop new methods of titanium production.

REFERENCES

1. Wartman et al. J. Electroch. Soc., Vol. 101, No. 10, p. 507, 1954.
2. Kroll, W.J. Metall, Vol. 9, 9/10 p. 366, 1955.
3. Winter, Ch. H. Patent USA, P2, No. 134, p. 586, 1952.
4. Ogurtsov, S. V. Izvestiya AN SSSR: Metallurgiya i toplivo [Metallurgy and Fuel], Vol. 4, No. 39, 1960.
5. Ogurtsov, S. V and V. A. Reznichenko. In the collection: Titan i yego splavy [Titanium and Its Alloys], No. 4, USSR Acad. Sci. Press, No. 122, 1960.
6. Reznichenko, V. A. and S. V. Ogurtsov. In the collection: Titan i yego splavy [Titanium and Its Alloys], No. 2, USSR Acad. Sci. Press, No. 82, 1959.
7. Bardin, I. P. and V. A. Reznichenko. In the collection: Metallurgiya SSSR, 1917-1957 [Metallurgy in the USSR, 1917-1957], Metallurgizdat, No. 611, 1958.
8. Ogurtsov, S. V., V. A. Reznichenko and A. I. Dedkov. In the collection: Titan i yego splavy [Titanium and Its Alloys], No. 8, USSR Acad. Sci. Press, No. 145, 1962.
9. Musiyenko, V. T. Metallurgiya titana [Metallurgy of Titanium], TsIIN ChM, 1958.
10. Gillemot, L. Acta Techn. Acad. Scient. Ind., Vol. 10, No. 1-2, 1955.
11. Sandler, R. A. Zhurnal prikladnoy khimii [Journal of Applied Chemistry], Vol. 33, No. 5, p. 1013, 1960.
12. Sandler, R. A. Zhurnal prikladnoy fiziki [Journal of Applied Physics], Vol. 33, No. 7, p. 1465, 1960.
13. Lukashenko, E. Ye. et al. In the collection: Titan i yego splavy [Titanium and Its Alloys], No. 6, USSR Acad. Sci. Press 14, 1961.
14. Savin, V. D. and V. A. Reznichenko. Zavodskaya laboratoriya [Plant Laboratory], No. 1, p. 63, 1964.
15. Glasstone, S., K. J. Laidler and H. Eyring. Teoriya absolyutnykh skorostey reaktsiy [Theory of Rate Processes], Translated from English, Foreign Lit. Press, 1948.
16. Kondrat'yev, V. N. Elementarnyye khimicheskiye protsessy [Elementary Chemical Processes], ONTI, Khimteoret., Leningrad, 1936.
17. Germain, J. E. Geterogenny kataliz [Catalyse Hétérogène]. Translated from French, Foreign Lit. Press, 1948.
18. Brunauer, S. Adsorbsiya gazov i parov [The Adsorption of Gases and Vapors]. Translated from English, Foreign Lit. Press, 1948.

SODIUM REDUCTION OF TITANIUM FROM TETRACHLORIDE

S. V. Ogurtsov, V. D. Savin, A. Ye. Nikitin, O. V. Perfil'yev

The magnesium and sodium methods for reducing titanium from titanium tetrachloride continue to remain the industrial methods for the production of titanium metal. The sodium method is completely competitive with the magnesium method, and abroad both these methods are widely employed industrially. Single-stage reduction with sodium makes it possible to obtain titanium of commercial purity. In the USSR semi-industrial studies of this process have achieved positive results [4].

The selection of the method of producing commercial metal on an industrial scale is contingent on market conditions.

A distinguishing feature of sodium reduction is the multiplicity of its some [1-9]. Depending on the conditions under which the process is carried out the reduction reaction may predominant either in the gas phase (production of disperse (finely divided) titanium) or at the surface of reaction products (formation of titanium sponge). Moreover, the process may occur in the molten pool between sodium and the lower chlorides of titanium dissolved in sodium chloride. The latter allows artificial division of the process into two stages.

/223

The two-stage method of conducting the reduction process, with the interaction between metallic sodium and the lower chlorides of titanium occurring under diffusion conditions during the second stage, makes it possible to obtain the greatest part of titanium metal in the form of large crystals which are not inferior in their properties to the properties of the titanium purified by the iodide process [5-7]. Unlike the single-stage method, however, the two-stage method cannot be considered competitive with the magnesium reduction method; it should rather be regarded as a method for obtaining high-purity metal in industrial apparatus. In other words, it may be considered a purification process. This process is difficult to conduct due to the complexity and relatively uninvestigated nature of the salt systems ($TiCl_2 - TiCl_3 - NaCl$) used for final reduction during the second stage as well as to the complexity of continuing this process in the diffusion region, the occurrence of reactions, side reaction of interaction between the lower chlorides of titanium and sodium chloride, etc. [5-14].

At present two distinct trends have arisen in research into this process as regards the composition of the chlorides used during the second stage: the use of a fused bath of titanium dichloride in sodium chloride containing various amounts of titanium trichloride [4, 5, 9] and the use of fused baths of complex compounds of the lower chlorides of titanium with sodium chloride [7].

A characteristic feature of the first orientation is the inconstant composition of the fused chloride baths employed and the general tendency to enrich the chloride bath with titanium dichloride at the expense of titanium trichloride. Thus a fused chloride bath used by American investigators [5], which they termed a "working mixture," contained 17-19% soluble titanium in the the form of subchlorides with predominance of titanium dichloride. The "mean effective valence," determined as the $TiCl_2:TiCl_3$ ratio, ranged from 2.5 to 2.2. The bath contained a small

amount of titanium metal. The ratio of soluble titanium to titanium metal and the "mean effective valence" were determined by the attainable degree of equilibrium of the following reaction



Socci [6] used a fused bath of titanium dichloride in sodium chloride, but he failed to specify the true composition of the bath.

Aleksandrovskiy and Gus'kov [9] placed emphasis on enriching the fused chloride bath with titanium dichloride when obtaining this bath during the first bath. The reagents were added in a stoichiometric mutual ratio in accordance with the reaction



The theoretical content of titanium chloride according to this reaction is 50.4%. The composition of the resulting reaction products markedly deviated from that calculated. In addition to TiCl_2 , whose concentration fluctuated within the limits of 13-50%, they contained a large amount of TiCl_3 (as much as 50%). The bath was heterogeneous over its height: its upper zone was richer in TiCl_3 and its lower zone, in TiCl_2 . In addition to the liquid reaction products, a block of titanium sponge also segregated in the bath; the titanium content of this block was 5-8% of the total amount of the metal. Finely divided (fine-disperse) titanium, the concentration of which in the lower zone of the bath was 1.3-1.8%, also segregated in the bath.

A positive aspect of the organization of the first stage is that baths of this composition greatly simplify the conduct of the first stage over a broad range of temperatures, from 600 to 900°C.

/224

The disadvantages of the two-stage process in which chlorides of this composition are employed lie in the following: considerable irretrievable losses of metal during the first stage (7-10% of total titanium); marked losses of metal during the second stage in the form of the finely divided titanium which segregates in the second-stage reaction vessel following the pressure-transfer of the fused bath (reaction (1)), since a bath of this composition, which during its pressure-transfer and filtration is deprived of the metal, becomes a non-equilibrium bath [10, 11]. Other disadvantages include: superposition of the disproportionation reaction and side reactions of the interaction between the lower chlorides of titanium and sodium chloride onto the final reduction reactions during the second stage of the process [8]; inhomogeneity of the chloride bath composition and the varying degree of development of the disproportionation and side reactions, which complicate the selection of technological regimes for the second stage and prevent obtaining stable results [5], etc. All this makes doubtful the possibility of organizing the two-stage process by using chlorides of varying composition.

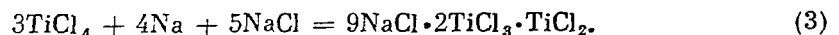
The two-stage sodium reduction method being developed by the present writers is to a large extent free of the above-mentioned shortcomings. Its principal distinguishing feature is that a congruently melting chemical compound is used as the intermediate product. Until the discovery of this compound only two incongruently melting compounds (NaTiCl_3 and Na_3TiCl_6), as well as two eutectic compositions [12, 13, 15, 16] were known in the system $\text{TiCl}_2\text{-TiCl}_3\text{-NaCl}$. No chemical systems were detected in this ternary system by the authors of [17] because, unfortunately, they confined themselves to plotting the liquidus curves.

The compound which we discovered corresponds to the approximate formula $9\text{NaCl}\cdot 2\text{TiCl}_3\cdot \text{TiCl}_2$. It was termed 'black salt' [7] and made it possible to begin to develop the method described here. The apparatus and technological regimes were developed by the Giredmet State Institute for the Design and Planning of the Rare Metals Industry.

The 'black salt' is stable in fused baths of sodium chloride, and disproportionation reactions do not occur in it [7, 8]; its melting point is 503°C , it crystallizes in one of the lower sygonies, its refractive index is $1.66\text{-}1.68$ and it displays distinct pleochroism. The most probable form in which it exists in fused baths of sodium chloride is the complex ion $[\text{Ti}_3\text{Cl}_{17}]^{9-}$.

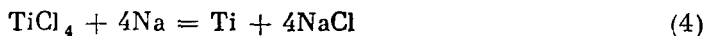
Composition of the 'black salt': 32.4 wt. % TiCl_3 , 12.5 wt. % TiCl_2 ; 55.1 wt. % NaCl .

The combined formula for the process of 'black salt' formation is the reaction

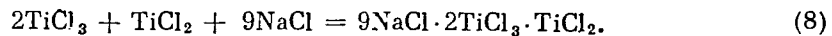


Synthesis of this compound requires prior charging of sodium chloride into the first-stage apparatus. For a long time the difference in pressures in the reaction vessel was a technological shortcoming in the synthesis of this compound. To clarify the cause of this effect, the kinetic features of individual stages of the process were investigated in laboratory conditions and a thermodynamic estimate of the occurrence probability of individual reactions were carried out on the basis of the data of [14].

It was established that synthesis of the 'black salt' requires the successive occurrence of the following principal reactions:



/225



Investigation of the processes occurring in first-stage apparatus provided a rough idea of the mechanism of their occurrence.

Reactions (4)–(6) develop only at the surface of the fused bath. The titanium metal forming in accordance with reaction (4) due to local excess of reduction agent and failure to interact with titanium tetrachloride in accordance with reaction (5) descends, due to its greater heaviness, in the fused chloride bath in which it interacts with titanium tetrachloride in accordance with reaction (7). Reaction (8) occurs within the volume of the fused bath. Thus a prerequisite for the development of the process is the predominant formation of titanium trichloride (reaction (6)) at the surface of the fused bath, its diffusion into the interior of the fused bath, its interaction there, resulting in the formation of "black salt," (reaction (8)) and its interaction with titanium metal (reaction (7)), as well as the diffusion of the resulting titanium dichloride toward the surface of the bath. The diffusion of reagents increases with temperature and is facilitated by the agitation of the bath due to the addition of reagents to the bath surface and the occurrence of the interaction reaction at the surface. The rate of reaction (7) increases with temperature increase. The limiting link in the process is reaction (6), since the thermodynamic probability of this reaction decreases with temperature increase, and at 730°C $\Delta F = 0$.

The study of kinetic features and the thermodynamic analysis made it possible to establish the optimal temperature regime (600 – 720°C).

Observance of this optimal temperature regime assured the synthesis of fused baths of "black salt" in laboratory conditions with simultaneous charging of reducing agent into the reaction vessel without development of appreciable pressures, while under semi-industrial conditions, during simultaneous admission of reagents, it made it possible to eliminate pressure from among the factors restricting the process.

A diagram of variation in technological parameters of the process of "black salt" synthesis in a semi-industrial reaction vessel is presented in Fig. 1. The temperature was measured with the aid of a five-junction thermocouple installed in the reaction vessel, with recording by means of an EPP-09 electronic potentiometer. Pressure was measured by means of an MV-100 vacuum pressure gauge. The admission rate of titanium tetrachloride was measured by means of an RS-5 rotameter and subsequently by means of an RD pickup with recording on an EPID-05 potentiometer, while the sodium level was measured by means of a float-type level gauge. The reagents began to be admitted at 600 – 650°C at the rate of 40–60 kg of TiCl_4 per hour, for a TiCl_4 :Na ratio of 6.0–6.1. At the beginning of the admission of reagents the pressure in the reaction vessel rose to 0.4–0.5 gauge atm but subsequently dropped to zero and then stayed within the limits of 0.2–0.3 gauge atm, slowly rising with increase in the occupation of the space of the

reaction vessel by the reaction products. The $TiCl_4:Na$ ratio was maintained within the limits of 6.0–6.1 throughout the process, with isolated deviations in readings (± 1 over 15 min). The temperature of the molten pool of reaction products throughout the process persisted at 600–670°C. The admission rate of titanium tetrachloride (and commensurately of sodium) continually increased and, following the formation of the fused bath, reached 200–250 kg/hr. Its further increase was in no way limited. The composition of the "black salt" synthesized is sufficiently homogeneous over its depth. The difference between Ti^{3+} concentrations in the upper and lower zones of the molten pool is less than 1.5%. In practice, its composition remains within the limits of: 31.5–33.5% $TiCl_3$, 11.5–13.5% $TiCl_2$, 54.0–56.0% NaCl.

/226

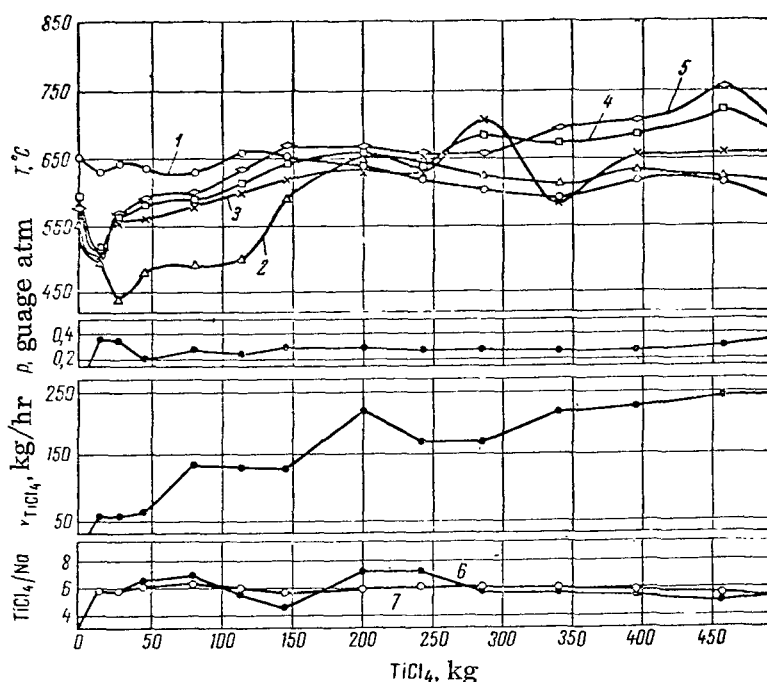


Figure 1. Diagram of Variation in Technological Parameters of the Process of "Black Salt" Synthesis Over 15 Min (6) and Since the Start of the Process (7):

1–5—Points of Five-Junction Thermocouple Vertically Spaced 300 mm Apart.

After the technology of production of homogeneous fused baths of the chlorides during the first stage of the process was worked out, the conditions for determining the technological regimes for the conduct of second stage of the process were created with the object of assuring a stable yield of crystalline titanium. The investigation established that in order to assure transition of the process to the diffusion region, in which titanium segregates in the form of large crystals, at the beginning of the process the surface of the fused bath of chlorides must be uniformly

coated with a layer of titanium sponge termed the "filter bed." The "filter bed" should maximally, completely and uniformly cover the surface of the fused bath of chlorides and its mechanical strength should be sufficient to assure continuity of its location throughout the process and its sufficient permeability with respect to sodium, which is chiefly determined by its structure. Conventional application of liquid sodium to the surface of the fused bath of chlorides, carried out at various rates and over a broad temperature range cannot produce a "filter bed" satisfying these conditions, as then it segregates in the form of compact titanium sponge incompletely covering the cross section of the reaction vessel, so that diffusion conditions of the process set in not initially but much later. Moreover, the dense sectors of the "filter bed" then prevent the migration of sodium to the reaction zone, thus resulting in instability of the processes and considerable scatter of results, with the yield of crystalline titanium ranging from 5 to 45%. The development of special technological regimes for producing the "filter bed" satisfying all the requirements enumerated above made it possible under laboratory conditions during admission of sodium to the surface of the fused bath to obtain a stable yield of crystalline titanium within the limits of 56-62%.

Figure 2 illustrates the contents of the reaction vessel (vertical cross section) with reaction products following the leaching of sodium chloride with weak solutions of hydrochloric acid.

The yield of crystalline titanium markedly depends on the temperature of the principal part of the process; the optimal temperatures are 860-870°C; lowering the temperature to 840-850°C or raising it slowly during variation in the admission rate of sodium (liquid instead of vapor) sharply reduces (to 20-35%) the crystalline titanium yield, while raising the temperatures to 880-890°C somewhat augments the yield of large crystals but reduces the total crystalline titanium yield to 40-42%.

/227

The yield of crystalline titanium depends on the concentration of dissolved titanium in the fused bath. Figure 3 illustrates the relation of this yield to the dilution of "black salt" by sodium chloride.

The total yield of crystalline titanium increases with increase in the dilution of "black salt" with sodium chloride until it reaches its maximum when the dilution is 40%, beyond which it sharply decreases. The same pattern is displayed by the yield of crystals measuring 10 to 20 mm in size. The yield of crystals of the >20 mm fraction (when the depth of the fused bath is 110 mm) increases insignificantly with increase in the above-mentioned dilution, reaching its maximum in the presence of 30% dilution, beyond which it decreases. A negative aspect of the dilution is the decrease in the productivity per cycle of the reduction apparatus (with respect to titanium), which is proportional to the dissolved titanium concentration. However, with "black salt" dilution the yield of crystalline titanium increases at a faster rate than the decrease in the titanium productivity cycle of the apparatus, and hence the cycle productivity of the apparatus with respect to the crystals also increases with increase in dilution and reaches its maximum in the presence of 35-40% dilution. Thus the optimal degree of dilution of "black salt" is 40%, as it maximizes both the crystalline titanium yield and the cycle productivity of the apparatus with respect to the crystals.

/228

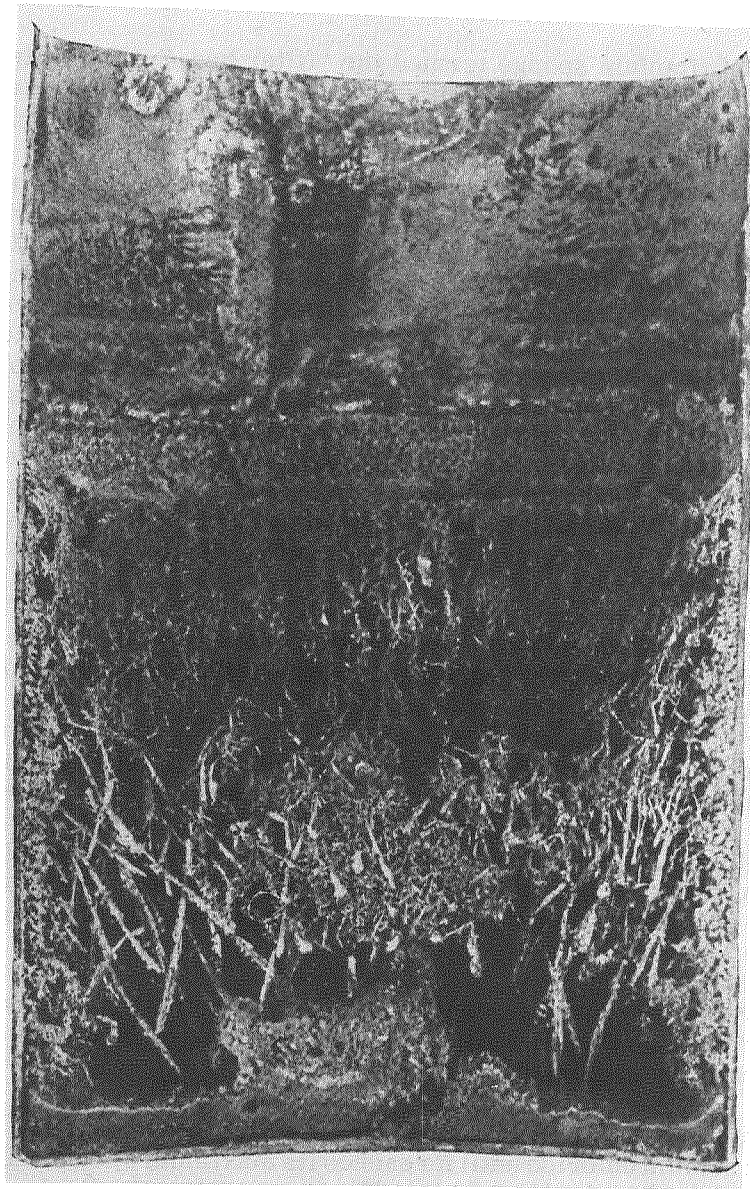


Figure 2. Reaction Products Following Leaching of Sodium Chloride With Water (Vertical Cross Section).

It may be assumed that the positive role of dilution (lowering of the concentration of valent titanium in the fused bath of chlorides) reduces to improving the conditions of formation and the structure of the "filter bed."

The crystalline titanium obtained by the two-stage sodium reduction process is not inferior in purity to the titanium purity to the titanium purified by the iodide process. The table below presents the results of an analysis of crystalline titanium (+ 10 mm fraction) and of an experimental specimen of iodide titanium with respect to the content of principal impurities.

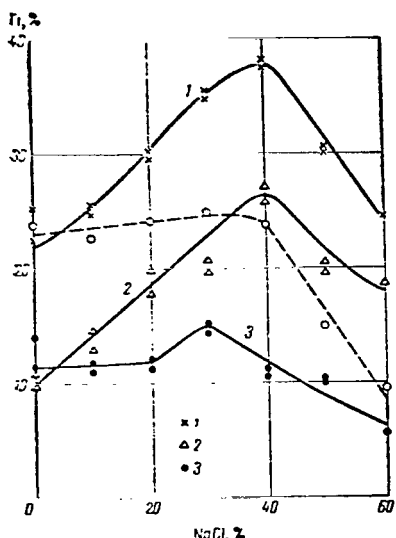


Figure 3. Relation of the Crystalline Titanium Yield to the "Black Salt" Dilution by Sodium Chloride:

Yield of Crystals: Total (1), Large, 10-mm (2), Extra-Large, 20-mm (3); Broken Line Denotes the Unit Yield of Crystalline Titanium Per Cycle.

conducted on using commercial-purity titanium tetrachloride and sodium. It is to be expected that purification of the raw components and hydrometallurgical treatment along with utilization of pure reagents will be a means of markedly enhancing the purity of crystalline titanium.

The two-stage sodium reduction method can be used to process the wastes of titanium sponge and Ti-based alloys into high-purity crystals. The wastes of titanium production are added during the first stage of the process. The resulting fused baths of chlorides are, following their filtration, subjected to final reduction by sodium.

To clarify the possibility of purifying titanium of its principal alloying elements, aluminum chloride was added to the "black salt" bath. Studies of this kind, too, will make it possible to further elucidate the mechanism of reduction as well as the mechanism of the growth of titanium crystals.

The results of preliminary studies showed that AlCl_3 , when present in the amount of $\sim 5\%$ in the fused bath, readily dissolves in the "black salt." The uniformity of its distribution is not vitiated by additional dilution of the bath with sodium chloride.

Comparison of these data shows that the content of such impurities as aluminum, vanadium, iron, silicon and nickel, the elimination of which by the iodide process is insufficiently effective, is lower in crystalline titanium by one of two orders of magnitude (and as regards zirconium, even by three orders of magnitude) than in iodide titanium. The total content of impurities (65 elements) in crystalline titanium is 0.07% lower than in iodide titanium. At the same time the content of calcium, manganese and chlorine in crystalline titanium is one order of magnitude higher and of cadmium, two orders higher, than in iodide titanium.

The mean hardness of melted specimens of crystalline titanium (averaged for five measurements) is 65.6 Brinell units. Oxygen content 0.03 wt. % and nitrogen content, 0.005 wt. %.

The hardness of melted specimens of microcrystalline titanium from the walls of the reaction vessel (10 + 3 mm fraction) is 98.3 Brinell units, and the hardness of the metal from the filter bed (3 mm fraction), 250.8 Brinell units.

/229

The data presented in the above table characterize metal obtained by the process

conducted on using commercial-purity titanium tetrachloride and sodium. It is to be expected that purification of the raw components and hydrometallurgical treatment along with utilization of pure reagents will be a means of markedly enhancing the purity of crystalline titanium.

The two-stage sodium reduction method can be used to process the wastes of titanium sponge and Ti-based alloys into high-purity crystals. The wastes of titanium production are added during the first stage of the process. The resulting fused baths of chlorides are, following their filtration, subjected to final reduction by sodium.

To clarify the possibility of purifying titanium of its principal alloying elements, aluminum chloride was added to the "black salt" bath. Studies of this kind, too, will make it possible to further elucidate the mechanism of reduction as well as the mechanism of the growth of titanium crystals.

The results of preliminary studies showed that AlCl_3 , when present in the amount of $\sim 5\%$ in the fused bath, readily dissolves in the "black salt." The uniformity of its distribution is not vitiated by additional dilution of the bath with sodium chloride.

TABLE 1. CONTENT OF PRINCIPAL IMPURITIES, %

Al	V	Fe	Cr	Ca	Si
Crystalline titanium produced by the two-stage process					
$3.0 \cdot 10^{-4}$	$5.1 \cdot 10^{-5}$	$5.8 \cdot 10^{-4}$	$4.7 \cdot 10^{-3}$	$4.1 \cdot 10^{-3}$	$6.0 \cdot 10^{-4}$
Iodide titanium					
$1.0 \cdot 10^{-3}$	$2.1 \cdot 10^{-2}$	$2.3 \cdot 10^{-3}$	$4.7 \cdot 10^{-3}$	$1.6 \cdot 10^{-4}$	$6.0 \cdot 10^{-3}$
Mn	Cl	Cr	Zr	Ni	Ti
Crystalline titanium produced by the two-stage process					
$2.2 \cdot 10^{-2}$	$1.4 \cdot 10^{-3}$	$2.2 \cdot 10^{-3}$	$1.9 \cdot 10^{-3}$	$7.2 \cdot 10^{-4}$	99.92
Iodide titanium					
$5.5 \cdot 10^{-3}$	$1.4 \cdot 10^{-4}$	$2.2 \cdot 10^{-3}$	$3.8 \cdot 10^{-2}$	$3.6 \cdot 10^{-3}$	99.85

Increasing the AlCl_3 content of the chloride bath to 6-8% markedly reduces the yield of macrocrystallizing titanium. The distribution of aluminum in various fractions of the metal is nonuniform; it is chiefly detected in the "filter bed" and at the bottom of the apparatus, while its content in crystalline titanium does not exceed 0.10-0.15 wt. % (30-40 times lower than in the metal of the "filter bed").

The above data convincingly demonstrate that the two-stage sodium reduction process is a means of obtaining crystalline titanium the aluminum content of which is approximately one order of magnitude lower than in the fused bath.

The obtained results have made it possible to begin trials on a semi-industrial scale. In connection with this, it was established that the first stage of the process, involving the synthesis of the "black salt" bath, is free of the development of pressures during admission at fast rates of titanium tetrachloride. The second-stage apparatus requires further improvements.

/230

It was shown that conducting the process in improved large-diameter apparatus assures the production of as much as 50% of the titanium in the form of large high-purity crystals.

REFERENCES

1. Ogurtsov, S. V., V. A. Reznichenko and S. I. Yegorov. In the collection: *Titan i yego splavy* [Titanium and Its Alloys], USSR Acad. Sci. Press, No. 6, p. 50, 1961.
2. Iochizawa, S., T. Hashino and S. Sakagushi. Technical reports on the Engineering Research Institute, Kioto University, IX, No. 4, p. 56, 1959.

3. Savin, V. D. and V. A. Reznichenko. Izvestiya AN SSSR, OTN: Metallurgiya i Gornoje Delo [Metallurgy and Mining], Vol. 3, No. 98, 1963.
4. Gus'kov, V. M., et al. Byull. TsNIItsvetmet, Vol. 4, No. 32, 1964.
5. Henrie, T. H. and D. H. Baker. Bureau of Mines, Report of Investigations, 5661, 1960.
6. Socci, M. La metallurgia italiana 8, 547, 1960.
7. Ogurtsov, S. V., et al. In the collection: Titan i yego splavy [Titanium and Its Alloys], USSR Acad. Sci. Press, No. 6, p. 60, 1961.
8. Savin, V. D. and V. A. Reznichenko. In the collection: Issledovaniya metallov v zhidkom i tverdom sostoyaniyakh [Studies of Metal in Liquid and Solid States], Nauka Press, No. 41, 1964.
9. Aleksandrovskiy, S. V. and V. M. Gus'kov. Izvestiya Vuzov: Tsvetnaya Metallurgiya, [Izvestiya of the Institutions: Nonferrous Metallurgy], Vol. 6, No. 74, 1965.
10. Markov, B. F. and Ye. P. Belyakova. Ukrainskiy khimicheskiy zhurnal [Ukrainian Chemical Journal], Vol. 27, No. 2, p. 46, 1961.
11. Gopiyenko, B. G. In the collection: Titan i yego splavy [Titanium and Its Alloys], No. 9, USSR Acad. Sci. Press, 205, 1963.
12. Ehrlich, Von P., G. Kaupa and K. Blankenstein. Z.anorg. allgem. Chemie, No. 290, p. 213, 1959.
13. Komarek, K. and P. Gerasymenko. J. Electrochem. Soc., Vol. 105, No. 4, p. 216, 1958.
14. Kelley, K. K. and Alla D. Mah. Bureau of mines. Report of Investigations No. 5490, Washington, 1959.
15. Kamenetskiy, V. M. Tsvetnyye metally [Nonferrous Metals], Vol. 2, No. 39, 1958.
16. Markov, B. F. and R. V. Chernov. Ukrainskiy khimicheskiy zhurnal [Ukrainian Chemical Journal], Vol. 25, No. 3, p. 279, 1959.
17. Korshunov, B. G. and V. I. Ionov. Izvestiya Vuzov: Tsvetnaya metallurgiya [Izvestiya of The Institutes: Nonferrous Metallurgy], Vol. 2, No. 102, 1961.

FEATURES OF THE PRODUCTION TECHNOLOGY OF SEMIFINISHED PRODUCTS OF TITANIUM AND ITS ALLOYS

I. N. Kaganovich

Titanium and its alloy display specific properties [1]: high chemical activity in heated state; resistance to corrosion in many corrosive media; a somewhat low plasticity and high strength*; presence of the polymorphic transformation $\alpha + \beta \rightleftharpoons \beta$ in the region of the optimal temperatures of hot deformation; marked difference in the properties of the α and β modifications; low heat condition.

These specific properties are taken into account in the flowsheets for the fabrication of semifinished products (sheets, forgings, tubes, rods, etc.) of titanium and its alloys.

The high chemical activity of titanium requires taking special steps to prevent or reduce gas absorption during heating, as well as to clean product surfaces of oxidation products.

/231

The high strength and low plasticity of titanium alloys at room temperatures restrict the possibilities for their deformation, and hence semifinished products are fabricated only following heating of the metal. The required heating temperature is higher the greater is the cross section of the products, the higher is the degree of treatment with alloying elements and the lower is the capacity of the equipment. An exception is represented by the fabrication of relatively thin products (wire, sheets, strip and tubes of unalloyed and low-alloy titanium), the deformation of which is accomplished in cold state with a large number of intermediate annealings or in "warm" state, i.e. after preheating to 500-800°C.

Deformation at high temperatures (in the region of the β modification) is accompanied by the formation of a coarse-grained macro- and microstructure with low mechanical properties. To assure a uniform micrograined structure the deformation of semifinished products to the finished size (during final heating) must be carried out at temperatures 40-50% below the temperature of phase transformation. In the process of preceding deformation the cast structure must be disintegrated and the large grains reduced in size.

Polymorphic transformation in a combination with low processability and low heat conduction may under certain conditions cause the formation of a consertal structure in semifinished products, thus reducing the stability of properties of the finished products. Correction of the structure by means of heat treatment, such as is applied to steels [2], is not feasible, and hence special thermo-mechanical treatment regimes must be developed in order to assure a homogeneous micrograined structure.

Treatment of titanium with β -stabilizing elements increases not only the amount and stability of the β phase but also the structural sensitivity of the alloy.

* As the impurity content decreases, the plasticity of titanium increases but the strength decreases.

This means that the deterioration of properties due to the presence of a non-fragmented β matrix in the structure is greater the higher is the degree of alloying of the β phase. The structural sensitivity of the alloys increases following their hardening heat treatment, and hence it is particularly important that products used in thermally hardened state should display a homogeneous fine-grained macro- and microstructure.

GENERAL TECHNOLOGICAL OPERATIONS

The fabrication of all kinds of semifinished products includes the following operations: reheating prior to deformation and cleaning of surface.

Reheating. The fabrication of semifinished products begins with the reheating of ingots (or billets) prior to their hot deformation. The high chemical activity and structural sensitivity of titanium and its alloys require a careful selection of reheating facilities, reheating regimes and methods of temperature measurement.

Furnaces of all kinds are used to reheat titanium: fuel oil-fired furnaces, gas-fired furnaces, induction and resistance furnaces based on electrical contact heating as well as on reheating in liquid media. The reheating of ingots and billets was considered in sufficient detail in the work [3], and hence here we will point out only the special features of reheating in induction furnaces. The use of induction furnaces makes it possible to markedly reduce the reheating time, but compared with other types of furnaces induction furnaces display a major shortcoming: electrical current is induced in the surface layers of metal, heating them to a high temperature, which leads to intense oxidation of the surface and in some cases to local burnout. In one of the experiments diffusion of oxygen into the metal to a considerable depth (8 mm) was discovered.

/232

When selecting the reheating regimes and the composition of the furnace atmosphere it must be borne in mind that the gas absorption of titanium sharply increases with increase in temperature and at the temperatures used in hot deformation it reaches a marked extent.

Light oxidation, endowing the metal with a slightly yellowish color, has been observed when heating titanium to 300°C , while heating at $> 500^{\circ}\text{C}$ causes the oxidized film to become blue. As the heating is continued, the color of the film changes depending on the composition of the alloy and its thickness markedly increases. On heating to $\geq 900^{\circ}\text{C}$ the scale on commercial titanium and its alloys with aluminum and tin acquires a yellowish color; the presence of vanadium, molybdenum or manganese in the alloy changes the color of the scale variously — from gray-green to cinnamon-brown. At the same time, oxygen diffuses across the scale into the metal, forming a brittle gas-saturated layer.

As shown by the experiments of Gulbransen and Andrew (cited in [4]), titanium without an appreciable oxide film on its surface readily absorbs hydrogen at 300°C . Hydrogen absorption by titanium during heating in a plasma furnace can begin at 500°C owing to the decomposition of water vapors and other hydrogen-containing gases [3]; this process may become significant as the heating temperature is raised and the amount of these gases in the furnace atmosphere are increased.

On heating in an electric furnace hydrogen content at the depth of 1 mm markedly increases at 900°C [5]. The absorption of hydrogen by titanium is a reversible process. In a number of cases vacuum annealing is applied to reduce the hydrogen content of the metal.

The interaction between titanium and nitrogen is of smaller significance, despite the high content of this gas in the furnace atmosphere, since the diffusion rate of nitrogen in titanium is low.

The fabrication of semifinished products from oxidized metal is difficult and in some cases impossible, hence the prevention of gas absorption by this metal during its reheating is a highly important problem. This problem can be solved by using inert-atmosphere furnaces (filled with argon or helium) or vacuum furnaces.

In this writer's opinion, immersion heating of medium-size billets for subsequent forging or extrusion is a promising method.

When furnaces with noncontrollable atmospheres are used, various protective coatings are employed to reduce oxidation of the metal (greases, enamels, metal spraying, etc.).

Surface treatment. The need for this operation is due to the oxidation of the metal during its reheating in furnaces with noncontrollable atmospheres.

In cases where semifinished products are subjected to mechanical treatment (e.g. forging) prior to their use in finished products, removal of scale may suffice. To this end, dry or liquid sand-blasting is more expedient.

The use of semifinished products without prior mechanical treatment necessitates removal of the brittle gas-saturated layer. This operation is, as a rule, carried out in two stages. During the first stage the scale is removed mechanically (liquid or dry sand-blasting, tumbling or abrasive cleaning) or by immersion (pickling) in a fused alkali bath.

During the production of sheets the first stage of cleaning is the crushing of scale and of the brittle oxidized layer by means of skin rolling with 3-6% reduction in area. The skin rolling may be replaced by pickling in a fused alkali bath.

The second stage of the descaling operation is the removal of the oxidized and gas-absorption layers in an acid solution (HCl , H_2SO_4 or HNO_3) treated with a fluorine compound (NaF , NH_4F or HF).

PRODUCTION OF SHEETS AND STRIP

When planning the flowsheets of the individual operations of the production of sheets and strip allowance is made for the processability of titanium alloys and the nature of their interaction with gases during reheating and pickling.

To determine processability, the deformation resistance of titanium alloys during rolling at various temperatures and their technological plasticity (permissible reduction of area between annealings during cold rolling) were investigated.

Rolling was carried out at 900°C (temperature characteristic of the initial or intermediate stage of the hot rolling of most titanium alloys) as well as at 600°C (characteristic of the warm rolling of these alloys).

To determine deformation resistance in reheated state, unit pressures of rolling were measured during the rolling of specimens measuring $12 \times 40 \times 200$ mm, selected from hot-rolled strip; the specimens were deformed to $\leq 20\%$. Specimens measuring $3 \times 30 \times 200$ mm were subjected to cold rolling with 10% deformation. The rolling was carried out in a Duo 260 mill. The results of these experiments make it possible to estimate the deformation resistance of different alloys under identical conditions (reduction of area, deformation rate and rolling temperature). The findings are collated in Table 1.

TABLE 1

Alloy	Unit rolling pressure, P, kg/mm ² , at			Alloy	Unit rolling pressure, P, kg/mm ² , at		
	900°	600°	Cold rolling		900°	600°	Cold rolling
VT1-1	5,2	23,5	109	VT6C	13,0	74,5	200
OT4-1	6,5	42,5	118	VT5-1	21,8	77,5	178
OT4	12,5	72,5	150	TS5	24,0	96,4	200
VT14	8,5	65	185	VT15	48,0	107,0	180

To determine the permissible degree of reduction in area during cold rolling, the specimens were annealed and subsequently cold rolling until the appearance of the first cracks. Table 2 presents the permissible degree of reduction in area.

As the data in Tables 1 and 2 imply, processability of the alloys decreases with increase in the degree of alloying of the α phase and increases with the formation of the β phase in the alloy but again begins to decrease when the degree of alloying of this phase also is increased; the lowest processability is displayed by the alloys with a high-alloy β phase.

Titanium alloys differ in the nature of their interaction with gases. During the operations of reheating and pickling, which are the most dangerous from the standpoint of gas absorption, the principal factor influencing this interaction is the phase composition of the alloys.

TABLE 1

/234

Alloy	Permissible deg. of reduction in area, %	Phase composition
VT1-1	60	Unalloyed α phase
OT4-1	25	Low-alloy α and β phases
OT4	20	The same
VT14	25	Medium-alloy α and β phases
VT6S	20	The same
VT5-1*	15	Medium-alloy α phase, high-alloy β phase
TS5*	12	Low-alloy β phase
VT15	35	High-alloy β phase, low-alloy α phase

*Rolling permissible only in warm state.

Taking as the basis the characteristics enumerated above, sheet titanium alloys may be divided into 4 groups:

1. All brands of technical titanium as well as alloys containing low-alloy α and β phases (OT4-1, OT4, etc.). These are distinguished by a high technological plasticity. The danger of oxidation during their heating is smaller than for alloys with a large amount of β phase; during pickling they do not absorb hydrogen.
2. Medium-alloy compositions (VT6S, VT14, VT2-1, etc.). Their technological plasticity is satisfactory; embrittlement during oxidation increases with increasing amount of β phase; they tend to absorb hydrogen during pickling; they are markedly hardened by heat treatment.
3. Alloys containing a high-alloy α phase; single-phase alloys (VT5, VT5-1, etc.) and alloys containing a small amount of β phase (TS5, VT20, etc.). Their technological plasticity is low; their gas absorption during heating is similar to that of alloys in group 1; α -alloys during pickling do not absorb hydrogen; α alloys containing a small amount of β phase tend to absorb some hydrogen during pickling.
4. Alloys containing a high-alloy β phase (VT15, VT16, etc.). Their technological plasticity is high; the danger of oxidation during heating is considerable; they tend to hydrogen absorption during pickling; heat treatment hardens them markedly.

The technology for the fabrication of sheets is selected depending on the properties of the alloy and the available equipment.

A high-productivity process for the fabrication of thin sheets of all the alloys by the strip rolling method may be organized given the availability of heavy-duty rolling equipment making it possible to roll coils in warm state and a number of alloys in cold state.

When medium-capacity equipment is used, sheets of alloys in group 1 can be fabricated by the strip rolling method. Sheets of alloys in groups 2-4 in this case are fabricated by the pack rolling method.

The rolling of titanium and titanium-alloy sheets does not fundamentally differ from similar operations of the rolling of the other metals.

An exception is represented by the operations of the technological process, the implementation of which involves the high chemical activity of titanium (the operations of hot rolling and pickling), as well as its high strength (the need for the warm rolling the skin rolling of most alloys).

HOT ROLLING

As was pointed out above, during its reheating prior to hot rolling titanium and its alloys actively absorb gases from the furnace atmosphere. Then oxygen diffuses across the layer of scale into the interior of the metal — over a continuous front in α -alloys and selectively in $(\alpha + \beta)$ -alloys: chiefly into the particles of the α phase and along grain boundaries. At 950-1000°C the maximum solubility of oxygen in the α phase is 12-14% and in the β phase, 0.5% [6].

The oxygen-enriched particles of the α phase embrittle the alloys to an extent that increases with decreasing proportion of the α phase in them, since their oxygen concentration then increases. The brittle particles represent "notches" along which the metal fractures during deformation. For this reason, during rolling, following heating of the noncontrollable-atmosphere furnace, the surface of the hot-rolled strip of $\alpha + \beta$ - and β -alloys fractures to a greater extent than the surface of α -alloy strip.

/235

As the degree of treatment of alloys with β -stabilizers increases, the danger of fracture of the oxygen-saturated surface of the metal increases.

Figure 1 illustrates the nature of gas-saturated layers of α - and $(\alpha + \beta)$ -alloys.

During the fabrication of thin sheets of alloys of group 1 the surface damage due to oxidization may be corrected by means of additional mechanical treatment (abrasive cleaning and other methods) and pickling.

The cracks formed during the hot rolling of alloys containing a large amount of β phase which were not protected against the action of the furnace atmosphere are practically impossible to eliminate, and hence the rolling of alloys of this kind is permissible only if they are protected against oxidation.

During the fabrication of plate from α -alloys and low-alloy $(\alpha + \beta)$ -composition a brittle oxidized layer may arise on their surface. Either measures should be taken to prevent the oxidation of blooms during their reheating prior to hot rolling or

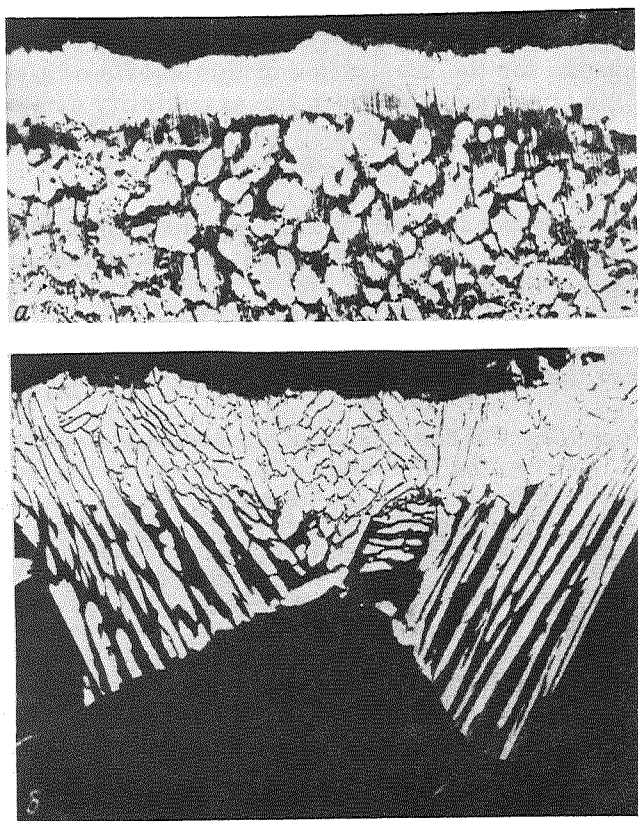


Figure 1. Gas-Saturated Layer in Specimens
Following Heating to 1000°C:

a—VT5-1 Alloy Magnified 340 Times; b—VT14
 $\alpha + \beta$ -Alloy, Magnified 200 Times.

the brittle layer should be removed from the plate surface by means of abrasive cleaning and subsequent pickling. During the fabrication of sheets this layer becomes thinned out in the process of rolling and removed by means of multistage pickling included in the production flowsheet. However, the elimination of this layer, as well as of the surface defects due to its disintegration is insufficiently reliable. Thus, protection of the metal against interaction with gases during prior reheating is highly recommended in all cases, and for the high-alloy ($\alpha + \beta$)- and β -compositions it is absolutely required.

/236

In addition to the methods for preventing or reducing the interaction between metal and the furnace atmosphere, as enumerated above, during the fabrication of sheets of high-alloy compositions cladding with unalloyed or low-alloy titanium is employed. The thickness of the cladding layer is 6-7% of the thickness of the bloom. The cladding layer not only protects the metal against oxidation but also prevents its hydrogen absorption during subsequent pickling. In a number of works, including [7], it is shown that the plastic cladding layer reduces the rolling pressure.

When working out the regime of heating prior to hot rolling allowance must be made for the following:

The temperature of the hot rolling is selected according to the plasticity diagram of the alloy and also after taking into account the unit power of the rolling mill and the final rolling temperature. If hot rolling is ended at or below the temperature of phase transformation, it results in the formation of a banded structure (in two-phase titanium alloys the transformation and recrystallization temperatures are fairly similar).

Banded structure is particularly evident in alloys with a large amount of β phase. It is not eliminated by subsequent rolling with $\leq 50\%$ deformation. The presence of this structure adversely affects the mechanical properties of the metal. In sheet fabrication the degree of deformation markedly exceeds 50% and hence banding may not be observed. In the presence of banding in the structure of hot-rolled stock the quality of sheets may be improved by annealing above the transformation temperature and subsequent deformation in the two-phase region with $\leq 50\%$ reduction in area.

The final thickness of hot-rolled stock is selected after taking into account the unit power of the rolling mill and the plasticity of the metal, with the object of rolling stock of minimum thickness; at the same time, during subsequent final rolling in warm or cold state a degree of deformation of at least 50% must be assured. Failure to observe this condition is a cause of deterioration in the mechanical properties of sheets.

This may be illustrated by the properties of 8 mm thick sheets of VT6S alloy fabricated from hot-rolled billets 13 and 20 mm thick which were rolled from a single ingot:

Billet, mm	13	20
σ_B , kg/mm ²	89	87
δ , %	11.5	13
Bending angle, deg	45	100

It follows hence that for the 20 mm thick billet elongation is 2% greater and bending angle, 55° greater, than for the 13 mm thick billet. The microstructure of these sheets (Fig. 2) shows that the deterioration in the properties of sheets fabricated from the 13 mm thick billet is due to the banding of structure, i. e. to insufficient working of the metal at the temperature of the $(\alpha + \beta)$ -region.

STRUCTURE OF SHEETS AND SUSCEPTIBILITY TO HYDROGEN ABSORPTION DURING PICKLING

/237

As was established by T. V. Shikhaleyeva during pickling of single-phase α -alloys containing a small amount of the β phase (alloys of the OT4-1 and OT4 types) in an acid solution having the composition of 10% HCl + 4% NaF, a hydrogen-saturated layer 0.01-0.02 mm thick forms at the metal surface. The amount of

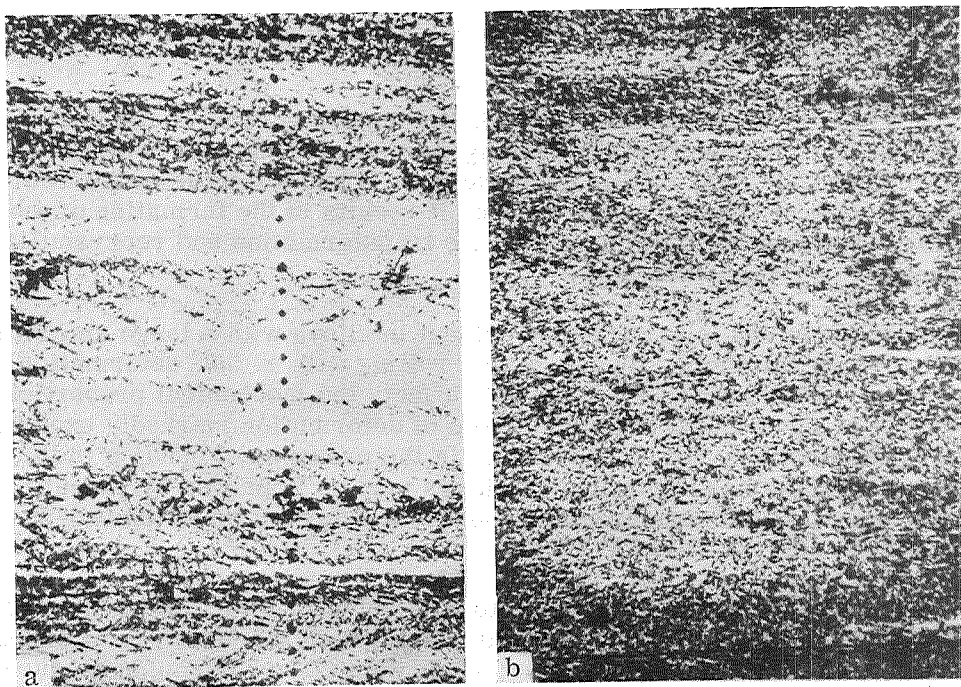


Figure 2. Microstructure of Sheets of VT6S Alloy Fabricated From 13 mm Thick Billet (a) and 20 mm Thick Billet (b); Sheet Thickness 0.8 mm. Magnified 70 Times.

hydrogen in the metal does not increase even after sufficiently prolonged pickling (as much as 12 hr). Pickling of alloys with a large amount of β phase (VT6, VT14, etc.), on the other hand, may lead to the diffusion hydrogen throughout the volume of the metal, with the hydrogen content reaching a significant extent (as much as tenths of one percent).

Subsequently it was shown [5] that the amount of hydrogen absorbed during pickling depends on the structure of the alloy, the amount of β phase and the shape of its particles, and the activity and duration of pickling.

It is known that the amount of β phase in the alloy varies within fairly broad limits depending on the reheating temperature. As the temperature of reheating in the $(\alpha + \beta)$ -region is raised, the amount of this phase increases; quenching from the β -region fixes the martensitic phase in alloys of the martensitic type. The greatest amount of β phase in the alloy is found in hot-rolled sheets and the smallest, following quenching from the β -region and following annealing at 400–700°C, depending on the composition of the alloys. Figure 3 presents the curves of the hydrogen content of specimens of various alloys following pickling as a function of the regime of prior heat treatment [5].

The obtained data made it possible to determine more precisely the regimes of thermomechanical treatment of the sheets of a number of titanium alloys.

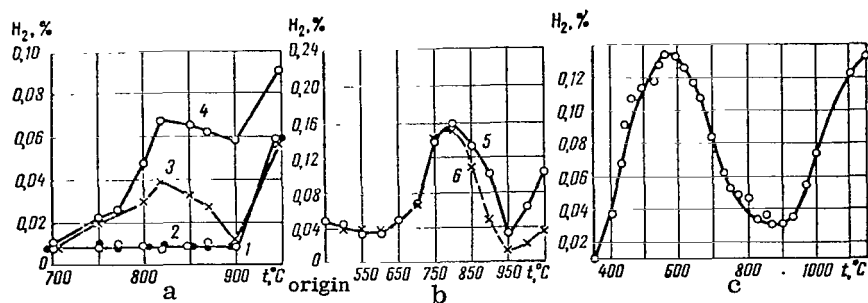


Figure 3. Relation of the Hydrogen Content of Specimens of the Alloys VT14 (a), VT16 (b) and VT15 (c) During Pickling to the Regime of Prior Heat Treatment [5]:

1—Original, Annealed; 2—Original, Quenched; 3—Quenched, Pickled for 25 Min at 50°C; 4—The Same as 3, Annealed; 5—Annealed; 6—Quenched.

PRODUCTION OF DROP AND DIE FORGINGS

The finished part must have minimum tolerances in order to preclude machining. This requirement is most readily met by raising the temperature of the metal in order to improve its deformability and facilitate the filling of molds. However, this adversely affects the final properties of the product. The selected conditions of thermomechanical treatment should be such as to assure precision of shape and the desired properties.

To obtain optimal mechanical properties of the macro- and microstructure of the semifinished products should be uniform, micrograined. This is achieved with relative ease when fabricating small cross section products whose production inevitably is accompanied by marked deformation of the ingot; the final operations of the fabrication of products of this kind are readily carried out at relatively low temperatures.

In the work [8] it was established that the deformation of a 40x40 mm specimen of VT14 alloy to at least 40% at the temperature of the $(\alpha + \beta)$ -region assures an optimal structure and high mechanical properties. This regime proved to be optimal for other alloys as well.

Attaining the desired structure in large cross section products, on the other hand, is difficult due to the specific properties of titanium and its alloys (low heat conduction conditions a significant temperature drop over the cross section of the billet during deformation; low plasticity at low heating temperatures complicates deformation and leads to the increase in surface defects; deformation at the high temperatures of the β region is accompanied by considerable grain growth; intense deformation on hammers [drop forging] heats the metal so that its temperature rises 50–150°C above the initial forging temperature; as the degree of alloying of the metal is increased, the possibility of heating during forging increase; the macrocrystalline structure of titanium ingots necessitates high-degree deformation in order to induce a microcrystalline structure).

The structure of large-diameter titanium billets often is consertal, which causes a deterioration in mechanical properties, particularly during the production of $(\alpha + \beta)$ -alloys. Following the hardening heat treatment of alloys of this kind, their mechanical properties, and particularly their plasticity characteristics, may decline quite markedly.

The use of billets having a consertal structure results in the retention of this structure by the finished product, even if the deformation at temperatures in the $(\alpha + \beta)$ -region was considerable. The production of die forgings with a uniform finegrained structure requires using billets (forged stock or rods) with a uniform fine-grained structure.

/239

It was established that rods, forgings and other types of billets for the production of die forgings having a desired structure can be obtained when deformation of the ingots is carried out by the following stages:

1. Forging of ingot into round or rectangular rods and their cutting into billets.
2. Working of all sides of the billet at a temperature $40-60^{\circ}\text{C}$ higher than the phase transformation temperature, by means of alternate double or triple upsetting and drawing or forging of successive sides and axes. This assures a uniform fine-grained recrystallized structure (characteristic of deformation in the β region) throughout the cross section of the billet. When the billets are fabricated by rolling in a billet mill, this treatment may be dispensed with.
3. Working of all sides of the billet, as during the preceding stage, or only upsetting or forming of the billet at a temperature $20-40^{\circ}\text{C}$ below the transformation temperature.

This results in fragmentation of the β matrix and its boundaries. The mechanical properties of the billet depend on the forging reduction ratio; the higher is this ratio, the greater becomes the increase in plasticity and strength characteristics. During low-temperature deformation on a hammer [drop forging] a provision must be made for the possibility of the attendant heating of the metal. Figure 4 shows the structure of an VTX-1 alloy forging fabricated from a billet obtained by the conventional technology, i. e. by drawing, as well as from a billet subjected to the working of all of its sides by the method described above. The data presented confirm the advantages of the newly developed technology.

During the production of billets exceeding 150-200 mm in diameter, the length of which is more than 2.5 times the diameter, low-temperature drop forging is difficult to implement and may lead to the formation of a consertal structure, deterioration of properties and formation of surface cracks. In certain cases, as regards large-diameter billets, the treatment is best confined to high-temperature forging, which preserves greater stability of properties compared to billets having a consertal structure.

Compared to drop forging, forging in presses assures the deformation in the $(\alpha + \beta)$ -region of billets of a somewhat larger diameter.

Given the currently used production methods, it is difficult to assure uniform structure in extra-long rods with a diameter of more than 80-120 mm when drop-forged and with a diameter of 120-150 mm when press-forged (die-forged). Die forgings with high and stable properties may be produced provided that the billets used are properly prepared in accordance with the technology described above.

The forging of billets should be effected at a temperature 20-40°C below the phase transformation temperature, with the maximum possible degree of deformation. This contributes to further fragmentation of the macro- and microstructure of the metal and improvement in its properties. Prior reheating to temperatures exceeding the phase transformation temperature, or the spontaneous heating of the metal to the temperature of the β region during its drop forging, may lead to the formation in the finished forging of a microstructure characteristic of high-temperature deformation, with the attendant sharp deterioration in properties.

The danger of the deterioration of properties during heating to high temperatures complicates the possibility of fabricating intricately shaped large forgings. In this connection, the possibility of deformation with multiple brief reheating to temperatures below the temperature of phase transformation has been established. This makes it possible to somewhat broaden the range of forgable products.

THERMOMECHANICAL TREATMENT

/240

One way of further increasing the mechanical properties of the forgings is their thermomechanical treatment (TMT), which combines hot working of the metal with its rapid cooling in water (quenching). This enhances the dispersity of structural components [9], creates a large number of stable crystal lattice defects [10] and fixes work hardening [11]. TMT is also a means of enhancing fatigue strength and high-temperature strength to a definite higher temperature, considering that it leads to the formation of a system of sub-boundaries which impede the migration of dislocations [12].

/241

Studies carried out in collaboration with Yu. I. Potapenko and Ye. D. Igumen'shchnev demonstrated the possibility of markedly increasing the mechanical properties of forgings of the alloys VT8, VT9 and VT14. First, the hardenability of titanium alloys was investigated, and it was established that the depth of hardenability varies depending on chemical composition of the alloy from 15 mm for the alloy VT14 to 30 mm for the alloy VTZ-1. These data must be taken into account when solving the question of the expediency of resorting to TMT. A flowsheet for the fabrication of forgings with application of TMT was worked out:

/242

1. Production of billets with a homogeneous fine-grained macro- and microstructure in accordance with the sequence described in the preceding section.
2. Heating to temperatures 30-50°C below the phase transformation temperatures.
3. Forging with 30-50% deformation.
4. Cooling in water, the temperature of which should not be above 50°C.

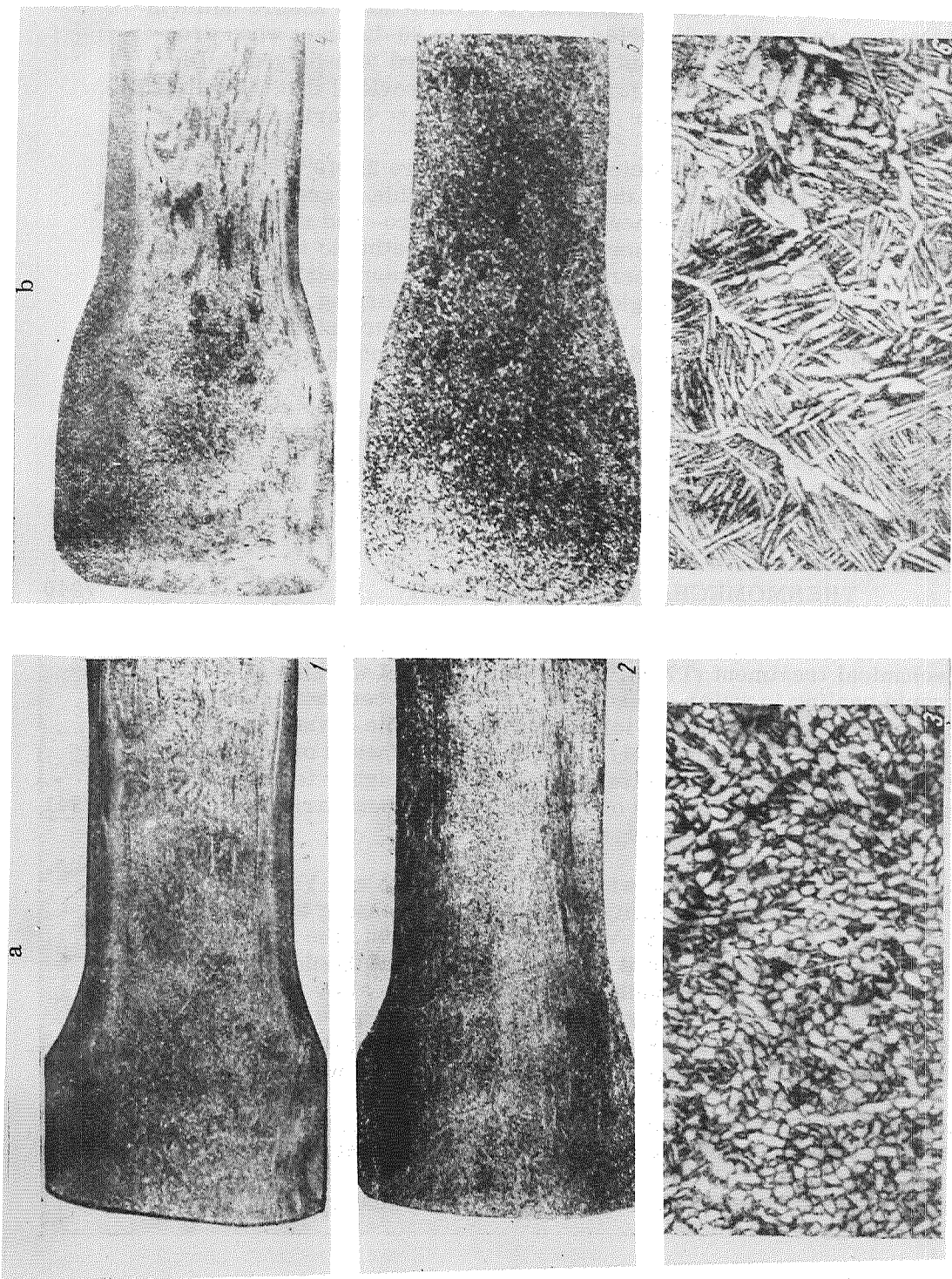


Figure 4. Structure and Properties of an VTZ-1 Alloy Product Forged by Two Different Methods:
a—Two-Stage Forging and Forming of All Sides of Billet; b—Drawing and Forming.

1—Macrostructure of Billet (1:2); 2—Macrostructure of Forging (1:2); 3—Microstructure of Forging (1:2); 4—Macrostructure of Billet (1:2); $\sigma_B = 102.9 \text{ kg/mm}^2$; $\delta = 17.1\%$; $\psi = 50.2\%$; 5—Macrostructure of Forging (1:2); 6—Microstructure of Forging (Magnified 450 Times); $\sigma_B = 109.1 \text{ kg/mm}^2$; $\delta = 13.2\%$; $\psi = 41.1\%$.

5. The interval of time between the ending of deformation and the quenching in water should not exceed 30 sec.

Table 4 presents the mechanical properties of VT8 and VT9 alloy forgings fabricated on using TMT.

TABLE 4

Alloy	Thickness, mm	σ_b , kg/mm ²	δ , %	ψ , %	a_{impact} , kg-m/cm ²
VT9	10-20	126-156	6-13	13-48	2.0-3.5
	40-50	120-140	9-16	22-48	3.2-4.4
	Accord. to tech. stand.	105	8	22	3
VT8	10-20	120-141	6-14	17-49	2.5-3.4
	40-70	120-137	9-15	35-50	3.1-4.4
	Accord. to tech. stand.	100	8	16	3

It can be seen from this table that TMT made it possible to increase ultimate strength by 15-20 kg/mm² above the level accepted in the pertinent technical standards, while at the same time resulting in some loss of plasticity.

In forgings of VT14 alloy TMT increases not only strength but also plasticity. This is confirmed by the data in Table 5, which presents the results of tests of specimens cut from VT14 alloy forgings and subjected to TMT.

TABLE 5

Thickness, mm	σ_b , kg/mm ²	δ , %	ψ , %	a_{impact} , kg-m/cm ²
18	122-133	9-12	37-54	2.5-4.1
20	130-132	11-13	39-49	2.2-2.8
Accord. to tech. stand.	112	5	12	2.5

Although TMT markedly increases the mechanical properties of forgings, its applicability to series-produced drop forgings is limited. When determining the expediency of using this method, allowance must be made for the low hardenability of titanium alloys, the buckling or warping which accompanies quenching may present sufficient difficulty when the forgings are of intricate configuration.

CONCLUSIONS

/243

In the fabrication of all kinds of semifinished products from titanium and its alloys allowance should be made for general rules stemming from the specific properties of this metal.

The principal conditions assuring the desired properties of the finished products are the prevention of gas absorption during the production process and intense deformation at temperatures of the $(\alpha + \beta)$ -region in order to obtain a homogeneous fine-grained macro-and microstructure.

To this end special equipment is needed: inert-atmosphere furnaces for reheating billets and heavy-duty equipment for deformation at temperatures of the $(\alpha + \beta)$ -region.

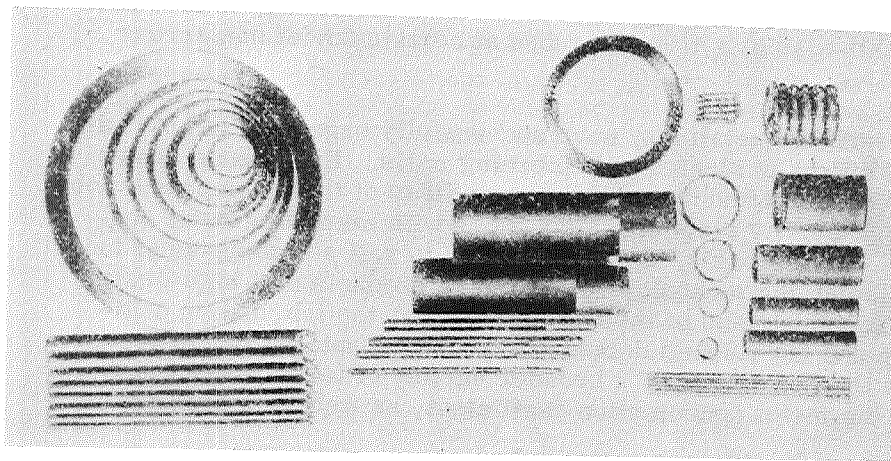
REFERENCES

1. McQuillan, A.D. and M.K. McQuillan. Titan [Titanium], Metallurgizdat, 1958.
2. Sadovskiy, V.D. Izvestiya AN SSSR: Metally [Metals], Vol. 5, No. 2, 1965.
3. Moroz, A.S., et al. Titan i yego splavy [Titanium and Its Alloys], Sudpromgiz, 1960.
4. Livanov, V.A., A.A. Bukhanova and B.A. Kolachev. Vodorod v titane [Hydrogen in Titanium], Metallurgizdat, 1962.
5. Kaganovich, I.N. and T.V. Shikhalevaya. Metallovedeniye i termicheskaya obrabotka metallov [Metallography and Thermal Treatment of Metals], Vol. 3, No. 5, 1963.
6. Molchanova, Ye.K. Atlas diagramm sostoyaniya titanovykh splavov [Atlas of Phases Diagrams of Titanium Alloys], Mashinostroyeniye Press, 1964.
7. Pavlov, I.M., et al. Tsvetnyy Metally [Nonferrous Metals], Vol. 4, No. 14, 1966.
8. Kaganovich, I.N. Titan v promyshlennosti [Titanium in Industry], Oborongiz, No. 18, 1961.
9. Kaganovich, I.N., Yu.I. Potapenko and Ye.D. Igumen'shchev. Tsvetnyye metally [Nonferrous Metals], Vol. 10, No. 21, 1965.
10. Zubov, V.Ya., et al. Fizika metallov i metallovedeniye [Metal Physics and Metallography], Vol. 20, No. 3, p. 21, 1965.
11. Bernshteyn, M.L., L.A. Yelagina and L.P. Fatkulina. Tsvetnyye metally [Nonferrous Metals], Vol. 12, No. 21, 1964.
12. Sokolov, Ye.N., Yu.P. Surkov and D.I. Gurfel'. Fizika metallov i metallovedeniye [Metal Physics and Metallography], Vol. 20, No. 4, p. 22, 1965.

PRODUCTION OF TUBES FROM TITANIUM AND ITS ALLOYS*

V. Ya. Ostrenko

Tubes of titanium as well as of the various alloys of titanium find increasing application in various branches of industry, including such branches as the chemical, aviation, shipbuilding and other industries [1, 2]. The production technology of these tubes should assure the possibility of their fabrication chiefly with the aid of currently existing equipment designed for the fabrication of steel tubes. It is worth noting that at present the production technology has been mastered of tubes of practically any titanium alloy, ranging from 0.5 to 465 mm in diameter [3]. Specimens of tubes of this kind are illustrated in Fig. 1.



/244

Figure 1. Titanium-Alloy Tubes Ranging From 0.5 to 465 mm in Diameter, the Production of Which has been Organized by the USSR Tube Industry.

Research into the properties of the titanium alloys has shown that small-diameter (≤ 60 mm) seamless tubes can be produced in two ways: 1) by extrusion of deep-drill stock followed by cold rolling and drawing; 2) by hot rolling in automatic tube mills, also followed by cold rolling and drawing. Large-diameter tubes can be produced with currently existing equipment only by means of hot

*The article presents the results of a comprehensive project for research into the organization of the production of titanium tubes, carried out with the direct creative participation of the author by the staff of the All-Union Scientific Research and Design Technology Institute of the Tube Industry (VNITI) in collaboration with the workers of the tube plants of ferrous metallurgy. The most active part in this project was taken by the associates of the VNITI: Ye. P. Akimova, N. V. Bogoyavlenskaya, A. G. Kravchenko, M. M. Bernshteyn, V. I. Shevchenko, V. K. Usov, L. N. Okhramovich, L. D. Bobrakov, V. A. Topal, R. L. Zaslavskiy, V. R. Tyr, L. A. Il'vovskaya, L. N. Kotenko, L. I. Guzevataya, A. I. Tyazhel'nikov, Ye. I. Chernenko, I. S. Stefanskiy, and others.

rolling (tubes of \geq 325 mm diameter, in automatic rolling mills and tubes of \geq 550 mm diameter, in pilger mills).

When selecting the method for the production of titanium tubes, the initial premises were as follows: a) the state of the equipment and technology for the production of tubes of analogous dimensions from alloy and high alloy steels and primarily from stainless steel; b) the possibilities of currently existing equipment; c) the results of laboratory research into the properties of titanium alloy; d) the data in the published literature.

It is known that the production technology used in the USSR of seamless, stainless-steel tubes differs considerably from the technology employed abroad, where the first and principal operation in the technological process of tube production—the piercing of the billet—is carried out in presses, with the billet usually first being drilled from one end to the other. This technology is also used in the fabrication of small-diameter titanium tubes at certain Soviet nonferrous metallurgy plants.

The tube plants of ferrous metallurgy have successfully organized the piercing of solid stainless-steel billets in slanted-roll piercing mills. Experience shows that this technology is expedient and assures the possibility of the mass production of a broad variety of high-quality stainless-steel tubes with minimum metal consumption coefficients. On this basis, the method used to roll stainless-steel tubes was adopted when developing the technology of the mass production of high-quality titanium-alloy tubes. A comparison of the two methods for the fabrication of titanium tubes (extrusion and hot rolling) demonstrates the advantages of the second method, which assures the fabrication of a broader variety of tubes without any significant increase in the metal consumption coefficient, as well as a high productivity of equipment.

Studies of the properties of titanium alloys under the conditions of the hot rolling of tubes established that all titanium alloys [4] regardless of their phase composition in cold state can be pierced at the temperature of existence of the β phase. Following piercing, during subsequent rolling and cooling, tubes fabricated from alloys of various groups can differ in structure. The most characteristic structure of hot-rolled tubes in post-rolled state is presented in Fig. 2.

/245

Hot-rolled tubes of α -alloys treated with aluminum and neutral hardners (Sn, Zr) and sometimes also tubes of alloys treated with some amount of β -stabilizers (Mn, V, Mo, etc.) display a "basket-weave" structure of the α phase with twins number of which, as a rule, increases with increasing content of alloying elements—chiefly, Al—in the alloy (Fig. 2, a-c).

/246

Tubes of two-phase alloys and β -alloys treated with Mn, V, Fe and Cr following cooling usually display an unstable structure and the α -phase content of this structure decreases with the increase in its content of β -stabilizers (Fig. 2, d, e); if the amount of β -stabilizers is substantial, the structure of the tubes may consist of the β phase (Fig. 2, f). If the piercing and rolling temperatures are sufficiently high, the tubes display sufficient plasticity, which is highly important if they subsequently have to be repaired, turned and bored.

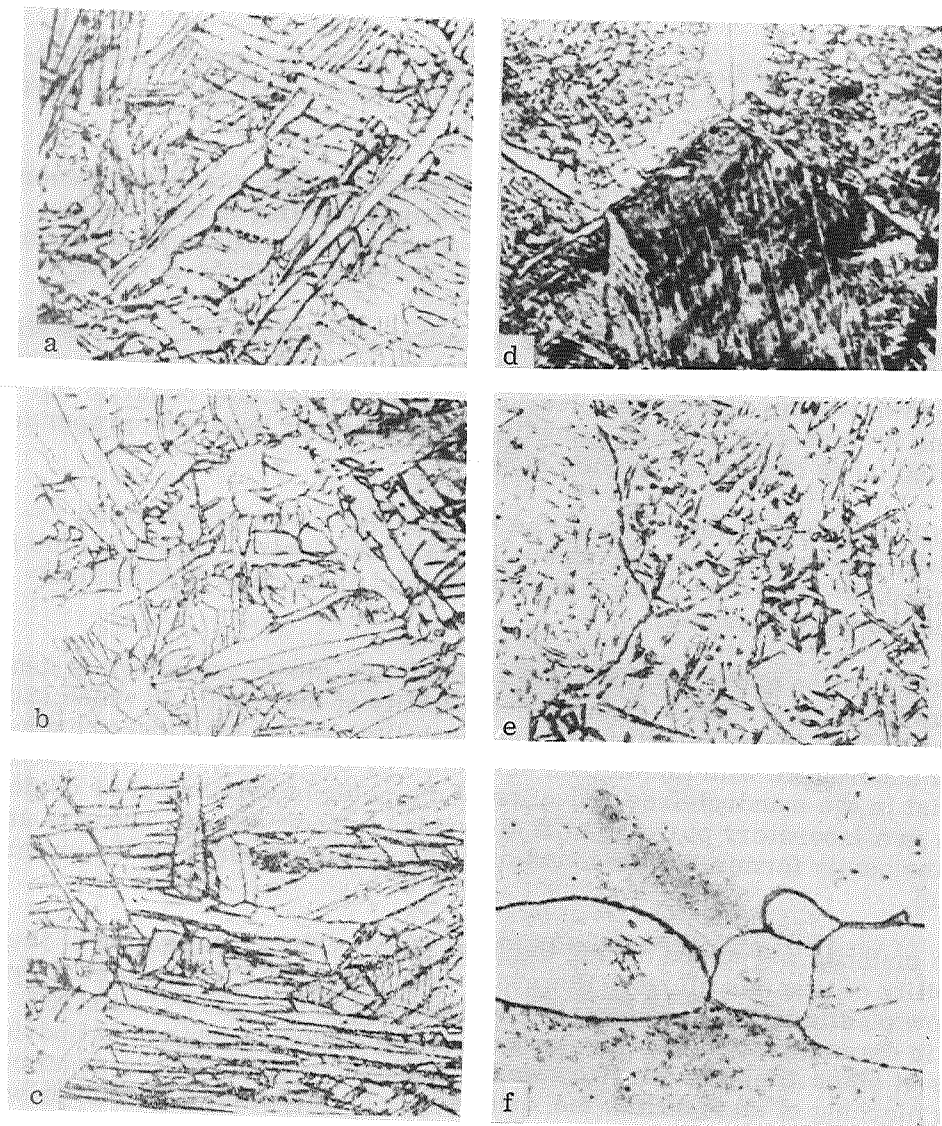


Figure 2. Characteristic Microstructure of Hot-Rolled Tubes,
Magnified 500 Times.

Figure section	Tube, mm	Alloy	Tempera-ture, °C
a	133x12	VT-1	1080-950
b	152x14	α -alloy	1160-1020
c	152x18	VT5	1140-1090
d	168x14	VT14	1160-1030
e	103x7	(α + β)-alloy	1070-970
f	133x8	VT15	1210-1000

The investigations also established that the structure and properties of α -alloy tubes change little during their subsequent heat treatment, and hence they usually are not subjected to subsequent heat treatment.

Hot-rolled tubes of $\alpha + \beta$ -alloys have an unstable structure and may become brittle in the course of their subsequent cold rolling, pickling in alkali baths, repairing, etc. The stabilizing treatment for tubes of these alloys is annealing at a temperature somewhat below the boundary of existence of the β region.

At higher temperatures, owing to the attendant marked softening, thinwalled tubes in the process of their heat treatment may get deformed in packs or even due to their own weight. Moreover, marked gas absorption may occur in the metal during its high-temperature annealing. On the other hand, the properties of thickwalled tubes can be sufficiently stable.

Hot-rolled tubes of β -alloys (e.g. the VT15 alloy) have high oxidation resistance, with the oxidation occurring along grain boundaries. Tubes of this alloy also may get embrittled during their processing and hence they must be heat-treated prior to their finishing.

The organization of the hot rolling of tubes of new steels and alloys is usually preceded by laboratory studies of the processability of the metal, to which end specific methods of technological tests (pierceability and hot twisting) are employed. In accordance with the method developed by the VNTI, the pierceability tests consist in the mandrel-free reduction of diameter of cylindrical or conical specimens in a laboratory piercing mill at various temperatures. The size and nature of the cavity forming in the interior of the specimen serve as the criteria of the metal.

These methods were used during the first stage of the investigation of the processability of titanium alloys. However, even specimens of titanium alloys having a low plasticity failed to fracture during tests at 950–1200°C with 15% reduction in diameter. Similar results were obtained during tests of cylindrical specimens of other titanium alloys as well. It should be noted that in practice during the piercing of steel billets the reduction in diameter until encounter with the mandrel tip usually does not exceed 4–6%. A 15% reduction in diameter during tests of specimens of any, even the most plastic, steel always leads to its extensive fracture.

To verify the effect of greater ($\leq 35\%$) reduction in diameter on the behavior of titanium alloys during their piercing, conical specimens were tested but even then, despite the much greater degree of deformation, the piercing of the specimen could not be completed (Fig. 3).

/247

Thus the pierceability test based on mandrel-free reduction of diameter of the specimen in the laboratory piercing mill is unsuitable for determining the piercing parameters of titanium alloys, since it does not assure complete piercing in titanium specimens, which display an extremely high plasticity over a broad range of the temperatures of hot deformation. Hence a new type of pierceability test was developed—piercing of cylindrical specimens on a mandrel

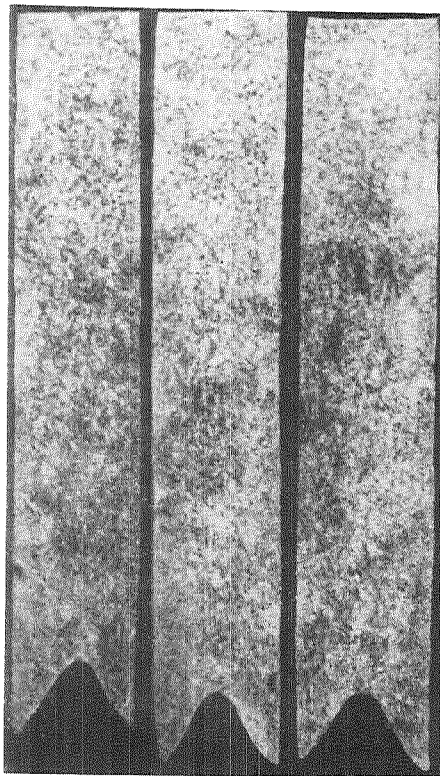


Figure 3. Conical Specimens of VT1-1 Alloy Following Tests With Reduction in Diameter from 0 to 35%.

was the piercing temperature: at 1000 and 1050°C the fissures occurred only at the butt ends, while at 1200 and 1250°C the internal surface of the specimens was completely smooth. Following piercing at 1200-1250°C damage to the mandrel tip was much smaller. However, at 1250°C the state of the external surface of the specimens deteriorated, due to the absorption of gases by the metal at such a high temperature. Therefore, the piercing temperature must be selected after an analysis of data on the structure of the specimen, the depth of the gas-saturated layer thereon and the load on the piercing mill.

Hot twist tests also were employed during the investigation of the processability of titanium alloys. Figure 5 presents the results of these tests for three groups of alloys (α , $\alpha + \beta$, β); for comparison, it also presents the curve plotted for the hot twist tests of specimens of Kh18N10T stainless steel, which is widely used in tube production. Analysis of the curves implies that the highest plasticity is displayed by technically pure titanium VT1-1. For all the alloys the number of twists initially sharply increases with rise in temperature, but decreases beyond 950°C for the alloy VT1-1 and beyond 1000-1050°C for all the other alloys. An exception is the alloy VT15 (β alloy), for which the number of twists steadily increases at all the test temperatures employed.

at various temperatures with various degrees of reduction in diameter. Then the criterions for processability of the metal are the state of the internal and external surface of the resulting hollow cylinders, their structure and gas absorption, the strength of the mandrels and the load exerted on the piercing mill. This method, which allows a sufficiently accurate assessment of the behavior of the metal during piercing, was used to investigate the processability of titanium alloys.

Figure 4 presents vertical cross sections of the pierced specimens and shows the state of the mandrels following piercing of specimens of the aforementioned two-phase alloy at 950-1250°C. It can be seen that at 950°C the specimen could not be pierced throughout due to the high deformation resistance of the metal and the consequent marked warping of the mandrel. The quality of the internal surface of the specimen at this temperature is unsatisfactory (fissures can be seen along the entire length of this surface). At higher temperatures (to 1250°C) all the specimens could be pierced through and the state of their internal surface was better the higher

/248

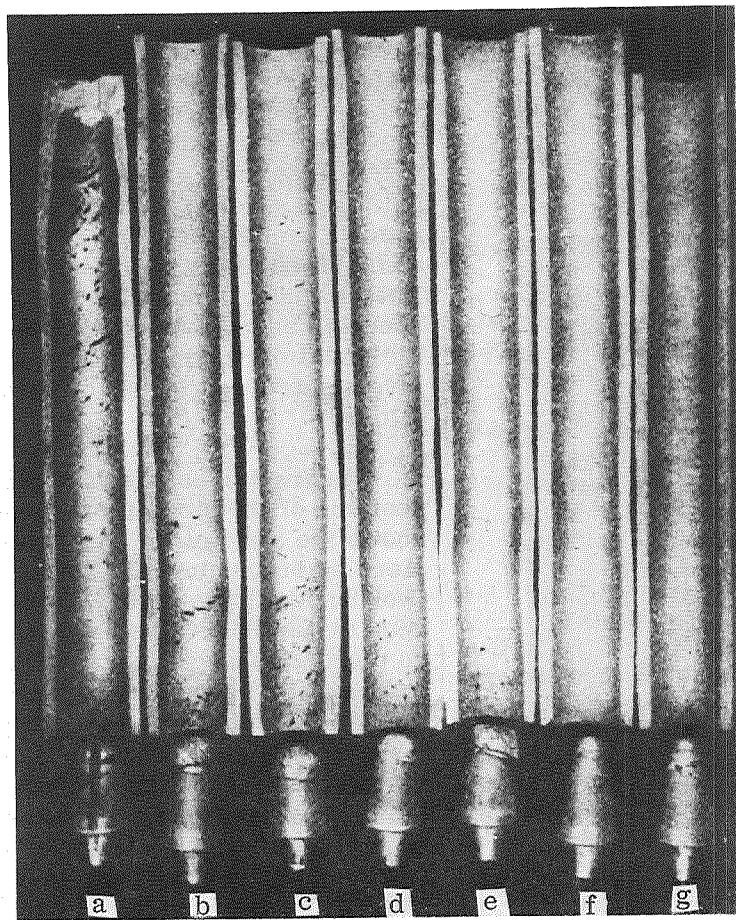


Figure 4. Hollow Cylinders Obtained by Piercing Specimens of Two-Phase Titanium Alloy at Various Temperature, $^{\circ}\text{C}$: 950 (a), 1000 (b), 1050 (c), 1100 (d), 1150 (e), 1200 (f), 1250 (g).

It is characteristic that the hot twist tests show the plasticity of titanium alloys to be much higher than the plasticity of Kh18N10T steel.

Further analysis showed that the principal cause of the decrease in the number of times the specimens can be twisted is the absorption of gases by the metal during heating to high temperatures. To verify this assumption, specimens of VT1-1 alloy were subjected to hot twist tests in conventional (air) and shielding (argon) atmospheres. The test results are presented in Fig. 6, which shows that a comparatively low test temperatures (up to 950°C), when the metal still does not absorb gases from air, the number of twists in both atmospheres is the same. At higher temperatures this number is much higher when the tests are carried out in the protective atmosphere.

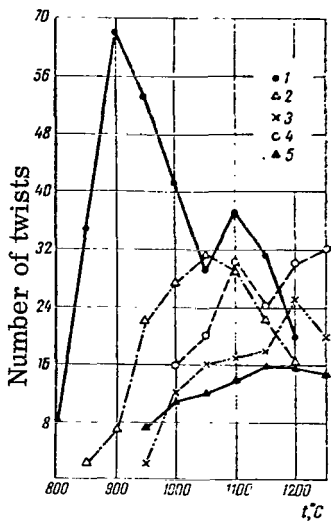


Figure 5. Relation of the Number of Twists of Specimens Until Fracture as a Function of Test Temperature.

Alloys: VT1-1 (1), α (2), $\alpha + \beta$ (3), β (4); Kh18N10T Steel (5).

industrial conditions.

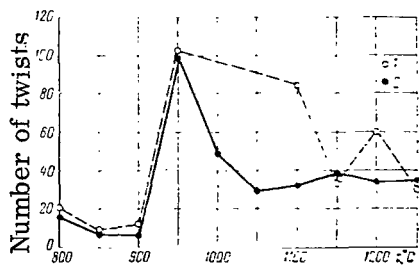


Figure 6. Twist Tests of VT1-1 Specimens in Air (1) and in Argon Atmosphere (2).

to the following factors: Certain protective coatings, e.g. the vitreous or colloidal-graphite lubricants used in extrusion, although providing satisfactory protection of titanium against gas absorption when the billets are in a stationary position, disintegrate during their manipulation in continuous furnaces. The bared pure layers of metal, on entering the zone of contact with the furnace atmosphere at a high temperature rapidly absorb gases. Coatings of other types,

The gases usually are absorbed only by relatively thin surface layers of the metal, but the rolling of tubes entails deformation of the entire cross sectional area of the billet and hence hot twist tests should be carried out in a protective atmosphere in order to assure correct selection of the piercing regime.

During the investigation of the processability of titanium alloys, in addition to piercing tests and hot twist tests, the effect of the temperature and degree of deformation was also studied by carrying out rollability tests of wedge-shaped specimens and determining the mechanical properties of the metal at various temperatures. The results of these tests were used to distribute the desired degrees of deformation among the elements of the tube mill and to determine the final rolling temperature.

The regimes of heating and piercing of billets and the parameters of tube rolling were ultimately selected on the basis of a combined analysis of the results of the pierceability and hot twist tests of titanium alloys, on also taking into account the results of supplementary tests. The thus established basic technological parameters of the hot rolling of titanium tubes were verified under

To prevent the absorption of gases by titanium, industrial plants employ various greases and ceramic and metal coatings for the billets. The use of special reheating facilities with a protective atmosphere or a vacuum is also effective. Protection of titanium by means of the Schoop process has become fairly widely used at certain plants.

However, our experiments showed that for the reheating of billets in the currently operating tube-rolling shops the use of protective coatings does not produce the desired effect. This is due

in their turn, although they may get firmly bounded to the heated metal, cause complications during entrainment of the billet by the rolls of the piercing mill as during subsequent hot deformation. Moreover, following rolling the coating has to be removed by a special procedure.

Studies carried out by the VNITI showed that, under present conditions, titanium billets can be successfully reheated in the currently existing furnaces for reheating steel billets. Titanium is highly viscous and hence it adheres to the rolling equipment, thus causing the formation on the external and internal tube surfaces of tiny defects reaching 0.8 mm in depth in the form of notches incised by the edges of the rolling mill, scratches due to the mandrels of the automatic mill, roll impressions, etc. Since shipments of titanium tubes are acceptable only if the tube surface is of high quality, the tubes must be machined (turned, bored or ground) and pickled. The thickness of the layer forming during the reheating of the billet is reduced during subsequent rolling, which entails considerable elongation (elongation coefficient reaches 8), and it decreases with increasing elongation, and hence after rolling the thickness of this layer on the tubes does not exceed the depth of occurrence of rolling-induced defects. This layer is readily removed by mechanical and chemical treatment.

/250

Thus the reheating of the titanium-alloy tube billets prior to their piercing is no major problem, even though it displays specific features of its own, and chiefly the need for prior thorough removal of iron scale from the furnace bottom and delivery chute. Therefore, a separate furnace for reheating titanium alloy and stainless-steel billets should be used when this reheating is carried out in the tube shops specializing in the production of steel tubes. In the shops where titanium tubes are fabricated fairly rarely the billets should be reheated in conventional furnaces on a track of pure refractory brick or in muffles. Rapid reheating in specialized devices reduces the metal loss due to scaling and it also reduces the thickness of the gas-absorbing layer.

In accordance with the requirements for the tubes technical conditions for the tube billet were drafted. In practice, solid forged and turned billets are used for the fabrication of all the currently manufactured titanium alloy tubes. Occasionally deep-drilled billets are used for the fabrication of large-diameter tubes rolled in pilger mills. Following the modernization of these facilities solid billets could be used, thus making it possible to reduce still further the metal consumption coefficients.

A special feature of the piercing of titanium billets is the absence of a cavity in front of the mandrel tip and hence also the absence of an internal film in the pierced billets regardless of the degree of reduction in their diameter. Another characteristic feature is the somewhat high axial stresses. During piercing of high-strength alloys the axial stresses reach a considerable magnitude which results in bending and vibration of the supporting rod of the piercing mill due to the more irregular wall thickness of the pierced billets. This may be attributed to the high ductility of titanium, which, compared with steel, conditions a different pattern of stresses in the area of deformation.

In addition, due to the high plasticity of titanium alloys in hot state, the pressure of metal on the rolls and the load on the main drive of the piercing mill

prove to be quite insignificant (much smaller than during the piercing of stainless steel billets); they become significant only during the piercing of high-strength alloys.

By contrast with piercing, the process of the rolling of titanium tubes in an automatic mill involves definite difficulties. The mandrel inside the tube, even though it is replaced following every rolling pass, complicates the process, since the metal adheres to it and thus tears occur on the internal surface of the tubes. In this connection, tubes within a series of sizes are rolled without using an automatic mill — the pierced billet is conveyed from the piercing mill to the reeling mill, thus assuring a high quality of the tube.

The parameters (diameter, wall thickness, variation of wall thickness) of the titanium-alloy tubes produced by the developed technology correspond to the tolerances specified in the standards for steel tubes.

For tubes subjected to turning and boring with the object of eliminating effects and the α -layer, the relative variation in wall thickness following such machining usually increases somewhat due to their curvature and ovalness. To eliminate this shortcoming the tubes should be subjected to warm straightening and the machine tools used should be equipped with a floating cutting head for removal of a uniform layer of metal from the tube surface.

/251

Investigation of mechanical properties of the tubes has shown that most indicators of >130 -mm diameter tubes are higher than for the original billet (see table below). The mechanical properties of tubes of smaller diameter, rolled from billets with a high forging reduction ratio, differ little from the properties of thickwalled and thinwalled tubes of the same alloy established that the short-time strength and yield point of thinwalled tubes are higher than required while their unit elongation is lower than required.

Investigation of hot-rolled α -alloy tubes of a single size has not established any relationship between mechanical properties and the final temperature of rolling or fluctuations in the chemical composition of the metal. This may be attributable to the fairly substantial deformation during rolling, which for thickwalled tubes reaches 40–60% and for thinwalled tubes, 80–85%, as well as to the high rate of drop in the temperature of metal. Within the 1000–700°C range, i.e. at the temperatures of the end of rolling, the decrease in temperature is very rapid so that there is not enough time for recrystallization to terminate.

Tubes of two-phase alloys following hot rolling are characterized by a high strength, while their unit elongation and impact strength remain roughly the same as in the billet.

In ferrous and nonferrous metallurgy plants thinwalled titanium tubes and small-diameter tubes are produced by cold rolling and drawing of hot-rolled or extruded billets. Many alloys in cold state display a comparatively low plasticity and high notch sensitivity and get hardened during their deformation, and hence when developing the production technology of tubes of these alloys considerable attention has been paid to determining the optimal roll pass design, the optimal method for preparing the metal for rolling, the optimal tube finishing operations

/252

TABLE 1. COMPARISON OF THE MECHANICAL PROPERTIES
 OF TECHNICAL-PURITY TITANIUM VT1-1 AND α -ALLOY
 OF TITANIUM IN THE BILLET AND IN THE TUBE

Alloy		Short-time tensile strength, kg/mm ²	Yield point, kg/mm ²	δ , %	ψ , %	Impact strength, kg-m/cm ²
VT1-6	Billet 260 mm	42.0—46.8	32.5—33.1	21.6—33.2	44.2—63.7	7—1.22
	Commercial tubes	45.0—63.0	33.0—55.0	20.0—33.5	46.0—63.0	6.1—17.7
	Billet 100 mm	45.3—63.4	36.5—51.8	23.7—38.7	32.2—66.8	17.2—17
	Processable tubes	44.6—62.7	37.4—52.8	26.7—28.4	55.0—67.6	5.7—8.6
α -alloy	Billet 260 mm	51.0—65.2	40.8—58.5	9.0—16.0	19.1—36.7	10.4—17.3
	Commercial tubes	61.5—69.0	57.5—63.5	14.0—24.0	38.5—57.0	6.3—17.2
	Billet 100 mm	57.8—64.5	50.4—59.7	21.9—25.8	30.0—44.4	8.8—11.9
	Processable tubes	62.2—65.5	57.0—60.5	22.5—29.5	43.5—51.0	4.6—8.9

[6, 9]. A highly important factor as regards tube quality is the thoroughness with which the tube billets are prepared for cold rolling. It was established that the presence of an α -layer at the surface or of traces of rough machining affects adversely the process of cold rolling and the quality of production. From this standpoint, the use of extruded tubes as billets, i.e. of tubes characterized by the presence of longitudinal scratches, is less desirable. The higher quality of cold-rolled tubes is assured by rolling them from hot rolled tube billets subjected to machining, deep pickling, clarification, and washing and by rigorously monitoring the state of the external and internal surfaces.

A comparison of the performance indicators of small-diameter tubes fabricated from hot-rolled and extruded billets also confirmed that hot-rolled billets are preferable as the material of tubes used for important purposes.

Thus, the technological flowsheet of the production of small-diameter (cold-rolled and cold-drawn) tubes in ferrous metallurgy plants consists of the following elements: a) hot rolling of tubes in automatic mills followed by warm straightening; b) boring, turning, pickling and preparation of the surface of hot-rolled tubes; c) cold rolling in KhPT or KhPTR cold-rolling tube mills and drawing with intermediate reheating and chemical treatments.

Operating experience of tube plants and data published on this problem show that the physical properties of titanium necessitate a corresponding modification of roll pass design in the cold-rolling tube mills, since the use of rolls and mandrels employed to cold-roll steel tubes did not produce positive results. It

was established that the roll pass design developed by the VNITI in collaboration with the YuTZ Southern Tube Plant is the most suitable for this purpose.

When developing the production technology of cold-deformed tubes of titanium alloys it was difficult to find a suitable lubricant, and the solution of this problem was complicated by the tendency of titanium to adhere to the rolls during its deformation. It was established that the best results were produced by coating the tube surface with an oxide film and with a lubricant consisting of a mixture of castor oil and talcum.

The oxide film is formed in a fused alkali bath [6].

A characteristic feature of the cold rolling of titanium-alloy tubes in KhPT mills is that their quality is greatly affected by the ratio between reduction of wall thickness and reduction in diameter [8]. The best results are obtained in cases where reduction in wall thickness is greater than reduction in diameter.

In this connection, endeavors are being made to reduce to a minimum the clearance between the mandrel and the internal surface of the tube. However, this is possible only in the rolling of thinwalled tubes, and therefore their quality is, as a rule, higher than the quality of tubes with thicker walls.

During the cold rolling of thickwalled tubes various defects occur on their internal surface and thus lower the quality of the tubes to an unacceptable level. The co-workers of the VNITI have developed and introduced into production the circulating-jet method of pickling, which assures the removal of minor defects from the internal surface of tubes. However, it must be pointed out that such a method for the cleaning of tube surfaces leads to loss of metal, which is removed by the jet of the pickling solution being pumped through the tube under pressure. This loss increases if circulating-jet pickling is carried out following every individual rolling pass, and hence it is expedient to introduce this operation only in extreme cases and only for nearly finished tubes.

/253

The production technology of titanium-alloy tubes, including tubes of the high-strength titanium alloys (VT14, VT15, etc.), that has been introduced at the tube plants of the USSR makes it possible to supply titanium tubes to various branches of industry.

The equipment currently used for the production of steel tubes can be used to produce titanium-alloy tubes of practically any size within the limits of the existing standards, at comparatively low metal consumption coefficients.

The experience gained by the tube plants and the VNITI warrants the issuance of a separate GOST All-Union State standard for titanium-alloy tubes.

REFERENCES

1. Shul'kin, S. M. In the collection: Goryachekatanyye truby iz titana [Hot-Rolled Titanium Tubes]. Metallurgiya [Metallurgy], 1, Sudpromgiz, 1958.
2. Engineer, No. 204, p. 5301, 1957.
3. Truby iz titana i yego splavov [Tubes of Titanium and Its Alloys], Tsvetmetinformatsiya, 1966.

4. Glazunov, S. G. Sovremennyye titanovyye splavy. Titan i yego splavy. Metallovedeniye i termicheskaya obrabotka metallov [Modern Titanium Alloys. Titanium and Its Alloys. Metallography and Heat Treatment of Metals], No. 2, 1963.
5. Smirnov, V. S., M. F. Nevezhin and G. S. Ponomarev. Issledovaniye usiliy i skol'zheniya pri proshivke gil'z iz titana [Study of Stresses and Slip During Piercing of Titanium Billets], Izvestiya Vuzov: Mashinostroyeniye, No. 1, 1950.
6. Ostrenko, V. Ya., et al. Razrabotka tekhnologii proizvodstva trub iz titanovogo splava AT-3 [Developing the Production Technology of AT-3 Titanium Alloys Tubes], In the collection: Titan i yego splavy [Titanium and Its Alloys], No. 10, Ussr Acad. Sci. Press, 1963.
7. Ostrenko, V. Ya., Ye. P. Akimova and L. A. Il'vovskaya. Issledovaniye svoystv titanovogo splava AT-4 primenitel'no k usloviyam trubnogo proizvodstva [Study of the Properties of AT-4 Titanium Alloy in Relation to the Conditions of Tube Production], In the collection: Titan i yego splavy [Titanium and Its Alloys], No. 10, USSR Acad. Sci. Press, 1963.
8. Rusinovich, Yu. I. O sootnoshenii deformatsii pri kholodnoy prokatke trub iz splavov titana. Tsvetnyye metally. [Deformation Ratio During Cold Rolling of Titanium Alloy Tubes. Nonferrous Metals, No. 9, 1962.
9. Rusinovich, Yu. I. and Yu. F. Shevakin. Kholodnaya prokatka trub iz titana i yego splavov. Tsvetnyye metally. [Cold Rolling of Tubes of Titanium and Titanium Alloys. Nonferrous Metals]. No. 1, 1962.

EXTRUSION OF TITANIUM ALLOY SHAPES

O. S. Mironov, M. F. Zakharov, Yu. I. Sobolev,
L. A. Yelagina and A. A. Gel'man

The extrusion of titanium and titanium-alloy shapes is a more complicated process than the extrusion of aluminum, copper and nickel alloys as well as of steels. This is due not only to the high prior reheating temperatures of the metal and the need to apply high unit pressures during extrusion but also and primarily to the nature of the extruded material itself.

The extruded material (titanium and its alloys) adheres to the working surface of the die, and hence a surface of satisfactory quality cannot be obtained in the extruded products, since deep scratches and tears form on it. Hence the conventional lubricant-free extrusion process (method 3 in the classification by S. I. Gubkin) is completely unsuitable for the extrusion of semifinished products of titanium and its alloys. Clearly, to obtain a surface of satisfactory quality on extruded titanium-alloy products it is necessary primarily to maximally isolate the extrusion billet from contact with the die material, i. e. to conduct extrusion under conditions of copious lubrication. The high temperature of the extrusion billet and the sharp drop in temperature between the billet and the press tools as well as the high unit pressures ($100-120 \text{ kg/mm}^2$) greatly complicate the selection of lubricants which can simultaneously assure a low friction coefficient and complete isolation of titanium from the die. Extrusion of long and fairly intricate shapes presents even greater difficulty.

/254

Some contact between titanium and the press tools in the course of extrusion is practically inevitable, and hence special attention must also be paid to the die material. The die should withstand high temperatures and pressures and be only minimally susceptible to interaction with the metal being extruded. The deformation of titanium and its alloys is accompanied by a considerable heat release, and hence the temperature of the extruded product emerging from the die may exceed the temperature of the eutectics Ti-Fe, Ti-Ni, which essentially precludes the possibility of using dies fabricated from Ni- and Fe-based alloys.

Using dies having a working surface of V2K or V3K stellite enhances the strength of the press tools, but this does not assure the desired surface quality of the extruded products, since the use of a flat-ended round billet entails, during the initial stage of extrusion, shear along the boundaries of "elastic ("dead") volume" and sliding of titanium over titanium.

The application of a lubricant to the side surface also does not produce satisfactory results, since the lubricant gets abraded by the metal of the "dead" volume so that the latter is practically bare of lubricant when entering the die hole.

The elimination of "dead" volumes and, hence, improvement in the surface quality of the extruded shapes can be assured by using dies with a cone-shaped bell and billets with tapering butt ends. Extrusion through dies with a cone-shaped inlet bell is ideal from the standpoint of the flow kinetics of the metal but difficult to implement in practice. First, fabrication of dies of this kind is much more

complicated than the fabrication of flat dies, particularly when materials not amenable to machining are used to make these dies. In addition, the selection of lubricant also is more difficult. The lubricant must perform satisfactorily also in the region of low pressures ahead of the area of deformation, as well as in the region of high pressures in the area of deformation. Allowance should also be made for some difference in the temperature of the metal before and after deformation.

The task is simplified if the extrusion is carried out in a flat die using special die inserts as well as billets, the ends of which are tapered by turning. If the special insert is made of a lubricant material then lubricant of one composition can be used in the low-pressure region and lubricant of another composition, in the high-pressure region. The first lubricant is applied to the side surface of the billet or to the working surface of the container bushing, while the second lubricant is represented by a dummy block of corresponding shape, inserted between the die and billet.

When developing the extrusion technology of titanium and titanium-alloy shapes we selected the method of extrusion through a flat die with an insert — a dummy block in front of the die. Glasses were used as lubricants. Glass No. 58 (softening point 440°C) was applied to the side surface of the billet, while the dummy block was made glass No. 15 (softening point 550°C).

Prior to extrusion the billets were reheated in induction furnaces. The reheated billet is rolled down a special inclined table coated with a layer of ground glass No. 58, whereupon it is conveyed to the container. A dummy block of glass No. 15 is first inserted in the space method is satisfactory. It must be borne in mind, however, that at lower temperatures the glass acts as an abrasive and hence the temperature of the internal surface of the container bushing should be higher than the softening temperature of the glass used as the lubricant of the side surface of the billet, as otherwise, when present at the surface of the container bushing, the glass would exist in solid state and cause premature breakdown of the bushing due to its increased wear.

/255

By way of an example, Fig. 1 shows the surface of shapes extruded by two different techniques.

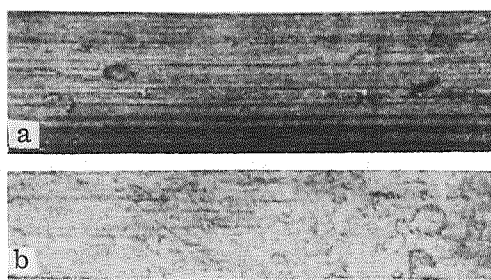


Figure 1. Surface of OT4 Alloy Shapes Extruded Without (a) and With (b) the Insertion of a Glass Dummy Block.

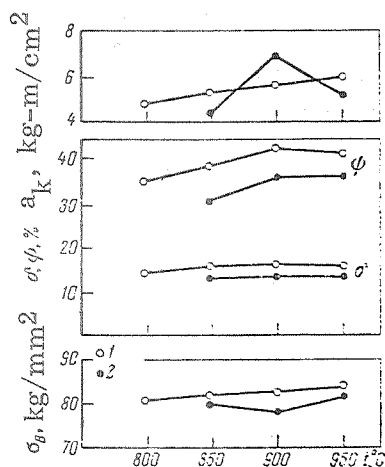


Figure 2. Effect of Reheat Temperature on the Mechanical Properties of Extruded OT4 Alloy Shapes. Degree of Deformation: 83.9% (1) and 91.8% (2).

of billets reheated at $> 900^{\circ}\text{C}$ also cannot be recommended.

From the standpoint of the surface quality of the extruded shapes and the strength of the press tools, extrusion should best be carried out at the lower limit of possible temperatures.

Investigation of the structure and properties of shapes extruded from the two-phase alloys OT4, VTZ-1 and VT8 at various temperatures established the optimal range of reheating temperatures for the extrusion billets ($900\text{--}950^{\circ}\text{C}$) (Fig. 2). The shapes extruded from such billets display a lamellar structure (Fig. 3, a) with $\leq 100 \mu$ grain size (the alloys VT8, VTZ-1) and a sufficiently high level of strength and plasticity properties.

Reheating at $> 950^{\circ}\text{C}$ leads to a sharp increase in grain size and is accompanied by a decrease in plasticity, which is particularly notable in the alloy VT-8, owing to the development of β -brittleness. Extrusion

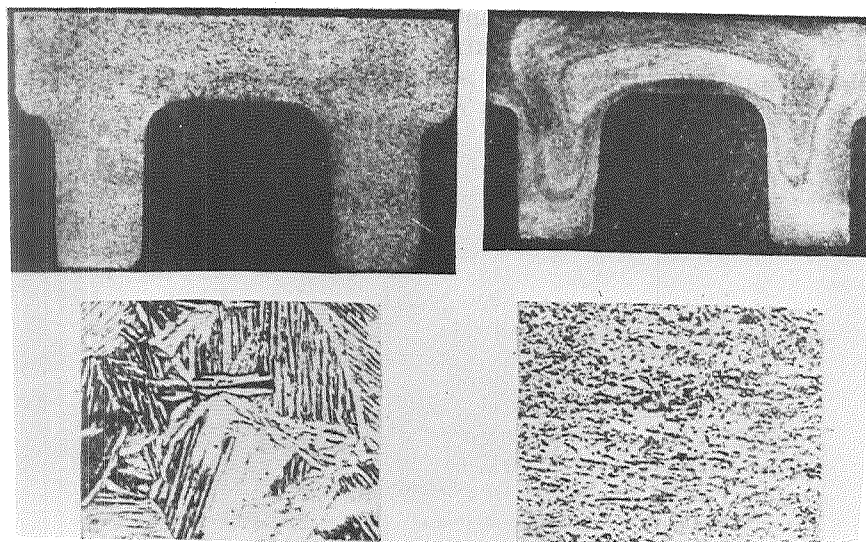


Figure 3. Structure of Extruded OT4 Alloy Shapes.
 Billet Reheat Temperature: $900\text{--}950^{\circ}\text{C}$ (a) and 900°C (b). Magnified 300 Times.

It was established that extrusion of OT4 alloy shapes from billets reheated at 800-850°C results in a decrease in the mean level of plasticity (Fig. 2) and intensifies the anisotropy of properties. In addition, in a number of cases, it leads to a marked decrease in transverse reduction of area with respect to the core of the broadest sections of the extruded shapes. The nonuniformity of plasticity over the cross section of the shapes is apparently associated with features of their fibrous structure.

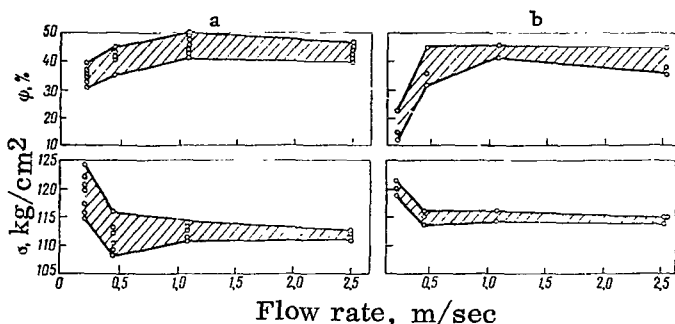


Figure 4. Mechanical Properties of VTZ-1 Alloy Shapes in Longitudinal (a) and Transverse (b) Directions as a Function of Flow Rate During Extrusion.

Structure and properties also are markedly affected by flow rate (Fig. 4). It was shown experimentally that during the extrusion of VT8 and VTZ-1 alloy shapes within the optimal range of temperatures the flow rate should exceed 0.5 m/sec. At lower flow rates certain extruded products develop anisotropy and the cross-sectional nonuniformity of their strength properties increases.

DEFORMABILITY OF CERTAIN ($\alpha + \beta$)- AND β -ALLOYS OF
 TITANIUM IN COLD STATE

/257

A. D. Lyuchkov, L. A. Il'vovskaya, V. I. Shevchenko and
 T. V. Kutsygina

The deformability in cold state of titanium alloys containing the β phase essentially depends on their structure and phase composition. It is known that $\alpha + \beta$ alloys in quenched state display a higher plasticity than in annealed state [1]. This manifests itself in the marked decrease in yield point and some increase in unit elongation and contraction during mechanical tests of quenched specimens [2, 3]. Quenching, in particular, leads to an improvement in the stampability of VT14 and VT6 alloy sheets.

It was of interest to investigate the effect of heat treatment on the deformability of alloys containing the β phase, under conditions of cold rolling. A group of alloys of this kind was selected; their chemical composition is given in Table 1.

TABLE 1

Сплав	Al	Mo	V	Cr	Fe	Temperature $\alpha + \beta \rightarrow \beta$ trans- formation, °C
VT14	4.2	2.7	1.2	—	0.1	950
VT8	5.9	3.2	—	—	—	1000
TiAl5V4Cr1.5Fe1.5	4.5	—	4.0	1.37	1.52	850
VT15	3.37	7.15	—	11.22	0.17	740
Ti-32Mo	—	33.5	—	—	—	—

Forged billets served as the original material. The quenching temperature of $(\alpha + \beta)$ -alloys was selected on the basis of the analysis of mechanical properties (Fig. 1) so that it would correspond to the lowest σ_S/σ_B ratio.

The phase composition of the heat-treatment specimens was determined radiographically according to the intensity ratio between the interferences of the (110) β and (010) α phases.

Rolling of the specimens was carried out in an PS-500 laboratory quarto mill by means of multiple deformation with a fixed 2% reduction in area per rolling pass. The peripheral speed of the rolls was 0.96 m/sec. The criterion of relative deformability was taken as the maximum degree of deformation preceding the formation of the first visually observable cracks on the side surfaces of the specimens.

/258

As determined in this manner, the suitability of the investigated alloys for cold plastic deformation differed. For the alloys VT15 and TiMo32 with a mechanically stable β -structure deformability proved to be extremely high (90%).

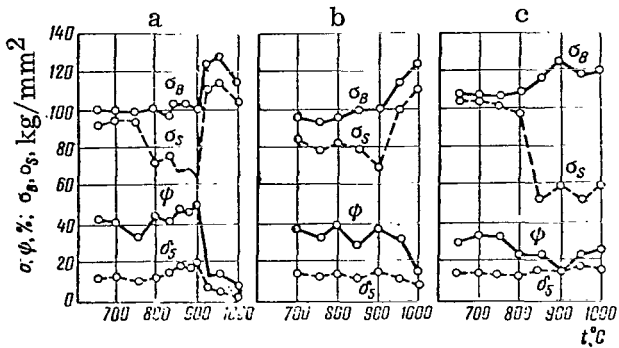


Figure 1. Mechanical Properties of $(\alpha + \beta)$ -Alloys as a Function of Quenching Temperature.

Alloys VT14 (a), VT8 (b), TiAl 4.5VCr1.5Fe1.5 (c).

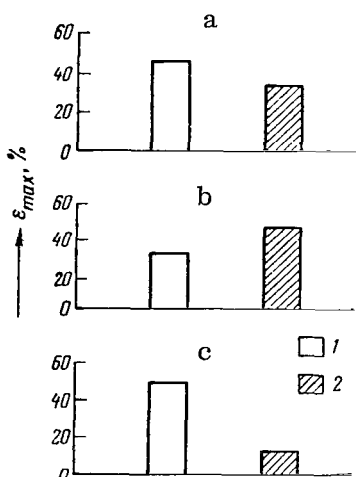


Figure 2. Limiting Deformability During the Rolling of Annealed (1) and Quenched (2) Alloys VT14 (a), VT8 (b), TiAl 4.5 V 4.0 Cr 1.5 Fe 1.5 (c).

composition and the σ_s/σ_B ratio are close to one another in the deformed quenched alloys. This indicates that during rolling in every case the quenching-induced decrease in yield point becomes exhausted toward the moment of commencement of fracture.

It was of interest to estimate the range of the degrees of deformation within which deformative decomposition of the mechanically unstable β phase is observed.

The results of the study of deformability of two-phase alloys containing the mechanically stable β phase in quenched state are presented in Fig. 2.

As can be seen from Fig. 2, the lowest deformability in annealed state (20%) is displayed by the alloy VT8 compared with 48% for the alloys VT14 and TiAl5V4Cr1.5Fe1.5. At the same time, when in quenched state this alloy displays the highest deformability whereas at this point the deformability of the quenched alloy VT14 is 35% and of the alloy TiAl 4.5VCr 1.5Fe1.5 is only 12%.

The results of the study of mechanical properties of the investigated alloys in original and maximally deformed state are shown in Fig. 3. All the alloys were annealed for 1 hr at 800°C.

As can be seen from Fig. 3, regardless of the extent of limiting (maximum) deformation and the σ_s/σ_B ratio in original state, the phase

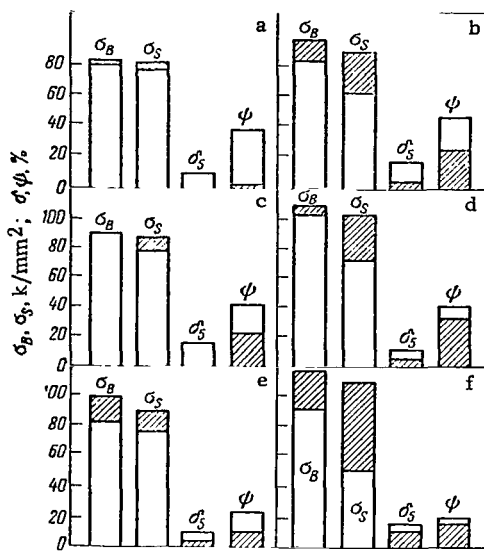


Figure 3. Properties of Alloys in Original Pre-deformation State and in Maximally Deformed State (Hatched Areas).

Figure	Annealing	Quenching-temperature, °C	ε _{max} %			σ_S/σ_B (original-deformed)
			ε ₁	ε ₂	ε ₃	
a	800° C, 1 hr	830	17	48	—	0.95-0.98
b	800° C, 1 hr	880	17	35	35	0.74-0.94
c	800° C, 1 hr	880	49	42	29	0.87-0.95
d	800° C, 1 hr	880	19	48	12	0.72-0.96
e	—	—	96	—	—	0.93-0.94
f	—	—	—	—	—	0.54-0.94

To this end, the mechanical properties of specimens of the alloy VT14 were investigated following quenching and annealing as well as following deformation by rolling (after quenching).

Noteworthy is the marked difference in the slope angles of the rectilinear segment of the diagram, corresponding to elastic deformation for annealed and quenched specimens. As the degree of prior deformation increases, the slope of the rectilinear segment also increases, but even at 30% deformation it does not reach the angle characteristic of annealed state.

A similar anomalous growth of elastic deformation was observed by Handros when investigating martensitic transformation in aluminum bronzes. The observed effect was explained as a result of macroscopically oriented displacement of micro-volumes having martensitic kinetics of transformation, due to the

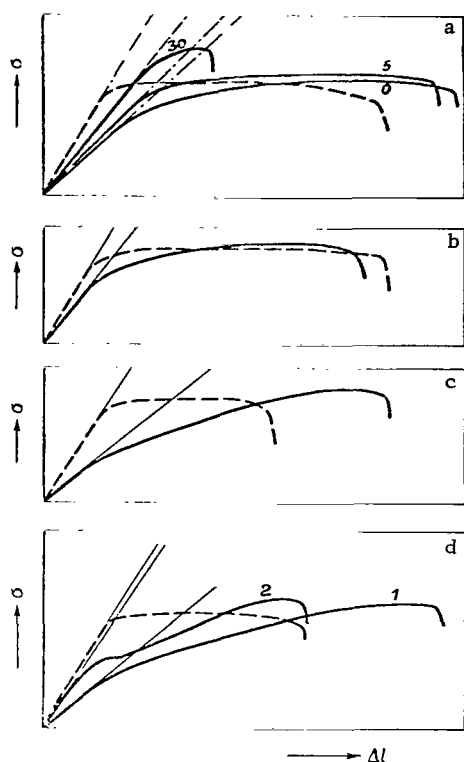


Figure 4. Tensile Diagrams of Specimens After Annealing (Broken Line) and After Quenching (Solid Lines).

a—VT14 Specimens Quenched With and Without Prior Deformation (Degree of Deformation in % is Shown by the Numerals on the Curves);
 b—VT8; c—TiAl 4.5V5Cr 1.5, Fe 1.5; d—TiAl 4.5V4Cr1.5, Tests were Conducted at Deformation Rates of 1 (1) and 20 (2) mm/min.

action of the external stress applied. The basis given for this explanation was the theories, developed in the works of Kurdumov, concerning the cooperative nature of the lattice rearrangement in martensitic transformations. Figure 5 shows the micro-structure of the quenched TiAl5V4Cr1.5Fe1.5 alloy following its 12% deformation (oriented growth of martensitic lamellae is readily visible). The peculiarity of martensitic transformation warrants regarding it as a possible independent mechanism of plastic deformation, since its realization requires the application of smaller stresses than those existing during slip and twinning. It is precisely the occurrence of the martensitic mechanism of plastic deformation that accounts for the drop in yield points within the temperature range of martensitic transformation.

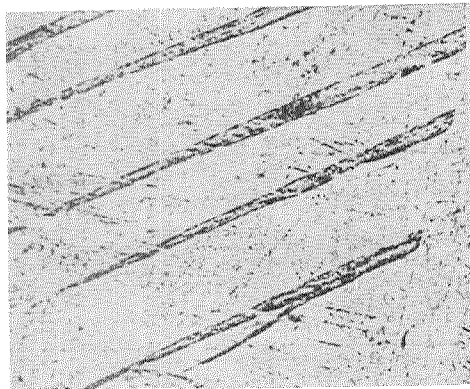


Figure 5. Microstructure of Quenched TiAl5V4Cr1.5, Fe1.5 Alloy Following 12% Deformation. Magnified 300 Times.

more or less broad (Fig. 4, a-c).

In particular, for the VT8 alloy this range is markedly narrower than for the VT14 and TiAl5V4Cr1.5Fe1.5 alloys; for the VT8 alloy following quenching the slope of the elastic-deformation segment of the curve becomes much smaller and the ratio σ_s/σ_B , higher. These findings indicate that the β phase of the alloy VT8 quenched from 880°C is relatively more stable when under static loading.

The deformation conditions during rolling are characterized not only by a distinctive stress pattern but also by a high rate of the deformation process itself which, as is known, can affect significantly the characteristics of the deformed material. To qualitatively assess the effect of increasing the deformation rate on the behavior of the investigated alloys under load, mechanical tests with 20-fold increase in the rate of advance of the moving clamp were carried out.

Figure 4, d presents the tensile diagrams of quenched specimens of the alloy TiAl5V4Cr1.5Fe1.5 (deformation rates during tests: 1 and 20 mm/min). For comparison the tensile strength curve of annealed metal is also presented. It can

Thus, the decrease in the slope angle of the elastic deformation curve, along with the collapse in σ_s , may be regarded as a proof of the presence in the structure of the alloy of a mechanically unstable phase undergoing martensitic transformation under load.

In the case considered here the slope of curves on the linear segment rises with increase in the degree of prior deformation, which points to a monotone course of the decrease in the amount of the β phase undergoing transformation.

The presented data give reason to believe that the process of decomposition of the β phase does not terminate during the initial stages of deformation and that the range within which it occurs can be

/260

be seen from Fig. 4, d that increasing the deformation rate by a factor of 20 already markedly alters the diagram: the slope at the beginning of the linear segment increases and an inflection point appears; the curve of the yield point reaches a plateau beyond which the slope of this curve increases, pointing to an increase in the hardening coefficient; elongation diminishes considerably.

From the presented data it follows that increasing the deformation rate reduces the deformation range within which the β -phase decomposes, displacing it chiefly in the direction of lower degrees of deformation. This leads to a rapid accumulation of decomposition products, the effect of which on the behavior of the material increases.

Table 2 presents the data of static mechanical tests characterizing the plasticity of the alloys and their deformability during cold rolling. For comparison, it also presents the values of the σ_s/σ_b ratio and data on phase composition in annealed and quenched states. /261

TABLE 2

Alloy	β , %	σ_s/σ_b	δ , %	ψ , %	ϵ_{max} , %
After quenching					
VT14	17	0,95	10,5	37	48
VT8	17	0,87	17,0	42,5	29
TiAl5V4Cr1.5Fe1.5	19	0,93	9,0	24,0	49
VT15	100	0,88	19,0	64,0	90
TiMo32	100	0,99	17,0	50,0	86
After quenching					
VT14	30	0,74	16,0	43	35
VT8	49	0,78	14,0	30,5	42
TiAl5V4Cr1.5Fe1.5	96	0,54	13,5	17,5	12
VT15	100	0,87	18,0	62,5	90
TiMo32	100	0,98	20,0	60,0	90

It can be seen from Table 2 that the highest plasticity in annealed and quenched states is displayed by the alloy VT15 and TiMo32 with a mechanically stable β -structure. The deformability of these alloys during rolling also is maximal. Then the σ_s/σ_b ratio is the highest, reaching 0.87 and 0.98 respectively.

The lowest deformability is displayed by the quenched alloy TiAl5V4Cr1.5Fe1.5, although in this (quenched) state it consists almost completely of the β -phase (96%) which moreover, in this alloy, displays the lowest mechanical stability ($\sigma_s/\sigma_b = 0.54$).

The highest deformability during rolling in the presence of a mechanically unstable β -phase in quenched state is displayed by the alloy VT8, an alloy whose

suitability for plastic deformation is the lowest when in annealed state. The amount of β phase in this alloy in annealed state is 17%, which practically equals its content in the two other alloys of this group. The low deformability level of this alloy in annealed state is probably due to its higher content of aluminum (6%, compared with 4.2% in the alloy VT14 and 4.5% in the alloy TiAl5V4Cr1.5Fe1.5; the deformability of the specimens of the last two alloys in annealed state is 48%. The higher deformability of the alloy VT8 in quenched state is associated with the increase in the amount of β phase in its structure, which apparently retains a higher mechanical stability than the β phases present in the other alloys of this group.

CONCLUSIONS

1. It was shown that the decrease in the σ_s/σ_b ratio and increase in unit elongation and concentration (reliable signs of the existence in the alloy structure of a mechanically unstable β phase) during the quenching of $(\alpha + \beta)$ -alloys of titanium do not necessarily point to satisfactory plasticity of the quenched alloys. In particular, this discrepancy is observed during plastic deformation under conditions of a high loading rate.
2. On deformation with a high loading rate the mechanically stable β phase assures a higher level of plasticity.
3. In some cases in the event of deformation at a high rate quenching may be applied to enhance the plastic properties of alloys of the VT8 type, with a high aluminum content. Then the amount of the β phase is increased without sharply reducing its mechanical stability.

REFERENCES

1. Jaffe, R. I. In the collection: Uspekhi fiziki metallov [Advances in Metal Physics], Vol. 4, No. 152, Metallurgizdat, 1961.
2. Glazunov, S. G. Metallovedeniye i termicheskaya obrabotka metallov [Metallography and Heat Treatment of Metals], Vol. 2, No. 2, 1963.
3. Moiseyev, V. N. and L. V. Geras'kova. Metallovedeniye i termicheskaya obrabotka metallov [Metallography and Thermal Treatment of Metals], Vol. 5, No. 5, 1965.

PROBLEMS OF THE WELDING OF TITANIUM AND ITS ALLOYS

/262

S. M. Gurevich

Modern technology has posed higher requirements for structural materials. Need has arisen for alloys displaying considerable high-temperature strength, resistance to corrosion in corrosive media and a number of other special properties. These requirements can be satisfied by using new metals and, primarily, titanium and its alloys. Within a short period of time, less than 20 years, titanium and its alloys have become accessible structural materials.

The effectiveness of the use of titanium and its alloys in industry largely depended on the successful introduction of their welding. Yet the welding of metals of this kind involves major difficulties due to the specific physicochemical properties of titanium and primarily to its high chemical activity at elevated temperatures and particularly in molten state, as well as to susceptibility to grain growth in heated state, structural transformations of alloyed titanium in the course of the thermal cycle of welding, which lead to the formation of brittle phases, etc.

The article briefly presents the results of the principal studies of the welding of titanium alloys carried out in recent years and points to the most urgent tasks in this field.

IMPROVEMENTS IN THE METHODS OF INERT GAS-SHIELDED WELDING. NEW METHODS AND TECHNIQUES OF CONSUMABLE- AND NONCONSUMABLE-ELECTRODE WELDING

The most common technique of the fusion welding of titanium and its alloys is inert gas-shielded welding. In recent years effective devices and attachments for automatic, semiautomatic and manual welding with consumable and nonconsumable electrodes (automatic and semiautomatic welding jigs, shielding sliders and chambers, torches, etc.) have been developed and introduced into production in this country. The new GOST All-Union State Standard for inert gas (GOST 10157-62), which specifies the provisions of brand-A argon, has contributed to improvements in the quality of welded joints. Airtight controllable-atmosphere chambers are increasingly used in the welding of titanium-alloy products. Positive experience has already been gained in the welding of products in large-sized chambers accommodating the welder himself. Chambers of this kind are highly effective for the welding of structural titanium-alloy elements by the manual method for which shielding of the reverse side of the weld (weld root) would otherwise be difficult if not impossible. As regards inert gas-shielded consumable-electrode welding, mention should primarily be made of the pulsed-arc welding technique. This new technique makes possible the welding under on-site conditions of joints located in various spatial positions (e.g. butt welds of tubes and columns in chemical machine building, etc.). The technique is based on control of magnetodynamic processes in the arc and, in particular, on application of drops of metal during melting of the electrode wire. Research carried out at the Institute of Electric Welding has made it possible to develop a new method for the programmed control of the formation of drops of the melting electrode and hence also of the dimensions and shape of the weld in any spatial position.



A diagram of the pulsed-arc consumable-electrode welding process is shown in Fig. 1. The application of powerful short current pulses of the d-c arc assures control of the formation of the drop of metal at the electrode tip.

/263

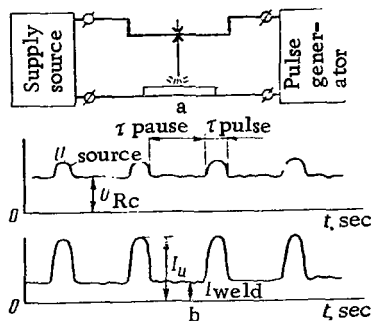


Figure 1. Diagram of the Process of Pulsed-Arc Consumable-Electrode Inert Gas-Shielded Welding (a) and Current Curves (b).

The use of an IIP-2 type pulse generator during the welding of titanium alloys with an electrode wire of 1.2-2 mm diameter has assured the application of one drop of metal for every current pulse. During non-pulsed (continuous) welding with 150-300 amp current the electrode metal gets spattered, the conditions for shielding the welding zone deteriorate and in the case of vertical welds the process is unstable. The employment of pulsed-arc welding, which made it possible to control, within certain limits, the transport of metal from the electrode tip to the weld pool, has practically completely eliminated spattering, stabilized the melting of the base metal and simplified the technology of the semiautomatic vertical welding. The periodic pulsed rise in arc current leads to a marked lowering of the lower limit of welding current during automatic and semiautomatic welding as well as to trans-

fer of metal in tiny drops. To titanium this is of particularly great significance from the standpoint of reliability of shielding of the welding zone. Our investigations have shown that the forced, oriented transfer of electrode metal during the welding of titanium alloys markedly improves the formation of welds produced by the semiautomatic method and makes possible semiautomatic welding in the vertical and even overhead positions. A difference in the microstructure of welds produced by the conventional argon-arc method and by the pulsed-arc method has been established. Thus, the metal of the weld of the Ti-based low-alloy composition AT-3, when applied by the pulsed-arc method is distinguished by the finely fragmented intragranular structure of the α' phase [1]. Further broadening of the range of applications of pulsed-arc consumable-electrode welding will make it possible to solve problems of importance to industry such as semiautomatic welding in various spatial positions without detriment to the high and stable quality of medium- and large-cross section metal weldments. Pulsed-arc nonconsumable-electrode welding assures a stable quality of thin ($\leq 2-3$ mm) alloy weldments [2].

Thus, for a pulse time of 0.2-0.3 sec and a pause time of 0.1-0.2 sec, the welding resembles a combination spot and lap welding, as it were, while at the same time markedly reducing the overheating of metal and the welding-induced deformations as well as, in a number of cases, improving the mechanical properties of the welded joint. Such a welding technique is highly promising for the fabrication of thinwalled structural elements of titanium alloys.

Of great importance to the further development of the fabrication of titanium and titanium-alloy weldments and particularly of weldments of high-strength heat-hardenable β alloys, is the new Soviet-developed method of submerged

argon-arc welding. Originally this method, which was proposed by O. A. Maslyukov, had been used only to eliminate weld porosity. This was accomplished by applying an extremely thin layer of a special single-component reagent to the surface of the edges to be joined.

Studies conducted at the Institute of Electric Welding showed that the use of special fluxes during nonconsumable-electrode welding makes it possible to markedly reduce the expenditure of running energy and to obtain narrower welds while at the same time considerably enhancing the depth of fusion and partially refining and inoculating the weld metal [3].

The requirements that must be met by the oxygen-free flux used in the non-consumable-electrode arc welding of titanium alloys also were established. The chief of these requirements are: good adhesion (liquid flux-solid titanium), correspondence between the melting and boiling points of the flux and the base metal, etc. These requirements are satisfied by certain systems of the fluorides and chlorides of alkali and alkali-earth metals.

/264

On the basis of these systems the fluxes AN-T15A, AN-T7A and others have been developed. These fluxes make it possible to produce with a single welding pass narrow non-V welds of ≤ 12 mm thick titanium on using 2.5-3 times less current than that required for conventional argon-arc nonconsumable-electrode welding. Figure 2 illustrates the decrease in running energy during the welding of 2-6 mm thick metal with the aid of fluxes of this kind.

Mechanized welding employing fluxes of the ANT-A series has passed pilot-industrial trials and has been introduced into the series production of weldments of titanium and a number of low-alloy compositions of titanium. Figure 3 presents the photograph of a spherical container welded from the alloy VT6S by the nonconsumable electrode method on using the flux ANT-15A.

/265

The rise in the cooling rate of the weld and near-weld zone due to the sharp decrease in the intensity of the current required to fuse the edges to be joined, as well as the refining and inoculating effect of the fluxes used, creates the conditions for favorable structural transformation in the weld metal of β -alloy of titanium (VT15) and precludes the formation of a second phase owing to the decomposition of the β phase in the post-welding state. Then the conditions for the formation of an intragranular chemical and structural inhomogeneity — which in the high-alloy composition VT15 may manifest itself in the formation of the intermetallic compound $TiCr_2$ and the depletion of chromium from the β -solid solution—also are eliminated. On using the fluxes it became possible for the first time to obtain, following a special postheating, a welded joint of VT15 alloy with an ultimate strength reaching 130 kg/mm 2 and satisfactory plasticity and impact strength.

The use of flux pastes makes it possible to solve a highly urgent task — the shielding of the weld root in relatively inaccessible sites in cases where shielding with inert gas is difficult or impossible.

New vistas are being opened by the deepened-arc method of welding medium- and large-cross section alloys, developed by A. P. Goryachev and associated [4].

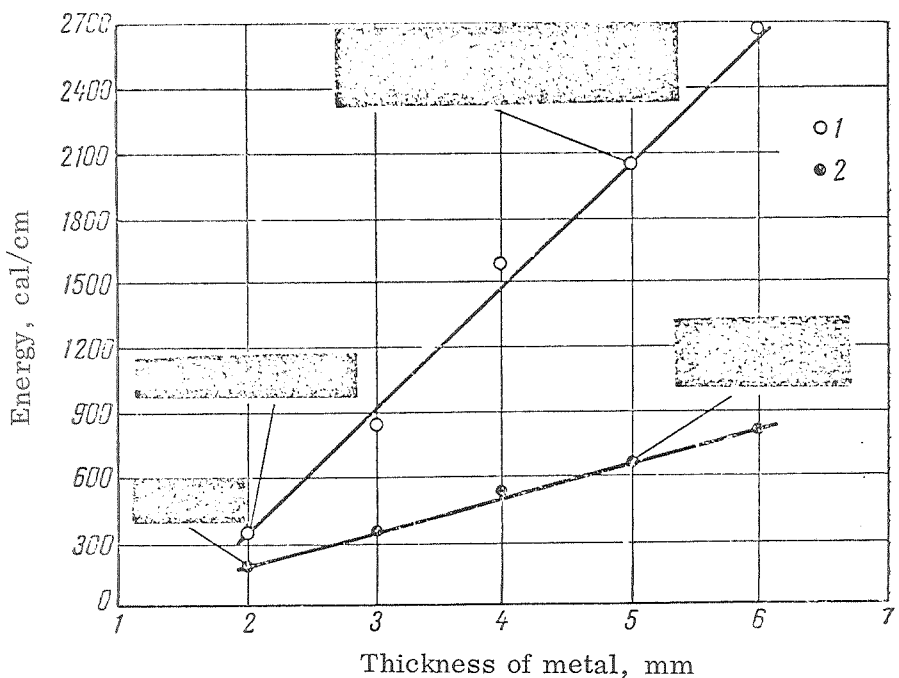


Figure 2. Expenditures of Running Energy and the Macrostructure of Weld During Welding of Titanium Without (1) and With the Use of Welding Flux (2).

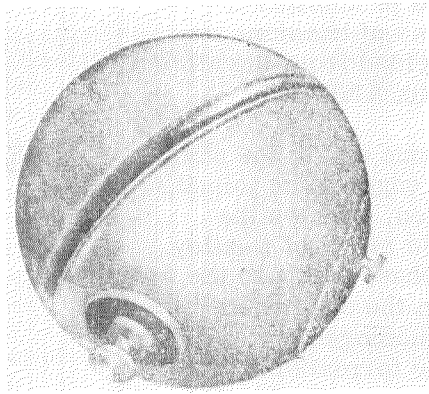


Figure 3. Container of VT6S Alloy, Wall Thickness 6 mm, Welded With a Nonconsumable Electrode in a Jet of Argon in the Presence of Welding Flux.

these fluxes are termed fluxes of the oxygen-free type. The principles for compounding these fluxes have been worked out and a new system of halogen fluxes of the ANT series has been developed, as has been, on their basis, an effective technology of the automatic submerged arc welding of titanium alloys of various thickness.

AUTOMATIC SUBMERGED ARC WELDING AND ELECTROSLAG WELDING

Initially it had been thought that of all the known methods of consumable-electrode welding only the inert gas-shielded method can be used to weld titanium. Foreign investigators, who based themselves on the experience of metallurgists who failed to find suitable materials for molds into which to cast titanium, due to its high chemical activity, denied the possibility of welding titanium by the submerged [flux] arc method.

Basic research, confirmed by experiments, made it possible to refute this opinion. The possibility of welding titanium under special refractory fluxes which contain practically no oxides was demonstrated;

The fluxes used to weld titanium must have sufficiently high melting and boiling points and they must assure protection against contamination with harmful impurities due to the possible highly intense exchange reactions between flux-slag and the weld metal, etc. In addition, fluxes of this kind, like any other welding fluxes, should assure a stable arc discharge during welding as well as produce a slag crust that can be readily separated following the completion of welding.

These requirements are most completely met by the fluxes based on pure chemical reagents of the refractory fluorides of alkali and alkali-earth metals treated with small amounts of chlorides.

Industry also employs the three-component fluxes ANT-1, ANT-3 and ANT-5 for medium-cross section welding of titanium and its alloys as well as the two-component flux ANT-7 for welding medium- and large-cross section metal.

Automatic submerged arc welding of titanium and its alloys is carried out with direct current of reverse polarity, on using standard supply sources and equipment. The automatic welding of titanium is characterized by high rates (as much as 50-60 m/hr), which is expedient for titanium from the standpoint of energy expenditures.

Automatic submerged arc welding is the principal technological process employed in welding the joints of equipment housings (longitudinal girth joints), as well as in flange welding, fabrication of large-diameter tubes, etc. The welding of products of technical titanium VT1 as well as of low-alloy titanium compositions has been mastered. Industry manufactures welded filters of various designs, including the LV-50T type large-size filters designed for the purification of molybdenum trisulfide slurry and chlorine-based corrosive suspensions, bag and bougie filters, pressure filters, mixers, electrolytic cells and other chemical equipment. Figure 4 shows a vessel of VT-1 titanium whose principal elements were welded automatically under ANT-7 flux.

/266

A major role in broadening the range of application of large-cross section titanium and its alloys has been played by the new method and equipment for electroslag welding [6]. Since, however, shielding with slag alone proved to be insufficient in assuring a satisfactory quality of joints welded by this method, a fundamentally new method of combined gas-slag welding had to be developed.

Electroslag welding of titanium and its alloys is carried out using the most refractory flux, ANT-2, having a high boiling point ($\sim 2500^{\circ}\text{C}$) which is particularly important to the electroslag process stability.

Industry has organized two methods for the electroslag welding of titanium alloys: the plate electrode method and the consumable guide-plate (plate-wire electrode) method. The former method is used to weld flanges, wheels, lids and other short-weld weldments reaching 150-200 mm in thickness.

The welding is carried out with the aid of an A-550 jig powered from a TShS-3000-1 transformer.

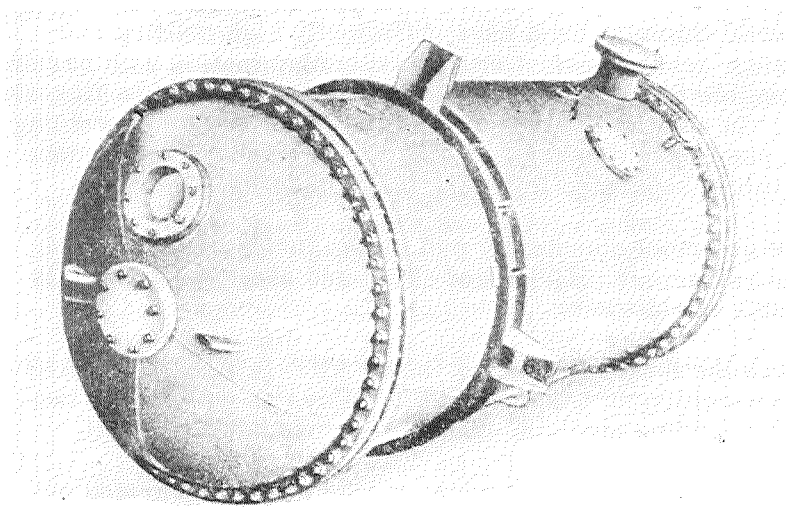
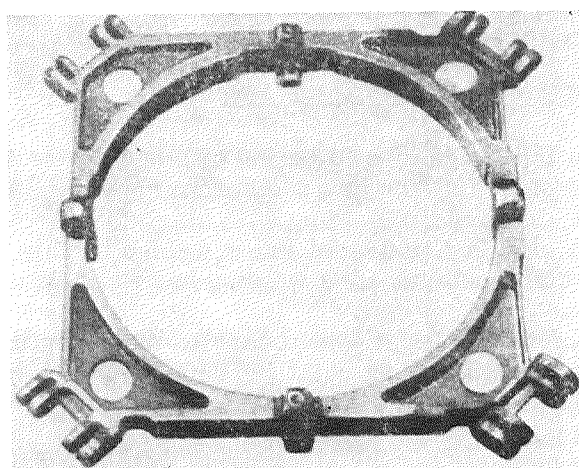


Figure 4. Apparatus Welded from VT-1 Technical Titanium.

At a chemical machine building plant this jug is used to weld flanges of the LV-50T filter from seven forged segments of VT1 alloy measuring 135x135 mm in cross section (outside diameter 2260 mm) and a ring of 60x120 mm forgings (outside diameter 800 mm). Butt joints are welded in an all-purpose R-939 water-cooled copper chill mold using a plate electrode of 8-12 mm thick titanium.



/267

Figure 5. Shaped Flange of Chemical Apparatus, Welded of OT-4 Alloy by the Electroslag Method.

Figure 5 presents a photograph of a weldment of this kind — a shaped OT4-alloy flange welded with the aid of an A-550 electroslag welding jig by the plate electrode method on using ANT-2 flux.

Consumable guide plate welding with the aid of the A-997 electroslag welding jig is applied to produce long welds of 200-250 mm thick titanium alloy. The jig is equipped with special attachments assuring reliable shielding with inert gas of the electrode and the slag and metal baths. Numerous studies of mechanical properties of large-cross section titanium welds produced by this method, carried out in laboratory and production conditions, showed that the strength of these welds equals the strength of the base metal and their plasticity and impact strength are satisfactory.

The problem is greatly complicated when it comes to arc and electroslag welding of high-strength titanium alloys. Using an unalloyed electrode in this case does not make it possible to obtain welds of a strength close to the strength of base metal.

Investigations showed that when the electrode used has the same composition as the base metal, the welds of certain high-strength alloys display low plasticity and impact strength. This raises a problem analogous to that which must be solved in the welding of alloy steels: the determination of the optimal chemical composition of the weld as well as a qualitative or quantitative alteration of its phase composition by means of postheating of the welded joint.

When selecting the weld composition in a number of cases (primarily as regards Ti-based single-phase α alloys and low-alloy ($\alpha + \beta$)-compositions) the alloying system can be preserved but the concentration of alloying elements in the weld metal decreases. The weld has an acicular, martensite-like structure characteristic of an alloyed α' phase, and hence its strength remains practically the same as the strength of the metal being joined. The plastic properties of the welds of certain alloys markedly increase when electrode wire of a composition different from that of the base metal is employed [7].

In large-cross section electroslag welding of two-phase alloys it is expedient to use composite plate electrodes or combined guide-plate electrodes. In the former case the electrode consists of strips of titanium alloy and unalloyed VT1 titanium in an optimal mutual ratio. In the latter case, wire of VT1 titanium is fed into the ducts in the consumable guide plate produced from the titanium alloy. Such a welding technique has been successfully used to weld a number of alloys [8].

/268

VACUUM WELDING

In recent years the welding of titanium and its alloys in vacuum chambers has been successfully employed. Of the methods of this kind the principal one is electron-beam welding, a variety of fusion welding which nevertheless qualitatively differs from all the other previously known methods. These differences stem from two principal causes: the use of a new powerful heat source and the practically total absence of gases around the welding zone.

A highly important feature of the electron flux used as the heat source is that the beam can be focused on an extremely tiny spot whose diameter is no larger than tenths of a millimeter. Such a concentration of energy, attainable by means of special focusing — contraction of the beam, makes possible welding

with unusual ratios between the weld width and the fusion depth (weld shape factors), e.g. 1:5, which cannot be attained by the electric-arc methods, as well as with narrow near-weld zones. Large-cross section welding by this method assures narrow and extremely deep fusion zones. "Dagger" welds of this kind make it possible to reduce the shape factor to as little as <0.1 .

Such a substantial reduction in the dimensions of the thermal influence zone is particularly important as regards titanium, a metal which is susceptible to grain growth when heated above the temperatures of its polymorphic transformation. The possibility of producing welded joints at a fraction of the running energy required by other methods such as arc welding, and the availability of a concentrated heat source make it possible to reduce to a minimum deformations of the joints being welded.

Vacuum welding eliminates the danger of the contamination of the weld with such harmful impurities as gases and assures a high plasticity and impact strength of welded joints. The electron-beam method can be used to produce butt, fillet and lap welds as well as flange joints. During welding by this method, by contrast with the arc in arc welding, the electron beam exerts only a negligible pressure on the molten weld pool, thus assuring satisfactory weld-formation even in cases where arc welding with a nonconsumable electrode does not make it possible to obtain uniform welds. For example, then it is possible to produce flanged girth welds with the flanged edges to be joined being parallel to the axis of rotation and the electron beam, perpendicular to this axis.

Welding with both continuous and intermittent application of the electron beam is possible. Pulsed electron beam welding of the latter kind can be applied during the welding of thinwalled titanium alloys.

Electron beam welding is applied under industrial conditions to weld not only small but large cross sections. Further improvements in electron beam guns and the development of all-purpose vacuum welding jigs will make it possible to broaden the range of applications of this promising welding method. As yet far from all the special features of the electron beam welding of titanium alloys have been elucidated. It is necessary to systematically investigate the effect of the principal elements of the process regime (current in beam, accelerating voltage, welding rate) on the weld parameters during medium- and large-cross section welding and to study the special features of thermal cycles as well as of the crystallization of narrow and deep welds during the welding of various types of titanium alloys, etc. It is likely that electron beam welding will become a means of fabricating structural members with joints of fundamentally new types.

An effective method for joining small-sized parts of titanium and titanium alloys is diffusion welding (diffusion bonding) [9, 11].

/269

The special feature of this process lies in the vacuum joining of metals without melting them, i.e. in welding under conditions which preclude the contamination of the joined surfaces with harmful impurities — gases, which is particularly important to such a chemically active metal as titanium.

The physicochemical properties of titanium, and primarily its mechanical properties at high temperatures, complicate the selection of optimal process parameters assuring minimal deformation of the parts being joined. However, research and production experience indicate that these difficulties are surmountable. Joints of technical titanium and a number of titanium alloys, whose welding is carried out by optimal technology display high mechanical properties and are successfully applied in important structural members.

The diffusion welding method makes it possible to solve problem of welding titanium to other structural metals. Direct welding of titanium to steel does not result in quality joints due to the formation of intermetallics which embrittle the zone of contact. To preclude the possibility of the formation of brittle phases, special interlayers are used. This makes it possible to obtain workable welded bimetal joints, for example, connecting tubes in piping, etc. Explosion welding also is highly promising for this purpose. This welding method, which utilizes the detonation wave, also requires the use of intermediate layers in order to join titanium to steel.

THE PROBLEM OF THE WELDABILITY OF TITANIUM ALLOYS AND SOME WAYS OF ITS SOLUTION

The assurance of the weldability of technical titanium has required the solution of a large number of problems, e.g. the fabrication of semifinished products (rolled stock electrode wire, etc.) with a limited content of harmful impurities (oxygen, nitrogen and hydrogen).

A major problem solved to be the susceptibility of welded joints to delayed fracture. Tightening the tolerances for the hydrogen content of the base metal as well as the introduction of the vacuum annealing of electrode wire with the object of its degassing made it possible to sharply enhance the resistance of weld metal to cold cracking.

In the welding of technical titanium the cardinal prerequisite for obtaining welded joints of satisfactory quality was the assurance of purity of the welding materials and reliable protection of the welding zone against interaction with ambient gases; in the welding of titanium alloys this condition, while also mandatory but, is no longer insufficient. Not infrequently there arise serious complications due to the specific nature of crystallization and structural transformations occurring in the weld metal and near-weld zone of alloyed titanium.

During the crystallization of titanium-alloy weld joints interacrustalline inhomogeneity may result in intensifying the tendency to embrittlement due to the formation and decomposition of metastable phases.

The patterns and nature of structural inhomogeneity in titanium-alloy welds still have not been adequately investigated. However, the results of certain investigation make it possible even now to point to the great significance of this matter. For example, consider the vanadium-rich boundary regions of crystallites during the electroslag welding of the VT6 alloy (system Ti-Al-V); the segregation of α phase along grain boundaries in the welds of titanium alloys

containing 6% Mn; the segregation of the intermetallic compound $TiCr_2$ in the boundary zones of crystallites of welds of the high-alloy β composition VT15, etc.

In addition to the customary transformations associated with the recrystallization of titanium, in alloyed titanium welds there may occur structural changes of another type. This primarily refers to the formation of the embrittling ω -phase. This phase, detectable electronmicroscopically, is usually encountered in welded joints in the form of round or, more often, elongated inclusions and it may occur in two cases: 1) directly following the welding of two-phase alloys having a concentration of a β -stabilizer that, though high, is still insufficient for complete stabilization of the β phase (e.g. alloys treated with Mn, V, etc.); 2) following the quenching and subsequent tempering (aging) of the welded joint.

/270

When selecting the optimal conditions for the heat treatment of welded joints, emphasis must therefore be placed on precluding the possibility of embrittlement as well. In a number of cases (e.g. as regards the alloy VT15) the regimes of heat treatment of the welded joints may differ from the regimes recommended for the base metal. Single-phase α alloys and low-alloy $\alpha + \beta$ compositions of titanium are mainly welded by the same regimes as technical titanium. In recent years, alloys of this type (VT5-1, OT4, OT4-1, ATZ, etc.) have been developed and are used in the fabrication of structural weldments. As the amount of metastable β phase increases, the susceptibility of the alloy to the variation in welding regime increases, the plasticity and impact strength of the welded joints markedly decrease and susceptibility to cold cracking of weld metal and near-weld zone increases; therefore, the welding of Ti-based high-strength $\alpha + \beta$ alloys entails additional complications; many of these alloys display limited or poor weldability. One effective way of improving weldability is treating the alloy with heterogeneous elements. For example, consider the alloys of the AT series, developed by I. I. Kornilov and associates. High-strength single-phase α alloys treated with an α -stabilizer (aluminum) and neutral hardeners (tin and zirconium) are satisfactorily weldable and highly promising.

A most complex aspect of the general problem of the weldability of titanium alloys proved to be the obtaining of high-strength and plastic welds of thermally hardenable β alloys of titanium (VT15, V 120VSA, etc.).

The welding of these alloys involves major difficulties due to the possibility of the formation in the welds and near-weld zones of intermediate brittle phases (ω phase, intermetallics of the $TiCr_2$ type) under the action of the thermal cycle of welding. During subsequent hardening heat treatment of the resulting welds with their macrocrystalline cast-metal structure characterized by microchemical inhomogeneity, the products of decomposition of the β phase embrittle the weld to an even greater degree while the strength of the weld is only slightly enhanced.

Thus, to obtain β -alloy welded joints of satisfactory quality it is necessary to determine not only the most favorable conditions of welding but also the optimal techniques of the hardening heat treatment of the welded joints.

For the alloy VT15 this problem can be solved by resorting to nonconsumable-electrode inert gas-shielded welding in the presence of an inoculating and refining

flux, as well as to hardening heat treatment precluding quenching [13]. To improve the weldability of Ti-based β alloys it is necessary to further refine the methods of their heat treatment with the object of limiting the gas concentration to a minimum and enhancing the stability of properties.

REFERENCES

/271

1. Gurevich, S. M., N. V. Podola and A. F. Tetervak. Impul'sno-dugovaya svarka titanovogo splava AT3 [Pulsed Arc Welding of AT3 Titanium Alloy], Avtomicheskaya Svarka, No. 5, 1966.
2. Petrov, A. V. and G. V. Slavin. Issledovaniye tekhnologicheskikh vozmozhnostey impul'snoy dugi [Study of the Technological Potential of the Pulsed Arc], Svarochnoye Proizvodstvo, No. 2, 1966.
3. Gurevich, S. M., V. N. Zamkov and N. A. Kushnirenko. Povysheniye effektivnosti poplavleniya titanovykh splavov pri argonodugovoy svarke [Increasing the Effectiveness of the Fusion of Titanium Alloys During Argon Arc Welding], Avtomicheskaya Svarka, No. 9, 1965.
4. Goryachev, A. P. and V. A. Zelenin. Mekhanizirovannaya svarka neplavyashchimsya ugлublennoy dugoy [Mechanized Nonconsumable-Electrode Deepened-Arc Welding], Avtomicheskaya Svarka, No. 12, 1964.
5. Gurevich, S. M. Nekotoryye osobennosti svarki titana pod flyusom [Certain Features of Submerged Arc Welding of Titanium], Avtomicheskaya Svarka, No. 5, 1967.
6. Gurevich, S. M. and V. P. Didkovskiy. Nekotoryye voprosy elektroshlakovoy svarki titana [Certain Problems of the Electroslag Welding of Titanium], Avtomicheskaya Svarka, No. 3, 1957.
7. Gurevich, S. M., N. A. Kushnirenko and V. Ye. Blashchuk. Puti polucheniya vysokoprochnykh titanovykh shvov bez uprochnyayushchey termicheskoy obrabotki [Ways of Obtaining High-Strength Titanium Welds Without Hardening Heat Treatment], In the collection: Novyye issledovaniya titanovykh splavov [New Studies of Titanium Alloys], Nauka Press, 1965.
8. Kompan, Ya. Yu. Elektroshlakovaya svarka titanovogo splava BT10 [Electro-slag Welding of the Titanium Alloy VT10], Avtomicheskaya Svarka, No. 4, 1965.
9. Kazakov, N. F., A. P. Shishkova and K. Ye. Charukhina. Soyedineniye titana diffuzionnoy svarkoy v vakuum [Vacuum Diffusion Welding of Titanium], Avtomicheskaya Svarka, No. 10, 1963.
10. Gorshkov, A. I. and F. Ye. Tret'yakov. Svarka pogruzhennoy dugoy titanovogo splava VT6C [Submerged Arc Welding of the Titanium Alloy VT6S], Svarochnoye Proizvodstvo, No. 1, 1966.
11. Kharchenko, G. K. Diffuzionnaya svarka [Diffusion Welding], Avtomicheskaya Svarka, No. 2, 1965.
12. Nazarov, G. V. and M. Kh. Shorshorov. Kharakteristiki svarivayemosti splavov titana AT3, AT4, AT6 and AT8 [Weldability Characteristics of the Titanium Alloys AT3, AT4, AT6 and AT8], In the collection: Titan i yego splavy [Titanium and Its Alloys], No. 7, USSR Acad. Sci. Press, 1962.
13. Gurevich, S. M., et al. Nekotoryye prichiny snizheniya plastichnosti svarnykh soyedineniy splava VT15 posle zakalki [Certain Causes of the Decrease in the Plasticity of Welded Joints of the Alloy VT15 Following Quenching], Avtomicheskaya Svarka, No. 8, 1966.

ABSTRACTS

UDC 669.295+661.882

Status and Developmental Prospects of the Production of Titanium Sponge, N. P. Sazhin, In the collection: Titanium Alloys for New Technology, Nauka Press, 1968, pp. 5-10.

The history of the development of titanium metallurgy as an autonomous branch of industry is presented. Problems of the creation of the principal technological processes are elucidated on selecting as the main orientation the chlorine method of processing the raw material. The chief tasks facing the titanium industry are formulated,

1 table, bibliography of 33 titles.

UDC 669.295

Status and Developmental Prospects of the Production of Ingots and Semifinished Products of Titanium alloys, A. F. Belov, In the collection: Titanium Alloys for New Technology, Nauka Press, 1968, pp. 10-13.

Certain most important problems in the development of the production of rolled titanium alloy stock are considered. The principal tasks of titanium production are substantiated: further expansion of the output of sponge and rolled stock, a sharp increase in the operating economy of production and a reduction in prices.

UDC 669.295

Modern Titanium Alloys, S. G. Glazunov, In the collection: Titanium Alloys for New Technology, Nauka Press, pp. 13-23.

A critical review of the specifications for titanium alloys existing in the USSR, United States and Great Britain is presented. The main trends of the development of titanium alloys are described and certain results of investigations of delayed fracture, cracking sensitivity and diagrams of stressed state are presented.

7 tables, 4 illustrations.

UDC 669.295+546.821

Status and Prospects of Research Into the Metal Chemistry of Titanium, I. I. Kornilov, In the collection: Titanium Alloys for New Technology, Nauka Press, 1968, pp. 24-34.

The principal results of studies of the metal chemistry of titanium are presented and the tasks of further research in this direction are outlined.

In addition, the methods of compounding and specific compositions of titanium-base alloys that remain highly plastic at cryogenic temperatures, as well as of high-strength, high-temperature and corrosion-resistant alloys and also of materials with special physical properties are examined.

2 tables, 7 illustrations, bibliography of 37 titles.

UDC 669.295

Certain Problems of Improving the Production Technology and Quality of Semi-finished Titanium Alloy Products, G. D. Agarkov, N. F. Anoshkin, V. I. Dobatkin, I. N. Kaganovich, V. A. Tsytsenko, In the collection: Titanium Alloys for New Technology, Nauka Press, 1968, pp. 35-38.

The results of refinements in the production technology and improvements in the quality of semifinished products are assessed. Main trends of the further development of production are discussed. The possibilities for expanding the production of stampings instead of forgings, welded wheels instead of forged and rolled wheels, and also of rolled rods, welded tubes and intricately shaped castings are considered. The rolling of merchant shapes as the most progressive method for fabricating semifinished products and intermediate billets of titanium alloys is analyzed. Problems of eliminating metallurgical defects in ingots, improving the surface quality of semifinished products, reducing the grain size of the structure of hot-deformed products and stabilizing and increasing properties are examined.

UDC 621.78.669.295

Heat Treatment of Titanium and Its Alloys, V. A. Livanov, B. A. Kolachev, N. S. Lyasotskaya, In the collection: Titanium Alloys for New Technology, Nauka Press, pp. 39-50.

The work establishes the heat treatment regimes of titanium alloys.

The authors examine the formation of metastable phases in titanium alloys (titanium with molybdenum and VTZ-1) on cooling from the β -phase region as well as the kinetics of their formation in the process of aging.

Diagrams of isothermal transformations of titanium alloys in relation to the content of β -isomorphic stabilizers are presented. Regimes of heat treatment of the alloys VT-15 and VTZ-1 are substantiated.

6 illustrations, bibliography of 26 titles.

UDC 621.78+621.77+699.295

Thermomechanical Treatment of Certain Titanium Alloys, I. M. Pavlov, A. Ye. Shelest, Yu. F. Tarasevich, In the collection: Titanium Alloys for New Technology, Nauka Press, 1968, pp. 51-61.

The effect of thermomechanical treatment on the strength and plasticity properties of α' -, $(\alpha+\beta)$ - and β -alloys of titanium is investigated. The variation in mechanical properties of single-phase titanium alloys is then found to be insignificant. In two-phase alloys the strength and plasticity properties increased. The high-alloy compositions based on two-phase Ti corresponded to a marked strengthening effect of thermomechanical treatment. It was established that the increase in the plasticity following thermomechanical treatment is associated with the variation in the pattern and nature of fracture in tensile-test specimens. Aspects of fracture during thermomechanical treatment are investigated.

8 illustrations, bibliography of 25 titles.

UDC 669.295

Problem of Utilizing Titanium Wastes and Secondary Titanium, A. I. Kanyuk, E. M. Strikha, O. M. Shapovalova, In the collection: Titanium Alloys for New Technology, Nauka Press, 1968, pp. 62-68.

The problem of utilizing the wastes of titanium industry, the quantities of which increase with each year, is considered. It is shown that the utilization of the wastes of titanium production makes it possible to reduce the cost of titanium ingots and to save a large amount of valuable alloying elements.

At present about one-third of all titanium wastes is utilized for the need of ferrous metallurgy, but such utilization is inefficient. The most efficient solution is the utilization of the wastes to produce secondary alloys of a composition close to that of the original raw material.

Bibliography of 9 titles.

/275

UDC 669.295

Status and Prospects for the Introduction of Titanium in Certain Branches of the National Economy, A. I. Kanyuk, E. M. Strikha, N. F. Ivanova-Stepanova, In the collection: Titanium Alloys for New Technology, Nauka Press, 1968, pp. 68-74.

The economic effectiveness of the introduction of titanium into various branches of the national economy is considered. The utilization of titanium as a corrosion-resistant metal (in the metallurgical, galvanotechnical, chemical and certain other branches of industry) is analyzed.

UDC 699.295+621

Prospects for the Application of New Titanium Alloys in Chemical Machine Building, Yu. M. Vinogradov, In the collection: Titanium Alloys for New Technology, Nauka Press, 1968, pp. 74-77.

Examples of successful operation of titanium-alloy apparatus in chemical machine building are presented. The corrosion resistance and possible range of applications of new alloys of titanium with molybdenum, with molybdenum and niobium, and also with tantalum, are described.

2 tables, 3 illustrations.

UDC 669.017.11

Phase Diagram of the Ternary System Ti-Al-V (up to 45% Al), I. I. Kornilov, M. A. Volkova, In the collection: Titanium Alloys for New Technology, Nauka Press, 1968, pp. 78-89.

Alloys of the ternary system Ti-Al-V containing 0-45% Al are investigated by methods of thermal, microstructural and x-ray analysis as well as of resistivity and hardness measurements.

Isothermal sections of the system are constructed for 1100, 800, 550°C, as are polythermal sections starting from the pure-Ti vertex, for Al/V ratios of 3:1, 1:1 and 1:3. The following phases are identified in the system: α , α_2 (Ti₃Al), β , γ (TiAl), δ (V₃Al). It is established that the phases γ and δ exist in equilibrium.

3 tables, 9 illustrations, bibliography of 11 titles.

UDC 669.017.11

Study of Phase Equilibrium and Certain Properties of Titanium-Rich Alloys of the System Ti-Al-Mo-Zr, I. I. Kornilov, N. G. Boriskina, M. A. Volkova, In the collection: Titanium Alloys for New Technology, Nauka Press, 1968, pp. 89-97.

Alloys of the system Ti-Al-Mo-Zr containing up to 30% Al + Mo + Zr are investigated by methods of microstructural and x-ray analysis and resistivity and hardness measurement.

The compositions of the alloys investigated were selected from two cross sections of the tetrahedron passing through the edge Ti-Al and the face Ti-Mo-Zr, with Mo/Zr ratios of 3:1 and 1:3 over the sections with 3, 6, 9, 12, 16 and 22% Al.

Isothermal sections of the system are constructed at 1100, 800 and 500°C. The existence of α -, β - and α_2 (Ti₃Al)-solid solutions and corresponding two- and three-phase regions is established.

1 table, 5 illustrations, bibliography of 7 titles.

UDC 669.017.11

Study of the Equilibrium and Properties of the Ti_3Sn -(Ti+5% Zr) section of the system Ti-Zr-Sn, N.I. Shirokova, T.T. Nartova, In the collection: Titanium Alloys for New Technology, Nauka Press, 1968, pp. 97-101.

The interaction between the intermetallic compound Ti_3Sn and the solid solution of Ti + 5% Zr is investigated for alloys prepared by the melting method in a helium-atmosphere arc furnace and remelting in suspended state.

A polythermal section from the composition of the Ti_3Sn compound to the composition of the Ti + 5% Zr alloy is constructed with the aid of methods of microstructural and thermal analyses. The established nature of chemical interaction of titanium with zirconium and tin resembles the interaction between titanium and the compound Ti_3Sn in the binary system Ti-Sn, as confirmed by investigation of the resistivity and hardness of various alloy compositions.

3 illustrations, bibliography of 9 titles.

UDC 669.017.11

Study of the Phase Equilibrium and Properties of Alloys of the Titanium Corner of the System Ti-Zr-Al, N.I. Shirokova, T.T. Nartova, In the collection: Titanium Alloys for New Technology, Nauka Press, 1968, pp. 101-106.

Two polythermal sections in the part of the system Ti-Ar-Al adjoining the Ti-Al side are constructed with the aid of methods of thermal and microstructural analysis: 1) radial, from the Ti + 5% Zr composition to the compound Ti_3Al ; 2) parallel to the Ti-Al side with 5% Zr.

It is established that interaction between titanium and zirconium and aluminum over both cross sections resembles the interaction between titanium and aluminum in the binary system Ti-Al. The established nature of chemical interaction of the components is confirmed by investigation of properties of the alloys.

With the aid of the centrifugal method of bending tests at $700^{\circ}C$ it is established that the maximum high-temperature strength is displayed by the alloy with 5% Zr and 9% Al.

6 illustrations, bibliography of 12 titles.

UDC 669.017:539.4+669.295

/276

Nature of the Hydrogen Embrittlement of Titanium and Its Alloys, B.A. Kolachev, V.A. Livanova, In the collection: Titanium Alloys for New Technology, Nauka Press, 1968, pp. 106-119.

A classification of the types of the hydrogen brittleness of metals, based on the origin of the sources of this brittleness, is presented.

Analytic formulas relating the basis parameters which determine hydrogen brittleness of titanium and its alloys are presented.

2 tables, 8 illustrations, bibliography of 26 titles.

UDC 669.017+669.295

Metastable Phases in Titanium Alloys, L. A. Petrova, In the collection: Titanium Alloys for New Technology, Nauka Press, 1968, pp. 119-131.

The published literature as well as the author's data on metastable phases in titanium alloys are examined. Depending on the β -alloying elements forming the eutectoid or isomorphic to β -Ti, the metastable α' , ω and β phases or α' , α'' , ω and β phases form in titanium alloys.

The martensitic α' phase has, like α -Ti, a hexagonal close-packed lattice, while the α'' phase, although it has a martensitic structure like the α' phase, displays a rhombic lattice; the ω phase occurs during quenching, its mechanism of formation is non-diffusive and it has a hexagonal structure; the β -solid solution forms in alloys in the presence of a specific electron concentration averaging 4.2 el./at.

1 table, bibliography of 51 titles.

UDC 669.017+669.295

Phase Transformations in Titanium Alloys Under Nonequilibrium Conditions, M. A. D'yakova, I. Ye. Bogachev, In the collection: Titanium Alloys for New Technology, Nauka Press, 1968, pp. 131-137.

The principal conditions for the formation of the metastable α' , α'' and ω phases in alloys of titanium with transitional elements are examined. It is shown that the metastable phases display a lower free energy than the high-temperature phase. The decomposition of β phase, which may occur through diffusive and nondiffusive displacement mechanisms, as well as due to an intermediate transformation, is examined. Depending on the temperature intervals, three stages of transformation are specified, as illustrated with a corresponding isothermal decomposition diagram of the β phase.

UDC 621.78:669.295

Effect of Tin and Zirconium on the Transformation Accompanying the Heat Treatment of the Alloy Ti+10%Cr, L. P. Luzhnikov, V. M. Novikova, A. P. Mareyev, I. S. Orlova, In the Collection: Titanium Alloys for New Technology, Nauka Press, 1968, pp. 137-145.

The effect of the α -stabilizers Sn (up to 14%) and Zr (up to 16%) on the transformations accompanying the heat treatment of the alloy Ti+10% Cr (0.15-0.17% O₂) is investigated.

The dilatometric method, the method of constructing kinetic curves of aging and of recovery during aging and partly also the method of metallographic analysis were employed.

The presence of 1% Sn or 2% Zr suppresses the formation of ω phase during quenching. Treatment with Sn and Zr to the maximum amounts practically does not harden the alloy in quenched state. A similar effect is produced by treatment with Al.

Tin and zirconium affect very significantly the processes of the decomposition of β -solid solution of the alloy during aging.

However, the maximum hardening that can be attained by the quenching and a aging of the alloy treated with Sn and Zr is no higher than the hardening of the alloy not treated with these elements.

The most marked effect on the processes of transformation during the aging of the investigated β alloy is produced by Sn and a less marked effect, by Zr and Al.

Tin and zirconium, along with aluminum, should find application as alloying elements for β -alloys.

2 tables, 6 illustrations, bibliography of 2 titles.

UDC 669.017+669.295

Study of Phase and Structural Transformation in Two-Phase Industrial Alloys,
M. I. Yermolova, E. V. Polyak, O. P. Solonina, In the collection: Titanium Alloys for New Technology, Nauka Press, 1968, pp. 145-154.

With the aid of x-ray structural and electronmicroscopic methods of analysis the phase transformations accompanying the quenching and aging of the titanium alloys VTZ-1, VT8, VT14 and VT16 are investigated.

In the investigated alloys were discovered three regions such that water-quenching from these regions results in fixing of the metastable phases β , α'' and α' , respectively. Depending on the degree of treatment with molybdenum these regions get displaced in position. The decomposition of the metastable phases β , α'' and α' owing to aging at 400-600°C leads to a rise in the hardness of the alloys, which is attributable to the formation of a fine-disperse mixture of α - and β -phases (according to electronmicroscopic examination); the β -phase decomposes at a lower temperature than the α'' and α' phases.

2 tables, 5 illustrations, bibliography of 12 titles.

UDC 621.78:669.295

Variation in the Amount and Composition of β Phase During Heat Treatment of the Alloy VTZ-1, Ye. I. Gus'kova, N. F. Lashko, L. M. Mirskiy, In the collection: Titanium Alloys for New Technology, Nauka Press, 1968, pp. 154-159.

The variation in the amount, composition and dispersity of the β phase electrolytically isolated from the $(\alpha + \beta)$ -titanium alloy VTZ-1 following quenching from 870 and 1000°C, as well as following high-temperature thermomechanical treatment and aging at 550°C, is investigated; following high-temperature thermomechanical treatment the β phase is more disperse than following conventional quenching.

Aging results in the decomposition of the $\alpha(\alpha'')$ phase into $(\alpha + \beta)$ phases; the residual β phase during aging coagulates and gets enriched with β -forming elements (Cr, Mo, Fe).

/277

UDC 621.78:669.017+669.295

Decomposition of Titanium-Vanadium Martensite During Heating, S. G. Fedotov, K. M. Konstantinov, Ye. P. Sinodova, In the collection: Titanium Alloys for New Technology, Nauka Press, 1968, pp. 159-164.

The decomposition of titanium-vanadium martensite during heating is investigated. This decomposition occurs by a displacive mechanism, within a specific range of temperatures. The start and end points of decomposition are determined by the chemical composition of martensite. As supersaturation increases, the start point of decomposition decreases.

The temperature of martensite decomposition during heating is closely linked to the temperature of martensite formation during quenching of the alloys.

The aging of martensite results in a marked hardening of alloys.

1 table, 5 illustrations, bibliography of 6 titles.

UDC 669.017:539.4:699.295

Study of Alloys of the System Ti-Al-Mo-Zr by the Bending Method at Elevated Temperatures, N. G. Boriskina, M. A. Volkova, In the collection: Titanium Alloys for New Technology, Nauka Press, 1968, pp. 164-171.

Alloys of the system Ti-Al-Mo-Zr, containing up to 30% (Al-Mo-Zr) were investigated by the centrifugal bending method under a load of 15 kg/mm² at 550, 600, 700 and 750°C. The compositions of the investigated alloys were selected from two cross sections of the tetrahedron passing through the Ti-Al edge and the Ti-Mo-Zr face with Mo/Zr ratio of 3:1 and 1:3 for the sections with 3, 6, 9, 12, 16 and 22% Al.

It is established that the alloy compositions with the greatest high-temperature strength are located in the neighborhood of the phase interfaces $\alpha/(\alpha + \beta)$ or $(\alpha + \alpha_2)/(\alpha + \alpha_2 + \beta)$ in the presence of a small amount of 1 phase.

4 illustrations, bibliography of 4 titles.

UDC 669.017:620.17

Study of the Properties of alloys of the Systems Ti-Zr and Ti-Zr-Al, Ye. A. Borisova, I. I. Shashenkova, In the collection: Titanium Alloys for New Technology, Nauka Press, 1968, pp. 171-176.

The work deals with alloys of titanium with 2, 4, 8, 12, 20, 40 and 65% Zr, without aluminum or containing 4, 6 and 7% Al.

All the alloys were vacuum-annealed and then subjected to tensile tests at (-196)-(+700°C). Impact strength and Rockwell hardness were determined at room temperature. The temperature boundaries of phase regions of alloys of the systems Ti-Zr and Ti-Zr-Al were determined by metallographic and dilatometric methods, as was the coefficient of linear thermal expansion for the alloys Ti-Zr.

The conducted investigation revealed that the alloys of the system Ti-Zr-Al containing 2-4% Al and 4-8% Zr are the most promising for further study with the object of developing a highly plastic alloy with $\sigma_B = 80-90$ kg/mm².

Alloys containing 6% Al and up to 20% Zr may prove to be promising for prolonged performance at $\leq 500\text{-}600^{\circ}\text{C}$.

2 tables, 6 illustrations, bibliography of 4 titles.

UDC 669.018.45:669.295

Certain Problems of the Physicochemical Theory of High-Temperature Strength and the New High-Temperature Titanium Alloys ST-1, ST-3, ST-4 and ST-5, T. T. Nartova, In the collection: Titanium Alloys for New Technology, Nauka Press, 1968, pp. 176-186.

In accordance with four basic types of equilibrium diagrams four types of "composition—high-temperature strength" diagrams are established. Binary titanium alloys are divided into these types according to the nature of the effect of alloying elements on the high-temperature strength of titanium. The established pattern of variation in the high-temperature strength of binary titanium systems is of significance to research into multicomponent titanium systems and to the determination of the optimal compositions of new high-temperature titanium alloys.

The phase structure and mechanical and high-temperature properties of the alloys ST-1, ST-3, ST-4 and ST-5, developed on the basis of multicomponent titanium systems for performance at temperatures exceeding 600°C , are investigated.

3 tables, 4 illustrations, bibliography of 16 titles.

UDC 669.018.8

Corrosion-Resistant Alloy of Titanium With 32% Mo, N. F. Anoshkin, N. G. Boriskina, P. B. Budberg, L. A. Yelyutina, S. I. Kushakevich, I. D. Nefedova, Ye. I. Oginskaya, Yu. M. Sigalov, G. L. Shvarts, In the collection: Titanium Alloys for New Technology, Nauka Press, 1968, pp. 186-195.

The results of an investigation of certain technological and mechanical properties of the alloy TM32, which is corrosion resistant in hydrochloric-acid media at high temperatures, are presented. Data on the thermal stability as well as weldability of this alloy also are given.

7 tables, 3 illustrations, bibliography of 6 titles.

UDC 669.018.45:699.295

Basic Properties of the Titanium Alloy AT-3 and the Prospects for Its Application, I. I. Kornilov, K. P. Markovich, V. S. Mikheyev, In the collection: Titanium Alloys for New Technology, Nauka Press, 1968, pp. 195-201.

The stress-rupture strength, creep and thermal stability of the titanium alloy AT-3 at 300, 350 and 400°C for 15,000-20,000 hr are investigated. Curves of stress-rupture strength and creep at 350 and 500°C under various loads are constructed. It is established that at 350°C the alloy displays a high stress-rupture strength which is close to its ultimate short-time strength (at 350°C

$\sigma_{10,000} = 56 \text{ kg/mm}^2$, $\sigma_B = 60 \text{ kg/mm}^2$). This points to insignificant softening of the alloys under conditions of prolonged creep at 350°C . Creep rate at this temperature is relatively independent of load.

During prolonged aging at $350\text{--}400^\circ\text{C}$ for 10,000 hr no embrittlement occurs. The strength and plasticity of the alloy remain unchanged.

4 tables, 6 illustrations, bibliography of 8 titles.

UDC 669.017:539.219.3

Diffusion Parameters of Oxygen in β -Ti, L. F. Sokiryanskiy, L. V. Ignatov, A. Ya. Shinyayev, I. V. Bogolybova, V. V. Latsh, M. S. Model', In the collection: Titanium Alloys for New Technology, Nauka Press, 1968, pp. 201-210.

The diffusion of oxygen in β -titanium at $950\text{--}1150^\circ\text{C}$ is investigated by the layer analysis method. The oxygen concentration was determined according to variation in the crystal lattice parameter. The results of the determination of diffusion coefficients D within the investigated range of temperatures are described by the equation

$$D_\beta = 0.63 \exp(-37,000/RT) \text{ cm}^2/\text{sec.}$$

This equation is satisfied for technical-purity titanium as well as for titanium purified by the iodide process. As shown by analysis of the structure of the obtained diffusion zones, oxygen diffusion in the α region of titanium proceeds more slowly than in the β region.

1 table, 8 illustrations, bibliography of 18 titles.

UDC 669.162.282:669.295

Magnesium Reduction of Titanium from Tetrachloride, N. P. Sazhin, S. V. Ogurtsov, K. N. Pavlova, V. L. Russo, V. S. Mirochnikov, Yu. N. Ol'khov, B. S. Gulyanitskiy, M. A. Losikova, V. D. Savin, In the collection: Titanium Alloys for New Technology, Nauka Press, 1968, pp. 211-222.

As a result of laboratory and industrial studies carried out over a broad range of temperatures and pressures, with simultaneous admission of reagents, on employing new specially developed test methods, the theories of the mechanism of the magnesium reduction of titanium from TiCl_4 are confirmed and markedly complemented. It is shown that this process is of an autocatalytic nature and may occur in the kinetic and diffusion regions of heterogeneous catalysis.

Under industrial conditions the relationship between the physical characteristics of titanium sponge and the principal technological parameters of the reduction process was determined, as were the apparent activation energy and the temperature of reaction surface; the mechanism of the process of reduction in industrial apparatus was more precisely determined.

The results of this investigation confirmed the validity and applicability of the working hypotheses based on autocatalytic nature of the process which makes it possible to improve the apparatus and technological regime of the magnesium reduction process.

7 illustrations, bibliography of 18 titles.

UDC 669.162.282:669.295

Sodium Reduction of Titanium From Tetrachloride, S. V. Ogurtsov, V.D. Savin, A. Ye. Nikitin, O. V. Perfil'yev, In the collection: Titanium Alloys for New Technology, Nauka Press, 1968, pp. 232-320.

The results of an investigation of the sodium reduction of titanium tetrachloride by the two stage method are investigated; during the first stage a molten pool of "black salt," a complex compound of the lower chlorides of titanium, is obtained, and during the second stage this compound is subjected to final reduction to metal in the form of large crystals. The technological parameters for conducting the stage of the process without developing pressure in the reaction vessel are determined. During the second stage conditions for obtaining in the laboratory a high and stable yield of macrocrystalline titanium within the limits of 55-60% were determined for the first time. The possibility of applying the technological regimes on an experimental-industrial scale with satisfactory results is demonstrated.

1 table, 4 illustrations, bibliography of 11 titles.

UDC 669.295+621.77

Aspects of the Production Technology of Semifinished Products of Titanium and Its Alloys, I. N. Kaganovich, In the collection: Titanium Alloys for New Technology, Nauka Press, 1968, pp. 230-243.

The process flowsheets and parameters for the fabrication of sheets, strip, forgings and stampings of various groups of titanium alloys are described. The effect of gas absorption and thermomechanical treatment on the properties of the semifinished products is examined.

3 tables, 4 illustrations, bibliography of 12 titles.

UDC 669.295+621.774

Production of Titanium and Titanium-Alloy Tubes, V.Ya. Ostrenko, In the collection: Titanium Alloys for New Technology, Nauka Press, 1968, pp. 243-253.

The current production technology of 0.5-465 mm diameter tubes of all the series-produced alloys, as practiced at Soviet plants, is reviewed.

Methods of further improving the production technology and quality of the tubes are illustrated.

1 table, 6 illustrations, bibliography of 9 titles.

UDC 621.777+669.295

Extrusion of Titanium Alloy Shapes, O.S. Mironov et al., In the collection: Titanium Alloys for New Technology, Nauka Press, 1968, pp. 253-256.

The technology of extrusion and the effect of temperature and rate parameters of deformation on the structure and properties of industrial titanium alloy shapes are described.

UDC 621.77+699.295

/279

Deformability of Certain ($\alpha + \beta$)- and β -Alloys of Titanium in Cold State,
A. D. Lyuchkov, L. A. Il'vovskaya, V. I. Shevchenko, T. V. Kutsygina, In the
collection: Titanium Alloys for New Technology, Nauka Press, 1968, pp. 257-261.

The results of an investigation of the effect of the structure and phase composition of the alloys VT14, VT8, TiAl5V4Cr1.5Fe1.5, VT15 and Ti-32 Mo on deformability at room temperature under high loading rates are presented.

It is concluded that in the presence of a high deformation rate the two-phase alloys VT14 and TiAl5V4Cr1.5Fe1.5 should be subjected to annealing and the alloy VT8, to quenching, in order to assure a higher plasticity level.

3 tables, 5 illustrations, bibliography of 3 titles.

UDC 621.791+669.295

Problems of the Welding of Titanium and Its Alloys, S. M. Gurevich, In the collection: Titanium Alloys for New Technology, Nauka Press, 1968, pp. 262-271.

The methods used to weld titanium and its alloys are analyzed. The advantages of pulsed-arc welding, submerged argon-arc welding, vacuum electron-beam welding and diffusion welding are described.

It is concluded that automatic submerged arc welding is the principal technological process for joining segments of apparatus housings.

5 illustrations, bibliography of 14 titles.

NATIONAL AERONAUTICS AND SPACE ADMINISTRATION
WASHINGTON, D. C. 20546
OFFICIAL BUSINESS

FIRST CLASS MAIL



POSTAGE AND FEES PAID
NATIONAL AERONAUTICS AND
SPACE ADMINISTRATION

000 001 42 51 305 70075 00403
AIR FORCE AERON. LABORATORY FACULTY
KIRKLAND AFB, NEW MEXICO 87147

RECORDED MAIL - AIR FORCE FACULTY

POSTMASTER: If Undeliverable (Section 158
Postal Manual) Do Not Return

"The aeronautical and space activities of the United States shall be conducted so as to contribute . . . to the expansion of human knowledge of phenomena in the atmosphere and space. The Administration shall provide for the widest practicable and appropriate dissemination of information concerning its activities and the results thereof."

— NATIONAL AERONAUTICS AND SPACE ACT OF 1958

NASA SCIENTIFIC AND TECHNICAL PUBLICATIONS

TECHNICAL REPORTS: Scientific and technical information considered important, complete, and a lasting contribution to existing knowledge.

TECHNICAL NOTES: Information less broad in scope but nevertheless of importance as a contribution to existing knowledge.

TECHNICAL MEMORANDUMS: Information receiving limited distribution because of preliminary data, security classification, or other reasons.

CONTRACTOR REPORTS: Scientific and technical information generated under a NASA contract or grant and considered an important contribution to existing knowledge.

TECHNICAL TRANSLATIONS: Information published in a foreign language considered to merit NASA distribution in English.

SPECIAL PUBLICATIONS: Information derived from or of value to NASA activities. Publications include conference proceedings, monographs, data compilations, handbooks, sourcebooks, and special bibliographies.

TECHNOLOGY UTILIZATION

PUBLICATIONS: Information on technology used by NASA that may be of particular interest in commercial and other non-aerospace applications. Publications include Tech Briefs, Technology Utilization Reports and Technology Surveys.

Details on the availability of these publications may be obtained from:

SCIENTIFIC AND TECHNICAL INFORMATION DIVISION
NATIONAL AERONAUTICS AND SPACE ADMINISTRATION
Washington, D.C. 20546